

EMERGING INFECTIOUS DISEASES[®]



Coronaviruses

February 2020

Artist Unknown. A Rajput Warrior with Camel, Possibly Maru Ragini from a Ragamala, 1650-80. Opaque watercolor, ink, and gold on paper. 10 1/4 in x 6 15/16 in/26 cm x 17.6 cm. Purchase and partial gift from the Catherine and Ralph Benkaim Collection; Severance and Greta Millikin Purchase Fund. Public domain digital image courtesy of The Cleveland Museum of Modern Art, Cleveland, Ohio



EMERGING INFECTIOUS DISEASES

EDITOR-IN-CHIEF

D. Peter Drotman

ASSOCIATE EDITORS

Charles Ben Beard, Fort Collins, Colorado, USA
 Ermias Belay, Atlanta, Georgia, USA
 David M. Bell, Atlanta, Georgia, USA
 Sharon Bloom, Atlanta, Georgia, USA
 Richard Bradbury, Melbourne, Australia
 Mary Brandt, Atlanta, Georgia, USA
 Corrie Brown, Athens, Georgia, USA
 Charles H. Calisher, Fort Collins, Colorado, USA
 Benjamin J. Cowling, Hong Kong, China
 Michel Drancourt, Marseille, France
 Paul V. Effler, Perth, Australia
 Anthony Fiore, Atlanta, Georgia, USA
 David O. Freedman, Birmingham, Alabama, USA
 Peter Gerner-Smith, Atlanta, Georgia, USA
 Stephen Hadler, Atlanta, Georgia, USA
 Matthew J. Kuehnert, Edison, New Jersey, USA
 Nina Marano, Atlanta, Georgia, USA
 Martin I. Meltzer, Atlanta, Georgia, USA
 David Morens, Bethesda, Maryland, USA
 J. Glenn Morris, Jr., Gainesville, Florida, USA
 Patrice Nordmann, Fribourg, Switzerland
 Johann D.D. Pitout, Calgary, Alberta, Canada
 Ann Powers, Fort Collins, Colorado, USA
 Didier Raoult, Marseille, France
 Pierre E. Rollin, Atlanta, Georgia, USA
 Frederic E. Shaw, Atlanta, Georgia, USA
 David H. Walker, Galveston, Texas, USA
 J. Todd Weber, Atlanta, Georgia, USA
 J. Scott Weese, Guelph, Ontario, Canada

Managing Editor

Byron Breedlove, Atlanta, Georgia, USA

Copy Editors Kristina Clark, Dana Dolan, Karen Foster,
 Thomas Gryczan, Amy Guinn, Michelle Moran, Shannon
 O'Connor, Jude Rutledge, P. Lynne Stockton, Deborah Wenger

Production Thomas Ehemann, William Hale, Barbara Segal,
 Reginald Tucker

Journal Administrator Susan Richardson

Editorial Assistant Kristine Phillips

Communications/Social Media Sarah Logan Gregory,
 Tony Pearson-Clarke, Deanna Altomara (intern)

Founding Editor

Joseph E. McDade, Rome, Georgia, USA

EDITORIAL BOARD

Barry J. Beaty, Fort Collins, Colorado, USA
 Martin J. Blaser, New York, New York, USA
 Andrea Boggild, Toronto, Ontario, Canada
 Christopher Braden, Atlanta, Georgia, USA
 Arturo Casadevall, New York, New York, USA
 Kenneth G. Castro, Atlanta, Georgia, USA
 Vincent Deubel, Shanghai, China
 Christian Drosten, Charité Berlin, Germany
 Isaac Chun-Hai Fung, Statesboro, Georgia, USA
 Kathleen Gensheimer, College Park, Maryland, USA
 Rachel Gorwitz, Atlanta, Georgia, USA
 Duane J. Gubler, Singapore
 Richard L. Guerrant, Charlottesville, Virginia, USA
 Scott Halstead, Arlington, Virginia, USA
 David L. Heymann, London, UK
 Keith Klugman, Seattle, Washington, USA
 Takeshi Kurata, Tokyo, Japan
 S.K. Lam, Kuala Lumpur, Malaysia
 Stuart Levy, Boston, Massachusetts, USA
 John S. Mackenzie, Perth, Australia
 John E. McGowan, Jr., Atlanta, Georgia, USA
 Jennifer H. McQuiston, Atlanta, Georgia, USA
 Tom Marrie, Halifax, Nova Scotia, Canada
 Nkuchia M. M'ikanatha, Harrisburg, Pennsylvania, USA
 Frederick A. Murphy, Bethesda, Maryland, USA
 Barbara E. Murray, Houston, Texas, USA
 Stephen M. Ostroff, Silver Spring, Maryland, USA
 Mario Raviglione, Milan, Italy, and Geneva, Switzerland
 David Relman, Palo Alto, California, USA
 Guenaël R. Rodier, Saône-et-Loire, France
 Connie Schmaljohn, Frederick, Maryland, USA
 Tom Schwan, Hamilton, Montana, USA
 Rosemary Soave, New York, New York, USA
 P. Frederick Sparling, Chapel Hill, North Carolina, USA
 Robert Swanepoel, Pretoria, South Africa
 David E. Swayne, Athens, Georgia, USA
 Phillip Tarr, St. Louis, Missouri, USA
 Duc Vugia, Richmond, California, USA
 Mary Edythe Wilson, Iowa City, Iowa, USA

Emerging Infectious Diseases is published monthly by the Centers for Disease Control and Prevention, 1600 Clifton Rd NE, Mailstop H16-2, Atlanta, GA 30329-4027, USA. Telephone 404-639-1960, fax 404-639-1954, email eideditor@cdc.gov.

The conclusions, findings, and opinions expressed by authors contributing to this journal do not necessarily reflect the official position of the U.S. Department of Health and Human Services, the Public Health Service, the Centers for Disease Control and Prevention, or the authors' affiliated institutions. Use of trade names is for identification only and does not imply endorsement by any of the groups named above.

All material published in *Emerging Infectious Diseases* is in the public domain and may be used and reprinted without special permission; proper citation, however, is required.

Use of trade names is for identification only and does not imply endorsement by the Public Health Service or by the U.S. Department of Health and Human Services.

EMERGING INFECTIOUS DISEASES is a registered service mark of the U.S. Department of Health & Human Services (HHS).

EMERGING INFECTIOUS DISEASES®

Coronaviruses

February 2020



On the Cover

Artist Unknown. *A Rajput Warrior with Camel*, possibly Maru Ragini from a Ragamala, 1650–80. Opaque watercolor, ink, and gold on paper. 10 1/4 in x 6 15/16 in/26 cm x 17.6 cm. Purchase and partial gift from the Catherine and Ralph Benkaim Collection; Severance and Greta Millikin Purchase Fund. Public domain digital image courtesy of The Cleveland Museum of Modern Art, Cleveland, Ohio

About the Cover p. 395

Perspective

Middle East Respiratory Syndrome Coronavirus Transmission

M.E. Killerby et al.

191

Synopses

Medscape
EDUCATION
ACTIVITY

Acute Toxoplasmosis among Canadian Deer Hunters Associated with Consumption of Undercooked Deer Meat Hunted in the United States

Health professionals should be aware that such outbreaks might be more common in the future.

C. Gaulin et al.

199

Public Health Program for Decreasing Risk for Ebola Virus Disease Resurgence from Survivors of the 2013–2016 Outbreak, Guinea

M. Keita et al.

206

Research

Medscape
EDUCATION
ACTIVITY

Characteristics of Patients with Acute Flaccid Myelitis, United States, 2015–2018

Differences in clinical and laboratory characteristics between years with and without increased activity suggest differences in viral etiologies.

N. McLaren et al.

212

Medscape
EDUCATION
ACTIVITY

Illness Severity in Hospitalized Influenza Patients by Virus Type and Subtype, Spain, 2010–2017

Influenza A(H1N1)pdm09 infections caused more hospitalizations, intensive care unit admissions, and deaths than influenza A(H3N2) or B infections.

C. Delgado-Sanz et al.

220

Exposure to Ebola Virus and Risk for Infection with Malaria Parasites, Rural Gabon

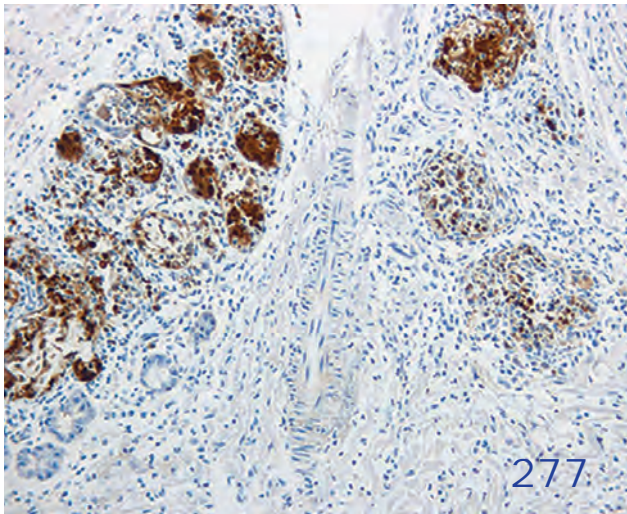
J.L. Abbate et al.

229

Cost-Effectiveness of Screening Program for Chronic Q Fever, the Netherlands

P.T. de Boer et al.

238



EMERGING INFECTIOUS DISEASES®

February 2020

Elizabethkingia anopheles Infection in Infants, Cambodia, 2012–2018

T.A.N. Reed et al. 320

Global Expansion of Pacific Northwest *Vibrio parahaemolyticus* Sequence Type 36

M. Abanto et al. 323

Surge in Anaplasmosis Cases in Maine, USA, 2013–2017

S.P. Elias et al. 327

Mycoplasma genitalium Antimicrobial Resistance in Community and Sexual Health Clinic Patients, Auckland, New Zealand

A. Vesty et al. 332

Early Detection of Public Health Emergencies of International Concern through Undiagnosed Disease Reports in ProMED-Mail

C. Rolland et al. 336

Ocular *Spiroplasma ixodetis* in Newborns, France

A. Matet et al. 340

Unique Clindamycin-Resistant *Clostridioides difficile* Strain Related to Fluoroquinolone-Resistant Epidemic BI/RT027 Strain

A.M. Skinner et al. 247

Porcine Deltacoronavirus Infection and Transmission in Poultry, United States

P.A. Boley et al. 255

Chronic Human Pegivirus 2 and Hepatitis C Virus Co-infection

K.E. Collier et al. 265

Interspecies Transmission of Reassortant Swine Influenza A Virus Containing Genes from Swine Influenza A(H1N1)pdm09 and A(H1N2) Viruses

H.E. Everett et al. 273

Multiplex Mediator Displacement Loop-Mediated Isothermal Amplification for Detection of *Treponema pallidum* and *Haemophilus ducreyi*

L. Becherer et al. 282

Novel Subclone of Carbapenem-Resistant *Klebsiella pneumoniae* Sequence Type 11 with Enhanced Virulence and Transmissibility, China

K. Zhou et al. 289

Neutralizing Antibodies against Enteroviruses in Patients with Hand, Foot and Mouth Disease

L.A. Nguyet et al. 298

Dispatches

Emergence of Chikungunya Virus, Pakistan, 2016–2017

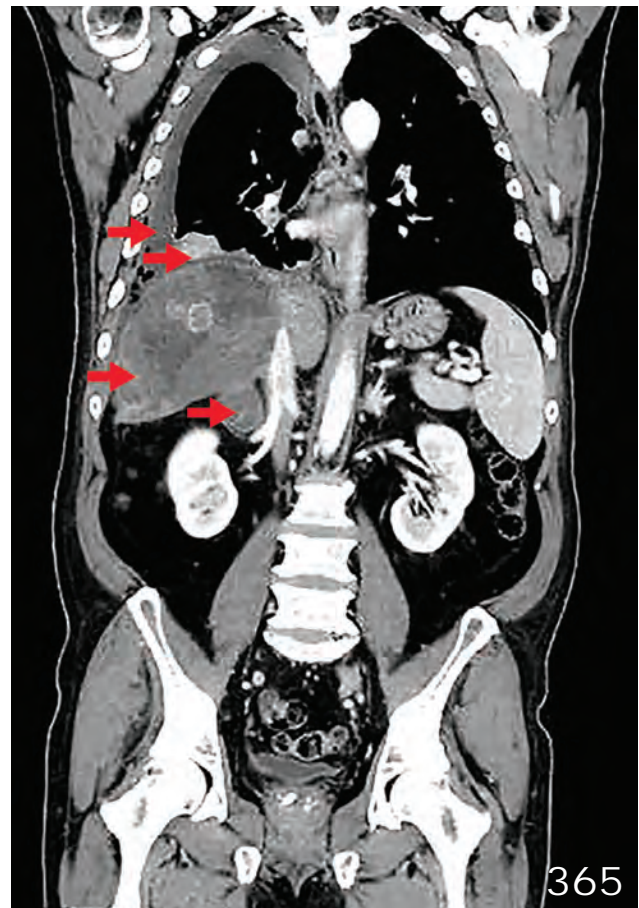
N. Badar et al. 307

Influence of Rainfall on *Leptospira* Infection and Disease in a Tropical Urban Setting, Brazil

K.P. Hacker et al. 311

Systematic Hospital-Based Travel Screening to Assess Exposure to Zika Virus

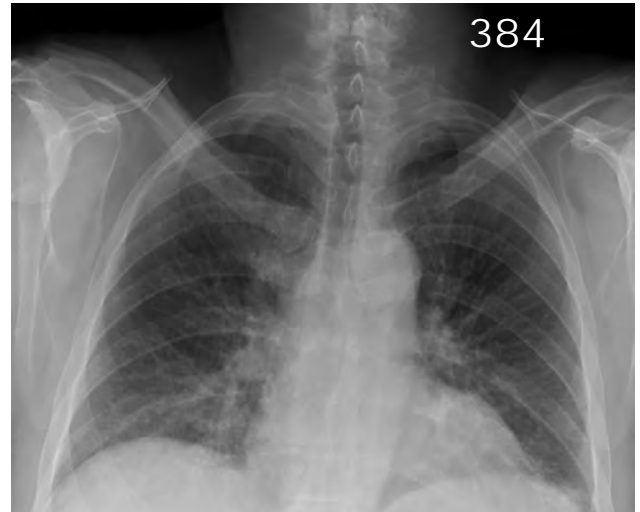
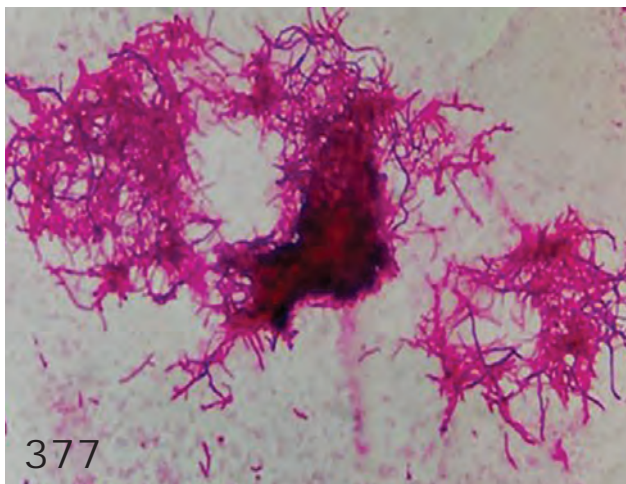
A. Iqbal et al. 315



Use of Surveillance Outbreak Response Management and Analysis System for Human Monkeypox Outbreak, Nigeria, 2017–2019 B.C. Silenou et al.	345
Human Norovirus Infection in Dogs, Thailand K. Charoenkul et al.	350
Hepatitis E Virus in Pigs from Slaughterhouses, United States, 2017–2019 H. Sooryanarain et al.	354
Rapid Nanopore Whole-Genome Sequencing for Anthrax Emergency Preparedness H.P. McLaughlin et al.	358

Research Letters

<i>Rickettsia mongolitimonae</i> Encephalitis, Southern France, 2018 M.D. Corbacho Loarte et al.	362
Human Alveolar Echinococcosis, Croatia D. Dušek et al.	364
Two Cases of a Newly Characterized <i>Neisseria</i> Species, Brazil M.M. Mustapha et al.	366
Hepatitis A Virus Genotype 1B Outbreak among Internally Displaced Persons, Syria M. Kaddoura et al.	369
<i>Rickettsia parkeri</i> and <i>Candidatus Rickettsia andeanae</i> in <i>Amblyomma maculatum</i> Group Ticks B.H. Noden et al.	371
Astrovirus in White-Tailed Deer, United States, 2018 L. Wang et al.	374
Actinomycetoma Caused by <i>Actinomadura mexicana</i>, a Neglected Entity in the Caribbean S. Bessis et al.	376
Antigenic Variant of Highly Pathogenic Avian Influenza A(H7N9) Virus, China, 2019 W. Jiang et al.	379



New Delhi Metallo-β-Lactamase-5-Producing <i>Escherichia coli</i> in Companion Animals, United States S.D. Cole et al.	381
Hantavirus Infection with Renal Failure and Proteinuria, Colorado, USA, 2019 S. Chand et al.	383
Persistence of Crimean-Congo Hemorrhagic Fever Virus RNA L. Mathengtheng et al.	385

Comment Letter

Non-<i>Leishmania</i> Parasite in Fatal Visceral Leishmaniasis-like Disease, Brazil M.A. Domagalska, J.-C. Dujardin	388
---	-----

Another Dimension

Social Responses to Epidemics Depicted by Cinema Q. Han, D.R. Curtis	389
--	-----

About the Cover

Veiled Dangers in an Idyllic Setting B. Breedlove	395
---	-----

Etymologia Pegivirus R. Henry	272
---	-----

DECENNIAL 2020

Global Solutions to Antibiotic Resistance in Healthcare



decennial2020.org • [#Decennial2020](https://twitter.com/Decennial2020)

6th Decennial International
Conference on Healthcare
Associated Infections

March 26–30, 2020
Marriott Marquis
Atlanta, GA

**REGISTER
TODAY!**

Co-Hosted by:



Middle East Respiratory Syndrome Coronavirus Transmission

Marie E. Killerby, Holly M. Biggs, Claire M. Midgley, Susan I. Gerber, John T. Watson

Middle East respiratory syndrome coronavirus (MERS-CoV) infection causes a spectrum of respiratory illness, from asymptomatic to mild to fatal. MERS-CoV is transmitted sporadically from dromedary camels to humans and occasionally through human-to-human contact. Current epidemiologic evidence supports a major role in transmission for direct contact with live camels or humans with symptomatic MERS, but little evidence suggests the possibility of transmission from camel products or asymptomatic MERS cases. Because a proportion of case-patients do not report direct contact with camels or with persons who have symptomatic MERS, further research is needed to conclusively determine additional mechanisms of transmission, to inform public health practice, and to refine current precautionary recommendations.

Middle East respiratory syndrome (MERS) coronavirus (MERS-CoV) was first detected in Saudi Arabia in 2012 (1). To date, >2,400 cases globally have been reported to the World Health Organization (WHO), including >850 deaths (case fatality rate ≈35%) (2). Illness associated with MERS-CoV infection ranges from asymptomatic or mild upper respiratory illness to severe respiratory distress and death.

MERS-CoV is a zoonotic virus, and dromedary camels are a reservoir host (3–5). Bats are a likely original reservoir; coronaviruses similar to MERS-CoV have been identified in bats (6), but epidemiologic evidence of their role in transmission is lacking. Infection of other livestock species with MERS-CoV is possible (7); however, attempts to inoculate goats, sheep, and horses with live MERS-CoV did not produce viral shedding (8), and no epidemiologic evidence has implicated any species other than dromedaries in transmission.

Sporadic zoonotic transmission from dromedaries has resulted in limited human-to-human transmission chains, usually in healthcare or household settings (9–14)

(Figure). MERS-CoV human cases result from primary or secondary transmission. Primary transmission is classified as transmission not resulting from contact with a confirmed human MERS case-patient (15) and can result from zoonotic transmission from camels or from an unidentified source. Conzade et al. reported that, among cases classified as primary by the WHO, only 191 (54.9%) persons reported contact with dromedaries (15). Secondary transmission is classified as transmission resulting from contact with a human MERS case-patient, typically characterized as healthcare-associated or household-associated, as appropriate. However, many MERS case-patients have no reported exposure to a prior MERS patient or healthcare setting or to camels, meaning the source of infection is unknown. Among 1,125 laboratory-confirmed MERS-CoV cases reported to WHO during January 1, 2015–April 13, 2018, a total of 157 (14%) had unknown exposure (15).

Although broad categories of exposure are associated with transmission (e.g., exposure to camels or to healthcare facilities with ill patients), exact mechanisms of MERS-CoV transmission are not fully understood. Little direct epidemiologic evidence exists regarding transmission routes or the efficacy of interventions in reducing transmission. However, other potentially important factors, including detection of virus in different secretions, detection and survival of virus in the environment, and detection of virus in aerosols, lend support for the biological plausibility of certain transmission pathways. We summarize the available evidence regarding camel-to-camel, camel-to-human, and human-to-human transmission of MERS-CoV, including direct epidemiologic evidence and evidence supporting biologically plausible transmission routes.

MERS-CoV in Camels

Evidence for Infection of Camels

MERS-CoV infection in camels has been demonstrated through serologic investigations, molecular evidence using real-time reverse transcription PCR

Author affiliation: Centers for Disease Control and Prevention, Atlanta, Georgia, USA

DOI: <https://doi.org/10.3201/eid2602.190697>

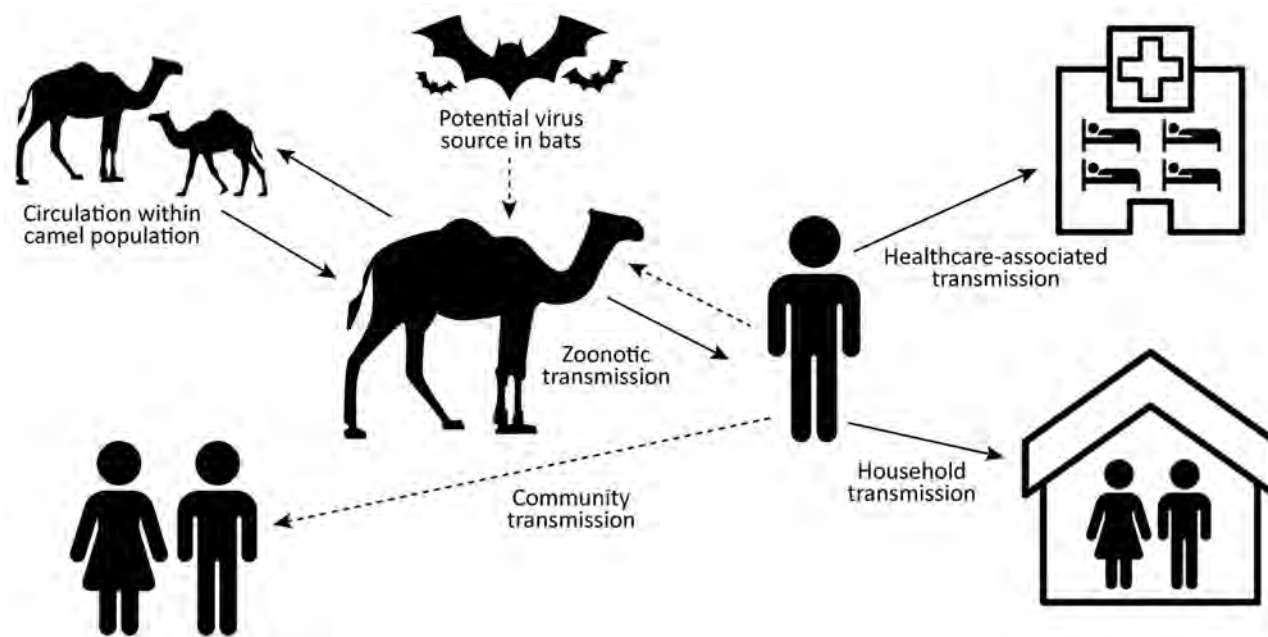


Figure. Summary of Middle East respiratory syndrome coronavirus transmission pathways. Solid lines indicate known transmission pathways; dashed lines indicate possible transmission pathways for which supporting evidence is limited or unknown.

(rRT-PCR), and by virus isolation, as described in recent reviews (16,17). Geographically wide-ranging seroprevalence studies have identified MERS-CoV-specific antibodies in camels in countries across the Middle East and North, West, and East Africa, often with >90% seroprevalence in adult camels (18). Studies in many of these countries have shown molecular evidence of MERS-CoV RNA and isolation of infectious MERS-CoV in camels (16,17,19–21).

Viral Shedding in Camels

In naturally or experimentally infected camels, MERS-CoV appears to cause an upper respiratory tract infection with or without symptoms, including nasal and lachrymal discharge, coughing, sneezing, elevated body temperature, and loss of appetite (20,22,23). In naturally infected camels, MERS-CoV RNA has been recovered most commonly from nasal swabs but also from fecal swabs, rectal swabs, and lung tissue (20,24). No evidence of viral RNA has been demonstrated in camel serum, blood, or urine using rRT-PCR (25,26). In experimentally infected camels, infectious virus and RNA was detected in nasal swab and oral samples but not in blood, serum, feces, or urine (23). MERS-CoV RNA has been detected in raw camel milk collected using traditional milking methods, including using a suckling calf as stimulus for milk letdown; presence of live virus was not evaluated (27). Viral RNA may therefore have been

introduced via calf saliva or nasal secretions or fecal contamination. Experimentally introduced virus can survive in milk but did not survive when heat treated (28). It is also not known if the virus would remain viable in milk from seropositive dams when antibodies could be found in the milk.

These shedding data indicate that contact with camel nasal secretions, saliva, and respiratory droplets carry potential risk for camel-to-human or camel-to-camel transmission. Contact with nasal secretions can occur when directly handling live camels, and virus from camel nasal secretions can contaminate fomites in the environment (29). Although rRT-PCR evidence of MERS-CoV and genome fragments have been detected in air samples from a camel barn (30), no live virus was detected, and no epidemiologic study has implicated airborne transmission. Transmission following exposure to camel feces may be biologically plausible, although no epidemiologic evidence indicates the likelihood of such transmission. Similarly, although transmission following consumption of raw camel milk may be biologically plausible, epidemiologic studies have not consistently identified milk consumption as a unique risk factor for MERS-CoV infection or illness, independent of other direct or indirect camel exposures (31,32). No epidemiologic evidence supports transmission associated with camel urine or meat.

Camel-to-Camel Transmission Dynamics

MERS-CoV RNA is detected most frequently in younger camels (22,25,33) but has been detected in camels >4 years of age (22). In a longitudinal study of a camel dairy herd, most calves became infected with MERS-CoV at 5–6 months of age, around the time maternal MERS-CoV antibodies wane. The calves then produced MERS-CoV antibodies by 11–12 months of age (34). In seroprevalence studies, camels <2 years of age demonstrated lower seroprevalence than camels >2 years of age (25,35). Across many countries, the seroprevalence of adult camels is >90% (16,17). Overall, these data suggest most camels are initially infected with MERS-CoV at <2 years of age. However, camels can shed virus despite preexisting MERS-CoV antibodies, suggesting that repeat infections are possible (36,37). Varying prevalence of MERS-CoV RNA in camels has been reported in different countries and settings, such as farms (33) and live animal markets (38). Risk for camel-to-camel or camel-to-human transmission may be influenced by crowding, mixing of camels from multiple sources, transportation, and characteristics of live animal markets (39). Phylogenetic modeling has provided supportive evidence that long-term MERS-CoV evolution has occurred exclusively in camels, with humans acting as a transient and usually terminal host (40).

Zoonotic Transmission

Evidence and Risk Factors for Zoonotic Transmission

Persons in Saudi Arabia with occupational exposure to camels demonstrated higher seroprevalence of MERS-CoV-specific antibodies (camel shepherds, 2.3%; slaughterhouse workers, 3.6%) compared with the general population (0.2%) (41). A case-control study of primary human cases and matched controls also showed that camel exposure was more likely among case-patients than matched controls (31). Further evidence supporting camel-to-human transmission includes identical or nearly identical MERS-CoV sequences found in camels and humans (41–45).

Occupational groups with frequent exposure to camels have been assessed through seroepidemiologic studies. In Qatar, a study of 9 seropositive and 43 matched seronegative camel workers showed that regular involvement in training and herding of camels, cleaning farm equipment, not handwashing before and after camel handling, and milking camels were associated with seropositivity (46). In a Saudi Arabia study of 30 camel workers in which 50% were seropositive for MERS-CoV, no association was identified between seropositivity and factors

including age, smoking, handwashing after camel contact, consuming camel meat or milk, or specific occupation (camel truck driver, handler, or herder) (47). Neither investigation controlled for possible confounding risk factors (e.g., age or duration of exposure to camels). In Abu Dhabi, an investigation of 235 market and slaughterhouse workers showed that 17% were seropositive for MERS-CoV and that daily contact with camels or their waste, working as a camel salesman, and self-reported diabetes were risk factors for seropositivity (32). Among market workers in the same study, handling live camels and either cleaning equipment (e.g., halters, water troughs, etc.) or administering medications to camels were risk factors on multivariable analysis (32). These studies generally support the hypothesis that direct physical contact with camels is a risk factor for transmission, although cleaning equipment could also result in indirect transmission.

Potential Seasonality of Human Cases

Previous findings suggest that MERS-CoV circulation among camels peaks in late winter through early summer (22,26,48). Initial MERS-CoV infection in camels is thought to occur at ≈6 months of age, after the typical winter calving season. Investigations have demonstrated different seasonal peaks for MERS-CoV infection in camels: November–January (22) and December–April (48) in Saudi Arabia, January–June in Egypt (26). A seasonal peak has been suggested to result in a corresponding peak in zoonotic transmission, and an April–July peak has been supported by phylogenetic modeling (40). However, camels have been found to be rRT-PCR positive for MERS-CoV throughout the year (22). Further investigations are needed to demonstrate seasonality of MERS-CoV infection in camels and link these patterns to seasonal peaks of zoonotic transmission.

Zoonotic MERS-CoV Transmission outside the Arabian Peninsula

Despite evidence of circulating MERS-CoV in camels in North, East, and West Africa (49), limited evidence of human infection exists from Africa. In Kenya, no MERS-CoV antibodies were detected among 760 persons with occupational exposure to camels (50). In a separate study in Kenya, 2 seropositive adults who kept other livestock but not camels were identified among 1,122 persons who were predominantly without occupational exposure to camels (Appendix reference 51, <https://wwwnc.cdc.gov/EID/article/26/2/19-0697-App1.pdf>). In Nigeria, no MERS-CoV antibodies were found in 261 slaughterhouse workers with exposure

to camels (Appendix reference 52). MERS-CoV sequences from camels in Africa phylogenetically cluster separately relative to camel and human MERS-CoV from the Arabian Peninsula, suggesting single or few introductions into Saudi Arabia and limited contact (19). Differences in virus growth have been shown between MERS-CoV strains isolated from West Africa and those isolated from the Middle East (19); relative to human and camel MERS-CoV from Saudi Arabia, virus isolates from Burkina Faso and Nigeria had lower virus replication competence in *ex vivo* cultures of human bronchus and lung. These findings may suggest regional variation in the potential for MERS-CoV replication in humans. Other factors contributing to the limited evidence of zoonotic MERS transmission in Africa may include differences between virus surveillance, human populations, camel populations, camel husbandry, and the type of human–camel interactions in these regions.

Prevention of Zoonotic Transmission

WHO recommends that anyone presumed at higher risk for severe illness (e.g., persons who are older, have diabetes, or are immunocompromised) should avoid contact with camels and raw camel products (Appendix reference 53). Although no evidence definitively links raw camel products with MERS-CoV infection, WHO presents these precautions in the context of considerable knowledge gaps surrounding MERS-CoV transmission. In addition, WHO recommends basic hygiene precautions for persons with occupational exposure to camels (Appendix reference 53).

Human-to-Human Transmission

After zoonotic introduction, human-to-human transmission of MERS-CoV can occur, but humans are considered transient or terminal hosts (40), with no evidence for sustained human-to-human community transmission. In addition to limited household transmission, large, explosive outbreaks in healthcare settings have been periodically documented. In South Korea in 2015, a single infected traveler returning from the Arabian Peninsula was linked to an outbreak of 186 cases, including 38 deaths (case-fatality rate 20%) (Appendix reference 54). Multiple other healthcare-associated outbreaks have been described in Saudi Arabia (Appendix references 55,56), Jordan (Appendix reference 57), and United Arab Emirates (Appendix reference 58). Healthcare transmission has also occurred outside the Arabian Peninsula from exported cases, including in the United Kingdom (Appendix reference 59) and France (Appendix reference 60). Given their size and scope, healthcare-

associated outbreaks have provided most of the context for investigation of risk factors for human-to-human transmission.

Viral Shedding in Humans

MERS-CoV shedding in humans appears to differ from the pattern of viral shedding in camels. In humans, MERS-CoV RNA and live virus have been detected in both upper (nasopharyngeal and oropharyngeal swab) and lower (sputum, tracheal aspirate, and bronchoalveolar lavage fluid) respiratory tract samples, although RNA levels are often higher in the lower respiratory tract (Appendix reference 61). In humans, MERS-CoV is predominantly thought to infect the lower respiratory tract (Appendix reference 62), where the MERS-CoV dipeptidyl peptidase-4 (DPP4) receptor predominates, in contrast to camels, where DPP4 is found predominantly in the upper respiratory tract (Appendix reference 63). More severely ill patients typically have higher MERS-CoV RNA levels, as indicated by rRT-PCR cycle threshold (Ct) values and more prolonged viral shedding (Appendix reference 64). MERS-CoV RNA has been detected from the lower respiratory tract >1 month after illness onset (Appendix references 65,66), and live virus has been isolated up to 25 days after symptom onset (Appendix reference 67). RNA detection is prolonged in the respiratory tract of patients with diabetes mellitus, even when adjusting for illness severity (Appendix reference 66). Among mildly ill patients, who might typically be isolated at home, viral RNA levels in the upper respiratory tract have been detected for several weeks (Appendix references 68,69). Infectious virus has been isolated from the upper respiratory tract of a patient with mild symptoms (Appendix reference 68), suggesting a potential for transmission among less severely ill patients. However, there is no definitive evidence of transmission from asymptomatic cases, and epidemiologic evidence suggests that transmission from mildly symptomatic or asymptomatic cases does not readily occur (Appendix reference 70).

In humans, MERS-CoV RNA has been detected outside of the respiratory tract (Appendix references 66,71,72). Viral RNA has been detected in the whole blood or serum of mildly or severely ill patients (Appendix references 66,72) and in the urine of patients who subsequently died (Appendix reference 66), although virus isolation attempts on urine samples (Appendix reference 66) and serum (Appendix reference 71) have been unsuccessful. MERS-CoV RNA has also been detected from the stool of mildly and severely ill patients (Appendix reference 66). Subgenomic MERS-CoV RNA, an intermediate in the virus replication

cycle, has been detected in stool, suggesting that MERS-CoV might replicate in the gastrointestinal tract (Appendix reference 73); however, it is not clear if this contributes to pathogenesis or transmission.

Reproduction Number and Attack Rates

The number of secondary cases resulting from a single initial case (reproduction number, R_0) (Appendix reference 74) ranges widely for MERS-CoV, e.g., from 8.1 in the South Korea outbreak, compared with an overall R_0 of 0.45 in Saudi Arabia (Appendix reference 74). Superspreading events, which generally describe a single MERS-CoV case epidemiologically linked to >5 subsequent cases, have been frequently described, particularly in healthcare-associated outbreaks (Appendix references 55,56). R_0 estimates, however, can vary depending on numerous biologic, sociobehavioral, and environmental factors, and must be interpreted with caution (Appendix reference 75). Most studies estimating R_0 across multiple areas, or at the end stage of an outbreak, result in estimates of $R_0 < 1$, consistent with the knowledge that the virus does not continue to circulate in humans and that outbreaks are eventually contained. A wide range in published attack rates (the proportion of exposed persons who are infected) has also been reported (Appendix reference 74).

Transmission in Healthcare Facilities

Multiple studies have examined risk factors for MERS-CoV transmission in healthcare facilities. Higher viral loads (rRT-PCR Ct values) in respiratory tract samples have been linked to transmission risk (Appendix reference 76). Kim et al. described heterogeneity of transmission in South Korea in 2015, where 22 of 186 cases were associated with further transmission of MERS-CoV and 5 superspreading events accounted for 150 of 186 cases (Appendix reference 54). On multivariable analysis, transmission was associated with lower Ct values (indicating higher viral RNA load) and preisolation hospitalization or emergency department visits. Superspreading events were associated with a higher number of preisolation contacts, increased preisolation emergency room visits, and visiting multiple healthcare providers.

Alraddadi et al. studied risk factors for MERS-CoV infection in 20 healthcare workers in Saudi Arabia using serologic testing (Appendix reference 77) and found that N95 respirator use among healthcare workers decreased the risk for seropositivity. Conversely, wearing a medical mask (as opposed to not wearing a medical mask) increased the risk for seropositivity, but this finding was observed in a small number of persons and was strongly correlated with

not wearing an N95 respirator. All 20 healthcare workers had been in the same room or automobile or within 2 m of a MERS patient. This study provided evidence to suggest that aerosol transmission of MERS-CoV may be possible at close range, as seen with other respiratory viruses (e.g., influenza) spread primarily by droplet or contact transmission, particularly during aerosol-generating procedures. Having participated in infection control training specific to MERS-CoV was associated with a decreased risk for seropositivity; in healthcare workers in South Korea, a lack of personal protective equipment (PPE) use was more likely in MERS-CoV-infected healthcare workers than among exposed uninfected healthcare workers (Appendix reference 78).

Studies have shown infection among persons without close and prolonged exposure to MERS case-patients during healthcare-associated outbreaks. In Jeddah during 2014, a total of 53 healthcare-associated cases were reported among hospitalized patients, of whom only 5 had documented presence in the same room as a MERS case-patient (Appendix reference 79). Among the remaining healthcare-associated cases, many shared common treatment locations (e.g., dialysis unit) but denied being in the same room as a MERS case-patient. Similar observations were documented during a multihospital outbreak in Jordan in 2015, and anecdotal evidence suggested a potential role for fomite transmission associated with a common imaging table and portable echocardiogram machine (Appendix reference 80).

MERS-CoV has been cultured from environmental objects, such as bed sheets, bedrails, intravenous fluid hangers, and radiograph devices, suggesting the potential for environmental transmission (Appendix reference 67). Viral RNA has also been identified in air samples from the hospital rooms of MERS patients (Appendix reference 81). MERS-CoV has also been shown to be relatively stable in the environment under various conditions (Appendix reference 82), supporting the possibility of fomite transmission, although definitive epidemiologic evidence implicating fomite or aerosol transmission is lacking.

Prevention of Healthcare-Associated Transmission

Studies have described delays in case recognition and establishment of infection control precautions as factors in healthcare-associated transmission (Appendix references 54,56,79). Triage practices that result in rapid isolation of suspected MERS case-patients and application of transmission-based precautions can decrease opportunities for early transmission. However, implementing triage procedures to quickly identify

potential MERS cases in areas with local MERS-CoV transmission (e.g., Arabian Peninsula) is challenging because signs and symptoms are often nonspecific (Appendix reference 83). In addition, complications or exacerbations of concurrent conditions, including chronic kidney or heart disease, can manifest with acute or worsening respiratory symptoms that delay suspicion for MERS. Patient crowding has been associated with transmission in healthcare facilities, particularly in emergency departments (Appendix references 54,79). In multiple outbreaks, inconsistent PPE use has been reported as contributing to transmission (Appendix references 56,58), and transmission to healthcare personnel despite reported use of appropriate PPE (Appendix references 56,78) suggests that improper PPE use may contribute to transmission. Transmission risk may be particularly high during aerosol-generating procedures, in which large quantities of virus might be aerosolized.

Household Transmission

Human-to-human transmission of MERS-CoV has been reported among household contacts. Drosten et al. described 12 probable cases among 280 household contacts of 26 index case-patients (13). Arwady et al. investigated MERS-CoV infections in an extended family of 79 relatives, of whom 19 (24%) tested positive for MERS-CoV by rRT-PCR or serology (Appendix reference 84). Risk factors for acquisition included sleeping in an index case-patient's room and touching their secretions. A study of MERS-CoV infection in a group of expatriate women housed in a dormitory in Riyadh, Saudi Arabia, showed an overall infection attack rate of 2.7% (Appendix reference 85). Risk factors for infection include direct contact with a confirmed case-patient and sharing a room with a confirmed case-patient; a protective factor was having an air conditioner in the bedroom. However, transmission among household contacts is variable; Hosani et al. found that none of 105 household contacts of 34 MERS-CoV case-patients showed antibodies to MERS-CoV (Appendix reference 70). Among those 34 patients, 31 were asymptomatic or mildly symptomatic, suggesting a lower risk for transmission among this group.

Viral Factors Affecting Human-to-Human Transmission

No evidence has been reported that mutations or recombinations in MERS-CoV have led to changes in human-to-human transmission. Recombination has been documented among coronaviruses (Appendix reference 86) and has been linked to increasing pathogenicity in strains of other animal RNA viruses (Appendix reference 87). Circulation of recombinant MERS-CoV

has been described in Saudi Arabia in camels (48) and humans (Appendix references 88,89) but no substantial change in human epidemiology was seen with this circulating variant (Appendix reference 89). Deletion variants of MERS-CoV were identified in humans in Jordan (Appendix reference 57), also without notable changes in epidemiology (Appendix reference 80).

Conclusions

In areas in which MERS-CoV actively circulates among camels, human cases can result from zoonotic transmission. In these areas, close contact with camels (e.g., handling or training) is an identified risk factor for infection. Direct or indirect contact with nasal secretions probably plays a role. Given limited knowledge of mechanisms of MERS-CoV transmission, current precautions to prevent zoonotic transmission, such as recommendations to avoid consumption of raw camel milk and meat, are prudent despite the lack of epidemiologic evidence linking these exposures to MERS-CoV infection. Such precautionary recommendations, while appropriate in the context of limited knowledge, should not be interpreted as evidence of an epidemiologic association with MERS-CoV transmission.

Human-to-human transmission of MERS-CoV most frequently occurs following close contact with MERS patients, predominantly in healthcare settings and less frequently in household settings. Specifically, contact with respiratory secretions, whether through direct contact or through aerosolization of secretions during aerosol-generating procedures, plays a role in transmission. Virus isolation from fomites suggests the potential for alternative mechanisms of transmission, but direct epidemiologic evidence is lacking. Although MERS-CoV has been isolated from a mildly ill case-patient, available evidence is not sufficient to conclusively state that asymptomatic patients play an appreciable role in MERS-CoV transmission. Given the knowledge gaps surrounding transmission from asymptomatic patients, WHO recommendations state "until more is known, asymptomatic RT-PCR positive persons should be isolated, followed up daily for development of any symptoms, and tested at least weekly—or earlier, if symptoms develop—for MERS-CoV" (Appendix reference 90). Available evidence supports published Centers for Disease Control and Prevention guidance for infection prevention and control for hospitalized MERS patients (Appendix reference 91).

Large, explosive MERS-CoV outbreaks have repeatedly resulted in devastating impacts on health systems and in settings where transmission

most frequently occurs. Sporadic community cases continue to be reported, and a small but consistent proportion of MERS cases have no camel, healthcare, or MERS-CoV exposure. Continuous epidemiologic and virologic monitoring is required to determine other exposures resulting in transmission and to assess for the possibility of improved virus fitness and adaptation. Until additional evidence is available to further refine recommendations to prevent MERS-CoV transmission, continued use of existing precautionary recommendations is necessary.

About the Author

Dr. Killerby is an epidemiologist in the Division of Viral Diseases, National Center for Immunization and Respiratory Diseases, Centers for Disease Control and Prevention. Her research interests include respiratory viruses, such as MERS-CoV, human coronaviruses, and adenoviruses.

References

- Zaki AM, van Boheemen S, Bestebroer TM, Osterhaus ADME, Fouchier RAM. Isolation of a novel coronavirus from a man with pneumonia in Saudi Arabia. *N Engl J Med*. 2012;367:1814–20. <https://doi.org/10.1056/NEJMoa1211721>
- World Health Organization. Middle East respiratory syndrome coronavirus (MERS-CoV) [cited 2019 Nov 1]. <http://www.who.int/emergencies/mers-cov>
- Paden C, Yusof M, Al Hammadi Z, Queen K, Tao Y, Eltahir Y, et al. Zoonotic origin and transmission of Middle East respiratory syndrome coronavirus in the UAE. *Zoonoses Public Health*. 2018;65:322–33.
- Wernery U, Lau SK, Woo PC. Middle East respiratory syndrome (MERS) coronavirus and dromedaries. *Vet J*. 2017;220:75–9. <https://doi.org/10.1016/j.tvjl.2016.12.020>
- Reusken CB, Raj VS, Koopmans MP, Haagmans BL. Cross-host transmission in the emergence of MERS coronavirus. *Curr Opin Virol*. 2016;16:55–62. <https://doi.org/10.1016/j.coviro.2016.01.004>
- Corman VM, Ithete NL, Richards LR, Schoeman MC, Preiser W, Drosten C, et al. Rooting the phylogenetic tree of Middle East respiratory syndrome coronavirus by characterization of a conspecific virus from an African bat. *J Virol*. 2014;88:11297–303. <https://doi.org/10.1128/JVI.01498-14>
- Kandeil A, Goma M, Shehata M, El-Taweel A, Kayed AE, Abiadh A, et al. Middle East respiratory syndrome coronavirus infection in non-camelid domestic mammals. *Emerg Microbes Infect*. 2019;8:103–8. <https://doi.org/10.1080/22221751.2018.1560235>
- Adney DR, Brown VR, Porter SM, Bielefeldt-Ohmann H, Hartwig AE, Bowen RA. Inoculation of goats, sheep, and horses with MERS-CoV does not result in productive viral shedding. *Viruses*. 2016;8:230. <https://doi.org/10.3390/v8080230>
- Assiri A, Abedi GR, Bin Saeed AA, Abdalla MA, al-Masry M, Choudhry AJ, et al. Multifacility outbreak of Middle East respiratory syndrome in Taif, Saudi Arabia. *Emerg Infect Dis*. 2016;22:32–40. <https://doi.org/10.3201/eid2201.151370>
- Balkhy HH, Alenazi TH, Alshamrani MM, Baffoe-Bonnie H, Arabi Y, Hijazi R, et al. Description of a hospital outbreak of Middle East Respiratory syndrome in a large tertiary care hospital in Saudi Arabia. *Infect Control Hosp Epidemiol*. 2016;37:1147–55. <https://doi.org/10.1017/ice.2016.132>
- Assiri A, McGeer A, Perl TM, Price CS, Al Rabeah AA, Cummings DA, et al.; KSA MERS-CoV Investigation Team. Hospital outbreak of Middle East respiratory syndrome coronavirus. *N Engl J Med*. 2013;369:407–16. <https://doi.org/10.1056/NEJMoa1306742>
- Oboho IK, Tomczyk SM, Al-Asmari AM, Banjar AA, Al-Mugti H, Aloraini MS, et al. 2014 MERS-CoV outbreak in Jeddah—a link to health care facilities. *N Engl J Med*. 2015;372:846–54. <https://doi.org/10.1056/NEJMoa1408636>
- Drosten C, Meyer B, Müller MA, Corman VM, Al-Masri M, Hossain R, et al. Transmission of MERS-coronavirus in household contacts. *N Engl J Med*. 2014;371:828–35. <https://doi.org/10.1056/NEJMoa1405858>
- Memish ZA, Zumla AI, Al-Hakeem RF, Al-Rabeah AA, Stephens GM. Family cluster of Middle East respiratory syndrome coronavirus infections. *N Engl J Med*. 2013;368:2487–94. <https://doi.org/10.1056/NEJMoa1303729>
- Conzade R, Grant R, Malik MR, Elkholy A, Elhakim M, Samhoury D, et al. Reported direct and indirect contact with dromedary camels among laboratory-confirmed MERS-CoV cases. *Viruses*. 2018;10:425. <https://doi.org/10.3390/v10080425>
- Sikkema RS, Farag EABA, Islam M, Atta M, Reusken CBEM, Al-Hajri MM, et al. Global status of Middle East respiratory syndrome coronavirus in dromedary camels: a systematic review. *Epidemiol Infect*. 2019;147:e84. <https://doi.org/10.1017/S095026881800345X>
- Dighe A, Jombart T, Van Kerkhove MD, Ferguson N. A systematic review of MERS-CoV seroprevalence and RNA prevalence in dromedary camels: Implications for animal vaccination. *Epidemics*. 2019;29:100350. <https://doi.org/10.1016/j.epidem.2019.100350>
- Hemida MG, Elmoslemany A, Al-Hizab F, Alnaeem A, Almuthen F, Faye B, et al. Dromedary camels and the transmission of Middle East respiratory syndrome coronavirus (MERS-CoV). *Transbound Emerg Dis*. 2017;64:344–53. <https://doi.org/10.1111/tbed.12401>
- Chu DKW, Hui KPY, Perera RAPM, Miguel E, Niemeyer D, Zhao J, et al. MERS coronaviruses from camels in Africa exhibit region-dependent genetic diversity. *Proc Natl Acad Sci U S A*. 2018;115:3144–9. <https://doi.org/10.1073/pnas.1718769115>
- Hemida MG, Chu DK, Poon LL, Perera RA, Alhammadi MA, Ng HY, et al. MERS coronavirus in dromedary camel herd, Saudi Arabia. *Emerg Infect Dis*. 2014;20:1231–4. <https://doi.org/10.3201/eid2007.140571>
- Raj VS, Farag EA, Reusken CB, Lamers MM, Pas SD, Voermans J, et al. Isolation of MERS coronavirus from a dromedary camel, Qatar, 2014. *Emerg Infect Dis*. 2014;20:1339–42. <https://doi.org/10.3201/eid2008.140663>
- Khalafalla AI, Lu X, Al-Mubarak AI, Dalab AH, Al-Busadah KA, Erdman DD. MERS-CoV in upper respiratory tract and lungs of dromedary camels, Saudi Arabia, 2013–2014. *Emerg Infect Dis*. 2015;21:1153–8. <https://doi.org/10.3201/eid2107.150070>
- Adney DR, van Doremalen N, Brown VR, Bushmaker T, Scott D, de Wit E, et al. Replication and shedding of MERS-CoV in upper respiratory tract of inoculated dromedary camels. *Emerg Infect Dis*. 2014;20:1999–2005. <https://doi.org/10.3201/eid2012.141280>
- Farag EA, Reusken CB, Haagmans BL, Mohran KA, Stalin Raj V, Pas SD, et al. High proportion of MERS-CoV shedding dromedaries at slaughterhouse with a potential epidemiological link to human cases, Qatar 2014. *Infect Ecol Epidemiol*. 2015;5:28305. <https://doi.org/10.3402/iee.v5.28305>

25. Alagaili AN, Briese T, Mishra N, Kapoor V, Sameroff SC, Burbelo PD, et al. Middle East respiratory syndrome coronavirus infection in dromedary camels in Saudi Arabia. *MBio*. 2014;5:01002-14. <https://doi.org/10.1128/mBio.01002-14>
26. Ali MA, Shehata MM, Gomaa MR, Kandeil A, El-Shesheny R, Kayed AS, et al. Systematic, active surveillance for Middle East respiratory syndrome coronavirus in camels in Egypt. *Emerg Microbes Infect*. 2017;6:1. <https://doi.org/10.1038/emi.2016.130>
27. Reusken CB, Farag EA, Jonges M, Godeke GJ, El-Sayed AM, Pas SD, et al. Middle East respiratory syndrome coronavirus (MERS-CoV) RNA and neutralising antibodies in milk collected according to local customs from dromedary camels, Qatar, April 2014. *Euro Surveill*. 2014;19:20829. <https://doi.org/10.2807/1560-7917.ES2014.19.23.20829>
28. van Doremalen N, Bushmaker T, Karesh WB, Munster VJ. Stability of Middle East respiratory syndrome coronavirus in milk. *Emerg Infect Dis*. 2014;20:1263-4. <https://doi.org/10.3201/eid2007.140500>
29. Omrani AS, Al-Tawfiq JA, Memish ZA. Middle East respiratory syndrome coronavirus (MERS-CoV): animal to human interaction. *Pathog Glob Health*. 2015;109:354-62.
30. Azhar EL, Hashem AM, El-Kafrawy SA, Sohrab SS, Aburizaiza AS, Farraj SA, et al. Detection of the Middle East respiratory syndrome coronavirus genome in an air sample originating from a camel barn owned by an infected patient. *MBio*. 2014;5:e01450-14. <https://doi.org/10.1128/mBio.1450-14>
31. Alraddadi BM, Watson JT, Almarashi A, Abedi GR, Turkistani A, Sadran M, et al. Risk factors for primary Middle East respiratory syndrome coronavirus illness in humans, Saudi Arabia, 2014. *Emerg Infect Dis*. 2016;22:49-55. <https://doi.org/10.3201/eid2201.151340>
32. Khudhair A, Killerby ME, Al Mulla M, Abou Elkheir K, Ternanni W, Bandar Z, et al. Risk factors for MERS-CoV seropositivity among animal market and slaughterhouse workers, Abu Dhabi, United Arab Emirates, 2014-2017. *Emerg Infect Dis*. 2019;25:927-35. <https://doi.org/10.3201/eid2505.181728>
33. Wernery U, Corman VM, Wong EY, Tsang AK, Muth D, Lau SK, et al. Acute middle East respiratory syndrome coronavirus infection in livestock dromedaries, Dubai, 2014. *Emerg Infect Dis*. 2015;21:1019-22. <https://doi.org/10.3201/eid2106.150038>
34. Meyer B, Juhasz J, Barua R, Das Gupta A, Hakimuddin F, Corman VM, et al. Time course of MERS-CoV infection and immunity in dromedary camels. *Emerg Infect Dis*. 2016;22:2171-3. <https://doi.org/10.3201/eid2212.160382>
35. van Doremalen N, Hijazeen ZS, Holloway P, Al Omari B, McDowell C, Adney D, et al. High prevalence of Middle East Respiratory coronavirus in young dromedary camels in Jordan. *Vector Borne Zoonotic Dis*. 2017;17:155-9. <https://doi.org/10.1089/vbz.2016.2062>
36. Hemida MG, Alnaeem A, Chu DK, Perera RA, Chan SM, Almathen F, et al. Longitudinal study of Middle East respiratory syndrome coronavirus infection in dromedary camel herds in Saudi Arabia, 2014-2015. *Emerg Microbes Infect*. 2017;6:e56.
37. Haagmans BL, van den Brand JM, Raj VS, Volz A, Wohlsein P, Smits SL, et al. An orthopoxvirus-based vaccine reduces virus excretion after MERS-CoV infection in dromedary camels. *Science*. 2016;351:77-81. <https://doi.org/10.1126/science.aad1283>
38. Yusof MF, Queen K, Eltahir YM, Paden CR, Al Hammadi ZMAH, Tao Y, et al. Diversity of Middle East respiratory syndrome coronaviruses in 109 dromedary camels based on full-genome sequencing, Abu Dhabi, United Arab Emirates. *Emerg Microbes Infect*. 2017;6:1. <https://doi.org/10.1038/emi.2017.89>
39. Fèvre EM, Bronsvoort BM, Hamilton KA, Cleaveland S. Animal movements and the spread of infectious diseases. *Trends Microbiol*. 2006;14:125-31. <https://doi.org/10.1016/j.tim.2006.01.004>
40. Dudas G, Carvalho LM, Rambaut A, Bedford T. MERS-CoV spillover at the camel-human interface. *eLife*. 2018;7:e31257. <https://doi.org/10.7554/eLife.31257>
41. Müller MA, Meyer B, Corman VM, Al-Masri M, Turkestani A, Ritz D, et al. Presence of Middle East respiratory syndrome coronavirus antibodies in Saudi Arabia: a nationwide, cross-sectional, serological study. *Lancet Infect Dis*. 2015;15:559-64. [https://doi.org/10.1016/S1473-3099\(15\)70090-3](https://doi.org/10.1016/S1473-3099(15)70090-3)
42. Haagmans BL, Al Dhahiry SHS, Reusken CBEM, Raj VS, Galiano M, Myers R, et al. Middle East respiratory syndrome coronavirus in dromedary camels: an outbreak investigation. *Lancet Infect Dis*. 2014;14:140-5. [https://doi.org/10.1016/S1473-3099\(13\)70690-X](https://doi.org/10.1016/S1473-3099(13)70690-X)
43. Al Hammadi ZM, Chu DK, Eltahir YM, Al Hosani F, Al Mulla M, Tarnini W, et al. Asymptomatic MERS-CoV infection in humans possibly linked to infected dromedaries imported from Oman to United Arab Emirates, May 2015. *Emerg Infect Dis*. 2015;21:2197-200. <https://doi.org/10.3201/eid2112.151132>
44. Memish ZA, Cotten M, Meyer B, Watson SJ, Alsahafi AJ, Al Rabeeah AA, et al. Human infection with MERS coronavirus after exposure to infected camels, Saudi Arabia, 2013. *Emerg Infect Dis*. 2014;20:1012-5. <https://doi.org/10.3201/eid2006.140402>
45. Azhar EL, El-Kafrawy SA, Farraj SA, Hassan AM, Al-Saeed MS, Hashem AM, et al. Evidence for camel-to-human transmission of MERS coronavirus. *N Engl J Med*. 2014;370:2499-505. <https://doi.org/10.1056/NEJMoa1401505>
46. Sikkema RS, Farag EABA, Himatt S, Ibrahim AK, Al-Romaihi H, Al-Marri SA, et al. Risk factors for primary Middle East respiratory syndrome coronavirus infection in camel workers in Qatar during 2013-2014: a case-control study. *J Infect Dis*. 2017;215:1702-5. <https://doi.org/10.1093/infdis/jix174>
47. Alshukairi AN, Zheng J, Zhao J, Nehdi A, Baharoon SA, Layqah L, et al. High prevalence of MERS-CoV infection in camel workers in Saudi Arabia. *MBio*. 2018;9:e01985-18. <https://doi.org/10.1128/mBio.01985-18>
48. Sabir JSM, Lam TT-Y, Ahmed MMM, Li L, Shen Y, Abo-Aba SEM, et al. Co-circulation of three camel coronavirus species and recombination of MERS-CoVs in Saudi Arabia. *Science*. 2016;351:81-4. <https://doi.org/10.1126/science.aac8608>
49. Miguel E, Chevalier V, Ayelet G, Ben Bencheikh MN, Boussini H, Chu DK, et al. Risk factors for MERS coronavirus infection in dromedary camels in Burkina Faso, Ethiopia, and Morocco, 2015. *Euro Surveill*. 2017;22:30498. <https://doi.org/10.2807/1560-7917.ES.2017.22.13.30498>
50. Munyua P, Corman VM, Bitek A, Osoro E, Meyer B, Müller MA, et al. No serologic evidence of Middle East respiratory syndrome coronavirus infection among camel farmers exposed to highly seropositive camel herds: a household linked study, Kenya, 2013. *Am J Trop Med Hyg*. 2017;96:1318-24. <https://doi.org/10.4269/ajtmh.16-0880>

Address for correspondence: Marie E. Killerby, Centers for Disease Control and Prevention, 1600 Clifton Rd NE, Mailstop H24-5, Atlanta, GA 30329-4027, USA; email: lxo9@cdc.gov

Acute Toxoplasmosis among Canadian Deer Hunters Associated with Consumption of Undercooked Deer Meat Hunted in the United States

Colette Gaulin, Danielle Ramsay, Karine Thivierge, Joanne Tataryn, Ariane Courville, Catherine Martin, Patricia Cunningham, Joane Désilets, Diane Morin, Réjean Dion

Medscape **EDUCATION** ACTIVITY

In support of improving patient care, this activity has been planned and implemented by Medscape, LLC and Emerging Infectious Diseases. Medscape, LLC is jointly accredited by the Accreditation Council for Continuing Medical Education (ACCME), the Accreditation Council for Pharmacy Education (ACPE), and the American Nurses Credentialing Center (ANCC), to provide continuing education for the healthcare team.

Medscape, LLC designates this Journal-based CME activity for a maximum of 1.00 **AMA PRA Category 1 Credit(s)**[™]. Physicians should claim only the credit commensurate with the extent of their participation in the activity.

Successful completion of this CME activity, which includes participation in the evaluation component, enables the participant to earn up to 1.0 MOC points in the American Board of Internal Medicine's (ABIM) Maintenance of Certification (MOC) program. Participants will earn MOC points equivalent to the amount of CME credits claimed for the activity. It is the CME activity provider's responsibility to submit participant completion information to ACCME for the purpose of granting ABIM MOC credit.

All other clinicians completing this activity will be issued a certificate of participation. To participate in this journal CME activity: (1) review the learning objectives and author disclosures; (2) study the education content; (3) take the post-test with a 75% minimum passing score and complete the evaluation at <http://www.medscape.org/journal/eid>; and (4) view/print certificate. For CME questions, see page 398.

Release date: January 17, 2020; Expiration date: January 17, 2021

Learning Objectives

Upon completion of this activity, participants will be able to:

- Analyze how humans may become infected with toxoplasma
- Assess the symptoms and consequences of toxoplasma infection
- Assess the clinical presentation of toxoplasmosis in a cohort of deer hunters
- Evaluate the laboratory evaluation of this cohort of deer hunters

CME Editor

Thomas J. Gryczan, MS, Technical Writer/Editor, Emerging Infectious Diseases. *Disclosure: Thomas J. Gryczan, MS, has disclosed no relevant financial relationships.*

CME Author

Charles P. Vega, MD, Health Sciences Clinical Professor of Family Medicine, University of California, Irvine School of Medicine, Irvine, California. *Disclosure: Charles P. Vega, MD, has disclosed the following relevant financial relationships: served as an advisor or consultant for Genentech, Inc.; GlaxoSmithKline; Johnson & Johnson Pharmaceutical Research & Development, L.L.C.; served as a speaker or a member of a speakers bureau for Shire.*

Authors

Disclosures: Colette Gaulin, MD, MSc; Danielle Ramsay, MSc; Karine Thivierge, PhD; Joanne Tataryn, DVM; Ariane Courville, MD, MSc; Catherine Martin, BSc; Patricia Cunningham, BSc(N); Joane Désilets, MD, MSc; Diane Morin, MD; and Réjean Dion, MD, have disclosed no relevant financial relationships.

Author affiliations: Ministère de la Santé et des Services Sociaux, Quebec City, Quebec, Canada (C. Gaulin); Ministère de l'Agriculture, des Pêcheries, et de l'Alimentation du Québec, Quebec City (D. Ramsay); Institut National de Santé Publique du Québec, Sainte-Anne-de-Bellevue, Quebec, Canada (K. Thivierge, R. Dion); Canadian Public Health Agency, Ottawa, Ontario, Canada (J. Tataryn); Direction de Santé Publique Gaspésie—

Îles-de-la-Madeleine, Gaspé, Quebec, Canada (A. Courville); Direction de la Santé Publique du Bas St-Laurent, Quebec City (C. Martin); Direction de Santé Publique Lanaudière, Joliette, Quebec, Canada (P. Cunningham, J. Désilets); Centre Intégré de Santé et de Services Sociaux de Chaudière-Appalaches, Sainte-Marie de Beauce, Quebec, Canada (D. Morin)

DOI: <https://doi.org/10.3201/eid2602.191218>

We conducted a recent investigation in Quebec, Canada, concerning Canadian deer hunters who went to the United States to hunt deer and returned with symptoms of fever, severe headache, myalgia, and articular pain of undetermined etiology. Further investigation identified that a group of 10 hunters from Quebec attended a hunting retreat in Illinois (USA) during November 22–December 4, 2018. Six of the 10 hunters had similar symptoms and illness onset dates. Serologic tests indicated a recent toxoplasmosis infection for all symptomatic hunters, and the risk factor identified was consumption of undercooked deer meat. Among asymptomatic hunters, 2 were already immune to toxoplasmosis, 1 was not immune, and the immune status of 1 remains unknown. Outbreaks of acute toxoplasmosis infection are rare in North America, but physicians should be aware that such outbreaks could become more common.

Toxoplasma gondii is one of the most common zoonotic parasites and can cause serious illness in humans and other animals worldwide (1–3). It can infect virtually all warm-blooded animals, including birds, livestock, marine mammals, and humans (2). Felids are the definitive hosts of *T. gondii*, meaning they are the only animals in which replication can result in the production of oocysts (eggs), which are then shed in the feces (2,3). Felids are essential to the epidemiology of this parasite (2).

Human *T. gondii* infection is caused by ingestion of tissue cysts in undercooked meat; ingestion of soil, water, or food contaminated with oocysts; or, less frequently, directly from feline feces (3–8). Frequency of human infection might vary substantially by region because of ecologic, social, and cultural factors (3).

T. gondii infection acquired after birth can be asymptomatic in humans. Symptoms appear mostly in immunocompromised persons. When symptoms develop, they are nonspecific and include malaise, fever, headache, sore throat, arthralgia, and myalgia.

Lymphadenopathy, frequently cervical, is the most common sign (3). Persons remain infected for life (3). Reactivation of the disease is possible sometimes years later. However, outbreaks of acute toxoplasmosis seem to be rare.

Cervids can be infected by *T. gondii* (2,7,9–12). Cases of clinical toxoplasmosis have been documented in humans who had consumed undercooked venison (13). Toxoplasmosis infection was documented in 1 Alabama and 2 South Carolina deer hunters during 1980 (14). A recent outbreak was reported in the United States during 2017 (15). However, it is quite rare to observe a cluster of cases related to undercooked deer meat, particularly related to consumption of venison. In addition, cysts and oocysts of

T. gondii are destroyed by freezing. We report an acute toxoplasmosis outbreak in Quebec, Canada, associated with consumption of venison. We conducted an investigation to determine the outbreak magnitude, describe illness-related factors, and coordinate *Toxoplasma* spp. diagnostic testing.

Background

On December 20, 2018, public health authorities in Quebec were alerted regarding a patient with fever, severe headache, myalgia, and articular pain of undetermined etiology. The first symptom onset occurred on December 8. The patient required hospitalization; medical history showed no chronic or immunologic disease.

Further investigation identified that this patient and 9 hunter companions from Quebec attended a hunting retreat in Illinois (USA) during November 22–December 4, ending the week before illness began. Six of the 10 hunters had similar symptoms and illness onset dates. Case-patients reported consuming undercooked venison during the retreat. Hunters were tested for Q fever, hepatitis E, leptospirosis, brucellosis, Lyme disease, and toxoplasmosis. Serologic tests indicated recent toxoplasmosis infections.

Material and Methods

Case Definition

A confirmed case was defined by serologic test results (IgM positive for toxoplasmosis and a low-avidity test result). These results were consistent with a recently acquired *Toxoplasma* spp. infection in a person who had clinical symptoms compatible with toxoplasmosis after attending the deer hunting retreat during November 22–December 4, 2018.

Epidemiologic Investigation

On December 20, 2018, the Direction de la Vigie Sanitaire at the Ministère de la Santé et des Services Sociaux (Ministry of Health in Quebec) initiated an investigation. This investigation was conducted in collaboration with the Ministère de l'Agriculture, des Pêcheries et de l'Alimentation du Québec (MAPAQ: Ministry of Agriculture, Fisheries, and Food of Quebec), public health units, and the Laboratoire de Santé Publique du Québec (LSPQ: Public Health Laboratory in Quebec).

All 10 hunting companions who attended the retreat in Illinois were interviewed. The following information was collected from each attendee, symptomatic or asymptomatic: demographic information; description of activities at the outfitter, including

deer hunting and evisceration; food consumed on site, including deer meat and how it was eaten (raw, undercooked, or well done); consumption of water; and possible exposure to ticks or other animals. For persons who had symptoms, we obtained information on onset dates and symptoms. Attendees were interviewed mostly by public health nurses or medical microbiologists and infectious disease physicians.

Food Inspection Services

Deer meat harvested during the trip was available, and we collected specimens from hunter households. Meat samples were collected by the food inspection services at the MAPAQ and analyzed by the Molecular Diagnosis Laboratory at the Veterinary School at the University of Montreal (Montreal, Quebec, Canada) by using standardized and adapted methods (16).

Serologic Tests

We tested symptomatic and asymptomatic hunters by using serologic analysis for toxoplasmosis, brucellosis, leptospirosis, Q fever, hepatitis E, West Nile virus (WNV), and Lyme disease. We detected *T. gondii* IgG and IgM by using VIDAS TOXO IgM and IgG II assays (bioMérieux, <https://www.biomerieux.com>). When *T. gondii* IgG was detected, we analyzed serum samples by using the Vidas Toxo IgG Avidity Assay (bioMérieux). Cutoff values used to interpret the results were those recommended by the manufacturers. All *Toxoplasma* spp. analyses were conducted at the LSPQ.

Other analyses were ordered. These analyses were detection of WNV IgM by ELISA using the WNV IgM Capture DxSelect (Focus Diagnostics, <https://www.focusdx.com>) at the LSPQ; detection of *Brucella* spp. IgM and IgG by using the standard tube *Brucella* agglutination test (in-house test at the LSPQ); detection of hepatitis E virus IgG and IgM by using a diagnostic assay (Wantai Biologic Pharmacy Enterprise, <http://www.ystwt.cn>); detection of *Leptospira* spp. IgM by using the Panbio *Leptospira* IgM ELISA (Abbott, <https://www.abbott.com>); detection of *Coxiella burnetii* IgG by using an immunofluorescence assay at the Centre Hospitalier Universitaire de Sherbrooke (Sherbrooke, Quebec, Canada); detection of *Borrelia burgdorferi* IgM and IgG by using the 2-tiered algorithm that included a screening ELISA conducted at Centre Hospitalier Universitaire de Sherbrooke (Zeus ELISA *Borrelia* VlsE1/pepC10 IgG/IgM test system; Alere, <https://www.alere.com>); an IgG Western blot assay (Anti-*Borrelia burgdorferi* U.S. EUROLINE-WB IgG; Euroimmun, <https://www.euroimmun.com>); and an IgM Line Blot Assay (Anti-*Borrelia* EUROLINE-RN-AT-adv IgM; Euroimmun) performed at the National Microbiology Laboratory in Winnipeg, Ontario, Canada.

euroimmun.com); and an IgM Line Blot Assay (Anti-*Borrelia* EUROLINE-RN-AT-adv IgM; Euroimmun) performed at the National Microbiology Laboratory in Winnipeg, Ontario, Canada.

Results

Epidemiologic Investigation

All 10 persons interviewed were men (age range 28–62 years). None of them had preexisting medical conditions. Clinical symptoms developed in 6 patients, including headache, fever, sweats, myalgia, and joint pain, during December 8–11, 2018; the earliest symptoms began a few days after the men returned home from Illinois. One case-patient was hospitalized because of severe headache, fever, and myalgia. Three other case-patients consulted a physician but were not hospitalized, and 2 other case-patients had similar symptoms but did not consult any physician.

We compiled results of *Toxoplasma* spp. testing and deer meat consumption for each hunter (Table). *Toxoplasma* spp. IgM was detected in 6 serum samples collected during the acute disease phase for the 6 symptomatic hunters. For 1 symptomatic hunter, *Toxoplasma* spp. IgM was detected when a second blood specimen was collected 3 weeks later. No IgG was detected in these serum samples, which suggested a recent infection in these hunters. We detected IgG with a low avidity index in the 6 serum samples collected from 6 case-patients during the convalescent phase, which enabled confirmation of a recent infection for all of these case-patients. For the 4 asymptomatic hunters, we analyzed 3 serum samples and detected IgG with a high avidity index in 2 samples, which suggested that both hunters were already immune to toxoplasmosis; 1 asymptomatic hunter was considered to be nonimmune. Even if this hunter consumed fresh deer meat that was undercooked, he did not show development of any disease and did not have any positive test results. One asymptomatic hunter did not participate in testing. When performed, serologic assays for hepatitis E, Q fever, leptospirosis, brucellosis, and Lyme disease all showed negative results.

We explored many possible risk factors to determine the most likely source of infection during the stay of the hunters, including water, food, and animal exposures. The hunters stayed at the camp for 12 days and during that time harvested and dressed 2–3 deer each. On November 30, the hunters prepared and consumed fresh deer steak that was cooked rare. Five of the 6 symptomatic hunters consumed rare steak, and 1 consumed steak cooked medium. Among the

SYNOPSIS

Table. Characteristics of 10 hunters who had suspected toxoplasmosis, Quebec, Canada, 2018*

Hunter	Illness	Signs/symptoms	Consumption of deer meat	Collection date	Test	Result	Conclusion
1	Yes	Fever, sweats, cephalalgia, muscular, joint pain, fatigue	Rare steak	2018 Dec 16	IgM IgG II IgG avidity	Negative Negative NA	No toxoplasmosis
				2019 Jan 11	IgM IgG II IgG avidity	Positive Positive Low avidity	Acute toxoplasmosis
2	Yes	Fever, sweats, cephalalgia, muscular, joint pain, fatigue	Rare steak	2018 Dec 21	IgM IgG II IgG avidity	Positive Negative NA	Acute toxoplasmosis
3	Yes	Fever, sweats, cephalalgia, muscular, joint pain, fatigue	Rare steak	2018 Dec 20	IgM IgG II IgG avidity	Positive Equivocal NA	Acute toxoplasmosis
				2019 Jan 14	IgM IgG II IgG avidity	Positive Positive Low avidity	Acute toxoplasmosis
4	Yes	Fever, cephalalgie, photophobic	Rare steak	2018 Dec 20	IgM IgG II IgG avidity	Positive Negative NA	Acute toxoplasmosis
				2019 Jan 14	IgM IgG II IgG avidity	Positive Positive Low avidity	Acute toxoplasmosis
5	Yes	Fever, sweats, cephalalgia, muscular, joint pain, fatigue	Medium steak	2018 Dec 19	IgM IgG II IgG avidity	Positive Negative NA	Acute toxoplasmosis
				2019 Jan 4	IgM IgG II IgG avidity	Positive Positive Low avidity	Acute toxoplasmosis
6	Yes	Fever, sweats, cephalalgia, muscular, joint pain, fatigue	Rare steak	2018 Dec 16	IgM IgG II IgG avidity	Positive Negative NA	Acute toxoplasmosis
				2019 Jan 4	IgM IgG II IgG avidity	Positive Positive Low avidity	Acute toxoplasmosis
7	No	Asymptomatic	Rare steak and heart	2019 Feb 7	IgM IgG II	Negative Negative	Asymptomatic and nonimmune
8	No	Asymptomatic	Well-done steak	2019 Jan 15	IgM IgG II IgG avidity	Negative Positive High avidity	Asymptomatic: absence of IgM and high IgG avidity index excluded recent <i>Toxoplasma</i> spp. infection
9	No	Asymptomatic	Well-done heart	2019 Jan 16	IgM IgG II IgG avidity	Negative Positive High avidity	Asymptomatic: absence of IgM and high IgG avidity index excluded recent <i>Toxoplasma</i> spp. infection
10	No	Asymptomatic	None	Did not participate	NA	NA	NA

*NA, not available.

remaining 4 hunters who did not show development of symptoms, 1 consumed the uncooked heart of a deer, 2 consumed deer meat that was cooked well done, and 1 did not consume any deer meat on site. All other potential exposures were determined to be unremarkable. The Illinois Department of Public Health received reports of no similar illnesses in this area during the study period.

When the stay in Illinois ended, the hunters divided the remaining harvested meat among themselves and brought it back to Quebec. It was

impossible to identify pieces of the deer partially consumed at the outfitter and possibly contaminated by *T. gondii*. At the beginning of the investigation, we recommended that the hunters not consume the deer meat until we knew more about the diagnosis. All deer meat was kept in freezers when the hunters returned home.

Food Inspection Services by MAPAQ

We collected 12 samples of frozen deer meat from 1 hunter household: 7 specimens of 300 g each and 5

specimens of 500 g each from the same freezer. Among the 12 deer meat specimens collected for analysis, no *T. gondii* parasites were detected. Parts of deer that were consumed at the outfitter were unrecognizable from other parts of deer not consumed on site.

Discussion

Outbreaks of acute toxoplasmosis infection are unusual in Quebec. In Illinois, no outbreaks were reported to the public health unit over a 20-year period. We identified a game meat-associated outbreak in Quebec involving travel to Illinois. Investigative findings identified consumption of fresh, undercooked deer meat as the most likely source of infection.

Sporadic cases associated with deer meat consumption have been reported (13). During 2017, acute toxoplasmosis developed in 8 of 10 hunters after they consumed fresh deer meat in Wisconsin, USA (15).

During the outbreak we report, symptoms were severe enough that 1 case-patient had to be hospitalized and 3 other companions consulted a physician. Primary acquired *Toxoplasma* spp. infection is predominantly asymptomatic in immunocompetent persons in North America (17). During the outbreak we report, 6 of 7 nonimmune hunters for whom we had the information showed development of symptoms after infection. The severity of infection might depend on the genotype of the strain. The severity of infection is usually low in North America, where genotype II strains predominate (18), in comparison to other parts of the world (19–21).

Another major outbreak of toxoplasmosis involving hundreds of persons was reported in 1995 in Victoria, British Columbia, Canada. The suspected source was an infected cougar that had defecated in the watershed; heavy rains had then washed a bolus of oocysts into the water reservoir. The outbreak included a high proportion of severe primary infections among immunocompetent persons (18). In the locations of that outbreak and the outbreak we report (British Columbia and Quebec), the genotype was not determined. We are not able to explain why so many cases were reported among the immunocompetent population.

In our investigation, we obtained serum samples from 3 of the 4 asymptomatic hunters. *Toxoplasma* IgG was detected in 2 serum samples. The absence of IgM and the high IgG avidity index suggest that both of those hunters were already immune to *T. gondii* by a past infection. One asymptomatic hunter did not show development of any disease and showed negative results for toxoplasmosis even after consuming fresh deer meat that was rare. We do not have immune information about the fourth patient.

Food specimens collected from 1 hunter were negative for *T. gondii*. Unfortunately, parts of the deer that were consumed at the outfitter were unrecognizable from parts of other deer harvested in Illinois during the same period of time, which might explain the negative results.

Little is known of the natural epidemiology of *T. gondii* infection in white-tailed deer. Given that deer are strict herbivores, it is believed that they become infected postnatally by ingesting oocysts from the environment (7). When ingested, the parasites form tissue cysts in the skeletal muscle and other tissues. When the infected deer die, tissues are scavenged by feline carnivore species, including bobcats and cougars (7). The life cycle then continues, and these cats shed more oocysts into the environment. Estimated *Toxoplasma* spp. prevalence among white-tailed deer varies across the United States from 15% to 74% (Ohio, Pennsylvania, and Minnesota) (7,9,10,12).

The MAPAQ website provides general recommendations to game meat hunters and their family about safe handling and preparation (22). Recommendations include not eating raw or undercooked game meat and cooking to an internal temperature of at least 160°F. They also recommend washing hands with soap and water after handling raw meat and cleaning all materials that come in contact with raw meat thoroughly after use. In addition, cysts and oocysts of toxoplasmosis might be destroyed by freezing the meat (23,24). Because the prevalence seems to be high in wild animals in which study prevalence was determined, freezing the meat seems to be efficient to destroy cysts and oocysts. Hunters should be aware of those recommendations. A person can be infected for life and disease can reactivate years after the initial infection.

Few studies have reported on the seroprevalence of *Toxoplasma* antibodies in humans in Canada. In the United States, a nationwide study conducted during 2009–2010 showed that the overall *T. gondii* antibody seroprevalence among persons >6 years of age was 13.2% (24). Other reports found that, although the presence of *T. gondii* is still relatively common, the prevalence in the United States decreased during 1988–1994 (25,26). Given the high prevalence of *Toxoplasma* spp. in white-tailed deer across some areas of the United States and the overall observed decrease in seroprevalence in humans, outbreaks like the one we reported might be more common in the future, and health professionals should be aware of this possibility.

In this investigation, we recommended to all hunters and their families that they not consume the

deer meat. This recommendation was given even if all hunters were immunocompetent. If hunters and their families decided to consume the deer meat despite our recommendations, they were advised to freeze it thoroughly, cook it, and avoid distribution of the meat to family members, pregnant women, or immunocompromised persons.

Acknowledgments

We thank Philippe Jutras, Jean Longtin, and public health unit nurses and physicians for interviewing all hunters; and Connie Austin and Isabelle Gagnon for their active contributions to this study.

About the Author

Dr. Gaulin is a physician and epidemiologist at the Protection Branch, Ministry of Health, Quebec City, Quebec, Canada. Her primary research interests are infectious diseases, enteric and nonenteric disease surveillance, and provincial outbreak investigations.

References

- Simon A, Bigras Poulin M, Rousseau AN, Dubey JP, Ogden NH. Spatiotemporal dynamics of *Toxoplasma gondii* infection in Canadian lynx (*Lynx canadensis*) in western Québec, Canada. *J Wildl Dis*. 2013;49:39–48. <https://doi.org/10.7589/2012-02-048>
- Dubey JP, editor. *Toxoplasmosis of animals and humans*, 2nd ed. Boca Raton (FL): CRC Press; 2010.
- American Academy of Pediatrics. Red book: 2012. Report of the committee on infectious diseases. Elk Grove Village (IL): The Academy [cited 2019 Nov 19]. https://redbook.solutions.aap.org/DocumentLibrary/RB12_interior.pdf
- Aramini JJ, Stephen C, Dubey JP, Engelstoff C, Schwantje H, Ribble CS. Potential contamination of drinking water with *Toxoplasma gondii* oocysts. *Epidemiol Infect*. 1999;122:305–15. <https://doi.org/10.1017/S0950268899002113>
- Shuhaiber S, Koren G, Boskovic R, Einarson TR, Soldin OP, Einarson A. Seroprevalence of *Toxoplasma gondii* infection among veterinary staff in Ontario, Canada (2002): implications for teratogenic risk. *BMC Infect Dis*. 2003;3:8. <https://doi.org/10.1186/1471-2334-3-8>
- Dubey JP. Toxoplasmosis in sheep, goats, pigs and cattle. In: Dubey J, Beattle C, editors. *Toxoplasmosis in animals and man*. Boca Raton (FL): CRC Press; 1988. p. 61–114.
- Dubey JP, Dennis PM, Verma SK, Choudhary S, Ferreira LR, Oliveira S, et al. Epidemiology of toxoplasmosis in white tailed deer (*Odocoileus virginianus*): occurrence, congenital transmission, correlates of infection, isolation, and genetic characterization of *Toxoplasma gondii*. *Vet Parasitol*. 2014;202:270–5. <https://doi.org/10.1016/j.vetpar.2014.01.006>
- Jones JL, Dargelas V, Roberts J, Press C, Remington JS, Montoya JG. Risk factors for *Toxoplasma gondii* infection in the United States. *Clin Infect Dis*. 2009;49:878–84. <https://doi.org/10.1086/605433>
- Dubey JP, Brown J, Verma SK, Cerqueira-Cézar CK, Banfield J, Kwok OC, et al. Isolation of viable *Toxoplasma gondii*, molecular characterization, and seroprevalence in elk (*Cervus canadensis*) in Pennsylvania, USA. *Vet Parasitol*. 2017;243:1–5. <https://doi.org/10.1016/j.vetpar.2017.05.030>
- Dubey JP, Jenkins MC, Kwok OC, Zink RL, Michalski ML, Ulrich V, et al. Seroprevalence of *Neospora caninum* and *Toxoplasma gondii* antibodies in white-tailed deer (*Odocoileus virginianus*) from Iowa and Minnesota using four serologic tests. *Vet Parasitol*. 2009;161:330–4. <https://doi.org/10.1016/j.vetpar.2009.01.002>
- Dubey JP, Velmurugan GV, Ulrich V, Gill J, Carstensen M, Sundar N, et al. Transplacental toxoplasmosis in naturally-infected white-tailed deer: isolation and genetic characterisation of *Toxoplasma gondii* from foetuses of different gestational ages. *Int J Parasitol*. 2008;38:1057–63. <https://doi.org/10.1016/j.ijpara.2007.11.010>
- Ballash GA, Dubey JP, Kwok OC, Shoben AB, Robison TL, Kraft TJ, et al. Seroprevalence of *Toxoplasma gondii* in white-tailed deer (*Odocoileus virginianus*) and free-roaming cats (*Felis catus*) across a suburban to urban gradient in northeastern Ohio. *EcoHealth*. 2015;12:359–67. <https://doi.org/10.1007/s10393-014-0975-2>
- Ross RD, Stec LA, Werner JC, Blumenkranz MS, Glazer L, Williams GA. Presumed acquired ocular toxoplasmosis in deer hunters. *Retina*. 2001;21:226–9. <https://doi.org/10.1097/00006982-200106000-00005>
- Sacks JJ, Delgado DG, Lobel HO, Parker RL. Toxoplasmosis infection associated with eating undercooked venison. *Am J Epidemiol*. 1983;118:832–8. <https://doi.org/10.1093/oxfordjournals.aje.a113701>
- Schumacher A, Kazmierczak J, Moldenhauer E, Hanhly T, Montoya J, Press C, et al. Toxoplasmosis associated with venison consumption during a retreat – Wisconsin, September–October 2017. Presented at: 67th Annual Epidemic Intelligence Service (EIS) Conference; 2018 Apr 16–19, 2018; Atlanta, Georgia, USA.
- Kasper DC, Sadeghi K, Prusa AR, Reischer GH, Kratochwill K, Förster-Waldl E, et al. Quantitative real-time polymerase chain reaction for the accurate detection of *Toxoplasma gondii* in amniotic fluid. *Diagn Microbiol Infect Dis*. 2009;63:10–5. <https://doi.org/10.1016/j.diagmicrobio.2008.09.009>
- Montoya JG, Parmley S, Liesenfeld O, Jaffe GJ, Remington JS. Use of the polymerase chain reaction for diagnosis of ocular toxoplasmosis. *Ophthalmology*. 1999;106:1554–63. [https://doi.org/10.1016/S0161-6420\(99\)90453-0](https://doi.org/10.1016/S0161-6420(99)90453-0)
- Howe DK, Sibley LD. *Toxoplasma gondii* comprises three clonal lineages: correlation of parasite genotype with human disease. *J Infect Dis*. 1995;172:1561–6. <https://doi.org/10.1093/infdis/172.6.1561>
- Carme B, Bissuel F, Ajzenberg D, Bouyne R, Aznar C, Demar M, et al. Severe acquired toxoplasmosis in immunocompetent adult patients in French Guiana. *J Clin Microbiol*. 2002;40:4037–44. <https://doi.org/10.1128/JCM.40.11.4037-4044.2002>
- Demar M, Ajzenberg D, Maubon D, Djossou F, Panchoe D, Punwasi W, et al. Fatal outbreak of human toxoplasmosis along the Maroni River: epidemiological, clinical, and parasitological aspects. *Clin Infect Dis*. 2007;45:e88–95. <https://doi.org/10.1086/521246>
- Mullens A. “I think we have a problem in Victoria”: MDs respond quickly to toxoplasmosis outbreak in BC. *CMAJ*. 1996;154:1721–4.
- Ministère de l’Agriculture, des Pêcheries et de l’Alimentation du Québec [cited 2019 Jul 29]. https://www.mapaq.gouv.qc.ca/fr/Publications/Fiche_Gibier_public_web.pdf
- Guo M, Buchanan RL, Dubey JP, Hill DE, Lambertini E, Ying Y, et al. Qualitative assessment for *Toxoplasma gondii* exposure risk associated with meat products in the United States. *J Food Prot*. 2015;78:2207–19. <https://doi.org/10.4315/0362-028X.JFP-15-270>

24. Jones JL, Kruszon-Moran D, Rivera HN, Price C, Wilkins PP. *Toxoplasma gondii* seroprevalence in the United States 2009–2010 and comparison with the past two decades. *Am J Trop Med Hyg.* 2014;90:1135–9. <https://doi.org/10.4269/ajtmh.14-0013>
25. Opsteegh M, Kortbeek TM, Havelaar AH, van der Giessen JW. Intervention strategies to reduce human *Toxoplasma gondii* disease burden. *Clin Infect Dis.* 2015;60:101–7. <https://doi.org/10.1093/cid/ciu721>
26. Jones JL, Kruszon-Moran D, Sanders-Lewis K, Wilson M. *Toxoplasma gondii* infection in the United States, 1999–2004, decline from the prior decade. *Am J Trop Med Hyg.* 2007;77:405–10. <https://doi.org/10.4269/ajtmh.2007.77.405>

Address for correspondence, Colette Gaulin, Ministère de la Santé et des Services Sociaux du Québec, 1075 Chemin Ste-Foy, QC, Québec G1S 2M1, Canada; email: colette.gaulin@msss.gouv.qc.ca



**EMERGING
INFECTIOUS DISEASES®**

December 2019

Zoonotic Infections

- Seroprevalence and Risk Factors Possibly Associated with Emerging Zoonotic Vaccinia Virus in a Farming Community, Colombia
- Patterns of Transmission and Sources of Infection in Outbreaks of Human Toxoplasmosis
- Global Epidemiology of Buruli Ulcer, 2010–2017, and Analysis of 2014 WHO Programmatic Targets
- Cost-effectiveness of Prophylactic Zika Virus Vaccine in the Americas
- Human Infection with Orf Virus and Description of Its Whole Genome, France, 2017
- High Prevalence of Macrolide-Resistant *Bordetella pertussis* and *ptxP1* Genotype, Mainland China, 2014–2016
- Avian Influenza A Viruses among Occupationally Exposed Populations, China, 2014–2016
- Genomic Analysis of Fluoroquinolone- and Tetracycline-Resistant *Campylobacter jejuni* Sequence Type 6964 in Humans and Poultry, New Zealand, 2014–2016
- *Streptococcus suis*–Associated Meningitis, Bali, Indonesia, 2014–2017
- Epidemiologic, Entomologic, and Virologic Factors of the 2014–15 Ross River Virus Outbreak, Queensland, Australia
- Multicountry Analysis of Spectrum of Clinical Manifestations in Children <5 Years of Age Hospitalized with Diarrhea
- Sheep as Host Species for Zoonotic *Babesia venatorum*, United Kingdom
- Half-Life of African Swine Fever Virus in Shipped Feed
- Zika Virus IgM 25 Months after Symptom Onset, Miami-Dade County, Florida, USA
- Divergent Barmah Forest Virus from Papua New Guinea
- Animal Exposure and Human Plague, United States, 1970–2017
- Sentinel Listeriosis Surveillance in Selected Hospitals, China, 2013–2017
- Economic Impact of Confiscation of Cattle Viscera Infected with Cystic Echinococcosis, Huancayo Province, Peru
- Predicting Dengue Outbreaks in Cambodia
- Cat-to-Human Transmission of *Mycobacterium bovis*, United Kingdom
- Evolution of Highly Pathogenic Avian Influenza A(H5N1) Virus in Poultry, Togo, 2018
- West Nile Virus in Wildlife and Nonequine Domestic Animals, South Africa, 2010–2018
- Highly Pathogenic Avian Influenza A(H5N8) Virus in Gray Seals, Baltic Sea
- Bagaza Virus in Himalayan Monal Pheasants, South Africa, 2016–2017
- Influenza A(H1N1)pdm09 Virus Infection in a Captive Giant Panda, Hong Kong
- Middle East Respiratory Syndrome Coronavirus Seropositivity in Camel Handlers and their Families, Pakistan
- Distantly Related Rotaviruses in Common Shrews, Germany, 2004–2014
- Molecular Confirmation of *Rickettsia parkeri* in *Amblyomma ovale* Ticks, Veracruz, Mexico
- Rhombencephalitis and Myeloradiculitis Caused by a European Subtype of Tick-Borne Encephalitis Virus
- *Aspergillus felis* in Patient with Chronic Granulomatous Disease
- Nodular Human Lagochilascariasis Lesion in Hunter, Brazil

To revisit the December 2019 issue, go to:

<https://wwwnc.cdc.gov/eid/articles/issue/25/12/table-of-contents>

Public Health Program for Decreasing Risk for Ebola Virus Disease Resurgence from Survivors of the 2013–2016 Outbreak, Guinea

Mory Keita, Sakoba Keita, Boubacar Diallo, Momo Camara, Samuel Mesfin, Koumpingnin Yacouba Nebie, N'Faly Magassouba, Seydou Coulibaly, Boubacar Barry, Mamadou Oury Baldé, Raymond Pallawo, Sadou Sow, Amadou Bailo Diallo, Pierre Formenty, Mamoudou Harouna Djingarey, Ibrahima Socé Fall, Lorenzo Subissi¹

At the end of the 2013–2016 Ebola virus disease outbreak in Guinea, we implemented an alert system for early detection of Ebola resurgence among survivors. Survivors were asked to report health alerts in their household and provide body fluid specimens for laboratory testing. During April–September 2016, a total of 1,075 (88%) of 1,215 survivors participated in the system; follow up occurred at a median of 16 months after discharge (interquartile range 14–18 months). Of these, 784 acted as focal points and reported 1,136 alerts (including 4 deaths among survivors). A total of 372 (91%) of 408 eligible survivors had >1 semen specimen tested; of 817 semen specimens, 5 samples from 4 survivors were positive up to 512 days after discharge. No lochia (0/7) or breast milk (0/69) specimens tested positive. Our findings underscore the importance of long-term monitoring of survivors' semen samples in an Ebola-affected country.

The 2013–2016 Ebola virus disease (EVD) outbreak was the largest outbreak since the discovery of Ebola virus in 1976. Overall, the outbreak caused >29,000 cases and >11,000 deaths and resulted in the

largest known cohort of EVD survivors in history (1). Currently, the second-largest EVD outbreak is ongoing in the Democratic Republic of the Congo, which has had 3,340 cases and 2,207 deaths as of December 12, 2019.

During mid-2015, after considering the high number of survivors in West Africa and several episodes of EVD reemergence linked to exposure to survivors' body fluids, the World Health Organization (WHO) adapted a strategy to manage survivors' sequelae and mitigate the risk of resurgence (i.e., EVD cases occurring after active chains of transmission stopped) posed by viral persistence in their body fluids (2), such as semen, vaginal fluids, sweat, aqueous humor, urine, and breastmilk (3–6). According to WHO, an intensive integrated program was necessary to address the medical needs of survivors and the risk for virus reintroduction, ideally a program that could be integrated into existing routine health services and facilities (2). Therefore, the national program coordinating EVD in Guinea, in collaboration with WHO and partners, developed and implemented a survivors' monitoring program (called SA-Ceint, derived from the French phrase “cordon sanitaire-based active surveillance”). In March 2016, when SA-Ceint was still in preparation, an episode of EVD resurgence occurred in Guinea during the WHO-endorsed 90-day period of enhanced surveillance following the declaration of the end of the outbreak. This resurgence was most likely caused by viral persistence in the semen of a survivor (7).

Author affiliations: World Health Organization Country Office, Conakry, Guinea (M. Keita, B. Diallo, S. Mesfin, K.Y. Nebie, S. Coulibaly, B. Barry, M.O. Baldé, R. Pallawo); National Agency for Health Security, Ministry of Health, Conakry (S. Keita, M. Camara); University Gamal Abdel Nasser, Conakry (N. Magassouba, S. Sow); World Health Organization Regional Office for Africa, Brazzaville, Republic of the Congo (A.B. Diallo, M.H. Djingarey, I.S. Fall); World Health Organization, Geneva, Switzerland (P. Formenty); Global Outbreak Alert and Response Network, Geneva (L. Subissi)

¹Current affiliation: World Health Organization, Geneva, Switzerland.

Similar cases from viral persistence were previously reported in Liberia, Sierra Leone, and Guinea (7–10).

The objective of SA-Ceint was to quickly detect any new EVD cases and stop transmission early. This project was conducted by using a community-based alert system and monitoring high-risk body fluids of survivors. Here we report on the findings of this public health program.

Methods

Implementation of the Household-Based Alert System

During December 8, 2015–March 31, 2016, the preparatory phase of SA-Ceint occurred. We attempted to contact all EVD survivors in Guinea present in the Ministry of Health database, conducted community engagement activities, and delivered the survivors package. The communication line between survivors and the SA-Ceint team was active during April 1–September 30, 2016.

Survivors were eligible to participate in the program if they were able to show the certificate of medical clearance that they were given at release from the Ebola treatment unit (ETU). Participants received a package that included monthly allowance as well as other forms of support such as rice and flour.

The smallest structure of the monitoring program was the ring unit. This unit was built around each survivor and included his or her family or household. In each ring unit, a focal point (the survivor, or a guardian for survivors <15 years of age) and a deputy (in case the focal point was not able to perform his or her tasks) were chosen. His or her task was to report all episodes of illness in the survivor's surroundings (i.e., episodes that involved the survivor, the immediate family, other relatives, and other persons living in proximity to the survivor). Sexually active men were prioritized as focal points because of their risk for shedding the virus in their semen.

Each focal point was given cell phone credit to call the district health authorities regularly to relay information on episodes of illness in his or her unit. Episodes of illness, also called case alerts, were defined as deaths, cases of unexplained hemorrhage, or episodes of acute unexplained fever and vomiting, diarrhea, muscle pain, weakness or fatigue, or stomach pain. The definition of a case alert roughly corresponded to that of EVD suspected cases used in phase 3 of the Ebola response, except that phase 3 definition included 2 additional criteria: no response to treatment to common febrile diseases (e.g., malaria) and any clinical suspicion of EVD (2). Once the case alert was sent, this episode was investigated to collect information on treatment failure and link it to the

body fluid testing results in the survivors of the concerned community, as was as any other complementary investigation considered of importance.

In each neighborhood, a platform was set up that consisted of all ring units plus the local elected representatives; this group met on a weekly basis. Its function was to resolve any type of conflict related to the program, to supervise and advise the focal point, and to inform on or validate episodes of illness occurring in the ring unit. All platform meetings were funded by the SA-Ceint program.

District data management units were responsible for communication to the central coordinating unit, the Ebola Response Coordination. Coordination of the program at this level was provided by the National Agency for Health Security, with the support of technical partners such as WHO, the US Centers for Disease Control and Prevention, the International Medical Corps, the International Federation of Red Cross and Red Crescent Societies, and the Red Cross in Guinea. A data management team was responsible for collecting and analyzing all information from health districts and laboratories. This system also monitored movement or relocation of the survivors between districts, and the ring unit was relocated according to the survivor's displacement so that surveillance could continue.

The National Agency for Health Security was responsible for the communication of the results of body fluid testing to the district health authorities. All male survivors >15 years of age were eligible for semen testing, and a subset of these men also was selected for urine testing. Female survivors who gave birth were eligible for body fluid testing (e.g., testing of blood, vaginal secretions, amniotic liquid, lochia, and breast milk) (Appendix Figure 1, <https://wwwnc.cdc.gov/EID/article/26/2/19-1235-App1.pdf>). Body fluid testing stopped after 2 negative tests by reverse-transcription PCR (RT-PCR) for the same body fluid, as recommended by WHO (2).

Sampling and Laboratory Analyses

A team consisting of an epidemiologist, a nurse, and a hygienist examined and sorted the alerts and were ready to be deployed to the ring units in cases of suspected EVD to carry out an Ebola rapid diagnostic test (OraQuick Ebola rapid antigen test kit, <https://www.oraquick.com>) (11) and collect specimens for quantitative RT-PCR using appropriate personal protective equipment. The ambulance of the district was mobilized in case safe transfer of patients or bodies was needed. The team was also in charge of routinely taking biological specimens from survivors' body fluids. Five laboratories processed biological specimens and covered the entire country of

Guinea: 3 were in the capital, Conakry; 1 in the forested region of Guinea (N'zerekore); and 1 in lower Guinea (Kindia) (Appendix Figure 1). According to the standard operating procedures, which were drafted and validated before the study began, specimens were stored in an icebox at 4°C–8°C after collection and tested within 24 hours at the nearest laboratory. Breast milk specimens were tested for Ebola virus RNA by using the RealStar ZEBOV RT-PCR Kit (Altona, <https://www.altona-diagnostics.com>) as previously described (12). Seminal fluid specimens were processed as previously described (13), and all other body fluids were processed as previously described (14). Any survivor with an RT-PCR-positive semen specimen was immediately counseled and included in the JIKI trial (15). Eligible family, other relatives, and other people living in proximity to a survivor were enrolled in the Ebola ça Suffit! trial, aiming at evaluating efficacy and effectiveness of a vaccine against EVD (16).

This study was considered public health practice and was implemented following the guidelines from the WHO Ebola response phase 3 strategic document (2). The study was integrated in the workflow of other research projects (i.e., Postebogui, the JIKI trial, EBOSEX, and the Ebola ça Suffit! vaccination trial), all of which had been approved by the National Committee for Ethics in Research and Health before their start. All the participants signed an informed consent form at the beginning of the program.

Results

Outcomes of the Community-Based Alert System

We were able to retrieve information on ≈1,130/1,270 EVD survivors in Guinea, 55 of whom died after ETU

discharge (late deaths) and before the program started and 140 of whom were unavailable for contact (lost to follow-up) (17). Excluding the 55 late deaths (and assuming no deaths occurred in the lost to follow-up category), we enrolled 1,075 of the 1,215 survivors who were known to be alive or who had been lost to follow-up (88% follow-up rate). The median starting point for follow-up was 16 months after discharge (interquartile range 14–18 months), and the median end point for follow-up was 22 months after discharge (interquartile range 20–24 months).

In total, 9,028 immediate family members, other relatives, and other persons living in proximity to a survivor were identified (an average of 11.5 persons/ring unit), of whom 6,929 were eligible to participate in the Ebola ça Suffit! trial; 727 (10.4%) were vaccinated. Of the enrolled survivors, 47% were male and 53% female; age distribution did not vary substantially by sex (Appendix Figure 2). Seventy-nine percent of the male survivors were 15–59 years of age, whereas 78% of female survivors were 15–59 years of age. Children <15 years of age accounted for 15% of male and 16% of female survivors; persons >60 years of age accounted for 5% of the male and 6% of the female survivors. Compared with the population of Guinea, the middle age group (15–59 years of age) was overrepresented (18).

The structure of the program was modeled on the existing health system, from the community level to the central level. A total of 784 ring units were established at the community level, and each was represented by 1 focal point (the survivor or a legal guardian). Then, 377 platforms (open to all survivors) were created at the neighborhood level, and 30 teams were formed at the district level. During the study period, the district teams received

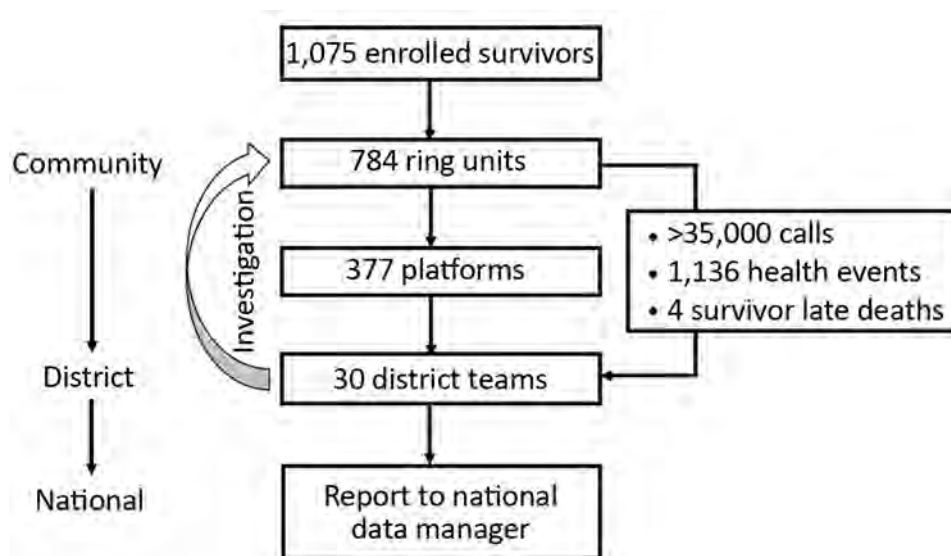


Figure 1. Structure of the SA-Ceint program to test body fluids from Ebola virus disease survivors to decrease risk for disease resurgence, Guinea, April–September 2016.

>35,000 calls (i.e., 6 calls/month from each focal point) (Figure 1). Focal points reported 1,136 episodes of illness. Of those events, 4 were late deaths of survivors. Assuming no one experienced illness more than once, the proportion of persons who experienced an episode of illness during the 6-month period was 10% of the total. However, none of these episodes was considered to meet the definition of a suspected EVD case; therefore, no one was sent to the ETU for testing.

Biological Monitoring of Survivors' Body Fluids

Of the 1,094 tested specimens, most (817 [74.7%]) were semen specimens. Urine, breast milk, vaginal secretions, blood, lochia, and amniotic liquid also were tested (Figure 2); however, date of delivery for pregnant women was not recorded. The SA-Ceint program was able to test 375 (91%) of all male survivors >15 years of age, of whom 224 were tested only once (60%), 101 (27%) twice, and 50 (13%) 3 times. The lowest proportion of male survivors whose semen specimen was tested at least once was registered in the districts of Boke (33%), Kouroussa (50%), Faranah (60%), and Siguiriri (78%). In all other districts, the proportion of male survivors tested was >80% (Table).

Of the semen specimens tested for Ebola virus, 4 (1%) of 375 survivors were positive. In total, 5 (1%) of 817 semen specimens (2 from the same survivor) tested positive. All 4 survivors were immediately treated with favipiravir after enrollment in the JKI trial (15). Three survivors' semen specimens were positive 276, 351, and 410 days after ETU release and then negative 1 month later. The fourth survivor had his first positive semen specimen (cycle threshold value 32) 494 days after ETU release, and despite favipiravir treatment, a second positive semen specimen (cycle threshold value 23) 512 days after ETU release. His 2 following specimens tested negative.

Discussion

We describe the experience of setting up and implementing a nationwide active surveillance program with EVD survivors in Guinea. The program aimed to mitigate the risk for EVD reintroduction from exposure to survivors' body fluids. We were able to enroll ≈90% of the survivors in Guinea and test the semen of >90% of the enrolled male survivors ≥15 years of age, an unprecedented rate compared with other survivor monitoring programs (19–25).

The number of focal points was ≈75% of the enrolled survivors because some survivors were from the same household. The fact that none of the >1,000 alerts were treated as a suspected EVD episode probably

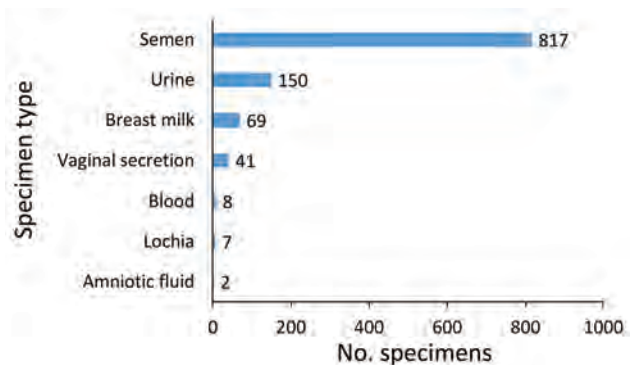


Figure 2. Number of specimens of body fluids from Ebola virus disease survivors tested for Ebola virus by reverse transcription PCR as part of the SA-Ceint program, Guinea, April–September 2016. All specimens tested negative except for 5 positive semen specimens from 4 survivors. Breast milk specimens were from 65 women; for all other sample types, no person had >1 samples taken.

means that the definition of an illness episode (which was broader than the definition of a suspected EVD case) was far from being specific. At this stage of the Ebola response, the need to investigate all alerts was more important than avoiding false-positive alerts (i.e., alerts that did not turn out to be suspected EVD cases). In fact, all 1,136 alerts were investigated. These investigations also used the available body fluid testing results. However, no alert was found to meet the definition of a suspected EVD case (i.e., none was sent to ETU for testing), in part because the case definition changed after the end of the outbreak to include cases

Table. Number of focal points and male survivors who were eligible for semen testing and were tested ≥1 time, by district, SA-Ceint program, Guinea, April–September 2016

District	No. focal points	No. eligible male survivors	No. male survivors tested ≥1 time	% Eligible survivors tested
Beyla	12	6	6	100
Boffa	6	4	4	100
Boke	6	3	1	33
Conakry	148	108	96	89
Coyah	82	36	35	98
Dubreka	35	20	20	100
Faranah	13	5	3	60
Forecariah	95	34	32	94
Fria	4	3	3	100
Gueckedou	47	18	16	89
Kankan	8	1	1	100
Kerouane	40	16	15	94
Kindia	23	10	9	90
Kissidougou	22	11	9	82
Kouroussa	5	2	1	50
Lola	11	8	8	100
Macenta	171	76	69	91
N'zerekore	24	27	26	97
Siguiriri	9	9	7	78
Telimele	15	4	4	100
Yomou	4	3	3	100
Unknown	4	4	4	100
Total	784	408	372	91

of treatment failure, with the objective of avoiding unnecessary anxiety in the population.

We believe that the outcome of zero suspected EVD cases did reflect the low incidence of Ebola in the community at the time SA-Ceint began, when most of the survivors had recovered for >1 year. However, the outcome also probably reflected the fear of creating panic in the affected communities, because testing would otherwise not be harmful. The stigma around Ebola is surely to some extent a hurdle to the successful implementation of a program such as SA-Ceint, and our experience underscores the importance of integrating social science into outbreak response activities to enable development of risk communication strategies adapted to the local context. Still, we believe that our strategy should be considered, if the resources allow it, by other Ebola-affected countries in the future, because our approach nevertheless enabled investigation of many health alerts and would likely have detected illnesses strongly suggestive of Ebola (e.g., hemorrhagic fever).

Of the tested specimens, only 5 (from 4 survivors) were positive, and all were semen specimens. Our findings (4 positive specimens from 375 survivors tested ≥ 1 time) were roughly in line with the prediction from Sissoko et al. (13) that <1 survivor from Guinea would have an RNA-positive semen specimen by July 2016. Furthermore, RNA detection does not mean the specimen contains infectious virus. Therefore, it is not surprising to see that EVD was never suspected, despite the number of alerts, during the SA-Ceint program. At that time, the risk for reintroduction of EVD was in fact very low. However, the finding that few semen specimens were positive >1 year after survivors' recovery confirms previous observations that male survivors' semen must be strictly and regularly monitored after ETU release (13).

The SA-Ceint program was not easy to implement. We experienced delays, and by the time the program was fully implemented, evidence suggested that the risk for EVD reintroduction from survivors in Guinea into the community was already very low (13). This hypothesis was confirmed by our laboratory findings. Moreover, we faced reluctance among survivors to provide semen specimens because of cultural and religious reasons. The program was costly, and all survivors were financially supported; this reimbursement was possible because of the international resources that the international outbreak response mobilized.

Overall, heightened awareness in the communities and platform meetings helped us to enroll a high number of eligible survivors. Because no

established network of community-based surveillance in Guinea had existed previously and because we wanted to minimize stigma among survivors, we empowered them to be the main actors in this program. We believe this was the best strategy to ensure regular reporting.

In conclusion, we successfully implemented a nationwide surveillance program for the early detection of resurgence of Ebola virus from persistently infected survivors. Our strategy could be implemented in future programs in similar contexts.

Acknowledgments

We thank all survivors and their communities for their active participation in the program. We thank the health authorities in Guinea, the World Health Organization field teams, and response partners; and the Global Outbreak Alert and Response Network for coordinated deployments in Guinea supported by the World Health Organization Ebola response support team at the regional offices and headquarters. We are also grateful to the reviewers for critical comments that substantially improved the manuscript.

Author contributions: S.K., B.D., M.C., M.H.D., I.S.F., A.B.D., M.O.B., R.P., L.S., and M.K. designed and performed the study. S.M., B.B., and S.C. managed the data. N.M. and K.Y.N. performed the laboratory investigations. M.K., M.C., and S.S. performed the appraisal of the program. M.K., P.F., and L.S. wrote the manuscript. All authors reviewed the final draft. The corresponding author had full access to all the data in the study and had final responsibility for the decision to submit for publication.

The study was co-funded by the World Health Organization, the International Medical Corps, and the International Federation of Red Cross and Red Crescent Societies in Guinea.

About the Author

Dr. Keita is a medical doctor and epidemiologist. During the 2013–2016 Ebola outbreak in Guinea, he worked as a World Health Organization field coordinator and regional coordinator. He currently works as field coordinator in the ongoing Ebola outbreak in the Democratic Republic of the Congo. He is interested in communicable diseases epidemiology and in strengthening health systems.

References

1. Coltart CEM, Lindsey B, Ghinai I, Johnson AM, Heymann DL. The Ebola outbreak, 2013–2016: old lessons for new epidemics. *Philos Trans R Soc Lond B Biol Sci*. 2017;372:372. <https://doi.org/10.1098/rstb.2016.0297>

2. World Health Organization. Ebola response phase 3: framework for achieving and sustaining a resilient zero [cited 2019 Dec 12]. http://apps.who.int/iris/bitstream/10665/184693/1/ebola_resilientzero_eng.pdf
3. Varkey JB, Shantha JG, Crozier I, Kraft CS, Lyon GM, Mehta AK, et al. Persistence of Ebola virus in ocular fluid during convalescence. *N Engl J Med*. 2015;372:2423–7. <https://doi.org/10.1056/NEJMoa1500306>
4. Rodriguez LL, De Roo A, Guimard Y, Trappier SG, Sanchez A, Bressler D, et al. Persistence and genetic stability of Ebola virus during the outbreak in Kikwit, Democratic Republic of the Congo, 1995. *J Infect Dis*. 1999;179(Suppl 1):S170–6. <https://doi.org/10.1086/514291>
5. Jacobs M, Rodger A, Bell DJ, Bhagani S, Cropley I, Filipe A, et al. Late Ebola virus relapse causing meningoencephalitis: a case report. *Lancet*. 2016;388:498–503. [https://doi.org/10.1016/S0140-6736\(16\)30386-5](https://doi.org/10.1016/S0140-6736(16)30386-5)
6. Deen GF, Broutet N, Xu W, Knust B, Sesay FR, McDonald SLR, et al. Ebola RNA persistence in semen of Ebola virus disease survivors—final report. *N Engl J Med*. 2017;377:1428–37. <https://doi.org/10.1056/NEJMoa1511410>
7. Diallo B, Sissoko D, Loman NJ, Bah HA, Bah H, Worrell MC, et al. Resurgence of Ebola virus disease in Guinea linked to a survivor with virus persistence in seminal fluid for more than 500 days. *Clin Infect Dis*. 2016;63:1353–6. <https://doi.org/10.1093/cid/ciw601>
8. Mate SE, Kugelman JR, Nyenswah TG, Ladner JT, Wiley MR, Cordier-Lassalle T, et al. Molecular evidence of sexual transmission of Ebola virus. *N Engl J Med*. 2015;373:2448–54. <https://doi.org/10.1056/NEJMoa1509773>
9. Keita M, Duraffour S, Loman NJ, Rambaut A, Diallo B, Magassouba N, et al. Unusual Ebola virus chain of transmission, Conakry, Guinea, 2014–2015. *Emerg Infect Dis*. 2016;22:2149–52. <https://doi.org/10.3201/eid2212.160847>
10. Subissi L, Keita M, Mesfin S, Rezza G, Diallo B, Van Gucht S, et al. Ebola virus transmission caused by persistently infected survivors of the 2014–2016 outbreak in West Africa. *J Infect Dis*. 2018;218(suppl_5):S287–S291.
11. World Health Organization. WHO emergency use assessment and listing for Ebola virus disease IVDs [cited 2017 Dec 21]. http://www.who.int/diagnostics_laboratory/160324_final_public_report_ea_0023_021_00.pdf
12. Rieger T, Kerber R, El Halas H, Pallasch E, Duraffour S, Günther S, et al. Evaluation of RealStar reverse transcription-polymerase chain reaction kits for filovirus detection in the laboratory and field. *J Infect Dis*. 2016;214(suppl 3):S243–9. <https://doi.org/10.1093/infdis/jiw246>
13. Sissoko D, Duraffour S, Kerber R, Kolie JS, Beavogui AH, Camara A-M, et al. Persistence and clearance of Ebola virus RNA from seminal fluid of Ebola virus disease survivors: a longitudinal analysis and modelling study. *Lancet Glob Health*. 2017;5:e80–8. [https://doi.org/10.1016/S2214-109X\(16\)30243-1](https://doi.org/10.1016/S2214-109X(16)30243-1)
14. Weidmann M, Mühlberger E, Hufert FT. Rapid detection protocol for filoviruses. *J Clin Virol*. 2004;30:94–9. <https://doi.org/10.1016/j.jcv.2003.09.004>
15. Sissoko D, Laouenan C, Folkesson E, M'Lebing A-B, Beavogui A-H, Baize S, et al.; JIKI Study Group. Experimental treatment with favipiravir for Ebola virus disease (the JIKI trial): a historically controlled, single-arm proof-of-concept trial in Guinea. *PLoS Med*. 2016;13:e1001967. <https://doi.org/10.1371/journal.pmed.1001967>
16. Henao-Restrepo AM, Camacho A, Longini IM, Watson CH, Edmunds WJ, Egger M, et al. Efficacy and effectiveness of an rVSV-vectored vaccine in preventing Ebola virus disease: final results from the Guinea ring vaccination, open-label, cluster-randomised trial (Ebola Ça Suffit!). *Lancet*. 2017;389:505–18. [https://doi.org/10.1016/S0140-6736\(16\)32621-6](https://doi.org/10.1016/S0140-6736(16)32621-6)
17. Keita M, Diallo B, Mesfin S, Marega A, Koumpingnin NY, N'Faly M, et al. Subsequent mortality of Ebola virus disease survivors in Guinea: a nationwide retrospective cohort study. *Lancet Infect Dis*. 2019;19:1202–8. [https://doi.org/10.1016/S1473-3099\(19\)30313-5](https://doi.org/10.1016/S1473-3099(19)30313-5)
18. Ministry of Health of Guinea. National Health Development Plan 2015–2024 [cited 2019 Dec 12]. http://www.nationalplanningcycles.org/sites/default/files/country_docs/Guinea/plan_national_developpement_sanitaire_2015-2024_guinee_fin.pdf
19. Soka MJ, Choi MJ, Baller A, White S, Rogers E, Purpura LJ, et al. Prevention of sexual transmission of Ebola in Liberia through a national semen testing and counselling programme for survivors: an analysis of Ebola virus RNA results and behavioural data. *Lancet Glob Health*. 2016;4:e736–43. [https://doi.org/10.1016/S2214-109X\(16\)30175-9](https://doi.org/10.1016/S2214-109X(16)30175-9)
20. Purpura LJ, Soka M, Baller A, White S, Rogers E, Choi MJ, et al. Implementation of a national semen testing and counseling program for male Ebola survivors—Liberia, 2015–2016. *MMWR Morb Mortal Wkly Rep*. 2016;65:963–6. <https://doi.org/10.15585/mmwr.mm6536a5>
21. Etard J-F, Sow MS, Leroy S, Touré A, Taverne B, Keita AK, et al.; Postebogui Study Group. Multidisciplinary assessment of post-Ebola sequelae in Guinea (Postebogui): an observational cohort study. *Lancet Infect Dis*. 2017;17:545–52. [https://doi.org/10.1016/S1473-3099\(16\)30516-3](https://doi.org/10.1016/S1473-3099(16)30516-3)
22. Subtil F, Delaunay C, Keita AK, Sow MS, Touré A, Leroy S, et al.; Postebogui Study Group. Dynamics of Ebola RNA persistence in semen: a report from the Postebogui cohort in Guinea. *Clin Infect Dis*. 2017;64:1788–90. <https://doi.org/10.1093/cid/cix210>
23. Deen GF, McDonald SLR, Marrison JE, Sesay FR, Ervin E, Thorson AE, et al.; Sierra Leone Ebola Virus Persistence Study Group. Implementation of a study to examine the persistence of Ebola virus in the body fluids of Ebola virus disease survivors in Sierra Leone: Methodology and lessons learned. *PLoS Negl Trop Dis*. 2017;11:e0005723. <https://doi.org/10.1371/journal.pntd.0005723>
24. Abad N, Malik T, Ariyaratnam A, Ongpin P, Hogben M, McDonald SLR, et al.; Sierra Leone Ebola Virus Persistence Study Group. Development of risk reduction behavioral counseling for Ebola virus disease survivors enrolled in the Sierra Leone Ebola Virus Persistence Study, 2015–2016. *PLoS Negl Trop Dis*. 2017;11:e0005827. <https://doi.org/10.1371/journal.pntd.0005827>
25. Sneller MC, Reilly C, Badio M, Bishop RJ, Eghrari AO, Moses SJ, et al.; PREVAIL III Study Group. A longitudinal study of Ebola sequelae in Liberia. *N Engl J Med*. 2019;380:924–34. <https://doi.org/10.1056/NEJMoa1805435>

Address for correspondence: Lorenzo Subissi, Global Outbreak Alert and Response Network, 22 Avenue Appia 1211, Geneva, Switzerland; email: subissil@who.int

Characteristics of Patients with Acute Flaccid Myelitis, United States, 2015–2018

Nilay McLaren, Adriana Lopez, Sarah Kidd, John X. Zhang, W. Allan Nix, Ruth Link-Gelles, Adria Lee, Janell A. Routh

Medscape **ACTIVITY** EDUCATION

In support of improving patient care, this activity has been planned and implemented by Medscape, LLC and Emerging Infectious Diseases. Medscape, LLC is jointly accredited by the Accreditation Council for Continuing Medical Education (ACCME), the Accreditation Council for Pharmacy Education (ACPE), and the American Nurses Credentialing Center (ANCC), to provide continuing education for the healthcare team.

Medscape, LLC designates this Journal-based CME activity for a maximum of 1.00 **AMA PRA Category 1 Credit(s)**[™]. Physicians should claim only the credit commensurate with the extent of their participation in the activity.

Successful completion of this CME activity, which includes participation in the evaluation component, enables the participant to earn up to 1.0 MOC points in the American Board of Internal Medicine's (ABIM) Maintenance of Certification (MOC) program. Participants will earn MOC points equivalent to the amount of CME credits claimed for the activity. It is the CME activity provider's responsibility to submit participant completion information to ACCME for the purpose of granting ABIM MOC credit.

All other clinicians completing this activity will be issued a certificate of participation. To participate in this journal CME activity: (1) review the learning objectives and author disclosures; (2) study the education content; (3) take the post-test with a 75% minimum passing score and complete the evaluation at <http://www.medscape.org/journal/eid>; and (4) view/print certificate. For CME questions, see page 399.

Release date: January 15, 2020; Expiration date: January 15, 2021

Learning Objectives

Upon completion of this activity, participants will be able to:

- Compare the clinical and laboratory characteristics of AFM cases reported in the United States during peak vs. nonpeak years from 2015 through 2018
- Compare the clinical and laboratory characteristics of AFM cases reported in the United States during peak years 2016 vs. 2018
- Describe the clinical and public health significance of differences in the clinical and laboratory characteristics of AFM cases reported in the United States during peak vs. nonpeak years from 2015 through 2018

CME Editor

Kristina B. Clark, PhD, Copyeditor, Emerging Infectious Diseases. *Disclosure: Kristina B. Clark, PhD, has disclosed no relevant financial relationships.*

CME Author

Laurie Barclay, MD, freelance writer and reviewer, Medscape, LLC. *Disclosure: Laurie Barclay, MD, has disclosed no relevant financial relationships.*

Authors

Disclosures: Nilay McLaren; Adriana Lopez, MHS; Sarah Kidd, MD, MPH; John X. Zhang, PhD; W. Allan Nix, BS; Ruth Link-Gelles, PhD, MPH; Adria Lee, MSPH; and Janell A. Routh, MD, MHS, have disclosed no relevant financial relationships.

Observed peaks of acute flaccid myelitis (AFM) cases have occurred biennially since 2014 in the United States. We aimed to determine if AFM etiology differed between peak and nonpeak years, considering that clinical features of AFM differ by virus etiology. We compared clinical and laboratory characteristics of AFM cases that occurred

during peak (2016 and 2018, n = 366) and nonpeak (2015 and 2017, n = 50) years. AFM patients in peak years were younger (5.2 years) than those in nonpeak years (8.3 years). A higher percentage of patients in peak years than nonpeak years had pleocytosis (86% vs. 60%), upper extremity involvement (33% vs. 16%), and an illness preceding limb weakness (90% vs. 62%) and were positive for enterovirus or rhinovirus RNA (38% vs. 16%). Enterovirus D68 infection was associated with AFM only in peak years. Our findings suggest AFM etiology differs between peak and nonpeak years.

Author affiliation: Centers for Disease Control and Prevention, Atlanta, Georgia, USA

DOI: <https://doi.org/10.3201/eid2602.191453>

Acute flaccid myelitis (AFM) is a clinical syndrome characterized by the acute onset of flaccid limb weakness accompanied by spinal cord gray matter lesions. AFM is a known complication of infection with certain viruses, including polioviruses, nonpolio enteroviruses, flaviviruses, herpesviruses, and adenoviruses (1–7). In the early 1950s, outbreaks of poliovirus caused >15,000 cases of paralysis each year in the United States, but after the introduction of poliovirus vaccines and the elimination of poliovirus in the United States, AFM caused by poliovirus became much less common (8). However, sporadic, poliovirus-negative cases continued to occur (9).

In August 2014, an unusual cluster of AFM in children was identified in Colorado (10). National surveillance was initiated in 2015 and subsequently led to the identification of heightened activity in 2016 and 2018; during these years, peak illness onset occurred during August–October. In contrast, in 2015 and 2017, the number of AFM cases remained low and did not vary by season (11). National experts agree that the AFM epidemiology observed in 2014 is new; this alternating pattern of high activity one year and low activity the next, referred to herein as peak and nonpeak years, with high activity typically in the late summer or early fall, has not been documented before 2014 (12–14) (M. Cortese, Centers for Disease Control and Prevention [CDC], Atlanta, GA, USA, pers. comm., 2017 Sep 27). This change suggests the emergence (beginning in 2014) of either a new cause of AFM or a known cause of AFM with a new epidemiologic pattern.

Determining the cause or causes of the biennial increases in AFM cases has implications for the development of treatment and prevention strategies. However, pathogen-specific laboratory testing has yielded limited insight into the underlying cause of this new epidemiology. Different viruses known to be associated with AFM development have been shown to produce distinctive sets of clinical features (15,16). If a single pathogen is responsible for most AFM cases in peak years, cases of illness onset in these years probably would have clinical manifestations distinct from those of illness onset in nonpeak years, when the etiology of cases is likely more mixed. We compared demographic, clinical, and laboratory characteristics of AFM cases in peak versus nonpeak years to evaluate this hypothesis.

Methods

Reporting and Classification

Beginning in August 2014, CDC received reports of patients meeting the clinical criterion for AFM (i.e., acute onset of flaccid limb weakness) through local

and state health departments. A panel of expert neurologists classified these patients according to the standardized case definition published by the Council of State and Territorial Epidemiologists in 2015 (17). We defined a confirmed case as an illness in a patient who met the clinical criterion and had magnetic resonance imaging (MRI) showing a spinal cord lesion largely restricted to the gray matter and spanning ≥ 1 spinal segment. Our analysis includes only confirmed AFM cases in patients <22 years of age and is limited to 4 complete years of AFM surveillance (January 1, 2015–December 31, 2018).

Laboratory Testing

CDC staff requested sterile site (e.g., blood, serum, and cerebrospinal fluid [CSF]) and nonsterile site (e.g., respiratory and fecal) specimens from each patient and tested these specimens using algorithms described previously (18,19). With specimens from 2015 and 2016, and starting in September 2018 with all received specimens, CDC staff tested for enterovirus/rhinovirus RNA using a 5' nontranslated region-targeted pan-*Enterovirus* real-time reverse transcription PCR assay (genus-level detection) and typed those that were positive. For specimens collected during January 2017–August 2018, only the specimens that had tested positive for enterovirus/rhinovirus RNA at an outside institution were requested by CDC staff for testing and typing. In our analysis, we report only the results from CDC laboratory testing.

Data Analysis

To assess trends in AFM activity over time, we assigned patients with confirmed cases to an epidemiologic week according to their date of onset of limb weakness. We compared cases of patients having AFM onset in peak years (i.e., 2016 and 2018) with those of patients having AFM onset in nonpeak years (i.e., 2015 and 2017) and compared cases between the 2 peak years (2016 vs. 2018). We analyzed the demographics, clinical characteristics, and laboratory results of AFM patients that had been systematically collected across all 4 years of surveillance. We defined AFM cases as severe if they included all 3 of the following clinical characteristics: respiratory distress requiring mechanical ventilation to manage, symptomatic cranial nerve involvement, and paralysis of all 4 limbs. We defined CSF pleocytosis as a leukocyte count of >5 cells/mm³.

We entered data into a Microsoft Access (for 2015–2017 data; <https://www.microsoft.com>) or REDCap (for 2018 data; <https://www.project-redcap.org>) database and performed descriptive analyses using R Studio version 3.4.1 (<https://rstudio.com>).

Table 1. Descriptive characteristics of confirmed AFM cases in patients <22 years of age from peak years versus nonpeak years, United States, January 2015–December 2018*

Characteristic	Peak years, n = 366†	Nonpeak years, n = 50‡	p value
Age, y, median (range) [IQR]	5.2 (0.4–21.9) [3.2–8.0]	8.3 (0.3–20.2) [3.9–11.9]	0.02
Sex			
M	217/366 (59)	32/50 (64)	0.54
F	149/366 (41)	18/50 (36)	0.54
Lumbar puncture	343/363 (94)	48/49 (98)	0.84
Pleocytosis§	283/328 (86)	28/47 (60)	<0.001
CSF, cells/mm ³ , median (range) [IQR]	75 (0–3,261) [24–150]	32 (0–1,081) [3–168]	0.07
Upper extremity involvement only	121/366 (33)	8/50 (16)	0.01
Lower extremity involvement only	49/366 (13)	16/50 (32)	<0.001
Paralysis of all 4 limbs	101/366 (28)	24/50 (48)	0.005
Severe AFM¶	9/366 (2)	9/50 (18)	<0.001
Cranial nerve lesion	96/366 (26)	10/50 (20)	0.39
Illness within previous 4 weeks			
Any fever	258/358 (72)	27/49 (55)	0.02
Any respiratory illness	282/360 (78)	21/49 (43)	<0.001
Any gastrointestinal illness	111/344 (32)	12/34 (35)	0.24
Any respiratory illness or fever	328/366 (90)	31/50 (62)	<0.001
Enterovirus/rhinovirus RNA positive	98/258 (38)	5/31 (16)	0.02
Enterovirus D68	53/98 (54)	0/5	0.02
Enterovirus A71	13/98 (13)	1/5 (20)	0.59

*Values are no./total (%), except where indicated otherwise. AFM, acute flaccid myelitis; CSF, cerebrospinal fluid; IQR, interquartile range.

†2016 and 2018.

‡2015 and 2017.

§Defined as leukocyte count >5 cells/mm³.

¶Defined as AFM cases of respiratory distress that required mechanical ventilation, cranial nerve involvement, and paralysis of all 4 limbs.

3), with a few notable exceptions. Cranial nerve lesions were less common in AFM patients in 2018 (19%) than in AFM patients in 2016 (37%; p<0.001). More cases in 2016 (6%) than 2018 (0%; p<0.001) were classified as severe AFM. Compared with AFM patients in 2016, more AFM patients in 2018 were reported to have an illness within the 4 weeks preceding the onset of limb weakness: any fever (68% in 2016 vs. 75%

in 2018; p<0.001), respiratory illness (76% in 2016 vs. 80% in 2018; p = 0.01), or gastrointestinal illness (26% in 2016 vs. 36% in 2018; p = 0.002). The percentage of confirmed AFM cases positive for enterovirus/rhinovirus RNA was similar in both peak years. Among all enterovirus/rhinovirus-positive specimens, EV-D68-positive specimens were more common in 2016 (71%) than in 2018 (45%; p = 0.02). However, AFM patients

Table 2. Descriptive characteristics of confirmed AFM cases in patients <22 years of age from peak months versus nonpeak months, United States, January 2015–December 2018*

Characteristic	All peak months, n = 268†	All nonpeak months, n = 148‡	p value
Age, y, median (range) [IQR]	5.2 (0.5–21.9) [3.3–7.8]	5.7 (0.3–21.9) [3.2–10.6]	0.18
Sex			
M	159/268 (59)	90/148 (61)	0.83
F	109/268 (41)	58/148 (39)	0.83
Lumbar puncture	251/267 (94)	140/145 (97)	0.35
Pleocytosis§	212/239 (89)	99/136 (73)	<0.001
CSF, cells/mm ³ , median (range) [IQR]	88 (0–814) [30–154]	44 (0–3,261) [4–118]	<0.001
Upper extremity involvement only	95/268 (35)	34/148 (23)	0.01
Lower extremity involvement only	29/268 (11)	36/148 (24)	0.001
Paralysis of all 4 limbs	67/268 (25)	58/148 (39)	0.004
Severe AFM¶	5/268 (2)	13/148 (9)	0.002
Cranial nerve lesion	72/268 (27)	34/148 (23)	0.41
Illness within previous 4 weeks			
Any fever	201/262 (77)	84/145 (58)	<0.001
Any respiratory illness	214/264 (81)	89/145 (61)	<0.001
Any gastrointestinal illness	80/256 (31)	43/122 (35)	0.46
Any respiratory illness or fever	246/268 (92)	113/148 (76)	<0.001
Enterovirus/rhinovirus RNA positive	73/192 (38)	30/97 (31)	0.25
Enterovirus D68	42/73 (58)	11/30 (37)	0.08
Enterovirus A71	6/73 (8)	8/30 (27)	0.02

*Values are no./total (%), except where indicated otherwise. AFM, acute flaccid myelitis; CSF, cerebrospinal fluid; IQR, interquartile range.

†August–October of 2016 and 2018.

‡January–July and November–December of 2016 and 2018, January–December of 2015 and 2017.

§Defined as leukocyte count >5 cells/mm³.

¶Defined as AFM cases of respiratory distress that required mechanical ventilation, cranial nerve involvement, and paralysis of all 4 limbs.

Table 3. Descriptive characteristics of confirmed AFM cases in patients <22 years of age from peak years, United States, January–December 2016 and 2018*

Characteristic	2016, n = 143	2018, n = 223	p value
Age, y, median (range) [IQR]	5.3 (0.4–21.2) [3.2–9.7]	5.2 (0.5–21.9) [3.2–7.8]	0.43
Sex			
M	86/143 (60)	131/223 (59)	0.83
F	57/143 (40)	92/223 (41)	0.83
Lumbar puncture	135/140 (96)	208/223 (93)	0.14
Pleocytosis†	114/135 (84)	169/208 (81)	0.47
CSF, cells/mm ³ , median (range) [IQR]	77 (0–3,261) [18–150]	74 (0–814) [27–152]	0.22
Upper extremity involvement only	48/143 (34)	73/223 (33)	0.91
Lower extremity involvement only	25/143 (17)	24/223 (11)	0.08
Paralysis of all 4 limbs	45/143 (31)	56/223 (25)	0.19
Severe AFM‡	9/143 (6)	0/223	<0.001
Cranial nerve lesion	53/143 (37)	43/223 (19)	<0.001
Illness within previous 4 weeks			
Any fever	93/137 (68)	165/221 (75)	<0.001
Any respiratory illness	106/139 (76)	176/221 (80)	0.01
Any gastrointestinal illness	33/126 (26)	78/218 (36)	0.002
Any respiratory illness or fever	122/143 (85)	206/223 (92)	0.04
Enterovirus/rhinovirus RNA positive	34/94 (36)	64/164 (39)	0.69
Enterovirus D68	24/34 (71)	29/64 (45)	0.02
Enterovirus A71	2/34 (6)	11/64 (17)	0.21

*Values are no./total (%), except where indicated otherwise. AFM, acute flaccid myelitis; CSF, cerebrospinal fluid; IQR, interquartile range.

†Defined as leukocyte count >5 cells/mm³.

‡Defined as AFM cases of respiratory distress that required mechanical ventilation, cranial nerve involvement, and paralysis of all 4 limbs.

in 2018 (17%) were more likely than those in 2016 (6%; $p = 0.21$) to be positive for EV-A71 because of a geographically limited outbreak of EV-A71 in Colorado.

To determine whether the differences in case characteristics between peak years could be explained by the EV-A71 outbreak, we conducted a subanalysis in which we removed all EV-A71–positive cases. Differences in clinical characteristics between years remained unchanged; however, the percentage of cases positive for EV-D68 was no longer significantly different (75% vs. 55%; $p = 0.07$) (Table 4).

Discussion

Five years of national AFM surveillance data show a seasonal, alternate-year pattern of AFM activity. The numbers of confirmed cases in peak years (2016 and 2018) was >5 times the numbers of cases in the previous year. Our analysis demonstrates key clinical differences between cases in peak years and nonpeak years. Patients with AFM onset in peak years were younger, more likely to have had fever or respiratory symptoms within the 4 weeks preceding AFM onset, and more likely to have pleocytosis and upper extremity weakness during hospitalization than those with AFM onset in nonpeak years. These clinical characteristics mirror the presentation of AFM described for cases of onset in 2014 (20). Patients with onset in nonpeak years were more severely affected during acute illness than those with onset in peak years. We also found differences between AFM patients with onset in 2016 and AFM patients with onset in 2018, the 2 peak years. Compared with AFM patients with onset in 2016, those with onset

in 2018 were less likely to have severe disease or cranial nerve lesions and were more likely to have a preceding illness before AFM onset.

Differences in the clinical presentation of AFM between peak and nonpeak years are suggestive of differences in AFM etiologies between those years. Likewise, the clinical differences between cases occurring during peak and nonpeak years might be indicative of different virus etiologies between peak and nonpeak years. In our analysis, enterovirus positivity among AFM cases was higher in peak years than in nonpeak years, and EV-D68 was detected only in the cases occurring during peak years. Although this difference disappeared in the sensitivity analysis (suggesting that the enteroviruses circulating in peak years varies slightly by month), EV-D68 detections remained exclusive to cases occurring in peak years. AFM case counts also vary slightly by month in different peak years; the escalation in cases began earlier in 2016 than they did in 2018, and the increase in case counts lasted slightly longer in 2018.

In peak years, overall enterovirus positivity among AFM cases was similar, but significant type-specific variations were noted. EV-D68 was detected more frequently in specimens from AFM patients with onset in 2016 and EV-A71 more often in those with onset in 2018. These variations might have contributed to differences in clinical characteristics seen between peak years. However, removal of EV-A71–positive cases did not eliminate the differences in clinical characteristics between peak years, suggesting that the greater number of EV-D68–positive cases in 2016 contributed to the clinical variability. Distinct AFM clinical presentations

Table 4. Descriptive characteristics of confirmed AFM cases in patients <22 years of age who were negative for enterovirus A71 during peak years, United States, January–December 2016 and 2018*

Characteristic	2016, n = 141	2018, n = 212	p value
Age, y, median (range) [IQR]	5.4 (0.4–21.2) [3.3–9.8]	5.3 (0.5–21.9) [3.4–7.8]	0.68
Sex			
M	86/141 (61)	120/212 (57)	0.44
F	55/141 (39)	92/212 (43)	0.44
Lumbar puncture	134/139 (96)	197/212 (93)	0.13
Pleocytosis†	113/132 (86)	158/184 (86)	1
CSF, cells/mm ³ , median (range) [IQR]	73 (0–3,261) [18–150]	73 (0–814) [25.5–149]	0.86
Upper extremity involvement only	48/141 (34)	71/212 (33)	1
Lower extremity involvement only	25/141 (18)	23/212 (11)	0.08
Paralysis of all 4 limbs	44/141 (31)	50/212 (24)	0.14
Severe AFM‡	9/141 (6)	0/212	<0.001
Cranial nerve lesion	52/141 (37)	42/212 (20)	<0.001
Illness within previous 4 weeks			
Any fever	91/135 (67)	154/210 (73)	<0.001
Any respiratory illness	104/137 (76)	172/210 (82)	0.004
Any gastrointestinal illness	32/124 (26)	72/207 (35)	0.003
Any respiratory illness or fever	120/141 (85)	195/212 (92)	0.05
Enterovirus/rhinovirus RNA positive	32/92 (35)	53/153 (35)	1
Enterovirus D68	24/32 (75)	29/53 (55)	0.07

*Values are no./total (%), except where indicated otherwise. AFM, acute flaccid myelitis; CSF, cerebrospinal fluid; IQR, interquartile range.

†Defined as leukocyte count >5 cells/mm³.

‡Defined as AFM cases of respiratory distress that required mechanical ventilation, cranial nerve involvement, and paralysis of all 4 limbs.

have been observed for different enterovirus etiologies (15,16). AFM caused by EV-A71 has been associated with myoclonus, ataxia, weakness, and autonomic instability. In an isolated outbreak in Colorado in 2018, AFM cases associated with EV-A71 were clinically distinct from those not associated with EV-A71 (15). Of note, paralytic syndrome caused by poliovirus is classically characterized by lower extremity weakness of an asymmetric distribution and a preceding mild gastrointestinal illness, features less common among AFM cases in peak years (16).

Although multiple viruses are associated with AFM, growing evidence suggests that nonpolio enteroviruses and specifically EV-D68 are linked to the changes in AFM epidemiology that started in 2014 (21,22). Enteroviruses were the most common viruses in nasopharyngeal, oropharyngeal, or fecal specimens from confirmed AFM patients identified by CDC researchers, and EV-D68 was the most frequent enterovirus typed (18–20). Unlike most other viruses known to cause AFM, enteroviruses routinely circulate and can cause outbreaks during the late summer and early fall months in the United States in a pattern corresponding with the observed seasonal AFM peaks (23,24). Although the United States does not have active national enterovirus surveillance, the enterovirus cases reported in 2 passive laboratory-based reporting systems (the National Enterovirus Surveillance System and the National Respiratory and Enteric Virus Surveillance System) demonstrate the presence of an annual enterovirus season with variation in the enterovirus types circulating each year (23,25,26). Climate, level of immunity in the host population, and viral fitness probably influence which

strains dominate each year (27). If >1 specific type of enterovirus causes AFM, differences in circulating types could account for changes in AFM epidemiology from year to year. EV-D68 might be one such type. Respiratory disease surveillance indicates that EV-D68 appears to have circulated in a biennial pattern since 2014, corresponding with trends in AFM. In 2014, 2016, and 2018, increases in respiratory disease caused by EV-D68 coincided with the increases in AFM (24,28–30). Since 2014, the correlation between EV-D68 circulation and AFM incidence has also been documented in Canada, Japan, Europe, and Argentina (31–34). Global collaborations for the investigation of AFM cases and ongoing, active enterovirus surveillance will enable a broader and more complete picture of enterovirus circulation patterns and their relationships to AFM in the future.

Sentinel surveillance of other enteroviruses, such as coxsackieviruses A2 and A4, have also demonstrated a biennial periodicity like that observed for EV-D68 (35), although neither of these coxsackieviruses have been implicated in clusters of AFM. Rotavirus has also been shown to have a biennial circulation pattern in the postvaccination era (36). These biennial circulation patterns might be caused by an increase in the number of young, unexposed persons during years of low circulation, which leads to a larger number of susceptible persons acquiring and transmitting the infection in the following year. However, this phenomenon cannot fully explain the periodicity seen with AFM. The median age of AFM patients in peak years (5 years) is higher than the median age of patients with respiratory EV-D68 infections (3 years) (24), possibly indicating that other factors besides

viral infection affect the risk for AFM development. Moreover, limited data show that persons across all age groups have robust neutralizing antibody titers against EV-D68 (37), including against both historical and contemporary outbreak strains, implying ongoing exposure and infection across the United States. The development of AFM in a small percentage of patients infected by this ubiquitous virus is likely to depend on other factors. Research into environmental or genetic risk factors for AFM development will provide insight into AFM pathogenesis.

Our findings are subject to limitations. First, differences in types of sterile and nonsterile specimens collected and sent to the CDC during 2015–2018 might have affected comparisons of enterovirus/rhinovirus positivity of cases in different years. However, because all enterovirus/rhinovirus-positive specimens were analyzed for enterovirus type, the percentage of type-specific (e.g., EV-D68 or EV-A71) cases among enterovirus/rhinovirus-positive cases would not have been affected. Second, we considered specimens enterovirus- or rhinovirus-positive only if the CDC laboratory confirmed this finding. Although CDC staff requested specimens for testing and confirmation, they might not have received all of them, thus influencing the results reported here. Last, the reporting of suspected cases to CDC public health staff is inconsistent, despite efforts to increase healthcare provider recognition of AFM. Year-to-year variation in reporting can occur, and more comprehensive reporting by healthcare providers might occur during peak years, when their awareness of this illness is heightened.

The alternate-year pattern in peak AFM activity since 2014 highlights a noteworthy shift in the epidemiology of this syndrome. Differences between AFM cases in peak years and nonpeak years provide additional evidence to support the hypothesis of a unique pathogen or pathogens contributing to this new epidemiology. Multiple lines of evidence support EV-D68 as a leading candidate, although additional research is needed. Frequent detection of EV-A71 in AFM cases in 2018 illustrates that >1 virus can cause outbreaks of AFM, and therefore AFM surveillance should not be restricted to detection of a specific pathogen. Healthcare providers thoroughly documenting clinical findings, including results of complete neurologic examinations, and reporting AFM cases to public health authorities, regardless of the pathogen implicated by test results, have implications for treatment and prevention. National AFM surveillance data can be used to characterize yearly variations in AFM cases (temporally, clinically, and etiologically) and illuminate the pathology of this emerging illness.

Acknowledgments

We thank the staff of state and local health departments, without whom this surveillance data would not have been collected. We thank our laboratory colleagues for providing enterovirus testing and typing data and Mary Ann Hall for her careful reading and editing of this manuscript.

About the Author

Mr. McLaren completed this work during a Student Worksite Experience Program internship in the Viral Vaccine Preventable Diseases Branch, Division of Viral Diseases, National Center for Immunization and Respiratory Diseases, CDC, in Atlanta, Georgia, USA, as a senior in high school at the Massachusetts Academy of Math and Science at Worcester Polytechnic Institute in Worcester, Massachusetts, USA. His primary research interests are neuroscience and infectious diseases.

References

- Solomon T, Willison H. Infectious causes of acute flaccid paralysis. *Curr Opin Infect Dis.* 2003;16:375–81. <https://doi.org/10.1097/00001432-200310000-00002>
- Ong KC, Wong KT. Understanding Enterovirus 71 neuropathogenesis and its impact on other neurotropic enteroviruses. *Brain Pathol.* 2015;25:614–24. <https://doi.org/10.1111/bpa.12279>
- Bitnun A, Yeh EA. Acute flaccid paralysis and enteroviral infections. *Curr Infect Dis Rep.* 2018;20:34. <https://doi.org/10.1007/s11908-018-0641-x>
- Saad M, Youssef S, Kirschke D, Shubair M, Haddadin D, Myers J, et al. Acute flaccid paralysis: the spectrum of a newly recognized complication of West Nile virus infection. *J Infect.* 2005;51:120–7. <https://doi.org/10.1016/j.jinf.2004.10.005>
- Wang Y, Yu CY, Huang L, Han YY, Liu YM, Zhu J. Acute longitudinal and hemorrhagic myelitis caused by varicella-zoster virus in an immunocompetent adolescent. *Neurologist.* 2015;19:93–5. <https://doi.org/10.1097/NRL.0000000000000016>
- Ivanova OE, Yurashko OV, Ereemeeva TP, Baikova OY, Morozova NS, Lukashov AN. Adenovirus isolation rates in acute flaccid paralysis patients. *J Med Virol.* 2012;84:75–80. <https://doi.org/10.1002/jmv.22265>
- Sejvar JJ, Bode AV, Marfin AA, Campbell GL, Ewing D, Mazowiecki M, et al. West Nile virus-associated flaccid paralysis. *Emerg Infect Dis.* 2005;11:1021–7. <https://doi.org/10.3201/eid1107.040991>
- Nathanson N. Eradication of poliomyelitis in the United States. *Rev Infect Dis.* 1982;4:940–50. <https://doi.org/10.1093/clinids/4.5.940>
- Nihei K, Naitoh H, Ikeda K. Poliomyelitis-like syndrome following asthmatic attack (Hopkins syndrome). *Pediatr Neurol.* 1987;3:166–8. [https://doi.org/10.1016/0887-8994\(87\)90085-3](https://doi.org/10.1016/0887-8994(87)90085-3)
- Pastula DM, Aliabadi N, Haynes AK, Messacar K, Schreiner T, Maloney J, et al.; Centers for Disease Control and Prevention. Acute neurologic illness of unknown etiology in children – Colorado, August–September 2014. *MMWR Morb Mortal Wkly Rep.* 2014;63:901–2.
- Centers for Disease Control and Prevention. AFM cases in U.S. [cited 2018 Nov 8]. <https://www.cdc.gov/acute-flaccid-myelitis/cases-in-us.html>

12. Van Haren K, Ayscue P, Waubant E, Clayton A, Sheriff H, Yagi S, et al. Acute flaccid myelitis of unknown etiology in California, 2012-2015. *JAMA*. 2015;314:2663-71. <https://doi.org/10.1001/jama.2015.17275>
13. Messacar K, Schreiner TL, Maloney JA, Wallace A, Ludke J, Oberste MS, et al. A cluster of acute flaccid paralysis and cranial nerve dysfunction temporally associated with an outbreak of enterovirus D68 in children in Colorado, USA. *Lancet*. 2015;385:1662-71. [https://doi.org/10.1016/S0140-6736\(14\)62457-0](https://doi.org/10.1016/S0140-6736(14)62457-0)
14. Uprety P, Curtis D, Elkan M, Fink J, Rajagopalan R, Zhao C, et al. Association of enterovirus D68 with acute flaccid myelitis, Philadelphia, Pennsylvania, USA, 2009-2018. *Emerg Infect Dis*. 2019;25:1676-82. <https://doi.org/10.3201/eid2509.190468>
15. Messacar KS, Spence-Davison E, Osborne C, Press C, Schreiner TL, Martin J, et al. Clinical characteristics of enterovirus A71 neurological disease during an outbreak in children in Colorado, USA, in 2018: an observational cohort study. *Lancet Infect Dis*. Online December 16, 2019. [http://dx.doi.org/10.1016/S1473-3099\(19\)30632-2](http://dx.doi.org/10.1016/S1473-3099(19)30632-2)
16. Pray LG. Observations on a poliomyelitis outbreak in North Dakota in 1946; with special consideration of spinal fluid findings. *J Lancet*. 1947;67:202-5.
17. Council of State and Territorial Epidemiologists. Revision to the standardized surveillance and case definition for acute flaccid myelitis. 2017 [cited 2018 Nov 8]. <https://cdn.ymaws.com/www.cste.org/resource/resmgr/2017PS/2017PSFinal/17-ID-01.pdf>
18. Lopez A, Lee A, Guo A, Konopka-Anstadt JL, Nisler A, Rogers SL, et al. Vital signs: surveillance for acute flaccid myelitis – United States, 2018. *MMWR Morb Mortal Wkly Rep*. 2019;68:608-14. <https://doi.org/10.15585/mmwr.mm6827e1>
19. Ayers T, Lopez A, Lee A, Kambhampati A, Nix WA, Henderson E, et al. Acute flaccid myelitis in the United States: 2015-2017. *Pediatrics*. 2019;144:e20191619. <https://doi.org/10.1542/peds.2019-1619>
20. Sejvar JJ, Lopez AS, Cortese MM, Leshem E, Pastula DM, Miller L, et al. Acute flaccid myelitis in the United States, August-December 2014: results of nationwide surveillance. *Clin Infect Dis*. 2016;63:737-45. <https://doi.org/10.1093/cid/ciw372>
21. Messacar K, Asturias EJ, Hixon AM, Van Leer-Buter C, Niesters HGM, Tyler KL, et al. Enterovirus D68 and acute flaccid myelitis-evaluating the evidence for causality. *Lancet Infect Dis*. 2018;18:e239-47. [https://doi.org/10.1016/S1473-3099\(18\)30094-X](https://doi.org/10.1016/S1473-3099(18)30094-X)
22. Mishra N, Ng TFF, Marine RL, Jain K, Ng J, Thakkar R, et al. Antibodies to enteroviruses in cerebrospinal fluid of patients with acute flaccid myelitis. *MBio*. 2019;10:e01903-19. <https://doi.org/10.1128/mBio.01903-19>
23. Khetsuriani N, Lamonte-Fowlkes A, Oberst S, Pallansch MA; Centers for Disease Control and Prevention. Enterovirus surveillance – United States, 1970-2005. *MMWR Surveill Summ*. 2006;55:1-20.
24. Midgley CM, Watson JT, Nix WA, Curns AT, Rogers SL, Brown BA, et al.; EV-D68 Working Group. Severe respiratory illness associated with a nationwide outbreak of enterovirus D68 in the USA (2014): a descriptive epidemiological investigation. *Lancet Respir Med*. 2015;3:879-87. [https://doi.org/10.1016/S2213-2600\(15\)00335-5](https://doi.org/10.1016/S2213-2600(15)00335-5)
25. Abedi GR, Watson JT, Pham H, Nix WA, Oberste MS, Gerber SI. Enterovirus and human parechovirus surveillance – United States, 2009-2013. *MMWR Morb Mortal Wkly Rep*. 2015;64:940-3. <https://doi.org/10.15585/mmwr.mm6434a3>
26. Abedi GR, Watson JT, Nix WA, Oberste MS, Gerber SI. Enterovirus and parechovirus surveillance – United States, 2014-2016. *MMWR Morb Mortal Wkly Rep*. 2018;67:515-8. <https://doi.org/10.15585/mmwr.mm6718a2>
27. Pons-Salort M, Oberste MS, Pallansch MA, Abedi GR, Takahashi S, Grenfell BT, et al. The seasonality of nonpolio enteroviruses in the United States: patterns and drivers. *Proc Natl Acad Sci U S A*. 2018;115:3078-83. <https://doi.org/10.1073/pnas.1721159115>
28. Messacar K, Robinson CC, Pretty K, Yuan J, Dominguez SR. Surveillance for enterovirus D68 in Colorado children reveals continued circulation. *J Clin Virol*. 2017;92:39-41. <http://dx.doi.org/10.1016/j.jcv.2017.05.009>
29. Naccache S, Bender J, Desai J, Van T, Meyers L, Jones J, et al. Acute flaccid myelitis cases presenting during a spike in respiratory enterovirus D68 circulation: case series from a single pediatric referral center. *Open Forum Infect Dis*. 2017;4(suppl_1):S305-6. <https://doi.org/10.1093/ofid/ofx163.708>
30. Kujawski SA, Midgley CM, Rha B, Lively JY, Nix WA, Curns AT, et al. Enterovirus D68-associated acute respiratory illness – new vaccine surveillance network, United States, July-October, 2017 and 2018. *MMWR Morb Mortal Wkly Rep*. 2019;68:277-80. <https://doi.org/10.15585/mmwr.mm6812a1>
31. Skowronski DM, Chambers C, Sabaiduc S, Murti M, Gustafson R, Pollock S, et al. Systematic community- and hospital-based surveillance for enterovirus-D68 in three Canadian provinces, August to December 2014. *Euro Surveill*. 2015;20:30047. <https://doi.org/10.2807/1560-7917.ES.2015.20.43.30047>
32. Hatayama K, Goto S, Yashiro M, Mori H, Fujimoto T, Hanaoka N, et al. Acute flaccid myelitis associated with enterovirus D68 in a non-epidemic setting. *IDCases*. 2019;17:e00549. <https://doi.org/10.1016/j.idcr.2019.e00549>
33. Knoester M, Helfferich J, Poelman R, Van Leer-Buter C, Brouwer OF, Niesters HGM; 2016 EV-D68 AFM Working Group. Twenty-nine cases of enterovirus-D68-associated acute flaccid myelitis in Europe 2016: a case series and epidemiologic overview. *Pediatr Infect Dis J*. 2019;38:16-21. <https://doi.org/10.1097/INF.0000000000002188>
34. Ruggieri V, Paz MI, Peretti MG, Rugilo C, Bologna R, Freire C, et al. Enterovirus D68 infection in a cluster of children with acute flaccid myelitis, Buenos Aires, Argentina, 2016. *Eur J Paediatr Neurol*. 2017;21:884-90. <http://dx.doi.org/10.1016/j.ejpn.2017.07.008>
35. Pons-Salort M, Grassly NC. Serotype-specific immunity explains the incidence of diseases caused by human enteroviruses. *Science*. 2018;361:800-3. <https://doi.org/10.1126/science.aat6777>
36. Hallowell BD, Parashar UD, Curns A, DeGroot NP, Tate JE. Trends in the laboratory detection of rotavirus before and after implementation of routine rotavirus vaccination – United States, 2000-2018. *MMWR Morb Mortal Wkly Rep*. 2019;68:539-43. <https://doi.org/10.15585/mmwr.mm6824a2>
37. Harrison CJ, Weldon WC, Pahud BA, Jackson MA, Oberste MS, Selvarangan R. Neutralizing antibody against enterovirus D68 in children and adults before 2014 outbreak, Kansas City, Missouri, USA. *Emerg Infect Dis*. 2019;25:585-8. <http://dx.doi.org/10.3201/eid2503.180960>

Address for correspondence: Janell A. Routh, Centers for Disease Control and Prevention, 1600 Clifton Rd NE, Mailstop H24-5, Atlanta, GA 30329-4027, USA; email: iyp1@cdc.gov

Illness Severity in Hospitalized Influenza Patients by Virus Type and Subtype, Spain, 2010–2017

Concepción Delgado-Sanz, Clara Mazagatos-Ateca, Jesús Oliva, Alin Gherasim, Amparo Larrauri

Medscape EDUCATION ACTIVITY

In support of improving patient care, this activity has been planned and implemented by Medscape, LLC and Emerging Infectious Diseases. Medscape, LLC is jointly accredited by the Accreditation Council for Continuing Medical Education (ACCME), the Accreditation Council for Pharmacy Education (ACPE), and the American Nurses Credentialing Center (ANCC), to provide continuing education for the healthcare team.

Medscape, LLC designates this Journal-based CME activity for a maximum of 1.00 **AMA PRA Category 1 Credit(s)**[™]. Physicians should claim only the credit commensurate with the extent of their participation in the activity.

Successful completion of this CME activity, which includes participation in the evaluation component, enables the participant to earn up to 1.0 MOC points in the American Board of Internal Medicine's (ABIM) Maintenance of Certification (MOC) program. Participants will earn MOC points equivalent to the amount of CME credits claimed for the activity. It is the CME activity provider's responsibility to submit participant completion information to ACCME for the purpose of granting ABIM MOC credit.

All other clinicians completing this activity will be issued a certificate of participation. To participate in this journal CME activity: (1) review the learning objectives and author disclosures; (2) study the education content; (3) take the post-test with a 75% minimum passing score and complete the evaluation at <http://www.medscape.org/journal/eid>; and (4) view/print certificate. For CME questions, see page 400.

Release date: January 16, 2020; Expiration date: January 16, 2021

Learning Objectives

Upon completion of this activity, participants will be able to:

- Compare clinical characteristics and epidemiology among SHCIC caused by different virus types and subtypes in Spain from 2010 to 2017, according to a retrospective cohort study
- Compare outcomes among SHCIC caused by different virus types and subtypes in Spain from 2010 to 2017, according to a retrospective cohort study
- Describe clinical implications of findings regarding SHCIC caused by different virus types and subtypes in Spain from 2010 to 2017, according to a retrospective cohort study

CME Editor

Jude Rutledge, BA, Technical Writer/Editor, Emerging Infectious Diseases. *Disclosure: Jude Rutledge has disclosed no relevant financial relationships.*

CME Author

Laurie Barclay, MD, freelance writer and reviewer, Medscape, LLC. *Disclosure: Laurie Barclay, MD, has disclosed no relevant financial relationships.*

Authors

Disclosures: Concepción Delgado-Sanz, MD, MPH; Clara Mazagatos-Ateca, MSc; Jesús Oliva Dominguez, MD, PhD; Alin Manuel Gherasim, MD; and Amparo Larrauri, MPharm, PhD, have disclosed no relevant financial relationships.

Author affiliations: European Centre for Disease Prevention and Control, Stockholm, Sweden (C. Delgado-Sanz); Institute of Health Carlos III, Madrid, Spain (C. Delgado-Sanz, C. Mazagatos-Ateca, J. Oliva, A. Gherasim, A. Larrauri); CIBER Epidemiología y

Salud Pública, Madrid (C. Delgado-Sanz, C. Mazagatos-Ateca, J. Oliva, A. Gherasim, A. Larrauri)

DOI: <https://doi.org/10.3201/eid2602.181732>

We conducted a retrospective cohort study to assess the effect of influenza virus type and subtype on disease severity among hospitalized influenza patients in Spain. We analyzed the cases of 8,985 laboratory-confirmed case-patients hospitalized for severe influenza by using data from a national surveillance system for the period 2010–2017. Hospitalized patients with influenza A(H1N1)pdm09 virus were significantly younger, more frequently had class III obesity, and had a higher risk for pneumonia or acute respiratory distress syndrome than patients infected with influenza A(H3N2) or B ($p < 0.05$). Hospitalized patients with influenza A(H1N1)pdm09 also had a higher risk for intensive care unit admission, death, or both than patients with influenza A(H3N2) or B, independent of other factors. Determining the patterns of influenza-associated severity and how they might differ by virus type and subtype can help guide planning and implementation of adequate control and preventive measures during influenza epidemics.

During the 2009 influenza pandemic, influenza surveillance activities were intensified in Spain (1). In accordance with international recommendations (2), Spain established surveillance of Severe Hospitalized Confirmed Influenza Case-patients (SHCIC) to monitor the evolution of severe influenza during pandemics and inter-pandemic influenza.

In the years since the 2009 influenza pandemic, SHCIC surveillance has become a consolidated severe influenza surveillance system that operates within the Spanish Influenza Surveillance System (3; Appendix, <https://wwwnc.cdc.gov/EID/article/26/2/18-1732-App1.pdf>). The system provides a standardized tool to monitor risk factors associated with severe influenza, identify influenza viruses associated with severe clinical manifestations, and monitor the disease burden of influenza epidemics. Sentinel hospitals belonging to the public health system of all 19 regions of Spain are involved in SHCIC surveillance (3).

The association of certain influenza virus types and subtypes with disease severity has been a major topic of influenza research in recent years (4–10). However, after the 2009 pandemic, findings on the severity of epidemics by type and subtype of influenza virus have varied widely. Some studies have reported no statistically significant differences in case-fatality rates and other markers of severity by type and subtype of influenza infections (4) and have shown that the risk for serious outcomes was not increased in hospitalized influenza patients infected with influenza A(H1N1)pdm09 (pH1N1) compared with seasonal influenza B viruses (5,6). In contrast, other authors have indicated that, in hospitalized influenza patients, pH1N1

infection is more clinically severe than influenza A(H3N2) or B infection (7–10).

SHCIC surveillance provides a reliable platform to monitor different influenza viruses associated with severe disease. By using the framework of this surveillance system, we aimed to explore disease severity of hospitalized influenza patients in Spain according to influenza virus type and subtype during the 7 influenza seasons that followed the 2009 pandemic.

Material and Methods

We conducted a retrospective cohort study by using SHCIC surveillance data obtained across the 7 postpandemic influenza seasons (2010–11 through 2016–17). The SHCIC surveillance system is a passive, hospital-based surveillance system that includes 90–181 reporting hospitals during the study period; these hospitals are located throughout Spain and serve 45%–60% of the population of Spain, depending on the influenza season.

Each influenza season was defined as lasting from week 40 of the first year to week 20 of the following year. As part of the surveillance, clinicians in the participating hospitals were advised to swab any person with clinical suspicion of influenza-like illness (without specific case definition) and who required hospital admission to any hospital ward. A severe hospitalized confirmed influenza case-patient was defined as any person with a clinical profile compatible with influenza-like illness who had laboratory confirmation of influenza infection (Appendix) and who was hospitalized according to ≥ 1 of the following clinical criteria: pneumonia, acute respiratory distress syndrome (ARDS), multiple organ dysfunction syndrome (MODS), septic shock, or admission to an intensive care unit (ICU). The case-patient definition was unchanged throughout the study period.

Variables collected for surveillance purposes included demographic characteristics (age and sex), dates of symptom onset and hospitalization, virus type and subtype, presence of underlying medical conditions (any chronic respiratory, cardiovascular, renal or liver disease, class III obesity, diabetes mellitus, or immunosuppression), complications (pneumonia, any laboratory-confirmed viral or bacterial coinfection, ARDS, or MODS), antiviral treatment, time from symptom onset to start of antiviral treatment, influenza vaccination status, date of vaccination, admission to ICU, outcome (alive or dead), region, and influenza season. Class III obesity was defined as a body mass index ≥ 40 kg/m². We obtained vaccination status by using clinical history and vaccination registries. We considered a patient to be correctly

vaccinated if she or he received the vaccine ≥ 15 days before symptom onset.

We calculated the percentage of patients with a specific condition by using the number of patients with available information regarding the condition. Our analysis excluded patients whose influenza A subtype was unknown. We calculated the percentage of pregnant women by using all women of childbearing age (15–49 years of age) as the denominator.

We used univariate multinomial logistic regression models to compare demographic and clinical characteristics across virus types and subtypes, including as a dependent variable the influenza virus type and subtype, with pH1N1 used as reference, and as independent variables each of the characteristics of interest. We measured the effect of each predictor in the model as a relative risk ratio (RRR). We also conducted univariate logistic regression models to estimate the odds ratios (ORs) and 95% confidence intervals for the risk for clinical complications or death, considering influenza virus type and subtype to be an explanatory variable and using influenza pH1N1 as reference. We compared patients infected with influenza A(H3N2) or B against patients infected with pH1N1.

In addition, we applied multivariable logistic regression models, stratified by age group, to explore the effect of influenza virus type and subtype as an independent factor for the following severe outcomes: ICU admission, death, or both, using pH1N1 as reference. We adjusted all of these models for potential confounding such as sex, age, influenza season, underlying medical conditions, pneumonia, antiviral treatment, and receipt of seasonal trivalent influenza vaccine.

For all statistical analyses, we considered 2-sided *p* values < 0.05 to be statistically significant.

We performed the analyses by using Stata 14.0 (<https://www.stata.com>)

This study was conducted within the framework of ongoing SHCIC surveillance by the Institute of Health Carlos III, National Epidemiology Centre. A formal ethics review was not required because the study was part of the routine surveillance activities in Spain. However, we collected anonymized data and obtained verbal consent from all patients before they were swabbed for surveillance purposes.

Results

During September 2010–May 2017, a total of 12,942 case-patients were reported in Spain. We included 8,985 patients with complete influenza virus type and subtype information in our study; 4,568 (51%) were infected with pH1N1, 3,091 (34%) with influenza A(H3N2), and 1,326 (15%) with influenza B.

SHCIC surveillance indicated week-by-week patterns that matched the epidemiologic patterns for influenza in the community based on the sentinel system for primary care. The identified influenza virus types and subtypes among case-patients were consistent with the type and subtype of influenza virus circulating within the general population (Figure 1). pH1N1 was the dominant subtype among case-patients during the 2010–11, 2013–14, and 2015–16 seasons; influenza A(H3N2) during the 2011–12, 2014–15, and 2016–17 seasons; and influenza B during the 2012–13 season. Also, we noted a substantial contribution from influenza B infections during the influenza A(H3N2)-dominant 2014–15 season and after the peak of the pH1N1-dominant 2015–16 influenza season (Figure 1).

The distribution of case-patients by age group varied according to the circulating virus type and

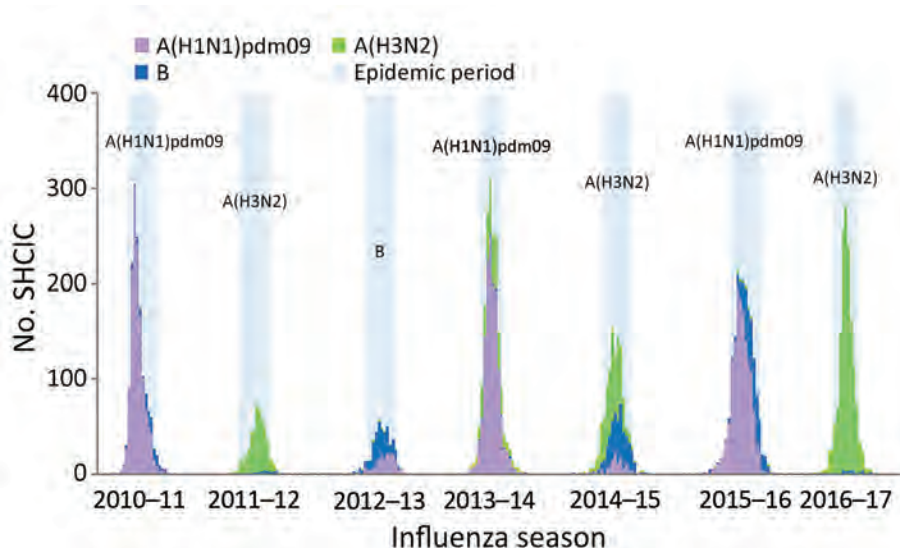


Figure 1. Number of patients hospitalized for laboratory-confirmed severe influenza, by influenza virus type or subtype and week of hospital admission, Spain, influenza seasons 2010–11 to 2016–17. Seasonal epidemic periods are labeled with dominant circulating virus.

subtype in each influenza season (Figure 2). In seasons with dominant pH1N1 circulation (Figure 2, panels A, C, and F), most patients (52%) were persons 15–64 years of age. Patients ≥ 65 years of age accounted for 65% of case-patients in those seasons with dominant influenza A(H3N2) circulation (Figure 2, panels B, E, and G); however, during the 2011–12 season, a relatively high percentage (33%) of case-patients were children. In the 2012–13 season, 54% of case-patients 15–64 years of age were infected with pH1N1, whereas 89% of case-patients 5–14 years of age were infected with influenza B (Figure 2, panel C). In general, case-patients infected with pH1N1 were significantly younger (median age 53 years [interquartile range (IQR) 37–66 years]) than those infected with influenza A(H3N2) (median age 73 years [IQR 56–83 years]) and influenza B (median age 60 years [22–74 years]) ($p < 0.001$).

Regarding the clinical characteristics, case-patients infected with influenza A(H3N2) or B virus were more likely to have ≥ 1 underlying medical conditions compared with those with pH1N1 infection (crude RRR [cRRR] 2.81 [95% CI 2.45–3.22] for influenza A[H3N2]-infected patients and cRRR 1.32 [95% CI 1.13–1.55] for influenza B-infected patients) (Table 1). This pattern also was observed for chronic respiratory, cardiovascular, and renal diseases. However, immunosuppression was less likely among influenza A(H3N2)-infected patients than pH1N1-infected patients (cRRR 0.72 [95% CI 0.63–0.84]). Class III obesity was less frequent among influenza A(H3N2)-infected patients (cRRR 0.66 [95% CI 0.55–0.78]) and influenza B-infected patients (cRRR 0.59 [95% CI 0.46–0.75]) than among pH1N1-infected patients. Among women 15–49 years of age, fewer pregnancies were observed among influenza A(H3N2)-infected patients

than pH1N1-infected patients (cRRR 0.33 [95% CI 0.17–0.64]). Patients infected with influenza A(H3N2) or B virus were less likely to receive antiviral treatment than those infected with pH1N1 (cRRR 0.48 [95% CI 0.42–0.54] for influenza A[H3N2]-infected patients and cRRR 0.30 [95% CI 0.26–0.34] for influenza B-virus infected patients) (Table 1). The median days from symptom onset to hospitalization was longer among pH1N1-infected patients (4 days [IQR 2–6 days]) than for influenza A(H3N2)-infected patients (3 days [IQR 1–5 days]) ($p < 0.001$).

The analysis of clinical complications and outcome revealed that patients with influenza A(H3N2) and B virus infection had lower risk for pneumonia (crude OR [cOR] 0.68 [95% CI 0.61–0.76] for influenza A[H3N2]-infected patients and cOR 0.77 [95% CI 0.67–0.89] for influenza B-virus infected patients), ARDS (cOR 0.69 [95% CI 0.61–0.77] for influenza A[H3N2]-infected patients and cOR 0.73 [95% CI 0.63–0.85] for influenza B-virus infected patients), and ICU admission (cOR 0.55 [95% CI 0.50–0.61] for influenza A[H3N2]-infected patients and cOR 0.64 [95% CI 0.56–0.73] for influenza B-virus infected patients) compared with patients with pH1N1 infection (Table 2). However, patients infected with influenza A(H3N2) or B had a higher risk for co-infection (cOR 1.23 [95% CI 1.09–1.38] for influenza A[H3N2]-infected patients and cOR 1.43 [95% CI 1.22–1.67] for influenza B-virus infected patients). The case-fatality rate was significantly higher among influenza A(H3N2)-infected patients (cOR 1.25 [95% CI 1.10–1.43]) than for pH1N1-infected patients. The risk for death was significantly lower for those patients infected with influenza B (cOR 0.76 [95% CI 0.62–0.93] for patients hospitalized and cOR 0.73 [95% CI 0.55–0.97] for those admitted to ICU) than patients with pH1N1 infection.

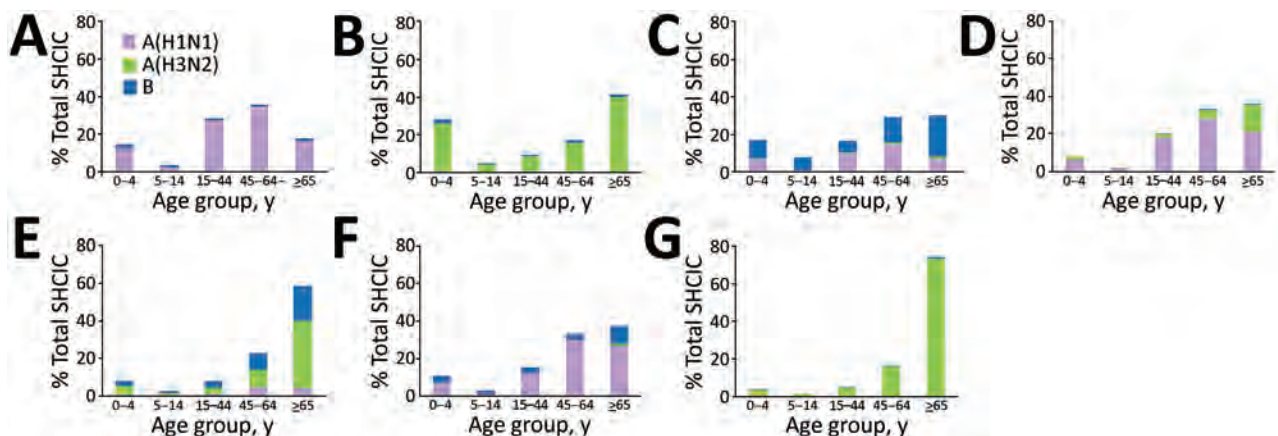


Figure 2. Number of patients hospitalized for laboratory-confirmed severe influenza, by influenza virus type or subtype and age group, Spain, influenza seasons 2010–11 to 2016–17. A) 2010–11 season. B) 2011–12 season. C) 2012–13 season. D) 2013–14 season. E) 2014–15 season. F) 2015–16 season. G) 2016–17 season.

Table 1. Demographic and clinical characteristics of patients hospitalized for laboratory-confirmed severe influenza, by influenza virus type or subtype, Spain, influenza seasons 2010–11 to 2016–17*

Characteristic	Influenza virus type or subtype				
	pH1N1		A(H3N2)		B
	No. (%)	No. (%)	Crude RRR† (95% CI)	No. (%)	Crude RRR‡ (95% CI)
Total no. patients	4,568 (100)	3,091 (100)	NA	1,326 (100)	NA
Age group, y					
<15	566 (12)	333 (11)	Referent	318 (24)	Referent
15–64	2,767 (61)	716 (23)	0.44 (0.38–0.52)	437 (33)	0.28 (0.24–0.33)
≥65	1,231 (27)	2,035 (66)	2.81 (2.41–3.27)	567 (43)	0.82 (0.69–0.97)
Missing data	4 (0.1)	7 (0.2)	NA	4 (0.3)	NA
Sex					
M	2,589 (57)	1,637 (53)	0.86 (0.78–0.94)	736 (56)	0.96 (0.85–1.08)
F	1,977 (43)	1,453 (47)	Referent	588 (44)	Referent
Missing data	2 (0.1)	1 (0.1)	NA	2 (0.2)	NA
Underlying medical condition§	2,334 (68)	2,055 (86)	2.81 (2.45–3.22)	754 (74)	1.32 (1.13–1.55)
Missing data	1,161 (25)	700 (23)	NA	310 (23)	NA
Class III obesity (BMI ≥40 kg/m ²)	447 (12)	205 (8)	0.66 (0.55–0.78)	80 (7)	0.59 (0.46–0.75)
Chronic respiratory diseases	686 (22)	680 (30)	1.53 (1.35–1.73)	238 (25)	1.20 (1.01–1.42)
Chronic cardiovascular diseases	800 (21)	1,051 (40)	2.49 (2.23–2.78)	308 (28)	1.45 (1.24–1.69)
Diabetes mellitus	696 (18)	755 (29)	1.81 (1.61–2.04)	225 (20)	1.15 (0.97–1.36)
Renal diseases	335 (9)	394 (15)	1.87 (1.60–2.18)	132 (12)	1.42 (1.14–1.75)
Chronic liver disease	212 (6)	147 (6)	1.02 (0.82–1.26)	58 (5)	0.94 (0.70–1.27)
Immunosuppression	632 (17)	327 (13)	0.72 (0.63–0.84)	170 (16)	0.92 (0.77–1.11)
Pregnancy¶	125 (24)	11 (10)	0.33 (0.17–0.64)	18 (24)	0.98 (0.56–1.73)
Missing data	134 (20)	30 (21)	NA	19 (20)	NA
Antiviral treatment	3,787 (86)	2,241 (75)	0.48 (0.42–0.54)	800 (64)	0.30 (0.26–0.34)
Missing data	165 (4)	86 (3)	NA	86 (6)	NA
Oseltamivir	3,709 (99.3)	2,209 (99.7)	NA	777 (99.4)	NA
Zanamivir	16 (0.4)	3 (0.1)	NA	4 (0.5)	NA
Other	11 (0.3)	5 (0.2)	NA	1 (0.1)	NA
Seasonal trivalent influenza vaccine	514 (14)	862 (36)	3.45 (3.05–3.91)	261 (27)	2.18 (1.84–2.58)
Missing data	961 (21)	727 (24)	NA	345 (26)	NA

*BMI, body mass index; RRR, relative risk ratio; NA, not applicable.

†Influenza A(H3N2) compared with pH1N1 (reference).

‡Influenza B compared with pH1N1 (reference).

§Underlying medical conditions defined as ≥1 of the following: class III obesity (BMI ≥40 kg/m²), chronic respiratory diseases, chronic cardiovascular diseases, diabetes mellitus, renal diseases, chronic liver disease, or immunosuppression.

¶Pregnancy among women of childbearing age (15–49 years).

We used a multivariable logistic regression analysis to explore the effect of influenza virus type and subtype on the severity of outcomes, such as ICU admission, death, or ICU admission and death, according to age group (Appendix Table 1). Case-patients >15 years of age who had influenza A(H3N2) or B infection showed less risk for death or ICU admission than patients infected with pH1N1, independent of other risk factors (Appendix Table 1). The pattern for all case-patient age groups combined was similar. When we compared pH1N1-infected patients with the other 2 patient groups, we observed significant differences in risk for ICU admission among influenza A(H3N2)-infected patients (adjusted OR [aOR] 0.56 [95% CI 0.44–0.71]) and influenza B-infected patients (aOR 0.51 [95% CI 0.41–0.63]); risk for death among influenza A(H3N2)-infected patients (aOR 0.56 [95% CI 0.40–0.77]) and influenza B-infected patients (aOR 0.38 [95% CI 0.26–0.54]); and risk for ICU admission and death among influenza A(H3N2)-infected patients (aOR 0.59 [95% CI 0.47–0.73]) and for

influenza B-infected patients (aOR 0.50 [95% CI 0.44–0.62]). However, among children <15 years of age, we observed no significant differences in the severity of outcome by virus type and subtype. In addition, we observed no difference in the risk for ICU admission between different influenza A subtypes among patients ≥65 years of age (Appendix Table 1).

Discussion

Our findings show that SHCIC surveillance has provided valuable information on disease severity by influenza virus type and subtype since the 2009 pandemic. We found that case-patients infected with pH1N1 were significantly younger than those infected with influenza A(H3N2) or B and had a higher risk for clinical complications and severe outcomes, such as ICU admission, death, or both compared with case-patients with influenza A(H3N2) or B virus infections.

During the 2011–12 and 2012–13 seasons, an unexpectedly low number of case-patients were reported compared with previous seasons. Similar

Table 2. Clinical complications and final outcomes of patients hospitalized for laboratory-confirmed severe influenza, by influenza virus type or subtype, Spain, influenza seasons 2010–11 to 2016–17*

Complication and outcome	Influenza virus type or subtype				
	pH1N1	A(H3N2)		B	
	No. (%)	No. (%)	Crude OR† (95% CI)	No. (%)	Crude OR‡ (95% CI)
Total no. patients	4,568 (100)	3,091 (100)	NA	1,326 (100)	NA
Pneumonia	3,529 (78)	2,154 (71)	0.68 (0.61–0.76)	951 (74)	0.77 (0.67–0.89)
Missing data	71 (2)	69 (2)	NA	36 (3)	NA
Co-infection	903 (26)	680 (31)	1.23 (1.09–1.38)	320 (34)	1.43 (1.22–1.67)
Missing data	1,153 (25)	873 (28)	NA	383 (29)	NA
ARDS	1,220 (29)	571 (22)	0.69 (0.61–0.77)	271 (23)	0.73 (0.63–0.85)
Missing data	405 (9)	528 (17)	NA	160 (12)	NA
MODS	405 (10)	236 (9)	0.94 (0.79–1.11)	107 (9)	0.94 (0.75–1.17)
Missing data	467 (10)	559 (18)	NA	177 (13)	NA
ICU admission	1,787 (41)	820 (28)	0.55 (0.50–0.61)	389 (31)	0.64 (0.56–0.73)
Missing data	245 (5)	146 (5)	NA	77 (6)	NA
Case-fatality rate					
Deaths in hospitalized patients	585 (14)	493 (16)	1.25 (1.10–1.43)	130 (11)	0.76 (0.62–0.93)
Deaths in ICU patients	405 (24)	180 (23)	0.90 (0.74–1.11)	68 (19)	0.73 (0.55–0.97)
Missing data	254 (6)	89 (3)	NA	109 (8)	NA

*ARDS, acute respiratory distress syndrome; ICU, intensive care unit; MODS, multiple organ dysfunction syndrome; NA, not applicable; OR, odds ratio.

†OR of influenza A(H3N2) compared with pH1N1 (reference).

‡OR of influenza B compared with pH1N1 (reference).

observations were reported during the 2011–12 influenza season in the United States (11) and France (8), where influenza A(H3N2) was also the predominant virus and caused excess mortality in the elderly (12–14). Given that the definition of case-patient was established in a season with almost exclusively pH1N1 circulation, the figures for the first postpandemic season with dominant influenza A(H3N2) virus might have been affected by lower definition sensitivity for identifying case-patients infected with other influenza types and subtypes. In addition, according to 2 international cohort studies conducted during 2009–2015 (15), outpatients with influenza A(H3N2) virus infection were less likely to be hospitalized than those infected with pH1N1 or influenza B virus, which might have influenced the numbers reported. Another aspect that could influence the higher number of pH1N1 infections recorded compared with other subtypes is the wider availability of the PCR assay for this virus subtype since the 2009 pandemic in all the laboratories of the hospitals participating in SHCIC surveillance.

Our results are similar to those from previous studies, which found that hospitalized influenza pH1N1-infected patients were younger than those infected with influenza A(H3N2) or B (15). Also, in the United States, a higher proportion of pH1N1 infections occurred in adults 15–64 years of age compared with influenza A(H3N2) and B infections (7). Several observations could be consistent with the differences on age by influenza virus type and subtype found in this study and others. The different susceptibility of each birth cohort is based on the likelihood that their influenza primary infections were with group 1 or 2

hemagglutinin. Individuals born before 1956 likely had their first infection with a group 1 virus and had preexisting cross-reactive antibodies against viruses of the same group as pH1N1 virus, whereas those born in 1968 or later appear protected against severe influenza A(H3N2) infection (16–18). Moreover, seasonal influenza A(H1N1) virus that circulated before 2009 provided some additional cross-reactive immunity protection in older patients against the newer pH1N1 virus (17,18). The younger patients, who have less exposure to this older seasonal influenza A(H1N1) virus, might have experienced more severe disease as a result of direct infection by pH1N1 and the resulting cytokine-induced inflammatory responses, an immune-mediated pathologic process which is believed to play an important role in the onset of severe disease (19–21).

In our study, case-patients infected with influenza A(H3N2) or B viruses were more likely to have underlying medical conditions than those infected with pH1N1. This observation is partly in line with findings from the aforementioned international cohort study (15) and could be consistent with the age difference between influenza virus type and subtype. However, when we stratified the analysis by age, the differences between those pH1N1-infected patients compared with influenza A(H3N2) and B remained significant, regardless of age (Appendix Tables 2–4). In contrast, a study in Argentina reported that the prevalence of underlying medical conditions did not differ between hospitalized patients with influenza A(H3N2) or pH1N1 infection (10).

We found that morbid obesity was more common among case-patients infected with pH1N1. This result

accords with a higher prevalence of obesity (18.2%) found by another study in hospitalized patients with pH1N1 infection compared with patients with influenza A(H3N2) or B infection (<10%) (7). Obesity was first identified as a novel independent risk factor for influenza severity in hospitalized adults during the 2009 pandemic in California (USA) (22). Furthermore, another study found a stronger association between obesity and ICU admission and death for pH1N1 infections (23).

Our results indicate that the likelihood of pneumonia was higher among patients with pH1N1 than patients with influenza A(H3N2) or B infections. However, patients with influenza A(H3N2) or B infections had a higher risk for bacterial or viral coinfection. Although our study lacks information on other clinical features or radiologic findings, the results seem to be in line with previous studies. A US study found that adults with pH1N1 infection had an increased risk for radiographically confirmed pneumonia compared with those with influenza A(H3N2) infection (24). A study in Japan showed that hospitalized patients with pH1N1 virus had primary viral pneumonia more frequently and had mixed bacterial or secondary bacterial pneumonia less frequently compared with patients with influenza A(H3N2) or B virus infections (25). Another study, conducted during the first postpandemic influenza season, showed that patients with pH1N1 pneumonia had similar clinical characteristics but slightly higher disease severity and stronger systemic inflammatory response than patients with influenza A(H3N2) pneumonia (26). In addition, in our study, ARDS occurred more frequently in patients infected with pH1N1 than those infected with influenza A(H3N2) or B viruses, which accords with previous reports from other countries (7,8).

Treatment with antiviral drugs was significantly less common in patients with influenza A(H3N2) or B infections than in patients with pH1N1 infection, regardless of age (Appendix Tables 2–4). We were unable to explain these data because antiviral treatment is recommended for everyone hospitalized with influenza in Spain (27), and the virus type and subtype should not have influenced treatment decisions (28).

Our results indicate that patients with influenza A(H3N2) or B infections were less likely to be admitted to an ICU, die, or both than were those with pH1N1 infections, after controlling for potential confounders. These findings are in agreement with other studies of disease severity by influenza virus type and subtype, which report higher ORs for ICU admission for pH1N1-infected patients (7,9,10,29).

The aforementioned international cohort study showed similar results to our own study for every age group except persons >65 years of age, for which they found higher hospitalization rates for outpatients infected with influenza B (15). In contrast, a study in South Africa showed no association between virus type and subtype and ICU admission or death (4). Other studies did not find differences in patient mortality between influenza A virus subtypes (10), or between other types or subtypes (8,25). In our study, we did not find differences in the risk for ICU admission by influenza A subtype in patients <65 years of age.

We should distinguish at this point the clinical seriousness caused by different influenza virus types and subtypes, as observed in severe influenza surveillance systems, from those results on the effect of influenza on population mortality rates obtained from population-based studies that use regression models. As previously reported, influenza A(H3N2)-dominant epidemics have a considerable impact on mortality, with highest excess mortality attributable to influenza occurring mainly in older adults (12–14,30,31). In addition, a study suggests that influenza B might also be more of a concern in terms of excess mortality in the influenza season 2017–18 (32). However, many of these deaths might have occurred in older persons who have a cascade of illness after an influenza infection, and influenza in older patients might not have a typical clinical profile. Moreover, many older patients might die at home or in managed care facilities and might not get to a hospital. The increase in deaths associated with influenza A(H3N2) at the population level might reflect greater population susceptibility or reduced vaccine effectiveness against influenza A(H3N2) that has become apparent in recent years (33), although it might not reflect the relative clinical seriousness of the individual infection. Therefore, our finding that pH1N1 infections caused a higher clinical seriousness in hospitalized patients than influenza A(H3N2) or B infections is fully congruent with the greater effect on the population mortality caused by influenza A(H3N2) seasons (12–14,30,31).

This study has several limitations. First, we cannot exclude a possible bias that results from using hospitalized case-based surveillance systems with many reporting sites that might have had different testing practices and might also have varied by season. However, because of the high percentage of the national population included in the SHCIC surveillance, the results obtained should be highly representative of the entire country. During the last 4 seasons, a relatively high proportion of influenza A

infections were not subtyped, probably because of the implementation of rapid tests for influenza confirmation. Influenza testing could also have been biased depending on age, severity of symptoms, changes in swabbing practices in the last few seasons, or even as a result of the selection of patients for swabbing based on physician-suspected influenza; however, these factors should not have influenced the virus type and subtype recorded. The multivariable analysis has been controlled for bias by season to avoid potential biases related to the inclusion of several seasons in the study (i.e., differing dominant influenza virus types and subtypes and their antigenic drifts and shifts, influenza vaccine uptake, and seasonal variations in match the vaccine to the circulating influenza strains could all complicate comparisons between seasons). However, a real strength of this study is its representativeness; it enrolled patients from hospitals throughout Spain and across every age group, it covered every influenza season since SHCIC surveillance began in 2009, and it benefited from substantial virus co-circulation and a large sample size.

In conclusion, our findings suggest that hospitalized patients infected with pH1N1 virus had a higher risk for ICU admission, death, or both than patients infected with influenza A(H3N2) or B infections, despite being younger and having fewer underlying medical conditions. Therefore, in those seasons with considerable circulation of pH1N1, more admissions to hospital ICUs should be expected, especially among hospitalized young adult patients. To decrease treatment delays, antiviral treatment should be started shortly after admission to hospital when influenza is suspected. These observations could be of crucial importance when planning resource deployment during influenza epidemics. Understanding the patterns of disease severity associated with influenza and how these patterns might differ among virus types and subtypes can help guide public health measures to control influenza. This knowledge can help in directing resource allocation in the healthcare system during each influenza season and thus can ensure an effective response to pressures on ICUs, especially during pH1N1 epidemics.

Acknowledgments

We thank members of the Spanish Influenza Surveillance System for their contribution to this work: Virtudes Gallardo, José María Navarro, Miriam García, Ana María Martínez, Ismael Huertas, Santiago Melón, Jaume Giménez, Joana M. Vanrell, Jordi Reina, Carmen Pérez, Luis Viloria, Mónica Gozalo, Sonia Humanes, María Victoria García, Tomás Vega, Socorro Fernández, Gregoria

Megias, Raúl Ortiz de Lejarazu, Iván Sanz, Silvia Rojo, Nuria Torner, María de los Ángeles Marcos, Javier Roig, Julián Mauro Ramos, María Jesús Purriños, Juan García Costa, Sonia Pérez-Castro, Luis García-Comas, Juan Carlos Galán, Ana García-Fulgueira, Antonio Moreno, Jesús Castilla, Mirian Fernández-Alonso, Carmen Ezpeleta, Fernando González-Carril, Gustavo Cilla, Eva Martínez-Ochoa, Carmen Quiñones, Miriam Blasco, Ana Rivas Daniel Castrillejo, Francisco Pozo, and Inmaculada Casas. We are also grateful to Christian Winter for his critical review of the manuscript.

The opinions expressed by authors contributing to this journal article do not necessarily reflect the opinions of the Institute of Health Carlos III or the institutions with which the authors are affiliated.

About the Author

Dr. Delgado-Sanz is medical epidemiologist at the National Centre of Epidemiology of the Carlos III Health Institute, Madrid, Spain. Her research interests focus on severity, impact, and disease burden of influenza virus.

References

1. Larrauri Cámara A, Jiménez-Jorge S, Mateo Ontañón S, Pozo Sánchez F, Ledesma Moreno J, Casas Flecha I; Spanish Influenza Surveillance System (SISS). Epidemiology of the 2009 influenza pandemic in Spain. *Enferm Infecc Microbiol Clin*. 2012;30(Suppl 4):2-9. [https://doi.org/10.1016/S0213-005X\(12\)70098-8](https://doi.org/10.1016/S0213-005X(12)70098-8)
2. World Health Organization. Report of the Review Committee on the Functioning of the International Health Regulations (2005) in relation to pandemic (H1N1) 2009 [cited 2018 Oct 10]. <https://apps.who.int/iris/handle/10665/3350>
3. Oliva J, Delgado-Sanz C, Larrauri A; Spanish Influenza Surveillance System. Estimating the burden of seasonal influenza in Spain from surveillance of mild and severe influenza disease, 2010-2016. *Influenza Other Respir Viruses*. 2018;12:161-70. <https://doi.org/10.1111/irv.12499>
4. Cohen AL, Hellferscee O, Pretorius M, Treurnicht F, Walaza S, Madhi S, et al. Epidemiology of influenza virus types and subtypes in South Africa, 2009-2012. *Emerg Infect Dis*. 2014;20:1162-9. <https://doi.org/10.3201/eid2007.131869>
5. Gutiérrez-Pizarra A, Pérez-Romero P, Alvarez R, Aydiillo TA, Osorio-Gómez G, Milara-Ibáñez C, et al. Unexpected severity of cases of influenza B infection in patients that required hospitalization during the first post-pandemic wave. *J Infect*. 2012;65:423-30. <https://doi.org/10.1016/j.jinf.2012.07.004>
6. Gubbels S, Krause TG, Bragstad K, Perner A, Mølbak K, Glismann S. Burden and characteristics of influenza A and B in Danish intensive care units during the 2009/10 and 2010/11 influenza seasons. *Epidemiol Infect*. 2013;141:767-75. <https://doi.org/10.1017/S0950268812001471>
7. Chaves SS, Aragon D, Bennett N, Cooper T, D'Mello T, Farley M, et al. Patients hospitalized with laboratory-confirmed influenza during the 2010-2011 influenza season: exploring disease severity by virus type and subtype.

- J Infect Dis. 2013;208:1305–14. <https://doi.org/10.1093/infdis/jit316>
8. Bonmarin I, Belchior E, Bergounioux J, Brun-Buisson C, Mégarbane B, Chappert JL, et al. Intensive care unit surveillance of influenza infection in France: the 2009/10 pandemic and the three subsequent seasons. *Euro Surveill*. 2015;20:30066. <https://doi.org/10.2807/1560-7917.ES.2015.20.46.30066>
 9. Boddington NL, Verlander NQ, Pebody RG. Developing a system to estimate the severity of influenza infection in England: findings from a hospital-based surveillance system between 2010/2011 and 2014/2015. *Epidemiol Infect*. 2017;145:1461–70. <https://doi.org/10.1017/S095026881700005X>
 10. Kuszniarz G, Carolina C, Manuel RJ, Sergio L, Lucila O, Julio B, et al. Impact of influenza in the post-pandemic phase: clinical features in hospitalized patients with influenza A (H1N1) pdm09 and H3N2 viruses, during 2013 in Santa Fe, Argentina. *J Med Virol*. 2017;89:1186–91. <https://doi.org/10.1002/jmv.24758>
 11. Centers for Disease Control and Prevention (CDC). Update: influenza activity – United States, 2011–12 season and composition of the 2012–13 influenza vaccine. *MMWR Morb Mortal Wkly Rep*. 2012;61:414–20.
 12. León-Gómez I, Delgado-Sanz C, Jiménez-Jorge S, Flores V, Simón F, Gómez-Barroso D, et al. Excess mortality associated with influenza in Spain in winter 2012 [in Spanish]. *Gac Sanit*. 2015;29:258–65.
 13. Mazick A, Gergonne B, Nielsen J, Wuillaume F, Virtanen MJ, Fouillet A, et al. Excess mortality among the elderly in 12 European countries, February and March 2012. *Euro Surveill*. 2012;17:20138.
 14. Mølbak K, Espenhain L, Nielsen J, Tersago K, Bossuyt N, Denissov G, et al. Excess mortality among the elderly in European countries, December 2014 to February 2015. *Euro Surveill*. 2015;20:21065. <https://doi.org/10.2807/1560-7917.ES2015.20.11.21065>
 15. Dwyer DE, Lynfield R, Losso MH, Davey RT, Cozzi-Lepri A, Wentworth D, et al.; INSIGHT Influenza Study Group. Comparison of the outcomes of individuals with medically attended influenza A and B virus infections enrolled in 2 international cohort studies over a 6-year period: 2009–2015. *Open Forum Infect Dis*. 2017;4:ofx212. <https://doi.org/10.1093/ofid/ofx212>
 16. Viboud C, Epstein SL. First flu is forever. *Science*. 2016; 354:706–7. <https://doi.org/10.1126/science.aak9816>
 17. Hancock K, Veguilla V, Lu X, Zhong W, Butler EN, Sun H, et al. Cross-reactive antibody responses to the 2009 pandemic H1N1 influenza virus. *N Engl J Med*. 2009;361:1945–52. <https://doi.org/10.1056/NEJMoa0906453>
 18. Goh EH, Jiang L, Hsu JP, Tan LWL, Lim WY, Phoon MC, et al. Epidemiology and relative severity of influenza subtypes in Singapore in the post-pandemic period from 2009 to 2010. *Clin Infect Dis*. 2017;65:1905–13. <https://doi.org/10.1093/cid/cix694>
 19. Lee CK, Lee HK, Loh TP, Lai FY, Tambyah PA, Chiu L, et al. Comparison of pandemic (H1N1) 2009 and seasonal influenza viral loads, Singapore. *Emerg Infect Dis*. 2011;17:287–91. <https://doi.org/10.3201/eid1702.100282>
 20. Bermejo-Martin JF, Martin-Loeches I, Rello J, Antón A, Almansa R, Xu L, et al. Host adaptive immunity deficiency in severe pandemic influenza. *Crit Care*. 2010;14:R167. <https://doi.org/10.1186/cc9259>
 21. Paquette SG, Banner D, Zhao Z, Fang Y, Huang SS, León AJ, et al. Interleukin-6 is a potential biomarker for severe pandemic H1N1 influenza A infection. *PLoS One*. 2012; 7:e38214. <https://doi.org/10.1371/journal.pone.0038214>
 22. Louie JK, Acosta M, Samuel MC, Schechter R, Vugia DJ, Harriman K, et al.; California Pandemic (H1N1) Working Group. A novel risk factor for a novel virus: obesity and 2009 pandemic influenza A (H1N1). *Clin Infect Dis*. 2011;52:301–12. <https://doi.org/10.1093/cid/ciq152>
 23. Fezeu L, Julia C, Henegar A, Bitu J, Hu FB, Grobbee DE, et al. Obesity is associated with higher risk of intensive care unit admission and death in influenza A (H1N1) patients: a systematic review and meta-analysis. *Obes Rev*. 2011;12:653–9. <https://doi.org/10.1111/j.1467-789X.2011.00864.x>
 24. Belongia EA, Irving SA, Waring SC, Coleman LA, Meece JK, Vandermause M, et al. Clinical characteristics and 30-day outcomes for influenza A 2009 (H1N1), 2008–2009 (H1N1), and 2007–2008 (H3N2) infections. *JAMA*. 2010;304:1091–8. <https://doi.org/10.1001/jama.2010.1277>
 25. Ishiguro T, Takayanagi N, Kanauchi T, Uozumi R, Kawate E, Takaku Y, et al. Clinical and radiographic comparison of influenza virus-associated pneumonia among three viral subtypes. *Intern Med*. 2016;55:731–7. <https://doi.org/10.2169/internalmedicine.55.5227>
 26. Yang SQ, Qu JX, Wang C, Yu XM, Liu YM, Cao B. Influenza pneumonia among adolescents and adults: a concurrent comparison between influenza A (H1N1) pdm09 and A (H3N2) in the post-pandemic period. *Clin Respir J*. 2014;8:185–91. <https://doi.org/10.1111/crj.12056>
 27. Centro Nacional de Epidemiología. Instituto de Salud Carlos III. Red Nacional de Vigilancia Epidemiológica. Protocolo de vigilancia de la Gripe. In: *Protocolos de la Red Nacional de Vigilancia Epidemiológica*. Madrid, 2013 [cited 2019 Jul 26]. https://www.isciii.es/QueHacemos/Servicios/VigilanciaSaludPublicaRENAVE/EnfermedadesTransmisibles/Documents/PROTOSCOLOS/PROTOSCOLOS%20EN%20BLOQUE/PROTOSCOLOS_RENAVE-ciber.pdf
 28. World Health Organization. Guidelines for pharmacological management of pandemic influenza A(H1N1) 2009 and other influenza viruses. Part I: recommendations [cited 2018 Oct 10]. http://www.who.int/csr/resources/publications/swineflu/h1n1_guidelines_pharmaceutical_mngt.pdf?ua=1
 29. Dimitrijević D, Ilić D, Rakić Adrović S, Šuljagić V, Pelemiš M, Stevanović G, et al. Predictors of hospitalization and admission to intensive care units of influenza patients in Serbia through four influenza seasons from 2010/2011 to 2013/2014. *Jpn J Infect Dis*. 2017;70:275–83. <https://doi.org/10.7883/yoken.JJID.2016.210>
 30. Kwok KO, Riley S, Perera RAPM, Wei VWI, Wu P, Wei L, et al. Relative incidence and individual-level severity of seasonal influenza A H3N2 compared with 2009 pandemic H1N1. *BMC Infect Dis*. 2017;17:337. <https://doi.org/10.1186/s12879-017-2432-7>
 31. Lytras T, Pantavou K, Mouratidou E, Tsiodras S. Mortality attributable to seasonal influenza in Greece, 2013 to 2017: variation by type and subtype and age, and a possible harvesting effect. *Euro Surveill*. 2019;24:1800118. <https://doi.org/10.2807/1560-7917.ES.2019.24.14.1800118>
 32. Nielsen J, Vestergaard LS, Richter L, Schmid D, Bustos N, Asikainen T, et al. European all-cause excess and influenza-attributable mortality in the 2017/18 season: should the burden of influenza B be reconsidered? *Clin Microbiol Infect*. 2019;25:1266–76. <https://doi.org/10.1016/j.cmi.2019.02.011>
 33. Belongia EA, McLean HQ. Influenza vaccine effectiveness: defining the H3N2 problem. *Clin Infect Dis*. 2019;69:1817–23. <https://doi.org/10.1093/cid/ciz411>

Address for correspondence: Concepción Delgado-Sanz, Institute of Health Carlos III, National Centre of Epidemiology, Monforte de Lemos 5, 28029 Madrid, Spain; email: cdelgados@isciii.es

Exposure to Ebola Virus and Risk for Infection with Malaria Parasites, Rural Gabon

Jessica L. Abbate, Pierre Becquart, Eric Leroy, Vanessa O. Ezenwa,¹ Benjamin Roche¹

An association between malaria and risk for death among patients with Ebola virus disease has suggested within-host interactions between *Plasmodium falciparum* parasites and Ebola virus. To determine whether such an interaction might also influence the probability of acquiring either infection, we used a large snapshot surveillance study from rural Gabon to test if past exposure to Ebola virus is associated with current infection with *Plasmodium* spp. during nonepidemic conditions. We found a strong positive association, on population and individual levels, between seropositivity for antibodies against Ebola virus and the presence of *Plasmodium* parasites in the blood. According to a multiple regression model accounting for other key variables, antibodies against Ebola virus emerged as the strongest individual-level risk factor for acquiring malaria. Our results suggest that within-host interactions between malaria parasites and Ebola virus may underlie epidemiologic associations.

Major outbreaks of infections with Ebola virus, such as the 2014–2016 West Africa epidemic and the ongoing 2018–2019 outbreak in eastern Democratic Republic of the Congo, pose several obvious and immediate threats to public health. Less obvious, but as concerning for public health, is the possibility that Ebola virus might also interact with common co-circulating infectious agents at both the population and within-host (individual) levels. Indeed, much attention has been paid to the relationship between malaria and Ebola virus disease (EVD), primarily because of the clinical resemblance between the 2

diseases (1) and the high frequency of *Plasmodium* spp. co-infection among patients undergoing treatment for confirmed EVD (2). At the individual level, several retrospective epidemiology studies of patients undergoing treatment for confirmed EVD have attempted to determine whether concurrent malaria affects patient outcomes. In Sierra Leone (3) and at 1 Ebola treatment center in Liberia (4), mortality risk was much higher among Ebola patients who were co-infected with *Plasmodium* parasites than among patients who were not co-infected, and a study in Guinea found that adverse outcomes were higher among EVD patients with higher *P. falciparum* parasite loads than among those with lower levels of parasitemia (5). A similar study of patients at several Ebola treatment centers in Liberia reported the opposite relationship, that the probability of survival for EVD patients was positively associated with both presence and level of *Plasmodium* spp. parasitemia (6). Together, these results point to a strong potential for biological interactions between *Plasmodium* parasites and Ebola virus that may influence the severity of EVD.

At the population level, interruption of normal public health services and disease control measures—including patient avoidance of healthcare facilities—during an EVD epidemic has been projected to cause increases in untreated cases and deaths from malaria, in addition to several otherwise preventable or treatable diseases (7–9). Yet whether biological interactions at the within-host level, such as inflammatory processes leading to prolonged post-Ebola syndrome symptoms common in acute EVD survivors (10), may also lead to a change in malaria transmission dynamics by influencing susceptibility remains unknown.

Knowledge of the extent of possible interactions between infection with *Plasmodium* parasites and Ebola virus is especially helpful because geographic regions where prevalence of antibodies against Ebola

Author affiliations: Institut de Recherche pour le Développement, Unité Mixte de Recherche MIVEGEC, Montpellier, France (J.L. Abbate, P. Becquart, E. Leroy, B. Roche); Institut de Recherche pour le Développement, Unité Mixte Internationale UMMISCO, Bondy, France (J.L. Abbate, B. Roche); CIRMF, Franceville, Gabon (E. Leroy); University of Georgia, Athens, Georgia, USA (V.O. Ezenwa); Universidad Nacional Autónoma de México, Mexico City, Mexico (B. Roche)

DOI: <https://doi.org/10.3201/eid2602.181120>

¹These senior authors contributed equally to this article.

virus (hereafter called Ebola antibodies) is high are also areas of high malaria endemicity (11), particularly the most severe form of malaria, caused by *P. falciparum* (12). Historically, small, typically rural, outbreaks of Ebola virus have been the norm; many such outbreaks across central Africa have been described since 1976 (13). However, the recent occurrence of large outbreaks involving multiple urban centers (14,15), including thousands of survivors and vaccinated persons, means that any interactions with malaria parasites have the potential to affect larger populations than in prior decades. Furthermore, it is estimated that less than half of the cross-species transmission events leading to a human EVD case are correctly identified by current surveillance systems, suggesting that most of these events are treated locally as an unknown fever or malaria (16).

To investigate the potential epidemiologic links between Ebola virus exposure and malaria parasites, we took advantage of a large snapshot surveillance study of 4,272 adults from 210 villages across Gabon, conducted during 2005–2008 (17–19), to test for populationwide and individual associations between the 2 infections during nonepidemic conditions. At both levels, we also tested for key cofactors that might influence detection of an association. With an Ebola antibody seroprevalence of 15.3% (17,18) and *Plasmodium* spp. prevalence of 52.1% (19), our study population offered the unique opportunity for testing such a link.

Materials and Methods

Study Population and Survey Methods

Our study was based on data previously generated from a snapshot surveillance study in rural Gabon (17–21). That study was conducted across 210 rural (population <300) villages in Gabon, located across a variety of open and forested habitats, and was designed specifically to test for the prevalence of undetected exposure to Ebola virus (17,18). Villages were selected by using a stratified random sampling method based on Gabon's 9 administrative provinces; each province was surveyed once during 1-month field missions from July 2005 through May 2008, generally during the dry season. All but 5 of Gabon's 49 administrative departments (grouping villages within provinces) were represented (Appendix Figure 1, <https://wwwnc.cdc.gov/EID/article/26/2/18-1120-App1.pdf>). In each village, all permanent residents >15 years of age were solicited for participation in the study if they were willing to complete a 2-page survey and provide a blood sample along with written consent.

The survey included questions about sociodemographics and medical history. All participants and nonparticipants in each village were offered information about the study, free medical examinations, malaria testing, blood typing, and medicines. Refusal to participate was low ($\approx 15\%$ of eligible persons). The study protocol was approved by the Gabonese Ministry of Health (research organization no. 00093/MSP/SG/SGAQM) and is described elsewhere (17–20).

Individual Pathogen Exposure and Cofactors

Study volunteers were tested for previous exposure to Ebola virus by use of a *Zaire ebolavirus* (ZEBOV) IgG-specific ELISA (17,18). Current infection with *Plasmodium* spp. was tested by using an in-field blood smear (17,18) and by high-throughput targeted sequencing of *Plasmodium*-specific cytochrome b mitochondrial DNA to identify species (single and mixed infections of *P. falciparum*, *P. malariae*, and *P. ovale* were identified) (19). For purposes of this study, we considered a person to be infected with malaria parasites if either blood smear or sequence amplification was positive (irrespective of the species) and to not be infected if both test results were negative.

In addition to participant sex and age group (16–30, 31–45, 46–60, >60 years), information was obtained about several cofactors that could be indicative of heterogeneous exposure or susceptibility to both infections (17,18). These cofactors included the presence of concurrent filarial worm infection (*Loa loa* and *Mansonella perstans*, each identified from blood samples as described in [20]), sickle cell hemoglobin genotype (carriers vs. noncarriers, as determined in [21]), participant education level (classified as less than secondary education or secondary education and above, serving as a proxy for socioeconomic status), participant regular contact with wild animals through primary occupation (classified as hunters or nonhunters), the keeping of wild animals as pets (yes or no), and specific exposure to bats by consumption (yes or no).

Population Cofactors

For determination of population-level influences on patterns of pathogen exposure, factors common to all persons in a given department or village were also examined. We obtained population density (no. persons/km²) at the department level by dividing population size (no. inhabitants/department based on 2003 national census data, <https://www.city-population.de/php/gabon-admin.php>) by department area (km²). Average household wealth and frequency of insecticide-treated mosquito net (ITN)

ownership per department were obtained from the Demographic and Health Surveys program 2012 survey for Gabon (22). Geographic displacement of households in these data remained within administrative boundaries; however, wealth and ITN data were missing for 7 departments (Appendix Table 1). Average household wealth was calculated by rescaling the wealth index for all rural households to positive integers and taking the geometric mean for each department. We calculated the frequency of ITN ownership per department by counting the number of rural households in each department with at least 1 ITN and dividing it by the number of households for which there were data. At the village level, the dominant habitat type was previously classified into 3 categories with statistically significant differences in terms of Ebola antibody prevalence: lakeland (including lakes, rivers, and coastal regions), savanna (including savanna and grassland areas), and forest (including northeastern forests, interior forests, and mountain forest areas) (17,18).

Statistical Analyses

We performed all statistical analyses in the R version 3.2.2 statistical programming environment (23). We tested for departure of malaria and Ebola antibody co-occurrence frequency from random expectations by using χ^2 analysis (`chisq.test` function in R). We tested the correlation between department-level prevalence of Ebola antibodies and malaria parasite infection by using the `cor.test` function in R, based on the nonparametric Spearman rank correlation coefficient. We tested department-level effects of population density, average wealth, and ITN ownership frequency on this correlation together as cofactors in a mixed-effects multiple linear regression model (function `lmer`, package `lme4`) by setting Ebola antibody prevalence as the main explanatory variable, *Plasmodium* spp. prevalence as the response variable, and province as a random variable to limit pseudoreplication. The inclusion of province as a random variable also enabled us to account for yearly and seasonal differences in prevalence because all departments within a given province were sampled within a single month-long field mission. To meet assumptions of normality, antibody prevalence, *Plasmodium* parasite prevalence, and ITN ownership frequency were arcsine square-root transformed, population density and average wealth were log-transformed, and data points were weighted by the number of persons tested in each department. Data for the 7 departments with missing wealth and ITN data were excluded from the multiple regression model.

At the individual level, we used multiple logistic regression (implemented as a generalized linear mixed effects model with binomial error distribution via the `glmer` function of package `lme4`) to test whether persons with Ebola antibodies were more or less likely than those without Ebola antibodies to also be infected with malaria parasites. *Plasmodium* parasite infection status (infected or not infected) was the response variable in the model, and we included province (also accounting for date sampled), department within province, and village (nested within department and province) of the person as random factors to control for pseudoreplication and spatial autocorrelation. Explanatory variables included ZEBOV-specific IgG seropositivity, individual cofactors (concurrent *L. loa* and *M. perstans* infection; sex; age group; sickle cell genotype; education level; and regular interaction with animals through hunting, keeping wild pets, or consuming bats), and population-level cofactors (village habitat and log-transformed population density of the administrative department). We tested the effect of each explanatory variable after correcting for all other model terms via likelihood ratio tests, reported as adjusted odds ratios, and used bootstrapping to calculate the 95% CIs of the coefficients by using the `bootMer` function (R `boot` package, no. Markov chain Monte Carlo simulations = 200). We removed from analysis those persons for whom values for any 1 variable were missing.

Results

A total of 4,272 volunteers from 210 villages were enrolled in the study. Among those sampled, we obtained data on both malaria status and Ebola antibodies from 4,170 persons: 2,199 (52.7%) female and 1,971 (47.8%) male participants, 16–90 (median 49) years of age. These data showed that across Gabon, 2,190 (52.5%) persons were infected with >1 species of *Plasmodium*, 638 (15.3%) were positive for ZEBOV-specific IgG, and an overabundance of 425 (10.2%) were in both categories (Figure 1; $\chi^2 = 59.4$, $df = 1$, $p < 0.0001$). Because of missing data, we analyzed individual-level risk factors for exposure to both pathogens on a subset of 3,912 persons (Table; Appendix Table 1).

At the population level, we found a striking positive correlation between the geographic distributions of Ebola virus exposure and *Plasmodium* parasite infection, measured as the prevalence of each across administrative departments (Figure 2; Spearman rank correlation coefficient $\rho = 0.43$, $df = 42$, $p < 0.01$). The direction and significance of this correlation was not qualitatively affected by population density, average household wealth, ITN ownership

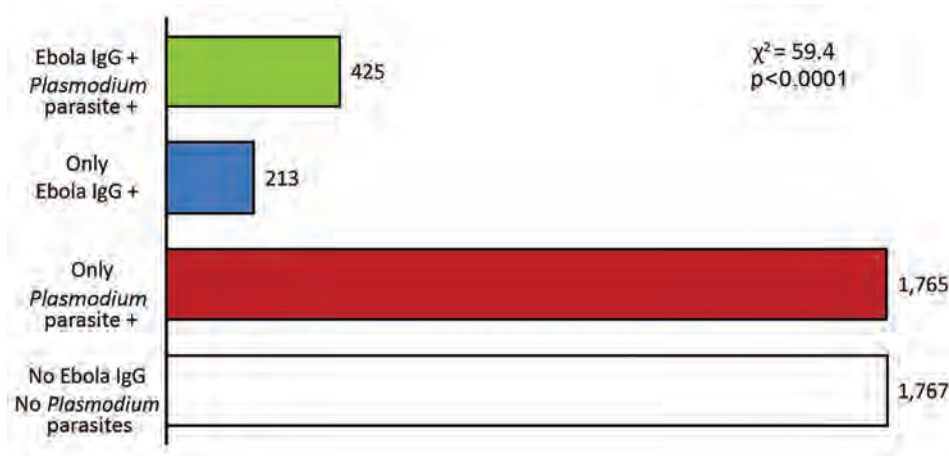


Figure 1. Frequency of *Plasmodium* spp. infection and Zaire ebolavirus-specific IgG seropositivity among participants in study of exposure to Ebola virus and risk for malaria, rural Gabon. +, positive.

frequency, or by controlling for random variance among provinces sampled on different dates (Appendix Table 2, Figures 2, 3).

At the individual level, we found that prior exposure to Ebola virus was strongly associated with an increased probability of current *Plasmodium* spp. infection, even after accounting for geographic location (administrative province, department, and village) and all other individual and population-level risk factors in the model (adjusted odds ratio [aOR] 1.741 [95% CI 1.400–2.143], $\chi^2 = 26.36$, $df = 1$, $p < 0.0001$; Figure 3; Appendix Table 3, Figure 4). This variable was a stronger risk factor for *Plasmodium* infection than any other individual trait, second only to living in a lakeland habitat (aOR 0.313 [95% CI 0.110–0.875], $\chi^2 = 11.64$, $df = 2$, $p < 0.01$) (Figure 3; Appendix Table 3). Other factors positively associated with *Plasmodium* parasite infection were concurrent infection with *M. perstans* (aOR 1.359 [1.056–1.727], $\chi^2 = 5.35$, $df = 1$, $p = 0.021$), male sex (aOR 1.335 [1.098–1.586], $\chi^2 = 10.5$, $df = 1$, $p = 0.0012$), and keeping a wild animal as a pet (aOR 1.308 [1.040–1.654], $\chi^2 = 4.55$, $df = 1$, $p = 0.033$). Being in an older age group was associated with a decline in *Plasmodium* parasite infection risk ($\chi^2 = 8.02$, $df = 1$, $p = 0.046$). From the individual-level model we excluded department-level wealth and ITN ownership frequency, which showed no evidence for influencing the association at the population level (Appendix Table 2) because these variables were confounded with department-level population density and because missing data were not randomly distributed (Appendix Table 1). These results for nonspecific malaria parasite infection risk factors were qualitatively identical when *P. falciparum* and *P. malariae* infections were considered separately (*P. ovale* infection was too rare to be tested; Appendix Tables 4, 5).

Discussion

At the population and individual levels across Gabon, we found a strong positive association between ZEBOV-specific IgG seropositivity and current malaria parasite infection. In geographic regions where Ebola virus exposure was high, prevalence of *Plasmodium* spp. infection was also high, and within these regions, having antibodies against Ebola virus increased the risk for current *Plasmodium* infection by nearly 75% after all other medical, demographic, social, behavioral, and ecologic cofactors for which we had data were controlled for. The magnitude of the association, particularly when compared with other risk factors (filarial worm infections, sex, age group, contact with wild animals, and village habitat type), was highly unexpected. This epidemiologic link between Ebola virus exposure and malaria is consistent with reports of high co-infection frequency during the 2014–2016 outbreak of EVD in West Africa (2) and suggests that ecologic processes between the 2 pathogens potentially influencing patient survival (3,4) may also influence susceptibility or transmission.

The public health implications of our findings are numerous. First, if Ebola virus infection renders patients and survivors more susceptible to malaria, healthcare providers should anticipate the need for additional malaria treatment and control measures after Ebola virus outbreaks beyond the increase predicted from disruption of healthcare services and reduced treatment-seeking behavior, which often accompany an outbreak. Second, if sublethal Ebola virus infections commonly co-occur with malaria, they may be missed because disease surveillance systems do not regularly screen for other causes of disease in *Plasmodium*-positive patients whose symptoms are consistent with malaria and resolve with malaria treatment. However, a trial in Liberia showed that antimalarial drugs inhibit Ebola virus infection of cells in culture (24–26)

Table. Characteristics of population in study of exposure to Ebola virus and risk for malaria parasite infection, rural Gabon*

Variable	No. (%) sampled	No. with <i>Plasmodium</i> spp. infection	No. ZEBOV-specific IgG+	No. with <i>Plasmodium</i> spp. infection and ZEBOV-specific IgG+
Sex				
F	2,058 (52.6)	1,017	277	180
M	1,854 (47.4)	1,022	323	218
Age, y				
16–30	604 (15.4)	343	93	71
31–45	1,062 (27.1)	584	170	117
46–60	1,554 (39.7)	801	234	152
≥60	692 (17.7)	311	103	58
Sickle cell genotype				
Carrier	811 (20.7)	424	118	83
Not carrier	3,101 (79.3)	1,615	482	315
<i>Loa loa</i>				
Infected	863 (22.1)	450	142	92
Not infected	3,049 (77.9)	1,589	458	306
<i>Mansonella perstans</i>				
Infected	391 (10.0)	230	70	48
Not infected	3,521 (90.0)	1,809	530	350
Education				
Less than secondary	2,909 (74.4)	1,478	446	292
More than secondary	1,003 (25.6)	561	154	106
Occupation				
Hunter	425 (10.9)	241	89	59
Not hunter	3,487 (89.1)	1,798	511	339
Pets				
Wild animal	450 (11.5)	263	62	46
No wild animals	3,462 (88.5)	1,776	538	352
Bat meat consumption				
Yes	522 (13.3)	273	92	53
No	3,390 (86.7)	1,766	508	345
Habitat (village)				
Forest	3,088 (78.9)	1,727	544	360
Lakeland	412 (10.5)	97	12	6
Savanna	412 (10.5)	215	44	32
Population density, department level, persons/km ²				
0.5–2	1,936 (49.5)	995	324	210
2–10	1,379 (35.3)	702	186	124
10–30	597 (15.3)	342	90	64

*ZEBOV, *Zaire ebolavirus*; +, positive.

and were associated with increased survival of EVD patients (4). This finding suggests that if active treatment for malaria helps modulate EVD severity, it may also result in Ebola virus infection frequencies being underestimated during epidemic and nonepidemic periods. Third, if the causal direction of the interaction is such that malaria increases susceptibility to Ebola virus, achieving malaria elimination goals across West and Central Africa may help prevent future EVD outbreaks. Indeed, our choice to consider past exposure to Ebola virus as an explanatory variable for current malaria parasite infection in our analysis was arbitrary, and additional analyses confirmed that reversing the positions of the 2 pathogens in the model did not qualitatively change the observed association pattern (Appendix Table 6, Figures 5, 6). Furthermore, a biological mechanism of interaction between the 2 pathogens with the potential to cause the association found here (such as persistent inflammatory processes

in EVD survivors [10,27,28] or damage to specific tissues targeted by both pathogens [29,30]) remains to be elucidated. We do, however, point out that the mechanism is not likely to be general or the result of immunosuppression (e.g., because of AIDS) because neither of the 2 common filarial infections included as co-factors (*L. loa* and *M. perstans*) were risk factors for infection with *Plasmodium* parasites (Figure 3) and Ebola virus exposure (Appendix Figure 5). Last, the World Health Organization has noted that the most recent EVD outbreak in the Nord Kivu Province of the Democratic Republic of the Congo coincided with a surge in malaria cases in the region (31). Even if the interaction is not biological and a common ecologic, epidemiologic, or even sociological factor not tested here is responsible for driving an increase in the probability of exposure to both pathogens, further study to identify that factor could prove helpful for predicting and preventing future EVD outbreaks.

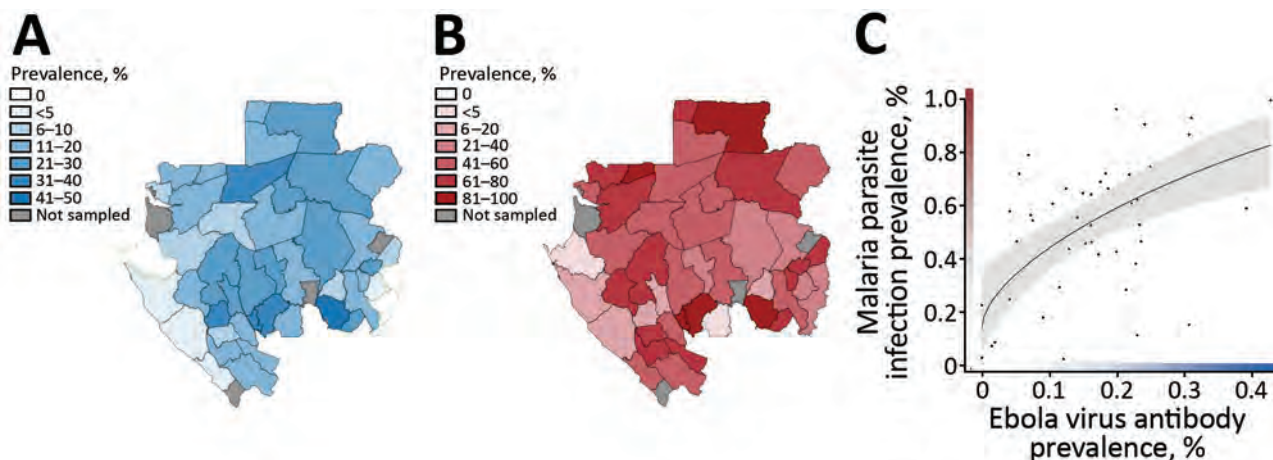


Figure 2. Association of Ebola virus exposure and *Plasmodium* spp. infection across rural communities in Gabon. A) Geographic distribution of Ebola virus antibody seroprevalence. B) Geographic distribution of malaria parasite (all *Plasmodium* species) prevalence. C) Correlation between these geographic distributions at the level of administrative department ($p = 0.43$, $p < 0.01$). The fitted curve and 95% CIs (gray shading) were generated by using the predict function from the basic stats package in the R version 3.2.2 statistical programming environment (23), based on a linear model between the 2 variables weighted by the number of persons sampled in each department.

One key challenge to understanding the drivers of the patterns we report in this study is determining what ZEBOV-specific IgG seropositivity means. Ebola virus-specific IgG is known to persist for at least a decade after acute disease (32). However, it is not entirely clear whether the surprisingly high seroprevalence of Ebola antibodies found in population studies such as ours during non-epidemic periods (17,18,33–36) are the result of undetected outbreaks, subclinical exposure to Ebola virus, or cross-reactivity with other unknown filoviruses. A recent modeling study estimated that nearly 75% of cross-species transmission events leading to a singular or small cluster of EVD cases go undetected (16), although widespread failure to detect acute EVD cases seems unlikely. Alternatively, evidence of subclinical antigenic stimulation has been documented, for example, by a survey of Ebola virus-specific IgG seroprevalence among domestic dogs. Frequency of Ebola virus-specific IgG was highest in dogs nearest to an outbreak epicenter in Gabon (37). Mild or asymptomatic Ebola virus infection is typically associated with low viral loads, limiting virus capacity for human-to-human transmission (38–40). Thus, evidence suggests that widespread seroprevalence of Ebola antibodies outside of known epidemic periods could reflect past subclinical infection contracted through exposure to natural reservoirs (such as frugivorous bats [41,42]); however, studies of humans have yielded only minimal support for this hypothesis (40,43,44). Whereas asymptomatic seroconversion of household contacts of acutely ill patients and high-risk exposure (direct physical contact with

blood or vomit) was demonstrated to occur at high frequency (11/24 persons) during the 1996 outbreak in Gabon (44), studies from the Democratic Republic of the Congo in 1995 (43) and during the 2014–2016 outbreak in Sierra Leone (40) found that this phenomenon was much more rare among household contacts with lower-risk exposure histories. Although these studies concluded that undiagnosed subclinical EVD and asymptomatic Ebola virus infections were evident during an outbreak, it has not yet been shown that they occur in the absence of diagnosed cases, let alone at sufficient frequency. Arguably, the most likely source of high Ebola antibody seroprevalence in the absence of large outbreaks is antibody cross-reactivity with an unknown and relatively asymptomatic virus; however, whereas IgG is largely cross-reactive among Ebola virus species (45), no such low-virulence Ebola-related virus has been identified circulating in these populations. Irrespective of the processes that govern the presence of Ebola-specific antibodies, the strong and consistent associations we found between antibody status and *Plasmodium* parasite infection risk suggest a need for additional investigation regarding the effect of the source of these antibodies on malaria epidemiology and vice versa.

In addition to resolving uncertainty around the provenance of Ebola-specific antibodies in the absence of known cases, future studies should aim to ascertain more detailed information on the timing, duration, and severity of *Plasmodium* infections. In particular, it would be very informative to know whether the positive association detailed here is also

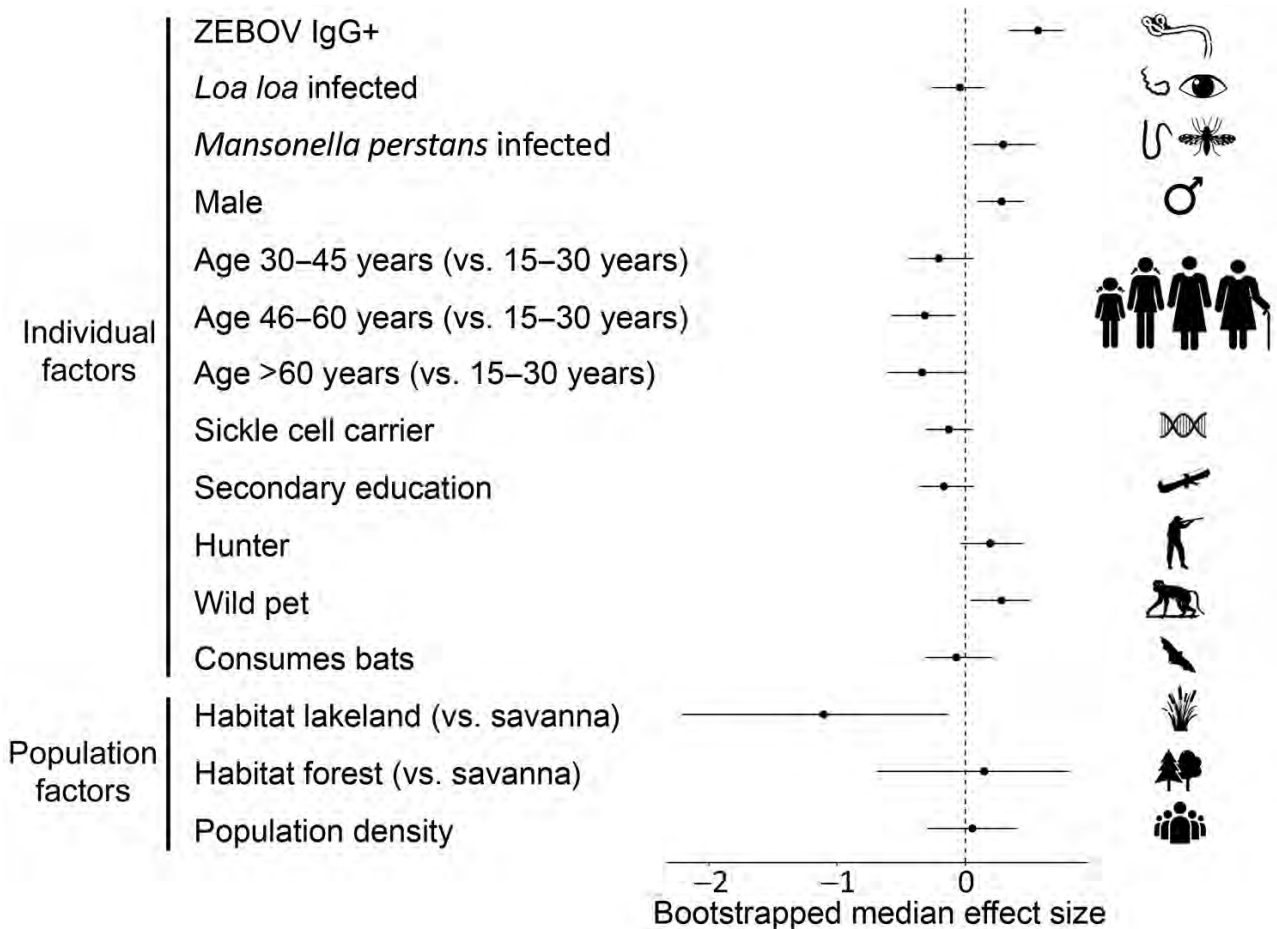


Figure 3. Malaria parasite infection risk factor effect sizes. The relationship between malaria and each individual or population-level risk factor was evaluated after accounting for all other variables, including geographic location (village within department within province) as a random factor, using a generalized linear mixed effects model. Effect sizes are presented as median adjusted odds ratios with bootstrapped 95% CIs. ZEBOV, Zaire ebolavirus; +, positive.

found in children (our study excluded persons <16 years of age) because the prevalence of acquired immunity against many pathogens, including Ebola virus (17) and *Plasmodium* spp. (46), increases with age because of accumulating exposure opportunities. A longitudinal cohort (following infection and immunity status of each individual through time) would produce results with more reliable interpretation than the cross-sectional (single time-point snapshot) design of our present study (47). Ultimately, only case-controlled experimental studies, such as vaccine trials, can provide the evidence necessary to claim a causal relationship between these 2 pathogens in humans.

The 2014–2016 Ebola virus outbreak in West Africa served as a wake-up call, highlighting the possibility of Ebola virus emergence into new and heavily populated regions and spurring the advancement of vaccine development and case-reactive ring

vaccination methods (48,49). However, with >17,000 EVD survivors across West Africa and an unknown number of asymptomatic seroconverted persons (50), it is important to clarify the mechanistic basis of our findings because this knowledge will help guide future investigations into public health implications, including the risk for acquiring malaria among EVD survivors and the potential for added benefits of both Ebola and malaria vaccination campaigns.

This study received a contribution from the Agence Nationale de la Recherche Programme Jeunes Chercheurs project STORY, granted to B.R. and supporting J.L.A. B.R. is supported by an Investissement d'Avenir grant from the Agence Nationale de la Recherche (CEBA ANR-10-LABX-2501). V.O.E. received support from a US Fulbright Scholar Award. The funders had no role in study design, data collection and analysis, decision to publish, or preparation of the manuscript.

About the Author

Dr. Abbate is a postdoctoral researcher at the French Institut de Recherche pour le Développement, where she has been investigating pathogen–pathogen associations from disease surveillance data by using empirical and theoretical tools. Her research interests include disease distributions, ecological interactions, host resistance evolution, and complex pathogen traits.

References

- Hartley M-A, Young A, Tran A-M, Okoni-Williams HH, Suma M, Mancuso B, et al. Predicting Ebola severity: a clinical prioritization score for Ebola virus disease. *PLoS Negl Trop Dis*. 2017;11:e0005265. <https://doi.org/10.1371/journal.pntd.0005265>
- Barry M, Traoré FA, Sako FB, Kpamy DO, Bah EI, Poncin M, et al. Ebola outbreak in Conakry, Guinea: epidemiological, clinical, and outcome features. *Med Mal Infect*. 2014;44:491–4. <https://doi.org/10.1016/j.medmal.2014.09.009>
- Waxman M, Aluisio AR, Rege S, Levine AC. Characteristics and survival of patients with Ebola virus infection, malaria, or both in Sierra Leone: a retrospective cohort study. *Lancet Infect Dis*. 2017;17:654–60. [https://doi.org/10.1016/S1473-3099\(17\)30112-3](https://doi.org/10.1016/S1473-3099(17)30112-3)
- Gignoux E, Azman AS, de Smet M, Azuma P, Massaquoi M, Job D, et al. Effect of artesunate-amodiaquine on mortality related to Ebola virus disease. *N Engl J Med*. 2016;374:23–32. <https://doi.org/10.1056/NEJMoa1504605>
- Carroll MW, Haldenby S, Rickett NY, Pályi B, Garcia-Dorival I, Liu X, et al. Deep sequencing of RNA from blood and oral swab samples reveals the presence of nucleic acid from a number of pathogens in patients with acute Ebola virus disease and is consistent with bacterial translocation across the gut. *MSphere*. 2017;2:e00325–17. <https://doi.org/10.1128/mSphereDirect.00325-17>
- Rosenke K, Adjemian J, Munster VJ, Marzi A, Falzarano D, Onyango CO, et al. *Plasmodium* parasitemia associated with increased survival in Ebola virus-infected patients. *Clin Infect Dis*. 2016;63:1026–33. <https://doi.org/10.1093/cid/ciw452>
- Walker PGT, White MT, Griffin JT, Reynolds A, Ferguson NM, Ghani AC. Malaria morbidity and mortality in Ebola-affected countries caused by decreased health-care capacity, and the potential effect of mitigation strategies: a modelling analysis. *Lancet Infect Dis*. 2015;15:825–32. [https://doi.org/10.1016/S1473-3099\(15\)70124-6](https://doi.org/10.1016/S1473-3099(15)70124-6)
- Takahashi S, Metcalf CJE, Ferrari MJ, Moss WJ, Truelove SA, Tatem AJ, et al. Reduced vaccination and the risk of measles and other childhood infections post-Ebola. *Science*. 2015;347:1240–2.
- Parpia AS, Ndeffo-Mbah ML, Wenzel NS, Galvani AP. Effects of response to 2014–2015 Ebola outbreak on deaths from malaria, HIV/AIDS, and tuberculosis, West Africa. *Emerg Infect Dis*. 2016;22:433–41. <https://doi.org/10.3201/eid2203.150977>
- Vetter P, Kaiser L, Schibler M, Ciglenecki I, Bausch DG. Sequelae of Ebola virus disease: the emergency within the emergency. *Lancet Infect Dis*. 2016;16:e82–91. [https://doi.org/10.1016/S1473-3099\(16\)00077-3](https://doi.org/10.1016/S1473-3099(16)00077-3)
- World Health Organization. World Malaria Report 2017 [cited 2019 Dec 5] <http://apps.who.int/iris/bitstream/10665/259492/1/9789241565523-eng.pdf>
- Hay SI, Guerra CA, Gething PW, Patil AP, Tatem AJ, Noor AM, et al. A world malaria map: *Plasmodium falciparum* endemicity in 2007. *PLoS Med*. 2009;6:e1000048. <https://doi.org/10.1371/journal.pmed.1000048>
- Pourrut X, Kumulungui B, Wittmann T, Moussavou G, Délicat A, Yaba P, et al. The natural history of Ebola virus in Africa. *Microbes Infect*. 2005;7:1005–14. <https://doi.org/10.1016/j.micinf.2005.04.006>
- Munster VJ, Bausch DG, de Wit E, Fischer R, Kobinger G, Muñoz-Fontela C, et al. Outbreaks in a rapidly changing Central Africa – lessons from Ebola. *N Engl J Med*. 2018;379:1198–201. <https://doi.org/10.1056/NEJMp1807691>
- Mbala-Kingebeni P, Aziza A, Di Paola N, Wiley MR, Makiala-Mandanda S, Caviness K, et al. Medical countermeasures during the 2018 Ebola virus disease outbreak in the North Kivu and Ituri Provinces of the Democratic Republic of the Congo: a rapid genomic assessment. *Lancet Infect Dis*. 2019;19:648–57. [https://doi.org/10.1016/S1473-3099\(19\)30118-5](https://doi.org/10.1016/S1473-3099(19)30118-5)
- Glennon EE, Jephcott FL, Restif O, Wood JLN. Estimating undetected Ebola spillovers. *PLoS Negl Trop Dis*. 2019;13:e0007428. <https://doi.org/10.1371/journal.pntd.0007428>
- Becquart P, Wauquier N, Mahlaköiv T, Nkoghe D, Padilla C, Souris M, et al. High prevalence of both humoral and cellular immunity to Zaire ebolavirus among rural populations in Gabon. *PLoS One*. 2010;5:e9126. <https://doi.org/10.1371/journal.pone.0009126>
- Nkoghe D, Padilla C, Becquart P, Wauquier N, Moussavou G, Akué JP, et al. Risk factors for Zaire ebolavirus – specific IgG in rural Gabonese populations. *J Infect Dis*. 2011;204(Suppl 3):S768–75. <https://doi.org/10.1093/infdis/jir344>
- Délicat-Loembet L, Rougeron V, Ollomo B, Arnathau C, Roche B, Elguero E, et al. No evidence for ape *Plasmodium* infections in humans in Gabon. *PLoS One*. 2015;10:e0126933. <https://doi.org/10.1371/journal.pone.0126933>
- Akue JP, Nkoghe D, Padilla C, Moussavou G, Moukana H, Mbou RA, et al. Epidemiology of concomitant infection due to *Loa loa* and *Mansonella perstans* in Gabon. *PLoS Negl Trop Dis*. 2011;5:e1329. <https://doi.org/10.1371/journal.pntd.0001329>
- Délicat-Loembet LM, Elguero E, Arnathau C, Durand P, Ollomo B, Ossari S, et al. Prevalence of the sickle cell trait in Gabon: a nationwide study. *Infect Genet Evol*. 2014;25:52–6. <https://doi.org/10.1016/j.meegid.2014.04.003>
- Demographic and Health Surveys Program. Survey summary: Gabon: standard DHS 2012 [cited 2019 Dec 5]. <http://www.measuredhs.com/what-we-do/survey/survey-display-402.cfm>
- R Core Team. R: a language and environment for statistical computing [cited 2019 Aug 14]. <https://www.r-project.org>
- Sakurai Y, Sakakibara N, Toyama M, Baba M, Davey RA. Novel amodiaquine derivatives potentially inhibit Ebola virus infection. *Antiviral Res*. 2018;160:175–82. <https://doi.org/10.1016/j.antiviral.2018.10.025>
- Madrid PB, Chopra S, Manger ID, Gilfillan L, Keepers TR, Shurtleff AC, et al. A systematic screen of FDA-approved drugs for inhibitors of biological threat agents. *PLoS One*. 2013;8:e60579. <https://doi.org/10.1371/journal.pone.0060579>
- Zilbermintz L, Leonardi W, Jeong S-Y, Sjødt M, McComb R, Ho C-LC, et al. Identification of agents effective against multiple toxins and viruses by host-oriented cell targeting. *Sci Rep*. 2015;5:13476. <https://doi.org/10.1038/srep13476>
- Clark DV, Kibuuka H, Millard M, Wakabi S, Lukwago L, Taylor A, et al. Long-term sequelae after Ebola virus disease in Bundibugyo, Uganda: a retrospective cohort study. *Lancet Infect Dis*. 2015;15:905–12. [https://doi.org/10.1016/S1473-3099\(15\)70152-0](https://doi.org/10.1016/S1473-3099(15)70152-0)

28. Etard J-F, Sow MS, Leroy S, Touré A, Taverne B, Keita AK, et al.; Postebogui Study Group. Multidisciplinary assessment of post-Ebola sequelae in Guinea (Postebogui): an observational cohort study. *Lancet Infect Dis.* 2017;17:545–52. [https://doi.org/10.1016/S1473-3099\(16\)30516-3](https://doi.org/10.1016/S1473-3099(16)30516-3)
29. Lanini S, Portella G, Vairo F, Kobinger GP, Pesenti A, Langer M, et al.; INMI-EMERGENCY EBOV Sierra Leone Study Group. Relationship between viremia and specific organ damage in Ebola patients: a cohort study. *Clin Infect Dis.* 2018;66:36–44. <https://doi.org/10.1093/cid/cix704>
30. Davis TME, Pongponratan E, Supanaranond W, Pukrittayakamee S, Helliwell T, Holloway P, et al. Skeletal muscle involvement in falciparum malaria: biochemical and ultrastructural study. *Clin Infect Dis.* 1999;29:831–5. <https://doi.org/10.1086/520444>
31. World Health Organization. Malaria control campaign launched in Democratic Republic of the Congo to save lives and aid Ebola response [cited 2019 May 3]. <https://www.afro.who.int/news/malaria-control-campaign-launched-democratic-republic-congo-save-lives-and-aid-ebola-response>
32. Wauquier N, Becquart P, Gasquet C, Leroy EM. Immunoglobulin G in Ebola outbreak survivors, Gabon. *Emerg Infect Dis.* 2009;15:1136–7. <https://doi.org/10.3201/eid1507.090402>
33. Busico KM, Marshall KL, Ksiazek TG, Roels TH, Fleerackers Y, Feldmann H, et al. Prevalence of IgG antibodies to Ebola virus in individuals during an Ebola outbreak, Democratic Republic of the Congo, 1995. *J Infect Dis.* 1999;179(Suppl 1):S102–7. <https://doi.org/10.1086/514309>
34. Gonzalez JP, Nakoune E, Slenczka W, Vidal P, Morvan JM. Ebola and Marburg virus antibody prevalence in selected populations of the Central African Republic. *Microbes Infect.* 2000;2:39–44. [https://doi.org/10.1016/S1286-4579\(00\)00287-2](https://doi.org/10.1016/S1286-4579(00)00287-2)
35. Gonzalez JP, Josse R, Johnson ED, Merlin M, Georges AJ, Abandja J, et al. Antibody prevalence against haemorrhagic fever viruses in randomized representative Central African populations. *Res Virol.* 1989;140:319–31. [https://doi.org/10.1016/S0923-2516\(89\)80112-8](https://doi.org/10.1016/S0923-2516(89)80112-8)
36. Steffen I, Lu K, Yamamoto LK, Hoff NA, Mulembakani P, Wemakoy EO, et al. Serologic prevalence of Ebola virus in equatorial Africa. *Emerg Infect Dis.* 2019;25:911–8. <https://doi.org/10.3201/eid2505.180115>
37. Allela L, Boury O, Pouillot R, Délicat A, Yaba P, Kumulungui B, et al. Ebola virus antibody prevalence in dogs and human risk. *Emerg Infect Dis.* 2005;11:385–90. <https://doi.org/10.3201/eid1103.040981>
38. Lanini S, Portella G, Vairo F, Kobinger GP, Pesenti A, Langer M, et al.; INMI-EMERGENCY EBOV Sierra Leone Study Group. Blood kinetics of Ebola virus in survivors and nonsurvivors. *J Clin Invest.* 2015;125:4692–8. <https://doi.org/10.1172/JCI83111>
39. de La Vega MA, Caleo G, Audet J, Qiu X, Kozak RA, Brooks JI, et al. Ebola viral load at diagnosis associates with patient outcome and outbreak evolution. *J Clin Invest.* 2015;125:4421–8. <https://doi.org/10.1172/JCI83162>
40. Glynn JR, Bower H, Johnson S, Houlihan CF, Montesano C, Scott JT, et al. Asymptomatic infection and unrecognised Ebola virus disease in Ebola-affected households in Sierra Leone: a cross-sectional study using a new non-invasive assay for antibodies to Ebola virus. *Lancet Infect Dis.* 2017;17:645–53. [https://doi.org/10.1016/S1473-3099\(17\)30111-1](https://doi.org/10.1016/S1473-3099(17)30111-1)
41. Caron A, Bourgarel M, Cappelle J, Liégeois F, De Nys HM, Roger F. Ebola virus maintenance: if not (only) bats, what else? *Viruses.* 2018;10:pii:E549. <https://doi.org/10.3390/v10100549>
42. De Nys HM, Kingebeni PM, Keita AK, Butel C, Thaurignac G, Villabona-Arenas C-J, et al. Survey of Ebola viruses in frugivorous and insectivorous bats in Guinea, Cameroon, and the Democratic Republic of the Congo, 2015–2017. *Emerg Infect Dis.* 2018;24:2228–40. <https://doi.org/10.3201/eid2412.180740>
43. Rowe AK, Bertolli J, Khan AS, Mukunu R, Muyembe-Tamfum JJ, Bressler D, et al. Clinical, virologic, and immunologic follow-up of convalescent Ebola hemorrhagic fever patients and their household contacts, Kikwit, Democratic Republic of the Congo. *Commission de Lutte contre les Epidémies à Kikwit. J Infect Dis.* 1999;179(Suppl 1):S28–35. <https://doi.org/10.1086/514318>
44. Leroy EM, Baize S, Volchkov VE, Fisher-Hoch SP, Georges-Courbot MC, Lansoud-Soukate J, et al. Human asymptomatic Ebola infection and strong inflammatory response. *Lancet.* 2000;355:2210–5. [https://doi.org/10.1016/S0140-6736\(00\)02405-3](https://doi.org/10.1016/S0140-6736(00)02405-3)
45. MacNeil A, Reed Z, Rollin PE. Serologic cross-reactivity of human IgM and IgG antibodies to five species of Ebola virus. *PLoS Negl Trop Dis.* 2011;5:e1175. <https://doi.org/10.1371/journal.pntd.0001175>
46. Baird JK. Host age as a determinant of naturally acquired immunity to *Plasmodium falciparum*. *Parasitol Today.* 1995; 11:105–11. [https://doi.org/10.1016/0169-4758\(95\)80167-7](https://doi.org/10.1016/0169-4758(95)80167-7)
47. Fenton A, Knowles SCL, Petchey OL, Pedersen AB. The reliability of observational approaches for detecting interspecific parasite interactions: comparison with experimental results. *Int J Parasitol.* 2014;44:437–45. <https://doi.org/10.1016/j.ijpara.2014.03.001>
48. Henao-Restrepo AM, Camacho A, Longini IM, Watson CH, Edmunds WJ, Egger M, et al. Efficacy and effectiveness of an rVSV-vectored vaccine in preventing Ebola virus disease: final results from the Guinea ring vaccination, open-label, cluster-randomised trial (Ebola Ça Suffit!). *Lancet.* 2017;389:505–18. [https://doi.org/10.1016/S0140-6736\(16\)32621-6](https://doi.org/10.1016/S0140-6736(16)32621-6)
49. Shiwani HA, Pharithi RB, Khan B, Egom CBA, Kruzliak P, Maher V, et al. An update on the 2014 Ebola outbreak in western Africa. *Asian Pac J Trop Med.* 2017;10:6–10. <https://doi.org/10.1016/j.apjtm.2016.12.008>
50. Bellan SE, Pulliam JRC, Dushoff J, Meyers LA. Ebola control: effect of asymptomatic infection and acquired immunity. *Lancet.* 2014;384:1499–500. [https://doi.org/10.1016/S0140-6736\(14\)61839-0](https://doi.org/10.1016/S0140-6736(14)61839-0)

Address for correspondence: Jessica L. Abbate, Laboratoire MIVEGEC, Institut de Recherche pour le Développement, 911 Ave Agropolis, 34090 Montpellier, France; email: jessie.abbate@gmail.com

Cost-effectiveness of Screening Program for Chronic Q Fever, the Netherlands

Pieter T. de Boer, Marit M.A. de Lange, Cornelia C.H. Wielders, Frederika Dijkstra, Sonja E. van Roeden, Chantal P. Bleeker-Rovers, Jan Jelrik Oosterheert, Peter M. Schneeberger, Wim van der Hoek

In the aftermath of a large Q fever (QF) epidemic in the Netherlands during 2007–2010, new chronic QF (CQF) patients continue to be detected. We developed a health-economic decision model to evaluate the cost-effectiveness of a 1-time screening program for CQF 7 years after the epidemic. The model was parameterized with spatial data on QF notifications for the Netherlands, prevalence data from targeted screening studies, and clinical data from the national QF database. The cost-effectiveness of screening varied substantially among subpopulations and geographic areas. Screening that focused on cardiovascular risk patients in areas with high QF incidence during the epidemic ranged from cost-saving to €31,373 per quality-adjusted life year gained, depending on the method to estimate the prevalence of CQF. The cost per quality-adjusted life year of mass screening of all older adults was €70,000 in the most optimistic scenario.

Chronic Q fever (CQF) is a potentially lethal condition that develops in 2% of Q fever (QF) patients (1). QF is caused by infection with *Coxiella burnetii*, a gram-negative bacterium that has its main reservoir in livestock and can infect humans by airborne transmission. CQF can become apparent months to years after infection and usually manifests as endocarditis or vascular infection (2). Risk factors for CQF include heart valve disorders, aortic aneurysms, vascular prostheses, older age, and a compromised immune system (3–5). Prognosis is poor despite long-term antimicrobial drug

treatment; 28% of patients need surgery, and 15% die from CQF-related complications (6).

During 2007–2010, the Netherlands faced the world's largest QF epidemic ever documented. More than 4,000 patients with acute QF were notified. However, QF often occurs asymptotically (1), and the total number of infections has been estimated at 50,000 (7). Through May 2016, a substantial number of CQF infections occurred, and at least 74 patients died (8). Because early detection of CQF might result in a better prognosis, local hospitals initiated multiple targeted screening studies for clinical risk groups living in areas affected by the epidemic. These studies revealed that 7%–20% of screened patients had serologic evidence of *C. burnetii* infection, of whom 5%–31% had CQF (9–11).

In 2017, new diagnoses of CQF continued to appear in the Netherlands, often with severe complications, and led to a call from multiple concerned parties, including politicians, the QF patient association, and medical doctors for a national CQF screening program. One aspect considered for such a screening program is whether its costs are economically balanced with the expenditure (12,13). To answer this question, we assessed the cost-effectiveness of a screening program for CQF in the Netherlands.

Methods

Overview

We developed a health-economic decision model to compare estimated costs and effects of a 1-time screening program for CQF with no such screening program (Figure 1). The screening was assumed to occur in 2017, seven years after the epidemic. We estimated comparative outcomes of the model in terms of clinical events, quality-adjusted life years (QALYs), and costs from a societal perspective. We used a lifetime time horizon. Costs were annually discounted at 4% and QALYs at 1.5% (14).

Author affiliations: National Institute for Public Health and the Environment, Bilthoven, the Netherlands (P.T. de Boer, M.M.A. de Lange, C.C.H. Wielders, F. Dijkstra, W. van der Hoek); University Medical Centre Utrecht, Utrecht, the Netherlands (S.E. van Roeden, J.J. Oosterheert); Radboud university medical center, Nijmegen, the Netherlands (C.P. Bleeker-Rovers); Jeroen Bosch Hospital, 's-Hertogenbosch, the Netherlands (P.M. Schneeberger)

DOI: <https://doi.org/10.3201/eid2602.181772>

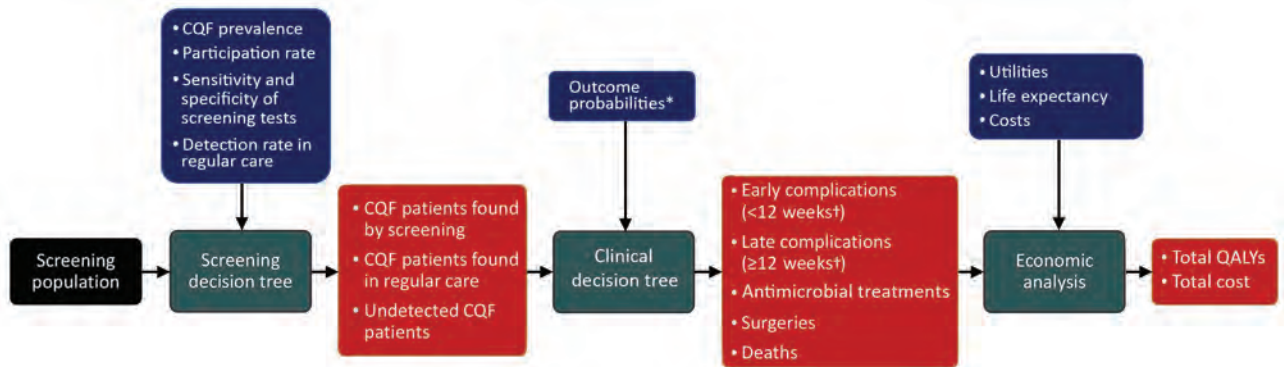


Figure 1. Schematic overview of the health-economic model in a study of the cost-effectiveness of screening for CQF, the Netherlands, 2017. Black square represents model input; green squares are model processes; blue squares are model parameters; and red squares are model outputs. Individual decision trees for screening and clinical outcomes are shown in Appendix Figure 1 (<https://wwwnc.cdc.gov/EID/article/26/2/18-1772-App1.pdf>). *Outcome probabilities differed among patients found by screening, patients found in regular care, and patients who remained undetected. †Weeks after diagnoses. CQF, chronic Q fever; QALY, quality-adjusted life year.

Screening Population

The analysis focused on adults ≥ 18 years of age. Because the prevalence of CQF is not uniformly distributed in the population (most QF patients resided in the south of the Netherlands; patients can have risk factors for CQF), we considered different subgroups for screening. We used the Netherlands population data from 2017 (15). First, we stratified the population on the basis of residence area between high, middle, and low QF incidence areas. For this stratification, we used spatial data on QF notifications and farms with QF outbreaks during the epidemic period (2007–2010). Next, we further divided these subgroups on the basis of a risk factor for CQF between persons with a cardiovascular risk factor, an immunocompromised status, or an unknown risk

status. The last group was labeled as unknown because the prevalences of heart valve disorders and aortic aneurysms are underreported. Because these cardiovascular prevalences increase with age, the unknown subgroup was split between persons < 60 years and ≥ 60 years of age. Thus, we considered 12 (3×4) subgroups (Table 1). We obtained prevalences of diagnosed and undiagnosed risk factors from the literature (16–21) (Appendix Table 1, <https://wwwnc.cdc.gov/EID/article/26/2/18-1772-App1.pdf>).

Model

We used a decision-tree model that consisted of 2 parts: a screening part and a clinical part (Appendix Figure 1). CQF is usually characterized by persistent high IgG against *C. burnetii* phase I, often in the

Table 1. Subgroup criteria in a study of the cost-effectiveness of screening for CQF, the Netherlands, 2017*

Category	Condition
Area of residence	
High incidence	≥ 50 acute QF notifications/100,000 inhabitants <i>and</i> > 2 acute QF notifications OR presence of a farm with QF abortion waves† within a 5-km range during the epidemic period.
Middle incidence	10–49 acute QF notifications/100,000 inhabitants <i>and</i> > 2 acute QF notifications OR presence of a farm that tested positive in the mandatory bulk tank milk monitoring initiated during the QF epidemic.
Low incidence	< 10 acute QF notifications/100,000 inhabitants OR < 2 notifications during the epidemic period.
Preexisting risk factor	
Diagnosed cardiovascular risk factor	Heart valve disorder (all types of defects), heart valve prosthesis, aortic aneurysm, prosthesis/stent, history of endocarditis and congenital heart anomalies.
Immunocompromised patients	HIV infection, asplenia, spleen disorder, malignancy or bone marrow transplantations and patients using immunosuppressant drugs. As proxy for patients using immunosuppressant drugs, prevalence data were used of rheumatoid arthritis patients and patients with inflammatory bowel disease, assuming these patients frequently use immunosuppressant medication.
Unknown, ≥ 60 y	Age ≥ 60 y AND no or undiagnosed cardiovascular risk factor, e.g., heart valve disorder, aortic aneurysm.
Unknown 18–59 y	Age 18–59 y AND no or undiagnosed cardiovascular risk factor, e.g., heart valve disorder, aortic aneurysm.

*The epidemic period was 2007–2010. QF, Q fever.

†Abortion of $> 5\%$ of pregnant goats in a farm over a 4-week period.

presence of high IgG against phase II (2,3). In the current clinical setting in the Netherlands, patients suspected of having CQF are tested with immunofluorescence assay (IFA) for IgG against phase I. However, IFA is a nonautomated and subjective test, and its use might not be feasible for a large-scale screening program (22). Therefore, we proposed an initial screening round with the ELISA for IgG against phase II, and positive samples were tested with IFA for IgG against phase I. In the sensitivity analysis, we explored a scenario with direct testing with IFA for IgG against phase I.

In the clinical part, patients were first classified among proven, probable, or possible CQF, according to the guideline of the Dutch Q Fever Consensus Group (23). This classification ranks the probability of having CQF based on PCR, serology, clinical parameters, imaging techniques, and pathologic findings (Appendix Table 2). Next, patients were divided by focus of infection and whether CQF led to an early complication (before diagnosis or within 12 weeks after diagnosis). Complications considered were heart failure, symptomatic aneurysm, arterial embolic complication, and other complications. After diagnosis, antimicrobial treatment can be initiated, possibly combined with a surgical procedure. Then, patients may have a late complication (≥ 12 weeks after diagnosis) and can die of CQF.

CQF Prevalence

The prevalence of CQF 7 years after the QF epidemic is uncertain because the average duration between infection and development of CQF is unknown. Therefore, we considered 2 scenarios, a low CQF prevalence scenario and a high CQF prevalence scenario. For both scenarios, we estimated the prevalence of CQF in 3 consecutive steps: 1) define the risk for *C. burnetii* infection per QF incidence area, 2) multiply by the risk for CQF given infection per risk group,

and 3) adjust the CQF prevalence from directly after the epidemic to the year of screening 7 years later. This final step accounts for a decrease of CQF prevalence over time, for instance, because of death or earlier diagnosis.

We selected parameter values for the low and high CQF prevalence scenarios (Table 2). In the low CQF prevalence scenario, we assumed that only patients with a *C. burnetii* infection during the epidemic period were at risk for CQF. We divided them among high, middle, and low QF incidence areas using small geographic areas (4-digit postal code) and used incidence rates of QF notifications during the epidemic period for each incidence area. To adjust for underreporting, we multiplied the incidence rates by 12.6 (7). In the high CQF prevalence scenario, we assumed that all patients who seroconverted after the epidemic can develop CQF. For this scenario, we used larger geographic areas (3-digit postal code areas) and *C. burnetii* seroprevalences for each incidence area from the literature (24,25). In the second step, we estimated the risk for CQF using targeted screening studies for CQF conducted during or immediately after the epidemic (Appendix Table 4) (9–11,26,27). In the third step, we based the adjustment of the CQF prevalence from directly after the epidemic to the year of screening for the low CQF prevalence scenario on the reduction of CQF patients in the national CQF database over time (28). For the high prevalence scenario, we estimated this adjustment factor on the risk for CQF among patients with a heart valve disorder in studies conducted immediately after the outbreak (9,10) and a study conducted in 2016–2017 (29) (Appendix).

Detection Rate of Screening and Regular Care

We assumed a participation rate in the screening program of 50%, which is the lower bound of previous targeted screening programs for CQF in the Netherlands (10,27,30). The prevalence of CQF was assumed

Table 2. Prevalence scenarios explored in a study of the cost-effectiveness of screening for CQF, the Netherlands, 2017*

Parameter	Low CQF prevalence scenario	High CQF prevalence scenario
Risk for <i>Coxiella burnetii</i> infection	Based on incidence rates of new infections during the epidemic period, adjusted for underreporting	Based on overall seroprevalences from the literature (24,25)
High incidence area, %	2.15	10.7
Middle incidence area, %	0.15	2.30
Low incidence area, %	0.027	1.00
Risk for CQF after <i>C. burnetii</i> infection	Equal for low and high CQF prevalence scenarios. Risk for CQF after infection is 7% for patients with heart valve disorders/prostheses, 29.3% for patients with vascular disorders/prostheses, and 6.9% for immunocompromised patients (probable or proven CQF). Risk for possible CQF in patients without risk factor is 0.2%.	
Adjustment factor to account for reduction of CQF prevalence from directly after epidemic (2010–2012) to year of screening (2017)	0.25	0.52

*The epidemic period was 2007–2010. CQF, chronic Q fever.

to be equal between participating and nonparticipating persons; hence, the participation rate affects only the number of CQF patients detected but not the cost-effectiveness of screening. We obtained sensitivity and specificity of ELISA from the literature; these values accounted for decreasing sensitivity over time after infection (31) (Appendix Table 5). CQF patients with high IgG against phase I were assumed to also have high IgG against phase II (C.C.H. Wielders, unpub. data [32]), which implies that all CQF patients test positive with ELISA. In the second screening round using IFA, patients with an IgG $\geq 1:512$ against phase I were clinically evaluated. The detection rate of CQF in regular care is unknown; we used a detection rate of 80% for proven CQF, 50% for probable CQF, and 10% for possible CQF.

Outcome Probabilities

We estimated outcome probabilities using data from the national CQF database (Appendix Table 6). This database contains information about 439 CQF patients in the Netherlands, of whom 249 had proven, 74 had probable, and 116 had possible CQF (6). To estimate the effectiveness of screening, we stratified outcome data between CQF patients detected by regular healthcare (358 patients) and CQF patients detected by screening (78 patients). Proven CQF patients detected through screening had a 4.0 (95% CI 3.3–4.7) times lower risk for an early complication, 2.8 (95% CI 2.2–3.3) times lower risk for surgery, and 1.8 (95% CI 1.1–2.5) times lower risk for CQF-related death compared with proven CQF patients detected through regular care. The risk for a late complication did not differ significantly (risk ratio 0.7 [95% CI 0.1–1.4]) and was assumed to be equal between screening and regular care. For probable CQF patients, outcome probabilities were not significantly lower for screened patients than for patients identified through regular care. To avoid overestimation of the effect of screening, we conservatively assumed no effectiveness of screening for probable CQF patients and explored a scenario in which probable CQF patients benefit from screening in the sensitivity analysis. No clinical events were assumed in possible CQF patients (6). For undetected CQF patients, we used a higher risk for a late complication and death than for patients found through regular care.

QALYs and Costs

We estimated QALYs by multiplying the utility value associated with a certain health status by the years lived in that status. We obtained utility data for CQF-related complications from the literature (33–36) (Appendix

Table 7). We applied a disutility for antimicrobial treatment (37,38). Average life expectancies of patients with premature CQF-related death were obtained from the national CQF database (6) (Appendix Table 8). For patients without premature CQF-related death, we assumed life expectancy to be half the life expectancy of a person at that age from the general population (39). We also obtained utility values for the general population from the literature (40) (Appendix).

We calculated costs in 2016 Euros (Appendix Table 9). Direct healthcare costs include costs of screening, diagnostic procedures, surgical procedures, antimicrobial drugs, specialist consultations, and lifelong costs of chronic complications. According to the national cost-effectiveness guideline (41), indirect healthcare costs (healthcare costs unrelated to CQF in life-years gained) should be taken into account, which we estimated using a prespecified tool (42). Because guidelines from other countries do not consider indirect healthcare costs, we show results without including indirect healthcare costs in the sensitivity analysis. Direct nonhealthcare costs include travel costs, and indirect nonhealthcare costs include productivity losses resulting from work absence (Appendix).

Cost-effectiveness and Sensitivity Analysis

We calculated the incremental cost-effectiveness ratio (ICER) of screening versus no screening by dividing the difference in costs by the difference in QALYs. We conducted a multivariate probabilistic sensitivity analysis using 10,000 simulations in which we varied a set of parameters at the same time within their uncertainty distributions. We conducted univariate sensitivity analyses, in which we varied several parameters one by one.

Results

CQF Prevalence

Depending on the size of the areas, 12% of the population (3-digit postal codes) or 16% of the population (4-digit postal codes) live in high QF incidence areas (Figure 2; Appendix Table 10). For the low CQF prevalence scenario, we estimated the number of *C. burnetii* infections at 42,143, resulting in 414 CQF patients directly after the epidemic and 102 CQF patients in the year of screening. For the high CQF prevalence scenario, the number of *C. burnetii*-infected persons was estimated to be 391,188, resulting in 3,842 CQF patients directly after the epidemic and 1,844 CQF patients in 2017. We also stratified the population by risk factor (Appendix Table 11). The prevalence of CQF varied substantially among risk groups and by

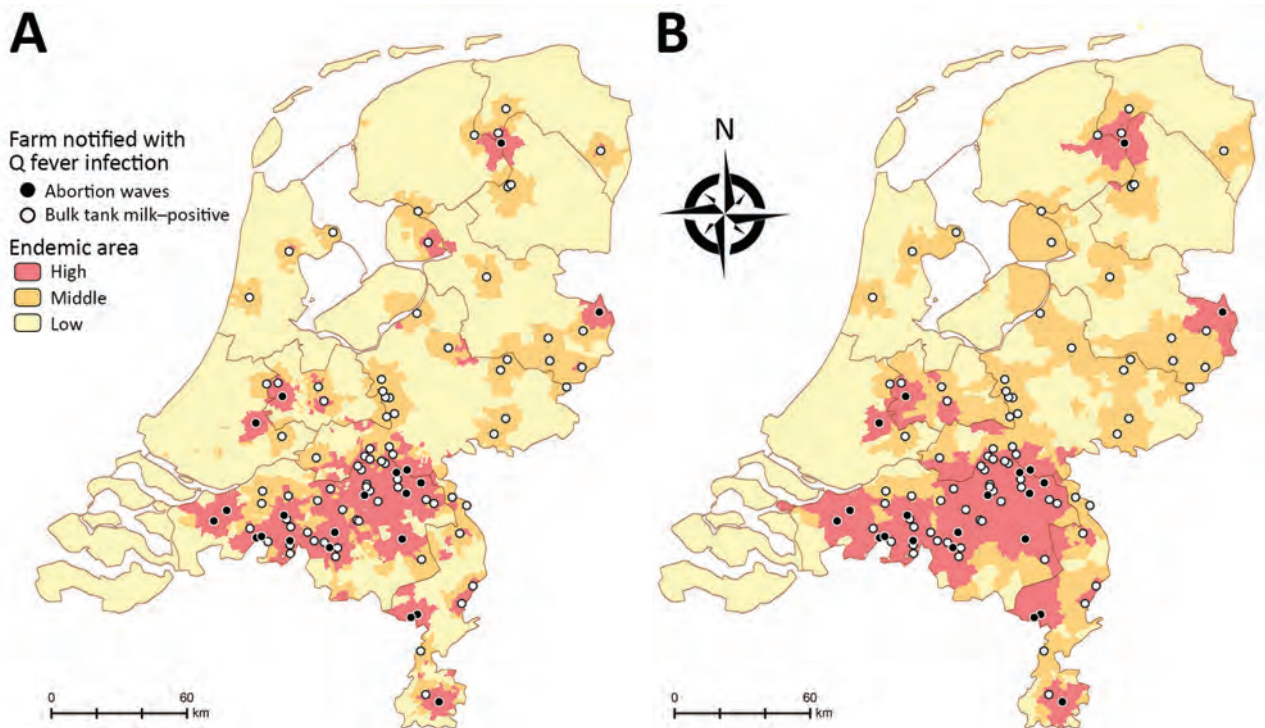


Figure 2. Geographic categorization of high, middle, and low Q fever incidence in the Netherlands using (A) 4-digit postal code areas and (B) 3-digit postal code areas. Incidence level was based on acute Q fever notifications and the proximity of farms with Q fever during the epidemic period (2007–2010).

residence area (Table 2); the highest prevalence occurred in cardiovascular risk patients living in high incidence areas (Appendix Table 12).

Clinical Impact

We determined the number of CQF patients and prevented clinical events for each subgroup (Table 3, <https://wwwnc.cdc.gov/EID/article/26/2/18-1772-T3.htm>; Appendix Tables 13, 14). Most CQF-related events are prevented by screening of cardiovascular risk groups living in high incidence areas. At an assumed participation rate of 50%, 8 complications, 4 surgeries, and 2 premature deaths are prevented for the low CQF prevalence scenario and 105 complications, 54 surgeries, and 26 premature deaths for the high CQF prevalence scenario. Screening of immunocompromised patients or all adults ≥ 60 years of age living in high-risk incidence areas, or screening of cardiovascular risk groups in middle-incidence areas, also could prevent a substantial number of clinical events.

Cost-effectiveness

We determined the incremental costs, incremental QALYs, and ICERs for each subgroup (Table 3; Appendix Tables 15–17). The ICER of screening of

cardiovascular risk groups living in high QF incidence areas was €31,737 per QALY for the low CQF prevalence scenario and cost-saving for the high CQF prevalence scenario. The next most cost-effective strategy would be screening of immunocompromised patients living in high incidence areas; ICERs were €66,145 per QALY for the low CQF prevalence scenario and €2,312 per QALY for the high CQF prevalence scenario. The ICER of screening for cardiovascular risk groups would increase substantially outside the high QF incidence area. For the high CQF prevalence scenario, the ICER increased from cost-saving to €12,929 per QALY in middle QF incidence areas and to €34,912 per QALY in low QF incidence areas. The ICER of screening for adults >60 years of age with an unknown risk factor living in high QF incidence areas was €679,136 per QALY in the low CQF prevalence scenario and €69,208 per QALY in the high CQF prevalence scenario. Screening of adults 18–59 years of age with an unknown risk factor was at least €8 million per QALY.

Sensitivity Analysis

We conducted a multivariate probabilistic sensitivity analysis (Figure 3; Appendix Figure 2). In the low

CQF prevalence scenario, screening of cardiovascular risk patients living in high incidence areas had a 3.1% chance of an ICER <€20,000 per QALY and 92.5% chance of an ICER <€50,000 per QALY (Figure 3, panel A). In the high CQF prevalence scenario, screening had a 54.4% chance of being cost-saving and 100% chance of an ICER <€20,000 per QALY (Figure 3, panel B) for this subgroup.

The ICER was most sensitive to the lifetime costs of complications, the life expectancy of CQF patients, and the effectiveness of the screening program. For the low CQF prevalence scenario, the ICER varied from €17,561 to €63,449 per QALY (Figure 3, panel C). Adding the effectiveness of screening for probable CQF patients changed the ICER from €31,737 to €29,585 per QALY. Exclusion of indirect healthcare costs reduced the ICER to €25,681 per QALY (ICERs without the inclusion of indirect healthcare costs of other subgroups are shown in Appendix Table 18). Adding additional program costs of €11.36 per participant increased the ICER to €53,639 per QALY. For the high CQF prevalence scenario, the ICER remained cost-saving in most scenarios explored, and the highest ICER found was €1,903 per QALY (Figure 3, panel D).

Discussion

We assessed the cost-effectiveness of a 1-time screening program for CQF in the Netherlands 7 years after a large QF epidemic. Cost-effectiveness varied substantially among areas and risk groups, and the results are highly sensitive to the prevalence of CQF. In a high CQF prevalence scenario, screening of cardiovascular risk patients living in high QF incidence areas during the epidemic was estimated cost-saving, whereas in a low CQF prevalence scenario the ICER was €31,737 per QALY for this subgroup. We found substantially higher ICERs for screening in areas with lower QF incidence during the epidemic or for screening of adults with an unknown risk factor for CQF.

A limitation is that the true prevalence of CQF 7 years after the epidemic is unknown. This prevalence can be affected by many factors, such as death from CQF or other causes, earlier diagnosis in regular care, and the background QF incidence after the epidemic. To account for uncertainty in CQF prevalence, we conducted a low and high CQF prevalence analysis. The estimated 42,000 new *C. burnetii* infections and 411 CQF patients during or after the epidemic low

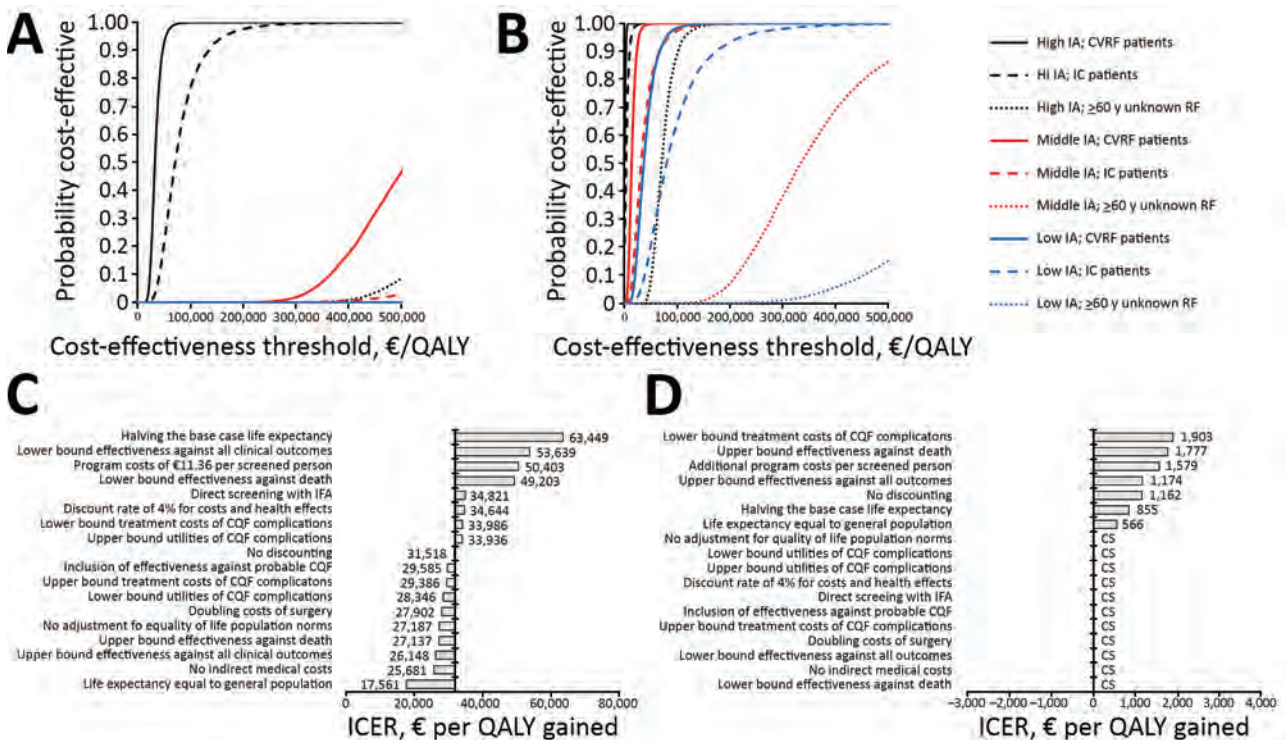


Figure 3. Sensitivity analysis of a screening program for CQF 7 years after the 2007–2010 epidemic, the Netherlands. A, B) Results of the multivariate probabilistic sensitivity analysis of screening in various target groups for a low CQF prevalence scenario (A) and a high CQF prevalence scenario (B). C, D) Results of a univariate sensitivity analysis of screening for chronic Q fever in patients with CVRFs living in high incidence areas for a low CQF prevalence scenario (C) and a high CQF prevalence scenario (D). CQF, chronic Q fever; CVRF, cardiovascular risk factor; IA, incidence area; IC, immunocompromised; ICER, incremental cost-effectiveness ratio; IFA, immunofluorescence assay; QALY, quality-adjusted life year; RF, risk factor.

CQF prevalence scenario estimated correspond with previous estimates from the literature (7) or CQF patients included in the national database until May 2016 (6). However, these numbers are thought to be the absolute minimum. Only 23% of the proven CQF patients had a diagnosed acute QF episode (6), and a postmortem study among patients with a history of heart valve surgery in the epidemic area indicates that CQF possibly contributed to the death in 15% of the patients (9). The high CQF prevalence scenario could be the upper range because it does not account for preexisting immunity from before the epidemic. It is therefore likely that the true prevalence falls within the reported ranges.

Recent seroprevalence studies performed outside high QF incidence areas are lacking. Underreporting of QF could be higher in these areas because medical doctors are less familiar with QF symptoms (7). Furthermore, the geographic division between high, middle, and low QF incidence areas is arbitrary. Persons could be infected while traveling, and the extent to which farms with positive bulk milk samples contribute to disease spread is uncertain because 1 infected goat could yield a positive result.

The effectiveness of screening on the prevention of CQF-related complications and premature death is not well documented. We estimated the effectiveness by comparing outcome data between patients detected by screening and by regular care. We did this comparison separately for different CQF categories (proven, probable, or possible), but the effectiveness of screening can still be biased by uncontrolled confounders, such as age and presence of underlying conditions. The effectiveness of antimicrobial treatment for CQF has never been assessed in a randomized clinical trial. Surgery is known to have a positive effect on survival of CQF patients with vascular infection (3).

Our cost-effectiveness analysis is based on data from several sources in the Netherlands, such as spatial data on notifications of acute QF, seroprevalence data of *C. burnetii* infections, risk factor-specific probabilities of CQF given infection, and clinical data from a large number of CQF patients. However, combining data from different sources could also introduce biases when study populations do not exactly overlap or screening studies are conducted at different time-points.

Results of our study could also be relevant for other countries, where CQF also might be underreported. For instance, the seroprevalence of *C. burnetii* infection in the United States was estimated

at 3.1% (43), representing millions of infections and potentially thousands of CQF cases, but no high numbers of CQF have been reported. An explanation may be that *C. burnetii* infections in the United States originate from cattle. The *C. burnetii* strains circulating in cattle differ from and are considered less pathogenic than the strains in small ruminants (3). In France, however, *C. burnetii* causes 5% of all endocarditis (44), and in Israel, *C. burnetii* infection was found in 9% of patients undergoing valve surgical procedure caused by endocarditis (45).

Cost-effectiveness is not the only criterion in deciding whether a screening program is justified (12). Screening for CQF is based on an antibody profile suggesting a chronic infection but cannot always be linked to a focus of infection (probable or possible CQF patients). Therefore, physicians must make difficult decisions about whether long-term antimicrobial treatment should be initiated when the outcome is uncertain and adverse events frequently occur. Raoult (46) has recently proposed alternative definition criteria for CQF from the consensus guideline in the Netherlands; these criteria could exclude most probable and possible CQF patients from follow-up but also may be less sensitive in the diagnosis of proven CQF (47).

When screening for CQF would be limited to subgroups for which screening is most cost-effective, a substantial proportion of CQF patients will remain undetected. Serologic follow-up for patients with acute QF is therefore recommended, even in absence of a risk factor for CQF (32). However, compliance with this recommendation was suboptimal during the epidemic (48), and many patients experience an acute infection asymptotically or do not have the infection diagnosed. Alongside a standalone screening program, case finding could be implemented in regular care, in which the physician decides whether a patient should be screened according to a risk profile. Also, a combination of case-finding and screening programs among high-risk groups could be initiated; this approach has also been suggested for hepatitis B and hepatitis C (49).

Acknowledgments

We thank Albert Jan van Hoek for providing useful comments on the methods and manuscript and Ben Bom for creating the Q fever incidence maps.

This study was financed from the regular budget of the Centre for Infectious Disease Control made available by the Ministry of Health, Welfare and Sport, project no. V/150207/17/RI.

About the Author

Mr. de Boer is a health economist at the Center of Infectious Diseases of the National Institute for Public Health and the Environment, the Netherlands. His work focuses on the cost-effectiveness of preventive interventions against infectious diseases, such as vaccination and screening programs.

References

- European Centre for Disease Prevention and Control. Risk assessment on Q fever. Stockholm: The Centre; 2010.
- Maurin M, Raoult D. Q fever. *Clin Microbiol Rev.* 1999;12:518–53. <https://doi.org/10.1128/CMR.12.4.518>
- Eldin C, Mélenotte C, Mediannikov O, Ghigo E, Million M, Edouard S, et al. From Q Fever to *Coxiella burnetii* infection: a paradigm change. *Clin Microbiol Rev.* 2017;30:115–90. <https://doi.org/10.1128/CMR.00045-16>
- Fenollar F, Fournier PE, Carrieri MP, Habib G, Messana T, Raoult D. Risks factors and prevention of Q fever endocarditis. *Clin Infect Dis.* 2001;33:312–6. <https://doi.org/10.1086/321889>
- Kampschreur LM, Dekker S, Hagenaars JC, Lestrade PJ, Renders NH, de Jager-Leclercq MG, et al. Identification of risk factors for chronic Q fever, the Netherlands. *Emerg Infect Dis.* 2012;18:563–70. <https://doi.org/10.3201/eid1804.111478>
- van Roeden SE, Wever PC, Kampschreur LM, Gruteke P, van der Hoek W, Hoepelman AIM, et al. Chronic Q fever-related complications and mortality: data from a nationwide cohort. *Clin Microbiol Infect.* 2019; 25:1390–8. <https://doi.org/10.1016/j.cmi.2018.11.023>
- van der Hoek W, Hogema BM, Dijkstra F, Rietveld A, Wijkmans CJ, Schneeberger PM, et al. Relation between Q fever notifications and *Coxiella burnetii* infections during the 2009 outbreak in the Netherlands. *Euro Surveill.* 2012;17:20058.
- National Institute for Public Health and the Environment. Q fever [in Dutch] [cited 2017 May 23]. http://www.rivm.nl/Onderwerpen/Q/Q_koorts
- Kampschreur LM, Oosterheert JJ, Hoepelman AI, Lestrade PJ, Renders NH, Elsmans P, et al. Prevalence of chronic Q fever in patients with a history of cardiac valve surgery in an area where *Coxiella burnetii* is epidemic. *Clin Vaccine Immunol.* 2012;19:1165–9. <https://doi.org/10.1128/CVI.00185-12>
- Wegdam-Blans MC, Stokmans RA, Tjhie JH, Korbeek JM, Koopmans MP, Evers SM, et al. Targeted screening as a tool for the early detection of chronic Q fever patients after a large outbreak. *Eur J Clin Microbiol Infect Dis.* 2013;32:353–9. <https://doi.org/10.1007/s10096-012-1749-9>
- Hagenaars JC, Wever PC, van Petersen AS, Lestrade PJ, de Jager-Leclercq MG, Hermans MH, et al. Estimated prevalence of chronic Q fever among *Coxiella burnetii* seropositive patients with an abdominal aortic/iliac aneurysm or aorto-iliac reconstruction after a large Dutch Q fever outbreak. *J Infect.* 2014;69:154–60. <https://doi.org/10.1016/j.jinf.2014.03.009>
- Wilson JMG, Jungner G. Principles and practice of screening for disease [cited 2017 Sep 1]. <http://apps.who.int/iris/handle/10665/37650>
- Andermann A, Blancaquaert I, Beauchamp S, Déry V. Revisiting Wilson and Jungner in the genomic age: a review of screening criteria over the past 40 years. *Bull World Health Organ.* 2008;86:317–9. <https://doi.org/10.2471/BLT.07.050112>
- National Health Care Institute. Guideline for economic evaluations in healthcare [cited 2017 Dec 1]. <https://english.zorginstituutnederland.nl/publications/reports/2016/06/16/guideline-for-economic-evaluations-in-healthcare>
- Statistics Netherlands. Population; gender, age, marital status and region, 1 January [in Dutch] [cited 2017 Dec 1]. <http://statline.cbs.nl/Statweb/publication/?DM=SLNL&PA=03759ned&D1=0-2&D2=0-117&D3=0&D4=l&HDR=T&STB=G2,G3,G1&VW=T>
- Vermeer-de Bondt PE, Schoffelen T, Vanrolleghem AM, Isken LD, van Deuren M, Sturkenboom MC, et al. Coverage of the 2011 Q fever vaccination campaign in the Netherlands, using retrospective population-based prevalence estimation of cardiovascular risk-conditions for chronic Q fever. *PLoS One.* 2015;10:e0123570. <https://doi.org/10.1371/journal.pone.0123570>
- van Hoek AJ, Andrews N, Waight PA, Stowe J, Gates P, George R, et al. The effect of underlying clinical conditions on the risk of developing invasive pneumococcal disease in England. *J Infect.* 2012;65:17–24. <https://doi.org/10.1016/j.jinf.2012.02.017>
- Volksgesondheidszorg.info. Reumatoïd artritis (RA) > numbers & context > current situation [in Dutch] [cited 2017 May 1]. <https://www.volksgesondheidszorg.info/onderwerp/reumato%C3%AFde-artritis-ra/cijfers-context/huidige-situatie#node-prevalentie-van-reumatoïde-artritis>
- de Groof EJ, Rossen NG, van Rhijn BD, Karregat EP, Boonstra K, Hageman I, et al. Burden of disease and increasing prevalence of inflammatory bowel disease in a population-based cohort in the Netherlands. *Eur J Gastroenterol Hepatol.* 2016;28:1065–72. <https://doi.org/10.1097/MEG.0000000000000660>
- d'Arcy JL, Coffey S, Loudon MA, Kennedy A, Pearson-Stuttard J, Birks J, et al. Large-scale community echocardiographic screening reveals a major burden of undiagnosed valvular heart disease in older people: the OxVALVE Population Cohort Study. *Eur Heart J.* 2016;37:3515–22. <https://doi.org/10.1093/eurheartj/ehw229>
- Pleumeekers HJ, Hoes AW, van der Does E, van Urk H, Hofman A, de Jong PT, et al. Aneurysms of the abdominal aorta in older adults. The Rotterdam Study. *Am J Epidemiol.* 1995;142:1291–9. <https://doi.org/10.1093/oxfordjournals.aje.a117596>
- van der Hoek W, Wielders CC, Schimmer B, Wegdam-Blans MC, Meekeleenkamp J, Zaaijer HL, et al. Detection of phase I IgG antibodies to *Coxiella burnetii* with EIA as a screening test for blood donations. *Eur J Clin Microbiol Infect Dis.* 2012;31:3207–9. <https://doi.org/10.1007/s10096-012-1686-7>
- Wegdam-Blans MC, Kampschreur LM, Delsing CE, Bleeker-Rovers CP, Sprong T, van Kasteren ME, et al.; Dutch Q Fever Consensus Group. Chronic Q fever: review of the literature and a proposal of new diagnostic criteria. *J Infect.* 2012;64:247–59. <https://doi.org/10.1016/j.jinf.2011.12.014>
- Pijnacker R, Reimerink J, Smit LAM, van Gageldonk-Lafeber AB, Zock JP, Borlée F, et al. Remarkable spatial variation in the seroprevalence of *Coxiella burnetii* after a large Q fever epidemic. *BMC Infect Dis.* 2017;17:725. <https://doi.org/10.1186/s12879-017-2813-y>
- Brandwagt DA, Herremans T, Schneeberger PM, Hackert VH, Hoebe CJ, Paget J, et al. Waning population immunity prior to a large Q fever epidemic in the south of the Netherlands. *Epidemiol Infect.* 2016;144:2866–72. <https://doi.org/10.1017/S0950268816000741>

26. Schoffelen T, Kampschreur LM, van Roeden SE, Wever PC, den Broeder AA, Nabuurs-Fransens MH, et al. *Coxiella burnetii* infection (Q fever) in rheumatoid arthritis patients with and without anti-TNF α therapy. *Ann Rheum Dis*. 2014;73:1436–8. <https://doi.org/10.1136/annrheumdis-2014-205455>
27. Morroy G, van der Hoek W, Albers J, Coutinho RA, Bleeker-Rovers CP, Schneeberger PM. Population screening for chronic Q-fever seven years after a major outbreak. *PLoS One*. 2015;10:e0131777. <https://doi.org/10.1371/journal.pone.0131777>
28. Buijs SB, Oosterheert JJ, Van Roeden SE, Kampschreur LM, Hoepelman AI, Wever PC, et al. Still new chronic Q fever cases diagnosed more than five years after a large Q fever outbreak [cited 2019 Sep 1]. https://www.escmid.org/escmid_publications/escmid_elibrary/material/?mid=67200
29. de Lange MMA, Scheepmaker A, van der Hoek W, Leclercq M, Schneeberger PM. Risk of chronic Q fever in patients with cardiac valvulopathy, seven years after a large epidemic in the Netherlands. *PLoS One*. 2019;14:e0221247. <https://doi.org/10.1371/journal.pone.0221247>
30. Schoffelen T, Joosten LA, Herremans T, de Haan AF, Ammerdorffer A, Rümke HC, et al. Specific interferon γ detection for the diagnosis of p=revious Q fever. *Clin Infect Dis*. 2013;56:1742–51. <https://doi.org/10.1093/cid/cit129>
31. Frosinski J, Hermann B, Maier K, Boden K. Enzyme-linked immunosorbent assays in seroprevalence studies of Q fever: the need for cut-off adaptation and the consequences for prevalence data. *Epidemiol Infect*. 2016;144:1148–52. <https://doi.org/10.1017/S0950268815002447>
32. Wielders CC, van Loenhout JA, Morroy G, Rietveld A, Notermans DW, Wever PC, et al. Long-term serological follow-up of acute Q-fever patients after a large epidemic. *PLoS One*. 2015;10:e0131848. <https://doi.org/10.1371/journal.pone.0131848>
33. Franklin M, Wailoo A, Dayer MJ, Jones S, Prendergast B, Baddour LM, et al. The cost-effectiveness of antibiotic prophylaxis for patients at risk of infective endocarditis. *Circulation*. 2016;134:1568–78. <https://doi.org/10.1161/CIRCULATIONAHA.116.022047>
34. Timmers TK, van Herwaarden JA, de Borst GJ, Moll FL, Leenen LP. Long-term survival and quality of life after open abdominal aortic aneurysm repair. *World J Surg*. 2013;37:2957–64. <https://doi.org/10.1007/s00268-013-2206-3>
35. Calvert MJ, Freemantle N, Cleland JG. The impact of chronic heart failure on health-related quality of life data acquired in the baseline phase of the CARE-HF study. *Eur J Heart Fail*. 2005;7:243–51. <https://doi.org/10.1016/j.ejheart.2005.01.012>
36. Stouthard ME, Essink-Bot ML, Bonsel GJ, Barendregt JJM, Kramers PGN, van de Water HPA, et al. Disability weights for diseases in the Netherlands [cited 2019 Sep 1]. https://pure.uva.nl/ws/files/3238153/3276_ddw.pdf
37. Million M, Thuny F, Richet H, Raoult D. Long-term outcome of Q fever endocarditis: a 26-year personal survey. *Lancet Infect Dis*. 2010;10:527–35. [https://doi.org/10.1016/S1473-3099\(10\)70135-3](https://doi.org/10.1016/S1473-3099(10)70135-3)
38. World Health Organization. Global burden of disease 2004 update: disability weights for diseases and conditions. Geneva: The Organization; 2004.
39. van Geldorp MW, Eric Jamieson WR, Kappetein AP, Ye J, Fradet GJ, Eijkemans MJ, et al. Patient outcome after aortic valve replacement with a mechanical or biological prosthesis: weighing lifetime anticoagulant-related event risk against reoperation risk. *J Thorac Cardiovasc Surg*. 2009;137:881–6, 886e1–5.
40. M Versteegh M, M Vermeulen K, M A A Evers S, de Wit GA, Prenger R, A Stolk E. Dutch tariff for the five-level version of EQ-5D. *Value Health*. 2016;19:343–52. <https://doi.org/10.1016/j.jval.2016.01.003>
41. Versteegh M, Knies S, Brouwer W. From good to better: new Dutch guidelines for economic evaluations in healthcare. *Pharmacoeconomics*. 2016;34:1071–4. <https://doi.org/10.1007/s40273-016-0431-y>
42. van Baal PH, Wong A, Slobbe LC, Polder JJ, Brouwer WB, de Wit GA. Standardizing the inclusion of indirect medical costs in economic evaluations. *Pharmacoeconomics*. 2011; 29:175–87. <https://doi.org/10.2165/11586130-000000000-00000>
43. Anderson A, Bijlmer H, Fournier PE, Graves S, Hartzell J, Kersh GJ, et al. Diagnosis and management of Q fever – United States, 2013: recommendations from CDC and the Q Fever Working Group. *MMWR Recomm Rep*. 2013;62 (RR-03):1–30.
44. Fournier PE, Casalta JP, Habib G, Messana T, Raoult D. Modification of the diagnostic criteria proposed by the Duke Endocarditis Service to permit improved diagnosis of Q fever endocarditis. *Am J Med*. 1996;100:629–33. [https://doi.org/10.1016/S0002-9343\(96\)00040-X](https://doi.org/10.1016/S0002-9343(96)00040-X)
45. Maor Y, Sternik L, Orlov B, Rahav G, Keller N, Raanani E, et al. *Coxiella burnetii* endocarditis and aortic vascular graft infection: an underrecognized disease. *Ann Thorac Surg*. 2016;101:141–5. <https://doi.org/10.1016/j.athoracsur.2015.06.075>
46. Raoult D. Chronic Q fever: expert opinion versus literature analysis and consensus. *J Infect*. 2012;65:102–8. <https://doi.org/10.1016/j.jinf.2012.04.006>
47. Kampschreur LM, Wegdam-Blans MC, Wever PC, Renders NH, Delsing CE, Sprong T, et al.; Dutch Q Fever Consensus Group. Chronic Q fever diagnosis – consensus guideline versus expert opinion. *Emerg Infect Dis*. 2015;21:1183–8. <https://doi.org/10.3201/eid2107.130955>
48. Morroy G, Wielders CC, Kruisbergen MJ, van der Hoek W, Marcelis JH, Wegdam-Blans MC, et al. Large regional differences in serological follow-up of Q fever patients in the Netherlands. *PLoS One*. 2013;8:e60707. <https://doi.org/10.1371/journal.pone.0060707>
49. Health Council of the Netherlands. Screening of risk groups for hepatitis B and C [In Dutch] [cited 2018 Sep 1]. <https://www.gezondheidsraad.nl/documenten/adviezen/2016/11/01/screening-van-risicogroepen-op-hepatitis-b-en-c>

Address for correspondence: Pieter T. de Boer, National Institute for Public Health and the Environment – Centre for Infectious Disease Control, Antonie Van Leeuwenhoeklaan 9, 3721 MA Bilthoven, the Netherlands; email: pieter.de.boer@rivm.nl

Unique Clindamycin-Resistant *Clostridioides difficile* Strain Related to Fluoroquinolone-Resistant Epidemic BI/RT027 Strain

Andrew M. Skinner, Laurica Petrella, Farida Siddiqui, Susan P. Sambol, Christopher A. Gulvik, Dale N. Gerding, Curtis J. Donskey, Stuart Johnson

During a surveillance study of patients in a long-term care facility and the affiliated acute care hospital in the United States, we identified a *Clostridioides difficile* strain related to the epidemic PCR ribotype (RT) 027 strain associated with hospital outbreaks of severe disease. Fifteen patients were infected with this strain, characterized as restriction endonuclease analysis group DQ and RT591. Like RT027, DQ/RT591 contained genes for toxin B and binary toxin CDT and a *tcdC* gene of identical sequence. Whole-genome sequencing and multilocus sequence typing showed that DQ/RT591 is a member of the same multilocus sequence typing clade 2 as RT027 but in a separate cluster. DQ/RT591 produced a similar cytopathic effect as RT027 but showed delayed toxin production in vitro. DQ/RT591 was susceptible to moxifloxacin but highly resistant to clindamycin. Continued surveillance is warranted for this clindamycin-resistant strain that is related to the fluoroquinolone-resistant epidemic RT027 strain.

As the leading cause of healthcare-associated infectious diarrhea and colitis, *Clostridioides* (formerly *Clostridium*) *difficile* continues to affect patients in hospitals and extended-care facilities in the United States (1–3). Among the numerous *C. difficile* strains, none have been more important to the healthcare community at large than the strain characterized as toxinotype III, restriction endonuclease analysis (REA) group BI, PCR ribotype (RT) 027, and sequence type (ST) 1, also known as pulsed-field gel electrophoresis type NAP1

(4,5). Because the BI/RT027 strain has been associated with numerous healthcare facility outbreaks and an increasing number of illnesses and deaths, it has been called hypervirulent (6). Factors that potentially contribute to increased virulence for this strain include increased sporulation, particular DNA gyrase mutations, the ability to survive in hostile environments, and increased toxin production (7–9).

The pathogenicity locus of BI/RT027 includes a characteristic 18-bp deletion and a single-base deletion at position 117 of the *tcdC* gene (4). These mutations result in a truncated TcdC protein that is rendered nonfunctional, leading to a lack of regulation of the *tcdA* and *tcdB* genes and potentially increased toxin A and B production (4). Virulence may be further affected by the binary toxin (CDT), which is coded for by genes located outside the pathogenicity locus, and its proposed role is to increase adherence of the bacterium to the epithelium (4,10).

Presumptive detection of the BI/RT027 strain by the Xpert *C. difficile* EPI assay (Cepheid, <https://www.cephid.com>) is based on PCR amplification of targets, including the deletion at position 117 within *tcdC* and sequences within *tcdB* and the binary CDT genes (11). During the past 10 years, non-RT027 strains have emerged that test positive by this assay because they have the same or similar gene targets (12,13). Several of these non-RT027 strains also have been associated with increased numbers of illnesses and deaths, suggesting that the gene targets for this assay may be related to increased virulence (12–14).

In 2012, during a surveillance study at 2 US Veteran Affairs (VA) long-term care facilities (LTCFs) and their affiliated acute care facilities, we detected a clonal *C. difficile* outbreak at 1 of the LTCFs and the affiliated acute care facility (15). The organism was initially identified as the epidemic strain BI/RT027 after it tested positive by Xpert *C. difficile* Epi assay

Author affiliations: Edward Hines, Jr. VA Hospital, Hines, Illinois, USA (A.M. Skinner, L. Petrella, F. Siddiqui, D.N. Gerding, S. Johnson); Loyola University Medical Center, Maywood, Illinois, USA (A.M. Skinner, S. Johnson); Centers for Disease Control and Prevention, Atlanta, Georgia, USA (C.A. Gulvik); Louis Stokes VA Hospital, Cleveland, Ohio, USA (C.J. Donskey); Case Western Reserve University, Cleveland (C.J. Donskey)

DOI: <https://doi.org/10.3201/eid2602.181965>

(15). However, further analysis identified this strain as REA group DQ and RT591. We report the microbiological and molecular characterization of this strain and the clinical findings of the infected patients.

Methods

During February 2012–August 2012, we obtained swab specimens from the perirectal area of asymptomatic LTCF patients at 2 VA facilities in Cleveland, Ohio, and Chicago, Illinois, USA, as part of a validation study comparing PCR using the Xpert *C. difficile* Epi assay and culture (15). In addition, fecal specimens from symptomatic patients with *C. difficile* infection (CDI) were cultured for *C. difficile* as part of a larger surveillance study of *C. difficile* in each LTCF and the associated acute care facility at these 2 sites (16). Specimens obtained from the perirectal area using BD BBL CultureSwabs (Becton Dickinson, <https://www.bd.com>) and submitted fecal specimens from symptomatic patients were cultured anaerobically on selective media as previously described (15). We reviewed medical records to obtain information about demographics, medical conditions, medications, CDI treatment, and outcomes. The severity of CDI and determination of initial versus recurrent cases were classified in accordance with the Infectious Diseases Society of America and Society for Healthcare Epidemiology of America *C. difficile* infection guidelines (17). The institutional review board of each hospital approved the study protocol.

REA

Recovered *C. difficile* isolates were first subjected to typing by REA. Using the methods provided by Clabots et al. (18), total cellular DNA was purified and subjected to *Hind*III restriction enzyme digestion and electrophoresis. The resulting banding patterns were then compared with a known database. All isolates representing a newly recognized REA type that corresponded to a presumptive BI/RT027 identified by the Xpert *C. difficile* Epi assay were subjected to PCR ribotyping, whole-genome sequencing (WGS), multilocus sequence typing (MLST), and PCR amplification of *cdtA*, *cdtB*, *tcdA*, and *tcdB* and an 18-bp deletion in *tcdC*. Sequencing of *tcdC* (1 isolate), toxinotyping (1 isolate), toxin production in vitro (1 isolate per REA strain group), and antimicrobial susceptibility testing (6 isolates) were performed on selected isolates.

PCR Ribotyping

We characterized recovered *C. difficile* isolates using high-resolution capillary gel electrophoresis–based PCR ribotyping. We analyzed these isolates against

a library of standard profiles, as described previously in the internationally validated consensus protocol from Fawley et al. (19).

Gene Analysis of Binary Toxin CDT, Toxins A and B, and the Negative Toxin Regulator

We conducted PCR amplification of *cdtA*, *cdtB*, *tcdA*, and *tcdB* and an 18-bp deletion in *tcdC* on all isolates identified as BI/RT027 and DQ/RT591 as previously described (20). In addition, by using primers previously described by Rupnik et al. (21), we amplified *cdtB* and *tcdB* by PCR to confirm the presence of CDT and toxin B on a representative DQ/RT591 isolate followed by amplification and sequencing of the *tcdC* gene. A full-length *tcdC* PCR was performed using the following primers to produce a 910-bp product: forward primer ACTGTTTATTGCAAT-TATAAAAACATCT; reverse primer TTACTT-TATTTTGTAATAATTATGCTTAGGG. PCR amplicons were gel purified, sequenced, and compared with BI and strain 630.

Toxinotyping

We conducted toxinotyping on a representative DQ/RT591 isolate by performing restriction fragment-length polymorphism PCR of the B1 and A3 fragment. We assessed for variation in the first 3-kbp of *tcdB* and a repetitive 3-kbp fragment in *tcdA* (21).

WGS and MLST

We conducted WGS using a Nextera kit (Illumina, <https://www.illumina.com>) to prepare genomic DNA libraries and sequenced the RT591 organism using an Illumina MiSeq producing 2×250-bp read sets in accordance with the manufacturer's protocols. Reads were filtered with SolexaQA++ 3.1 by dynamic trimming bases lower than Phred 30 and discarding reads <50-bp long. (22) We then assembled high-fidelity filtered reads into contigs at least 500 bp long with SPAdes 3.6.2 (22,23). Isolates that met the following 5 molecular testing criteria (positive for *cdtA*, *cdtB*, *tcdA*, and *tcdB* and an 18-bp deletion in *tcdC*) were then analyzed by genomewide average nucleotide identity (ANI). We computed pairwise ANI values between genomes from NUCmer v3.1 alignments aided by PyANI version 0.1 (24). Pairwise identity values were sorted into a 2-dimensional matrix with pandas version 0.15.2 in Python, and a heatmap of identity values with hierarchical clustering linkages was visualized with gplots version 2.16.0 in R (25). DQ/RT591 genomes also had single-nucleotide polymorphisms (SNPs) identified with Parsnp version 1.3.

We retrieved all STs on PubMLST's webserver (<https://pubmlst.org/cdifficile>) (351 as of June 28, 2016) to compare distances among STs. The database of profiles was based on the first scheme created for *C. difficile*, which uses the loci of *adk*, *atpA*, *dxr*, *glyA*, *recA*, *sodA*, and *tpi*. Of the 3,501-bp length for each ST, 524 positions were found to have a nucleotide variant among the 351 STs. The variable sites were given to RAxML version 8.1.17 with the generalized time-reversible substitution model, and the tree was visualized in Figtree version 1.4.2 (26).

In Vitro Toxin Production and Antimicrobial Susceptibility Testing

We determined toxin production on *C. difficile* isolate supernatants of representative isolates of 5 different REA group strains after 24, 48, and 72 hours of growth in brain heart infusion broth media (27). Toxin concentrations were determined by enzyme immunoassay (*C. difficile* toxA/B II EIA; TechLab, <https://www.techlab.com>) and interpolation from a standard curve using a toxin A standard of known concentration. Assays were performed in triplicate on a representative DQ isolate and compared with supernatants from toxigenic strains BI (RT027), J (RT001), AF (RT244), and a nontoxigenic strain, REA group T. A qualitative cytotoxin analysis was performed on the representative isolate supernatants using human fibroblast cells (Bartels cytotoxicity assay; Trinity Biotech, <https://trinitylifesciences.com>). We determined antimicrobial susceptibilities by Etest (bioMérieux, <https://www.biomerieux-usa.com>) for moxifloxacin, ceftriaxone, azithromycin, and clindamycin on taurocholate fructose agar plates (28,29). We confirmed the susceptibility results for moxifloxacin and clindamycin by testing 5 additional unique strains of BI and DQ recovered from patients at the VA site where the DQ outbreak occurred. We used Clinical and Laboratory Standards Institute guidelines for resistance cut-off values (30,31).

Statistical Analysis

We compared characteristics and outcomes of patients colonized or infected with BI/NAP1/027 and other strain types with those of patients colonized or infected with DQ/591 strains. Student *t*-test was used for normally distributed data and Fisher exact test for categorical data. We analyzed data using SPSS Statistics 10.0 (IBM, <https://www.ibm.com>).

Results

REA group BI strains were the most common strains recovered from both VA sites and accounted

for 33 (40%) of the 83 isolates at the Cleveland site. In addition, 16 (19%) of the isolates from 15 Cleveland patients were identified as REA strain DQ, even though the corresponding Xpert *C. difficile* EPI assay results indicated the presence of the NAP1 strain (i.e., REA group BI). No DQ strains were found at the Chicago site.

We compared baseline characteristics and outcomes of the 15 patients with fecal cultures positive for the DQ strain with those of the 22 patients with BI/NAP1/027 strains and 27 with other strain types (Table). Ten (67%) of the 15 patients with the DQ strain were LTCF residents, 4 (27%) were on the spinal cord injury unit, and 1 was hospitalized on a medical ward. Of the 7 patients with CDI caused by DQ strains, 3 (43%) met criteria for severe CDI, but none had fulminant CDI. All 7 CDI cases were healthcare associated; 3 of these patients had onset in the hospital, and 4 had onset in the LTCF. In all patients with CDI caused by DQ strains, diarrhea resolved with therapy, but CDI recurred in 3. Patients colonized or infected with DQ strains were significantly more likely than those with BI/NAP1/027 or other strain types to be LTCF residents and to have received antimicrobial drugs during the past 90 days. Patients with other strain types were significantly less likely than patients with DQ strains to have a recent intensive care unit admission, to have healthcare-associated CDI, or to die within 6 months after the CDI diagnosis.

The *Hind*III REA banding patterns differed between the DQ and BI strains (Figure 1, panel A). The PCR ribotype patterns were more similar, except for the RT591 pattern (DQ), which was missing 2 major bands present in RT027 pattern (BI) (Figure 1, panel B).

PCR amplification of *tcdB* and *cdtB* in a representative DQ isolate indicated the presence of genes for toxin B and binary toxin CDT, consistent with the profile of the epidemic BI/RT027 strain (data not shown). In addition, amplification and sequencing of the *tcdC* gene showed complete alignment with *tcdC* from a reference BI strain, both of which contained an 18-bp deletion from positions 316 to 333 and a single base deletion at position 117 that resulted in a stop codon at position 196, unlike the reference *C. difficile* strain, 630 (data not shown) (32). The similarities to the BI/RT027 strain were further validated because toxinotyping indicated the DQ/591 strain was toxinotype III (data not shown).

WGS and MLST results showed that, although the strains are closely related and reside within the same clade (MLST clade 2), they form a separate cluster (Figure 2). ANI showed a clear separation of the BI/027 and DQ/591 isolates at the whole genome level

Table. Comparison of baseline characteristics and outcomes of patients colonized or infected with *Clostridioides difficile* DQ/591, BI/027, and other strain types in study of *C. difficile* at 2 US Veteran Affairs long-term care facilities and their affiliated acute care facilities*

Characteristic	Strain type		
	DQ/591, n = 15	BI/027, n = 22	Other, n = 27
Age, y (range)	67.9 (49–85)	68.9 (57–89)	67.4 (48–91)
Sex			
M	15 (100)	22 (100)	26 (96)
F	0	0	1 (4)
Residence			
Long-term care facility	10 (67)	7 (32)†	8 (30)†
Spinal cord injury unit	4 (27)	8 (36)	7 (26)
Drugs received			
Proton pump inhibitor	12 (80)	11 (50)	19 (70)
Antimicrobial drug treatment in past 90 d	15 (100)	14 (64)†	15 (56)†
Fluoroquinolone in past 90 d	5 (33)	6 (27)	6 (22)
Clindamycin in past 90 d	1 (7)	0	0
Azithromycin in past 90 d	1 (7)	0	0
Intensive care unit admission in past 30 d	4 (27)	4 (18)	0†
Medical conditions			
Chronic lung disease	6 (40)	4 (18)	5 (19)
Cancer	5 (33)	5 (23)	5 (19)
Major surgery in past 90 d	3 (20)	1 (4.5)	5 (19)
End-stage renal disease	3 (20)	4 (18)	4 (15)
Disease classification, no. (%)			
<i>C. difficile</i> infection	7 (47)	13 (59)	16 (59)
Severe	3 (43)	3 (23)	1 (6)
Fulminant	0	0	0
Recurrent	3 (43)	2 (15)	4 (25)
Healthcare-associated	7 (100)	11 (85)	8 (50)†
Asymptomatic carrier	8 (53)	9 (41)	11 (41)
Died within 6 mo after CDI diagnosis	4 (27)	6 (27)	1 (4)†

*Values for BI/027 and for other strain types were compared with values for DQ/591 strains.

† $p < 0.05$.

(Appendix Figure 1, <https://wwwnc.cdc.gov/EID/article/26/2/18-1965-App1.pdf>). By MLST analysis, the DQ/RT591 isolates were ST41, whereas BI/RT027 were ST1. Although the STs are closely related, there is a 4-SNP separation in the MLST loci.

Supernatant from the DQ/RT591 strain produced typical cellular rounding on fibroblasts similar to BI/RT027, whereas the AF/RT244 strain produced a different phenotype, clumping and rounding of cells (Appendix Figure 2). Strain AF/RT244 is also related to RT027 and was responsible for an outbreak of severe disease in Australia (12). DQ/RT591 showed minimal toxin production in vitro at 24 hours; by 48 hours, toxin levels were similar to those of strain J/RT001 but still less than levels produced by BI/RT027 (Figure 3).

The DQ/RT591 strain was highly resistant to clindamycin (MIC >256 µg/mL) and azithromycin (MIC >256 µg/mL) but was susceptible to moxifloxacin (MIC range 1–2 µg/mL) and ceftriaxone (MIC 16 µg/mL). BI/RT027 was resistant to moxifloxacin (MIC >32 µg/mL) and azithromycin (MIC >256 µg/mL) and variably resistant to clindamycin (MIC range 6–32 µg/mL). Furthermore, WGS revealed that all DQ/RT591 isolates contained a variant *ermB* sequence known to confer clindamycin resistance (33).

Discussion

During a surveillance study of *C. difficile* in asymptomatic LTCF patients and symptomatic patients in the affiliated acute care hospitals at 2 VA facilities (16), we detected a clonal outbreak of a newly recognized *C. difficile* strain at the Cleveland facility. This strain, identified as REA group DQ, ribotype 591, is closely related to the BI/RT027 strain, and a commercial PCR erroneously identified it as the epidemic NAP1 strain (i.e., BI/RT027). The strain was misidentified as NAP1 by Xpert *C. difficile* PCR (Cepheid) because of the similar genetic findings within the *C. difficile* pathogenicity locus, and the presence of the binary toxin CDT gene *cdtB* (33). Our findings and previous reports of other non-RT027 strains show that these genetic targets are not specific to NAP1 (12,13). Even though the outbreak of RT244 in Melbourne, Australia, was misidentified as NAP1 (RT027) by the same commercial PCR, it was associated with severe disease in the infected patients (12), suggesting the possibility of shared virulence determinants.

DQ/RT591 and BI/RT027 share several characteristics, including *tcdB*, *cdtB*, the 18-bp and position 117 *tcdC* deletions, and a similar cytotoxic phenotype. Despite these shared genetic and phenotypic characteristics, in vitro toxin production appeared

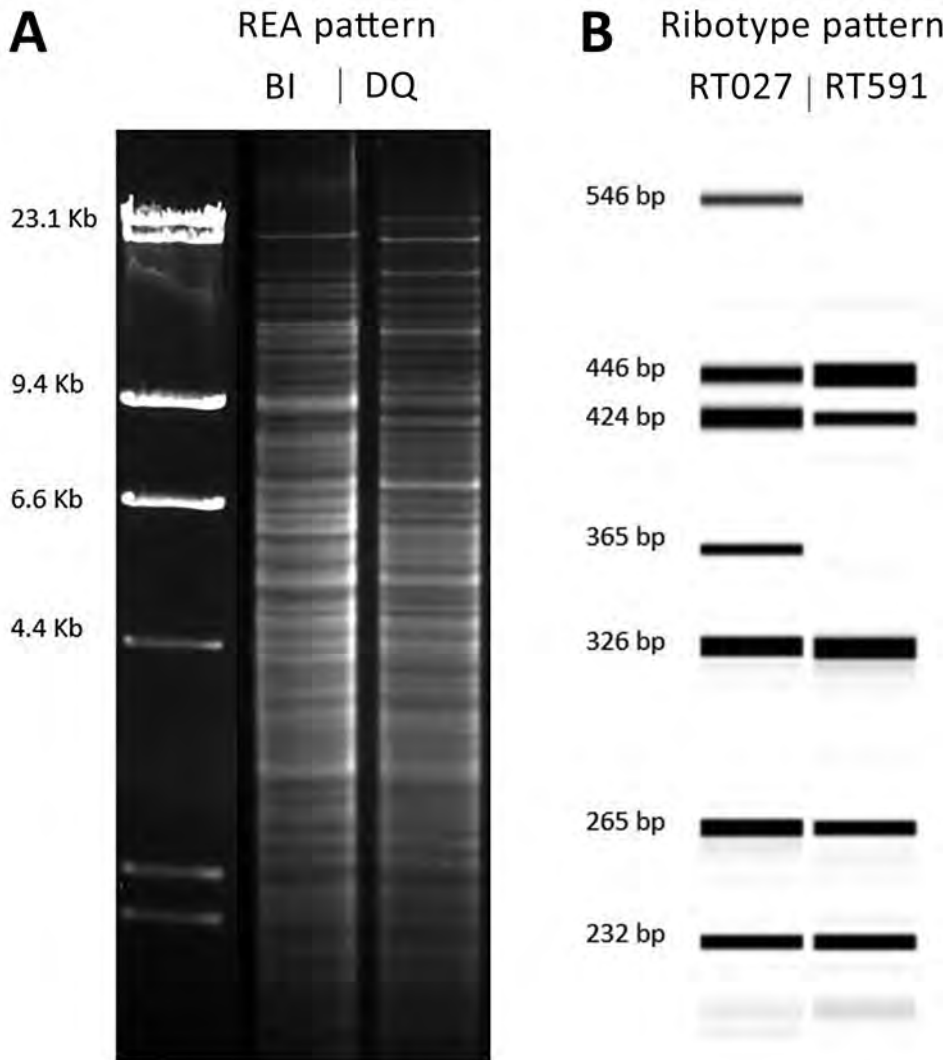


Figure 1. Comparison of the molecular characteristics of *Clostridioides difficile* strain DQ/591 and the epidemic BI/027 strain in study of *C. difficile* at 2 US Veteran Affairs long-term care facilities and their affiliated acute care facilities. The *Hind*III REA (A) and PCR ribotype (B) banding patterns were distinct between REA strain DQ/RT591 and REA strain BI/RT027. Molecular weight markers (in kb) are shown adjacent to the REA gel pattern. An internal spiked LIZ 1200 standard was used for fragment length calibrations (in bp) of the PCR ribotype gel patterns. REA, restriction endonuclease analysis.

to be delayed and somewhat lower in the DQ/RT591 strain than in BI/RT027. The clinical manifestations of the patients colonized or infected with DQ/RT591 were not unusual and did not differ substantially from those of patients with BI/NAP1/027 and other strain types in the cohort reported here. In nearly half (47%) of the patients, symptoms developed that were consistent with CDI. Although no fulminant CDI cases or deaths directly related to *C. difficile* were recognized, in CDI that developed because of DQ/591, 43% were classified as severe CDI in accordance with Infectious Diseases Society of America and Society for Healthcare Epidemiology of America guidelines. Likewise, no fulminant CDI cases or CDI-related deaths were recognized among the patients infected with BI/RT027 during this same study. However, all-cause mortality was lower for persons with non-DQ/RT591 and non-BI/RT027

infections. All the documented transmission events occurred in the BI/RT027 patients (34). Despite the fact that all the CDI cases caused by DQ/RT591 were healthcare associated, WGS did not identify any transmission events between patients because core genome SNP differences were >8 among DQ isolates (Appendix Figure 3) (34).

All patients in whom DQ/RT591 was confirmed had received antimicrobial drugs within 90 days before testing, and all patients with a CDI were classified as having a healthcare-associated infection; nearly all cases occurred in the LTCF or spinal cord injury unit. No specific antimicrobial drug was highly associated with infection by this strain. Fluoroquinolones have been associated with CDI outbreaks with the BI/RT027 strain, which is highly resistant to fluoroquinolones in vitro (35). Among the DQ/RT591- and BI/RT027-infected patients, receipt of fluoroquinolones or

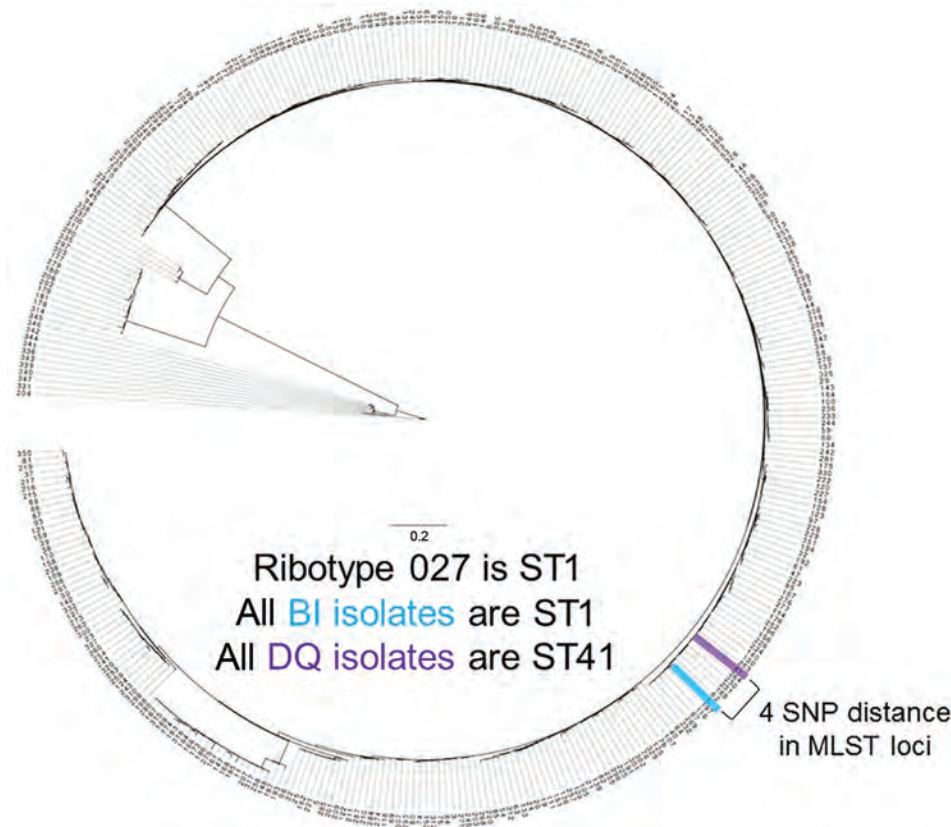


Figure 2. MLST loci map for *Clostridioides difficile* strains DQ/RT591 and BI/RT027 in study of *C. difficile* at 2 US Veteran Affairs long-term care facilities and their affiliated acute care facilities. The 2 strains are 4 SNPs apart. Scale bar indicates nucleotide substitutions per variable site of loci. MLST, multilocus sequence typing; SNP, single-nucleotide polymorphism; ST, sequence type.

clindamycin was limited. Despite high-level resistance to clindamycin in vitro and the presence of *ermB* in DQ/RT591, only 1 patient infected with this strain had received clindamycin.

Our experience was limited, but DQ/RT591 did not appear to carry the same level of clinical severity that BI/RT027 has exhibited (6). This difference in severity might be attributable to delayed toxin

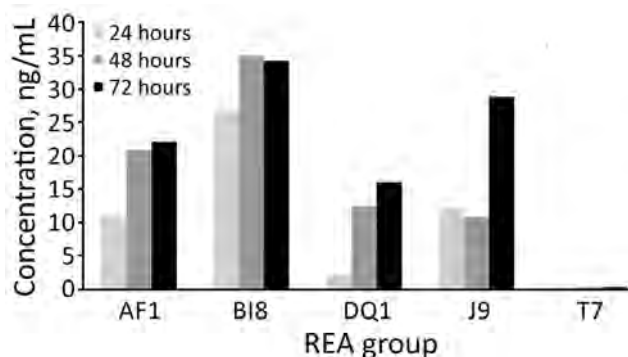


Figure 3. Quantitative in vitro total toxin production in study of *C. difficile* at 2 US Veteran Affairs long-term care facilities and their affiliated acute care facilities. Results at 24, 48, and 72 hours of incubation are shown for REA strains AF (ribotype 244), BI (ribotype 027), DQ (ribotype 591), J (ribotype 001), and T (a nontoxigenic *Clostridioides difficile* strain). REA, restriction endonuclease analysis.

production in vivo (Figure 3). Although increased toxin production has been proposed as the reason for increased virulence with the BI/RT027 strain (4,29), increased toxin production was not demonstrated for the AF/RT244 strain, which nevertheless was associated with an outbreak of increased severity in Australia (12). AF/RT244 also shows a different cytopathic effect than BI/027, which suggests the presence of a variant toxin B in AF/RT244 (4,12). Factors associated with increased virulence associated with these strains are still incompletely defined.

Because REA DQ/RT591 is closely related to BI/027, further monitoring is required to determine whether this strain carries risk for increased illness and death or has the capability of widespread dissemination. Since we completed this work, RT591 was reported as the most prevalent *C. difficile* strain in 3 tertiary hospitals in Colombia. These RT591 isolates were also mostly resistant to clindamycin (85%) (36).

Acknowledgments

The RT244 strain was a gift from T. Riley. We thank Adam Cheknis for technical support with the toxin and susceptibility assays. We also thank Brandi M. Limbago, Maria Karlsson, and Ashley L. Paulick for their support on this project.

This study was supported by the Centers for Disease Control and Prevention and by the Department of Veterans Affairs.

About the Author

Dr. Skinner is an infectious diseases fellow at Loyola University Medical Center and the Hines Veterans Affairs Hospital. His research interests include *C. difficile* epidemiology, treatment, host response, and molecular characterization.

References


- Dallal RM, Harbrecht BG, Boujoukas AJ, Sirio CA, Farkas LM, Lee KK, et al. Fulminant *Clostridium difficile*: an underappreciated and increasing cause of death and complications. *Ann Surg*. 2002;235:363-72. <https://dx.doi.org/10.1097/00000658-200203000-00008>
- McDonald LC, Killgore GE, Thompson A, Owens RC Jr, Kazakova SV, Sambol SP, et al. An epidemic, toxin gene-variant strain of *Clostridium difficile*. *N Engl J Med*. 2005;353:2433-41. <http://dx.doi.org/10.1056/NEJMoa051590>
- Lessa FC, Mu Y, Bamberg WM, Beldavs ZG, Dumyati GK, Dunn JR, et al. Burden of *Clostridium difficile* infection in the United States. *N Engl J Med*. 2015;372:825-34. <https://dx.doi.org/10.1056/NEJMoa1408913>
- O'Connor JR, Johnson S, Gerding DN. *Clostridium difficile* infection caused by the epidemic BI/NAP1/027 strain. *Gastroenterology*. 2009;136:1913-24. <https://dx.doi.org/10.1053/j.gastro.2009.02.073>
- Brazier JS, Raybould R, Patel B, Duckworth G, Pearson A, Charlett A, et al.; HPA Regional Microbiology Network. Distribution and antimicrobial susceptibility patterns of *Clostridium difficile* PCR ribotypes in English hospitals, 2007-08. *Euro Surveill*. 2008;13:19000. <https://dx.doi.org/10.2807/ese.13.41.19000-en>
- See I, Mu Y, Cohen J, Beldavs ZG, Winston LG, Dumyati G, et al. NAP1 strain type predicts outcomes from *Clostridium difficile* infection. *Clin Infect Dis*. 2014;58:1394-400. <https://dx.doi.org/10.1093/cid/ciu125>
- Merrigan M, Venugopal A, Mallozzi M, Roxas B, Viswanathan VK, Johnson S, et al. Human hypervirulent *Clostridium difficile* strains exhibit increased sporulation as well as robust toxin production. *J Bacteriol*. 2010;192:4904-11. <https://dx.doi.org/10.1128/JB.00445-10>
- He M, Miyajima F, Roberts P, Ellison L, Pickard DJ, Martin MJ, et al. Emergence and global spread of epidemic healthcare-associated *Clostridium difficile*. *Nat Genet*. 2013;45:109-13. <https://dx.doi.org/10.1038/ng.2478>
- Jump RLP, Pultz MJ, Donskey CJ. Vegetative *Clostridium difficile* survives in room air on moist surfaces and in gastric contents with reduced acidity: a potential mechanism to explain the association between proton pump inhibitors and *C. difficile*-associated diarrhea? *Antimicrob Agents Chemother*. 2007;51:2883-7. <https://dx.doi.org/10.1128/AAC.01443-06>
- Gerding DN, Johnson S, Rupnik M, Aktories K. *Clostridium difficile* binary toxin CDT: mechanism, epidemiology, and potential clinical importance. *Gut Microbes*. 2014;5:15-27. <https://dx.doi.org/10.4161/gmic.26854>
- Scardina T, Labuszewski L, Pacheco SM, Adams W, Schreckenberger P, Johnson S. *Clostridium difficile* infection (CDI) severity and outcome among patients infected with the NAP1/BI/027 strain in a non-epidemic setting. *Infect Control Hosp Epidemiol*. 2015;36:280-6. <https://dx.doi.org/10.1017/ice.2014.45>
- Lim SK, Stuart RL, Mackin KE, Carter GP, Kotsanas D, Francis MJ, et al. Emergence of a ribotype 244 strain of *Clostridium difficile* associated with severe disease and related to the epidemic ribotype 027 strain. *Clin Infect Dis*. 2014;58:1723-30. <https://dx.doi.org/10.1093/cid/ciu203>
- Kok J, Wang Q, Thomas LC, Gilbert GL. Presumptive identification of *Clostridium difficile* strain 027/NAP1/BI on Cepheid Xpert: interpret with caution. *J Clin Microbiol*. 2011;49:3719-21. <https://dx.doi.org/10.1128/JCM.00752-11>
- Wehrhahn MC, Keighley C, Kurtovic J, Knight DR, Hong S, Hutton ML, et al. A series of three cases of severe *Clostridium difficile* infection in Australia associated with a binary toxin producing clade 2 ribotype 251 strain. *Anaerobe*. 2019;55:117-23. <https://dx.doi.org/10.1016/j.anaerobe.2018.11.009>
- Donskey CJ, Sunkesula VC, Jencson AL, Stone ND, Gould CV, McDonald LC, et al. Utility of a commercial PCR assay and a clinical prediction rule for detection of toxigenic *Clostridium difficile* in asymptomatic carriers. *J Clin Microbiol*. 2014;52:315-8. <https://dx.doi.org/10.1128/JCM.01852-13>
- Pacheco SM, Donskey CJ, Samore M, Mayer J, Stone ND, Gould CV, et al. *Clostridium difficile* strains colonizing long-term care facility (LTCF) residents are similar to strains causing infection in both LTCF and hospital patients suggesting a shared continuum of transmission. *Open Forum Infect Dis*. 2014;1(Suppl 1):S437-8. <https://dx.doi.org/10.1093/ofid/ofu052.1184>
- McDonald LC, Gerding DN, Johnson S, Bakken JS, Carroll KC, Coffin SE, et al. Clinical practice guidelines for *Clostridium difficile* infection in adults and children: 2017 update by the Infectious Diseases Society of America (IDSA) and Society for Healthcare Epidemiology of America (SHEA). *Clin Infect Dis*. 2018;66:987-94. <https://dx.doi.org/10.1093/cid/ciy149>
- Clabots CR, Johnson S, Bettin KM, Mathie PA, Mulligan ME, Schaberg DR, et al. Development of a rapid and efficient restriction endonuclease analysis typing system for *Clostridium difficile* and correlation with other typing systems. *J Clin Microbiol*. 1993;31:1870-5.
- Fawley WN, Knetsch CW, MacCannell DR, Harmanus C, Du T, Mulvey MR, et al. Development and validation of an internationally-standardized, high-resolution capillary gel-based electrophoresis PCR-ribotyping protocol for *Clostridium difficile*. *PLoS One*. 2015;10:e0118150. <https://dx.doi.org/10.1371/journal.pone.0118150>
- Abrahamian FM, Talan DA, Krishnadasan A, Citron DM, Paulick AL, Anderson LJ, et al.; EMERGENCY ID NET Study Group. EMERGENCY ID NET Study Group. EMERGENCY ID NET Study Group. *Clostridium difficile* infection among US emergency department patients with diarrhea and no vomiting. *Ann Emerg Med*. 2017;70:19-27.e4. <https://dx.doi.org/10.1016/j.annemergmed.2016.12.013>
- Rupnik M, Brazier JS, Duerden BI, Grabnar M, Stubbs SL. Comparison of toxinotyping and PCR ribotyping of *Clostridium difficile* strains and description of novel toxinotypes. *Microbiology*. 2001;147:439-47. <https://dx.doi.org/10.1099/00221287-147-2-439>
- Cox MP, Peterson DA, Biggs PJ, Solexa QA. SolexaQA: At-a-glance quality assessment of Illumina second-generation sequencing data. *BMC Bioinformatics*. 2010;11:485. <https://dx.doi.org/10.1186/1471-2105-11-485>
- Bankevich A, Nurk S, Antipov D, Gurevich AA, Dvorkin M, Kulikov AS, et al. SPAdes: a new genome assembly algorithm and its applications to single-cell sequencing. *J Comput Biol*. 2012;19:455-77. <https://dx.doi.org/10.1089/cmb.2012.0021>
- Kurtz S, Phillippy A, Delcher AL, Smoot M, Shumway M, Antonescu C, et al. Versatile and open software for

- comparing large genomes. *Genome Biol.* 2004;5:R12. <https://dx.doi.org/10.1186/gb-2004-5-2-r12>
25. Warnes GR, Bolker B, Bonebakker L, Gentleman R, Liaw WHA, Lumley T, et al. *gplots*: Various R programming tools for plotting data. R package version 2.16.0. 2016 [cited 2018 Nov 18]. <https://CRAN.R-project.org/package=gplots>
 26. Stamatakis A. RAxML version 8: a tool for phylogenetic analysis and post-analysis of large phylogenies. *Bioinformatics.* 2014;30:1312–3. <https://dx.doi.org/10.1093/bioinformatics/btu033>
 27. Warny M, Pepin J, Fang A, Killgore G, Thompson A, Brazier J, et al. Toxin production by an emerging strain of *Clostridium difficile* associated with outbreaks of severe disease in North America and Europe. *Lancet.* 2005;366:1079–84. [https://dx.doi.org/10.1016/S0140-6736\(05\)67420-X](https://dx.doi.org/10.1016/S0140-6736(05)67420-X)
 28. Sambol SP, Tang JK, Merrigan MM, Johnson S, Gerding DN. Infection of hamsters with epidemiologically important strains of *Clostridium difficile*. *J Infect Dis.* 2001;183:1760–6. <https://dx.doi.org/10.1086/320736>
 29. Razaq N, Sambol S, Nagaro K, Zukowski W, Cheknis A, Johnson S, et al. Infection of hamsters with historical and epidemic BI types of *Clostridium difficile*. *J Infect Dis.* 2007;196:1813–9. <https://dx.doi.org/10.1086/523106>
 30. Clinical and Laboratory Standards Institute. *Methods for antimicrobial susceptibility testing of anaerobic bacteria; approved standard: eighth edition (M11-A8)*. Wayne (PA): The Institute; 2012.
 31. Clinical and Laboratory Standards Institute. *Performance standards for antimicrobial susceptibility testing; twenty-seventh edition (M100-S27)*. Wayne (PA): The Institute; 2017.
 32. Curry SR, Marsh JW, Muto CA, O'Leary MM, Pasculle AW, Harrison LH. *tcdC* genotypes associated with severe TcdC truncation in an epidemic clone and other strains of *Clostridium difficile*. *J Clin Microbiol.* 2007;45:215–21. <https://dx.doi.org/10.1128/JCM.01599-06>
 33. Gupta SK, Padmanabhan BR, Diene SM, Lopez-Rojas R, Kempf M, Landraud L, et al. ARG-ANNOT (antibiotic resistance gene-ANNOTation), a new bioinformatic tool to discover antibiotic resistance genes in bacterial genomes. *Antimicrob Agents Chemother.* 2014;58:212–20. <https://dx.doi.org/10.1128/AAC.01310-13>
 34. Donskey CJ, Sunkesula VCK, Stone ND, Gould CV, McDonald LC, Samore M, et al. Transmission of *Clostridium difficile* from asymptotically colonized or infected long-term care facility residents. *Infect Control Hosp Epidemiol.* 2018;39:909–16. <https://dx.doi.org/10.1017/ice.2018.106>
 35. Wiczorkiewicz JT, Lopansri BK, Cheknis A, Osmolski JR, Hecht DW, Gerding DN, et al. Fluoroquinolone and macrolide exposure predict *Clostridium difficile* infection (CDI) with the highly fluoroquinolone- and macrolide-resistant epidemic *C. difficile* strain, BI/NAP1/027. *Antimicrob Agents Chemother.* 2015;60:418–23. <https://dx.doi.org/10.1128/AAC.01820-15>
 36. Salazar CL, Reyes C, Atehortua S, Sierra P, Correa MM, Paredes-Sabja D, et al. Molecular, microbiological and clinical characterization of *Clostridium difficile* isolates from tertiary care hospitals in Colombia. *PLoS One.* 2017; 12:e0184689. <https://dx.doi.org/10.1371/journal.pone.0184689>

Address for correspondence: Stuart Johnson, Edward Hines, Jr. VA Hospital, Infectious Diseases, Research Service/151, 5000 S 5th Ave, Hines, IL 60141, USA; email: stuart.johnson2@va.gov; Andrew M. Skinner, Loyola University Medical Center, 2160 S 1st Ave, Maywood, IL 60153, USA; email: andrew.skinner@lumc.edu

April 2018

**EMERGING
INFECTIOUS DISEASES**



Antimicrobial Resistance

- Seroprevalence of Chikungunya Virus in 2 Urban Areas of Brazil 1 Year after Emergence
- Two Infants with Presumed Congenital Zika Syndrome, Brownsville, Texas, USA, 2016–2017
- Reemergence of Intravenous Drug Use as Risk Factor for Candidemia, Massachusetts, USA
- Rickettsial Illnesses as Important Causes of Febrile Illness in Chittagong, Bangladesh
- Influence of Population Immunosuppression and Past Vaccination on Smallpox Reemergence
- Emerging Coxsackievirus A6 Causing Hand, Foot and Mouth Disease, Vietnam
- Influenza A(H7N9) Virus Antibody Responses in Survivors 1 Year after Infection, China, 2017
- Genomic Surveillance of 4CMenB Vaccine Antigenic Variants among Disease-Causing *Neisseria meningitidis* Isolates, United Kingdom, 2010–2016
- Evolution of Sequence Type 4821 Clonal Complex Meningococcal Strains in China from Prequinolone to Quinolone Era, 1972–2013
- Avirulent *Bacillus anthracis* Strain with Molecular Assay Targets as Surrogate for Irradiation-Inactivated Virulent Spores
- Phenotypic and Genotypic Characterization of *Enterobacteriaceae* Producing Oxacillinase-48–Like Carbapenemases, United States
- Bacterial Infections in Neonates, Madagascar, 2012–2014
- Artemisinin-Resistant *Plasmodium falciparum* with High Survival Rates, Uganda, 2014–2016
- Carbapenem-Nonsusceptible *Acinetobacter baumannii*, 8 US Metropolitan Areas, 2012–2015
- Cooperative Recognition of Internationally Disseminated Ceftriaxone-Resistant *Neisseria gonorrhoeae* Strain

To revisit the April 2018 issue, go to:
<https://wwwnc.cdc.gov/eid/articles/issue/24/4/table-of-contents>

Porcine Deltacoronavirus Infection and Transmission in Poultry, United States¹

Patricia A. Boley, Moyasar A. Alhamo, Geoffrey Lossie, Kush Kumar Yadav, Marcia Vasquez-Lee, Linda J. Saif, Scott P. Kenney

Coronaviruses cause respiratory and gastrointestinal diseases in diverse host species. Deltacoronaviruses (DCoVs) have been identified in various songbird species and in leopard cats in China. In 2009, porcine deltacoronavirus (PDCoV) was detected in fecal samples from pigs in Asia, but its etiologic role was not identified until 2014, when it caused major diarrhea outbreaks in swine in the United States. Studies have shown that PDCoV uses a conserved region of the aminopeptidase N protein to infect cell lines derived from multiple species, including humans, pigs, and chickens. Because PDCoV is a potential zoonotic pathogen, investigations of its prevalence in humans and its contribution to human disease continue. We report experimental PDCoV infection and subsequent transmission among poultry. In PDCoV-inoculated chicks and turkey poults, we observed diarrhea, persistent viral RNA titers from cloacal and tracheal samples, PDCoV-specific serum IgY antibody responses, and antigen-positive cells from intestines.

Coronaviruses (CoVs) cause respiratory and gastrointestinal disease in humans, poultry, swine, and cattle. CoVs (family *Nidovirales*, subfamily *Coronaviridae*, subfamily *Coronavirinae*) are composed of 4 genera, *Alphacoronavirus*, *Betacoronavirus*, *Gammacoronavirus*, and *Deltacoronavirus* (1). Viruses from each CoV genus have been detected in diverse host species, but gammacoronaviruses and deltacoronaviruses (DCoVs) have been isolated primarily in birds (2). Two members of the *Gammacoronavirus* genus, transmissible gastroenteritis coronavirus (TGEV) and porcine epidemic diarrhea virus (PEDV), cause severe diarrhea in swine. TGEV and PEDV infections have caused severe economic losses in many countries,

including the United States (3–5). The *Betacoronavirus* genus includes the notable human pathogens OC43, HKU1, severe acute respiratory syndrome (SARS) CoV, and Middle East respiratory syndrome (MERS) CoV, which mostly cause respiratory symptoms (6–9). *Gammacoronavirus* includes avian enteric coronavirus and infectious bronchitis virus that mainly infect avian species (10). DCoVs previously were identified primarily in multiple songbird species and in leopard cats (*Prionailurus bengalensis*) (11).

Porcine deltacoronavirus (PDCoV) was initially detected in 2009 in fecal samples from pigs in Asia, but its etiologic role was not identified until 2014, when it caused diarrhea in pigs in the United States (11,12). The origin of PDCoV is unknown, but because of the widespread prevalence of DCoV in songbird species and genomic similarities, researchers suspect that PDCoV may have originated from an ancestral avian DCoV (11).

In experiments, PDCoV caused diarrhea and gut lesions in infected piglets (13,14). It was detected in pigs in Hong Kong in 2012 (11) and the United States in February 2014 (15–17). Although not considered as deadly to pigs as PEDV (13,18), PDCoV continues to circulate and cause illness in swine herds worldwide. How PDCoV emerged in swine and how it spreads remain unknown.

In vitro studies have shown that PDCoV utilizes a conserved region of the protein aminopeptidase N (APN) gene to infect cell lines derived from multiple species, including humans, pigs, and chickens (19). As a potentially emerging zoonotic pathogen, studies of PDCoV prevalence in humans and its contribution to human disease are ongoing. The ability of PDCoV to infect cells of multiple species and cause illness and death in pigs makes it a priority pathogen that should be studied further.

Author affiliations: The Ohio State University, Wooster, Ohio, USA (P.A. Boley, M.A. Alhamo, K.K. Yadav, M. Vasquez-Lee, L.J. Saif, S.P. Kenney); The Ohio State University, Columbus, Ohio, USA (G. Lossie)

¹Preliminary results of this study were presented at the Conference of Research Workers in Animal Diseases, December 1–4, 2018, Chicago, Illinois, USA.

DOI: <https://doi.org/10.3201/eid2602.190346>

In vivo studies could validate cell culture susceptibility findings and determine whether PDCoV causes infection and disease in species other than pigs. Virus cross-species transmission among hosts plays a major role in the evolution and diversification of viruses, appearing in many instances to be preferential to coevolving within an initial host (20). CoVs already have demonstrated a propensity for crossing species barriers, both in animal-to-animal spread and animal-to-human spread. Initial evidence of CoVs jumping from mammalian to avian species was reported from bovine CoV infecting turkeys but not chickens (21,22). As a zoonotic CoV transmission, SARS-CoV is believed to have jumped from bats or palm civets (*Paguma larvata*) to humans in 2002, causing 8,098 cases in 37 countries and 774 deaths (11). MERS-CoV emerged more recently, jumping from dromedary camels (*Camelus dromedarius*) to humans, and has caused 1,879 cases of respiratory illness in humans and 666 deaths (10).

Understanding how cross-species transmission of CoVs occurs is critical to our ability to predict which viruses might be on the verge of SARS- or MERS-like pandemics. In addition, studies of CoV cross-species transmission can inform development of novel therapeutics and strategies to combat CoVs in susceptible animal hosts before they pose an imminent human health threat. We conducted experiments to determine the prevalence of PDCoV infection in and transmissibility among poultry.

Materials and Methods

Animals

We obtained 25 fourteen-day-old chickens (*Gallus gallus domesticus*) and 25 fourteen-day-old turkey poults (*Meleagris gallopavo*) from the specific pathogen-free flock of the Ohio Agricultural Research and Development Center of The Ohio State University (Wooster, Ohio, USA). This flock has no prior exposure to swine or to PDCoV, PEDV, or TGEV. After acclimating in Biosafety Level 2 (BSL-2) facilities for 1 day, all birds appeared healthy with no evidence of diarrhea or other clinical signs. Animal protocols used in this study were approved by the Institutional Laboratory Animal Care and Use Committee of The Ohio State University.

Titration of PDCoV

We determined PDCoV titers from intestinal contents of pigs by 50% tissue culture infectious dose (TCID₅₀) assay (23). We seeded LLC porcine kidney (LLC-PK) cells at 5×10^4 cells/well in a 96-well plate (BD

Biosciences, <https://www.bdbiosciences.com>). We washed 100% confluent monolayers once with 200 μ L of maintenance media (MM): minimal essential media (MEM), 4-(2-hydroxyethyl)-1-piperazineethanesulfonic acid (HEPES), GlutaMAX (GIBCO, <https://www.thermofisher.com>) consisting of MEM with 1% antibiotic-antimycotic solution, 1% nonessential amino acids, and 1% HEPES. We inoculated 100 μ L from 10-fold dilutions of PDCoV in 8 replicates per dilution. Each plate included 1 row of negative control MM only with 5 μ g/mL of Trypsin (Corning, <https://www.corning.com>). After absorption for 1 h, we added another 100 μ L of MM with 5 μ g/mL of Trypsin to each well. We monitored cytopathic effects for 3–7 days, calculated virus titers after immunofluorescent (IF) staining by using the Reed-Muench method (24), and expressed results as log₁₀ TCID₅₀/mL (23).

Study Design

Birds were floor housed in a temperature-controlled BSL-2 containment room with wood litter shavings and provided ad libitum access to food and water. In consecutive experiments of poults and chicks, we randomly divided the flock of 25 birds into 2 groups, 15 uninfected and 10 infected birds. Each group was housed separately and inoculated through the choanal cleft. The uninfected group was inoculated with 200 μ L of unfiltered, undiluted small intestine contents (SIC) from an uninfected gnotobiotic pig (GP-8). The infected group was inoculated with SIC from a PDCoV-infected pig (DC175) with 6.87 log₁₀ TCID₅₀/mL. One poult in the uninfected group died of unknown causes unrelated to known pathogens before inoculation.

After inoculation, we observed chicks and poults for clinical signs 2 times each day. We scored fecal consistency as follows: 0, solid; 1, pasty; 2, semiliquid; and 3, liquid (25). We considered a fecal consistency score of >2 as diarrhea. At 2 days postinoculation (dpi), we randomly assigned 5 birds from each uninfected group as sentinels and allowed them to comingle with the infected group for the duration of the experiment. We recorded body weights and collected cloacal swab, tracheal swab, and serum samples at 2, 4, 7, 9, 11, and 14 dpi. Except for sentinel birds, we euthanized 2 chicks and 2 poults from each group at 3 and 7 dpi for blood and tissue collection. We concluded the study at 14 dpi and euthanized the remaining 33 birds, including sentinels, for blood and tissue collection.

Serum Antibody Detection

We modified and optimized an ELISA (26) to detect PDCoV-specific IgY antibodies in serum from

PDCoV-inoculated chicks and poults. We added 50 μ L of serum diluted 1:1,000 to the PDCoV antigen-coated and mock antigen-coated wells and incubated for 90 m at 37°C, then added 100 μ L of biotin-conjugated antichickens IgY (Invitrogen Goat anti-Chicken IgY [H+L] Secondary Antibody, Biotin; ThermoFisher, <https://www.thermofisher.com>) or biotin-conjugated antiturkey IgY (Goat Anti-Turkey IgY (H+L) Biotin pAb; Cell Sciences, <https://www.cellsciences.com>) at a dilution of 1:10,000 and incubated at 37°C for 1 h. We added 100 μ L of HRP-Conjugated Streptavidin (ThermoFisher) to each well at a dilution of 1:5,000 and incubated at 37°C for 1 h. We washed wells with phosphate buffered saline solution with 0.05% Tween-20 (\times 5) between each step. We added 3,3',5,5'-tetramethylbenzidine substrate (SureBlue TMB 1-Component Microwell Peroxidase Substrate; Seracare, <https://www.seracare.com>), then added 100 μ L of 0.3 mol/L sulfuric acid to stop the reaction. We read plates at an absorbance of 450 nm by using a SpectraMax F5 (Molecular Devices, <https://www.moleculardevices.com>) plate reader. We conducted statistical analysis by using Prism software (GraphPad, <https://www.graphpad.com>). We used analysis of variance to compare multiple groups and a 1-tailed Student *t*-test to compare groups of 2.

Histopathology and IF Staining

We examined gross tissues from small intestines, duodenum to ileum, and large intestines, cecum and colon, as well as other organs, including bursa, lung, liver, kidney, proventriculus, and spleen, and then fixed tissues in 10% neutral formalin for 1–2 days at room temperature for histopathology (27). We embedded, sectioned, and then stained samples with hematoxylin and eosin for light microscopy examination. We measured mean jejunal or ileal ratios of villus height and crypt depth (VH:CD) by using MetaMorph software (MetaMorph, Inc., <https://www.metamorph-software.com>), as described previously (18). We tested prepared tissues by IF staining to detect PDCoV antigen using a polyclonal rabbit antiserum against PDCoV (provided by E. Nelson, South Dakota State University, Brookings, SD, USA) (28). We also tested tissues from a PDCoV-infected pig for comparison.

Real-Time Reverse Transcription PCR

We suspended cloacal swabs, tracheal swabs, SIC, and large intestine contents (LIC) in 1–4 mL MEM as a 10% suspension. We extracted RNA by using GenCatch Viral RNA Miniprep Kit (Epoch Life Science, <https://www.fishersci.com>). We further processed samples containing fecal matter by using OneStep

PCR Inhibitor Removal Kit (Zymo Research Corporation, <https://www.zymoresearch.com>).

We determined viral RNA titers by real-time reverse transcription-PCR (rRT-PCR), as reported previously (23). In brief, we amplified a 541-bp fragment of the M gene that covered the quantitative RT-PCR-amplified fragment. We designed 5'-CGCGTAATCGTGTGATCTATGT-3' and 5'-CCGGCCTTTGAAGTGTTAT-3' primers according to the sequence of a strain from the United States, Illinois121/2014 (GenBank accession no. KJ481931). We purified the PCR products by using a QIAquick PCR Purification Kit (QIAGEN Inc., <https://www.qiagen.com>), sequenced, and then used these as the template to construct a quantitative RT-PCR standard curve. The detection limit of the rRT-PCR was 10 genomic equivalents (GEs)/reaction, which corresponded to 4.6 log₁₀ GE/mL of PDCoV in cloacal and tracheal samples.

Results

Clinical Signs

By 2 dpi, 70% of infected chicks had diarrhea and fecal scores >2; that percentage decreased to 17% by 9 dpi (Table 1). By 14 dpi, most (5/6) of the remaining infected chicks had normal feces. The 5 uninfected sentinel chicks that comingled with the infected birds at 2 dpi demonstrated mild to moderate diarrhea 2 days after comingling (4 dpi); diarrhea peaked 5 days after comingling (7 dpi). At 14 dpi, only 2 sentinel chicks had abnormal feces. Two chicks in the uninfected group had transient diarrhea during the study but tested negative for known pathogens, including PDCoV.

In poults, 50% exhibited diarrhea at 2 dpi. During the study, the rate of diarrhea increased, and poults did not recover by 14 dpi. (Table 1). Sentinel poults began exhibiting mild to moderate diarrhea 5 days after comingling (7 dpi), and by 9 dpi, 60% were affected. At 14 dpi, all 5 sentinel poults had moderate diarrhea.

Two infected chicks necropsied at 3 dpi had distended gastrointestinal tracts containing a mixture of yellow liquid and gas. Similar but less extensive findings were seen in infected chicks at 7 dpi. No gross pathology was detected in infected chicks or sentinel chicks at 14 dpi. In necropsies of infected poults, we observed distended gastrointestinal tracts containing a mixture of yellow liquid and gas at all time points.

Weights

Birds were weighed before inoculation and then at 2, 4, 7, 9, 11, and 14 dpi. PDCoV infection greatly affected the chicks' weight at 2 dpi (Figure 1, panel A). At

Table 1. Prevalence of diarrhea in uninfected birds and birds experimentally inoculated with porcine deltacoronavirus*

Group	Days postinoculation					
	2	4	7	9	11	14
Birds, total†	n = 49	n = 41	n = 41	n = 33	n = 33	n = 33
Chicks, n = 25						
Uninfected	0/15	1/8‡	2/8‡	1/6‡	0/6	0/6
Infected	7/10	5/8	5/8	1/6	0/6	1/6
Sentinel§	NA	1/5	3/5	1/5	0/5	0/5
Poult, n = 25						
Uninfected	0/14¶	0/7	0/7	0/5	0/5	0/5
Infected	5/10	2/8	6/8	5/6	4/6	5/6
Sentinel§	NA	0/5	1/5	4/5	5/5	5/5

*Uninfected birds were inoculated with small intestine contents from uninfected gnotobiotic pig. Fecal consistency scored on a scale of 0–3: 0, solid; 1, pasty; 2, semiliquid; 3, liquid. Values expressed as number of birds with a cloacal swab score of ≥ 2 /total number of birds in the room on the indicated day postinoculation (dpi). NA, not applicable.

†Two birds from each group, excluding sentinels, were randomly removed for necropsy at 3 dpi and 7 dpi.

‡One chick in uninfected group consistently had a score of 3 for 7 d, another briefly scored a 2 at 7 dpi; both tested negative for porcine deltacoronavirus, *Salmonella*, and for parasites via fecal float analysis. Cause of diarrhea was unknown.

§We removed 5 uninfected birds as sentinels and allowed them to come in contact with infected birds at 2 dpi for the duration of the experiment.

¶One poult in uninfected group died before inoculation.

4 and 7 dpi, weight gain averages in infected chicks were comparable to those in uninfected birds, but at 9 and 11 dpi, infected chicks had gained much less weight than the uninfected chicks. By 14 dpi, infected chicks rebounded and showed compensatory weight gain at higher levels than uninfected chicks.

Poult weight gain responses differed from those of the chicks. At 2 dpi, infected poult were gaining weight at a much higher rate than uninfected poult (Figure 1, panel B). However, by 4 dpi, poult weight gain was severely curtailed; several lost weight, and the average weight gain for the infected group was 0.5 g, compared with almost 10 g for uninfected poult. By 7 dpi, the infected poult recovered and gained weight at a slightly higher, but not statistically significantly different, rate than the uninfected poult. This trend continued until the end of the study.

Histopathology and IF Staining

We examined tissue sections by using light microscopy. We noted suspect zymogen depletion in several poult in both the infected and uninfected groups, suggesting possible inanition. We conducted

VH:CD measurements of the ileum and jejunum of intestinal tissues from chicks at 14 dpi (Table 2). Infected chicks had a VH:CD ratio of 4.26:1 compared with a ratio of 6.15:1 for uninfected chicks. The VH:CD ratio was lower in sentinel chicks than in uninfected chicks but the difference was not statistically significant.

We could not obtain enough measurements for poult tissues to provide accurate comparisons. IF tissue staining in infected poult demonstrated PDCoV antigen detectable in the epithelial cells lining the villi of the jejunum, although at reduced levels from the ileum and from infected porcine tissue (Figure 2, panel A). We also detected PDCoV antigen in numerous epithelial cells that had sloughed off and remained in the lumen of infected poult when compared with stained tissue sections from uninfected poult (Figure 2, panel B and C). We were unable to visualize a signal in tissues from chicks.

Serum IgY Antibody Responses

We analyzed serum samples collected at 2, 4, 7, 9, 11, and 14 dpi. We used indirect ELISA to test samples

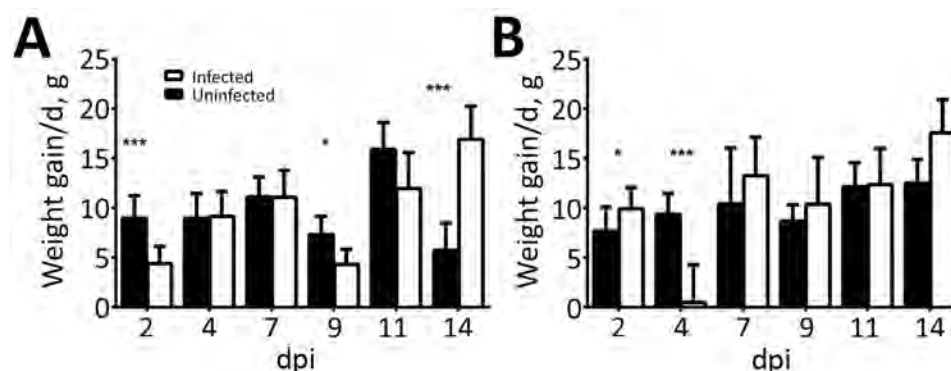


Figure 1. Average weight gain/day of (A) chicks and (B) turkey poult in a study of infection and transmission of porcine deltacoronavirus in poultry. Weights were taken at 2, 4, 7, 9, 11, and 14 dpi and differences were averaged by the number of days between time points. Weights for sentinel birds are excluded after 2 dpi. Error bars indicate upper half of SD. Statistically significant values are indicated: * $p < 0.05$; ** $p < 0.01$; *** $p < 0.001$. dpi, days postinoculation.

Table 2. Effect of porcine deltacoronavirus on villus height:crypt depth ratios of ileum or jejunum in experimental chicks*

Characteristics	Uninfected, n = 6	Infected, n = 6	Sentinel, n = 5
Villous height	370	353	547
Crypt depth	64	84	94
Ratio of villous height to crypt depth	6.15	4.26	5.87

*Values are expressed in millimeters and represent the average of ≤ 10 measurements/bird at 14 d postinoculation with porcine deltacoronavirus. Bold text indicates statistically significant difference, $p = 0.04$.

at 2 and 14 dpi for PDCoV-specific IgY antibodies in all birds from each group, including sentinel birds. We assigned experimental values by averaging 3 replicates. Because we did not have positive controls in chicks and poults, we established a cutoff by using the average final optical density value of uninfected birds at 2 dpi plus 2 SD. We established a separate cutoff value for sentinel birds.

At 14 dpi, infected chicks had increased IgY antibody levels in serum, demonstrating an antibody response to PDCoV (Figure 3, panel A), but sentinel chicks did not have antibody levels demonstrating exposure to PDCoV (Figure 3, panel B). Serum samples from poults exhibited a similar range of IgY values. The average IgY values were much higher in infected birds at 14 dpi compared with infected birds at 2 dpi and uninfected birds (Figure 3, panel C). The IgY greatly increased in sentinel poults at 14 dpi compared with IgY values at 2 dpi, but were still below the cutoff value (Figure 3, panel D).

rRT-PCR on Samples from Chicks

All experimentally infected chicks rapidly shed detectable viral RNA postinoculation, and viral RNA titers remained relatively constant through 11 dpi (Figure 4, panels A, B). Viral RNA from cloacal swabs reached $6.52 \log_{10}$ GE/mL by 2 dpi and remained $>6.5 \log_{10}$ GE/mL until 11 dpi, when levels at $7.14 \log_{10}$ GE/mL at 9 dpi, then decreased to $5.82 \log_{10}$ GE/mL at 14 dpi. Despite an absence of noticeable

respiratory signs, tracheal swab specimens also showed high levels of PDCoV RNA throughout the study (Figure 4, panel B). PDCoV spread rapidly from infected to naive birds, and all 5 sentinel chicks became positive for PDCoV RNA in both tracheal and cloacal swabs within 2 days of comingling with infected birds (Figure 4, panels C, D).

We calculated titers and viral RNA loads in SIC and LIC from infected and sentinel chicks at 3, 7, and 14 dpi (Figure 5). We used RNA isolated at 14 dpi from SIC of 1 infected and 1 sentinel bird to amplify an $\approx 1,300$ -bp portion of the nucleocapsid (N) gene of PDCoV, then gel extracted and sequenced the resulting product. The samples sequenced had $>99\%$ identity with the original inoculum, Ohio FD22 strain of PDCoV. We tested infectivity of intestinal contents of infected and sentinel chicks by using TCID₅₀ assay at 7 and 14 dpi (Figure 5, panel A).

rRT-PCR on Samples from Poults

Similar to the results from chicks, results for infected poults showed all had high levels of PDCoV RNA in cloacal and tracheal swabs through 14 dpi (Figure 6, panels A, B). Poults appeared to have higher initial viral loads, averaging $8.07 \log_{10}$ GE/mL by 2 dpi, decreasing to $\approx 6 \log_{10}$ GE/mL at 4 dpi, and persisting through 14 dpi (Figure 6, panel A). Naive birds also were susceptible to infection, and cloacal and tracheal swab specimens from all sentinel poults were positive for PDCoV RNA within 2 days after comingling with

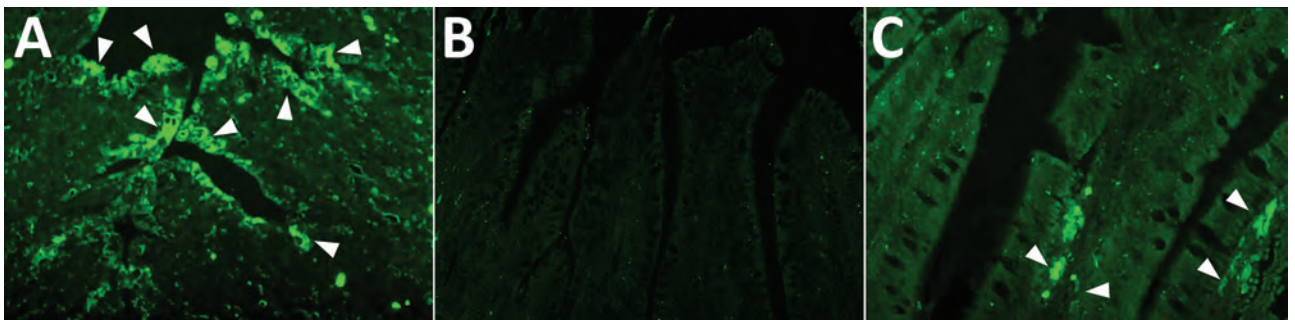


Figure 2. Detection of porcine deltacoronavirus (PDCoV) antigen in poultry by immunofluorescent (IF) staining in the intestines of poults inoculated with intestinal contents of a PDCoV-infected GF pig (DC175) ($6.87 \log_{10}$ 50% tissue culture infectious dose/mL) or a mock inoculate in a study of infection and transmission of porcine deltacoronavirus in poultry. A) PDCoV-infected pig intestine used as positive control; white arrows indicate widespread antibody staining. B) IF-stained jejunum of a poults (no. 42) at 14 dpi with no antigen-positive cells. C) IF-stained jejunum of a poults (no. 63) at 14 days postinoculation (dpi); white arrows indicate several PDCoV antigen-positive cells in the villous epithelial cells. Original magnification $\times 300$.

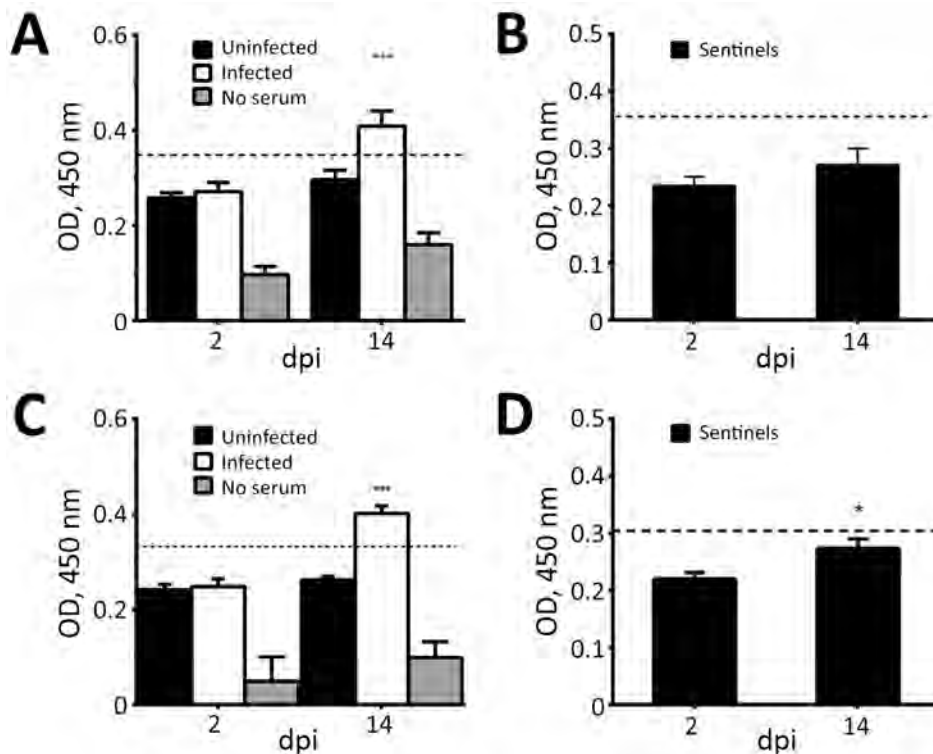


Figure 3. Detection of porcine deltacoronavirus (PDCoV)-specific IgY antibody titers in serum collected from chicks and turkey poults in a study of infection and transmission of porcine deltacoronavirus in poultry. A) Uninfected ($n = 6$) and infected chicks ($n = 6$). B) Sentinel chicks ($n = 5$). C) Uninfected ($n = 5$) and infected poults ($n = 6$). D) Sentinel poults ($n = 5$). OD values are blanked against a control of uncoated wells (carbonate buffer only). Values represent the average of 3 replicates; error bars represent upper half of SEM. Dashed line indicates cutoff, which was determined by using the mean of uninfected birds at 2 dpi +2 SDs. Statistically significant values: * $p < 0.05$; *** $p < 0.001$. dpi, days postinoculation; OD, optical density.

infected poults (Figure 6, panels C, D, E). We calculated titers and viral RNA loads in SIC and LIC from infected and sentinel poults at 3, 7, and 14 dpi (Figure 5, panel B). We tested infectivity of intestinal contents of infected and sentinel poults by using TCID₅₀ assay at 7 and 14 dpi (Figure 5, panel B).

We isolated viral RNA from the SIC of 1 infected and 1 sentinel bird at 14 dpi and used it to amplify an $\approx 1,300$ -bp portion of the N gene of PDCoV, then gel extracted and sequenced the resulting product. As we noted in chicks, the samples sequenced had >99% identity with the original inoculum, the Ohio FD22 strain of PDCoV.

Discussion

Emerging viruses in at least 2 genera of porcine CoVs have exhibited increased propensity for interspecies transmission (2,29). Porcine APN was identified as a major cell entry receptor for PDCoV (19,30). APN is a protein that exhibits enzymatic activity, peptide processing, cholesterol uptake, and chemotaxis to cell signaling and cell adhesion (31). APN is widely distributed and highly conserved in amino acid sequences across species of the Animalia kingdom (19) and is expressed in a wide range of tissues, including epithelial cells of the kidneys (31), respiratory tract (32,33), and gastrointestinal tract (34).

Our data suggest that chicks and poults are susceptible to infection with PDCoV. In addition, the rapid transmission of PDCoV to the sentinel birds that comingled with infected birds demonstrates that the virus could spread easily. The length of our pilot study did not allow us to determine how long the chicks and poults would be affected by PDCoV or how long they might shed viral RNA. The chicks appeared to recover more rapidly than poults; clinical signs diminished or were completely absent by 14 dpi. However, chicks still were shedding low viral RNA titers at 14 dpi. Poults did not recover by the end of the study and still exhibited gross pathology and mild to moderate diarrhea. PDCoV RNA shedding titers were higher in poults than in the chicks. Cloacal shedding titers in chicks peaked at 9 dpi and then decreased. In poults, cloacal viral RNA shedding titers were multiphasic, peaking at 2 dpi, with additional smaller peaks at 9 and 14 dpi. The rapid onset of viral RNA shedding correlates with previous *in vitro* data in which the PDCoV S1 domain bound most efficiently to APN of galline origin (19) and cytopathic effects were observed more rapidly in leghorn male hepatoma and DF1 chicken cell lines compared with swine testicular cells (S.P. Kenney, unpub. data).

ELISA results showed that both chicks and poults developed PDCoV antibodies by 14 dpi. Pig infection dynamics have demonstrated a similar serum

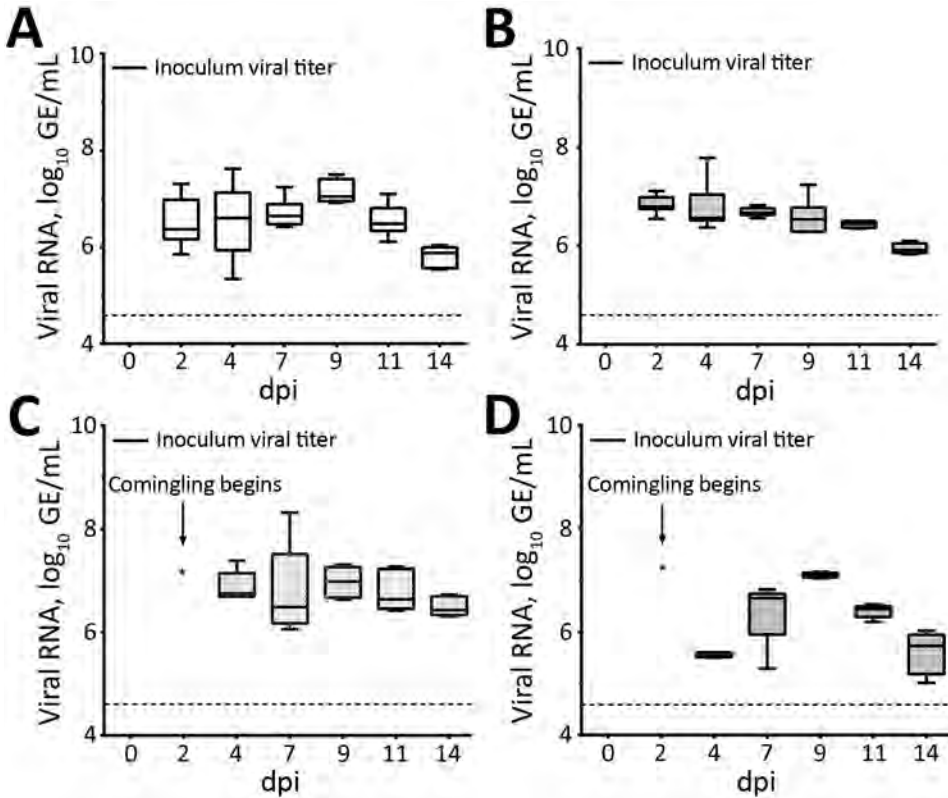


Figure 4. Porcine deltacoronavirus (PDCoV) viral RNA shedding patterns in samples collected from cloaca (A) and trachea (B) of infected and uninfected chicks, and from cloaca (C) and trachea (D) of sentinel chicks in a study of infection and transmission of porcine deltacoronavirus in poultry. Inoculum viral titer represents the genomic equivalent (GE) of inoculum administered at onset, 9.71 log₁₀ GE/mL. Box plots represent distribution of values; tops and bottoms of boxes represent 10%–90% range of values; horizontal lines within boxes indicate medians; error bars represent SEM. Dashed line indicates detection limit of 4.6 log₁₀ GE/mL of PDCoV in samples. dpi, days postinoculation; GE, genomic equivalent.

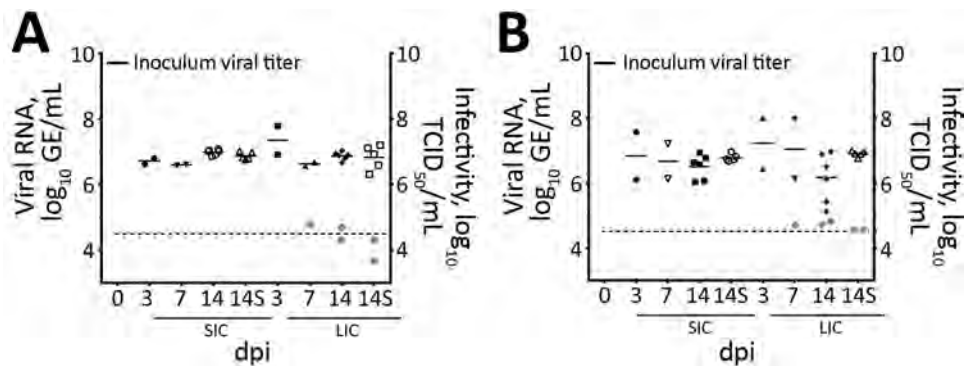
neutralizing antibody titer increase at 7–14 days (12,25). Sentinel birds had low or undetectable antibody responses compared with experimentally challenged birds, likely because of the passive infection method and because less time passed between exposure to the virus and the end of the study.

Recent studies demonstrated that PDCoV can infect and kill cells of other species through APN receptors (19,35). PDCoV has been reported to infect commercial chickens in vivo (36). The differences in susceptibility to PDCoV infection between chicks and

poult we observed could be related to differences in APN expression levels between the species.

The true incidence rates for PDCoV infection, natural host range, reservoirs, and routes of transmission are still relatively unknown, and no plans for vaccine development have been reported (37). DCoV RNA has been detected in fecal samples from wild birds (38,39), Chinese ferret badgers (*Melogale moschata*), and leopard cats (40). In addition to swine, calves have been shown by experimental testing to be susceptible to PDCoV infection (41). These data, coupled with the

Figure 5. Viral RNA titers and infectivity of intestinal contents of (A) chicks and (B) poult in a study of infection and transmission of porcine deltacoronavirus in poultry. Inoculum viral titer represents the genomic equivalent (GE) of inoculum administered at onset, 9.71 log₁₀ GE/mL. Gray dots represent infectivity at 7 and 14 dpi, expressed in log₁₀ TCID₅₀/mL, as indicated on the right y-axis. Dashed line indicates detection limit of 4.6 log₁₀ GE/mL of PDCoV in samples. Shapes represent individual birds necropsied at each time point. Solid bars represent the mean. dpi, days postinoculation; GE, genomic equivalent; LIC, large intestine contents; S, sentinel birds necropsied; SIC, small intestine contents; TCID₅₀, 50% tissue culture infectious dose.



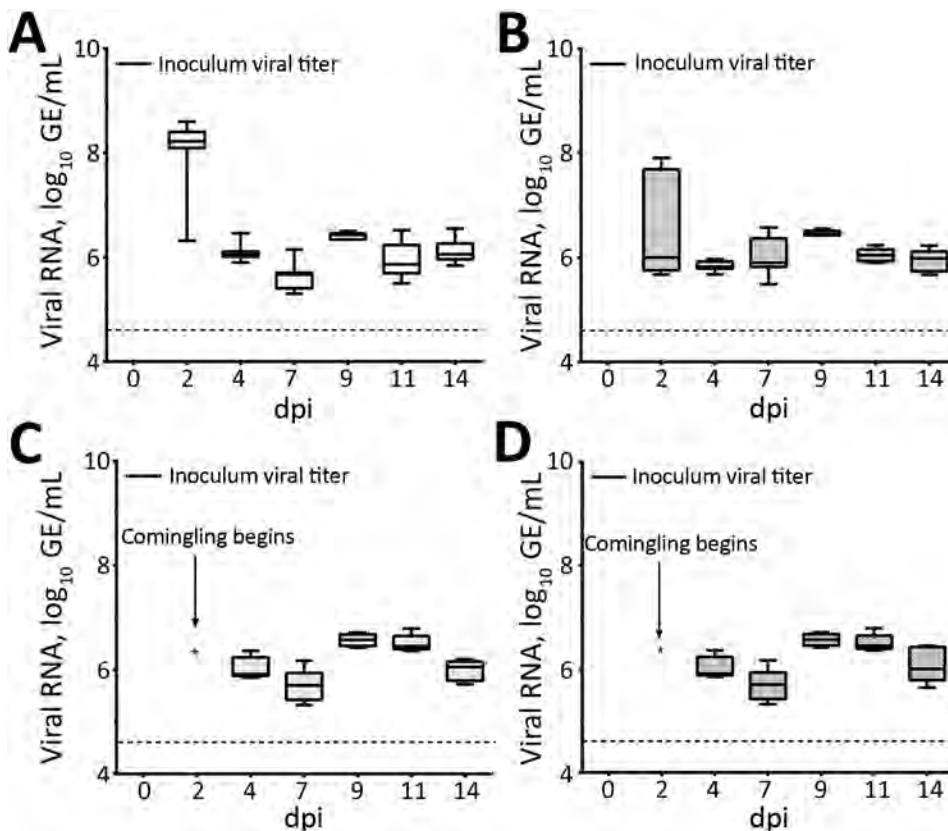


Figure 6. Porcine deltacoronavirus (PDCoV) viral RNA shedding patterns in samples collected from cloaca (A) and trachea (B) of infected and uninfected poulters and from cloaca (C) and trachea (D) of sentinel poulters in a study of infection and transmission of porcine deltacoronavirus in poultry. Inoculum viral titer represents the genomic equivalent (GE) of inoculum administered at onset, $9.71 \log_{10}$ GE/mL. Box plots represent distribution of values; tops and bottoms of boxes represent 10%–90% range of values; horizontal lines within boxes indicate medians; error bars represent SEM. Dashed line indicates detection limit of $4.6 \log_{10}$ GE/mL of PDCoV in samples. dpi, days postinoculation.

PDCoV binding receptor APN being conserved across many species, suggest that the host range for PDCoV is broader than initially expected (19). The close sequence homology between DCoV isolates from mammalian and wild bird species implies a transmission cycle in which PDCoV regularly crosses from wild birds and mammals into animal production systems, including the swine and poultry industries. More epidemiologic data are required to understand the full extent to which DCOVs are threatening food production systems and whether they pose a direct threat to human health.

Our results are consistent with the likelihood that avian species act as potential passthrough or intermediate hosts for PDCoV. In vivo confirmation of avian susceptibility to PDCoV suggests that in vitro data implicating human susceptibility should be evaluated further. Research regarding how PDCoV is adapting and mutating in different species and whether it infects humans is critical to determining if PDCoV poses a pandemic health risk to commercial poultry or humans.

Acknowledgments

We thank the animal care staff of the Ohio Agricultural Research and Development Center (OARDC) of The Ohio State University for assisting in the rearing and care of birds used in this study, Xiaohong Wang for assistance

with rRT-PCR, Anastasia Vlasova and lab for insightful discussions and protocols, John Ngunjiri for training on inoculation of chickens, and Tea Meulia for assisting with immunofluorescent image processing.

The National Institute of Food and Agriculture provided funding through the Food Animal Health Research Program (project number OHO0005-AH).

About the Author

Dr. Boley currently investigates emerging zoonotic coronaviruses in the Ohio Agricultural Research and Development Center (OARDC) of The Ohio State University. Her research interests include coronaviruses, emerging zoonotic diseases, and chemoprevention of liver cancer.

References

1. Masters PS, Perlman S. Coronaviridae. In: Knipe DM, Howley PM, eds. *Fields virology*, 6th ed. Philadelphia: Lippincott Williams & Wilkins; 2013. p. 825–58.
2. Chan JF, To KK, Tse H, Jin DY, Yuen KY. Interspecies transmission and emergence of novel viruses: lessons from bats and birds. *Trends Microbiol.* 2013;21:544–55. <https://doi.org/10.1016/j.tim.2013.05.005>
3. Schwegmann-Wessels C, Herrler G. Transmissible gastroenteritis virus infection: a vanishing specter. *Dtsch Tierarztl Wochenschr.* 2006;113:157–9.

4. Song D, Zhou X, Peng Q, Chen Y, Zhang F, Huang T, et al. Newly emerged porcine deltacoronavirus associated with diarrhoea in swine in China: identification, prevalence and full-length genome sequence analysis. *Transbound Emerg Dis.* 2015;62:575–80. <https://doi.org/10.1111/tbed.12399>
5. Huang YW, Dickerman AW, Piñeyro P, Li L, Fang L, Kiehne R, et al. Origin, evolution, and genotyping of emergent porcine epidemic diarrhea virus strains in the United States. *MBio.* 2013;4:e00737–13. <https://doi.org/10.1128/mBio.00737-13>
6. Memish ZA, Zumla AI, Al-Hakeem RF, Al-Rabeeh AA, Stephens GM. Family cluster of Middle East respiratory syndrome coronavirus infections. *N Engl J Med.* 2013;368:2487–94. <https://doi.org/10.1056/NEJMoa1303729>
7. de Wit E, van Doremalen N, Falzarano D, Munster VJ. SARS and MERS: recent insights into emerging coronaviruses. *Nat Rev Microbiol.* 2016;14:523–34. <https://doi.org/10.1038/nrmicro.2016.81>
8. Jean A, Quach C, Yung A, Semret M. Severity and outcome associated with human coronavirus OC43 infections among children. *Pediatr Infect Dis J.* 2013;32:325–9. <https://doi.org/10.1097/INF.0b013e3182812787>
9. Lau SK, Woo PC, Yip CC, Tse H, Tsoi HW, Cheng VC, et al. Coronavirus HKU1 and other coronavirus infections in Hong Kong. *J Clin Microbiol.* 2006;44:2063–71. <https://doi.org/10.1128/JCM.02614-05>
10. Fehr AR, Perlman S. Coronaviruses: an overview of their replication and pathogenesis. *Methods Mol Biol.* 2015;1282:1–23. https://doi.org/10.1007/978-1-4939-2438-7_1
11. Woo PC, Lau SK, Lam CS, Lau CC, Tsang AK, Lau JH, et al. Discovery of seven novel mammalian and avian coronaviruses in the genus *Deltacoronavirus* supports bat coronaviruses as the gene source of alphacoronavirus and betacoronavirus and avian coronaviruses as the gene source of gammacoronavirus and deltacoronavirus. *J Virol.* 2012;86:3995–4008. <https://doi.org/10.1128/JVI.06540-11>
12. Zhang J. Porcine deltacoronavirus: overview of infection dynamics, diagnostic methods, prevalence and genetic evolution. *Virus Res.* 2016;226:71–84. <https://doi.org/10.1016/j.virusres.2016.05.028>
13. Jung K, Hu H, Eyerly B, Lu Z, Chepngeno J, Saif LJ. Pathogenicity of 2 porcine deltacoronavirus strains in gnotobiotic pigs. *Emerg Infect Dis.* 2015;21:650–4. <https://doi.org/10.3201/eid2104.141859>
14. Vitosh-Sillman S, Loy JD, Brodersen B, Kelling C, Doster A, Topliff C, et al. Experimental infection of conventional nursing pigs and their dams with porcine deltacoronavirus. *J Vet Diagn Invest.* 2016;28:486–97. [PubMed https://doi.org/10.1177/1040638716654200](https://doi.org/10.1177/1040638716654200)
15. Wang L, Byrum B, Zhang Y. Detection and genetic characterization of deltacoronavirus in pigs, Ohio, USA, 2014. *Emerg Infect Dis.* 2014;20:1227–30. <https://doi.org/10.3201/eid2007.140296>
16. Marthaler D, Jiang Y, Collins J, Rossow K. Complete genome sequence of strain SDCV/USA/Illinois121/2014, a porcine deltacoronavirus from the United States. *Genome Announc.* 2014;2:e00218–14. <https://doi.org/10.1128/genomeA.00218-14>
17. Li G, Chen Q, Harmon KM, Yoon KJ, Schwartz KJ, Hoogland MJ, et al. Full-length genome sequence of porcine deltacoronavirus strain USA/IA/2014/8734. *Genome Announc.* 2014;2:e00278–14. <https://doi.org/10.1128/genomeA.00278-14>
18. Jung K, Wang Q, Scheuer KA, Lu Z, Zhang Y, Saif LJ. Pathology of US porcine epidemic diarrhea virus strain PC21A in gnotobiotic pigs. *Emerg Infect Dis.* 2014;20:662–5. <https://doi.org/10.3201/eid2004.131685>
19. Li W, Hulswit RJG, Kenney SP, Widjaja I, Jung K, Alhano MA, et al. Broad receptor engagement of an emerging global coronavirus may potentiate its diverse cross-species transmissibility. *Proc Natl Acad Sci U S A.* 2018;115:E5135–43. <https://doi.org/10.1073/pnas.1802879115>
20. Geoghegan JL, Duchêne S, Holmes EC. Comparative analysis estimates the relative frequencies of co-divergence and cross-species transmission within viral families. *PLoS Pathog.* 2017;13:e1006215. <https://doi.org/10.1371/journal.ppat.1006215>
21. Ismail MM, Tang AY, Saif YM. Pathogenicity of turkey coronavirus in turkeys and chickens. *Avian Dis.* 2003;47:515–22. <https://doi.org/10.1637/5917>
22. Ismail MM, Cho KO, Ward LA, Saif LJ, Saif YM. Experimental bovine coronavirus in turkey poults and young chickens. *Avian Dis.* 2001;45:157–63. <https://doi.org/10.2307/1593023>
23. Hu H, Jung K, Vlasova AN, Chepngeno J, Lu Z, Wang Q, et al. Isolation and characterization of porcine deltacoronavirus from pigs with diarrhea in the United States. *J Clin Microbiol.* 2015;53:1537–48. <https://doi.org/10.1128/JCM.00031-15>
24. Reed LJ, Muench H. A simple method of estimating fifty percent endpoints. *Am J Epidemiol.* 1938;37:493–7.
25. Jung K, Miyazaki A, Hu H, Saif LJ. Susceptibility of porcine IPEC-J2 intestinal epithelial cells to infection with porcine deltacoronavirus (PDCoV) and serum cytokine responses of gnotobiotic pigs to acute infection with IPEC-J2 cell culture-passaged PDCoV. *Vet Microbiol.* 2018;221:49–58. <https://doi.org/10.1016/j.vetmic.2018.05.019>
26. Hu H, Jung K, Vlasova AN, Saif LJ. Experimental infection of gnotobiotic pigs with the cell-culture-adapted porcine deltacoronavirus strain OH-FD22. *Arch Virol.* 2016;161:3421–34. <https://doi.org/10.1007/s00705-016-3056-8>
27. Jung K, Kim J, Ha Y, Choi C, Chae C. The effects of transplacental porcine circovirus type 2 infection on porcine epidemic diarrhoea virus-induced enteritis in preweaning piglets. *Vet J.* 2006;171:445–50. <https://doi.org/10.1016/j.tvjl.2005.02.016>
28. Okda F, Lawson S, Liu X, Singrey A, Clement T, Hain K, et al. Development of monoclonal antibodies and serological assays including indirect ELISA and fluorescent microsphere immunoassays for diagnosis of porcine deltacoronavirus. *BMC Vet Res.* 2016;12:95. <https://doi.org/10.1186/s12917-016-0716-6>
29. Vlasova AN, Saif LJ. Biological aspects of the interspecies transmission of selected coronaviruses. In: Singh SK, editor. *Viral infections and global change.* Hoboken (NJ): John Wiley & Sons; 2013. p. 393–418.
30. Ji CM, Wang B, Zhou J, Huang YW. Aminopeptidase-N-independent entry of porcine epidemic diarrhea virus into Vero or porcine small intestine epithelial cells. *Virology.* 2018;517:16–23. <https://doi.org/10.1016/j.virol.2018.02.019>
31. Mina-Osorio P. The moonlighting enzyme CD13: old and new functions to target. *Trends Mol Med.* 2008;14:361–71. <https://doi.org/10.1016/j.molmed.2008.06.003>
32. van der Velden VH, Wierenga-Wolf AF, Adriaansen-Soeting PW, Overbeek SE, Möller GM, Hoogsteden HC, et al. Expression of aminopeptidase N and dipeptidyl peptidase IV in the healthy and asthmatic bronchus. *Clin Exp Allergy.* 1998;28:110–20. <https://doi.org/10.1046/j.1365-2222.1998.00198.x>
33. Dijkman R, Jebbink MF, Koekoek SM, Deijs M, Jónsdóttir HR, Molenkamp R, et al. Isolation and characterization of current human coronavirus strains in primary human epithelial cell cultures reveal differences

- in target cell tropism. *J Virol*. 2013;87:6081–90. <https://doi.org/10.1128/JVI.03368-12>
34. Kenny AJ, Maroux S. Topology of microvillar membrane hydrolases of kidney and intestine. *Physiol Rev*. 1982;62:91–128. <https://doi.org/10.1152/physrev.1982.62.1.91>
 35. Wang B, Liu Y, Ji CM, Yang YL, Liang QZ, Zhao P, et al. Porcine deltacoronavirus engages the transmissible gastroenteritis virus functional receptor porcine aminopeptidase N for infectious cellular entry. *J Virol*. 2018;92:e00318-18. <https://doi.org/10.1128/JVI.00318-18>
 36. Liang Q, Zhang H, Li B, Ding Q, Wang Y, Gao W, et al. Susceptibility of chickens to porcine deltacoronavirus infection. *Viruses*. 2019;11:E573. <https://doi.org/10.3390/v11060573>
 37. Wang Q, Vlasova AN, Kenney SP, Saif LJ. Emerging and re-emerging coronaviruses in pigs. *Curr Opin Virol*. 2019;34:39–49. <https://doi.org/10.1016/j.coviro.2018.12.001>
 38. Chen Q, Wang L, Yang C, Zheng Y, Gauger PC, Anderson T, et al. The emergence of novel sparrow deltacoronaviruses in the United States more closely related to porcine deltacoronaviruses than sparrow deltacoronavirus HKU17. *Emerg Microbes Infect*. 2018;7:105. <https://doi.org/10.1038/s41426-018-0108-z>
 39. Hu H, Jung K, Wang Q, Saif LJ, Vlasova AN. Development of a one-step RT-PCR assay for detection of pancoronaviruses (α -, β -, γ -, and δ -coronaviruses) using newly designed degenerate primers for porcine and avian fecal samples. *J Virol Methods*. 2018;256:116–22. <https://doi.org/10.1016/j.jviromet.2018.02.021>
 40. Dong BQ, Liu W, Fan XH, Vijaykrishna D, Tang XC, Gao F, et al. Detection of a novel and highly divergent coronavirus from Asian leopard cats and Chinese ferret badgers in southern China. *J Virol*. 2007;81:6920–6. <https://doi.org/10.1128/JVI.00299-07>
 41. Jung K, Hu H, Saif LJ. Calves are susceptible to infection with the newly emerged porcine deltacoronavirus, but not with the swine enteric alphacoronavirus, porcine epidemic diarrhea virus. *Arch Virol*. 2017;162:2357–62. <https://doi.org/10.1007/s00705-017-3351-z>

Address for correspondence: Scott P. Kenney, The Ohio State University, Food Animal Health Research Program, 1680 Madison Ave, Hayden Hall Wooster, Wooster, OH 44691, USA; email: kenney.157@osu.edu



EMERGING INFECTIOUS DISEASES®

December 2018

Zoonotic Infections

- Outbreak of HIV Infection Linked to Nosocomial Transmission, China, 2016–2017
- Autochthonous Human Case of Seoul Virus Infection, the Netherlands
- Restaurant Inspection Letter Grades and *Salmonella* Infections, New York City
- Spatial Analysis of Wildlife Tuberculosis Based on a Serologic Survey Using Dried Blood Spots, Portugal
- Comparison of Highly Pathogenic Avian Influenza H5 Guangdong Lineage Epizootic in Europe (2016–17) with Previous HPAI H5 Epizootics
- *Capnocytophaga canimorsus* Capsular Serovar and Disease Severity, Helsinki, Finland, 2000–2017
- Rat Lungworm Infection in Rodents Across Post-Katrina New Orleans, Louisiana
- Emerging Multidrug-Resistant Hybrid Pathotype Shiga toxin-producing *Escherichia coli* O80 and Related Strains of Clonal Complex 165, Europe
- Terrestrial Bird Migration and West Nile Virus Circulation, United States
- Substance Use and Adherence to HIV Preexposure Prophylaxis for Men Who Have Sex with Men
- Genomic Characterization of β -Glucuronidase-Positive *Escherichia coli* O157:H7 Producing Stx2a
- Highly Pathogenic Clone of Shiga Toxin-producing *Escherichia coli* O157:H7, England and Wales
- CTX-M-65 Extended-Spectrum β -Lactamase-Producing *Salmonella* Serotype Infantis, United States
- Novel Type of Chronic Wasting Disease Detected in Moose (*Alces alces*), Norway
- Survey of Ebola Viruses in Frugivorous and Insectivorous Bats in Guinea, Cameroon, and the Democratic Republic of the Congo, 2015–2017
- Prevalence of Avian Influenza A(H5) and A(H9) Viruses in Live Bird Markets, Bangladesh

To revisit the December 2018 issue, go to:

<https://wwwnc.cdc.gov/eid/articles/issue/24/12/table-of-contents>

Chronic Human Pegivirus 2 without Hepatitis C Virus Co-infection

Kelly E. Collier, Veronica Bruce, Michael Cassidy, Jeffrey Gersch, Matthew B. Frankel, Ana Vallari, Gavin Cloherty, John Hackett, Jr., Jennifer L. Evans, Kimberly Page, George J. Dawson

Most human pegivirus 2 (HPgV-2) infections are associated with past or current hepatitis C virus (HCV) infection. HPgV-2 is thought to be a bloodborne virus: higher prevalence of active infection has been found in populations with a history of parenteral exposure to viruses. We evaluated longitudinally collected blood samples obtained from injection drug users (IDUs) for active and resolved HPgV-2 infections using a combination of HPgV-2-specific molecular and serologic tests. We found evidence of HPgV-2 infection in 11.2% (22/197) of past or current HCV-infected IDUs, compared with 1.9% (4/205) of an HCV-negative IDU population. Testing of available longitudinal blood samples from HPgV-2-positive participants identified 5 with chronic infection (>6 months viremia in >3 timepoints); 2 were identified among the HCV-positive IDUs and 3 among the HCV-negative IDUs. Our findings indicate that HPgV-2 can establish chronic infection and replicate in the absence of HCV.

The recently identified second human pegivirus (HPgV-2 or HHpgV-1) is a bloodborne flavivirus: little is known about the potential clinical significance of infection (1,2). Active or resolved HPgV-2 infection has been detected worldwide in cohorts associated with risk for parenteral exposure to bloodborne pathogens (1,3–5). In a study in which hepatitis C virus (HCV) status was determined (3), 1.2% of HCV positive were actively infected with HPgV-2; none of the 1,306 HCV-negative participants (volunteer blood donors, HBV infected, HIV infected) were actively infected. In another study, participants with concurrent HIV/HCV infection or injection drug users (IDUs) had a higher prevalence (3.0%–5.7%) of active HPgV-2 infection (4–6). Although active HPgV-2 has been found in other populations (e.g., hemophiliacs or others,

with risk for parenteral exposure), their HCV antibody status was not determined (6,7).

Previous studies indicate that HPgV-2 can establish a chronic infection characterized by detectable viremia for >6 months (2,6). Most chronic HPgV-2 cases are associated with active HCV infection (2,6). In chronic HPgV-2 cases in which HCV RNA has not been detected, the presence of HCV antibodies (indicating a resolved infection) was not determined; thus, it is unclear whether previous HCV infection played a role in the initial HPgV-2 infection. Despite observations of HCV and HPgV-2 co-infection, no evidence has been reported that HPgV-2 infection exacerbates HCV infection (5,6,8) or that co-infection influences the replication of either virus.

We examined a cohort of IDUs for whom longitudinal samples were available. We monitored the cohort for HCV status by HCV antibodies, RNA, or both, with the intent of capturing nascent HCV infections (9). We performed initial testing for HPgV-2 (RNA and antibodies) on baseline and last collected samples. We further characterized longitudinal samples from available participants that showed active or resolved HPgV-2 infection upon testing initial or last timepoints. We hypothesized that the IDUs would have similar prevalence of HPgV-2 as shown in a previous study of HCV-infected persons with unknown IDU status, and that by studying IDUs without HCV infection we would uncover HPgV-2 infection in the absence of HCV. Last, we hypothesized that longitudinal samples from IDUs would reveal whether HPgV-2 can establish a persistent infection in the absence of HCV co-infection.

Materials and Methods

Samples

We obtained samples from the U-Find-Out (UFO) Study, an ongoing prospective observational study of young adult active injectors, <30 years of age at enrollment, that was initiated in 2003 in the San Francisco Bay area (California, USA). Details of enrollment

Author affiliations: Abbott Laboratories, Abbott Park, Illinois, USA (K.E. Collier, M. Cassidy, J. Gersch, M.B. Frankel, A. Vallari, G. Cloherty, J. Hackett, Jr., G.J. Dawson); University of New Mexico, Albuquerque, New Mexico, USA (V. Bruce, K. Page); University of California San Francisco, San Francisco, California, USA (J.L. Evans)

DOI: <https://doi.org/10.3201/eid2602.190434>

methods and follow-up have been described previously (9,10). In brief, young adult IDUs were recruited from neighborhoods where IDUs were known to congregate and invited to participate in a field study for eligibility screening. Eligible persons were those who reported injection drug use in the prior 30 days, were <30 years of age, spoke English, had no plans to travel outside of the San Francisco Bay area for >3 months, and had negative or unknown HCV status. HCV antibody-positive persons were admitted into the study if their HCV RNA status was negative or unknown; those identified as HCV infected (RNA positive) at baseline were not enrolled into follow-up.

Eligible consenting participants were asked to complete a baseline interviewer-administered structured questionnaire that queried sociodemographics, parenteral and sexual risk behaviors and exposures, injecting exposures (e.g., frequency of injecting, number of persons injected with, types of drugs injected), alcohol use, and prevention and health service use. They were also asked to provide blood samples for HCV testing, including both HCV antibodies and HCV RNA, and for storage. Before 2012, all participants provided samples for HCV antibodies (using standard laboratory-based testing) and for a qualitative HCV RNA status determination using a nucleic acid amplification test (Proclix HIV-1/HCV assay; Gen-Probe Inc., <https://www.novartis.com>). Beginning in May 2012, HCV antibody testing was primarily conducted using a rapid test (OraSure Technologies, <https://www.orasure.com>) by fingerstick capillary blood collection; however, venipuncture was still used to collect specimens for RNA testing and sample storage. Baseline samples on 402 participants were selected as the initial sample set (Figure). A total of 205 (51.0%) samples were negative and 197 (49.0%) positive for HCV antibodies and HCV RNA at baseline. HCV-positive in this current study is defined as any evidence of HCV infection (RNA

or HCV antibodies), past or present; HCV-negative is defined as no evidence (RNA or HCV antibodies), past or present.

HPgV-2 Prevalence Study Design

We used previously described HPgV-2 molecular (11) and serologic (3) assays to test all samples for determining HPgV-2 prevalence. We divided them into 3 testing groups: sample set 1, initial blood samples ($n = 402$); sample set 2, all last available follow-up samples ($n = 200$); and sample set 3, any longitudinal samples available for samples that were HPgV-2 (RNA or antibody) positive at initial or last draw timepoint ($n = 70$) (Figure). Because the initial study collection targeted incident HCV infection, a limited number of participants who were HCV positive at initial collection had follow-up samples available; only 8 HCV-positive and 192 HCV-negative participants from sample set 1 had follow-up (last) draw available for testing, constituting sample set 2.

HPgV-2 Molecular Assay

We used a modified version of the HPgV-2 reverse transcription PCR (RT-PCR) to determine HPgV-2 viremia (11). The RT-PCR targets 2 conserved regions of the HPgV-2 genome within the 5' untranslated region (UTR) and the nonstructural (NS) 2–3 coding region (11). We modified the assay to replace detection of HPgV RNA with an internal control. The internal control was derived from the hydroxypyruvate reductase gene from the pumpkin plant, *Cucurbita pepo*, and is delivered in an Armored RNA (Ambion, Inc., <https://www.thermofisher.com>) particle that has been diluted in negative human plasma (nonreactive for HBsAg, HIV RNA, HCV RNA, HBV DNA, HIV-1/-2 antibodies, and HCV antibodies). We introduced the internal control into each specimen at the beginning of sample preparation as a control for extraction and amplification. We extracted samples from plasma using

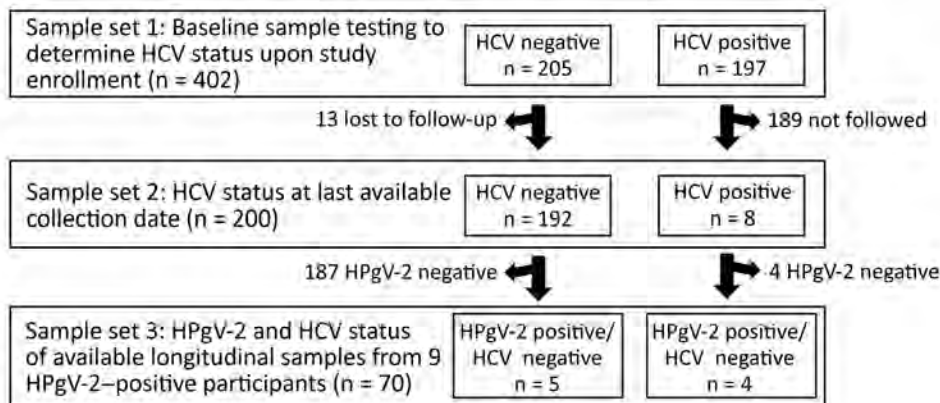


Figure. Design of study of chronic human pegivirus-2 and hepatitis C virus co-infection in injection drug users in the San Francisco Bay area, California, USA. Samples were tested using HPgV-2 molecular and serologic assays in 3 sample sets. HCV, hepatitis C virus; HPgV-2, human pegivirus 2.

the Abbott *m2000sp* instrument (Abbott Molecular, <https://www.molecular.abbott>) (open mode protocol m2000-RNA-Plasma-LL-500-110-v71408, version 1.0). We used eluted nucleic acids immediately for subsequent PCR analysis or stored them in the deep well plate at -80°C .

HPgV-2 Antibody Testing

We screened research use-only assays to detect IgG response to HPgV-2 proteins for HPgV-2 seroconversion (3). In brief, we built 2 separate indirect IgG assays for use on the ARCHITECT instrument (Abbott Laboratories). The capture antigen for the E2 assay was mammalian expressed glycoprotein E2, and for the NS4AB assay a portion of the NS4AB region. We generated signal to cutoff values for each assay by determining a provisional cutoff from testing a population of low-risk volunteer donors and calculating the median + 10 SD of relative light units (RLU) generated using the individual assays (3). Both E2 and NS4AB assays detected active and resolved HPgV-2 infection (3).

Statistical Analyses

We used the Fisher exact test to examine differences in prevalence of HPgV-2 between subgroups (for example, by HCV status). We performed unpaired Student *t*-tests to determine if there was a significant difference ($p < 0.05$) between the average HPgV-2 log copies/mL (NS2/3 or 5'UTR) of the HCV positive and negative groups. We used GraphPad Prism version 6.04 for Windows (GraphPad Software, <https://www.graphpad.com>).

Results

Baseline Sample Testing

The overall prevalence of HPgV-2 (presence of RNA or antibodies) among baseline samples in the IDU cohort was 6.5% (Table 1; Figure). We determined a higher HPgV-2 prevalence in the HCV-positive group (11.2%) compared with the HCV-negative group (1.9%) ($p = 0.0002$ by Fisher exact test). We observed HPgV-2 infection (HPgV-2 RNA) more frequently in the HCV-positive group (6.1%; 12/197 samples) than in the HCV-negative group (1.0%; 2/197 samples).

Last Sample Testing

Follow-up specimens were available for some study participants (sample set 2), primarily those who were HCV negative, due to the prospective design of the study that did not require follow-up samples from HCV-positive participants (Figure). However, the study also included persons with newly detected HCV infection whom we followed to examine natural history and resolution of incident HCV infection (9). A total of 200 participants from baseline collection had a final follow-up sample available for evaluation in the HPgV-2 RNA and antibody assays; this group included 8 HCV-positive and 192 HCV-negative participants (Figure). Although 26 participants were HPgV-2 positive (by RNA or antibodies) at baseline (Table 1), only 4 participants were available for follow-up; they provided 3 HPgV-2 RNA-positive samples and 1 HPgV-2 RNA-negative seropositive sample.

We saw evidence of HPgV-2 infection (antibodies or RNA) in 9 samples in set 2, 6 HCV-negative samples and 3 HCV-positive samples (Table 2). Among the HCV-negative participants, 3 (QM0003, VH0052, VP0295) showed active HPgV-2 infection during either the baseline or last draw timepoint. Participant QM0003 showed chronic (>6 mos viremia) HPgV-2 infection during the study, with detection of HPgV-2 RNA at time points spanning 832 days (Table 2). Participant VH0052 was actively infected with HPgV-2 at baseline and resolved infection by the last draw date (201 days elapsed), whereas participant VP0295 acquired HPgV-2 infection during the study and was RNA positive at the last draw date (on study for 553 days). Three participants (GG0012, RM0095, RM0337) were HPgV-2 RNA and antibody negative at enrollment and had seroconverted to have HPgV-2 antibodies by the last draw. One participant, VH0044, was HPgV-2 seropositive at baseline but was seronegative (seroreverted) by the final draw (250 days elapsed).

In the HCV-positive group, 1 participant (VH0085) was HPgV-2 RNA positive both on the first and last draw dates (2,805 days elapsed). The other 2 HCV-positive participants (GG0038 and VT0031) were HPgV-2 RNA negative on the first draw dates but showed active HPgV-2 infection at the last draw date. A single participant (RM0337) acquired both

Table 1. Prevalence of HPgV-2 antibodies or RNA, initial blood draw samples from study of chronic HPgV-2 infection and HCV co-infection in injection drug users in the San Francisco Bay area, California, USA*

HCV status	No. tested	No. HPgV-2 Ab+	No. HPgV-2 Ab+/RNA+	No. HPgV-2 Ab-/RNA+	Total RNA+	Total HPgV-2 RNA or Ab+ (%)
HCV positive	197	18	8	4	12	22 (11.2)
HCV negative	205	3	1	1	2	4 (1.9)
Totals	402	21	9	5	14	26 (6.5)

*Ab, antibody; HCV, hepatitis C virus; HPgV-2, human pegivirus 2; +, positive; -, negative.

Table 2. Evidence of HPgV-2 infection in most recent samples from study of chronic HPgV-2 infection and HCV co-infection in injection drug users in the San Francisco Bay area, California, USA*

HCV RNA status at initial draw	Sample ID	HPgV-2 status at initial blood draw		HPgV-2 status at last blood draw		HCV RNA status	No. days†	Comments‡
		RNA	Antibody	RNA	Antibody			
Negative	QM0003	Pos	Neg	Pos	Pos	Neg	832	Chronic
	VH0052	Pos	Pos	Neg	Pos	Neg	201	Resolved
	VP0295	Neg	Neg	Pos	Pos	Neg	553	Active
	GG0012	Neg	Neg	Neg	Pos	Neg	689	Resolved
	RM0095	Neg	Neg	Neg	Pos	Neg	201	Resolved
	RM0337§	Neg	Neg	Neg	Pos	Pos	1,680	Resolved
	VH0044	Neg	Pos	Neg	Neg	Neg	250	Resolved
Positive	VH0085	Pos	Pos	Pos	Pos	Neg	2,805	Chronic
	GG0038	Neg	Neg	Pos	Neg	Neg	461	Active
	VT0031	Neg	Neg	Pos	Pos	Pos	818	Active

*HCV, hepatitis C virus; HPgV-2, human pegivirus 2; neg, negative; pos, positive.

†Days elapsed between initial and last blood draw.

‡Comments of HPgV-2 status based on initial and last draw testing. Chronic indicates >6 months with detectable active viremia. Active indicates viremia at last draw. Resolved indicates no viremia detected at last draw, but antibodies were present.

§Participant RM0337 acquired HCV during the study.

HPgV-2 and HCV during the course of the study, with HPgV-2 infection preceding HCV infection by 280 days (Table 3). Within the last sample set, 6 participants demonstrated HPgV-2 infection after initial collection. Three of the participants showed active HPgV-2 viremia and 3 showed resolved HPgV-2 infection as indicated by detection of antibodies only.

Longitudinal Sample Testing

We tested longitudinal samples (N = 70, sample set 3) from 9/10 participants (Table 2) for HPgV-2 antibodies and RNA (Tables 3, 4; Figure). We reported data available for age, sex, years of injection drug use, HIV status, HCV RNA, HCV antibodies, alanine aminotransferase (HCV-positive only), and HCV drug treatment therapy. We did not follow up with additional HPgV-2 testing on participant VH0044, who was negative for HPgV-2 RNA and antibodies (seroreverted) by last sample date (Table 2). We found chronic HPgV-2 (active viremia >6 months) in 5 different IDU participants, 3 male and 2 female; 3 (QM0003, VP0295, RM0095) were HCV negative and 2 (VH0085, GG0038) HCV positive. None of the participants demonstrating chronic HPgV-2 infection or seroconversion had evidence of HIV infection. Among the participants who demonstrated chronic HPgV-2 infection and were HCV negative, participant QM0003 had a longer (>5 y) history of exposure to injection drug use than the other participants, RM0095 and VP0295 (<5 y). Both participants with active HPgV-2 and HCV co-infection (GG0038 and VH0085) had long histories of injecting exposure (>5 y) and maintained HPgV-2 after HCV infection was resolved.

All chronic HPgV-2 infections demonstrated active viremia despite the presence of HPgV-2 antibodies, with most participants generating an IgG

response to the glycoprotein E2 (Tables 3, 4). E2 antibodies developed in all participants with chronic HPgV-2 samples and observed seroconversion (GG0038, QM0003, VP0295, and RM0095) before the other marker, NS4AB antibody (Tables 3, 4). One chronically infected sample, VH0085, contained antibodies to both E2 and NS4AB, but we did not observe the initial seroconversion. Compared with the other samples in this study, VH0085 had the highest signal to cutoff values for both E2 and NS4AB antibody assays, and the HPgV-2 RNA log copies/mL were higher than in most other samples (Table 3). Some participants (VP0295, RM0095, GG0038) demonstrated seroconversion after several months of initial HPgV-2 RNA detection; these participants were chronically infected with HPgV-2.

The median using the NS2/3 assay was 3.26 HPgV-2 log₁₀ copies/mL for the HCV-negative group and 3.21 HPgV-2 log₁₀ copies/mL for the HCV-positive group; using the 5' UTR, results were 1.71 log₁₀ copies/mL for the HCV-negative group and 1.60 log₁₀ copies/mL for the HCV-positive group (Table 5). HCV co-infection did not appear to influence HPgV-2 viral load; the average value showed no significant difference between the HCV-positive and HCV-negative groups (NS2/3, p = 0.11; 5' UTR, p = 0.36). One HCV-positive participant, VH0085, was positive for HPgV-2 and HCV RNA at baseline, received HCV treatment (8 weeks ledipasvir/sofosbuvir), and cleared HCV infection. After clearance of HCV, the participant remained HPgV-2 viremic and went on to establish a chronic HPgV-2 infection that lasted 8 years (2,805 days). Participant GG0038 acquired HPgV-2 infection after spontaneous resolution of HCV infection (RNA negative and HCV antibody positive) and maintained active HPgV-2 infection for >232 days.

Conclusions

The recently identified human pegivirus HPgV-2 has yet to be linked with any disease in humans. Several groups have shown HPgV-2 infection associated with HCV co-infection (1,3–6). HPgV-2 is a bloodborne virus, and a higher HPgV-2 prevalence is observed among HCV-positive IDUs (4,6). We decoupled the behavior of injection drug use from HCV status by monitoring HCV-negative or HCV-positive IDUs for HPgV-2 infection (RNA and antibodies). We also observed the enrichment of HPgV-2 infection in HCV-positive IDUs (Table 1), as was reported previously (4,6). We found, through longitudinal surveillance of both HCV-negative participants, that HPgV-2 can establish infection and maintain chronic infection in the absence of HCV. We defined chronic infection as detectable HPgV-2 viremia for >6 months in >3 timepoints that was not associated with particular symptoms. Of 9 participants with evidence of HPgV-2

infection (by RNA or serology), 2 HCV-infected participants demonstrated chronic HPgV-2 infection (Table 3), and 3 participants demonstrated chronic HPgV-2 without evidence of past or present HCV infection (Table 4).

Several limitations can contribute to the underestimation of chronic HPgV-2 infection. We identified HPgV-2 in baseline samples from 12 HCV-positive participants; but because of the study design most HCV-positive participants were not followed through subsequent timepoints. Three of these participants did provide longitudinal samples; 2 participants demonstrated chronic HPgV-2 infection. A second limitation is that participants testing negative for HPgV-2 during the timepoints evaluated may become positive following the last timepoint sampled, if they continue the risk behavior of intravenous drug use. Alternatively, false-positive chronic infections could result from long lapses in sampling, in which

Table 3. Information about participants with HPgV-2 infection with HCV co-infection in study of injection drug users in the San Francisco Bay area, California, USA*

Sample ID	Participant age, y/sex	No. years drug use†	Collection date	HCV RNA	HCV antibody	NS2/3 log ₁₀ copies/mL	5' UTR log ₁₀ copies/mL	NS4AB S/CO‡	E2 S/CO‡
RM0337	25.6/F	11.1	2013 Jul 10	Neg	Neg	Neg	Neg	0.16	0.14
			2013 Oct 9	Neg	Neg	Neg	Neg	0.14	0.13
			2014 Jan 29	Neg	Neg	Neg	Neg	0.13	0.12
			2016 Jul 27	Neg	Neg	Neg	Neg	0.12	0.11
			2016 Oct 26	Neg	Neg	Neg	Neg	0.12	0.13
			2017 Jan 18	Neg	Neg	Neg	Neg	0.13	0.13
			2017 Apr 26	Neg	Neg	0.96	0.42	0.13	1.46
			2017 Jul 19	Neg	Neg	Neg	Neg	0.09	1.34
			2017 Oct 18	Neg	Neg	Neg	Neg	0.13	0.88
			2018 Jan 31	Pos	Neg	Neg	Neg	0.14	1.02
2018 Feb 14	Pos	Neg	Neg	Neg	0.25	1.26			
VH0085§	22.2/F	9.9	2010 May 14	Pos	Pos	3.22	2.3	1.38	9.37
			2017 Feb 15	Neg	Not tested	3.14	2.07	2.96	12.92
			2017 May 17	Neg	Not tested	1.87	0.69	3.33	12.35
			2017 Aug 9	Neg	Not tested	4.30	2.25	6.13	18.71
			2017 Nov 1	Neg	Not tested	3.40	1.68	5.13	19.45
			2018 Jan 17	Neg	Not tested	3.86	2.26	3.75	16.16
GG0038§	26.5/M	8.8	2016 Jul 14	Pos	Pos	Neg	Neg	0.16	0.12
			2017 Mar 1	Pos	Not tested	3.04	1.02	0.17	¶
			2017 May 3	Pos	Not tested	2.14	0.64	0.20	0.37
			2017 May 23	Neg	Not tested	3.01	1.16	0.18	0.36
			2017 Oct 18	Neg	Not tested	4.15	1.91	0.16	2.96
VT0031	19.8/M	1.8	2005 Feb 2	Pos	Pos	Neg	Neg	0.09	0.22
			2005 May 24	Pos	Pos	Neg	Neg	0.11	0.15
			2005 Jun 14	Pos	Pos	Neg	Neg	0.10	0.17
			2005 Aug 9	Pos	Pos	Neg	Neg	0.12	0.14
			2005 Nov 8	Pos	Pos	Neg	Neg	0.08	0.13
			2006 Jan 31	Pos	Pos	Neg	Neg	0.14	0.13
			2006 May 9	Pos	Pos	Neg	Neg	0.09	0.19
			2006 Aug 8	Pos	Pos	Neg	Neg	0.21	1.25
			2007 Feb 6	Pos	Pos	2.30	0.53	0.14	1.19
			2007 May 1	Pos	Pos	0.48	0.41	0.14	1.82

*Participants were determined positive for HCV by RNA or antibody test. HCV, hepatitis C virus; HPgV-2, human pegivirus 2; ID, identification; neg, negative; NS, nonstructural protein; pos, positive; S/CO, signal to cutoff value; UTR, untranslated region.

†Number of years participant had injected drugs as of the time of the initial blood draw.

‡S/CO > 1.0 is considered positive.

§Participants VH0085 and GG0038 demonstrate resolved HCV infection. VH0085 was administered direct active antiviral drugs (8 weeks ledipasvir/sofosbuvir, LDV-SOF), and GG0038 spontaneously cleared HCV infection.

¶Volume not available for testing.

RESEARCH

the participant could become infected, clear the infection, then become reinfected with HPgV-2. The molecular and serologic assays cannot distinguish reinfection from chronic infection.

We observed HPgV-2 seroconversion in the longitudinal surveillance of 7 participants; the detectable IgG response occurred several months after initial HPgV-2 RNA detection in several of the chronically infected participants (Tables 3, 4). Similar to HCV infection, which demonstrates a seronegative viremic window period of 50–60 days (12–14), the detection of HPgV-2-specific antibodies lagged behind detectable HPgV-2 RNA (Tables 3, 4). In this study, all participants demonstrating chronic HPgV-2 viremia did so in the presence of antibodies to the glycoprotein E2, which suggests that E2 antibodies are not neutralizing. In contrast, active viremia and

E2 IgG are rarely co-detected in persons with the closest human virus, human pegivirus-1 (HPgV, GBV-C); the presence of E2 antibodies in HPgV infection often indicates resolution of infection (3,15–17).

Our data indicate that chronic HPgV-2 infection among IDUs does not require active HCV to establish infection or maintain chronic infection. It is possible that participants with no detectable HCV antibodies were seroreverters from previous cleared HCV infections; however, this is unlikely in our study because the cohort of active IDUs had ongoing exposure to HCV, and because seroreversion in immunocompetent persons has been shown to occur after a long time (>7 years) (18), exceeding the observation period of this study. Furthermore, 2 participants showed spontaneous (GG0038) or therapeutic (VH0085) resolution of

Table 4. Information about participants with HPgV-2 infection without HCV co-infection in study of injection drug users in the San Francisco Bay area, California, USA*

Sample ID	Age, y/sex	No. years drug use†	Collection date	NS2/3 log ₁₀ copies/mL	5' UTR log ₁₀ copies/mL	NS4AB S/CO‡	E2 S/CO‡
QM0003	28.4/F	14.4	2015 Oct 10	3.76	2.84	0.12	0.08
			2015 Nov 4	0.93	0.55	0.08	0.08
			2016 Jan 27	2.66	1.10	0.16	0.72
			2016 Apr 18	3.56	1.62	0.07	0.85
			2016 Jul 13	3.66	1.61	§	§
			2016 Oct 5	3.22	1.74	0.13	2.76
			2017 Jan 4	4.22	2.30	0.25	4.67
			2017 Apr 10	3.85	2.10	0.17	3.58
			2017 Jul 5	4.08	2.39	0.28	3.73
			2018 Feb 7	3.41	1.34	0.37	2.66
VP0295	24.6/M	3.1	2016 Jan 6	Neg	Neg	0.10	0.12
			2016 Apr 6	Neg	Neg	0.09	0.11
			2016 Aug 24	Neg	Neg	0.12	0.11
			2017 Jan 4	4.44	2.82	0.11	0.14
			2017 Apr 12	3.19	1.06	0.09	0.89
GG0012	23.4/F	3.4	2017 Jul 12	1.42	0.82	0.15	5.51
			2016 Apr 29	Neg	Neg	0.23	0.52
			2016 Aug 17	Neg	Neg	1.77	3.28
			2016 Nov 29	Neg	Neg	3.18	5.76
			2017 Mar 1	Neg	Neg	4.90	8.90
			2017 May 31	Neg	Neg	2.60	4.51
			2017 Sep 20	Neg	Neg	4.05	10.94
2017 Dec 13	Neg	Neg	6.03	11.04			
VH0052	23.7/M	3.5	2018 Mar 19	Neg	Neg	3.77	6.67
			2006 Dec 14	2.13	1.23	2.00	1.91
RM0095	27.1/M	1.1	2007 Jul 3	Neg	Neg	0.81	1.63
			2011 Jan 19	Neg	Neg	0.06	0.06
			2011 Jul 27	0.02	0.14	0.07	0.09
			2011 Oct 19	2.33	1.54	0.06	0.29
			2012 Jan 11	0.20	0.50	0.09	0.59
			2012 Apr 11	0.02	0.16	0.24	0.50
			2012 Jul 3	Neg	Neg	0.14	0.59
			2012 Oct 23	0.03	0.27	0.12	1.09
			2013 Jan 15	0.45	0.61	0.15	2.45
			2013 Apr 10	1.37	1.08	0.13	2.37
			2013 Jul 2	Neg	Neg	0.17	3.53
			2013 Sep 18	0.46	0.55	0.14	2.64
			2013 Dec 11	Neg	Neg	0.14	3.07

*Participants were determined negative for HCV by RNA or antibody test. HCV, hepatitis C virus; HPgV-2, human pegivirus 2; ID, identification; neg, negative; NS, nonstructural protein; pos, positive; S/CO, signal to cutoff value; UTR, untranslated region.

†Number of years participant had injected drugs as of the time of the initial blood draw.

‡S/CO >1.0 is considered positive.

§No blood sample available for testing.

Table 5. Characteristics of findings in study of chronic HPgV-2 infection for participants with and without HCV co-infection in injection drug users in the San Francisco Bay area, California, USA*

Finding	HCV negative, n = 3	HCV positive, n = 2	p value
Average HPgV-2, log ₁₀ copies/mL			
NS2/3	3.26	3.21	0.11
5' UTR	1.71	1.60	0.36
Average years injection drug use†	5.5	7.9	NA
Average age at detection of HPgV-2 RNA, y†	25.6	26.1	NA

*HCV, hepatitis C virus; HPgV-2, human pegivirus 2; NS, nonstructural protein.

†No p values available because of low number of samples.

HCV infection but HPgV-2 chronic infection remained (Table 3); thus, there appeared to be no reliance on HCV to establish or maintain HPgV-2 infection. We observed no difference in HPgV-2 viral loads whether HCV was present or absent (Table 5). The relative ratio of resolved to active infections between the HCV-positive and HCV-negative cohorts was similar (Table 1).

As noted in this and other studies, high-risk populations that are exposed to parenterally transmitted viruses experience an increase in HPgV-2 prevalence (4,6,7). We observed similar higher incidence of both active and resolved HPgV-2 infection in the HCV-positive IDU cohort (Table 1). The HCV-positive and HCV-negative infected persons within the IDU cohort share many common behaviors with no discernable characteristics, except total number of years of injection drug use (average 7.6 y for HCV-positive users, 4.7 y for HCV-negative users). Similarly, the HCV-positive HPgV-2 carriers identified in this study demonstrated injection drug use behavior longer (average 7.9 y) than the HCV-negative group (average 4.4 y). The greater number of potential exposures to parentally transmitted bloodborne viruses is probably a major contributing factor for increased prevalence of HPgV-2 in the HCV-positive IDU cohort.

The pathogenic potential of HPgV-2 in humans remains unknown; no clinical symptoms have been associated with HPgV-2 infection. We gathered no additional clinical information from HCV-negative study participants. Most HPgV-2 studies have shown the virus is associated with HCV co-infection, which can mask any pathogenicity associated with HPgV-2 infection. Identifying populations that show higher prevalence of HPgV-2 monoinfection and monitoring these persons over time may help identify clinical symptoms associated with HPgV-2 infection, thus enabling researchers to categorize HPgV-2 as human pathogen or benign infection.

Acknowledgments

We acknowledge the ongoing support and efforts of the Blood Systems Research Institute, especially Michael Busch, Mars Stone, and Honey Dave, for their expert management of the UFO Study specimen bank.

About the Author

Dr. Collier is a research scientist at Abbott Laboratories, Abbott Diagnostics Division. Her research interests include developing serologic assays for the detection of emerging infectious diseases.

References

- Berg MG, Lee D, Collier K, Frankel M, Aronsohn A, Cheng K, et al. Discovery of a novel human pegivirus in blood associated with hepatitis C virus co-infection. *PLoS Pathog.* 2015;11:e1005325. <https://doi.org/10.1371/journal.ppat.1005325>
- Kapoor A, Kumar A, Simmonds P, Bhuva N, Singh Chauhan L, Lee B, et al. Virome analysis of transfusion recipients reveals a novel human virus that shares genomic features with hepaciviruses and pegiviruses. *MBio.* 2015;6:e01466-15. <https://doi.org/10.1128/mBio.01466-15>
- Collier KE, Berg MG, Frankel M, Forberg K, Surani R, Chiu CY, et al. Antibodies to the novel human pegivirus 2 are associated with active and resolved infections. *J Clin Microbiol.* 2016;54:2023-30. <https://doi.org/10.1128/JCM.00515-16>
- Wang H, Wan Z, Sun Q, Zhu N, Li T, Ren X, et al. Second human pegivirus in hepatitis C virus-infected and hepatitis C virus/HIV-1-co-infected persons who inject drugs, China. *Emerg Infect Dis.* 2018;24:908-11. <https://doi.org/10.3201/eid2405.161162>
- Wang H, Wan Z, Xu R, Guan Y, Zhu N, Li J, et al. A novel human pegivirus, HPgV-2 (HHpgV-1), is tightly associated with hepatitis C virus (HCV) infection and HCV/human Immunodeficiency virus type 1 coinfection. *Clin Infect Dis.* 2018;66:29-35. <https://doi.org/10.1093/cid/cix748>
- Kandathil AJBF, Thomas DL, Balagopal A, Mehta SH, Timp W, Salzberg SL, et al. Presence of human hepegivirus-1 in a cohort of people who inject drugs. *Ann Intern Med.* 2018;168:158-9. <https://doi.org/10.7326/L17-0527>
- Bonsall D, Gregory WF, Ip CLC, Donfield S, Iles J, Ansari MA, et al. Evaluation of viremia frequencies of a novel human pegivirus by using bioinformatic screening and PCR. *Emerg Infect Dis.* 2016;22:671-8. <https://doi.org/10.3201/eid2204.151812>
- Bijvand Y, Aghasadeghi MR, Sakhaee F, Pakzad P, Vaziri F, Saraji AA, et al. First detection of human hepegivirus-1 (HHpgV-1) in Iranian patients with hemophilia. *Sci Rep.* 2018;8:5036. <https://doi.org/10.1038/s41598-018-23490-4>
- Page K, Hahn JA, Evans J, Shiboski S, Lum P, Delwart E, et al. Acute hepatitis C virus infection in young adult injection drug users: a prospective study of incident infection, resolution, and reinfection. *J Infect Dis.* 2009;200:1216-26. <https://doi.org/10.1086/605947>
- Hahn JA, Page-Shafer K, Lum PJ, Bourgeois P, Stein E, Evans JL, et al. Hepatitis C virus seroconversion among

- young injection drug users: relationships and risks. *J Infect Dis.* 2002;186:1558–64. <https://doi.org/10.1086/345554>
11. Frankel M, Forberg K, Collier KE, Berg MG, Hackett J Jr, Cloherty G, et al. Development of a high-throughput multiplexed real time RT-PCR assay for detection of human hepatitis B and C. *J Virol Methods.* 2017;241:34–40. <https://doi.org/10.1016/j.jviromet.2016.12.013>
 12. Cox AL, Netski DM, Mosbrugger T, Sherman SG, Strathdee S, Ompad D, et al. Prospective evaluation of community-acquired acute-phase hepatitis C virus infection. *Clin Infect Dis.* 2005;40:951–8. <https://doi.org/10.1086/428578>
 13. Maheshwari A, Ray S, Thuluvath PJ. Acute hepatitis C. *Lancet.* 2008;372:321–32. [https://doi.org/10.1016/S0140-6736\(08\)61116-2](https://doi.org/10.1016/S0140-6736(08)61116-2)
 14. Glynn SA, Wright DJ, Kleinman SH, Hirschhorn D, Tu Y, Heldebrandt C, et al. Dynamics of viremia in early hepatitis C virus infection. *Transfusion.* 2005;45:994–1002. <https://doi.org/10.1111/j.1537-2995.2005.04390.x>
 15. Tanaka T, Hess G, Schlueter V, Zdunek D, Tanaka S, Kohara M. Correlation of interferon treatment response with GBV-C/HGV genomic RNA and anti-envelope 2 protein antibody. *J Med Virol.* 1999;57:370–5. [https://doi.org/10.1002/\(SICI\)1096-9071\(199904\)57:4<370::AID-JMV8>3.0.CO;2-K](https://doi.org/10.1002/(SICI)1096-9071(199904)57:4<370::AID-JMV8>3.0.CO;2-K)
 16. Gutierrez RA, Dawson GJ, Knigge MF, Melvin SL, Heynen CA, Kyrk CR, et al. Seroprevalence of GB virus C and persistence of RNA and antibody. *J Med Virol.* 1997;53:167–73. [https://doi.org/10.1002/\(SICI\)1096-9071\(199710\)53:2<167::AID-JMV10>3.0.CO;2-G](https://doi.org/10.1002/(SICI)1096-9071(199710)53:2<167::AID-JMV10>3.0.CO;2-G)
 17. Dille BJ, Surowy TK, Gutierrez RA, Coleman PF, Knigge MF, Carrick RJ, et al. An ELISA for detection of antibodies to the E2 protein of GB virus C. *J Infect Dis.* 1997;175:458–61. <https://doi.org/10.1093/infdis/175.2.458>
 18. Lefrère JJ, Girot R, Lefrère F, Guillaume N, Lerable J, Marrec NL, et al. Complete or partial seroreversion in immunocompetent individuals after self-limited HCV infection: consequences for transfusion. *Transfusion.* 2004;44:343–8. <https://doi.org/10.1111/j.1537-2995.2004.00656.x>

Address for correspondence: Kelly E. Collier, Abbott Laboratories, Abbott Diagnostics Division, 100 Abbott Park Rd, Abbott Park, IL 60064-6400, USA; email: kelly.collier@abbott.com

etymologia

Pegivirus [peg^ˈi-vi^ˈrəs]

Ronnie Henry

In 1967, researchers studying non-A, non-B hepatitis identified a transmissible agent in the serum of a surgeon (initials G.B.) with acute hepatitis and named it the GB agent. In the 1990s, researchers from Abbott Laboratories identified 3 GB viruses (A, B, and C) at the same time as a group at Genelabs isolated RNA from patients with non-A, non-B hepatitis and named it hepatitis G virus. Later research showed that GB virus C and hepatitis G virus were the same species.

Subsequent phylogenetic analysis showed that GB viruses A and C (and GB virus D, later identified in bats) should be classified under a new genus, *Pegivirus* (because they cause persistent infection and because of the historic association with hepatitis G), and GB virus B should be classified as a second species (with hepatitis C virus) in the genus *Hepacivirus*. As of 2016, 11 species of *Pegivirus* had been identified (*Pegivirus* A–K).

Sources

1. Linnen J, Wages J Jr, Zhang-Keck ZY, Fry KE, Krawczynski KZ, Alter H, et al. Molecular cloning and disease association of hepatitis G virus: a transfusion-transmissible agent. *Science.* 1996;271:505–8. <https://doi.org/10.1126/science.271.5248.505>
2. Simons JN, Leary TP, Dawson GJ, Pilot-Matias TJ, Muerhoff AS, Schlauder GG, et al. Isolation of novel virus-like sequences associated with human hepatitis. *Nat Med.* 1995;1:564–9. <https://doi.org/10.1038/nm0695-564>
3. Smith DB, Becher P, Bukh J, Gould EA, Meyers G, Monath T, et al. Proposed update to the taxonomy of the genera *Hepacivirus* and *Pegivirus* within the *Flaviviridae* family. *J Gen Virol.* 2016;97:2894–907. <https://doi.org/10.1099/jgv.0.000612>
4. Stapleton JT, Fong S, Muerhoff AS, Bukh J, Simmonds P. The GB viruses: a review and proposed classification of GBV-A, GBV-C (HGV), and GBV-D in genus *Pegivirus* within the family *Flaviviridae*. *J Gen Virol.* 2011;92:233–46. <https://doi.org/10.1099/vir.0.027490-0>

Address for correspondence: Ronnie Henry, Centers for Disease Control and Prevention, 1600 Clifton Rd NE, Mailstop E28, Atlanta, GA 30333, USA; email: boq3@cdc.gov

DOI: <https://doi.org/10.3201/eid2602.ET2602>

Interspecies Transmission of Reassortant Swine Influenza A Virus Containing Genes from Swine Influenza A(H1N1)pdm09 and A(H1N2) Viruses

Helen E. Everett, Bethany Nash, Brandon Z. Londt,¹ Michael D. Kelly, Vivien Coward, Alejandro Nunez, Pauline M. van Diemen, Ian H. Brown, Sharon M. Brookes

Influenza A(H1N1)pdm09 (pH1N1) virus has become established in swine in the United Kingdom and currently co-circulates with previously enzootic swine influenza A virus (IAV) strains, including avian-like H1N1 and human-like H1N2 viruses. During 2010, a swine influenza A reassortant virus, H1N2r, which caused mild clinical disease in pigs in the United Kingdom, was isolated. This reassortant virus has a novel gene constellation, incorporating the internal gene cassette of pH1N1-origin viruses and hemagglutinin and neuraminidase genes of swine IAV H1N2 origin. We investigated the pathogenesis and infection dynamics of the H1N2r isolate in pigs (the natural host) and in ferrets, which represent a human model of infection. Clinical and virologic parameters were mild in both species and both intraspecies and interspecies transmission was observed when initiated from either infected pigs or infected ferrets. This novel reassortant virus has zoonotic and reverse zoonotic potential, but no apparent increased virulence or transmissibility, in comparison to pH1N1 viruses.

The ability of swine to support replication of phylogenetically diverse influenza A virus (IAV) strains from avian and mammalian origin poses a public health risk because of the potential for viral antigenic change resulting in variants with zoonotic properties (1). This risk was highlighted by emergence of the influenza A(H1N1)pdm09 (pH1N1) swine-origin influenza virus during 2009 (2).

In swine herds from Europe, the classical swine influenza virus A(H1N1) lineage 1A (3), was the only lineage detected before 1979. This strain has a common origin with the progenitor virus that

caused the human 1918 influenza pandemic. However, in the early 1980s, the classical swine H1N1 strain was displaced by a new European enzootic swine IAV strain, the Eurasian, avian-like H1N1 (H1avN1) lineage 1C (3), probably after cross-species transmission directly from birds to mammals (1). H1avN1 virus underwent rapid and sustained adaptation to mammals, as shown by phylogenetic as well as phenotypic changes, including enhanced mammalian replication and transmission (4). This H1avN1 lineage is now enzootic and has also undergone reassortment resulting in emergence of multiple genotypes and 2 main enzootic subtypes, H1N2 (H1huN2), also designated lineage IB (3), and H3N2, through acquisition of human seasonal influenza virus-origin hemagglutinin (HA) or neuraminidase (NA) gene segments (1).

Since the global dissemination of pH1N1 virus, this lineage has also undergone reassortment with swine IAV strains endemic to the corresponding geographic region (5). Within Europe, this diversification of pH1N1 virus in pigs has increased the circulating swine IAVs from 4 to ≥ 25 genotypes (6,7). Diversification has been rapid; pH1N1 reassortant viruses incorporating enzootic swine virus HA and NA, or NA alone, detected during 2010 in the United Kingdom (8) and Italy (9), have emerged. The NA segment was N2 subtype in both instances. Subsequently, viruses have been identified that contain the NA segment from European enzootic H3N2 strains and the remaining 7 segments from pH1N1-origin viruses (10,11) or a further reassortant containing H3 of human seasonal origin (12).

Author affiliation: Animal and Plant Health Agency, Weybridge, UK

DOI: <https://doi.org/10.3201/eid2601.190486>

¹Current affiliation: hVIVO Services Limited, London, UK.

Reassortment between enzootic and pH1N1 influenza viruses was also rapidly detected elsewhere, including Asia, where a reassortant swine IAV containing pH1N1-origin NA was described during 2010 (13), and in North America, where several reassortants containing HA and NA segments from enzootic viruses have been maintained since 2011 (14). These swine IAV reassortants from North America incorporate different combinations of the pH1N1 internal gene cassette (gene segments other than HA and NA) and invariably carry the pH1N1-origin matrix (M) protein gene.

Swine IAV H1N2 virus reassortment strains circulating in Brazil acquired NA gene segments from independent introductions of human seasonal H3N2 strains similar to those circulating in the late 1990s and an HA segment derived from human H1 strains circulating in the early 2000s. These lineages have subsequently reassorted with co-circulating pH1N1 strains (15) and viruses with a pH1N1-origin internal gene cassette have been isolated from wild boar (16) and swine (17).

One such H1N2 reassortant gave rise to a human clinical case of influenza in a worker on a swine farm (18). A reassortant H1N2 virus strain was also isolated from pigs in Chile; this virus incorporated human-origin HA and NA gene segments prevalent in the 1990s and the pH1N1 internal gene cassette (19). Human infection with swine-origin H1N2 viruses (H1N2v infection) has been reported in the United States, most notable being 3 human influenza cases linked to infection with a related co-circulating H1N2 swine IAV virus incorporating a pH1N1-origin M gene segment (20).

Genetic reassortment between enzootic swine and pH1N1 strains giving rise to H1N2 virus diversification has also been reported in Asia, including lineages in South Korea containing Eurasian avian-like swine HA and Korean swine H1N2 NA gene segments and the pH1N1-like internal gene cassette (21)

and another reassortant strain associated with pig respiratory disease in China incorporating the HA, basic polymerase protein 2, and M genes of swine pH1N1 virus origin; the remaining gene segments were derived from a swine H3N2 strain (22).

We characterized a prototypical reassortant swine influenza A virus, A/swine/England/1382/2010 (H1N2r) (23), which has become enzootic in the pig population in the United Kingdom (6). This virus incorporates the genes encoding the envelope glycoproteins, HA and NA, from a European swine H1N2 subtype (which themselves derive from human-origin strains) and the remaining gene cassette encoding the internal proteins from swine-origin pandemic 2009 strains (8). Serologic assessment of potential exposure of pig industry workers in the United Kingdom to swine viruses during 2009–2010 showed that antibodies to H1N2 swine IAVs were present in 24% of persons, and this prevalence was increased relative to a comparator population (24). Because the potential risks associated with a novel combination of gene segments in the H1N2r isolate were unknown, we investigated the pathogenesis and infection dynamics of this virus in pigs, the natural host, and in ferrets, which are widely established as an animal model for investigating influenza and pandemic risk in humans (25,26).

Materials and Methods

Viruses

We isolated H1N2r virus A/swine/England/1382/2010 from nasal swab specimens from pigs that had clinical signs of mild influenza-like disease (8). Virus was propagated in embryonated specific pathogen-free chicken eggs according to standard methods (27), passaged once to obtain a virus stock, and characterized by using whole-genome sequencing (8) using reference influenza A virus strains (Table).

Table. Influenza virus strains of swine or human origin used for analysis of swine influenza A virus containing genes from pH1N1 and swine influenza A(H1N2) viruses*

Virus strain	Abbreviation	Gene segment origin†		Use	Reference
		HA + NA	Internal cassette		
A/swine/England/1382/2010	H1N2r	H1 _{hu} N2‡	pH1N1	In vivo, in vitro	(8)
A/swine/England/1353/2009	Sw/pdm09	pH1N1	pH1N1	In vitro	(28)
A/swine/England/997/2008	H1 _{hu} N2‡	H1 _{hu} N2‡	H1 _{av} N1	In vitro	(6)
A/England/195/2009	Hu/pdm09	pH1N1	pH1N1	HI	(29)
A/swine/England/201635/1992	H3N2	H3N2‡	H1 _{av} N1	HI	(30)
A/swine/England/195852/1992	H1 _{av} N1	H1 _{av} N1	H1 _{av} N1	HI	(31)
A/swine/England/104270/2011	H1 _{hu} N2‡	H1 _{hu} N2‡	H1 _{av} N1	HI	(Animal and Plant Health Agency, unpub. data)

*Av, avian; HA, hemagglutinin; HI, hemagglutination inhibition; hu, human; NA, neuraminidase; pH1N1, influenza A(H1N1)pdm09; Sw, swine.

†Gene segment origin refers to the virus lineage origin of gene segments encoding the HA and NA envelope proteins or the remaining gene segments of the internal gene cassette.

‡Swine virus gene segments previously derived from human-origin viruses.

Organ Culture

Ferret organ cultures were prepared as described (Appendix, <https://wwwnc.cdc.gov/EID/article/26/2/19-0486-App1.pdf>). Organ cultures were inoculated by adsorbing virus for 1 h at 37°C onto the air interface of triplicate tissue sections. The culture was then washed and replenished with supplemented Dulbecco modified Eagle medium and incubated before virus detection 24–48 hours postinoculation (hpi) in combined supernatant and tissue lysate per sample. Control organ cultures were mock inoculated. Influenza A virus nucleoprotein (NP) was detected in tissues by using immunohistochemical (IHC) analysis as described (32).

Real-Time Reverse Transcription Quantitative PCR Analysis

Virus RNA was extracted by using a QIAmp Viral RNA Biorobot Kit (QIAGEN, <https://www.qiagen.com>) and assayed by using a real-time quantitative reverse transcription PCR (qRT-PCR) (33). Virus RNA was quantified as relative equivalent units (REUs) (34) against a 10-fold dilution series of RNA prepared from the inoculum stock with a titer of 10^6 50% egg infectious dose (EID_{50})/mL. REU measures the amount of virus RNA present and not infectivity. However, it can be inferred from the linear relationship with the dilution series that REU values are proportional to the amount of infectious virus present.

We used Prism software (GraphPad, <https://www.graphpad.com>) for statistical analyses. We determined the area under the curve of the shedding profile for each animal and compared between groups by using the Tuckey multiple comparisons test and 1-way analysis of variance. Positive-sense RNA encoding the virus M gene was quantified by using a positive strand-specific real-time qRT-PCR (Appendix).

In Vivo Studies

All animal studies were reviewed and approved by the Animal and Plant Health Agency Ethical Review Panel. Studies were conducted according to the Animal (Scientific Procedures) Act of 1986 and Animal Research: Reporting of In Vivo Experiments guidelines.

High health status, 6–8-week-old, male Landrace hybrid pigs and male fitch ferrets (weight range 750–1,000 g, maximum age 3 months) were bred in the United Kingdom. Before infection, all animals were confirmed free of influenza A virus RNA by performing real-time qRT-PCR analysis of nasal swab specimens (pigs) or nasal washes (ferrets) (33). These animals also showed negative results in a hemagglutination inhibition (HI) test (35) using 4 influenza A virus antigens (pH1N1, H1avN1, H3N2, and H1N2

viruses) appropriate for the pig population in the United Kingdom (Table). Animals were subcutaneously implanted with a biothermal idENTiCHIP (Destron Fearing, <http://destronfearing.com>) for daily temperature monitoring, and a clinical scoring system was used for daily clinical monitoring (36,37).

Experimental Infection

We intranasally infected animals by using protocols appropriate for the species and nasal structure. We infected pigs by using a MAD Nasal Intranasal Mucosal Atomization Device (Wolfe-Tory Medical Inc., <https://www.lmaco.com>) to deliver droplets with a diameter of 30–100 μ m. A total dose of 10^6 EID_{50} units diluted in phosphate-buffered saline to a final volume of 4 mL (2 mL/nostril) was administered. We anesthetized ferrets and infected them by intranasal droplet instillation of a total dose of 10^6 EID_{50} in 0.4 mL inoculum (0.2 mL/nostril).

Pathologic Analysis

For each species, postmortem examination was conducted for 4 animals at 3 days postinoculation (dpi) and 5 dpi, as well as for 2 animals at 7 dpi. Gross pathology was assessed and tissue samples were collected in 10% (vol/vol) phosphate-buffered formalin for histopathologic analysis. Lesions were scored as described for ferrets (37) and pigs (36). Influenza A virus NP was detected in tissues by using IHC analysis as described (36,37).

Experimental Infection and Transmission Studies

Six animals of each species were directly infected for study I (intraspecies transmission) and study II (interspecies transmission). In study I, immunologically naive animals ($n = 6$) of the same species were placed in direct contact at 1 dpi. In study II, animals of 1 species ($n = 6$) were infected and immediately thereafter cohoused animals of the other species ($n = 6$) were reintroduced. Pigs were housed on the floor and immediately adjacent to ferret cages (minimum distance 30 cm), and the floor of the ferret cage was at the height of the heads of the pigs. Virus shedding was monitored daily from 1 dpi through 12 dpi in nasal swab specimens from pigs (1/nostril) or nasal wash samples from ferrets (1 mL/animal). Serum samples were obtained before infection and at the end of the study at 21 dpi. An overdose of barbiturates was used for euthanasia of all animals.

Swab and Tissue Specimen Processing

Daily nasal swab specimens, which were pooled for each pig, were eluted in 1 mL Leibovitz L-15 medium

with l-glutamine supplemented with 100 U/mL penicillin, 1,000 µg/mL streptomycin, and 1% fetal bovine serum (all from GIBCO). Ferret nasal wash samples were obtained by using 1 mL phosphate-buffered saline (GIBCO). Tissues were analyzed by preparing a 10%–20% [wt/vol] homogenate in 1 mL supplemented Leibovitz-15 medium by using an Omni GLH Homogenizer (Omni International, <https://www.omni-inc.com>).

Serologic Analysis

Serum samples were analyzed by using an influenza A virus NP competitive ELISA (IDVet) according to the manufacturer's specifications and dilutions of 1:40 for pig serum samples and 1:10 for ferret serum samples. Antibody titers to the H1N2r virus were measured by HI as described for pig (35) or ferret (38) serum samples.

Results

H1N2r Virus Ex Vivo Replication

To investigate H1N2r virus replication in the ferret animal model, we inoculated ferret organ cultures with virus strains at the same viral multiplicity of infection or mock-inoculated. We quantified influenza A virus replication by using real-time qRT-PCR for virus RNA at 24 hpi and 48 hpi. Replication of the H1N2r isolate was comparable to that of swine pH1N1 and H1N2 strains and a human-origin pH1N1 strain in tracheal cultures (Figure 1, panel A). We also detected comparable amounts of virus RNA in lung cultures at 24 hpi; these amounts decreased slightly by 48 hpi for some strains (Appendix Figure). We confirmed H1N2r virus replication in tracheal cultures by positive IHC

labeling for influenza A virus NP (Figure 1, panel B). A strand-specific PCR detected replicating virus-positive sense RNA in infected tracheal cultures (Figure 1, panel C), which decreased between 24 hpi and 48 hpi, most likely reflecting virus replication kinetics. These in vitro assay results showed productive replication of the swine-origin H1N2r virus in ferret cells, but we observed no selective growth advantage linked to the novel gene constellation.

Pathologic Assessment

We then investigated the pathogenicity profile after H1N2r infection of pigs, the natural host, or ferrets, which represent a surrogate model for human infection. We assessed pathologic changes at 3, 5, and 7 dpi in both species and observed gross pathologic changes at 3 dpi in 2 of 4 directly infected pigs. In 1 of these pigs, a large portion of a single lung lobe was consolidated by lesions consistent with influenza A virus infection. We also found gross pathologic changes in the lungs in all pigs at 5 dpi, with a reduction by 7 dpi. In infected ferrets, small sporadic lesions common to influenza A virus infection occurred, and individual animals had lesions in the respiratory turbinates (5 dpi) and salivary glands (7 dpi), as well as in the left cranial lung lobe in 2 directly infected ferrets at 3 dpi and 5 dpi.

Histopathologic changes were consistent with mild inflammatory disease. For pigs (Figure 2, panel A), inflammation was evident throughout the respiratory tract at all timepoints (e.g., in respiratory turbinates [upper respiratory tract] and lung lobes [lower respiratory tract]) at 3, 5, and 7 dpi. In contrast, for ferrets, most pronounced inflammation occurred in



Figure 1. Infection and replication of swine H1N2r virus in ferret tracheal organ cultures. A) Quantity of influenza A virus RNA in ferret tracheal ex vivo organ cultures at 24 h and 48 h postinoculation with swine viruses H1N2r (A/swine/England/1382/2010), Sw/pdm09 (A/swine/England/1353/2009), H1N2 (A/swine/England/997/2009), and Hu/pdm09 (A/England/195/2009). Results are log₁₀ REU in combined supernatants and tissue lysates for each sample. Error bars indicate upper end of SEM for triplicate cultures. B) Immunohistochemical labeling of influenza A virus nucleoprotein in ferret tracheal cultures infected with H1N2r reassortant virus (original magnification ×20). C) Detection of virus-positive strand replicative intermediate RNA in ferret tracheal and lung cultures at 24 and 48 h postinoculation with H1N2r virus. Error bars indicate upper end of SEM for triplicate cultures. C_t, cycle threshold; hpi, hours postinoculation; hu, human; H1N2r, reassortant swine influenza A virus; pdm09, influenza A(H1N1)pdm09; REU, relative equivalent unit; sw, swine; +, positive.

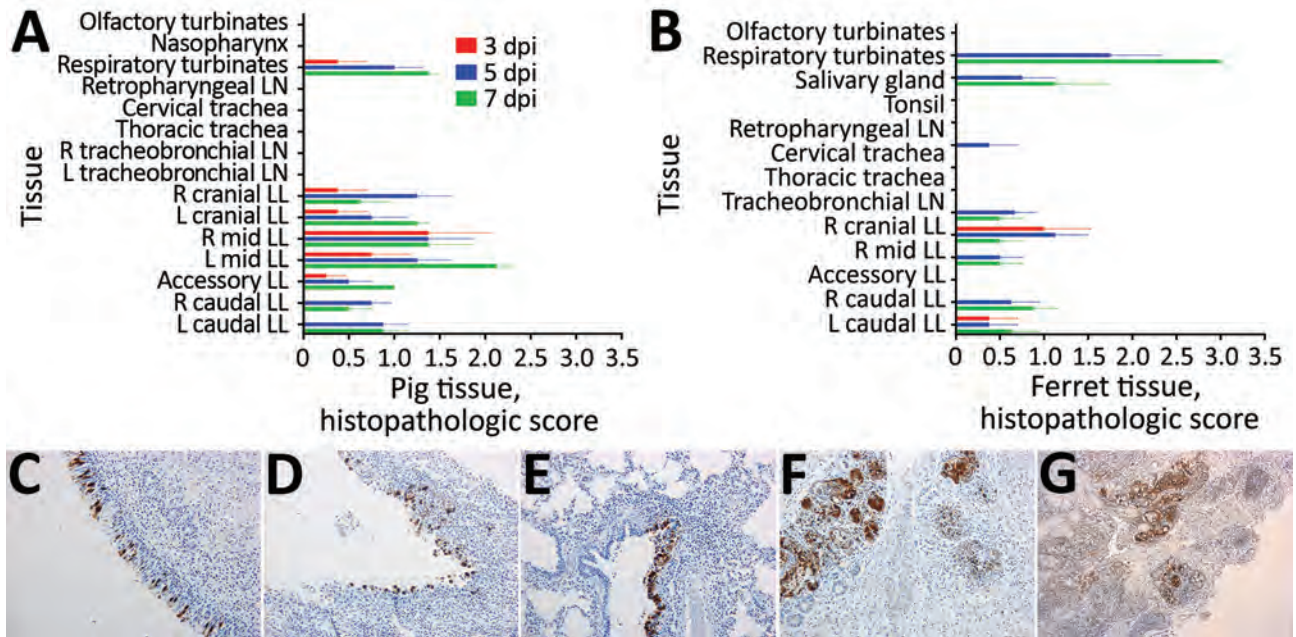


Figure 2. Histopathologic and immunohistochemical analyses of tissues from pigs or ferrets directly infected with swine influenza A(H1N2) reassortant virus showing mild disease. A, B) Histopathologic scores for pigs (A) or ferrets (B) are calculated as mean for 4 animals at 3 dpi and 5 dpi or 2 animals at 7 dpi. Error bars indicate SEM. Tissues are indicated in anatomic order from the upper to lower respiratory tract. C–G) Immunohistochemical labeling for influenza A virus nucleoprotein (brown) is shown for tissue sections from pig respiratory turbinates at 5 dpi (C), ferret respiratory turbinates at 7 dpi (D), pig lung at 5 dpi (E), and ferret lung at 7 dpi (F) (original magnification $\times 20$ for C, D, E, and F). Ferret salivary gland tissue at 76 dpi (G) shows intense labeling (original magnification $\times 10$). dpi, days postinoculation; L, left; LL, lung lobe; LN, lymph node; mid, middle; R, right.

the respiratory turbinates and in the salivary glands, initially at 5 dpi and increasing by 7 dpi, which indicated a predominantly upper respiratory tract infection (Figure 2, panel B).

Influenza A virus NP labeling showed replicating virus in pig and ferret tissues, notably in pig respiratory turbinates, at 5 dpi (Figure 2, panel C). For pig lung tissues, we detected virus in the right mid lung at 3 dpi and in all lung lobes at 5 dpi (Figure 2, panel E), with evidence of virus clearing by 7 dpi. For ferret tissues, virus NP labeling was more pronounced at 7 dpi, as shown for respiratory turbinates (Figure 2, panel D) and lungs (Figure 2, panel F). We observed intense IHC virus labeling in salivary glands of ferrets. These animals showed an increase in virus labeling from 3 dpi through 7 dpi (Figure 2, panel G).

H1N2r Virus Infection

In study I (Figure 3, panel A), we directly infected 6 animals and then placed them in direct contact with 6 uninfected animals of the same species 1 day later. Clinical signs from H1N2r infection were unapparent or mild (1–2 days) in pigs and ferrets, whether directly infected or contact animals, and there was no major change in body temperature ($<1^{\circ}\text{C}$ above

baseline). We observed clinical signs in 3 of 12 pigs: 2 pigs had mild rhinitis at 1 dpi, and 1 pig had mild respiratory signs (sneezing) at 5 dpi. Clinical signs in ferrets were limited to transient rhinitis in some animals and could have been caused by infection or other factors, such as sampling.

Shedding and Transmission Profile of H1N2r Virus

We monitored virus RNA shedding daily in nasal swab specimens (pigs) or washes (ferrets) and quantified results by using real-time qRT-PCR. Nasal shedding started in directly infected animals at <1 dpi and in uninfected contacts at 1–2 days after contact (Figure 3, panels B, C). These results from study I confirmed transmission between infected and uninfected animals of the same species. Peak amounts of virus RNA were shed by directly infected animals at 2–5 dpi. In comparison with directly infected or contact pigs (Figure 3, panel B), directly infected or contact ferrets (Figure 3, panel C) shed virus for a longer duration and also shed a larger total quantity of virus. Significantly greater ($p < 0.0001$) quantities of virus RNA were shed by directly infected ferrets in comparison with all other groups, and also by contact

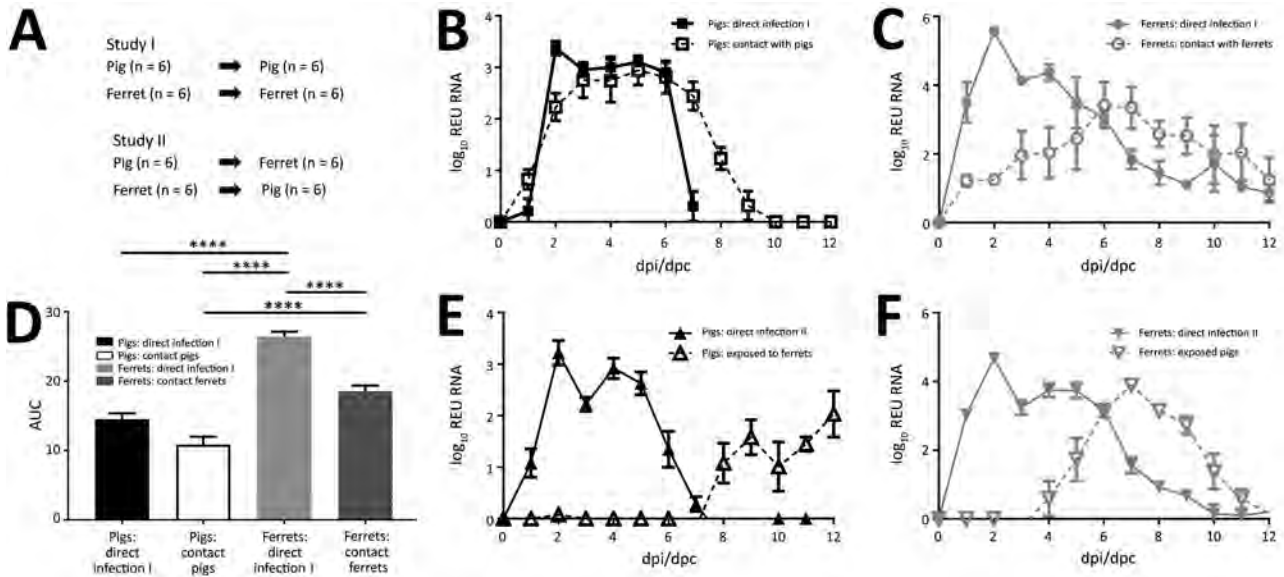


Figure 3. Nasal shedding and transmission of swine influenza A(H1N2) reassortant virus from infected animals. A) Schematic outline of study design. B, C) In study I, virus RNA in nasal swab specimens from directly infected or contact pigs (B) and directly infected or contact ferrets (C) was quantified by using real-time reverse transcription quantitative PCR. Values are indicated as REU at each dpi or dpc. Error bars indicate SEM. D) AUC for virus shedding profiles in study I in pigs or ferrets, showing significant differences (**** $p < 0.0001$) in virus shedding by directly infected ferrets compared with all other groups and between contact pigs and ferrets. Error bars indicate upper end of SEM. E, F) In study II, virus RNA in nasal swab specimens from infected or cohoused pigs (E) or nasal washes from infected or cohoused ferrets (F) was quantified as REU. Error bars indicate SEM. AUC, area under the curve; dpi, days postinfection; dpc, days postcontact; REU, relative equivalent unit.

ferrets in comparison with contact pigs, as shown by area under the curve analysis (Figure 3, panel D). A greater variation in shedding occurred between individual ferrets than between pigs, particularly among contact animals.

In study II (Figure 3, panel A), directly infected pigs or ferrets (representing a human model) were cohoused with animals of the other species to assess interspecies transmission of the H1N2r virus and zoonotic potential. Direct infection of pigs (Figure 3, panel E) or ferrets (Figure 3, panel F) resulted in similar infection dynamics as for intraspecies study I. When infected ferrets were cohoused with uninfected pigs (Figure 3, panel E), the pigs became infected after a considerable 8–10-day lag, and virus shedding profiles differed between recipient pigs. These infection kinetics might indicate that some pigs became infected from their penmates, demonstrating possible onward transmission of virus and potential for the H1N2r virus to disseminate in a susceptible population. Ferrets were readily infected within 4 days when cohoused with infected pigs (Figure 3, panel F), and the infection profile was similar to that observed for intraspecies transmission, suggesting that all ferrets were infected synchronously by the infected pigs. Nasal shedding profiles observed for animals infected directly with H1N2r

were comparable with profiles for human pH1N1 influenza viruses A/England/195/2009 and A/California/07/2009 (36,37,39,40).

Serologic Analysis

Serologic analysis by competitive ELISA for NP, which is present within virions, demonstrated that, in interspecies transmission study II, infected and contact ferrets seroconverted by 21 dpi/days after contact (Figure 4, panel A). Most infected pigs also seroconverted and showed lower final antibody titers, although 2 of 6 pigs cohoused with infected ferrets did not seroconvert within the study period. HI titers, which measure exposure to the viral envelope HA protein, were positive against the H1N2r challenge strain, indicating seroconversion of all infected or contact animals (Figure 4, panel B). Both assays showed that the antibody response was stronger in ferrets than pigs, perhaps corresponding to the higher virus load and more prolonged infection in ferrets.

Discussion

Our study showed that pigs and ferrets were susceptible to infection with the H1N2r virus and showed clinical signs and virologic parameters indicating mild disease. Longitudinal postmortem analysis

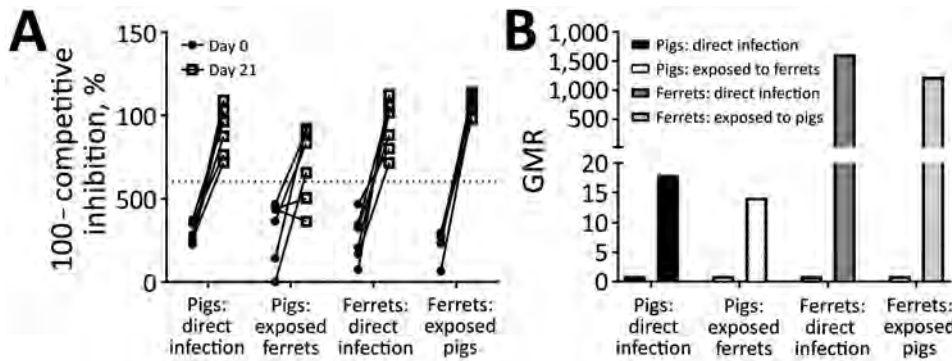


Figure 4. Serum antibody levels monitored in groups of pigs and ferrets in interspecies transmission study II to assess seroconversion after infection. A) Influenza A virus nucleoprotein competitive ELISA, showing inverse of competitive inhibition, %. Dotted line indicates lower limit for the positive threshold. B) GMR of hemagglutination-inhibition titer to the A/swine/England/1382/2010 challenge strain. GMR, geometric mean ratio.

indicated that this virus could be more adapted to a swine host because infection disseminated more rapidly throughout the respiratory tract, and distribution of infection in the lung on all postmortem days was more evident in pigs than in ferrets. However, in contrast to pigs, ferrets shed a larger total quantity of virus for an extended duration, and seroconversion occurred in all infected and contact ferrets by 21 dpi. However, interpretation of data is limited by the different intranasal infection protocols and nasal sampling techniques for the 2 species. All animals had increased specific antibody titers postinfection. However, in comparison with ferrets, titers in pigs were lower and, in some contact pigs, were below the positive threshold. These findings are comparable with outcomes reported for pH1N1 virus infection of pigs and ferrets (36,37,39,40) and a comparison of swine H1 viruses, including H1N2v strains, when infecting ferrets (41). A North American reassortant H1N1 swine IAV incorporating pH1N1-origin polymerase acidic, NP, and M genes also reportedly showed similar replication kinetics to a swine IAV pH1N1 isolate when infecting ferrets (14). We conclude that there are no apparent phenotypic changes associated with the novel combination of genes in the H1N2r reassortant virus.

Intraspecies transmission by direct contact was demonstrated in our study in pigs and ferrets. Previous studies have focused on ferret-to-ferret transmission of reassortant viruses as a means of assessing risk because the ferret is an accepted small animal model for human influenza, and this animal has comparable anatomic properties, such as respiratory tract distribution of virus receptors, clinical manifestations, and transmission patterns (25). The reassortant H1N2 virus isolated in Denmark incorporates all pH1N1 genes except the NA segment (10). However, ferret-to-ferret transmission consistently occurred only by direct contact and not by the airborne respiratory droplet route. In contrast, an H1N2 strain from South

Korea that had the pH1N1 internal gene cassette was found to infect directly inoculated and contact ferrets and also be transmitted at a lower efficiency, to ferrets indirectly exposed to airborne respiratory droplets (42). In a similar fashion, an H1N2 reassortant strain from Chile containing the pH1N1 internal gene cassette was also transmitted between ferrets by direct and indirect routes (19).

Swine are known to support replication of viruses with a wide range of HA activation pH values, whereas ferrets support replication of a narrower pH activation range for HA (40). In addition, it has been suggested that successful transmission of influenza A viruses requires a balance between the HA and NA activities (43). Therefore, the HA and NA combination of the H1N2r isolate that we studied is compatible with replication and transmission in both mammalian hosts.

In our study, we modeled the zoonotic and reverse-zoonotic infection potential of the H1N2r virus by investigating virus transmission from infected pigs or infected ferrets to cohoused animals of the other species. Transmission by the indirect respiratory droplet route occurred, whether pigs or ferrets were the infection source. Transmission of virus from pigs occurred more rapidly in comparison with ferrets. This finding could have occurred as a consequence of the room layout, the different degree of aerosolization of virus shed from ferrets or pigs, or the anatomic and physiologic differences in the pig and ferret nasal tract. Once animals became infected, whether directly or indirectly, the shedding profile was consistent within the same species. These findings indicate that the threat associated with pH1N1 reassortant viruses from swine or human origin is no greater from either donor species, although zoonotic infection is clearly plausible and might be augmented by the presence of the pH1N1 internal gene cassette.

In conclusion, our study demonstrates that a swine H1N2r virus can be readily transmitted

between mammalian species. Although this virus does not display enhanced virulence compared with other swine IAV or human pH1N1 viruses (36,39), it nevertheless shows high interspecies and intraspecies transmissibility. This virus strain represents a newly emergent reassortant virus that could enhance the genetic diversity of circulating strains and contribute to influenza A virus genotypic change at the human-animal interface, thereby increasing the potential for generating new viruses with altered disease phenotype or fitness for new host species.

Acknowledgment

We thank the Animal and Plant Health Agency Animal Sciences Unit for providing expertise during this study.

This study was supported under research project SE2202 by the Department for Environment, Food, and Rural Affairs and the devolved governments of Scotland and Wales.

About the Author

Dr. Everett is a research scientist at the Animal and Plant Health Agency, Weybridge, UK. Her research interests are the pathogenesis of mammalian influenza viruses, mechanisms of immune-mediated protection from influenza, and strategies for assessing and controlling outbreak risk.

References

1. Brown IH. History and epidemiology of swine influenza in Europe. *Curr Top Microbiol Immunol*. 2013;370:133–46. https://doi.org/10.1007/82_2011_194
2. Smith GJ, Vijaykrishna D, Bahl J, Lycett SJ, Worobey M, Pybus OG, et al. Origins and evolutionary genomics of the 2009 swine-origin H1N1 influenza A epidemic. *Nature*. 2009;459:1122–5. <https://doi.org/10.1038/nature08182>
3. Anderson TK, Macken CA, Lewis NS, Scheuermann R, Van Reeth K, Brown IH, et al. A phylogeny-based global nomenclature system and automated annotation tool for H1 hemagglutinin genes from swine influenza A viruses. *MSphere*. 2016;1:e00275–16. <https://doi.org/10.1128/mSphere.00275-16>
4. Bhatt S, Lam TT, Lycett SJ, Leigh Brown AJ, Bowden TA, Holmes EC, et al.; Combating Swine Influenza Consortium. The evolutionary dynamics of influenza A virus adaptation to mammalian hosts. *Philos Trans R Soc Lond B Biol Sci*. 2013;368:20120382. <https://doi.org/10.1098/rstb.2012.0382>
5. Lewis NS, Russell CA, Langat P, Anderson TK, Berger K, Bielejec F, et al.; ESNIP3 consortium. The global antigenic diversity of swine influenza A viruses. *eLife*. 2016;5:e12217. <https://doi.org/10.7554/eLife.12217>
6. Watson SJ, Langat P, Reid SM, Lam TT, Cotten M, Kelly M, et al.; ESNIP3 Consortium. Molecular epidemiology and evolution of influenza viruses circulating within European swine between 2009 and 2013. *J Virol*. 2015;89:9920–31. <https://doi.org/10.1128/JVI.00840-15>
7. Henritzi D, Hoffmann B, Wacheck S, Pesch S, Herrler G, Beer M, et al. A newly developed tetraplex real-time RT-PCR for simultaneous screening of influenza virus types A, B, C and D. *Influenza Other Respir Viruses*. 2018.
8. Howard WA, Essen SC, Strugnell BW, Russell C, Barass L, Reid SM, et al. Reassortant pandemic (H1N1) 2009 virus in Ppigs, United Kingdom. *Emerg Infect Dis*. 2011;17:1049–52. <https://doi.org/10.3201/eid1706.101886>
9. Moreno A, Di Trani L, Faccini S, Vaccari G, Nigrelli D, Boniotti MB, et al. Novel H1N2 swine influenza reassortant strain in pigs derived from the pandemic H1N1/2009 virus. *Vet Microbiol*. 2011;149:472–7. <https://doi.org/10.1016/j.vetmic.2010.12.011>
10. Fobian K, Fabrizio TP, Yoon SW, Hansen MS, Webby RJ, Larsen LE. New reassortant and enzootic European swine influenza viruses transmit efficiently through direct contact in the ferret model. *J Gen Virol*. 2015;96:1603–12. <https://doi.org/10.1099/vir.0.000094>
11. Starick E, Fereidouni SR, Lange E, Grund C, Vahlenkamp T, Beer M, et al. Analysis of influenza A viruses of subtype H1 from wild birds, turkeys and pigs in Germany reveals interspecies transmission events. *Influenza Other Respir Viruses*. 2011;5:276–84. <https://doi.org/10.1111/j.1750-2659.2011.00201.x>
12. Krog JS, Hjulsgaard CK, Larsen MA, Larsen LE. Triple-reassortant influenza A virus with H3 of human seasonal origin, NA of swine origin, and internal A(H1N1) pandemic 2009 genes is established in Danish pigs. *Influenza Other Respir Viruses*. 2017;11:298–303. <https://doi.org/10.1111/irv.12451>
13. Vijaykrishna D, Poon LL, Zhu HC, Ma SK, Li OT, Cheung CL, et al. Reassortment of pandemic H1N1/2009 influenza A virus in swine. *Science*. 2010;328:1529. <https://doi.org/10.1126/science.1189132>
14. Ducatez MF, Hause B, Stigger-Rosser E, Darnell D, Corzo C, Juleen K, et al. Multiple reassortment between pandemic (H1N1) 2009 and endemic influenza viruses in pigs, United States. *Emerg Infect Dis*. 2011;17:1624–9. <https://doi.org/10.3201/1709.110338>
15. Nelson MI, Schaefer R, Gava D, Cantão ME, Ciacci-Zanella JR, Influenza A. Influenza A viruses of human origin in swine, Brazil. *Emerg Infect Dis*. 2015;21:1339–47. <https://doi.org/10.3201/eid2108.141891>
16. Biondo N, Schaefer R, Gava D, Cantão ME, Silveira S, Mores MA, et al. Genomic analysis of influenza A virus from captive wild boars in Brazil reveals a human-like H1N2 influenza virus. *Vet Microbiol*. 2014;168:34–40. <https://doi.org/10.1016/j.vetmic.2013.10.010>
17. Schaefer R, Rech RR, Gava D, Cantão ME, da Silva MC, Silveira S, et al. A human-like H1N2 influenza virus detected during an outbreak of acute respiratory disease in swine in Brazil. *Arch Virol*. 2015;160:29–38. <https://doi.org/10.1007/s00705-014-2223-z>
18. Resende PC, Born PS, Matos AR, Motta FC, Caetano BC, Debur MD, et al. Whole-genome characterization of a novel human influenza A(H1N2) virus variant, Brazil. *Emerg Infect Dis*. 2017;23:152–4. <https://doi.org/10.3201/eid2301.161122>
19. Bravo-Vasquez N, Karlsson EA, Jimenez-Bluhm P, Meliopoulos V, Kaplan B, Marvin S, et al. Swine influenza virus (H1N2) characterization and transmission in ferrets, Chile. *Emerg Infect Dis*. 2017;23:241–51. <https://doi.org/10.3201/eid2302.161374>
20. Komadina N, McVernon J, Hall R, Leder K. A historical perspective of influenza A(H1N2) virus. *Emerg Infect Dis*. 2014;20:6–12. <https://doi.org/10.3201/eid2001.121848>
21. Pascua PN, Lim GJ, Kwon HI, Kim YI, Kim EH, Park SJ, et al. Complete genome sequences of novel reassortant

- H1N2 swine influenza viruses isolated from pigs in the Republic of Korea. *Genome Announc.* 2013;1:e00552-13. <https://doi.org/10.1128/genomeA.00552-13>
22. Peng X, Wu H, Xu L, Peng X, Cheng L, Jin C, et al. Molecular characterization of a novel reassortant H1N2 influenza virus containing genes from the 2009 pandemic human H1N1 virus in swine from eastern China. *Virus Genes.* 2016;52:405-10. <https://doi.org/10.1007/s11262-016-1303-4>
 23. Williamson SM, Tucker AW, McCrone IS, Bidewell CA, Brons N, Habernoll H, et al.; COSI. Descriptive clinical and epidemiological characteristics of influenza A H1N1 2009 virus infections in pigs in England. *Vet Rec.* 2012;171:271. <https://doi.org/10.1136/vr.100673>
 24. Fragaszy E, Ishola DA, Brown IH, Enstone J, Nguyen-Van-Tam JS, Simons R, et al.; Flu Watch Group; Combating Swine Influenza (COSI) Consortium. Increased risk of A(H1N1)pdm09 influenza infection in UK pig industry workers compared to a general population cohort. *Influenza Other Respir Viruses.* 2016;10:291-300. <https://doi.org/10.1111/irv.12364>
 25. Belser JA, Katz JM, Tumpey TM. The ferret as a model organism to study influenza A virus infection. *Dis Model Mech.* 2011;4:575-9. <https://doi.org/10.1242/dmm.007823>
 26. Trock SC, Burke SA, Cox NJ. Development of framework for assessing influenza virus pandemic risk. *Emerg Infect Dis.* 2015;21:1372-8. <https://doi.org/10.3201/eid2108.141086>
 27. Brauer R, Chen P. Influenza virus propagation in embryonated chicken eggs. *J Vis Exp.* 2015;Mar 19:doi:10.3791/52421. <https://doi.org/10.3791/52421>
 28. Hemmink JD, Morgan SB, Aramouni M, Everett H, Salguero FJ, Canini L, et al. Distinct immune responses and virus shedding in pigs following aerosol, intra-nasal and contact infection with pandemic swine influenza A virus, A(H1N1)09. *Vet Res (Faisalabad).* 2016;47:103. <https://doi.org/10.1186/s13567-016-0390-5>
 29. Baillie GJ, Galiano M, Agapow PM, Myers R, Chiam R, Gall A, et al. Evolutionary dynamics of local pandemic H1N1/2009 influenza virus lineages revealed by whole-genome analysis. *J Virol.* 2012;86:11-8. <https://doi.org/10.1128/JVI.05347-11>
 30. Brown IH, Harris PA, Alexander DJ. Serological studies of influenza viruses in pigs in Great Britain 1991-2. *Epidemiol Infect.* 1995;114:511-20. <https://doi.org/10.1017/S0950268800052225>
 31. Brown IH, Harris PA, McCauley JW, Alexander DJ. Multiple genetic reassortment of avian and human influenza A viruses in European pigs, resulting in the emergence of an H1N2 virus of novel genotype. *J Gen Virol.* 1998;79:2947-55. <https://doi.org/10.1099/0022-1317-79-12-2947>
 32. van den Brand JM, Stittelaar KJ, van Amerongen G, Reperant L, de Waal L, Osterhaus AD, et al. Comparison of temporal and spatial dynamics of seasonal H3N2, pandemic H1N1 and highly pathogenic avian influenza H5N1 virus infections in ferrets. *PLoS One.* 2012;7:e42343. <https://doi.org/10.1371/journal.pone.0042343>
 33. Slomka MJ, Densham AL, Coward VJ, Essen S, Brookes SM, Irvine RM, et al. Real time reverse transcription (RRT)-polymerase chain reaction (PCR) methods for detection of pandemic (H1N1) 2009 influenza virus and European swine influenza A virus infections in pigs. *Influenza Other Respir Viruses.* 2010;4:277-93. <https://doi.org/10.1111/j.1750-2659.2010.00149.x>
 34. Löndt BZ, Nunez A, Banks J, Nili H, Johnson LK, Alexander DJ. Pathogenesis of highly pathogenic avian influenza A/turkey/Turkey/1/2005 H5N1 in Pekin ducks (*Anas platyrhynchos*) infected experimentally. *Avian Pathol.* 2008;37:619-27. <https://doi.org/10.1080/03079450802499126>
 35. Kitikoon P, Gauger PC, Vincent AL. Hemagglutinin inhibition assay with swine sera. *Methods Mol Biol.* 2014;1161:295-301. https://doi.org/10.1007/978-1-4939-0758-8_24
 36. Brookes SM, Núñez A, Choudhury B, Matrosovich M, Essen SC, Clifford D, et al. Replication, pathogenesis and transmission of pandemic (H1N1) 2009 virus in non-immune pigs. *PLoS One.* 2010;5:e9068. <https://doi.org/10.1371/journal.pone.0009068>
 37. Vidaña B, Martínez J, Martínez-Orellana P, García Migura L, Montoya M, Martorell J, et al. Heterogeneous pathological outcomes after experimental pH1N1 influenza infection in ferrets correlate with viral replication and host immune responses in the lung. *Vet Res (Faisalabad).* 2014;45:85. <https://doi.org/10.1186/s13567-014-0085-8>
 38. Martínez-Orellana P, Martorell J, Vidaña B, Majó N, Martínez J, Falcón A, et al. Clinical response to pandemic H1N1 influenza virus from a fatal and mild case in ferrets. *Virology.* 2015;12:48. <https://doi.org/10.1186/s12985-015-0272-x>
 39. Janke BH. Influenza A virus infections in swine: pathogenesis and diagnosis. *Vet Pathol.* 2014;51:410-26. <https://doi.org/10.1177/0300985813513043>
 40. Russier M, Yang G, Marinova-Petkova A, Vogel P, Kaplan BS, Webby RJ, et al. H1N1 influenza viruses varying widely in hemagglutinin stability transmit efficiently from swine to swine and to ferrets. *PLoS Pathog.* 2017;13:e1006276. <https://doi.org/10.1371/journal.ppat.1006276>
 41. Pulit-Penalosa JA, Pappas C, Belser JA, Sun X, Brock N, Zeng H, et al. Comparative in vitro and in vivo analysis of H1N1 and H1N2 variant influenza viruses isolated from humans between 2011 and 2016. *J Virol.* 2018;92:e01444-18. <https://doi.org/10.1128/JVI.01444-18>
 42. Lee JH, Pascua PN, Decano AG, Kim SM, Park S-J, Kwon H-I, et al. Evaluation of the zoonotic potential of a novel reassortant H1N2 swine influenza virus with gene constellation derived from multiple viral sources. *Infect Genet Evol.* 2015;34:378-93. <https://doi.org/10.1016/j.meegid.2015.06.005>
 43. Yen H-L, Liang C-H, Wu C-Y, Forrest HL, Ferguson A, Choy K-T, et al. Hemagglutinin-neuraminidase balance confers respiratory-droplet transmissibility of the pandemic H1N1 influenza virus in ferrets. *Proc Natl Acad Sci U S A.* 2011;108:14264-9. <https://doi.org/10.1073/pnas.1111000108>

Address for correspondence: Helen E. Everett, Animal and Plant Health Agency, New Haw, Addlestone, Surrey KT15 3NB, UK; email: helen.everett@apha.gov.uk

Multiplex Mediator Displacement Loop-Mediated Isothermal Amplification for Detection of *Treponema pallidum* and *Haemophilus ducreyi*

Lisa Becherer, Sascha Knauf, Michael Marks, Simone Lueert, Sieghard Frischmann, Nadine Borst, Felix von Stetten, Sibauk Bieb, Yaw Adu-Sarkodie, Kingsley Asiedu, Oriol Mitjà,¹ Mohammed Bakheit¹

Yaws, a neglected tropical disease caused by the bacterium *Treponema pallidum* subspecies *pertenue*, manifests as ulcerative skin lesions. Nucleic acid amplification tests, like loop-mediated isothermal amplification (LAMP), are versatile tools to distinguish yaws from infections that cause similar skin lesions, primarily *Haemophilus ducreyi*. We developed a novel molecular test to simultaneously detect *T. pallidum* and *H. ducreyi* based on mediator displacement LAMP. We validated the *T. pallidum* and *H. ducreyi* LAMP (TPHD-LAMP) by testing 293 clinical samples from patients with yaws-like lesions. Compared with quantitative PCR, the TPHD-LAMP demonstrated high sensitivity and specificity for *T. pallidum* (84.7% sensitivity, 95.7% specificity) and *H. ducreyi* (91.6% sensitivity, 84.8% specificity). This novel assay provided rapid molecular confirmation of *T. pallidum* and *H. ducreyi* DNA and might be suitable for use at the point of care. TPHD-LAMP could support yaws eradication by improving access to molecular diagnostic tests at the district hospital level.

Author affiliations: University of Freiburg, Freiburg, Germany (L. Becherer, N. Borst, F. von Stetten); Georg-August-University of Goettingen, Goettingen, Germany (S. Knauf); German Primate Centre, Goettingen (S. Knauf, S. Lueert); London School of Hygiene & Tropical Medicine, London, UK (M. Marks); Hospital for Tropical Diseases, London (M. Marks); Mast Diagnostica GmbH, Reinfeld, Germany (S. Frischmann, M. Bakheit); Hahn-Schickard, Freiburg, Germany (N. Borst, F. von Stetten); Papua New Guinea Department of Health, Port Moresby, Papua New Guinea (S. Bieb); Kwame Nkrumah University of Science and Technology, Kumasi, Ghana (Y. Adu-Sarkodie); World Health Organization, Geneva, Switzerland (K. Asiedu); Lihir Medical Centre-International SOS, Newcrest Mining, Lihir Island, Papua New Guinea (O. Mitjà); Fundacio Lluita contra la Sida-Hospital Universitari Germans Trias i Pujol, Badalona, Spain (O. Mitjà); Barcelona Institute for Global Health-Hospital Clinic-University of Barcelona, Barcelona, Spain (O. Mitjà)

DOI: <https://doi.org/10.3201/eid2602.190505>

Yaws, a neglected tropical disease caused by the bacterium *Treponema pallidum* subspecies *pertenue*, predominantly affects children living in low-income, rural communities of warm and humid regions (1). Clinical manifestations include lesions of the skin, bone, and cartilage, progressing to severe destructive lesions if left untreated (2). Manifestations of primary yaws include papillomas or ulcerative lesions; manifestations of secondary yaws include a wide range of rashes, often accompanied by bone and joint involvement (2). Currently, 15 countries in West and Central Africa, Southeast Asia, and the Pacific region are known to be yaws-endemic. The World Health Organization (WHO) released a yaws eradication strategy (the Morges strategy) in 2012 (3). The mainstay of the strategy is mass drug administration (MDA) with single-dose azithromycin in yaws-endemic communities, followed by routine surveillance and retreatment for 3–6 months until no cases remain (3).

Serologic tests, including the *T. pallidum* particle agglutination and rapid plasma reagin tests, remain the primary diagnostic tools for yaws (2). Newer point-of-care serologic tests have replaced traditional laboratory-based serologic assays in many settings (4–7). Despite their central role in yaws diagnosis, serologic assays have several limitations. First, treponemal serologic assays usually remain positive over a patient's lifetime, and these tests cannot distinguish previous from current infection. Second, studies in Africa and in countries in the Pacific region have demonstrated that *Haemophilus ducreyi* causes cutaneous lesions similar to those observed in yaws (8–11). Persons with clinically suspicious lesions caused by

¹These senior authors contributed equally to this article.

H. ducreyi can have a reactive serologic test for yaws because of latent *T. pallidum* infection. Nucleic acid amplification tests (NAATs) can distinguish active yaws, involving a lesion with detectable *T. pallidum* DNA, from latent yaws, in which patients will have reactive serology without detectable *T. pallidum* DNA from lesions. In addition, before seroconversion, a small proportion of patients with early active yaws will have a positive NAAT but negative serologic results.

NAATs could play a central role in yaws eradication efforts, particularly for diagnosis and surveillance after MDA in yaws-endemic areas (12). PCR has been standard for molecular diagnosis and has a high specificity and sensitivity for *T. pallidum* and *H. ducreyi*, but the process is time-consuming and requires expensive laboratory equipment. Most yaws-endemic countries have limited access to PCR to aid national yaws eradication programs. A point-of-care NAAT could provide reliable post-MDA molecular surveillance, as well as help in monitoring for azithromycin resistance. Loop-mediated isothermal amplification (LAMP) is an alternative for molecular diagnosis that might be more suitable than PCR as a point-of-care NAAT in resource-limited environments. LAMP has fast processing times and high specificity and can be performed on less expensive devices than those needed for PCR.

Multiplex technologies, such as mediator displacement (MD) LAMP (13), have extended the usability of LAMP for simultaneous detection of >1 target and could be an efficient and cost-effective solution. MD detection uses an MD probe composed of a generic mediator attached to a generic overhang of a DNA target-specific sequence and a universal reporter molecule with a fluorophore and quencher for detection. We developed and validated a biplex MD LAMP assay to simultaneously identify *T. pallidum* and *H. ducreyi*.

Methods

Participants

We obtained samples from larger trials conducted on Lihir Island (n = 57) and Karkar Island (n = 184), Papua New Guinea; and in Ghana (n = 52). Details of the studies in which the samples were collected are provided elsewhere (14,15). In brief, samples were collected as part of a randomized control trial comparing azithromycin doses of 30 mg/kg against doses of 20 mg/kg to treat patients in a pilot study for yaws elimination (14,15). Swabs were collected from persons with yaws-like ulcers and placed in AssayAssure Multilock (Sierra Molecular, <https://sierramolecular.com>) transport medium, then frozen

at -20°C until transported to Mast Diagnostica GmbH laboratory in Reinfeld, Germany. DNA was extracted from the samples by using innuPREP MP Basic Kit A (Analytik Jena, <https://www.analytik-jena.com>) according to manufacturer's instructions. Isolated DNA was kept frozen at -20°C until it was used for biplex *T. pallidum* and *H. ducreyi* LAMP (TPHD-LAMP), singleplex *T. pallidum* and *H. ducreyi* LAMP assays, and quantitative PCR (qPCR) testing.

Ethics Approval

Participants, or parents or guardians of persons <18 years of age, provided written consent for inclusion in clinical surveys and etiologic studies. Children also provided assent when appropriate. The studies were approved by the National Medical Research Advisory Committee of the Papua New Guinea Ministry of Health (MRAC nos. 12.36 and 14.31), the Ghana Health Service (approval no. GHS 13/11/14), the London School of Hygiene & Tropical Medicine (approval no. 8832), and WHO (approval no. RPC720).

TPHD-LAMP Assay

We devised the TPHD-LAMP assay on the basis of 2 previously published assays: a singleplex LAMP assay (16), which we modified by adding an MD probe; and a biplex LAMP assay of *T. pallidum* and *H. ducreyi* (13). TPHD-LAMP primers target the polymerase I (polA) gene of *T. pallidum* and the 16S ribosomal RNA (16S rRNA) of *H. ducreyi*. We further optimized the assays for improved functionality by redesigning primers and probes and modifying reagent concentrations (Appendix Tables 1–3, <https://wwwnc.cdc.gov/EID/article/26/2/19-0505-App1.pdf>).

We performed a 2-step validation of the TPHD-LAMP assay. In the first step, we assessed the analytical sensitivity and specificity of the assay. In the second step, we used clinical samples collected in Ghana and Papua New Guinea to compare the performance of TPHD-LAMP against qPCR for individual targets. In a secondary analysis, we compared the performance of singleplex LAMP assays for each individual target against qPCR assays.

Assessment of Analytical Performance

We determined the analytical limit of detection (LOD) for the TPHD-LAMP assay by using target sequences cloned into plasmids. We determined the LOD of each of the 2 components separately, as well as the LOD of the biplex TPHD-LAMP assay (Appendix). We varied the plasmid DNA concentrations between 3×10^1 copies/reaction and 3×10^5 copies/reaction in 8 replicates to reproduce the *Treponema*

bacterial load in skin infections, which ranges from 10^2 – 10^4 copies/reaction (17). In addition, we tested the TPHD-LAMP in the presence of a high number of copies, 3×10^5 copies/reaction, of *H. ducreyi* or *T. pallidum* in the presence of a low number of copies of the second target to optimize each component and to simulate clinical samples that might contain both targets. We conducted primer titration experiments to minimize the preferential amplification of *H. ducreyi* DNA targets in persons with both infections. We estimated the LOD by counting the fraction of positive amplifications and performed probit regression analysis by using SPSS Statistics 25 (IBM, <https://www.ibm.com>).

We assessed the analytical specificity of the primer sets in silico by using ortholog target gene sequences from GenBank (Appendix Table 4) and found all primer sets were highly specific for *T. pallidum* and *H. ducreyi*. Based on these results, we tested the specificity of TPHD-LAMP in vitro against endemic pathogens associated with cutaneous ulcerative syndromes by using a panel of 13 organisms: *Escherichia coli*, *Klebsiella pneumoniae*, *Acinetobacter baumannii*, *Pseudomonas aeruginosa*, *Enterobacter cloacae*, *Salmonella enterica* (Paratyphi and Typhi), *Streptococcus pneumoniae*, *Streptococcus pyogenes*, *Staphylococcus aureus*, *Corynebacterium diphtheria*, *Corynebacterium ulcerans*, *Proteus mirabilis*, and *Enterococcus faecalis* (Appendix). We calculated interassay and intraassay variability of the TPHD-LAMP assay by using 3 batches of the TPHD-LAMP mix, prepared individually on 3 separate days and processed in different runs of 3 replicates per batch (Appendix).

Clinical Performance of the TPHD-LAMP

We performed clinical validation by comparing the performance of the TPHD-LAMP and qPCR assays to identify *T. pallidum* and *H. ducreyi* in patient samples collected in Ghana and Papua New Guinea. TPHD-LAMP reactions (10 μ L per assay) were composed of 1 \times RM MPM buffer (MAST Diagnostica GmbH, <https://mast-group.com>), 8 U Bst 2.0 WarmStart DNA Polymerase (New England Biolabs, <https://www.neb.com>), 0.05 μ mol/L universal reporter, and MD primer mix (Appendix). We incubated primer mixes for 5 m at 70°C before LAMP to prevent non-specific amplification initiated by primer dimerization. We performed real-time TPHD-LAMP reactions at 64°C in a Rotor-Gene Q (QIAGEN, <https://www.qiagen.com>) and acquired fluorescence signals every minute by using the Cy5-readout gain for *T. pallidum* and the FAM-readout gain for *H. ducreyi*. The single-

plex LAMP reactions (10 μ L per assay) using intercalating dye were composed of 1 \times RM MPM buffer, 8 U Bst 2.0 WarmStart DNA Polymerase, and 1 μ L of 10 \times SYBR Green staining reagent, DNA free (AppliChem, <https://www.applichem.com>) and primer mix (Appendix Table 1). We also performed singleplex LAMP reactions in a Rotor-Gene Q at 63°C with the FAM-readout gain. We used a cutoff of 60 m for biplex TPHD-LAMP and singleplex LAMP assays and considered samples with amplification beyond 60 m negative.

For performance analyses, we compared the TPHD-LAMP assay against TaqMan qPCR assays targeting *polA* of *T. pallidum* (18) and an optimized TaqMan qPCR assay targeting the 16S rRNA gene of *H. ducreyi* on the same DNA extract (Appendix Table 4, Figure 1). The 16S rRNA gene has been previously used in qPCR assays to detect *H. ducreyi* (19). We ran all tests in duplicate and included positive controls and DNA-free negative controls in each run. We used an identical sample volume, 2.5 μ L/reaction, for TPHD-LAMP, singleplex LAMP, and qPCR. For samples that tested negative by qPCR but positive by TPHD-LAMP, we repeated qPCR in a single reaction with higher sample volumes (3 μ L) to identify true negative test results.

Statistical Analysis

For clinical validation, we compared the sensitivity and specificity of the TPHD-LAMP assay against TaqMan qPCR assays. In a secondary analysis, we compared the performance of singleplex LAMP assays to qPCR. We performed all analysis by using R version 3.4.3 (<https://www.R-project.org>).

Results

Analytical Sensitivity and Specificity

The LOD for the TPHD-LAMP assay was 357 copies/reaction (95% CI 265–535 copies/reaction) for *T. pallidum* and 293 copies/reaction (95% CI 199–490 copies/reaction) for *H. ducreyi*. When we added the second target at the higher concentration of 3×10^5 copies/reaction to simulate clinical samples from persons infected with both bacteria, the LOD increased to 808 copies/reaction (95% CI 550–2,128 copies/reaction) for *T. pallidum* and 622 copies/reaction (95% CI 415–1,687 copies/reaction) for *H. ducreyi* (Appendix Figure 2). The TPHD-LAMP assay was negative for all other pathogens tested within 60 m, demonstrating high analytical specificity (Appendix Figure 3). We observed a minimal interassay or intraassay variation (Appendix Figure 4).

Validation of TPHD-LAMP in Clinical Samples

For clinical validation, we used a sample set consisting of 293 lesion swabs collected from patients with suspected *T. pallidum* infection. Samples were collected in Lihir Island (n = 57; 19.5%) and Karkar Island (n = 184; 62.8%), Papua New Guinea; and in Ghana (n = 52; 17.7%). A total of 184 (62.8%) cases were in male patients and 109 (37.2%) in female patients; the median age of case-patients was 10 years (interquartile range [IQR] 8–12 years).

Using qPCR, we detected *T. pallidum* in 59 (20.1%) samples, *H. ducreyi* in 155 (52.9%) samples, and *T. pallidum* and *H. ducreyi* co-infection in 19 (6.5%) samples. When tested by TPHD-LAMP, we detected *T. pallidum* in 60 (20.5%) samples and *H. ducreyi* in 163 (55.6%) samples. We detected both targets in 12 (4.1%) samples. Taking qPCR as the reference standard, the diagnostic sensitivity of the TPHD-LAMP assay for *T. pallidum* was 84.7% and the specificity was 95.7%. For *H. ducreyi*, the sensitivity of the TPHD-LAMP assay was 91.6% and the specificity was 84.8% (Table 1). Kappa coefficients (κ), ranging from 0.7 to 0.9 for the detection of *T. pallidum* and from 0.7 to 0.8 for *H. ducreyi*, show substantial to excellent agreement between qPCR and TPHD-LAMP. Moderate agreement between qPCR and TPHD-LAMP ($\kappa = 0.5$) also was demonstrated for the simultaneous detection of both targets. The median time to amplification of *T. pallidum* was 11 min (IQR 9–15 min) and the median time to amplification of *H. ducreyi* was 10 min (IQR 8–24 min).

For samples in which only 1 organism was detected by qPCR, the sensitivity of the TPHD-LAMP assay was higher for both *T. pallidum* (92.5%) and *H. ducreyi* (94.1%) than for samples with both organisms confirmed by qPCR. For samples confirmed to contain both bacteria by qPCR, sensitivity for *T. pallidum* was 68.4% ($p = 0.048$) and sensitivity for *H. ducreyi* was 73.7% ($p = 0.01$) (Table 1).

Using qPCR as the reference standard, the singleplex *T. pallidum* LAMP assay had a sensitivity of 78.0% and specificity of 97.9%; for the singleplex *H. ducreyi* LAMP assay the sensitivity was 91.0% and specificity was 75.3% (Table 2). We did not see a noticeable variation in the performance of the biplex TPHD-LAMP and singleplex LAMP assays between locations from which samples were collected (Tables 1 and 2).

Discussion

We provide data demonstrating a high analytical performance of a multiplex LAMP assay for *T. pallidum* and *H. ducreyi* and a high sensitivity and specificity comparable to qPCR. The TPHD-LAMP assay also performed better than singleplex LAMP assays, likely reflecting better performance of the MD technology used in the biplex LAMP compared with standard intercalating dyes used in singleplex LAMP assays.

The LOD of the TPHD-LAMP assay was 300 copies/reaction for both targets, which is comparable to qPCR, which has standard reproducibility in a range

Table 1. Comparison of clinical performance of biplex loop-mediated isothermal amplification for detection of *Treponema pallidum* and *Haemophilus ducreyi* (TPHD-LAMP) against singleplex TaqMan quantitative PCR*

Characteristics	Sample size	<i>Treponema pallidum</i>	<i>Haemophilus ducreyi</i>
Total samples, no.	293		
No. positive		60	163
Sensitivity, % (95% CI)		84.7 (72.5–92.4)	91.6 (85.8–95.3)
Specificity, % (95% CI)		95.7 (92.0–97.8)	84.8 (77.4–90.1)
Lesions containing a single pathogen†	195		
No. positive		48	151
Sensitivity, % (95% CI)		92.5 (78.5–98.0)	94.1 (88.4–97.2)
Specificity, % (95% CI)		95.7 (92.0–97.8)	84.8 (77.4–90.1)
Lesions containing both pathogens†	19		
No. positive		12	12
Sensitivity, % (95% CI)		68.4 (43.5–86.4)	73.7 (48.6–89.9)
Specificity, % (95% CI)		NA	NA
Samples from Lihir Island, no.	57		
No. positive		21	13
Sensitivity, % (95% CI)		90.5 (68.2–98.3)	76.5 (50.0–92.2)
Specificity, % (95% CI)		94.4 (80.0–99.0)	100.0 (89.1–100)
Samples from Karkar Island, no.	184		
No. positive		33	119
Sensitivity, % (95% CI)		78.1 (59.6–90.1)	94.2 (87.5–97.7)
Specificity, % (95% CI)		94.7 (89.5–97.5)	74.7 (63.4–83.5)
Samples from Ghana, no.	52		
No. positive		6	31
Sensitivity, % (95% CI)		100.0 (51.7–100)	90.9 (75.5–97.6)
Specificity, % (95% CI)		100.0 (90.4–100)	94.7 (71.9–99.7)

*NA, not applicable.

†Determined by quantitative PCR.

Table 2. Comparison of clinical performance of singleplex loop-mediated isothermal amplification for detection of *Treponema pallidum* and *Haemophilus ducreyi* against singleplex TaqMan quantitative PCR*

Characteristics	Sample size	<i>Treponema pallidum</i>	<i>Haemophilus ducreyi</i>
Total samples, no.	293		
No. positive		51	175
Sensitivity, % (95% CI)		78.0 (64.9–87.3)	91.0 (85.0–94.8)
Specificity, % (95% CI)		97.9 (94.8–99.2)	75.3 (67.2–82.1)
Lesions containing a single pathogen†	195		
No. positive		34	158
Sensitivity, % (95% CI)		82.5 (66.6–92.1)	92.6 (86.5–96.2)
Specificity, % (95% CI)		97.9 (94.8–99.2)	75.4 (67.2–82.1)
Lesions containing both pathogens†	19		
No. positive samples		17	17
Sensitivity, % (95% CI)		68.4 (43.5–86.4)	78.9 (53.9–93.0)
Specificity, % (95% CI)		NA	NA

*NA, not applicable.

†Determined by quantitative PCR.

of 10^1 – 10^6 copies/reaction. The LOD increased to ≈ 600 copies/reaction in samples that contained both targets, which is consistent with our clinical validation of the TPHD-LAMP; sensitivity for both bacteria was slightly higher when samples contained only a single target. Kappa coefficients confirmed substantial agreement ($\kappa > 0.7$) for the individual targets and moderate agreement ($\kappa = 0.5$) for simultaneous detection of both targets in a sample.

Detection of *T. pallidum* is the programmatic priority, but detection of *H. ducreyi* is beneficial for clinical management of patients with suspected yaws. The median time to amplification was < 15 m for both *T. pallidum* and *H. ducreyi*, indicating the TPHD-LAMP assay could provide rapid, molecular confirmation of the presence of *T. pallidum* or *H. ducreyi*. Further optimization of the assay to enhance the performance of the *T. pallidum* component, particularly in the context of co-infection, will be required to ensure cases of yaws are not missed.

Implementing qPCR at the point of care is operationally challenging because it requires relatively expensive equipment, in particular thermocyclers, which can cost up to 10 times as much as a tubescanner capable of performing the TPHD-LAMP assay. Because qPCR is available only in a limited number of national and international reference laboratories, TPHD-LAMP might be an alternative molecular test to support expansion of yaws eradication activities. We did not conduct a cost-effectiveness analysis of the TPHD-LAMP assay, but such an assessment should consider equipment costs, cost per assay, and the relative performance of each assay to assess the cost per case diagnosed. However, our data suggest that the TPHD-LAMP assay might be a cost-saving alternative to qPCR, especially at the point of care.

Our study had some limitations. We tested samples from only 2 geographic regions for clinical

validation of the TPHD-LAMP. Primer binding site mutations have affected the performance of other diagnostic assays for *T. pallidum* strains. Although we selected conserved genomic regions when designing the TPHD-LAMP primers, further experimental validation of the TPHD-LAMP assay with samples from a broader range of settings is needed. We conducted clinical validation of the assay in a controlled laboratory setting, but conditions at the point of care, including temperature, humidity, and a range of other environmental factors, might affect reagents in storage and in performing assays. Further optimization, including freeze-dried reagents in combination with dried oligonucleotides, might improve robustness and facilitate rollout of the assay in yaws-endemic countries.

In yaws-endemic countries, clinical manifestations combined with serologic tests are still the standard tool for the clinical management of yaws, but serologic tests have limitations and molecular assays are needed to support WHO yaws eradication efforts (12). Molecular assays also can detect mutations in the 23S RNA gene associated with azithromycin resistance (15,20,21), which is essential to monitor for drug resistance as yaws eradication efforts expand. qPCR is the most common NAAT currently available but remains restricted to a small number of laboratories in yaws-endemic countries. MD LAMP could facilitate surveillance for resistance and we plan further studies to evaluate a modified TPHD-LAMP assay for this purpose. Further, multicountry evaluations are warranted to assess performance of the assay when deployed in yaws-endemic countries and to assess the role the test could play in support of national yaws eradication programs. Nonetheless, the performance characteristics of the TPHD-LAMP suggest it has the potential to increase access to molecular diagnosis of yaws, especially at the point of care.

Acknowledgments

We thank members of the study teams and communities who participated in the field studies from which we obtained samples.

Financial support: The trial conducted in Ghana and Karkar Island, Papua New Guinea, was funded by a grant from the Neglected Tropical Diseases Support Center to WHO (no. NTD-SC/NCT 053). M.M. was supported by the Wellcome Trust under grant no. 102807. The study was partially funded by a grant from the German Research Foundation (no. KN 1097/3-2) to S.K. This work was partially funded by a grant from the German Federal Ministry of Education and Research (EuroTransBio no. 031B0132B) to L.B. The authors alone are responsible for the views expressed in this article and they do not necessarily represent the views, decisions, or policies of the institutions with which they are affiliated.

Author contributions: L.B. conducted laboratory work, analyzed the data, and wrote the first draft of the manuscript. M.M. and O.M. designed the field studies and analyzed the data. S.K., S.L., S.F., and N.B. contributed to laboratory work or analysis. S.B., Y.A.-S., and K.A. led the field studies. M.B. contributed to laboratory work and analyzed the data. All authors revised the manuscript.

Potential conflicts of interest: S.F. and M.B. are employees of Mast Diagnostica GmbH, which produces and sells LAMP kits and products. A patent covering the technique described in the paper has been applied for by the University of Freiburg, Freiburg, Germany, and Hahn-Schickard, Villingen-Schwenningen, Germany.

About the Author

Ms. Becherer is a scientific researcher in the nucleic acid analysis group at the Department of Microsystems Engineering, University of Freiburg, Freiburg, Germany. Her work focuses on the development of novel methods for nucleic acid amplification, with a special focus on isothermal amplification.

References

- Marks M, Solomon AW, Mabey DC. Endemic treponemal diseases. *Trans R Soc Trop Med Hyg.* 2014;108:601-7. <https://doi.org/10.1093/trstmh/tru128>
- Mitjà O, Asiedu K, Mabey D. Yaws. *Lancet.* 2013;381:763-73. [https://doi.org/10.1016/S0140-6736\(12\)62130-8](https://doi.org/10.1016/S0140-6736(12)62130-8)
- The World Health Organization. Eradication of yaws – the Morges strategy. *Wkly Epidemiol Rec.* 2012;87:189-94.
- Ayove T, Houniei W, Wangnapi R, Bieb SV, Kazadi W, Luke L-N, et al. Sensitivity and specificity of a rapid point-of-care test for active yaws: a comparative study. *Lancet Glob Health.* 2014;2:e415-21. [https://doi.org/10.1016/S2214-109X\(14\)70231-1](https://doi.org/10.1016/S2214-109X(14)70231-1)
- Marks M, Goncalves A, Vahi V, Sokana O, Puiahi E, Zhang Z, et al. Evaluation of a rapid diagnostic test for yaws infection in a community surveillance setting. *PLoS Negl Trop Dis.* 2014;8:e3156. <https://doi.org/10.1371/journal.pntd.0003156>
- Fitzpatrick C, Asiedu K, Sands A, Gonzalez Pena T, Marks M, Mitja O, et al. The cost and cost-effectiveness of rapid testing strategies for yaws diagnosis and surveillance. *PLoS Negl Trop Dis.* 2017;11:e0005985. <https://doi.org/10.1371/journal.pntd.0005985>
- Marks M, Yin Y-P, Chen X-S, Castro A, Causer L, Guy R, et al. Metaanalysis of the performance of a combined treponemal and nontreponemal rapid diagnostic test for syphilis and yaws. *Clin Infect Dis.* 2016;63:627-33. <https://doi.org/10.1093/cid/ciw348>
- González-Beiras C, Marks M, Chen CY, Roberts S, Mitjà O. Epidemiology of *Haemophilus ducreyi* infections. *Emerg Infect Dis.* 2016;22:1-8. <https://doi.org/10.3201/eid2201.150425>
- Marks M, Chi K-H, Vahi V, Pillay A, Sokana O, Pavluck A, et al. *Haemophilus ducreyi* associated with skin ulcers among children, Solomon Islands. *Emerg Infect Dis.* 2014;20:1705-7. <https://doi.org/10.3201/eid2010.140573>
- Mitjà O, Lukehart SA, Pokowas G, Moses P, Kapa A, Godornes C, et al. *Haemophilus ducreyi* as a cause of skin ulcers in children from a yaws-endemic area of Papua New Guinea: a prospective cohort study. *Lancet Glob Health.* 2014;2:e235-41. [https://doi.org/10.1016/S2214-109X\(14\)70019-1](https://doi.org/10.1016/S2214-109X(14)70019-1)
- Ghinai R, El-Duah P, Chi K-H, Pillay A, Solomon AW, Bailey RL, et al. A cross-sectional study of ‘yaws’ in districts of Ghana which have previously undertaken azithromycin mass drug administration for trachoma control. *PLoS Negl Trop Dis.* 2015;9:e0003496. <https://doi.org/10.1371/journal.pntd.0003496>
- Marks M, Mitjà O, Vestergaard LS, Pillay A, Knauf S, Chen C-Y, et al. Challenges and key research questions for yaws eradication. *Lancet Infect Dis.* 2015;15:1220-5. [https://doi.org/10.1016/S1473-3099\(15\)00136-X](https://doi.org/10.1016/S1473-3099(15)00136-X)
- Becherer L, Bakheit M, Frischmann S, Stinco S, Borst N, Zengerle R, et al. Simplified real-time multiplex detection of loop-mediated isothermal amplification using novel mediator displacement probes with universal reporters. *Anal Chem.* 2018;90:4741-8. <https://doi.org/10.1021/acs.analchem.7b05371>
- Marks M, Mitjà O, Bottomley C, Kwakye C, Houine W, Bauri M, et al.; study team. Comparative efficacy of low-dose versus standard-dose azithromycin for patients with yaws: a randomised non-inferiority trial in Ghana and Papua New Guinea. *Lancet Glob Health.* 2018;6:e401-10. [https://doi.org/10.1016/S2214-109X\(18\)30023-8](https://doi.org/10.1016/S2214-109X(18)30023-8)
- Mitjà O, Godornes C, Houine W, Kapa A, Paru R, Abel H, et al. Re-emergence of yaws after single mass azithromycin treatment followed by targeted treatment: a longitudinal study. *Lancet.* 2018;391:1599-607. [https://doi.org/10.1016/S0140-6736\(18\)30204-6](https://doi.org/10.1016/S0140-6736(18)30204-6)
- Knauf S, Lüert S, Šmajš D, Strouhal M, Chuma IS, Frischmann S, et al. Gene target selection for loop-mediated isothermal amplification for rapid discrimination of *Treponema pallidum* subspecies. *PLoS Negl Trop Dis.* 2018;12:e0006396. <https://doi.org/10.1371/journal.pntd.0006396>
- Tipple C, Hanna MOF, Hill S, Daniel J, Goldmeier D, McClure MO, et al. Getting the measure of syphilis: qPCR to better understand early infection. *Sex Transm Infect.* 2011;87:479-85. <https://doi.org/10.1136/sti.2011.049494>
- Chen C-Y, Chi K-H, George RW, Cox DL, Srivastava A, Rui Silva M, et al. Diagnosis of gastric syphilis by direct

RESEARCH

- immunofluorescence staining and real-time PCR testing. *J Clin Microbiol.* 2006;44:3452–6. <https://doi.org/10.1128/JCM.00721-06>
19. Orle KA, Gates CA, Martin DH, Body BA, Weiss JB. Simultaneous PCR detection of *Haemophilus ducreyi*, *Treponema pallidum*, and herpes simplex virus types 1 and 2 from genital ulcers. *J Clin Microbiol.* 1996;34:49–54.
20. Chen C-Y, Chi K-H, Pillay A, Nachamkin E, Su JR, Ballard RC. Detection of the A2058G and A2059G 23S rRNA gene point mutations associated with azithromycin resistance in *Treponema pallidum* by use of a TaqMan real-time multiplex PCR assay. *J Clin Microbiol.* 2013;51:908–13. <https://doi.org/10.1128/JCM.02770-12>
21. Lukehart SA, Godornes C, Molini BJ, Sonnett P, Hopkins S, Mulcahy F, et al. Macrolide resistance in *Treponema pallidum* in the United States and Ireland. *N Engl J Med.* 2004;351:154–8. <https://doi.org/10.1056/NEJMoa040216>

Address for correspondence: Mohammed Bakheit, Mast Diagnostica GmbH, Feldstraße 20, 23858 Reinfeld, Germany; email: bakheit@mast-diagnostica.de



@CDC_EIDjournal

Want to stay updated on the latest news in *Emerging Infectious Diseases*? Let us connect you to the world of global health. Discover groundbreaking research studies, pictures, podcasts, and more by following us on Twitter at @CDC_EIDjournal.

Novel Subclone of Carbapenem-Resistant *Klebsiella pneumoniae* Sequence Type 11 with Enhanced Virulence and Transmissibility, China

Kai Zhou,¹ Tingting Xiao,¹ Sophia David,¹ Qin Wang, Yanzi Zhou, Lihua Guo, David Aanensen, Kathryn E. Holt, Nicholas R. Thomson, Hajo Grundmann,² Ping Shen,² Yonghong Xiao²

We aimed to clarify the epidemiologic and clinical importance of evolutionary events that occurred in carbapenem-resistant *Klebsiella pneumoniae* (CRKP). We collected 203 CRKP causing bloodstream infections in a tertiary hospital in China during 2013–2017. We detected a subclonal shift in the dominant clone sequence type (ST) 11 CRKP in which the previously prevalent capsular loci (KL) 47 had been replaced by KL64 since 2016. Patients infected with ST11-KL64 CRKP had a significantly higher 30-day mortality rate than other CRKP-infected patients. Enhanced virulence was further evidenced by phenotypic tests. Phylogenetic reconstruction demonstrated that ST11-KL64 is derived from an ST11-KL47-like ancestor through recombination. We identified a pLVPK-like virulence plasmid carrying *ompA* and *peg-344* in ST11-KL64 exclusively from 2016 onward. The pLVPK-like-positive ST11-KL64 isolates exhibited enhanced environmental survival. Retrospective screening of a national collection identified ST11-KL64 in multiple regions. Targeted surveillance of this high-risk CRKP clone is urgently needed.

The global dissemination of carbapenem-resistant *Enterobacteriaceae* (CRE) has become an urgent public health concern (1,2). In 2016, the World Health

Organization included CRE in a list of antimicrobial-resistant priority pathogens on which to concentrate future drug development strategies. Of note, carbapenem-resistant *Klebsiella pneumoniae* (CRKP) account for 60%–90% of clinical CRE infections in the United States, Europe, and China (1–3), resulting in an increased mortality rate of up to 40%–50% in nosocomial settings (4).

The dissemination of CRKP is mostly clonal, and the population structure is geographically specific. Since its emergence during the early to mid-2000s, sequence type (ST) 258 has become the most prevalent CRKP clone in North America, Latin America, and Europe (5). However, in Asia, especially China, ST11 is the predominant clone, accounting for up to 60% of CRKP (3). ST11 is a single-locus (*tonB*) variant of ST258, and both types belong to the clonal group 258. A recombination event is thought to have occurred between a recipient ST11 and a donor ST442-like strain, giving rise to ST258 during 1985–1997 (6,7). A phylogenomic study revealed that the ST258 population consists of >2 clades, resulting from an ~215-kb recombination event that includes the capsule polysaccharide (*cps*) synthesis locus (6). The genetic differences generated by the resulting capsular switch are supposed to be primarily responsible for the ST258 diversification (8). Likewise, a segregation was identified in the ST11 population, resulting in >3 clades with different capsular loci (KL) (9–11). These studies consistently indicate that *cps* is a recombination hotspot in *K. pneumoniae*. However, the K-type distribution within ST11 in clinical settings is unclear. More important, the biological, epidemiologic, and

Author affiliations: First Affiliated Hospital of Southern University of Science and Technology (Shenzhen People's Hospital), Shenzhen, China (K. Zhou); The Second Clinical Medical College of Jinan University, Shenzhen (K. Zhou); Zhejiang University, Hangzhou, China (T. Xiao, Q. Wang, Y. Zhou, L. Guo, P. Shen, Y. Xiao); Centre for Genomic Pathogen Surveillance, Cambridge, UK (S. David, D. Aanensen); University of Melbourne, Melbourne, Victoria, Australia (K.E. Holt); London School of Hygiene and Tropical Medicine, London, UK (K.E. Holt, N.R. Thomson); Wellcome Trust Sanger Centre, Cambridge (N.R. Thomson); University of Freiburg, Freiburg, Germany (H. Grundmann)

DOI: <https://doi.org/10.3201/eid2602.190594>

¹These first authors contributed equally to this article.

²These senior authors contributed equally to this article.

clinical importance of capsular switches in ST11 remains poorly understood.

Of greater concern, a carbapenem-resistant hypervirulent *K. pneumoniae* ST11 outbreak clone was recently reported in eastern China (12). The outbreak strain was KL47 and hypermucoid and harbored a virulence plasmid carrying *rmpA2* and the aerobactin synthesis locus. Loss of the plasmid substantially alleviated virulence in a *Galleria mellonella* moth model. This finding indicates a worrying convergence of carbapenem resistance and hypervirulence in an already epidemic lineage of *K. pneumoniae*. Although incidence of carbapenem-resistant hypervirulent *K. pneumoniae* has remained low (13–15), understanding how this lineage emerged and evolved is crucial in controlling its further dissemination.

In this study, we measured the occurrence and clinical outcomes of bloodstream infections (BSI) caused by CRKP in a tertiary hospital in China during 2013–2017. We characterized the genomic alterations in the dominant ST11 population and ascertained associated changes in phenotype and pathogenicity traits.

Materials and Methods

Setting and Study Design

We performed a retrospective study in a 2,500-bed tertiary care hospital in China during January 2013–June 2017. We reviewed medical records of any patient with a blood culture positive for *K. pneumoniae* and a clinical course consistent with bacteremia (upon notification of the patient). Patients <16 years of age were excluded. If 1 patient had >1 episode of BSI caused by *K. pneumoniae* (BSI-KP), we included only the first episode. This study was approved by the institutional review board of the First Affiliated Hospital of Zhejiang University in China (approval no. 2017–442). Definitions of terms are detailed in Appendix 1 (<https://wwwnc.cdc.gov/EID/article/26/2/19-0594-App1.pdf>).

Microbiological Assessment

We determined antimicrobial susceptibility by using the VITEK-II system (bioMérieux, <https://www.biomerieux.com>) and further confirmed by using the broth microdilution method. We defined carbapenem nonsusceptibility as MIC >2 mg/L for imipenem or meropenem or MIC >1 mg/L for ertapenem (16). We used multilocus sequence typing to identify ST11 (17). We estimated the pathogenicity of *K. pneumoniae* by testing *G. mellonella* infection, biofilm production, and neutrophil-killing resistance, as previously described (18–20) (Appendix 1). We evaluated the

capacity of CRKP to survive on dry surfaces over time by using previously described methods (21), except that the stainless steel discs were replaced by Corning 24-well polystyrene microplates (Merck, <https://www.sigmaaldrich.com>) and the concentration of bacteria was adjusted to 1×10^8 CFU/mL.

Whole-Genome Sequencing and Analyses

We sequenced 154 ST11 isolates by using an Illumina HiSeq2500 instrument (Illumina, <https://www.illumina.com>) with 2×125 -bp paired-end libraries. We performed de novo assembly of the short-read data by using CLC Genomics Workbench version 10.0 (QIAGEN, <https://www.qiagen.com>) after quality trimming (Phred quality score >20). We performed long-read sequencing on 2 isolates (KP16932 and KP47434) by using the PacBio RSII platform (Pacific Biosciences, <https://www.pacb.com>) with a 10-kb library. A hybrid assembly of these 2 isolates was generated by using Unicycler 0.4.0 (22) with the short and long reads. We annotated the assemblies by using the RAST server (<https://rast.nmpdr.org>) and conducted multilocus sequence typing by using the CGE server (<https://cge.cbs.dtu.dk>). We performed plasmid analysis by Southern blotting and Blast (Appendix 1). We determined the presence or absence of resistance and virulence genes by using Ariba (23) with a custom gene database (<https://figshare.com/s/94437a301288969109c2>) and identified K-type by using Kleborate (<https://github.com/katholt/Kleborate>). We further detected mutations in *rmpA* and *rmpA2* by using blastn (<https://blast.ncbi.nlm.nih.gov/Blast.cgi>). We included genome assemblies of the isolates sequenced in this study and the 62 isolates published elsewhere (10–12,24–26) in the phylogenetic and temporal analysis (Appendix 2 Table 1, <https://wwwnc.cdc.gov/EID/article/26/2/19-0594-App2.xlsx>).

Statistical Analysis

Statistical analyses are described in Appendix 1. We conducted all statistical analyses by using SPSS Statistics 23 (IBM, <https://www.ibm.com>) and SAS 9.4 (SAS institute, <https://www.sas.com>).

Results

Capsular Switch in CRKP-ST11 over a 4-Year Period

We retrospectively screened 10,134 *K. pneumoniae* isolates to determine the proportion of BSI-CRKP. Of 705 nonrepetitive bloodstream isolates, 203 were CRKP. The proportion of *K. pneumoniae* and CRKP in BSIs increased from 17.1% to 45.5% during the study period (Table 1). ST11 was the predominant

Table 1. Prevalence trend of *Klebsiella pneumoniae* causing BSIs in a tertiary hospital, China, 2013–2017*

Isolate type	2013	2014	2015	2016	2017 (half year)	Score test	
						for trend	p value†
Primary BSI/non-BSI isolates	123/610	133/635	201/723	149/687	99/398	1.3934	0.1635
CRKP/non-CRKP	21/102	35/98	53/148	49/100	45/54	6.0697	<0.001
CRKP-ST11/non-ST11 CRKP	20/1	28/7	46/7	39/10	41/4	-0.3116	0.7553
ST11-KL47/ST11-KL64	18/1	20/4	22/23	11/28	5/36	-7.5463	<0.001

*BSI, bloodstream infection; CRKP, carbapenem-resistant *Klebsiella pneumoniae*; ST, sequence type.

†Calculated by using Cochran–Armitage trend test.

clone among BSI-CRKP isolates, accounting for 85.7% (n = 174); annual distribution was relatively stable (95.2%–91.1%).

Five KLS were detected in the BSI-CRKP-ST11 population: KL47 (n = 76), KL64 (n = 92), KL31 (n = 3), KL103 (n = 2), and KL105 (n = 1). The ratio of ST11-KL47 to CRKP-ST11 dropped from 90% (18/20) in 2013 to 12.2% (5/41) in 2017, whereas that of ST11-KL64 increased from 4.6% (1/20) in 2013 to 87.8% (36/41) in 2017. Thus, the ratio of ST11-KL47 to ST11-KL64 decreased substantially in the study period (Table 1), suggesting a KL shift among the CRKP-ST11 population over the 4-year period.

ST11-KL64 Infections as Cause of Higher 30-Day Mortality

To evaluate the clinical importance of ST11-KL47 and ST11-KL64, we analyzed 162 ST11-infected patients with complete clinical data, 72 patients with ST11-KL47 and 90 with ST11-KL64 (Appendix 2 Table 2); 4 ST11-KL47-infected and 2 ST11-KL64-infected outpatients were excluded. ST11-KL47 patients had a significantly longer stay than did ST11-KL64 patients, with respect to both the total hospital stay (p = 0.001) and hospital stay before the BSI onset (p = 0.029). More ST11-KL47-infected patients acquired lung infections and received invasive procedures, devices, or both before and after BSI; they also had received hemodialysis and chemotherapy or radiotherapy within 30 days before BSI. However, the Charlson comorbidity score was identical for patients of both groups. Patients infected with ST11-KL64 showed significantly higher overall 30-day mortality than those with ST11-KL47 (62.2% vs. 52.8%; 2 = 4.252; p = 0.039) (Figure 1).

We further included 29 patients infected with non-ST11 CRKP in the analysis to evaluate whether CRKP-ST11 caused higher mortality than non-ST11 CRKP. We found no significant differences in 30-day mortality between patients infected with CRKP-ST11 and those with non-ST11 CRKP (57.1% vs. 44.8%; $\chi^2 = 0.833$; p = 0.176). Cox regression multivariate analysis revealed 3 factors independently associated with a higher risk for ST11-caused mortality: lower platelet at time of BSI, Acute Physiology and Chronic Health Evaluation

(APACHE II) score, and tigecycline as the empirical therapy (Table 2; Appendix 2 Table 3). We also found no significant difference in 30-day mortality between patients infected with ST11-KL47 and those with non-ST11 CRKP (52.8% vs. 44.8%; 2 = 0.395; p = 0.529). However, the ST11-KL64-infected patients showed significantly higher 30-day mortality than those with non-ST11 CRKP (62.2% vs. 44.8%; 2 = 3.771; p = 0.05).

Recombination-Mediated Evolutionary Diversification in CRKP-ST11

We performed phylogenomic analysis to understand the evolutionary diversification in the CRKP-ST11 population. We included 154 newly sequenced genomes (excluding the remaining 20 isolates without *rmpA* or *rmpA2*); 62 previously published ST11 genomes from diverse origins; and an ST1731 genome (accession no. ERR1541319) as an outgroup. We identified 429 recombined regions, including 348 that were >1 kb. The length of sequence removed per isolate ranged from 505,312 to 1,276,214 bp (median 947,836 bp). The phylogenetic tree, which was rooted using the ST1731 outgroup isolate that was later removed (Appendix 1 Figure 1), showed division of ST11 isolates into 2 major clades (Figure 2). One clade consists of isolates of KL47, KL64, and KL31 exclusively obtained from China, whereas the second clade consists of isolates possessing diverse K-types from elsewhere. These findings suggest that KL47 and KL64 have emerged and undergone local expansion in China.

Root-to-tip regression analysis of the 154 newly sequenced genomes demonstrated a correlation between the genetic distances and sampling dates ($R^2 = 0.64$) (Appendix 1 Figure 2). By using a Bayesian dating method implemented in BactDating (27), we found that KL64 isolates probably evolved from a KL47 ancestor around 2011 (Appendix 1 Figure 3). A high substitution rate also was found (15.3 single-nucleotide polymorphisms (SNPs)/genome/y, 95% CI 12.4–19.0 SNPs/genome/y).

The number of SNPs separating ST11-KL47 and ST11-KL64 isolates was 907–3,098 before and 30–220 after removal of recombination regions. This finding suggests that recombination largely contributed to the diversification of ST11-KL47 and ST11-KL64. Indeed,

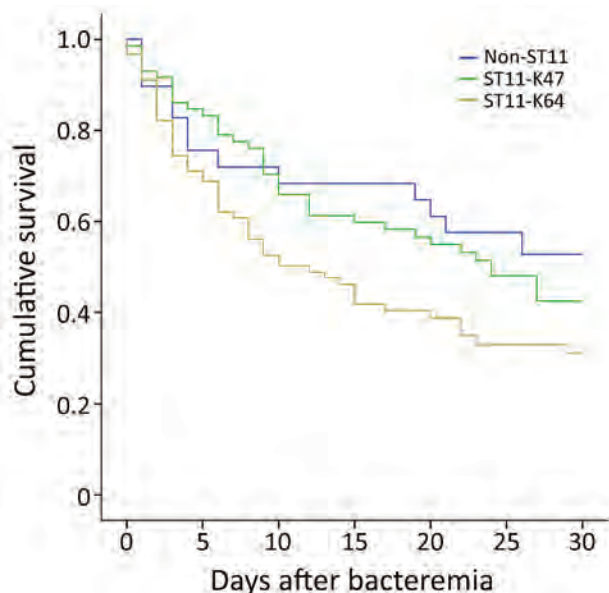


Figure 1. Kaplan–Meier survival estimates for patients with bloodstream infections caused by ST11-KL47, ST11-KL64, and non-ST11 CRKP, China, 2013–2017. A significant difference was found in the 30-day mortality among the 3 groups ($p = 0.039$). ST11-KL64–infected patients showed significantly higher overall 30-day mortality than ST11-KL47–infected patients (62.2% vs. 52.8%; $p = 0.039$) and non-ST11 CRKP–infected patients (62.2% vs. 44.8%; $p = 0.05$). No significant difference in 30-day mortality was found between patients infected with ST11-KL47 and non-ST11 CRKP (52.8% vs. 44.8%, $p = 0.529$). CRKP, carbapenem-resistant *Klebsiella pneumoniae*; KL, capsular loci; ST, sequence type.

we detected 4 recombination events of >1 kb on the branch coinciding with the switch from KL47 to KL64 (regions with respect to the reference genome [isolate KP47434]: 307,448–322,057; 4,060,806–4,154,013; 4,173,036–4,186,742; and 4,197,111–4,217,597) (Appendix 1 Figure 4; Appendix 2 Table 4). Three of these events were localized around the cps region, suggesting that the capsule switch was likely the result of recombination. Another recombination event in the cps region also corresponds with the capsule switch from KL47 to KL31 (Appendix 1 Figure 4).

Emergence of *rmpA-rmpA2*-Positive ST11-KL64 Isolates

Analysis of virulence genes showed that the 154 ST11 isolates possessed yersiniabactin genes (*ybtAE PQS-TUX*, *irp1*, *irp2*, and *fyuA*) located on ICEKp3, and the core type III fimbrial cluster *mrkABCDEF*, except for 4 ST11-KL64 isolates. Of 76 ST11-KL47 isolates, 29 (36.3%) carried an *rmpA2* gene, and only 2 were positive for the string test, suggesting that *rmpA2* was inactive in most isolates. *rmpA2*-positive ST11-KL47 isolates have been detected since 2013 and are interspersed

Table 2. Multivariable analysis of risk factors for 30-day mortality in 191 BSI patients infected with carbapenem-resistant *Klebsiella pneumoniae*, China, 2013–2017*

Variable	p value†	OR (95% CI)
Platelets at time of BSI	0.001	0.996 (0.994–0.998)
APACHE II score at time of BSI	0.012	1.041 (1.009–1.074)
Tigecycline as empirical therapy	0.003	1.920 (1.257–2.935)

*APACHE, Acute Physiology and Chronic Health Evaluation; BSI, bloodstream infection; OR, odds ratio.

†Calculated by using Cox regression.

among *rmpA2*-negative isolates in the phylogenetic tree (Figure 2). A frameshift *rmpA2* gene (*rmpA2**) was identified in 48 of 92 ST11-KL64 isolates (52.2%). *rmpA2**-positive ST11-KL64 isolates were first detected in 2015, and most of them are monophyletic (Figure 2). An *rmpA* gene was also found in 42 of the 48 *rmpA2**-positive ST11-KL64 isolates, of which 6 had in-frame truncations resulting in 2 variants (555 bp and 624 bp) and 12 were positive for the string test. The *rmpA-rmpA2**-positive ST11-KL64 isolates were detected from 2016 onward. The prevalence trend of *rmpA/rmpA2*-positive isolates is accordant with that of each subclone (Appendix 1 Figure 5).

All *rmpA/rmpA2**-positive isolates also carried aerobactin genes *iucABCD-iutA*, implying that they might co-locate on the same plasmid. A plasmid-borne virulence factor *peg-344* was exclusively found in 45 of 48 *rmpA2**-positive ST11-KL64 isolates. The salmonelisin cluster *iroBCDN* was also detected in 5 *rmpA-rmpA2**-positive and in 1 classic ST11-KL64 isolate (Figure 2).

Diversity of Virulence Plasmids

We further analyzed the vectors of *rmpA/rmpA2* genes to understand how they were captured. The *rmpA/rmpA2* gene of both subclones was detected on plasmids by using southern blot (Appendix 1 Figure 6). Higher diversity of the virulence plasmids was found in ST11-KL64 through classifying the plasmids by size; 5 types were detected in ST11-KL47 with sizes ranging from 110 to 217 kb, and 13 types were in ST11-KL64, ranging from 110 to 230 kb (Appendix 2 Table 5). The *rmpA* and *rmpA2** genes coexisted on the same plasmid in ST11-KL64.

Virulence plasmids detected in KP16932 (KL47) and KP47434 (KL64) were circularized to evaluate their structural variations. The *rmpA2* gene of KP16932 was carried by an IncFIB(K)-IncHI1B-type plasmid (pVir-KP16932) with a size of 177.8 kb, which is almost identical to a virulence plasmid pVir-CR-HvKP4 (MF437313) recently detected in a KL47 clone that caused a fatal outbreak in China (Appendix 1 Figure

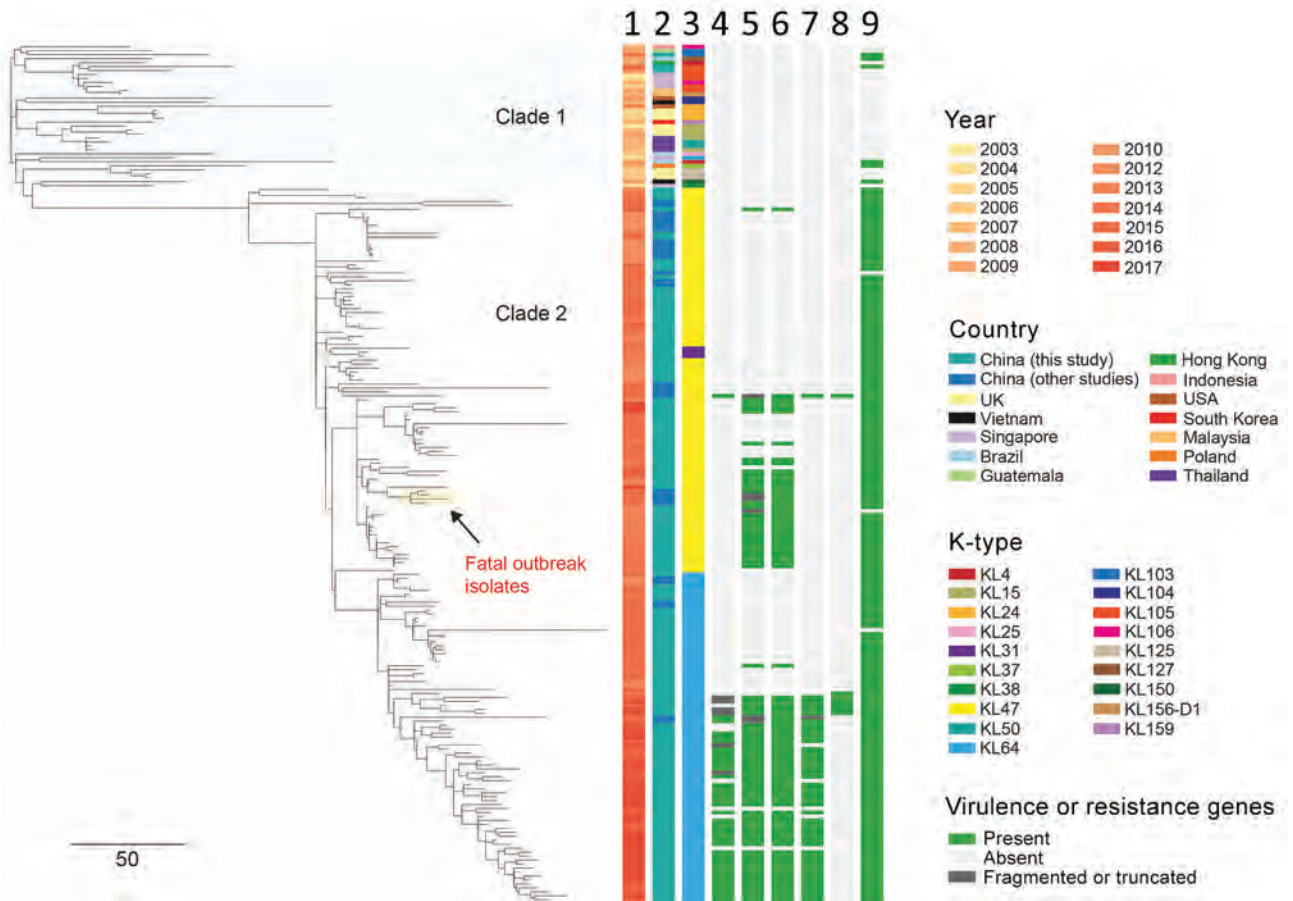


Figure 2. Phylogenetic analysis of 216 CRKP ST11 isolates, China, 2013–2017, including 154 CRKP isolates collected during 2012–2017 in study of bloodstream infections in a tertiary hospital and 62 isolates that were sequenced in previous studies (Appendix 2 Table 1, <https://wwwnc.cdc.gov/EID/article/26/2/19-0594-App2.xlsx>). The phylogenetic tree was obtained by mapping all sequence reads to the hybrid assembly of KP47434 and removing the recombinant regions from the alignment. The tree was rooted using ST1731 isolate EuSCAPE_ES29 (ERR1541319), which was included in this analysis but later removed from the tree (a tree including this outgroup is shown in Appendix 1 Figure 1, <https://wwwnc.cdc.gov/EID/article/26/2/19-0594-App1.pdf>). Five capsular types (KL31, KL47, KL64, KL103, and KL105) were detected in our ST11 collection, which are indicated in different colors as shown in the legend. Some of virulence genes detected are shown here. The *rmpA2* gene carried by KL64 isolates was frameshifted, namely *rmpA2**. Aerobactin and salmochelin represent the *iucABCD-iatA* and *iroBCDN* gene clusters, respectively. The fatal outbreak clone reported in China recently (12) is highlighted on the tree. Lanes: 1, year; 2, country; 3, K-type; 4, *rmpA*; 5, *rmpA2*; 6, aerobactin; 7, *peg-344*; 8, salmochelin; 9, *blaKPC*. Scale bar indicates single-nucleotide polymorphisms. CRKP, carbapenem-resistant *Klebsiella pneumoniae*; KL, capsular loci; ST, sequence type.

7). The *rmpA* and *rmpA2** genes of KP47434 existed in an IncFIB(K)-IncHI1B-type plasmid (pVir-KP47434) with a size of 201.8 kb, which shares a high homology with a virulence plasmid pVir-CR-HvKP267 (accession no. MG053312). Compared with pVir-KP47434, a 24-kb and an 18-kb region were absent in pVir-KP16932 (Appendix 1 Figure 7), which encodes genes involved in metabolic processes such as carbon utilization (*OppA-B-F* and *DppC*) (28) and virulence (*H-NS* protein) (29). The virulence plasmids carried by *rmpA2*-KL47 and *rmpA/rmpA2**-KL64 isolates possessed the highly similar backbone sequences with the pVir-KP16932 and pVir-KP47434 plasmids, respectively, and the

intra-subclonal variations were mainly caused by gain or loss of gene clusters involved in heavy metal resistance and mobile genetic elements (Appendix 1 Figure 8).

Virulence Plasmids and Infections

To evaluate whether the acquisition of virulence plasmids carrying *rmpA/rmpA2* and aerobactin genes has an effect on clinical outcomes, we stratified the cohort described according to the existence of virulence plasmids in ST11-KL47 and ST11-KL64. No significant differences in mortality were evident between patients infected by ST11-KL64-pVir-KP47434-like or classical ST11-KL64 isolates (i.e., without virulence plasmids)

(60.4% vs. 64.3%; $p = 0.983$) or those infected by ST11-KL47-pVir-KP16932 or classical ST11-KL47 isolates (51.7% vs. 53.5%; $p = 0.931$) (Appendix 2 Table 6, 7). However, the Charlson comorbidity scores for patients with ST11-KL47-pVir-KP16932-like infections (median 1 [range 0.5–2]) were significantly lower than scores for patients with ST11-KL47 infections (median 3 [range 1–4]; $p = 0.003$); similarly, scores for ST11-KL64-pVir-KP47434-like patients (median 1 [range 0–2]) were significantly lower than scores for ST11-KL64 patients (median 2 [range 1–3]; $p = 0.003$). These findings indicate that the virulence plasmids could promote infections in healthier patients.

Various Resistomes in ST11-KL47 and ST11-KL64

The resistome of ST11-KL47 was different from that of ST11-KL64 (Appendix 1 Figure 9). Genes *floR*, *arr-3*, *dfrA27*, and *aac(6)-Ib-cr* were exclusively detected in ST11-KL47, whereas *blaSHV-12* and *dfrA14* were unique for ST11-KL64, suggesting the 2 subclones might have been selected for in different niches. For each subclone, the resistomes of *rmpA/rmpA2*-positive isolates were much more consistent than those of classical isolates (Appendix 1 Figure 9). This finding is consistent with the phylogeny and the fact that the *rmpA/rmpA2*-positive isolates were relatively more clonal.

Enhanced Virulence in ST11-KL64

The *rmpA/rmpA2*-encoding virulence plasmids carried by each subclone shared an intrasubclonal similarity as described previously (i.e., the intrasubclonal variations were mainly caused by gain or loss of heavy metal resistance gene clusters and mobile genetic elements). ST11-KL64 isolates produced significantly more biofilm than ST11-KL47 isolates (optical density at 595 nm: 0.54 ± 0.09 vs. 3.08 ± 0.11 ; $p < 0.0001$) (Appendix 1 Figure 10, panel A). We evaluated the virulence potential by using a human neutrophil assay. The ST11-KL64 isolates had an average survival of 91.2% after incubation with the human neutrophils for 60 min, which was significantly higher than that of the ST11-KL47 strains (65.8%; $p = 0.0011$) (Appendix 1 Figure 10, panel B). Compared with the ST11-KL64 isolates, the ST23-K1 isolates showed lower survival (70.3%) and the ST86-K2 isolates comparable survival (91.8%). The ST35 isolate had the lowest survival, 37.2%.

We further estimated pathogenicity by infecting *G. mellonella* larvae with an inoculum of 1×10^6 CFU. At 48 h postinfection, the 4 ST11-KL64 isolates (1 classic [isolate KP33068], 1 *rmpA2**-positive [isolate KP33130], and 2 *rmpA-rmpA2**-positive [isolates KP33229 and KP33367]) showed comparable virulence resulting in

10% survival, whereas survival was 40%–60% for the 4 ST11-KL47 isolates (2 classic [isolates KP9343 and KP29407] and 2 *rmpA2*-positive [isolates KP10042 and KP16932]). K1 survival 40% and K2 30%; survival of a classic CRKP isolate (ST35) reached 70% (Appendix 1 Figure 10, panel C).

To determine the underlying mechanisms of enhanced transmissibility obtained by *rmpA-rmpA2**-positive ST11-KL64, we randomly selected 6 ST11-KL47 isolates (3 classic [KP8369, KP29407, and KP30412] and 3 *rmpA2*-positive [KP9343, KP10042, and KP16932]) and 6 ST11-KL64 isolates (2 classic [KP28367 and KP33068], 2 *rmpA2**-positive [KP33130 and KP45812], and 2 *rmpA-rmpA2**-positive [KP47434 and KP39615]) to evaluate the capacity of survival on a dry polystyrene surface. Only viable cells of 2 *rmpA-rmpA2**-KL64 isolates were recovered after overnight drying; the average recovered loads were 90 ± 31.09 CFU/mL and 115 ± 20.62 CFU/mL. This finding suggests that the enhanced transmissibility of the newly emerged subclone was associated with enhanced environmental survival.

National Prevalence of BSI-CRKP-ST11

To estimate the national prevalence of BSI-CRKP-ST11, we further retrospectively screened 1,098 clinical BSI-KP strains collected from 13 provinces in China during 2014–2016 (Table 3). In total, 46 of 83 CRKP strains were ST11; ST11-KL47 accounted for 80.4% and ST11-KL64 19.6%. The *rmpA2* gene was detected in 11 ST11-KL47 and 1 ST11-KL64 isolates, and 1 isolate of each subclone also co-harbored an *rmpA* gene. The *rmpA2*-positive isolates were detected from Anhui and Zhejiang provinces. Most (9/12) *rmpA2*-positive CRKP isolates appeared after 2015.

Discussion

The global dissemination of CRKP poses a serious threat to public health. Control of CRKP in populations and healthcare networks thus becomes an urgent issue. However, efforts are often complicated by rapid evolution, especially among epidemic clones (e.g., ST11 and ST258). Therefore, tracking of evolutionary events and understanding their clinical importance are critical. We performed a comprehensive study to provide insight into the evolution of key virulence features of BSI-CRKP collected in China. We found 2 major Ks (KL47 and KL64) in the dominant clone BSI-CRKP-ST11. Capsule is known as an important immune-evasion molecule, and thus has become a popular target for vaccine design. Determining the prevalence of Ks is crucial for the development of capsule-based vaccines and phage-derived exopolysaccharide-depolymerase treatments, which are

Table 3. Prevalence of CRKP-ST11 causing BSIs, China, 2014–2016*

Year	KP	CRKP	CRKP-ST11	CRKP-ST11-KL47, <i>rmpA/rmpA2</i> -positive	CRKP-ST11-KL64, <i>rmpA/rmpA2</i> -positive
2014	224	10	7	5 (1)	2 (0)
2015	345	31	19	16 (2)	3 (0)
2016	529	42	20	16 (8)	4 (1)
Total	1,098	83	46	37 (11)	9 (1)

*Isolates were collected as part of national surveillance for BSIs. BSI, bloodstream infection; CRKP, carbapenem-resistant *Klebsiella pneumoniae*; KL, capsular loci; KP, *Klebsiella pneumoniae*; ST, sequence type.

considered as novel approaches for the treatment of CRKP infections (30). Our study provides useful data for assisting the development of an immunotherapy for ST11-CRKP infections in China.

In this study, ST11 was partitioned into 2 clades, 1 consisting of ST11-KL47, ST11-KL64, and ST11-KL31, suggesting that these strains were diversified from a common ancestor. We found that sequences within the *cps* region of ST11-KL64 and ST11-KL31 were imported through recombination indicating the occurrence of capsule switching. By using a Bayesian approach, we found that ST11-KL64 might have emerged from an ST11-KL47-like ancestor in 2011. We further noted that the 2 ST11 subclones (ST11-KL47 and ST11-KL64) have spread nationally by interregional transmission. However, the lack of genome data about ST11-KL47 and ST11-KL64 from different origins hampers our understanding of spatial evolution at a global scale.

The notion of a rapid evolution of the ST11 population is supported by numerous *cps* variants ($n = 19$) and the very high evolutionary rate (15.3 SNPs/genome/year) detected in this study and others (9). Capsule switching has been suggested to be a common event across the wider *K. pneumoniae* population through large recombination events (9–11). We suppose that generating numerous descendants with various combinations of evolved chromosomes and capsules heavily contributes to the success of ST11 and its descendants (e.g., ST258). Of note, our study identified a clonal replacement in the CRKP-ST11 population over a 4-year period in a hospital. ST11-KL47, the dominant subclone before 2015, was progressively replaced by ST11-KL64. The population structure of ST11-K64 was monophyletic, implying that ST11-KL64 might have gained fitness and was ready to disseminate clonally like ST258. Also, KL64 is a more commonly observed capsule type than KL47, and has been detected in Brazil (25), Taiwan (31), Singapore (32), the United States, and Europe (33).

To understand the clinical importance of the clonal replacement that coincided with the capsular switch in the ST11 population, we analyzed the metadata of 162 infected patients. Patients infected

by ST11-KL64 had significantly higher mortality rates than those infected by ST11-KL47 and non-ST11 CRKP. This finding is supported by the results of our phenotypic assays, which showed that ST11-KL64 was more virulent than ST11-KL47. Our findings suggest that the acquisition of virulence plasmids promotes the infection in healthier patients but is not associated with the increased mortality, indicating that other virulence factors might be involved. Capsular switching in the ST11 population might contribute to increased mortality. The capsule type is thought to be an important determinant for the pathogenicity of *K. pneumoniae*, like the notorious capsular serotypes K1 and K2. Similar associations are also identified in other species, such as *Acinetobacter baumannii* (34) and *Streptococcus* spp. (35,36). We also cannot exclude that the enhanced virulence and increased mortality might be associated with other chromosomal and plasmid variations.

We further noted that the newly emerged *rmpA2**-positive ST11-KL64 isolates exclusively carried an *rmpA* gene. The presence of a truncated variant might confer an advantage through a more subtle activation of capsule expression in comparison to a strain with 2 fully functional variants present (37). In addition, the combination of *RmpA* and truncated *RmpA2* was previously found predominantly in clinical isolates with a hypervirulent or hypermucoviscous phenotype (38). This finding is consistent with our study, given that *rmpA-rmpA2**-ST11-KL64 isolates become the dominant clone after they emerged. We suppose that such combination might confer fitness to the population resulting in the replacement of *rmpA2*-ST11-KL47 by *rmpA-rmpA2**-ST11-KL64. This supposition can be supported by the fact that *rmpA-rmpA2**-ST11-KL64 isolates survive longer than ST11-KL47 in vitro, which largely facilitates a better dissemination of the population under nosocomial conditions. Besides the isolates found in Anhui and Zhejiang provinces in our study, 2 *rmpA-rmpA2**-ST11-KL64 isolates have been detected in Shanghai and Henan provinces (9), suggesting that the newly emerged subclone has widely disseminated in China.

In summary, our study identified the emergence of a high-risk subclone of CRKP-ST11, resulting in

enhanced virulence and transmissibility. The newly emerging descendant obtained enhanced environmental survival and poses a substantial threat to healthcare networks, suggesting the urgent need for tailor-made surveillance and stricter infection-control measures to prevent further dissemination in nosocomial settings.

Acknowledgments

We thank Jinru Ji and Chaoqun Ying for their assistance during sample collection and data analysis.

This work was supported by the National Key Research and Development Program of China (grant no. 2017YFC1200200), Major Infectious Diseases such as AIDS and Viral Hepatitis Prevention and Control Technology Major Projects (grant no. 2018ZX10712-001), and the National Natural Science Foundation of China (81702045, 81361138021).

We deposited the 2 scaffolded genome sequences in GenBank under the accession nos. QVAN000000000 (KP16932) and QURI000000000 (KP47434); accession numbers of the other genome sequences are listed in Appendix 2 Table 1. The datasets supporting the conclusions of this article are included in the article and in Appendix 2.

About the Author

Dr. Kai Zhou is an associate professor at the First Affiliated Hospital of Southern University of Science and Technology, Shenzhen, China. His research interests are epidemiology and drug-resistance mechanisms of carbapenem-resistant *Enterobacteriaceae*.

References

- Guh AY, Bulens SN, Mu Y, Jacob JT, Reno J, Scott J, et al. Epidemiology of carbapenem-resistant *Enterobacteriaceae* in 7 US communities, 2012–2013. *JAMA*. 2015;314:1479–87. <https://doi.org/10.1001/jama.2015.12480>
- Grundmann H, Glasner C, Albigier B, Aanensen DM, Tomlinson CT, Andrasević AT, et al.; European Survey of Carbapenemase-Producing Enterobacteriaceae (EuSCAPE) Working Group. Occurrence of carbapenemase-producing *Klebsiella pneumoniae* and *Escherichia coli* in the European survey of carbapenemase-producing *Enterobacteriaceae* (EuSCAPE): a prospective, multinational study. *Lancet Infect Dis*. 2017;17:153–63. [https://doi.org/10.1016/S1473-3099\(16\)30257-2](https://doi.org/10.1016/S1473-3099(16)30257-2)
- Zhang R, Liu L, Zhou H, Chan EW, Li J, Fang Y, et al. Nationwide surveillance of clinical carbapenem-resistant *Enterobacteriaceae* (CRE) strains in China. *EBioMedicine*. 2017;19:98–106. <https://doi.org/10.1016/j.ebiom.2017.04.032>
- Patel G, Huprikar S, Factor SH, Jenkins SG, Calfee DP. Outcomes of carbapenem-resistant *Klebsiella pneumoniae* infection and the impact of antimicrobial and adjunctive therapies. *Infect Control Hosp Epidemiol*. 2008;29:1099–106. <https://doi.org/10.1086/592412>
- Pitout JDD, Nordmann P, Poirel L. Carbapenemase-producing *Klebsiella pneumoniae*, a key pathogen set for global nosocomial dominance. *Antimicrob Agents Chemother*. 2015;59:5873–84. <https://doi.org/10.1128/AAC.01019-15>
- Chen L, Mathema B, Pitout JDD, DeLeo FR, Kreiswirth BN. Epidemic *Klebsiella pneumoniae* ST258 is a hybrid strain. *MBio*. 2014;5:e01355–14.
- Gaiarsa S, Comandatore F, Gaibani P, Corbella M, Dalla Valle C, Epis S, et al. Genomic epidemiology of *Klebsiella pneumoniae* in Italy and novel insights into the origin and global evolution of its resistance to carbapenem antibiotics. *Antimicrob Agents Chemother*. 2015;59:389–96.
- DeLeo FR, Chen L, Porcella SF, Martens CA, Kobayashi SD, Porter AR, et al. Molecular dissection of the evolution of carbapenem-resistant multilocus sequence type 258 *Klebsiella pneumoniae*. *Proc Natl Acad Sci U S A*. 2014;111:4988–93. <https://doi.org/10.1073/pnas.1321364111>
- Wyres KL, Gorrie C, Edwards DJ, Wertheim HFL, Hsu LY, Van Kinh N, et al. Extensive capsule locus variation and large-scale genomic recombination within the *Klebsiella pneumoniae* clonal group 258. *Genome Biol Evol*. 2015;7:1267–79. <https://doi.org/10.1093/gbe/evv062>
- Jiang Y, Wei Z, Wang Y, Hua X, Feng Y, Yu Y. Tracking a hospital outbreak of KPC-producing ST11 *Klebsiella pneumoniae* with whole genome sequencing. *Clin Microbiol Infect*. 2015;21:1001–7. <https://doi.org/10.1016/j.cmi.2015.07.001>
- Dong N, Zhang R, Liu L, Li R, Lin D, Chan EW-C, et al. Genome analysis of clinical multilocus sequence type 11 *Klebsiella pneumoniae* from China. *Microb Genom*. 2018;4:54–12. <https://doi.org/10.1099/mgen.0.000149>
- Gu D, Dong N, Zheng Z, Lin D, Huang M, Wang L, et al. A fatal outbreak of ST11 carbapenem-resistant hypervirulent *Klebsiella pneumoniae* in a Chinese hospital: a molecular epidemiological study. *Lancet Infect Dis*. 2018;18:37–46. [https://doi.org/10.1016/S1473-3099\(17\)30489-9](https://doi.org/10.1016/S1473-3099(17)30489-9)
- Du P, Zhang Y, Chen C. Emergence of carbapenem-resistant hypervirulent *Klebsiella pneumoniae*. *Lancet Infect Dis*. 2018;18:23–4. [https://doi.org/10.1016/S1473-3099\(17\)30625-4](https://doi.org/10.1016/S1473-3099(17)30625-4)
- Yao H, Qin S, Chen S, Shen J, Du X-D. Emergence of carbapenem-resistant hypervirulent *Klebsiella pneumoniae*. *Lancet Infect Dis*. 2018;18:25. [https://doi.org/10.1016/S1473-3099\(17\)30628-X](https://doi.org/10.1016/S1473-3099(17)30628-X)
- Wong MHY, Shum H-P, Chen JHK, Man M-Y, Wu A, Chan EW-C, et al. Emergence of carbapenem-resistant hypervirulent *Klebsiella pneumoniae*. *Lancet Infect Dis*. 2018;18:24. [https://doi.org/10.1016/S1473-3099\(17\)30629-1](https://doi.org/10.1016/S1473-3099(17)30629-1)
- Xiao T, Yu W, Niu T, Huang C, Xiao Y. A retrospective, comparative analysis of risk factors and outcomes in carbapenem-susceptible and carbapenem-nonsusceptible *Klebsiella pneumoniae* bloodstream infections: tigecycline significantly increases the mortality. *Infect Drug Resist*. 2018;11:595–606. <https://doi.org/10.2147/IDR.S153246>
- Diancourt L, Passet V, Verhoef J, Grimont PAD, Brisse S. Multilocus sequence typing of *Klebsiella pneumoniae* nosocomial isolates. *J Clin Microbiol*. 2005;43:4178–82. <https://doi.org/10.1128/JCM.43.8.4178-4182.2005>
- McLaughlin MM, Advincula MR, Malczynski M, Barajas G, Qi C, Scheetz MH. Quantifying the clinical virulence of *Klebsiella pneumoniae* producing carbapenemase *Klebsiella pneumoniae* with a *Galleria mellonella* model and a pilot study to translate to patient outcomes. *BMC Infect Dis*. 2014;14:31. <https://doi.org/10.1186/1471-2334-14-31>
- Naparstek L, Carmeli Y, Navon-Venezia S, Banin E. Biofilm formation and susceptibility to gentamicin and colistin of extremely drug-resistant KPC-producing *Klebsiella*

- pneumoniae*. J Antimicrob Chemother. 2014;69:1027–34. <https://doi.org/10.1093/jac/dkt487>
20. Wang L, Shen D, Wu H, Ma Y. Resistance of hypervirulent *Klebsiella pneumoniae* to both intracellular and extracellular killing of neutrophils. PLoS One. 2017;12:e0173638. <https://doi.org/10.1371/journal.pone.0173638>
 21. Havill NL, Boyce JM, Otter JA. Extended survival of carbapenem-resistant *Enterobacteriaceae* on dry surfaces. Infect Control Hosp Epidemiol. 2014;35:445–7. <https://doi.org/10.1086/675606>
 22. Wick RR, Judd LM, Gorrie CL, Holt KE. Unicycler: Resolving bacterial genome assemblies from short and long sequencing reads. PLoS Comput Biol. 2017;13:e1005595. <https://doi.org/10.1371/journal.pcbi.1005595>
 23. Henson SP, Boinett CJ, Ellington MJ, Kagia N, Mwarumba S, Nyongesa S, et al. Molecular epidemiology of *Klebsiella pneumoniae* invasive infections over a decade at Kilifi County Hospital in Kenya. Int J Med Microbiol. 2017;307:422–9. <https://doi.org/10.1016/j.ijmm.2017.07.006>
 24. Holt KE, Wertheim H, Zadoks RN, Baker S, Whitehouse CA, Dance D, et al. Genomic analysis of diversity, population structure, virulence, and antimicrobial resistance in *Klebsiella pneumoniae*, an urgent threat to public health. Proc Natl Acad Sci U S A. 2015;112:E3574–81. <https://doi.org/10.1073/pnas.1501049112>
 25. Bowers JR, Kitchel B, Driebe EM, MacCannell DR, Roe C, Lemmer D, et al. Genomic analysis of the emergence and rapid global dissemination of the clonal group 258 *Klebsiella pneumoniae* pandemic. PLoS One. 2015;10:e0133727. <https://doi.org/10.1371/journal.pone.0133727>
 26. Moradigaravand D, Martin V, Peacock SJ, Parkhill J. Evolution and epidemiology of multidrug-resistant *Klebsiella pneumoniae* in the United Kingdom and Ireland. MBiol 2017;8:e01976–16.
 27. Didelot X, Croucher NJ, Bentley SD, Harris SR, Wilson DJ. Bayesian inference of ancestral dates on bacterial phylogenetic trees. Nucleic Acids Res. 2018;46:e134–4. <https://doi.org/10.1093/nar/gky783>
 28. Lee E-M, Ahn S-H, Park J-H, Lee J-H, Ahn S-C, Kong I-S. Identification of oligopeptide permease (*opp*) gene cluster in *Vibrio fluvialis* and characterization of biofilm production by *oppA* knockout mutation. FEMS Microbiol Lett. 2004;240:21–30. <https://doi.org/10.1016/j.femsle.2004.09.007>
 29. Ares MA, Fernández-Vázquez JL, Rosales-Reyes R, Jarillo-Quijada MD, von Bargen K, Torres J, et al. H-NS nucleoid protein controls virulence features of *Klebsiella pneumoniae* by regulating the expression of type 3 pili and the capsule polysaccharide. Front Cell Infect Microbiol. 2016;6:13. <https://doi.org/10.3389/fcimb.2016.00013>
 30. Kobayashi SD, Porter AR, Freedman B, Pandey R, Chen L, Kreiswirth BN, et al. Antibody-mediated killing of carbapenem-resistant ST258 *Klebsiella pneumoniae* by human neutrophils. MBio. 2018;9:1198. <https://doi.org/10.1128/mBio.00297-18>
 31. Pan Y-J, Lin T-L, Lin Y-T, Su P-A, Chen C-T, Hsieh P-F, et al. Identification of capsular types in carbapenem-resistant *Klebsiella pneumoniae* strains by wzc sequencing and implications for capsule depolymerase treatment. Antimicrob Agents Chemother. 2015;59:1038–47. <https://doi.org/10.1128/AAC.03560-14>
 32. Koh TH, Cao D, Shan QY, Bacon A, Hsu LY, Ooi EE. Acquired carbapenemases in *Enterobacteriaceae* in Singapore, 1996–2012. Pathology. 2013;45:600–3. <https://doi.org/10.1097/PAT.0b013e3283650b1e>
 33. Cryz SJ Jr, Mortimer PM, Mansfield V, Germanier R. Seroepidemiology of *Klebsiella* bacteremic isolates and implications for vaccine development. J Clin Microbiol. 1986; 23:687–90.
 34. Jones CL, Clancy M, Honnold C, Singh S, Snedrud E, Onmus-Leone F, et al. Fatal outbreak of an emerging clone of extensively drug-resistant *Acinetobacter baumannii* with enhanced virulence. Clin Infect Dis. 2015;61:145–54. <https://doi.org/10.1093/cid/civ225>
 35. Melin M, Trzcirski K, Meri S, Käyhty H, Väkeväinen M. The capsular serotype of *Streptococcus pneumoniae* is more important than the genetic background for resistance to complement. Infect Immun. 2010;78:5262–70. <https://doi.org/10.1128/IAI.00740-10>
 36. Rukke HV, Kalluru RS, Repnik U, Gerlini A, José RJ, Periselneris J, et al. Protective role of the capsule and impact of serotype 4 switching on *Streptococcus mitis*. Infect Immun. 2014;82:3790–801. <https://doi.org/10.1128/IAI.01840-14>
 37. Struve C, Roe CC, Stegger M, Stahlhut SG, Hansen DS, Engelthaler DM, et al. Mapping the evolution of hypervirulent *Klebsiella pneumoniae*. MBio. 2015;6:e00630. <https://doi.org/10.1128/mBio.00630-15>
 38. Hsu C-R, Lin T-L, Chen Y-C, Chou H-C, Wang J-T. The role of *Klebsiella pneumoniae rmpA* in capsular polysaccharide synthesis and virulence revisited. Microbiology. 2011;157:3446–57. <https://doi.org/10.1099/mic.0.050336-0>

Address for correspondence: Yonghong Xiao, First Affiliated Hospital of Zhejiang University, Qingchun Rd 79, Hangzhou, Zhejiang 330003, China; email: xiaoyonghong@zju.edu.cn

Neutralizing Antibodies against Enteroviruses in Patients with Hand, Foot and Mouth Disease

Lam Anh Nguyet, Tran Tan Thanh, Le Nguyen Thanh Nhan, Nguyen Thi Thu Hong, Le Nguyen Truc Nhu, Hoang Minh Tu Van, Nguyen Thi Han Ny, Nguyen To Anh, Do Duong Kim Han, Ha Manh Tuan, Vu Quang Huy, Ho Lu Viet, Hoang Quoc Cuong, Nguyen Thi Thanh Thao, Do Chau Viet, Truong Huu Khanh, Louise Thwaites, Hannah Clapham, Nguyen Thanh Hung, Nguyen Van Vinh Chau, Guy Thwaites, Do Quang Ha, H. Rogier van Doorn, Le Van Tan

Hand, foot and mouth disease (HFMD) is an emerging infection with pandemic potential. Knowledge of neutralizing antibody responses among its pathogens is essential to inform vaccine development and epidemiologic research. We used 120 paired-plasma samples collected at enrollment and >7 days after the onset of illness from HFMD patients infected with enterovirus A71 (EV-A71), coxsackievirus A (CVA) 6, CVA10, and CVA16 to study cross-neutralization. For homotypic viruses, seropositivity increased from <60% at enrollment to 97%–100% at follow-up, corresponding to seroconversion rates of 57%–93%. Seroconversion for heterotypic viruses was recorded in only 3%–23% of patients. All plasma samples from patients infected with EV-A71 subgenogroup B5 could neutralize the emerging EV-A71 subgenogroup C4. Collectively, our results support previous reports about the potential benefit of EV-A71 vaccine but highlight the necessity of multivalent vaccines to control HFMD.

Since 1997, hand, foot and mouth disease (HFMD) has emerged as a serious childhood infection in the Asia-Pacific region (1,2) with the potential of spreading to other parts of the world. Indeed, HFMD epidemics, especially those caused by enterovirus A71

(EV-A71), have increasingly been reported worldwide, including in the United States and Europe (3–5). Although HFMD is a mild infection in most cases, severe clinical complications (e.g., central nervous system involvement as brainstem encephalitis) may happen and can be fatal (1,6). However, no antiviral drugs are available to the affected patients, including those with severe clinical phenotypes.

HFMD is caused by various serotypes of enterovirus A of the family Picornaviridae. Of these, EV-A71, coxsackievirus A (CVA) 6, CVA10, and CVA16 are the most common pathogens isolated from patients with clinically suspected HFMD, with CVA6 being increasingly reported (7–9). In Vietnam, our recent report showed that of 1,547 patients with HFMD enrolled in a clinical study, EV-A71 was detected in 24.4%, followed by CVA6 (21.8%), CVA16 (10.8%), and CVA10 (7.9%). Other enteroviruses detected sporadically included CVA4 (1.7%), CVA12 (1.4%), and CVA2 (0.6%) (10). Infection with EV-A71 has received more attention because it frequently causes severe HFMD, especially in recent outbreaks recorded in the Asia-Pacific region since 1997 (6,11). Consequently, inactivated monovalent vaccines for EV-A71 have been successfully developed and licensed in China (12–14). The use of those vaccines, however, has been voluntary and restricted within mainland China.

Because the viruses causing HFMD are diverse, ongoing efforts exist to develop multivalent vaccines, especially those including antigens of the aforementioned common serotypes (15). Results from these preclinical studies using animal models showed a lack of cross-reactivity among EV-A71, CVA6, CVA10, and CVA16 (16,17). There is, however, scarce information about to what extent human infection with 1 HFMD-causing enterovirus serotype can elicit (cross-)neutralizing antibodies

Author affiliations: Oxford University Clinical Research Unit, Ho Chi Minh City, Vietnam (L.A. Nguyet, T.T. Thanh, N.T.T. Hong, L.N.T. Nhu, H.M.T. Van, N.T.H. Ny, N.T. Anh, D.D.K. Han, L. Thwaites, H. Clapham, G. Thwaites, D.Q. Ha, H.R. van Doorn, L.V. Tan); Children's Hospital 1, Ho Chi Minh City (L.N.T. Nhan, T.H. Khanh, N.T. Hung); Children's Hospital 2, Ho Chi Minh City (H.M. Tuan, H.L. Viet, D.C. Viet); University of Medicine and Pharmacy, Ho Chi Minh City (H.M. Tuan, V.Q. Huy); Pasteur Institute, Ho Chi Minh City (H.Q. Cuong, N.T.T. Thao); University of Oxford, Oxford, UK (L. Thwaites, H. Clapham, G. Thwaites, H.R. van Doorn); Hospital for Tropical Diseases, Ho Chi Minh City (N.V.V. Chau)

DOI: <https://doi.org/10.3201/eid2602.190721>

against homotypic and heterotypic enterovirus serotypes. Such data are of paramount importance to support the development of intervention strategies (including vaccines) and the design of epidemiologic research on surveillance and transmission dynamics of HFMD and will contribute to the expanded knowledge about host–pathogen and pathogen–pathogen interaction of this emerging clinical problem. We aim to fill the existing gaps in knowledge about seropositivity and (cross-)neutralization elicited as a consequence of human infection by EV-A71, CVA6, CVA10, and CVA16, the 4 most common serotypes responsible for the ongoing epidemic of HFMD worldwide, especially in Asia.

Materials and Methods

Settings

The clinical and patient data used in this study were derived from an ongoing clinical study of HFMD that has been conducted at Children’s Hospital (CH) 1, CH2, and the Hospital for Tropical Diseases (HTD) in Ho Chi Minh City, Vietnam, since 2013 (6,8). These hospitals are tertiary referral centers for children with HFMD in Ho Chi Minh City and southern Vietnam, covering a catchment population of >40 million.

Patient Enrollment and Data Collection

We screened all patients <12 years of age who came to outpatient departments or were admitted to inpatient wards of CH1, CH2, or HTD with a clinical diagnosis of HFMD and, if outpatients, an illness of <3 days for enrollment in our study. We excluded any patient for whom the attending physician believed another diagnosis was more likely.

We collected information regarding demographics, clinical signs/symptoms, clinical grades, treatments, laboratory tests, length of hospital stay, and outcomes. In addition, for enterovirus serotype determination, we sampled acute throat and rectal swabs at enrollment and collected a plasma sample from each participant at enrollment and 7–14 days after enrollment.

HFMD Clinical Grade Classification

According to the Vietnamese Ministry of Health, HFMD is clinically divided into 4 major grades. Grade 1 is assigned to patients with mouth ulcers or vesicles/papules on hands, feet, or buttocks, with or without mild fever (<39°C). Grade 2 is further divided into grade 2A (central nervous system [CNS] involvement, myoclonus reported by parents or caregivers only, fever >39°C or ataxia), grade 2B1

(myoclonus observed by medical staff or history of myoclonus and lethargy or pulse >130 bpm), and grade 2B2 (ataxia, cranial nerve palsies, limb weakness, nystagmus, persistent high fever, or pulse >150 bpm). Grade 3 involves autonomic dysfunction with sweating, hypertension, tachycardia, and tachypnea. Grade 4 is for disease with additional cardiopulmonary compromise with pulmonary edema or shock syndrome (18). Patients with grade 2B1 or above are considered to have severe HFMD, and often require intravenous immunoglobulin administration.

Determination of Enterovirus Serotype and EV-A71 Subgenogroup

We determined enterovirus serotype using a combination of PCR and sequencing approaches (19–21). In brief, we first extracted viral RNA from throat/rectal swab specimens. We then used a 1-step multiplex real-time reverse transcription PCR assay to simultaneously detect all enterovirus serotypes and EV-A71 (19). We then tested all specimens positive for enterovirus serotype or EV-A71 to further identify specific enterovirus serotypes or EV-A71 subgenogroups, using a combination of viral protein (VP) 1 PCR and sequencing of the obtained PCR amplicon (18,20,21). Finally, we analyzed the obtained VP1 sequences using a previously described online tool to determine enterovirus serotype or EV-A71 subgenogroup (22).

Selection of Patients and Plasma Sample for Microneutralization Assay

From this study, we selected a convenience sample of 120 patients (30 per serotype CVA6, CVA10, CVA16, and EV-A71) who had plasma samples collected at enrollment and follow-up and were available for immunological response analysis. In addition, for assessment of antigenic difference between subgenogroup B5 (circulating in Vietnam during 2013–2015) and C4 (circulating in Vietnam in 2018), we included 1 available follow-up plasma sample collected from a fatal case, in which the patient was infected with subgenogroup C4 during the 2018 outbreak (6).

Viral Strains

We isolated representative samples of CVA10, CVA16, and EV-A71 (including EV-A71 subgenogroup B5 in 2013 and C4 in 2018) used for microneutralization assay from patients with HFMD who were enrolled in the clinical study (7,8,10). We obtained a CVA6 isolate from the virus archive of Pasteur Institute in Ho Chi Minh City. For EV-A71, unless specified, all neutralization experiments were carried out using EV-A71 subgenogroup B5.

Microneutralization Assay

We performed the microneutralization as previously described (23). In brief, we first inactivated plasma samples at 56°C for 30 min, and we then diluted the samples in serial ratios from 1:8 to 1:512 in maintenance medium (Sigma-Aldrich, <https://www.sigmaaldrich.com>). Accordingly, the lower limit of detection of the assay was 1:8 and the upper limit was 1:512. Next, we incubated plasma dilutions with an equal volume of 100 times the median culture of infectious dose (TCID₅₀) of the virus at 37°C for 1 hour, and then transferred them into a 96-well plate pre-coated with human rhabdomyosarcoma (RD) cells (American Type Culture Collection, <https://www.atcc.org>). The plate was then incubated in a 5% carbon dioxide incubator at 37°C. Cells were observed daily for cytopathic effects. The antibody titer of the sample was determined by the highest plasma dilution that prevented cytopathic effects in 50% of the wells. We tested each dilution in quadruplicate and included negative and positive controls in each experiment. We defined seropositivity as neutralizing antibody titer >1:8. We defined seroconversion as a change from seronegativity to seropositivity, or at least a 4-fold rise in the neutralizing antibody titer between enrollment and follow-up time points.

Statistical Analysis

We performed statistical analyses of clinical data using IBM SPSS Statistics 23 (IBM Corp., <https://www.ibm.com>). We compared categorical variables using a χ^2 test or Fisher exact test and compared continuous variables using the Mann-Whitney U-test, 1-way analysis of variance (ANOVA) test, or Kruskal-Wallis test. We tested the difference in neutralizing antibody titers between samples obtained at enrollment and follow-up using the Wilcoxon matched-pairs signed rank test, available in Prism 5.04 (GraphPad Software, <https://www.graphpad.com>).

The institutional review boards of CH1, CH2, and HTD, as well as the Oxford Tropical Research Ethics Committee (OxTREC), approved the study. We obtained written informed consent from a parent or guardian of each enrolled patient.

Results

Baseline Characteristics of Patients

We compiled the baseline characteristics and clinical outcome of 120 patients included for analysis of neutralizing antibody responses to all 4 enterovirus serotypes (EV-A71, CVA6, CVA10, and CVA16) (Table 1). All patients were enrolled in the clinical study during

July 2013–March 2017. Male patients were predominant (female/male ratio 45/75). Thirteen (10.8%) patients had severe HFMD (grade 2B1 or above); 119 patients (99.2%) made a complete recovery. Following the onset of illness, 50% of the patients were admitted to hospital within 1 day (range 0–5 days) and were enrolled in the clinical study within 2 days (range 0–6 days). All second/follow-up plasma samples included for analysis were collected at day >7 (median 9 days, range 7–17) after the illness onset.

Of the 30 patients infected with EV-A71, detailed information about subgenogroup was successfully generated for 13 patients, who were all positive for subgenogroup B5. Of the patients with EV-A71 infections, 20% had severe clinical phenotypes (grade 2B1 or above), whereas severe outcome was recorded in 3.3% of patients infected with CVA6, 6.7% of patients infected with CVA10, and 13.3% of patients infected with CVA16 (Table 1). Mouth lesion distributions and C-reactive protein levels were statistically different among serotypes. Otherwise, there were considerable similarities between groups of patients who were infected with EV-A71, CVA6, CVA10, or CVA16 in terms of clinical characteristics and outcome, as well as blood biochemistry parameters (Table 1), in agreement with a previous report (8).

Seropositivity and Seroconversion

We compiled the results of seropositivity testing at enrollment (baseline) and follow-up (Table 2). Although 60% (18/30) of patients infected with EV-A71 had specific antibodies to EV-A71 at the measured level (>1:16) or above in their blood samples, most of the patients (>70%) infected with CVA6, CVA10, or CVA16 had no specific antibodies to the infecting viruses at enrollment. The proportion of patients with antibodies against heterotypic viruses ranged from 7% (2/30) of CVA6 patients having neutralizing antibodies against EV-A71 to 57% (17/30) of EV-A71 patients having antibodies against CVA10.

At follow-up (>7 days after the onset of illness), seropositivity for homotypic viruses reached 97%–100% in all patient groups; comparisons for seropositivity rates at enrollment and follow-up were all significant ($p < 0.001$) (Table 2), corresponding to seroconversion rates of 57% (17/30) for EV-A71, 77% (23/30) for CVA16, 83% (25/30) for CVA10, and 93% (28/30) for CVA6 (Table 2). We found no difference in antibody responses (seropositivity and seroconversion) between the groups of patients who were positive for EV-A71 subgenogroup B5 and those from whom EV-A71 subgenogroup was not available (data not shown).

Table 1. Baseline characteristics and clinical outcome of the patients included in study of patients with hand, foot and mouth disease, Vietnam*

Characteristics	All, N = 120	EV-A71, N = 30	CVA6, N = 30	CVA10, N = 30	CVA16, N = 30	p value†
Demographics						
Sex ratio, F/M	45/75	8/22	8/22	14/16	15/15	0.12
Median age, mo (range)	16.2 (1.8–59)	16.7 (4.9–58.6)	16.4 (5.3–59)	14.7 (1.8–41.4)	19 (5.8–46.5)	0.11
Median day of illness from onset (range)						
To hospital admission	1 (0–5)	2 (0–4)	1 (0–3)	1 (0–3)	1 (0–5)	0.058
To enrollment in study	2 (0–6)	2 (0–4)	1.5 (0–3)	2 (0–6)	2 (0–6)	0.802
To collection of second plasma	9 (7–17)	9 (7–12)	9 (7–14)	9 (7–14)	9 (8–17)	0.211
Median day of hospitalization‡	3 (1–12)	4 (2–10)	3 (1–8)	3 (1–6)	4 (2–12)	0.3
Inpatient/outpatient ratio	77/43	17/13	18/12	25/5	17/13	0.08
Clinical characteristics, no. (%)						
Fever	87 (72.5)	24 (80)	17 (56.7)	24 (80)	17 (56.7)	0.16
Cough	26 (21.7)	6 (20)	2 (6.7)	8 (26.7)	10 (33.3)	0.06
Runny nose	21 (17.5)	6 (20)	3 (10)	5 (16.7)	7 (23.3)	0.63
Vomiting	25 (20.8)	7 (23.3)	5 (16.7)	5 (16.7)	8 (26.7)	0.77
Diarrhea	14 (11.7)	3 (10)	3 (10)	3 (10)	5 (16.7)	0.89
Drowsiness	6 (5)	2 (6.7)	0	2 (6.7)	2 (6.7)	0.6
Irritability	14 (11.7)	5 (16.7)	2 (6.7)	5 (16.7)	2 (6.7)	0.46
Myoclonus	30 (25)	10 (33.3)	3 (10)	9 (30)	8 (27)	0.13
Sweating	4 (3.3)	1 (3.3)	1 (3.3)	1 (3.3)	1 (3.3)	1
Lethargy	2 (1.7)	0	0	2 (6.7)	0	0.24
Conjunctivitis	1 (0.8)	0	1 (3.3)	0	0	1
Rash	106 (88.3)	30 (100)	30 (100)	17 (56.7)	19 (63.3)	0
Mouth lesion	111 (92.5)	28 (93.3)	23 (76.7)	30 (100)	30 (100)	0.001
Limb weakness	4 (3.3)	1 (3.3)	1 (3.3)	1 (3.3)	1 (3.3)	0.80
Median pulse, bpm (range)	120 (96–180)	120 (96–180)	120 (100–167)	125 (100–165)	120 (100–170)	0.632
Median blood pressure, mm Hg (range)						
Systolic	90 (75–128)	90 (75–100)	90 (80–120)	90 (80–120)	90 (80–128)	0.661
Diastolic	60 (40–80)	55 (50–62)	55 (40–80)	60 (50–80)	60 (50–77)	0.551
Blood biochemistry results, median (range)						
Leukocyte count, × 10 ⁹ cells/L	13.1 (1–50.6)	13.6 (7.8–50.6)	12.5 (1–25.9)	14.3 (5–24.7)	12.4 (4.5–24.4)	0.638
Neutrophils, %	51 (2.1–92.7)	51.2 (19.7–72.8)	52.7 (7.7–92.7)	47.6 (2.1–76.3)	50.9 (24.2–86.1)	0.658
Lymphocytes, %	37.1 (3.7–80.2)	37.1 (18.4–65.5)	33.9 (3.7–80.2)	37.6 (17.6–71.2)	36.5 (6.1–60.3)	0.846
Platelet count, × 10 ⁹ /L	322.5 (96–597)	360 (189–522)	341.5 (150–513)	297 (96–452)	293.5 (175–597)	0.086
Glucose, mg/dL	107 (0–212)	112 (62–170)	108.5 (0–154)	108.5 (68–212)	98.5 (51–164)	0.324
C-reactive protein, mg/dL	12.4 (0–102)	4.1 (0–100)	13.7 (0–102)	23.3 (3–58)	9.9 (0–39)	<0.001
Clinical grade, no. (%)						
Mild	107 (89.2)	24 (80)	29 (96.7)	28 (93.3)	26 (86.7)	0.2
Severe	13 (10.8)	6 (20)	1 (3.3)	2 (6.7)	4 (13.3)	
IVIg administration, no. (%)	8 (6.7%)	3 (10)	1 (3.3)	1 (3.3)	3 (10)	0.5
Outcome, no. (%)						
Full recovery	119 (99.2)	30 (100)	29 (96.7)	30 (100)	30 (100)	0.17
Incomplete recovery	1 (0.8)	0	1 (3.3)	0	0	

*CV, coxsackievirus; EV, enterovirus; IVIg, intravenous immunoglobulin.

†Results of statistical analyses comparing individual groups of patients infected with EV-A71, CVA6, CVA10, or CVA16.

‡Inpatients only.

The difference in the proportion of patients who were seropositive for heterotypic viruses was not statistically significant between the enrollment and follow-up time points (Table 2). At follow-up, seroconversion for heterotypic viruses was recorded in only 3% (1/30) to 23% (7/30) of the patients, with comparable rates across serotypes (Table 2). For example, of the 30 patients infected with CVA16, seroconversions for CVA6 were recorded in 10%, seroconversions for CVA10 in 7%, and seroconversions for EV-A71 in 7%. Similarly, of the 30 patients infected with EV-A71, seroconversions for CVA6 were recorded in 13%, seroconversions for CVA10 in 3%, and seroconversions

for CVA16 in 10%. Five patients became seronegative for heterotypic viruses at follow-up (Figures 1, 2; Appendix Figures 1, 2, <https://wwwnc.cdc.gov/EID/article/26/2/19-0721-App1.pdf>).

Seropositivity versus Illness Day at Enrollment and Patient Age

We found a significant difference in illness days at enrollment between the groups of patients who were seropositive by neutralization testing for any homotypic virus and those who were negative, median day of illness 2 (range 1–6 days) versus 1 (0–6 days) ($p < 0.001$) (Figure 3). Despite the small sample size,

Table 2. Seropositivity and seroconversion in plasma from hand, foot and mouth disease patients infected with EV-A71, CVA6, CVA10, and CVA16 viruses, Vietnam*

Virus	Immunity status	Virus, no. (%) samples			
		CVA6	CVA10	CVA16	EV-A71
CVA6	Seropositivity				
	At enrollment	2 (7)	10 (33)	5 (17)	2 (7)
	At follow-up	30 (100)	9 (30)	9 (30)	3 (10)
	p value	<0.001	1.0	0.36	1.0
	Seroconversion	28 (93)	1 (3)	7 (23)	2 (7)
CVA10	Seropositivity				
	At enrollment	4 (13)	9 (30)	3 (10)	3 (10)
	At follow-up	6 (20)	29 (97)	4 (13)	5 (17)
	p value	0.73	<0.001	1.0	0.71
	Seroconversion	4 (13)	25 (83)	3 (10)	2 (7)
CVA16	Seropositivity				
	At enrollment	7 (23)	10 (33)	8 (27)	5 (17)
	At follow-up	9 (30)	11 (37)	30 (100)	7 (23)
	p value	0.77	1.0	<0.001	0.75
	Seroconversion	3 (10)	2 (7)	23 (77)	2 (7)
EV-A71	Seropositivity				
	At enrollment	5 (17)	17 (57)	6 (20)	18 (60)
	At follow-up	7 (23)	14 (47)	8 (27)	30 (100)
	p value	0.75	0.61	0.76	<0.001
	Seroconversion	4 (13)	1 (3)	3 (10)	17 (57)

*n = 30 for each virus. p values reflect the results of statistical analysis comparing the seropositive rates between the 2 time points (enrollment and follow-up) of the corresponding enterovirus serotypes. CV, coxsackievirus; EV, enterovirus.

subgroup analysis demonstrated a similar association between illness day and seropositivity at enrollment among patients infected with EV-A71 and those infected with CVA6 (Appendix Figure 3). We found no difference in age (months) between the groups of patients with and without neutralizing antibodies at enrollment (data not shown).

Kinetics of Neutralizing Antibody Titers

To further shed light on the kinetics of neutralizing antibody titers over the course of illness, we plotted and compared the neutralizing antibody titers against homotypic and heterotypic enterovirus serotypes at enrollment and follow-up time points (Table 3; Figures 1, 2; Appendix Figures 1, 2). Overall, the antibody

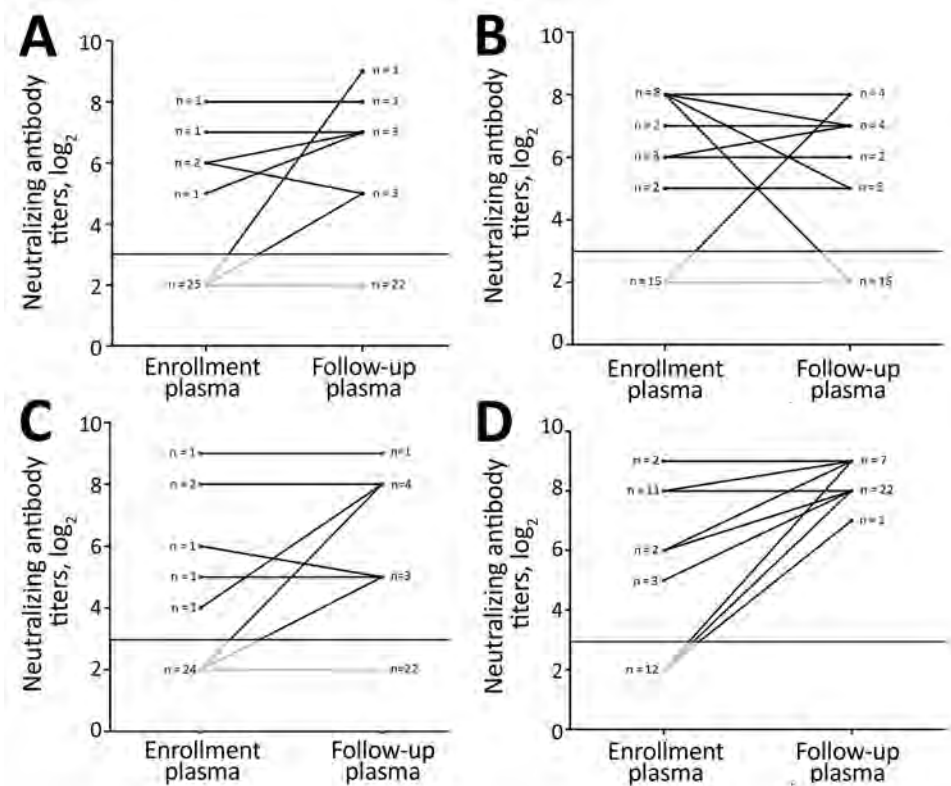


Figure 1. Kinetics of neutralizing antibody titers in plasma samples collected at enrollment and follow-up from patients infected with EV-A71 in study of patients with hand, foot and mouth disease, Vietnam. A) CVA6 (p = 0.073); B) CVA10 (p = 0.347); C) CVA16 (p = 0.250); D) EV-A71 (p<0.001). CV, coxsackievirus; EV, enterovirus.

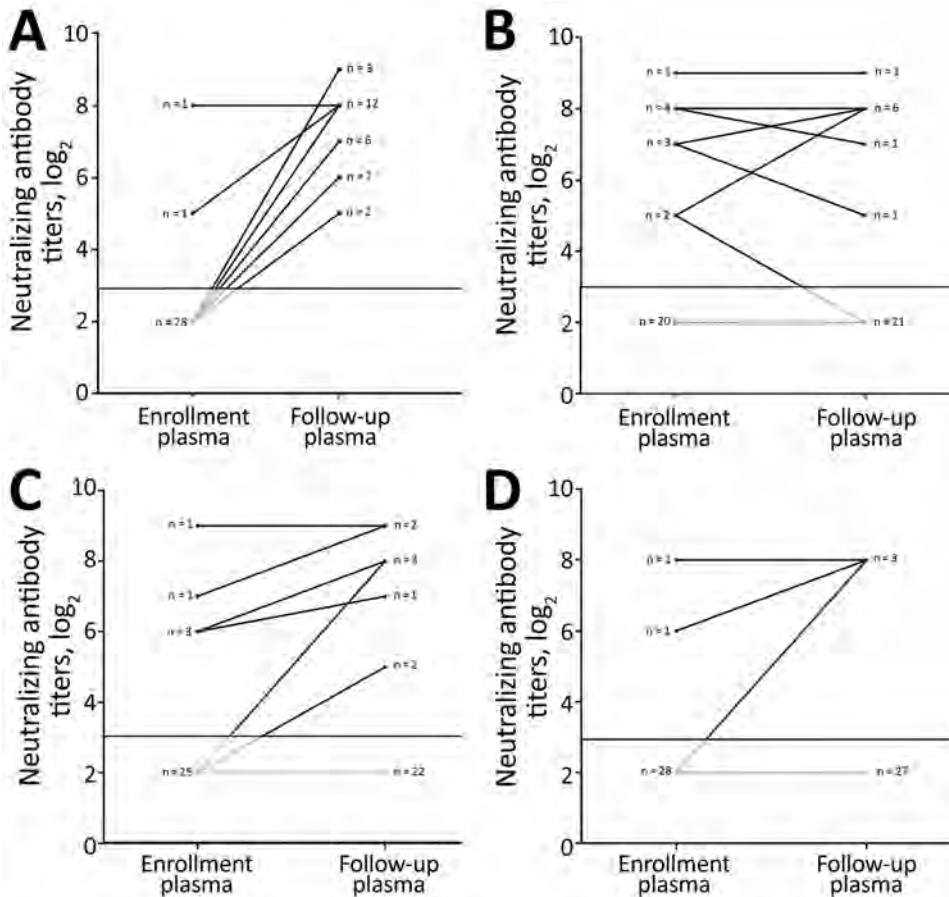


Figure 2. Kinetics of neutralizing antibody titers in plasma samples collected at enrollment and follow-up from patients infected with CVA6 in study of patients with hand, foot and mouth disease, Vietnam. A) CVA6 ($p < 0.001$); B) CVA10 ($p = 0.915$); C) CVA16 ($p = 0.021$); D) EV-A71 ($p = 0.5$). CV, coxsackievirus; EV, enterovirus.

titers to homotypic enteroviruses at follow-up were significantly higher than those measured at enrollment ($p < 0.001$; Table 3). All patients at follow-up had antibody titers against homotypic viruses ranging from 32 to 512, well above the protective level as defined from vaccine trials (12–14) (Appendix Figures 1, 2).

Neutralizing antibody titers against heterogeneous serotypes measured at the 2 time points were not statistically different, with most patients (15/50–27/30 [50%–90%]) having antibody titers below the assay cutoff (i.e., below the protective level). There was, however, a significant difference in antibody titer against CVA16 between the 2 time points among patients infected with CVA6 ($p = 0.021$; Table 3). Sub-analysis did not show that samples positive for CVA6 were more likely to be positive for CVA16 or any other serotypes than samples that were negative for CVA6 (Appendix Table 1).

Antigenic Difference between Subgenogroup B5 and Emerging Subgenogroup C4

To assess the extent to which infection with subgenogroup B5 circulating during 2013–2015 could elicit cross-neutralizing antibody responses against

subgenogroup C4, which emerged in 2018 and caused a large outbreak of >130,000 hospitalizations and 17 deaths in Vietnam (6), we performed a complementary analysis using 6 follow-up plasma samples from the aforementioned group of patients infected with subgenogroup B5. Subsequently, all the included plasma samples could neutralize 2018 subgenogroup C4, and there was no difference in neutralizing antibody titers against the EV-A71 subgenogroups C4 and B5 (Figure 4). Likewise, the only available follow-up plasma sample collected from a patient infected with 2018 subgenogroup C4 had a neutralizing antibody titer of 1:512 against both subgenogroups.

Discussion

Despite the public health threat of HFMD, scarce information exists for pathogen–pathogen and host–pathogen interactions, from the immunity perspective, to inform the development and implementation of intervention strategies, especially vaccines, and the design of epidemiologic research on disease surveillance and transmission dynamics. Here we report on the seropositivity, seroconversion, and neutralization in HFMD patients infected with EV-A71, CVA6,

CVA10, or CVA16, the 4 most common enterovirus serotypes responsible for the ongoing HFMD epidemic in Vietnam and the Asia-Pacific region over the past few decades.

In terms of seropositivity, our results showed that antibody response against homotypic viruses at or above the titer of the protective level developed quickly after the onset of illness, with seropositivity for homotypic viruses changing from <60% at day 0–6 after illness onset (at enrollment) to 97%–100% at follow-up (7–19 days after the onset of illness). We could find no existing data obtained from natural infection to compare with our results. However, results obtained from phase 3 vaccine trials have shown that at day 56 after the administration of the first 2 doses of inactivated EV-A71 vaccine, 98.5–99.9% of the volunteers had neutralizing antibody against EV-A71 at titers of >1:16 (12–14). Collectively, these data expand our knowledge about immunogenicity elicited as a consequence of EV-A71 vaccination and natural infection. Coxsackievirus vaccine development has not gone beyond animal experiments; thus, no similar data exist for CVA6, CVA10, or CVA16 (15,17).

In contrast to the observed data for homotypic viruses, seropositive rates for heterotypic viruses were recorded in <57% of the patients during the course of illness. Furthermore, at follow-up, only a small proportion (3%–23%) of the patients had seroconverted for heterotypic viruses, suggesting that cross-neutralization among EV-A71, CVA6, CVA10, and CVA16 is absent or occurs in only a small proportion of patients (24,25). It cannot, however, be ruled out that these seropositive and seroconversion rates, especially among CVA6 patients, were attributable to previous exposure or co-infection with other serotypes (e.g., CVA16 in the case of CVA6 patients), which may have been undetected by PCR. Our data support a recent report about recurrent HFMD episodes

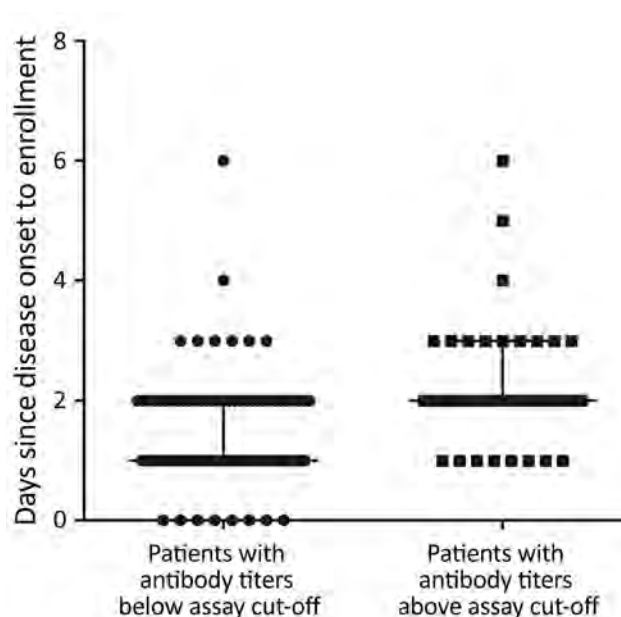


Figure 3. Association between antibody response (seropositive) and illness days at enrollment ($p < 0.001$) in study of patients with hand, foot and mouth disease, Vietnam. There were 82 patients with antibody titers below assay cutoff, and 38 patients with antibody titers above assay cutoff.

resulting from reinfection with heterotypic serotypes in China (9) and the absence of cross-neutralization among these 4 enterovirus serotypes observed in vaccine studies (13,16,17). As such, multivalent vaccines are needed to control HFMD.

EV-A71 exists as a single serotype but is genetically divided into several genogroups (e.g., A, B, and C) and subgenogroups (e.g., C1–C5 and B1–B5). In Vietnam, HFMD has been a major public health concern since 2011, causing an average of 80,000 hospitalizations per year. The switches between predominant EV-A71 subgenogroups have been well documented; C4 was responsible for the 2011–2012

Table 3. Geometric mean titers of neutralizing antibodies against enteroviruses in study of patients with hand, foot and mouth disease, Vietnam*

Virus	Samples	Geometric mean titer (95% CI) of neutralizing antibodies			
		CVA6	CVA10	CVA16	EV-A71
CVA6	Enrollment	4.9 (3.6–6.7)	13.3 (6.8–26.1)	6.9 (4.3–11.3)	5.0 (3.6–7.0)
	Follow-up	151.4 (113.0–202.8)	13.0 (6.4–26.2)	10.8 (5.6–20.8)	6.0 (3.8–9.7)
	p value	<0.001	0.83	0.021	0.50
CVA10	Enrollment	6.2 (3.9–9.7)	10.1 (5.7–17.7)	5.3 (3.8–7.2)	5.9 (3.8–9.7)
	Follow-up	8.7 (4.8–16.1)	245.5 (181.1–332.7)	6.3 (4.0–10.1)	7.6 (4.3–13.8)
	p value	0.063	<0.001	0.098	0.50
CVA16	Enrollment	9.0 (5.0–16.0)	13.6 (6.9–26.7)	10.5 (5.7–18.6)	7.4 (4.3–12.9)
	Follow-up	10.3 (5.7–18.7)	14.6 (7.5–28.5)	141.2 (104.547–191.0)	9.8 (5.1–18.7)
	p value	0.25	1.0	<0.001	0.098
EV-A71	Enrollment	6.6 (4.2–10.4)	23.2 (11.5–46.7)	7.6 (4.4–13.0)	37.7 (17.9–79.4)
	Follow-up	9.4 (5.3–16.7)	18.8 (10.0–35.4)	10.1 (5.4–18.7)	295.1 (260.6–334.2)
	p value	0.073	0.31	0.25	<0.001

*p values reflect the results of statistical analysis comparing the geometric mean titers between the 2 time points (enrollment and follow-up) of the corresponding enterovirus serotypes. CV, coxsackievirus; EV, enterovirus; HFMD, hand, foot and mouth disease.

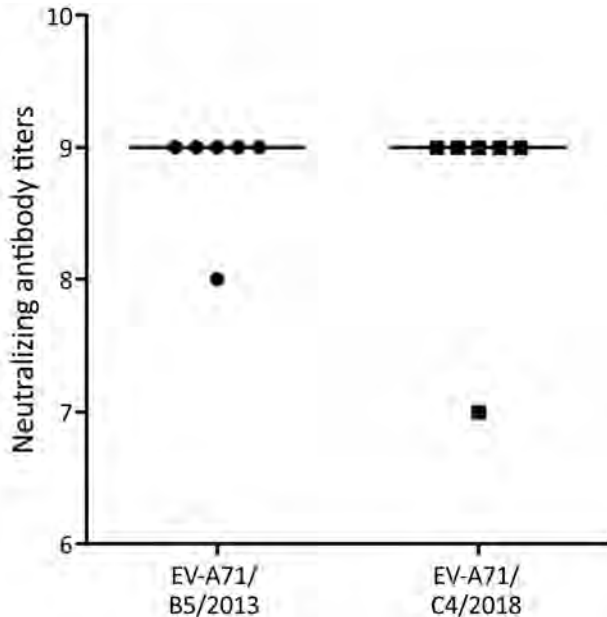


Figure 4. Neutralizing antibody titers (in binary logarithm) against subgenogroups C4 and B5 in follow-up plasma samples collected from 6 patients infected with EV-A71 subgenogroup B5 ($p = 1.0$) in study of patients with hand, foot and mouth disease, Vietnam. Information about years of collection is shown alongside the EV-A71 subgenogroup on the x-axis. EV, enterovirus.

outbreak (18) followed by the predominance of B5 during 2013–2015 (10) and the reemergence of C4 in 2018 (6). Of note, the emergence of C4 in 2018 resulted in a severe outbreak that caused >130,000 hospitalizations and 17 deaths. The underlying mechanism that determines the emergence of certain subgenogroups in specific localities remains a puzzle; it may be a consequence of a complex interplay among the pathogen, the hosts, and public health response, of which antigenic evolution might play a role (26,27). The fact that all serum samples from subgenogroup B5—infected patients collected before 2018 could neutralize the 2018 C4 virus suggests that immunity developed as a consequence of natural infection with subgenogroup B5 could provide protection against subgenogroup C4. However, the extent to which waning immunity (28), as observed from vaccine trials, may influence the long-term protection and overall population immunity, in turn resulting in possible reinfection, which has previously been reported in China (9), as well as disease emergence, remains unknown. The underlying mechanism determining the emergence of subgenogroup C4 in Vietnam in 2018 warrants further research.

Our study has some limitations. We based our analysis on only the 4 predominant serotypes currently responsible for the ongoing HFMD epidemics

in the Asia-Pacific region, whereas >20 enterovirus serotypes have been reported to be associated with HFMD in the region. Furthermore, because of the unavailability of plasma samples, we were not able to informatively assess the antigenic relationship between EV-A71 subgenogroups responsible for major HFMD outbreaks in Vietnam since 2011 (C4 and B5) with proper sample size. Likewise, our syndromic hospital-based surveillance may have missed atypical HFMD cases. Together with the convenience sample used, these limitations may lower the level of generalizability of the obtained results to some extent. In addition, we were unable to obtain long-term follow-up blood samples from HFMD cases after hospital discharge. Therefore, evaluation of antibody kinetics and the waning antibody profiles of the natural infection beyond the sampling period of the current study remain unknown.

In summary, because human infection with 1 HFMD-causing enterovirus serotype can elicit neutralizing antibodies against homotypic viruses, our results support previous reports about the potential benefit of monovalent EV-A71 vaccine in reducing the incidence of EV-A71-associated HFMD (29). The data also emphasize the requirement for multivalent vaccines to control HFMD. Our results offer evidence that is essential for the development of intervention strategies, especially multivalent vaccines, and the design of seroepidemiologic studies.

Acknowledgments

We thank Le Kim Thanh for her logistics support. We are indebted to the patients who participated in this study.

This study was funded by the Wellcome Trust of Great Britain (grant nos.106680/B/14/Z and 204904/Z/16/Z).

About the Author

Ms. Nguyet is a research assistant at Oxford University Clinical Research Unit in Ho Chi Minh City, Vietnam. She is particularly interested in the application of classical virology methods as virus isolation and neutralization to study viruses responsible for emerging infections (hand, foot and mouth disease) in Vietnam and the region.

References

- Ooi MH, Wong SC, Lewthwaite P, Cardosa MJ, Solomon T. Clinical features, diagnosis, and management of enterovirus 71. *Lancet Neurol.* 2010;9:1097–105. [https://doi.org/10.1016/S1474-4422\(10\)70209-X](https://doi.org/10.1016/S1474-4422(10)70209-X)
- Solomon T, Lewthwaite P, Perera D, Cardosa MJ, McMinn P, Ooi MH. Virology, epidemiology, pathogenesis, and control of enterovirus 71. *Lancet Infect Dis.* 2010;10:778–90. [https://doi.org/10.1016/S1473-3099\(10\)70194-8](https://doi.org/10.1016/S1473-3099(10)70194-8)

3. Österback R, Vuorinen T, Linna M, Susi P, Hyypiä T, Waris M. Coxsackievirus A6 and hand, foot, and mouth disease, Finland. *Emerg Infect Dis*. 2009;15:1485–8. <https://doi.org/10.3201/eid1509.090438>
4. Abedi GR, Watson JT, Nix WA, Oberste MS, Gerber SI. Enterovirus and parechovirus surveillance – United States, 2014–2016. *MMWR Morb Mortal Wkly Rep*. 2018;67:515–8. <https://doi.org/10.15585/mmwr.mm6718a2>
5. Kimmis BD, Downing C, Tyring S. Hand-foot-and-mouth disease caused by coxsackievirus A6 on the rise. *Cutis*. 2018;102:353–6.
6. Nhan LNT, Hong NTT, Nhu LNT, Nguyet LA, Ny NTH, Thanh TT, et al. Severe enterovirus A71 associated hand, foot and mouth disease, Vietnam, 2018: preliminary report of an impending outbreak. *Euro Surveill*. 2018;23. <https://doi.org/10.2807/1560-7917.ES.2018.23.46.1800590>
7. Anh NT, Nhu LNT, Van HMT, Hong NTT, Thanh TT, Hang VIT, et al. Emerging coxsackievirus A6 causing hand, foot and mouth disease, Vietnam. *Emerg Infect Dis*. 2018;24:654–62. <https://doi.org/10.3201/eid2404.171298>
8. Hoang MTV, Nguyen TA, Tran TT, Vu TTH, Le NTN, Nguyen THN, et al. Clinical and aetiological study of hand, foot and mouth disease in southern Vietnam, 2013–2015: inpatients and outpatients. *Int J Infect Dis*. 2019;80:1–9. <https://doi.org/10.1016/j.ijid.2018.12.004>
9. Huang J, Liao Q, Ooi MH, Cowling BJ, Chang Z, Wu P, et al. Epidemiology of recurrent hand, foot and mouth disease, China, 2008–2015. *Emerg Infect Dis*. 2018;24. <https://doi.org/10.3201/eid2403.171303>
10. Van HMT, Anh NT, Hong NTT, Nhu LNT, Nguyet LA, Thanh TT, et al. Enterovirus A71 phenotypes causing hand, foot and mouth disease, Vietnam. *Emerg Infect Dis*. 2019;25:788–91. <https://doi.org/10.3201/eid2504.181367>
11. Xing W, Liao Q, Viboud C, Zhang J, Sun J, Wu JT, et al. Hand, foot, and mouth disease in China, 2008–12: an epidemiological study. *Lancet Infect Dis*. 2014;14:308–18. [https://doi.org/10.1016/S1473-3099\(13\)70342-6](https://doi.org/10.1016/S1473-3099(13)70342-6)
12. Zhu F-C, Meng F-Y, Li J-X, Li XL, Mao QY, Tao H, et al. Efficacy, safety, and immunology of an inactivated alum-adjuvant enterovirus 71 vaccine in children in China: a multicentre, randomised, double-blind, placebo-controlled, phase 3 trial. *Lancet*. 2013;381:2024–32. [https://doi.org/10.1016/S0140-6736\(13\)61049-1](https://doi.org/10.1016/S0140-6736(13)61049-1)
13. Li R, Liu L, Mo Z, Wang X, Xia J, Liang Z, et al. An inactivated enterovirus 71 vaccine in healthy children. *N Engl J Med*. 2014;370:829–37. <https://doi.org/10.1056/NEJMoa1303224>
14. Zhu F, Xu W, Xia J, Liang Z, Liu Y, Zhang X, et al. Efficacy, safety, and immunogenicity of an enterovirus 71 vaccine in China. *N Engl J Med*. 2014;370:818–28. <https://doi.org/10.1056/NEJMoa1304923>
15. Fang CY, Liu CC. Recent development of enterovirus A vaccine candidates for the prevention of hand, foot, and mouth disease. *Expert Rev Vaccines*. 2018;17:819–31. <https://doi.org/10.1080/14760584.2018.1510326>
16. Zhang W, Dai W, Zhang C, Zhou Y, Xiong P, Wang S, et al. A virus-like particle-based tetraavalent vaccine for hand, foot, and mouth disease elicits broad and balanced protective immunity. *Emerg Microbes Infect*. 2018;7:1–12. <https://doi.org/10.1038/s41426-018-0094-1>
17. Lim H, In HJ, Lee JA, Sik Yoo J, Lee SW, Chung GT, et al. The immunogenicity and protection effect of an inactivated coxsackievirus A6, A10, and A16 vaccine against hand, foot, and mouth disease. *Vaccine*. 2018;36:3445–52. <https://doi.org/10.1016/j.vaccine.2018.05.005>
18. Khanh TH, Sabanathan S, Thanh TT, Thoa PK, Thuong TC, Hang V, et al. Enterovirus 71-associated hand, foot, and mouth disease, southern Vietnam, 2011. *Emerg Infect Dis*. 2012;18:2002–5. <https://doi.org/10.3201/eid1812.120929>
19. Thanh TT, Anh NT, Tham NT, Van HM, Sabanathan S, Qui PT, et al. Validation and utilization of an internally controlled multiplex real-time RT-PCR assay for simultaneous detection of enteroviruses and enterovirus A71 associated with hand foot and mouth disease. *Virology*. 2015;12:85. <https://doi.org/10.1186/s12985-015-0316-2>
20. Nix WA, Oberste MS, Pallansch MA. Sensitive, seminested PCR amplification of VP1 sequences for direct identification of all enterovirus serotypes from original clinical specimens. *J Clin Microbiol*. 2006;44:2698–704. <https://doi.org/10.1128/JCM.00542-06>
21. Tan V, Tuyen NT, Thanh TT, Ngan TT, Van HM, Sabanathan S, et al. A generic assay for whole-genome amplification and deep sequencing of enterovirus A71. *J Virol Methods*. 2015;215-216:30–6. <https://doi.org/10.1016/j.jviromet.2015.02.011>
22. Kroneman A, Vennema H, Deforche K, van der Avoort H, Peñaranda S, Oberste MS, et al. An automated genotyping tool for enteroviruses and noroviruses. *J Clin Virol*. 2011;51:121–5. <https://doi.org/10.1016/j.jcv.2011.03.006>
23. Tran CB, Nguyen HT, Phan HT, Tran NV, Wills B, Farrar J, et al. The seroprevalence and seroincidence of enterovirus71 infection in infants and children in Ho Chi Minh City, Viet Nam. *PLoS One*. 2011;6:e21116. <https://doi.org/10.1371/journal.pone.0021116>
24. Takahashi S, Metcalf CJE, Arima Y, Fujimoto T, Shimizu H, Rogier van Doorn H, et al. Epidemic dynamics, interactions and predictability of enteroviruses associated with hand, foot and mouth disease in Japan. *J R Soc Interface*. 2018;15:20180507. <https://doi.org/10.1098/rsif.2018.0507>
25. Pons-Salort M, Grassly NC. Serotype-specific immunity explains the incidence of diseases caused by human enteroviruses. *Science*. 2018;361:800–3. <https://doi.org/10.1126/science.aat6777>
26. Huang SW, Tai CH, Fonville JM, Lin CH, Wang SM, Liu CC, et al. Mapping enterovirus A71 antigenic determinants from viral evolution. *J Virol*. 2015;89:11500–6. <https://doi.org/10.1128/JVI.02035-15>
27. Huang SW, Hsu YW, Smith DJ, Kiang D, Tsai HP, Lin KH, et al. Reemergence of enterovirus 71 in 2008 in Taiwan: dynamics of genetic and antigenic evolution from 1998 to 2008. *J Clin Microbiol*. 2009;47:3653–62. <https://doi.org/10.1128/JCM.00630-09>
28. Liu L, Mo Z, Liang Z, Zhang Y, Li R, Ong KC, et al. Immunity and clinical efficacy of an inactivated enterovirus 71 vaccine in healthy Chinese children: a report of further observations. *BMC Med*. 2015;13:226. <https://doi.org/10.1186/s12916-015-0448-7>
29. Takahashi S, Liao Q, Van Boeckel TP, Xing W, Sun J, Hsiao VY, et al. Hand, foot, and mouth disease in China: modeling epidemic dynamics of enterovirus serotypes and implications for vaccination. *PLoS Med*. 2016;13:e1001958. <https://doi.org/10.1371/journal.pmed.1001958>

Address for correspondence: Lam Anh Nguyet or Le Van Tan, Oxford University Clinical Research Unit, Ho Chi Minh City, Vietnam; email: nguyetla@oucru.org or tanlv@oucru.org

Emergence of Chikungunya Virus, Pakistan, 2016–2017

Nazish Badar, Muhammad Salman, Jamil Ansari, Uzma Aamir,
Muhammad Masroor Alam, Yasir Arshad, Nighat Mushtaq, Aamer Ikram, Javaria Qazi

During December 2016–May 2017, an outbreak of chikungunya virus infection occurred across Pakistan. The East/Central/South African genotype was predominant. This study provides baseline data on the virus strain and emphasizes the need for active surveillance and implementation of preventive interventions to contain future outbreaks.

Chikungunya is a vectorborne viral disease that causes large outbreaks, mainly in tropical and subtropical countries (1). The term chikungunya is derived from a word in the Makonde language (spoken in parts of Tanzania and Mozambique, Africa), *kungunyala*, meaning “that which bends up,” referring to the stooped posture and impaired gait patients exhibit because of severe joint pain (2). Chikungunya virus (CHIKV; family *Togaviridae*, genus *Alphavirus*) is an enveloped, single-strand, positive-sense RNA virus transmitted through the bite of infected *Aedes* mosquitoes, predominantly *Ae. aegypti* and *Ae. albopictus* (2).

West African, East/Central/South African (ECSA), and Asian CHIKV genotypes are distinguished by envelope 1 (E1) glycoprotein phylogeny. In 2005, a major outbreak in countries around the Indian Ocean was caused by the ECSA genotype (3). Virus mutations facilitated its replication in *Ae. albopictus* mosquitoes and its rapid spread by *Ae. albopictus* and *Ae. aegypti* mosquitoes (3), species prevalent in Pakistan during and after monsoon season, May–September.

In Pakistan, CHIKV was reported to be circulating in rodents as early as 1983 (4), but few human cases were reported. During a 2011 dengue outbreak in Lahore, some patients also had CHIKV antibodies. CHIKV emerged in Karachi during 2016, and an outbreak eventually was declared when evidence of local transmission was confirmed (5). We

reviewed the epidemiologic and evolutionary links of CHIKV detected during December 2016–May 2017 across Pakistan.

The Study

We tested serum samples from 584 patients with suspected CHIKV infection, according to the World Health Organization case definition (6). Patients were seen in different hospitals and clinics during December 20, 2016–May 31, 2017. Patients had acute onset fever (temperature $>38.5^{\circ}\text{C}$), rash, and severe arthralgia or arthritis ≤ 7 days after a mosquito bite. Clinical signs and symptoms included fever in 90% (523/584) of persons with suspected cases, headache in 65% (382/584), joint pain in 85% (497/584), and rash in 24% (141/584) (Appendix Table 1, <https://wwwnc.cdc.gov/EID/article/26/2/17-1636-App1.pdf>).

We used a predesigned form to collect patient demographic data, clinical information, and travel histories. We identified 495 (84.7%) suspected cases in Sindh, 52 (8.9%) in Baluchistan, 10 (1.7%) in Federal Capital Territory, 10 (1.7%) in Punjab, and 17 (2.9%) in Khyber Pakhtunkhwa (Figure 1).

We used the QIAmp Viral RNA Mini Kit (QIAGEN, <https://www.qiagen.com>) to extract RNA from serum samples, according to the manufacturer’s protocol. We conducted one-step real-time reverse transcription-PCR (rRT-PCR) on the ABI7500 platform (Applied Biosystems, <https://www.thermofisher.com>) following guidelines from the U.S. Centers for Disease Control and Prevention emergency use authorization for Trioplex Real-Time RT-PCR assay (7). We used CHIKV-specific oligonucleotide primers to detect and sequence the envelope 1 (E1) and nonstructural protein 1 (NSP1) genes (8). We conducted phylogenetic analysis of partial E1 ($n = 12$) and NSP1 ($n = 21$) by the maximum-likelihood method in MEGA version 6 (<https://www.megasoftware.net>). We detected CHIKV IgM by using Anti-Chikungunya Virus ELISA (Euroimmune, <https://www.euroimmun.com>) commercial kits.

We collected and analyzed epidemiologic data, conducted bivariate analysis, and calculated p values

Author affiliations: National Institute of Health, Islamabad, Pakistan (N. Badar, M. Salman, J. Ansari, U. Aamir, M.M. Alam, Y. Arshad, N. Mushtaq, A. Ikram); Quaid-I-Azam University, Islamabad (N. Badar, J. Qazi)

DOI: <https://doi.org/10.3201/eid2602.171636>

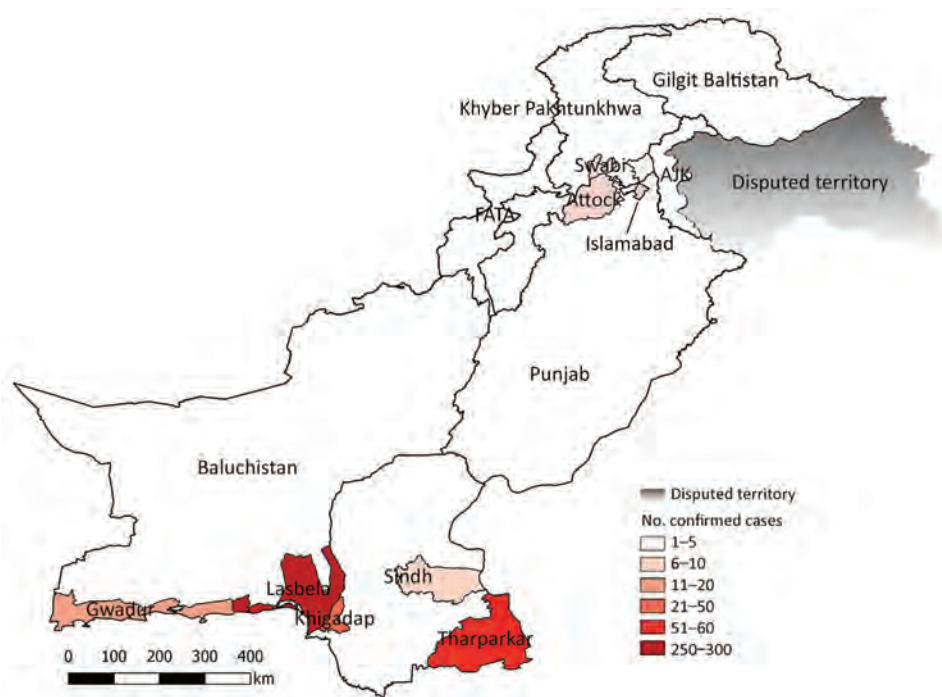


Figure 1. Geographic distribution of chikungunya-positive cases in Pakistan, December 20, 2016–May 31, 2017. AJK, Azad Jammu and Kashmir; FATA, Federally Administered Tribal Areas.

by using SPSS Statistics 16.0 (IBM, <https://www.ibm.com>). We predicted the atomic structure of the E1 protein by using the Semiliki Forest virus (PDB ID: 2XFC) as a model in UCSF Chimera version 1.11.2 (University of California, San Francisco, <https://www.cgl.ucsf.edu/chimera>).

We confirmed CHIKV by real-time reverse transcription PCR in 411 (70.3%) patients. The mean age of CHIKV-positive case-patients was 31.8 years (SD \pm 15.7 years); most (25.5%) were 21–40 years of age (Appendix Figure 1). Children \leq 10 years of age had more rashes (42%) than adults, but 91% of patients 11–20 years of age and 40% of patients 21–30 years of age had joint pain and swelling.

Of representative samples ($n = 154$), 85% (131/154) were positive by PCR; 67% (88/131) by IgM ELISA, of which 33% (43/131) had detectable CHIKV IgM; and 6% (8/131) of cases were confirmed by both methods. PCR was more sensitive \leq 3 days after fever onset; IgM ELISA was more sensitive $>$ 3 days after fever onset.

Partial E1 (294 bp) and nsP1 (354 bp) gene sequences showed 99.9% similarity to strains of Indian Ocean lineage from the ECSA genotype (Figure 2). CHIKV strains in Pakistan had 99.9% homology with viruses from India, Singapore, and Bangladesh. The E1 protein of isolates from Pakistan diverged only 0.01% from prototype S-27 from Africa.

We noted substitutions in E1 genes at T98A, S111T, A145T, and K157N (Table 2) and at K128T in the NSP1 genes. We analyzed potential glycosylation

sites in E1 and compared these with an o'nyong-nyong virus strain (GenBank accession no. AF079456). The E1 gene revealed a single conserved N-linked glycosylation site at N141 (Appendix Figure 2).

Conclusions

We noted a high rate of CHIKV infection, 70% (411/584), among suspected cases; most, 37% (153/411), occurred during May, early in monsoon season, similar to a 1963 outbreak in India that coincided with monsoon season, July–December. Another study in India noted an increase in CHIKV infections during and after monsoon season, possibly reflecting the favorable breeding conditions for *Ae. albopictus* and *Ae. aegypti* mosquitoes (9).

With a population of \geq 180 million, Pakistan is the world's sixth most populous country and the second most urbanized nation in South Asia; 36% of the population resides in cities. Pakistan and other countries in Asia are experiencing harsher summers and milder winters, conditions that increase outbreaks of arboviruses likely by expanding arthropod vector breeding seasons (10). In addition, outbreaks can intensify in poor sanitary conditions in parts of the region. CHIKV could also be introduced into nonendemic areas by travelers with viremia, leading to local transmission (11). Speculated risk factors in Sindh during 2016 included population movement across the country, as well as high vector density, poor sanitation, and susceptible populations (10).

Genomic and serologic assays confirmed CHIKV infection 3–5 days after patients' fever onset. We noted more CHIKV cases in persons ≥ 20 years of age. However, persons ≤ 20 years of age more frequently exhibited rashes and arthralgia, similar to results from a previous study during a 2007 outbreak in Kerala, India (12).

CHIKV Asian genotype circulates in Southeast Asia, where *Ae. albopictus* mosquitoes have been expanding during the previous 60 years (13). In CHIKV-endemic settings in Asia, 2 independent E1 gene mutations in A226V and T98A could enable virus adaptation to this mosquito species. In contrast, for Indian Ocean lineage strains, the same fitness advantage and selection efficiency could be gained by the acquisition of a single T98A amino acid substitution (13).

Chikungunya should be considered as a diagnosis in persons who report fever, rash, or arthralgia,

especially those returning from travel to virus-endemic areas (14). Chikungunya cases increased in Karachi and adjoining areas of Pakistan within months after massive outbreaks in India in 2016 (15). CHIKV in those outbreaks had high sequence homology to isolates from Pakistan, ascribing to the ECSA Indian Ocean lineage. Because no licensed CHIKV vaccine is available, public health officials should urge adoption of measures to prevent mosquito bites, such as use of repellents and mosquito nets.

Our study had some limitations. We did not obtain information on patient outcomes or clinical management. Our results might also underreport cases because Pakistan does not have a nationwide surveillance system for CHIKV.

In summary, we report on the molecular epidemiology of CHIKV genotypes circulating in Pakistan during 2016–2017. Sustained surveillance for CHIKV

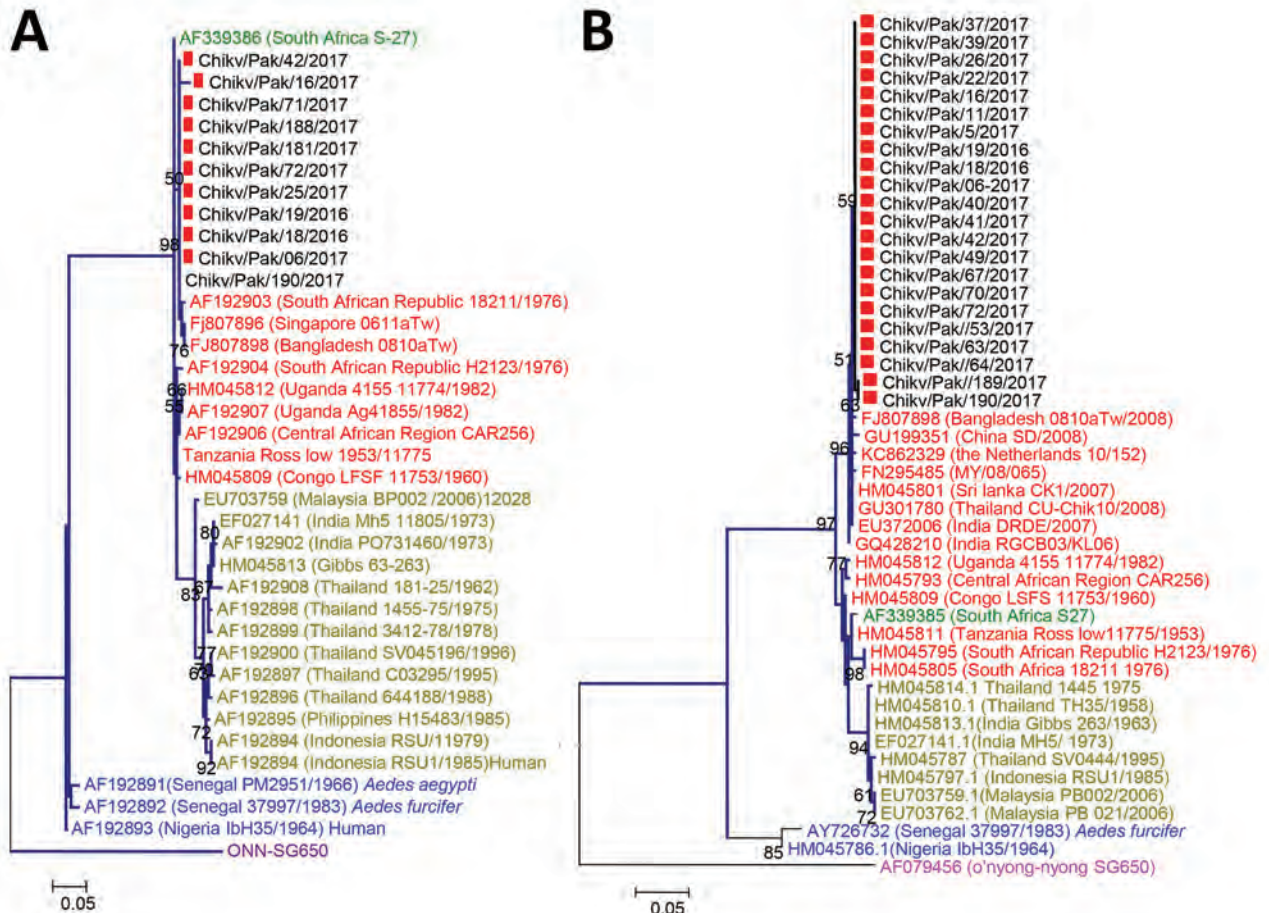


Figure 2. Phylogenetic tree of chikungunya viruses collected from patients in Pakistan, December 20, 2016–May 31, 2017 (red squares), and reference viruses. The tree was generated by the maximum-likelihood method based on the nucleotide sequence of the partial envelope 1 (A) and nonstructural protein 1 (B) genes. Red text indicates East/Central/South African genotype; yellow text indicates Asian genotype; green text indicates South African genotype; blue text indicates West African genotype; and purple text indicates o'nyong-nyong virus ancestral strain. GenBank accession numbers are provided for reference viruses. Scale bars indicate nucleotide substitutions per site.

is needed to monitor the extent of virus circulation in subsequent years. Identification of genotypes and monitoring for mutations that might facilitate transmission fitness for CHIKV in mosquito vectors can improve public health response.

Molecular graphics and analyses were performed with UCSF Chimera, developed by the Resource for Biocomputing, Visualization, and Informatics at the University of California, San Francisco, with support from NIH P41-GM103311.

About the Author

Dr. Nazish is molecular biologist and technical supervisor of the Center for Disease Control-Global Health Security Agenda laboratory for dengue and other arboviruses, Virology Department, National Institute of Health, Pakistan. Her research interests include the epidemiology, diagnosis, and molecular characterization of arboviral infections.

References

- Weaver SC, Osorio JE, Livengood JA, Chen R, Stinchcomb DT. Chikungunya virus and prospects for a vaccine. *Expert Rev Vaccines*. 2012;11:1087–101. <https://doi.org/10.1586/erv.12.84>
- Burt FJ, Rolph MS, Rulli NE, Mahalingam S, Heise MT. Chikungunya: a re-emerging virus. *Lancet*. 2012;379:662–71. [https://doi.org/10.1016/S0140-6736\(11\)60281-X](https://doi.org/10.1016/S0140-6736(11)60281-X)
- Thiberville S-D, Moyen N, Dupuis-Maguiraga L, Nougairede A, Gould EA, Roques P, et al. Chikungunya fever: epidemiology, clinical syndrome, pathogenesis and therapy. *Antiviral Res*. 2013;99:345–70. <https://doi.org/10.1016/j.antiviral.2013.06.009>
- Darwish MA, Hoogstraal H, Roberts TJ, Ahmed IP, Omar F. A sero-epidemiological survey for certain arboviruses (Togaviridae) in Pakistan. *Trans R Soc Trop Med Hyg*. 1983;77:442–5. [https://doi.org/10.1016/0035-9203\(83\)90106-2](https://doi.org/10.1016/0035-9203(83)90106-2)
- Aamir UB, Badar N, Salman M, Ahmed M, Alam MM. Outbreaks of chikungunya in Pakistan. *Lancet Infect Dis*. 2017;17:483. [https://doi.org/10.1016/S1473-3099\(17\)30191-3](https://doi.org/10.1016/S1473-3099(17)30191-3)
- World Health Organization. Guidelines on clinical management of chikungunya fever. Geneva: The Organization; 2008.
- US Food and Drug Administration. Triplex real-time RT-PCR assay: U.S. Centers for Disease Control and Prevention instructions for use [cited 2017 Mar 14]. <https://www.fda.gov/downloads/MedicalDevices/Safety/EmergencySituations/UCM491592.pdf>
- Hasebe F, Parquet MC, Pandey BD, Mathenge EG, Morita K, Balasubramaniam V, et al. Combined detection and genotyping of chikungunya virus by a specific reverse transcription-polymerase chain reaction. *J Med Virol*. 2002;67:370–4. PubMed <https://doi.org/10.1002/jmv.10085>
- Lahariya C, Pradhan SK. Emergence of chikungunya virus in Indian subcontinent after 32 years: a review. *J Vector Borne Dis*. 2006;43:151–60.
- Rauf M, Fatima-tuz-Zahra, Manzoor S, Mehmood A, Bhatti S. Outbreak of chikungunya in Pakistan. *Lancet Infect Dis*. 2017;17:258. [https://doi.org/10.1016/S1473-3099\(17\)30074-9](https://doi.org/10.1016/S1473-3099(17)30074-9)
- Napoli C, Salcuni P, Pompa MG, Declich S, Rizzo C. Estimated imported infections of chikungunya and dengue in Italy, 2008 to 2011. *J Travel Med*. 2012;19:294–7. <https://doi.org/10.1111/j.1708-8305.2012.00640.x>
- Kumar NP, Suresh A, Vanamail P, Sabesan S, Krishnamoorthy KG, Mathew J, et al. Chikungunya virus outbreak in Kerala, India, 2007: a seroprevalence study. *Mem Inst Oswaldo Cruz*. 2011;106:912–6. <https://doi.org/10.1590/s0074-02762011000800003>
- Tsetsarkin KA, Chen R, Leal G, Forrester N, Higgs S, Huang J, et al. Chikungunya virus emergence is constrained in Asia by lineage-specific adaptive landscapes. *Proc Natl Acad Sci U S A*. 2011;108:7872–7. <https://doi.org/10.1073/pnas.1018344108>
- Shiferaw B, Lam P, Tuthill S, Choudhry H, Syed S, Ahmed S, et al. The chikungunya epidemic: a look at five cases. *IDCases*. 2015;2:89–91. <https://doi.org/10.1016/j.idcr.2015.08.004>
- Kaur N, Jain J, Kumar A, Narang M, Zakaria MK, Marcello A, et al. Chikungunya outbreak in Delhi, India, 2016: report on coinfection status and comorbid conditions in patients. *New Microbes New Infect*. 2017;20:39–42. <https://doi.org/10.1016/j.nmni.2017.07.007>

Address for correspondence: Javaria Qazi, Quaid-I-Azam University, Department of Biotechnology, Islamabad, 44000, Pakistan; email: javariaq@yahoo.com

Influence of Rainfall on *Leptospira* Infection and Disease in a Tropical Urban Setting, Brazil

Kathryn P. Hacker,¹ Gielson A. Sacramento,¹ Jaqueline S. Cruz, Daiana de Oliveira, Nivison Nery, Jr., Janet C. Lindow, Mayara Carvalho, Jose Hagan, Peter J. Diggle, Mike Begon, Mitermayer G. Reis, Elsie A. Wunder, Jr., Albert I. Ko,¹ Federico Costa¹

The incidence of hospitalized leptospirosis patients was positively associated with increased precipitation in Salvador, Brazil. However, *Leptospira* infection risk among a cohort of city residents was inversely associated with rainfall. These findings indicate that, although heavy rainfall may increase severe illness, *Leptospira* exposures can occur year-round.

Leptospirosis, a leading zoonotic cause of illness and death (1), has emerged as a major health problem due to the global expansion of urban slum communities (2–4). The disease is associated with severe manifestations such as Weil’s disease and pulmonary hemorrhage syndrome (5), for which case-fatality rates are 10%–50% or even higher (6). Transmission to slum residents occurs in the peridomestic environment, in which exposures to sewers, floodwater, and contaminated soil are risk factors (3,7,8). Extreme weather events may precipitate outbreaks (3–6), as recently experienced during the aftermath of Hurricane Maria in Puerto Rico (9). Similarly, seasonal periods of heavy rainfall and flooding are a contributing factor to the risk for urban leptospirosis (4,10).

In urban slum settings, contact with rats and *Leptospira*-contaminated water and soil occur year-round (3). Prior studies have shown, consistently, positive

associations between heavy rainfall and hospitalized leptospirosis case-patients (4,10). However, this relationship may be affected by differences in case definitions used by diverse surveillance systems. In the few prospective cohort studies available, estimates of severe disease accounted for only a small proportion of the total disease burden (6). Thus, little is known about the role of rainfall in overall infection rates. To characterize the seasonal pattern of leptospirosis and *Leptospira* infection in a tropical urban setting and evaluate the influence of meteorological factors on seasonal risk, we conducted a prospective investigation of *Leptospira* infection rates among slum residents while actively surveying for hospitalized leptospirosis case-patients within Salvador, Brazil, during seasonal periods of high and low rainfall.

The Study

During February 2013–April 2015, we identified patients >5 years old with suspected leptospirosis at the state infectious disease hospital in Salvador, Brazil (4,5), and those reported in the public health surveillance database by other hospitals in Salvador. We estimated the probable date of infection as 15 days before the hospital admission date. We evaluated suspected leptospirosis cases according to the WHO case definition standard (4,6,11) using the microscopic agglutination test (MAT), lipL32 real-time PCR assay (11), IgM-ELISA (6), or a combination. We defined laboratory-confirmed cases of leptospirosis as those with >4-fold rise in MAT titers in paired serum samples, MAT titers >1:800 in a single sample, or positive PCR (Appendix Tables 1, 2, <https://wwwnc.cdc.gov/EID/article/26/2/19-0102-App1.pdf>).

A linear regression model identified that cumulative monthly rainfall (Figure 1, panel A) was significantly associated with the monthly number

Author affiliations: University of Pennsylvania, Philadelphia, Pennsylvania, USA (K.P. Hacker); Yale University, New Haven, Connecticut, USA (K.P. Hacker, J.C. Lindow, J. Hagan, E.A. Wunder, Jr., A.I. Ko, F. Costa); Fundação Oswaldo Cruz, Salvador, Brazil (G.A. Sacramento, J.S. Cruz, D. de Oliveira, N. Nery, Jr., J.C. Lindow, M. Carvalho, J. Hagan, M.G. Reis, A.I. Ko, F. Costa); Montana State University Bozeman, Bozeman, Montana, USA (J.C. Lindow); Lancaster University, Lancaster, UK (P.J. Diggle); Johns Hopkins University, Baltimore, Maryland, USA (P.J. Diggle); University of Liverpool, Liverpool, UK (M. Begon); Universidade Federal da Bahia, Salvador (M.G. Reis, F. Costa)

DOI: <https://doi.org/10.3201/eid2602.190102>

¹These authors contributed equally to this article.

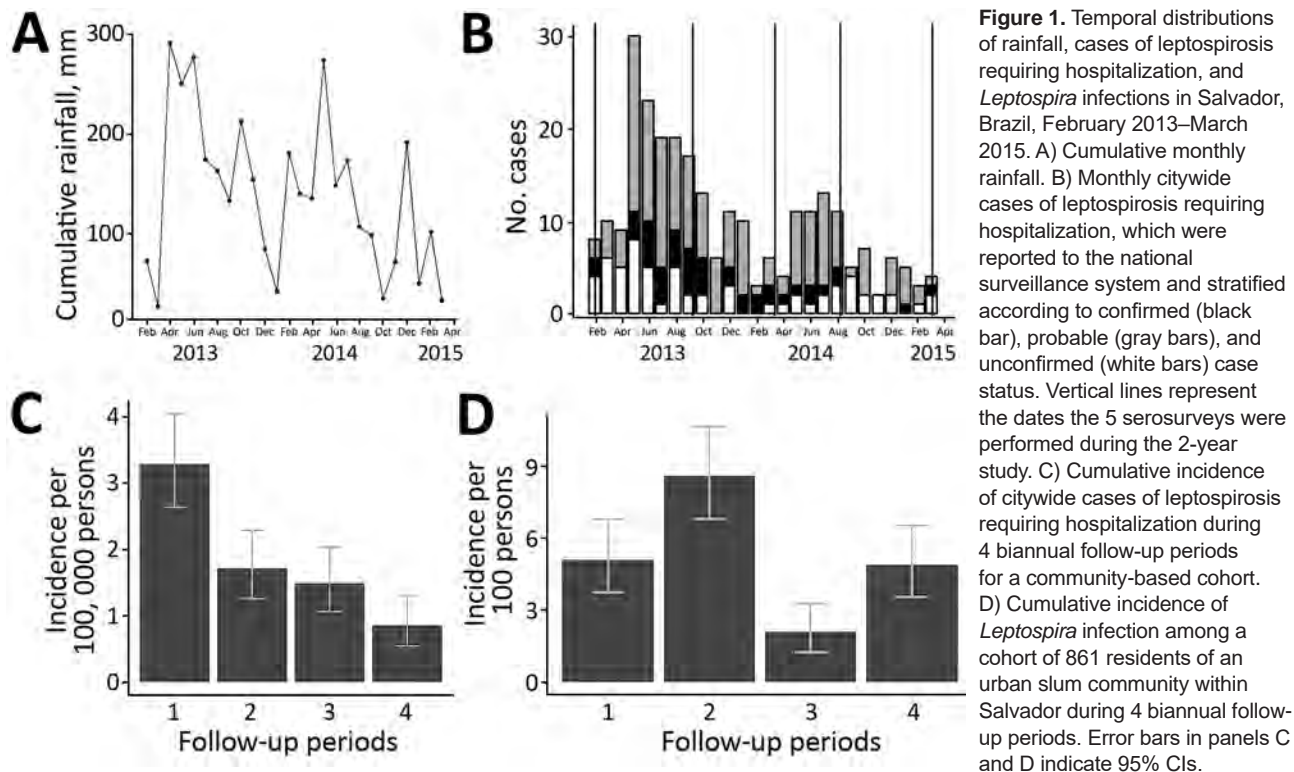


Figure 1. Temporal distributions of rainfall, cases of leptospirosis requiring hospitalization, and *Leptospira* infections in Salvador, Brazil, February 2013–March 2015. A) Cumulative monthly rainfall. B) Monthly citywide cases of leptospirosis requiring hospitalization, which were reported to the national surveillance system and stratified according to confirmed (black bar), probable (gray bars), and unconfirmed (white bars) case status. Vertical lines represent the dates the 5 serosurveys were performed during the 2-year study. C) Cumulative incidence of citywide cases of leptospirosis requiring hospitalization during 4 biannual follow-up periods for a community-based cohort. D) Cumulative incidence of *Leptospira* infection among a cohort of 861 residents of an urban slum community within Salvador during 4 biannual follow-up periods. Error bars in panels C and D indicate 95% CIs.

of hospitalized cases ($r^2 = 0.22$, $p < 0.007$) (Figure 2). The highest hospitalized disease incidence occurred during the first period (February–September 2013; 3.29 cases/100,000 population; 95% CI 2.67–4.01 cases/100,000 population) and decreased across the next periods (Table 1; Figure 1, panels B, C).

Concurrently, we conducted a prospective cohort study assessing serologic evidence of *Leptospira* infection among urban slum residents of Pau da Lima, northwestern Salvador. We enrolled 2,421 of 3,716 eligible residents, ≥ 5 years of age and with written informed

consent, of whom 821 participated in all serologic surveys performed twice annually during August–September (dry season) and February–March (rainy season) during 2013–2015 (Figure 1, panel A). Using panels with the 2 most common *Leptospira* species in Salvador (4), *L. interrogans* serogroup Icterohaemorrhagiae serovar Copenhageni (strain Fiocruz L130) and *L. kirsheri* serogroup Cynopteri serovar Cynopteri (strain 3522C), we defined serologic evidence of *Leptospira* infection by a MAT titer increase from negative to $\geq 1:50$ (seroconversion) or ≥ 4 -fold increase between sequential, paired samples. During the study period, 29% of the infected participants reported fever.

To assess the association between rainfall and laboratory-confirmed *Leptospira* infection, we calculated the cumulative amount of rainfall that each study participant experienced between sequential samples. We used a generalized estimating equation and incorporated explanatory variables for gender, age, time period, and cumulative rainfall that each participant experienced. In contrast to the hospitalized cases, we found *Leptospira* infection risk in the urban area had an inverse association with cumulative rainfall (0.986 cm, 95% CI 0.977–0.995 per cm) (Table 2; Figure 1, panel D). We additionally assessed various rainfall metrics, as well as the number of severe rainfall events each participant experienced above the mean rainfall, and the resulting patterns remained

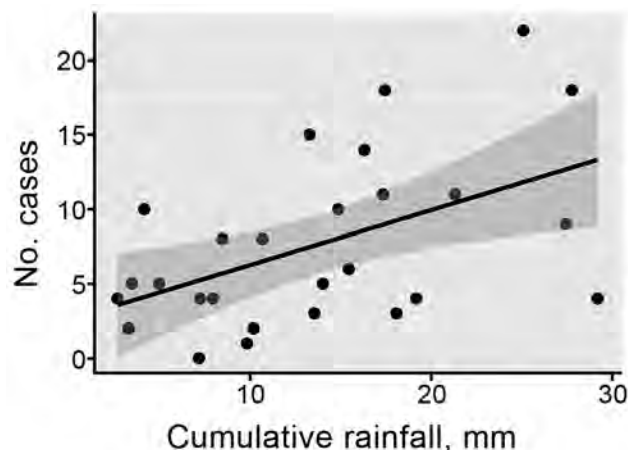


Figure 2. Correlation between cumulative monthly rainfall and monthly citywide cases of leptospirosis requiring hospitalization.

Table 1. Cumulative rainfall, citywide incidence of leptospirosis requiring hospitalization, and incidence of *Leptospira* infection among a community-based cohort in Salvador, Brazil, 2013–2015*

Follow-up period (dates)*	Cumulative rainfall, cm (\pm SD)†	Hospitalizations/100,000 population‡		<i>Leptospira</i> infection in period§	
		No. cases	Incidence (95% CI)	No. infected	Incidence (95% CI)
1 (2013 Feb 2–Sep 10)	126 (\pm 13)	88	3.29 (2.67–4.01)	44	5.11 (3.74–6.80)
2 (2013 Sep 10–2014 Mar 14)	81 (\pm 21)	46	1.72 (1.26–2.29)	74	8.60 (6.81–10.67)
3 (2014 Mar 14–2014 Aug 8)	93 (\pm 16)	40	1.50 (1.07–2.04)	18	2.09 (1.24–3.28)
4 (2014 Aug 8–2015 Mar 3)	57 (\pm 11)	23	0.86 (0.54–1.29)	42	4.88 (3.54–6.54)

*We conducted 5 semiannual follow-up surveys for a community-based cohort of 861 residents of a community within Salvador, Brazil. A period was defined as the interval between 2 consecutive surveys.

†The source of rainfall data is 4 weather stations maintained by the Brazilian Institute for the Environment and Water Resources (Instituto do Meio Ambiente e Recursos Hidricos), located 1.6 km from the study site.

‡Cases of hospitalized leptospirosis per 100,000 population in the city of Salvador, Brazil (pop. 2,675,656 in 2010), during the follow-up period.

§We performed microscopic agglutination test to evaluate serologic evidence of *Leptospira* infections between 2 consecutive surveys. Cumulative incidence was calculated as the number of infections per 861 cohort subjects multiplied by 100.

consistent. Increasing age and male sex were associated with higher infection risk.

Conclusions

Leptospirosis is traditionally associated with heavy rainfall and flooding events in Brazil (5,9) and worldwide (7,10). Our findings support the association between extreme weather events and clinical leptospirosis. During the study period, the risk of acquiring leptospirosis that required hospitalization was significantly higher in periods with elevated rainfall. However, this finding is in contrast to *Leptospira* infection in nonhospitalized persons.

Our findings indicate that *Leptospira* infections occur year-round in this urban tropical setting and the cumulative incidence of *Leptospira* infection is high (2%–9% per period). This finding differs from patterns that we and others have identified for leptospirosis requiring hospitalization (2,4,9,12). Although this study does not specifically assess subclinical symptomatic infection, it provides further evidence that the impact of leptospirosis is underestimated, and physicians should be aware that leptospirosis infection may manifest clinically year-round.

The patterns of *Leptospira* exposure incidence and infection severe enough to require hospitalization, when taken together, suggest that rainfall may promote exposures of greater inocula, which in turn may increase the risk of developing severe clinical outcomes, such as severe pulmonary hemorrhage syndrome and Weil's disease. For example, heavy rainfall may diffuse *Leptospira* from the soil, resulting in higher concentrations of bacteria in the media to which humans are exposed (sewer water) and so to a higher inoculum dose, thus increasing hospitalized disease incidence and perhaps decreasing the environmental exposure risk in and around households (mud and exposed soil) and decreasing infection risk. However, additional studies are needed to assess the specific contribution of inoculum dose to disease severity.

The 2-year study period was atypical because rainfall was lower than expected during the rainy seasons (Figure 1, panel A; Appendix Figure 1). Of note, we observed a significant inverse association between cumulative rainfall and the risk for infection during biannual sampling periods. Thus, these trends may not apply to periods with higher amounts of rainfall or extreme climatic events, such as El Niño. This study was also limited because we used seroconversion to identify infection and therefore could not determine the precise timing of exposure events; furthermore, we conducted serologic surveys only in a single urban slum community. However, most hospitalized cases occur in similar communities (4), and therefore Pau da Lima is likely to be representative. Last, although the surveillance hospitals were able to capture a variety of febrile illnesses, they did not capture mild febrile illness, which may account for a missing proportion of leptospirosis cases.

Our findings demonstrate that, despite the association of leptospirosis hospitalization with rainfall, *Leptospira* exposure continues year-round. Although we did not evaluate mild subclinical or clinical infections, it is possible that participants experience symptomatic illness that may be unrecognized or misdiagnosed as dengue or other febrile disease (12,13). Clinicians should be aware that leptospirosis may

Table 2. Association of cumulative rainfall and semiannual follow-up period with risk for *Leptospira* infection, Salvador, Brazil, 2013–2015*

Variable	Odds ratio (95% CI)
Per year of age	1.02 (1.02–1.03)
Male sex	1.98 (1.48–2.64)
Cumulative rainfall, cm†	0.986 (0.977–0.995)
Period	
1	Referent
2	1.15 (0.63–2.10)
3	0.30 (0.15–0.59)
4	0.44 (0.20–0.97)

*We used Generalized Estimating Equation to evaluate the association of rainfall, follow-up period, and patient age and sex on *Leptospira* infection, as ascertained by serologic evidence, assuming a dependence on the individual level across the 4 repeated measures.

†Cumulative amount of rainfall experienced by participant between sequential samples.

manifest clinically outside of normal seasonal periods of heavy rainfall. In addition, the differences observed during the time periods independent from rainfall indicate that other unexplained factors may influence the temporal risk for *Leptospira* infection. Identifying these factors will help enhance intervention strategies in urban slum environments.

Acknowledgments

We thank the Community Health Council of Pau da Lima and the members of the Pau da Lima community in Salvador, Brazil. We also thank team members from the Urban Health Council of Pau da Lima and Oswaldo Cruz Foundation.

The study was supported by grants from the Fogarty International Center (R25 TW009338, R01 TW009504) and National Institute of Allergy and Infectious Diseases (F31 AI114245, R01 AI121207) from the National Institutes of Health; the UK Medical Research Council (MR/P0240841); the Wellcome Trust (102330/Z/13/Z); and the Fulbright Foundation.

About the Author

While developing this work, Dr. Hacker was a PhD candidate in the Department of Epidemiology of Microbial Disease at Yale University. She is a postdoctoral fellow at the University of Pennsylvania focusing on risk mapping of zoonotic diseases in complex urban settings in the Department of Biostatistics, Epidemiology, and Informatics. Mr. Sacramento is pursuing a PhD in biotechnology in health and investigative medicine at Fiocruz Brazil. His research interests include the epidemiology of zoonotic disease, transmission dynamics, and environmental dynamics affecting the transmission of disease in urban communities.

References

- Costa F, Hagan JE, Calcagno J, Kane M, Torgerson P, Martinez-Silveira MS, et al. Global morbidity and mortality of leptospirosis: a systematic review. *PLoS Negl Trop Dis*. 2015;9:e0003898. <https://doi.org/10.1371/journal.pntd.0003898>
- Bharti AR, Nally JE, Ricaldi JN, Matthias MA, Diaz MM, Lovett MA, et al.; Peru-United States Leptospirosis Consortium. Leptospirosis: a zoonotic disease of global importance. *Lancet Infect Dis*. 2003;3:757–71. [https://doi.org/10.1016/S1473-3099\(03\)00830-2](https://doi.org/10.1016/S1473-3099(03)00830-2)
- Hagan JE, Moraga P, Costa F, Capián N, Ribeiro GS, Wunder EA Jr, et al. Spatiotemporal determinants of urban leptospirosis transmission: four-year prospective cohort study of slum residents in Brazil. *PLoS Negl Trop Dis*. 2016;10:e0004275. <https://doi.org/10.1371/journal.pntd.0004275>
- Ko AI, Galvão Reis M, Ribeiro Dourado CM, Johnson WD Jr, Riley LW; Salvador Leptospirosis Study Group. Urban epidemic of severe leptospirosis in Brazil. *Lancet*. 1999;354:820–5. [https://doi.org/10.1016/S0140-6736\(99\)80012-9](https://doi.org/10.1016/S0140-6736(99)80012-9)
- Gouveia EL, Metcalfe J, de Carvalho AL, Aires TS, Villasboas-Bisneto JC, Queiroz A, et al. Leptospirosis-associated severe pulmonary hemorrhagic syndrome, Salvador, Brazil. *Emerg Infect Dis*. 2008;14:505–8. <https://doi.org/10.3201/eid1403.071064>
- McBride AJA, Athanzio DA, Reis MG, Ko AI. Leptospirosis. *Curr Opin Infect Dis*. 2005;18:376–86. <https://doi.org/10.1097/01.qco.0000178824.05715.2c>
- Felzemburgh RD, Ribeiro GS, Costa F, Reis RB, Hagan JE, Melendez AX, et al. Prospective study of leptospirosis transmission in an urban slum community: role of poor environment in repeated exposures to the *Leptospira* agent. *PLoS Negl Trop Dis*. 2014;8:e2927. <https://doi.org/10.1371/journal.pntd.0002927>
- Reis RB, Ribeiro GS, Felzemburgh RDM, Santana FS, Mohr S, Melendez AXTO, et al. Impact of environment and social gradient on *Leptospira* infection in urban slums. *PLoS Negl Trop Dis*. 2008;2:e228. <https://doi.org/10.1371/journal.pntd.0000228>
- Centers for Disease Control and Prevention. 2017 hurricane key messages. Atlanta: Centers for Disease Control and Prevention; 2017 [cited 2019 Dec 17]. https://www.cdc.gov/disasters/KeyMessages_Harvey/docs/2017_Hurricane_Key_Messages_9.8.2017.pdf
- Maskey M, Shastri JS, Saraswathi K, Surpam R, Vaidya N. Leptospirosis in Mumbai: post-deluge outbreak 2005. *Indian J Med Microbiol*. 2006;24:337–8. <https://doi.org/10.4103/0255-0857.29413>
- Riediger IN, Stoddard RA, Ribeiro GS, Nakatani SM, Moreira SDR, Skraba I, et al. Rapid, actionable diagnosis of urban epidemic leptospirosis using a pathogenic *Leptospira lipL32*-based real-time PCR assay. *PLoS Negl Trop Dis*. 2017;11:e0005940. <https://doi.org/10.1371/journal.pntd.0005940>
- Lau CL, Smythe LD, Craig SB, Weinstein P. Climate change, flooding, urbanisation and leptospirosis: fuelling the fire? *Trans R Soc Trop Med Hyg*. 2010;104:631–8. <https://doi.org/10.1016/j.trstmh.2010.07.002>
- Flannery B, Pereira MM, Velloso L de F, Carvalho C de C, De Codes LG, Orrico G de S, et al. Referral pattern of leptospirosis cases during a large urban epidemic of dengue. *Am J Trop Med Hyg*. 2001;65:657–63. <https://doi.org/10.4269/ajtmh.2001.65.657>

Address for correspondence: Federico Costa, Universidade Federal da Bahia, R. Basílio da Gama, 316 Canela, Salvador, 40110-040, Bahia, Brazil; email: federico.costa@ufba.br

Systematic Hospital-Based Travel Screening to Assess Exposure to Zika Virus¹

Aftab Iqbal, Robert Colgrove, Vito Iacoviello, Barbra M. Blair, Lin H. Chen

We queried hospital patients about international travel in the previous 30 days to assess potential importation of emerging infections. We used 12 months of deidentified data to analyze patient demographics, travel destinations, and diagnoses for exposure to Zika virus. Our approach could be used to analyze potential infectious disease exposures.

Incidence of Zika virus (ZIKV) infections rose rapidly in early 2015, and local transmission was confirmed in 84 countries and territories by March 2017 (1). Although ZIKV typically causes mild symptoms (2,3), in utero infection can cause congenital Zika syndrome (4,5). The threat of in utero infection, along with sexual transmission (6,7), led to advisories for women who were pregnant, or might become pregnant, and their partners to avoid travel to countries or areas with ZIKV transmission (7–10).

After implementing reactive screening during several global infectious disease outbreaks, including the 2014 Ebola outbreak, Mount Auburn Hospital (Cambridge, Massachusetts, USA) incorporated a standardized screening question regarding international travel into all hospital visits beginning in September 2015. To detect potential travel-associated exposures, patients were asked, “Have you traveled outside of the U.S. within the past 30 days?” Each quarter during November 1, 2015–October 31, 2016, we aggregated deidentified patient data to estimate the proportion of patients with potential ZIKV exposure and the possibility for congenital Zika syndrome.

Author affiliations: Providence Community Health Centers, Providence, Rhode Island, USA (A. Iqbal); Mount Auburn Hospital, Cambridge, Massachusetts, USA (A. Iqbal, R. Colgrove, V. Iacoviello, L.H. Chen); Beth Israel Deaconess Medical Center, Boston, Massachusetts, USA (B.M. Blair); Harvard Medical School, Boston (R. Colgrove, V. Iacoviello, B.M. Blair, L.H. Chen)

DOI: <https://doi.org/10.3201/eid2602.190292>

The Study

During November 1–December 31, 2016, we retrospectively analyzed deidentified patient demographic, travel destination, and medical services data from the hospital database. We analyzed records from patients admitted as inpatients, and those seen in the emergency department/walk-in center (ED/WIC) and by other services during November 1, 2015–October 31, 2016. We included data from patients who responded “yes” to the travel screening question and provided a travel history and for whom diagnostic data were available. We categorized destination countries according to the World Health Organization 2016 classification for ZIKV transmission (11): category 1, countries that reported outbreaks from 2015 onward; category 2, countries with possible endemic transmission or evidence of local mosquito-borne ZIKV infections in 2016; and category 3, countries with evidence of local mosquito-borne ZIKV infections during or before 2015, but without documentation of cases in 2016, or designated as outbreak terminated. We defined reproductive age as 15–49 years of age for female patients and ≥15 years of age for male patients (12). We extracted records with International Classification of Diseases, 10th Revision, codes applicable to pregnancy, including Z33.1, Z34.91, Z34.92, Z34.93, and Z34.90, and diagnosis descriptions that met the Zika disease case definition (3), which includes fever, rash, arthralgia, conjunctivitis, complication of pregnancy, or Guillain-Barré syndrome. We performed analyses by using IBM SPSS Statistics 17.0 (IBM, <https://www.ibm.com>). The Mount Auburn Hospital Institutional Review Board determined the activity to be exempt from review and approval.

We identified 5,642 patients who reported travel ≤30 days before their hospital visit. Of 5,004

¹Preliminary results were presented at the 65th Annual Meeting of the American Society of Tropical Medicine and Hygiene, Atlanta, Georgia, November 12–17, 2016.

Table 1. Countries visited most frequently in the previous 30 days by 5,004 travelers and Zika-affected countries visited by 1,570 travelers, Cambridge, Massachusetts, USA

Rank	All destinations visited		Destinations with ZIKV transmission*	
	Destination	No. (%) travelers	Destination	No. (%) travelers
1	Canada	778 (15.5)	Mexico	318 (20.2)
2	United Kingdom	363 (7.2)	Dominican Republic	119 (7.5)
3	Mexico	318 (6.4)	Aruba	102 (6.4)
4	France	315 (6.3)	Brazil	85 (5.4)
5	Italy	265 (5.3)	Costa Rica	84 (5.3)
6	Germany	227 (4.5)	Puerto Rico	83 (5.2)
7	China	200 (4.0)	Bahamas	81 (5.1)
8	Ireland	158 (3.2)	Virgin Islands	57 (3.6)
9	India	155 (3.1)	Colombia	48 (3.1)
10	Spain	150 (3.0)	Cuba	45 (2.8)

*According to the World Health Organization (11). ZIKV, Zika virus.

patients who had complete demographic, destination, and diagnostic data, 3,109 (62.1%) were female and 1,895 (37.9%) male; patients were 10 months–94 years of age. A total of 959 (19%) were evaluated in the ED/WIC, and 161 (3.2%) with recent travel were hospitalized. The most frequently visited destinations were Canada, the United Kingdom, and Mexico (Table 1).

Among female patients, 1,579 (50.8%) were of reproductive age and 176 (5.7%) were pregnant. Among male patients, 1,850 (97.6%) were of reproductive age. Overall, 475 (30%) female and 514 (28%) male patients of reproductive age traveled to countries with ZIKV transmission. Of 176 pregnant women, 38 (22%) had

traveled to countries with ZIKV transmission within the previous 30 days; 21 were in the first trimester (Figure).

When analyzed for destinations in WHO categories 1–3 (11), 1,492 travelers, 963 female and 529 male, visited 1,570 destinations with ZIKV transmission. Mexico, the Dominican Republic, Aruba, Brazil, and Costa Rica (Table 1) were the most frequently visited destinations, and the Caribbean was the most frequently visited region ($n = 648$).

Among patients who traveled to countries with ZIKV transmission whose admitting diagnosis or description was available, 42 listed symptoms compatible with ZIKV infection (Table 2). We did not

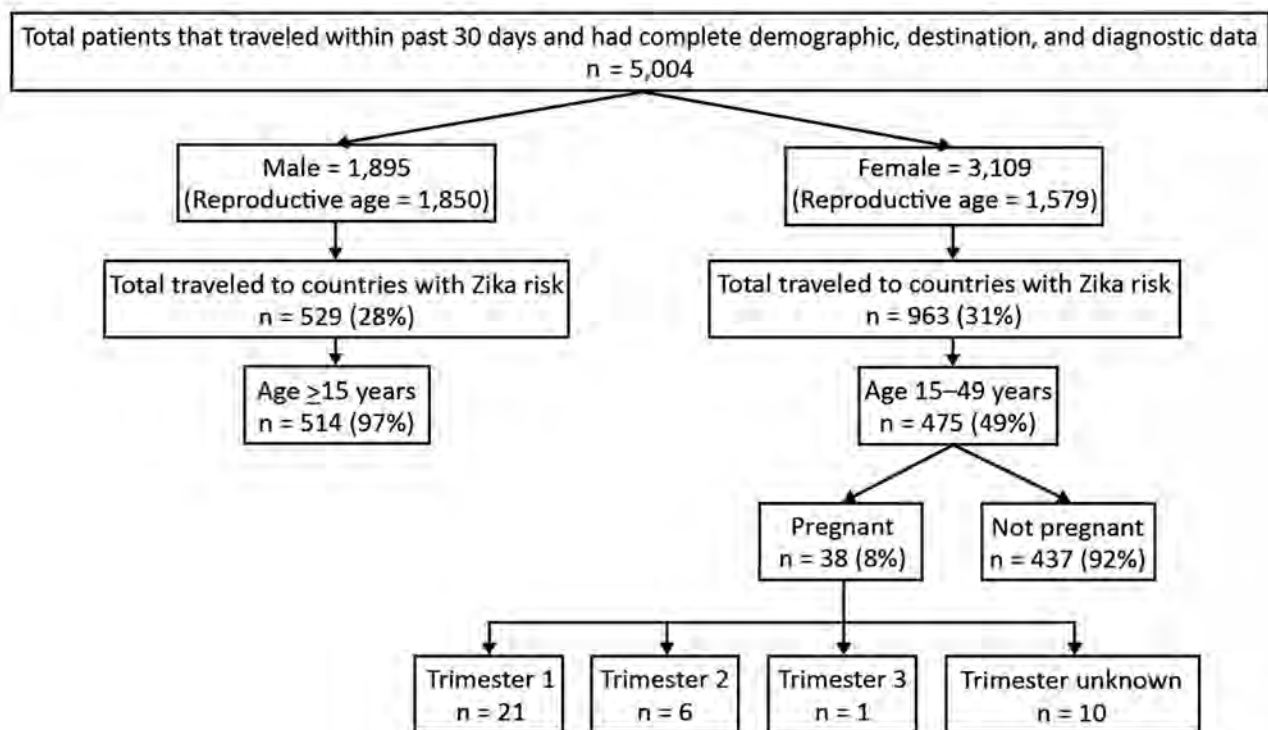


Figure. Flowchart of possible Zika virus exposure based on travel destination, sex, and pregnancy status in patients responding to a question on international travel ≤ 30 days before seeking care at a hospital, Cambridge, Massachusetts, USA.

Table 2. Results of search for symptoms compatible with Zika virus clinical criteria in a study of travel screening for Zika virus infection, Cambridge, Massachusetts, USA*

Patient age, y/sex	Date of hospital visit	Destinations visited	Diagnosis and symptoms at admission
40/F	2015 Nov	Malaysia	Rash and other nonspecific skin eruption
49/F	2015 Nov	Thailand	Pruritus, unspecified; rash and other nonspecific skin eruption
59/F	2015 Nov	Malaysia, Indonesia	Fever, unspecified
15/F	2015 Nov	Costa Rica	Fever, unspecified; rash and other nonspecific skin eruption; myalgia
29/M	2015 Nov	Mexico	Unidentified influenza virus with other respiratory manifestations; fever, unspecified
5/M	2015 Dec	Brazil	Viral infection, unspecified; rash and other nonspecific skin eruption; fever, unspecified
48/M	2015 Dec	Mexico	Acute pharyngitis, unspecified; rash and other nonspecific skin eruption
40/M	2015 Dec	Mexico	Acute pharyngitis, unspecified; fever, unspecified
28/F	2016 Jan	Indonesia	Fever, unspecified; acute pharyngitis, unspecified; cough; myalgia
34/F	2016 Jan	The Bahamas	Viral infection, unspecified; fever, unspecified
61/F	2016 Jan	Mexico	Rash and other nonspecific skin eruption
39/F	2016 Jan	Argentina	Rash and other nonspecific skin eruption
1/M	2016 Jan	Mexico	Rash and other nonspecific skin eruption; fever, unspecified
33/M	2016 Jan	Colombia	Rash and other nonspecific skin eruption
55/M	2016 Jan	Costa Rica	Fever, unspecified; rash and other nonspecific skin eruption
58/F	2016 Feb	Mexico	Acute pharyngitis, unspecified; fever, unspecified; myalgia
UNK/M	2016 Feb	Brazil	Rash, cough, fever, sneezing; viral infection, unspecified
31/M	2016 Feb	Brazil	Viral infection, unspecified; rash and other nonspecific skin eruption
31/M	2016 Feb	Brazil	Posttravel follow-up; requested screening for other viral diseases; rash and other nonspecific skin eruption
28/F	2016 Mar	Costa Rica	Influenza-like symptoms; viral infection, unspecified
28/F	2016 Mar	Mexico	Rash and other nonspecific skin eruption
46/F	2016 Mar	Jamaica, Mexico	Influenza-like symptoms; cough; unidentified influenza virus with unspecified type of pneumonia
21/M	2016 Mar	Mexico	Influenza-like symptoms; viral infection, unspecified
32/M	2016 Mar	The Bahamas	Headache, back pain, vomiting; fever, unspecified; nausea with vomiting, unspecified
30/F	2016 Apr	Brazil	Fever and aches; viral infection, unspecified
69/F	2016 Apr	Haiti	Fever, unspecified
26/M	2016 Apr	Dominican Republic	Headache with rash; viral infection, unspecified
26/F	2016 May	Thailand	Fever, unspecified
39/F	2016 Jun	Mexico	Rash and other nonspecific skin eruption; nonvenomous insect bites on left and right upper arm
25/M	2016 Jun	Puerto Rico	Rash and other nonspecific skin eruption; other fatigue
44/F	2016 Jul	Dominican Republic	Rash and other nonspecific skin eruption
29/M	2016 Jul	Dominican Republic	Influenza-like symptoms Viral infection, unspecified
15/M	2016 Jul	Trinidad and Tobago	Rash and other nonspecific skin eruption Fever, unspecified; acute pharyngitis, unspecified
44/F	2016 Aug	Nicaragua	Rash and other nonspecific skin eruption
51/F	2016 Aug	Dominican Republic	Cough; fever, unspecified
51/M	2016 Aug	Malaysia, Turkey	Cough; fever, unspecified
36/M	2016 Aug	Brazil	Posttravel screening; fever, unspecified; unspecified conjunctivitis
28/F	2016 Sep	Chile	Influenza-like symptoms
34/F	2016 Sep	Indonesia	Acute pharyngitis, unspecified; fever, unspecified
28/F	2016 Sep	Virgin Islands	Rash; unspecified viral infection
39/M	2016 Sep	Dominican Republic	Rash and other nonspecific skin eruption
30/M	2016 Sep	Colombia	Possible Zika virus; patient was ill after travel

*Symptoms include rash, fever, conjunctivitis, arthralgia or myalgia, complications in pregnancy, or Guillain-Barré syndrome. Patients were asked, "Have you traveled outside the U.S. in the past 30 days?" UNK, unknown.

identify Guillain-Barré syndrome or any complications of pregnancy among the 42 patients, but 2 had laboratory-confirmed ZIKV infection.

Our results approximate the Global Travel Epidemiology Network analysis of pretravel consultations (13), in which 28% of 22,736 travelers planned trips to ZIKV-affected countries and >75% were of reproductive age. Another study retrospectively reviewed 46 patients for possible ZIKV infection and found 17%

had laboratory evidence of infection (14). Applying this seropositivity rate to our study, if testing had been done, 7 patients with symptoms compatible with ZIKV clinical criteria might have had laboratory-confirmed ZIKV infection.

We found that a standardized question to screen for international travel provided a description of travel patterns for this patient community. Data from the 12-month period coincided with the rapid

spread of ZIKV and revealed the sizable portion of patients who might have been exposed to ZIKV during travel. Population-based analysis of travel-related ZIKV exposure could provide estimates of at-risk populations and diagnostic testing needs, especially for pregnant women. The application is especially promising with newer electronic health record systems. However, limited testing capability might have underestimated the actual number of travel-associated cases (15), even when clinicians suspected ZIKV.

Our study had some limitations. Because we only reviewed the population at 1 hospital during a single 12-month period, our results might not be generalizable to the US population. Our analysis relied on recent travel to countries and territories that reported ZIKV transmission, but some travelers might have visited risk-free settings, such as locations at higher altitudes, resulting in overestimation of the number of possible infections. Infectious ZIKV has been detected in semen mainly ≤ 30 days after fever onset, but its presence in semen has been documented longer (10,15); therefore, the potential number of ZIKV infections might exceed our estimate because sexual partners could become infected. Also, we did not have information on whether the patients of reproductive age were sexually active, fertile, had pregnant partners, or were planning conception. We might have missed cases for the following reasons: we relied on diagnoses and diagnostic descriptions, but omission of symptoms in these fields might not represent truly absent symptoms; some infected persons might have been unaware of ZIKV and might not have sought medical evaluation; the incubation period of sexually transmitted ZIKV might be >30 days and patients might have become ill after being seen; we did not collect or record ZIKV infections identified after the study period; only patients strongly suspected of ZIKV were tested due to limited laboratory capacity; and the travel screening question would not have identified sexually transmitted ZIKV infection in a patient who had not traveled internationally.

Conclusions

We used a systematic travel screening question to analyze potential exposure to ZIKV in a hospital population. Because up to 80% of ZIKV infections are asymptomatic (2), we used travel to Zika-affected countries as a proxy for potential ZIKV exposure. In patients with international travel ≤ 30 days before seeking treatment, 31.4% visited countries with ZIKV transmission. Half of the female patients

and most male patients were of reproductive age. In this population, 30% of female patients who were of reproductive age or pregnant reported travel with potential exposure to ZIKV; male patients similarly were affected. Despite severe restrictions on testing for ZIKV infection at the time of the study, our analysis demonstrated the ability to identify patients with clinical findings that fit the ZIKV case definition even if they were not tested. We also identified a large proportion of patients who should have received Zika pretravel counseling.

Analysis of the hospitalwide data for recent travel history provided a tool to assess the proportion of the population that might have been exposed to ZIKV. These data could inform population-based ZIKV vaccination needs in the future. In addition, systematic travel screening also could be applied to other imported emerging infections in the future.

Acknowledgments

The authors thank Mary Elizabeth Wilson for her advice and Andrew Gardner for his assistance on data download and aggregation.

This project is supported in part by the Mount Auburn Hospital Medical Staff Executive Committee Research Grant 2015.

Disclosures: L.H.C. reports past advisor fees from Shoreland, Inc., and past Data Safety Monitoring Board service for Valneva, Inc., outside the submitted work. Other authors report no financial relationship.

About the Author

Dr. Iqbal currently is a primary care physician at Providence Community Health Centers, Providence, Rhode Island, USA. His primary research interest is in the health of globally mobile residents, including recent and first generation immigrants.

References

1. World Health Organization. Situation report: Zika virus, microcephaly, Guillain-Barre syndrome, 10 March 2017 [cited 2017 Nov 13]. <https://www.who.int/emergencies/zika-virus/situation-report/10-march-2017>
2. Petersen LR, Jamieson DJ, Powers AM, Honein MA. Zika Virus. *N Engl J Med*. 2016;374:1552-63. <https://doi.org/10.1056/NEJMra1602113>
3. Council of State and Territorial Epidemiologists. Zika virus disease and congenital Zika virus infection interim case definition and addition to the nationally notifiable diseases list [cited 2016 Apr 22]. http://www.cste2.org/docs/Zika_Virus_Disease_and_Congenital_Zika_Virus_Infection_Interim.pdf

4. Rasmussen SA, Jamieson DJ, Honein MA, Petersen LR. Zika virus and birth defects—reviewing the evidence for causality. *N Engl J Med*. 2016;374:1981–7. <https://doi.org/10.1056/NEJMSr1604338>
5. Johansson MA, Mier-y-Teran-Romero L, Reefhuis J, Gilboa SM, Hills SL. Zika and the risk of microcephaly. *N Engl J Med*. 2016;375:1–4. <https://doi.org/10.1056/NEJMp1605367>
6. Hamer DH, Wilson ME, Jean J, Chen LH. Epidemiology, prevention, and potential future treatments of sexually transmitted Zika virus infection. *Curr Infect Dis Rep*. 2017;19:16. <https://doi.org/10.1007/s11908-017-0571-z>
7. World Health Organization. Prevention of sexual transmission of Zika virus: interim guidance update, 6 September 2016. WHO/ZIKV/MOC/16.1 Rev.3 [cited 2016 September 6]. <https://www.who.int/csr/resources/publications/zika/sexual-transmission-prevention>
8. Petersen EE, Polen KND, Meaney-Delman D, Ellington SR, Oduyebo T, Cohn A, et al. Update: interim guidance for health care providers caring for women of reproductive age with possible Zika virus exposure—United States, 2016. *MMWR Morb Mortal Wkly Rep*. 2016;65:315–22. <https://doi.org/10.15585/mmwr.mm6512e2>
9. Oduyebo T, Petersen EE, Rasmussen SA, Mead PS, Meaney-Delman D, Renquist CM, et al. Update: Interim guidelines for health care providers caring for pregnant women and women of reproductive age with possible Zika virus exposure—United States, 2016. *MMWR Morb Mortal Wkly Rep*. 2016;65:122–7. <https://doi.org/10.15585/mmwr.mm6505e2>
10. Oster AM, Russell K, Stryker JE, Friedman A, Kachur RE, Petersen EE, et al. Update: Interim guidance for prevention of sexual transmission of Zika virus—United States, 2016. *MMWR Morb Mortal Wkly Rep*. 2016;65:323–5. <https://doi.org/10.15585/mmwr.mm6512e3>
11. World Health Organization. Situation report: Zika virus, microcephaly, Guillain-Barré syndrome, 3 November 2016 [cited 2017 Nov 13]. <https://www.who.int/emergencies/zika-virus/situation-report/3-november-2016>
12. World Health Organization. Reproductive health indicators: guidelines for their generation, interpretation and analysis for global monitoring [cited 2017 Nov 13]. https://apps.who.int/iris/bitstream/handle/10665/43185/924156315X_eng.pdf
13. Lammert S, Walker AT, Erskine S, Rao SR, Esposito DH, Ryan ET, et al. Characteristics of US travelers to Zika virus-affected countries in the Americas, March 2015–October 2016. *Emerg Infect Dis*. 2017;23:324–7. <https://doi.org/10.3201/eid2302.161292>
14. Valle J, Eick SM, Fairley JK, Waggoner JJ, Goodman RA, Rosenberg E, et al. Evaluation of patients for Zika virus infection in a travel clinic in the southeast United States, 2016. *South Med J*. 2019;112:45–51. <https://doi.org/10.14423/SMJ.0000000000000917>
15. Graciaa DS, Collins MH, Wu HM. Zika in 2018: advising travelers amid changing incidence. *Ann Intern Med*. 2018;169:337–8. <https://doi.org/10.7326/M18-1112>

Address for correspondence: Lin H. Chen, Mount Auburn Hospital, Division of Infectious Diseases and Travel Medicine, 330 Mount Auburn St, Cambridge, MA 02138, USA; email: lchen@hms.harvard.edu

EID SPOTLIGHT TOPIC Zika virus



Zika virus is spread to people through mosquito bites. Outbreaks of Zika have occurred in areas of Africa, Southeast Asia, the Pacific Islands, and the Americas. Because the *Aedes* species of mosquitoes that spread Zika virus are found throughout the world, it is likely that outbreaks will spread to new countries. In May 2015, the Pan American Health Organization issued an alert regarding the first confirmed Zika virus infection in Brazil. In December 2015, Puerto Rico reported its first confirmed Zika virus case.

<https://wwwnc.cdc.gov/eid/page/zika-spotlight>

**EMERGING
INFECTIOUS DISEASES®**

Elizabethkingia anophelis Infection in Infants, Cambodia, 2012–2018

Thomas A.N. Reed, Gabriella Watson, Chheng Kheng, Pisey Tan, Tamalee Roberts, Clare L. Ling, Thyl Miliya, Paul Turner

We describe 6 clinical isolates of *Elizabethkingia anophelis* from a pediatric referral hospital in Cambodia, along with 1 isolate reported from Thailand. Improving diagnostic microbiological methods in resource-limited settings will increase the frequency of reporting for this pathogen. Consensus on therapeutic options is needed, especially for resource-limited settings.

Elizabethkingia anophelis is a recently identified aerobic, nonmotile, oxidase-positive, indole-positive species of gram-negative bacillus (1,2) that has been implicated in nosocomial and community outbreaks and associated with high mortality rates (3,4). We report a case of *E. anophelis* bacteremia in an infant in Cambodia in October 2018 and a retrospective study to identify previously misidentified isolates and describe the clinical features of *E. anophelis*-associated pediatric illness in Cambodia.

The Study

A 7-day-old girl was brought to her local hospital with difficulty in breathing and poor feeding. She was a twin, born vaginally at 36 weeks' gestation, with no antenatal or delivery complications. Both her mother and twin were in good health. Hospital staff administered ampicillin (50 mg/kg 2×/d) and gentamicin (5 mg/kg/36 h).

The patient was transferred to the pediatric intensive care unit of Angkor Hospital for Children, a non-governmental pediatric hospital in Siem Reap, Cambodia, with presumed late-onset neonatal sepsis. Upon arrival, she was cyanotic with recurrent apneas, requiring intubation, and had jaundice. Clinical examination and vital signs were otherwise unremarkable. Blood tests showed a leukocyte count of $8.5 \times 10^9/L$ (neutrophils $6.4 \times 10^9/L$); hemoglobin 16.9 g/dL; platelet count

$45 \times 10^9/L$; C-reactive protein 195 mg/L; and total bilirubin 252 $\mu\text{mol/L}$. Lumbar puncture was omitted due to thrombocytopenia. A blood culture was transferred with her from the local hospital.

The day after transfer, she experienced symptoms of meningitis, including fever and seizures. We initiated anticonvulsant therapy and changed her antimicrobial therapy to intravenous meropenem (40 mg/kg 3×/d). Blood culture microscopy subsequently showed gram-negative bacilli, identified as *E. anophelis* on hospitalization day 3 by matrix-assisted laser desorption/ionization time-of-flight (MALDI-TOF) mass spectrometry using bioMérieux VITEK MS in an in vitro diagnostic mode using the spectrum knowledge base version 3.2.0 (bioMérieux, <https://www.biomerieux.com>). At this stage antimicrobial drugs were changed to intravenous ciprofloxacin (10 mg/kg, 2×/d) and vancomycin (15 mg/kg, 1×/d); a blood culture collected before the change confirmed bacteremia caused by *E. anophelis*.

The patient was extubated on day 6 and underwent lumbar puncture because her platelet count had improved. Cerebrospinal fluid was cloudy, with a leukocyte count of 265 cells/ μL (75% polymorphs), glucose of 1 mmol/L, and protein of 13 g/L. Gram stain microscopy revealed no organisms, and culture was negative. After 28 days of ciprofloxacin/vancomycin, she was clinically well and discharged home.

At her 1-month follow-up appointment, she displayed clinical features of raised intracranial pressure, including neurologic deficits. Cranial ultrasound showed hydrocephalus, a suspected sequela of meningitis, and she was referred for neurosurgical opinion.

After the case described was identified, we retrieved all isolates in -80°C storage that had been identified since January 2012 as *Chryseobacterium meningosepticum*, *C. miricola*, or *Elizabethkingia* spp. We included in our study the first isolates from a given clinical episode: 4 identified as *C. meningosepticum*, 3 as *E. meningoseptica*, and the isolate already identified as *E. anophelis*. From subculture, we analyzed these using VITEK MS MALDI-TOF mass spectrometry. We identified

Author affiliations: Angkor Hospital for Children, Siem Reap, Cambodia (T.A.N. Reed, G. Watson, C. Kheng, P. Tan, T. Miliya, P. Turner); Lao-Oxford-Mahosot Hospital, Vientiane, Laos (T. Roberts); Mahidol University, Mae Sot, Thailand (C.L. Ling); University of Oxford, Oxford, UK (C.L. Ling, P. Turner)

DOI: <https://doi.org/10.3201/eid2602.190345>

6 isolates as *E. anophelis* and 1 as *E. meningoseptica*. MALDI-TOF was unable to return an identification for 1 isolate, previously identified as *C. meningosepticum*.

We determined MICs to antimicrobial drugs for all *E. anophelis* isolates using Etest (bioMérieux). MIC₅₀ result for ceftriaxone was 64 µg/mL; for sulfamethoxazole/trimethoprim, 0.25 µg/mL; for ciprofloxacin, 0.5 µg/mL; and for vancomycin, 12 µg/mL (Table).

To provide regional context for these results, 2 microbiology laboratories in Mae Sot, Thailand, and Vientiane, Laos, also reanalyzed stored clinical isolates as we described. In Mae Sot, a single isolate of *E. meningoseptica* from a neonatal blood culture was reidentified as *E. anophelis*. In Vientiane, 9 isolates of *C. meningosepticum* were reidentified as *E. meningoseptica*, and the identity of 1 *E. meningoseptica* isolate remained the same.

Conclusions

Although reports of *E. anophelis* are rare, cases are reported from countries in southern Asia, including Singapore (3), Taiwan (5), and Hong Kong (6). Our findings are consistent with reports of *E. anophelis* infection from other countries demonstrating it to be an opportunistic organism affecting more vulnerable patient groups (6). The mortality rate associated with

E. anophelis is high (50%), and isolation of *E. anophelis* from blood in two thirds of the children in this study demonstrates its importance as a human pathogen.

Previous reports of community- and hospital-acquired *E. anophelis* infection among infants have proposed a range of transmission routes, including vectorborne (*Anopheles* mosquitoes) (1,2,7), waterborne (8), and vertical transmission (9). With no temporal clustering, and with most cases occurring among older infants, we suspect that unidentified environmental reservoirs are possible sources of these cases.

Previously, studies relied on 16S rRNA testing to identify *E. anophelis*, with biochemical phenotypic methods unable to distinguish between *Elizabethkingia* spp. (10). Although this method provides high discriminatory power, its use in diagnostic microbiology is limited to established laboratory settings. It also requires highly trained staff to interpret results, which are rarely available within a clinically useful timeframe. Until late 2017, oxidase-positive gram-negative isolates were identified at the microbiology laboratory at Angkor Hospital for Children by biochemical phenotypic methods (API 20NE, bioMérieux); identification is now done by MALDI-TOF mass spectrometry. Misidentification of *Elizabethkingia* spp. using biochemical methods has been reported (2,6); however, updated MALDI-TOF databases

Table. Characteristics of *Elizabethkingia anophelis* isolates from Cambodia and Thailand*

Characteristic	Isolate no.						
	1 (this study)	2	3	4	5	6	7
Patient characteristics							
Sex	F	M	F	M	F	M	F
Age at admission	6 d	8 mo	15 wk	0 d	51 d	0 d	0 d
Concurrent condition	Prematurity†	Duodenal atresia	Failure to thrive	Prematurity†	Ventricular septal defect	Prematurity†	Prematurity†
Country	Cambodia	Cambodia	Cambodia	Cambodia	Cambodia	Cambodia	Thailand
Clinical features							
Diagnosis	Meningitis	VAP	Meningitis	Sepsis	VAP	Sepsis	Sepsis
Treatment	CIP/VAN	MER	CAX	AMP/GM	CIP	IMP	AMP/GM
Outcome	Survived	Died	Unknown‡	Died	Died	Survived	Died
Length of admission, d	31	16	1	5	79	35	25
Specimen details							
Collection date	2018 Oct	2018 Jan	2015 Aug	2013 Aug	2012 Sep	2012 Mar	2017 Apr
Specimen type	Blood	Respiratory secretion	Blood	Blood	Respiratory secretion	Blood	Blood
Hospitalization day collected	1	16	1	5	64	21	22
Isolate details							
First ID	<i>E. anophelis</i>	<i>E. meningoseptica</i>			<i>C. meningosepticum</i>		<i>E. meningoseptica</i>
Initial ID method	MALDI-TOF	MALDI-TOF	API 20NE	API 20NE	API 20NE	API 20NE	API 20NE
MIC (µg/mL)							
VAN	8	16	16	16	8	16	8
SXT	0.25	0.25	0.25	0.5	0.25	0.5	NA§
CAX	32	64	>256	64	64	>256	>256
CIP	1	0.5	0.5	0.5	0.5	0.5	1

*AMP, ampicillin; CAX, ceftriaxone; CIP, ciprofloxacin; F, female; GM, gentamicin; ID, identification; IMP, imipenem; M, male; MER, meropenem; SXT, sulfamethoxazole/trimethoprim; VAN, vancomycin; VAP, ventilator-associated pneumonia.

†It was not possible to retrieve gestational age for all patients.

‡Patient left hospital against medical advice.

§Sulfamethoxazole/trimethoprim MIC testing not available in the Thailand laboratory.

provide reliable differentiation (10). As the resolution that MALDI-TOF mass spectrometry provides in pathogen identification expands, and its use becomes available in low- and middle-income countries, we expect to see higher reported incidence of *E. anophelis* infection. Conversely, it may become apparent that the burden of *E. meningoseptica* is not as high as previously thought, with retrospective studies already showing *E. anophelis* as the predominant species of its genus (6,10,11). In our study, this possibility was not found to be the case in Laos, suggesting possible regional variation.

E. anophelis demonstrates phenotypic and genotypic resistance to multiple antimicrobial drugs, and, without epidemiologically based interpretive cutoffs, selection of therapeutic options is challenging (4,5,10,12). High MICs to ceftriaxone are consistent with β -lactam resistance reported elsewhere, and carbapenem resistance should also be expected (4,5,10,12). Following Clinical and Laboratory Standards Institute guidelines (M100–29; 2019) (13) for “other non-*Enterobacteriaceae*,” these isolates were susceptible to ciprofloxacin and sulfamethoxazole/trimethoprim. This finding is not consistent with other regional data that show greater rates of resistance to these drugs (5,10). *E. anophelis* has been shown to be susceptible to piperacillin/tazobactam and to rifampin (4,10), which were not tested against in this study and are not currently available as therapeutic options in the study setting. It is unusual for gram-negative organisms to exhibit susceptibility to vancomycin, and interpretation of MICs to this drug should be approached with caution. Use of Etest in this study was a methodological limitation; the preferred method of broth microdilution was not available.

In summary, updates of mass spectrometry platforms have enabled identification of clinical *E. anophelis* isolates in Cambodia and Thailand. As diagnostic microbiology capacity expands in low- and middle-income countries, further reports of this organism are expected. Because of the associated high mortality rates for this pathogen, consensus on therapeutic options for infection caused by *E. anophelis* is needed, especially in resource-limited settings with restricted choices for antimicrobial drugs.

Acknowledgments

We thank Verena Carrara and the microbiology department of Shoklo Malaria Research Unit for their assistance in laboratory work and collecting of clinical details.

About the Author

Dr. Reed is a research clinician at the Cambodia-Oxford Medical Research Unit, Angkor Hospital for Children, Siem Reap, Cambodia. His primary research interest is antimicrobial resistance.

References

- Kämpfer P, Matthews H, Glaeser SP, Martin K, Lidders N, Faye I. *Elizabethkingia anophelis* sp. nov., isolated from the midgut of the mosquito *Anopheles gambiae*. *Int J Syst Evol Microbiol*. 2011;61:2670–5. <https://doi.org/10.1099/ijs.0.026393-0>
- Frank T, Gody JC, Nguyen LBL, Berthet N, Le Fleche-Mateos A, Bata P, et al. First case of *Elizabethkingia anophelis* meningitis in the Central African Republic. *Lancet*. 2013;381:1876. [https://doi.org/10.1016/S0140-6736\(13\)60318-9](https://doi.org/10.1016/S0140-6736(13)60318-9)
- Teo J, Tan SY, Tay M, Ding Y, Kjelleberg S, Givskov M, et al. First case of *E. anophelis* outbreak in an intensive-care unit. *Lancet*. 2013;382:855–6. [https://doi.org/10.1016/S0140-6736\(13\)61858-9](https://doi.org/10.1016/S0140-6736(13)61858-9)
- Perrin A, Larsonneur E, Nicholson AC, Edwards DJ, Gundlach KM, Whitney AM, et al. Evolutionary dynamics and genomic features of the *Elizabethkingia anophelis* 2015 to 2016 Wisconsin outbreak strain. *Nat Commun*. 2017;8:15483. <https://doi.org/10.1038/ncomms15483>
- Lin JN, Lai CH, Yang CH, Huang YH. Comparison of clinical manifestations, antimicrobial susceptibility patterns, and mutations of fluoroquinolone target genes between *Elizabethkingia meningoseptica* and *Elizabethkingia anophelis* isolated in Taiwan. *J Clin Med*. 2018;7:538. <https://doi.org/10.3390/jcm7120538>
- Lau SK, Chow WN, Foo CH, Curreem SO, Lo GC, Teng JL, et al. *Elizabethkingia anophelis* bacteremia is associated with clinically significant infections and high mortality. *Sci Rep*. 2016;6:26045. <https://doi.org/10.1038/srep26045>
- Raygoza Garay JA, Hughes GL, Koundal V, Rasgon JL, Mwangi MM. Genome sequence of *Elizabethkingia anophelis* strain EaAs1, isolated from the Asian malaria mosquito *Anopheles stephensi*. *Genome Announc*. 2016;4:e00084-16. <https://doi.org/10.1128/genomeA.00084-16>
- Yung CF, Maiwald M, Loo LH, Soong HY, Tan CB, Lim PK, et al. *Elizabethkingia anophelis* and association with tap water and handwashing, Singapore. *Emerg Infect Dis*. 2018;24:1730–3. <https://doi.org/10.3201/eid2409.171843>
- Lau SK, Wu AK, Teng JL, Tse H, Curreem SO, Tsui SK, et al. Evidence for *Elizabethkingia anophelis* transmission from mother to infant, Hong Kong. *Emerg Infect Dis*. 2015;21:232–41. <https://doi.org/10.3201/eid2102.140623>
- Han MS, Kim H, Lee Y, Kim M, Ku NS, Choi JY, et al. Relative prevalence and antimicrobial susceptibility of clinical isolates of *Elizabethkingia* species based on 16S rRNA gene sequencing. *J Clin Microbiol*. 2017;55:274–80. <https://doi.org/10.1128/JCM.01637-16>
- Chew KL, Cheng B, Lin RTP, Teo JWP. *Elizabethkingia anophelis* is the dominant *Elizabethkingia* species found in blood cultures in Singapore. *J Clin Microbiol*. 2018;56:e01445-17. <https://doi.org/10.1128/JCM.01445-17>
- Breurec S, Criscuolo A, Diancourt L, Rendueles O, Vandenbogaert M, Passet V, et al. Genomic epidemiology and global diversity of the emerging bacterial pathogen *Elizabethkingia anophelis*. *Sci Rep*. 2016;6:30379. <https://doi.org/10.1038/srep30379>
- Clinical and Laboratory Standards Institute (CLSI). Performance standards for antimicrobial susceptibility testing; 29th edition (M100–29). Wayne (PA): The Institute; 2019.

Address for correspondence: Thomas A.N. Reed, Cambodia-Oxford Medical Research Unit, Angkor Hospital for Children, Tep Vong (Achamean) Rd and Oum Chhay St, Svay Dangcum, PO Box 50, Siem Reap, Cambodia; email: tanreed@gmail.com

Global Expansion of Pacific Northwest *Vibrio parahaemolyticus* Sequence Type 36

Michel Abanto, Ronnie G. Gavilan, Craig Baker-Austin, Narjol Gonzalez-Escalona, Jaime Martinez-Urtaza

We report transcontinental expansion of *Vibrio parahaemolyticus* sequence type 36 into Lima, Peru. From national collections, we identified 7 isolates from 2 different Pacific Northwest complex lineages that surfaced during 2011–2016. Sequence type 36 is likely established in environmental reservoirs. Systematic surveillance enabled detection of these epidemic isolates.

Compared with other major foodborne illnesses, *Vibrio parahaemolyticus* infections have been steadily increasing (1); thus, *V. parahaemolyticus* has become the leading cause of seafood-related bacterial infections globally. The US Centers for Disease Control and Prevention estimated that the average annual incidence of all *Vibrio* infections increased by 54% during 2006–2017 (2), and *V. parahaemolyticus* infections were responsible for a large percentage of this increase in the later years (3). *V. parahaemolyticus* is believed to be responsible for ≈35,000 human infections each year in the United States alone (4) and has been identified as the leading cause of foodborne infections in China since the 1990s (5).

In some areas of the world, the steady increase in local numbers of cases associated with *V. parahaemolyticus* has coincided with the overall geographic expansion of *V. parahaemolyticus* disease. *V. parahaemolyticus* cases are now being regularly reported in areas with little previous incidence, including South America and northern Europe (6,7). Although the precise circumstances and factors driving the growth in case numbers are unclear, the transition of *V. parahaemolyticus* disease from a regional to a more global pathogen has been directly connected with the emergence of isolates with epidemic potential.

Author affiliations: University of La Frontera, Temuco, Chile (M. Abanto); Instituto Nacional de Salud, Lima, Peru (R.G. Gavilan); The Centre for Environment, Fisheries and Aquaculture Science, Weymouth, UK (C. Baker-Austin, J. Martinez-Urtaza); US Food and Drug Administration, College Park, Maryland, USA (N. Gonzalez-Escalona)

DOI: <https://doi.org/10.3201/eid2602.190362>

V. parahaemolyticus and *V. cholerae* represent the only 2 documented instances of global expansion of human pathogenic marine bacteria (8). Pandemic *V. cholerae* emerged >50 years ago, and intercontinental expansion of *V. parahaemolyticus* began ≈25 years ago. *V. parahaemolyticus* sequence type (ST) 3 emerged in India in 1996 and rapidly underwent transcontinental dissemination, reaching almost all continents (9). ST3 causes infections worldwide and persists as the dominant type in some countries of Asia, including China (5).

ST3 was the only known example of *V. parahaemolyticus* transcontinental expansion until 2012, when a new type, ST36, was identified outside its endemic region (the Pacific Northwest of North America) (10). ST36 infections were initially reported in the northeastern United States, increasing the number of *V. parahaemolyticus* infections in this region (3). A few months later, they were reported in a single large outbreak in Spain (11). An in-depth genomewide analysis of representative isolates from the Pacific Northwest, northeastern United States, and Spain showed that ST36 is a highly dynamic population and that the *V. parahaemolyticus* strains causing infections in the northeastern United States had diverged from the original lineage in the Pacific Northwest over the course of the cross-continent eastward expansion (12). The strains in the northeastern United States and Spain arose from 2 distinctive ST36 populations. Although the international spread of this population is a concern, ST36 has not been documented outside of the United States since the outbreak in Spain in 2012 (11).

The Study

After the emergence of cholera in 1991 in Peru and re-emergence in 1998, both concurrent with El Niño events, the Peruvian National Institute of Health (Lima, Peru) implemented a contingency plan for preparedness to respond to every El Niño episode. This contingency plan involves intensive investigations of all *Vibrio* isolates acquired in clinical settings and enhanced monitoring

of environmental sources. Among the characterized *V. parahaemolyticus* isolates obtained over the course of surveillance, we identified 5 clinical ST36 isolates (3 in 2015 and 2 in 2016) from Lima (Table). After reviewing the *V. parahaemolyticus* isolates deposited in the historical collection of the Peruvian National Institute of Health over the past 30 years, we were able to identify 2 additional isolates (1 from a seawater sample collected in 2011 and 1 from a clinic in 2012).

Table. Sequence type 36 isolates identified in clinical settings and from environmental sources, Lima, Peru, 2011–2016

Isolate	Alias	Year	Source
CFSAN062371	3.369–15	2011	Environmental
CFSAN062362	1.004–13	2012	Clinical
CFSAN062300	3.252–16	2015	Clinical
CFSAN062366	1.147–15	2015	Clinical
CFSAN062373	1.146–15	2015	Clinical
CFSAN062273	1.210–16	2016	Clinical
CFSAN062350	1.166–15	2016	Clinical

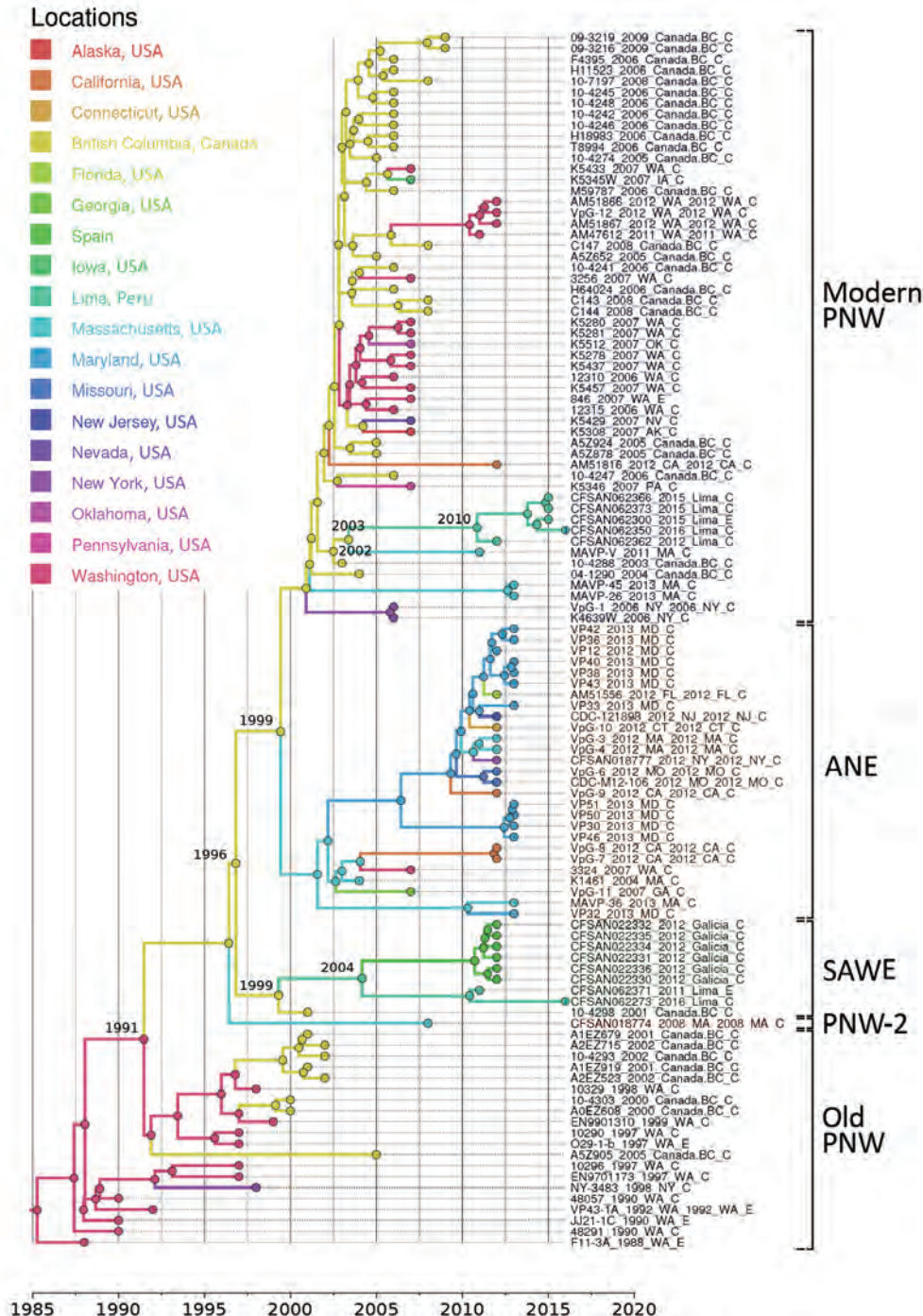


Figure 1. Phylogenetic reconstruction of transcontinental spread of *Vibrio parahaemolyticus* sequence type 36, North America, Peru, and Spain, 1985–2016. Timeline was estimated with BEAST (<https://beast.community>) by applying a Bayesian skyline demographic model and uncorrelated lognormal molecular clock. Single-nucleotide polymorphisms were identified in core genomes after the removal of recombination. Branch colors represent the most probable geographic origin of the last common ancestor of the group. Dates at nodes show estimated divergence dates from most recent common ancestor. Old PNW is the ancestral population (last strain identified in 2002) of the PNW lineage complex, and the modern PNW lineage is the currently circulating PNW population. *Vibrio* classifications are indicated. ANE, Atlantic Northeast; PNW, Pacific Northwest; SAWE, South America–West Europe.

We performed a genomewide phylogenetic analysis of a global collection of 111 ST36 isolates (Appendix Table, <https://wwwnc.cdc.gov/EID/article/26/2/19-0362-App1.pdf>) obtained during the past 30 years from the United States (west and east coasts), Canada, Spain, and Peru. Results indicated that the isolates from Peru were of 2 different genetic variants (Figures 1, 2): 5 clustered with the modern (i.e., currently circulating) Pacific Northwest lineage, and 2 clustered in a distinctive group comprising isolates from the 2012 outbreak in Spain. Analysis of the phylodynamics of transmission by Bayesian inference suggested the existence of 2 independent and almost contemporary introductions of ST36 into Peru in 2011, both originating from 2 distinct modern Pacific Northwest variants. The group comprising isolates from Peru and Spain appeared to have diverged from a common ancestor around 2004. Considering the number of years from the last common ancestor of both Peru

lineages and that other closely related genetic variants are absent from the dataset, intermediary populations might exist in regions not yet scrutinized.

The identification of ST36 in Peru provides additional evidence of the extraordinary dynamics of *Vibrio* infections in this region. Since the emergence of cholera in 1991 and the subsequent implementation of an active surveillance system for *Vibrio* diseases in Peru, several instances of emergence of major epidemic clones of *V. parahaemolyticus* have been reported in the country. Although the sources and routes of introduction of these foreign clones remain yet undetermined, a growing body of evidence has linked the epidemic dynamics and spreading of disease in this particular region of South America to El Niño (13). During the past 30 years, the emergence of cases in Peru associated with new clones of *Vibrio* has been sharply influenced by the onset of El Niño conditions, which has also shaped the extent and severity of epidemics

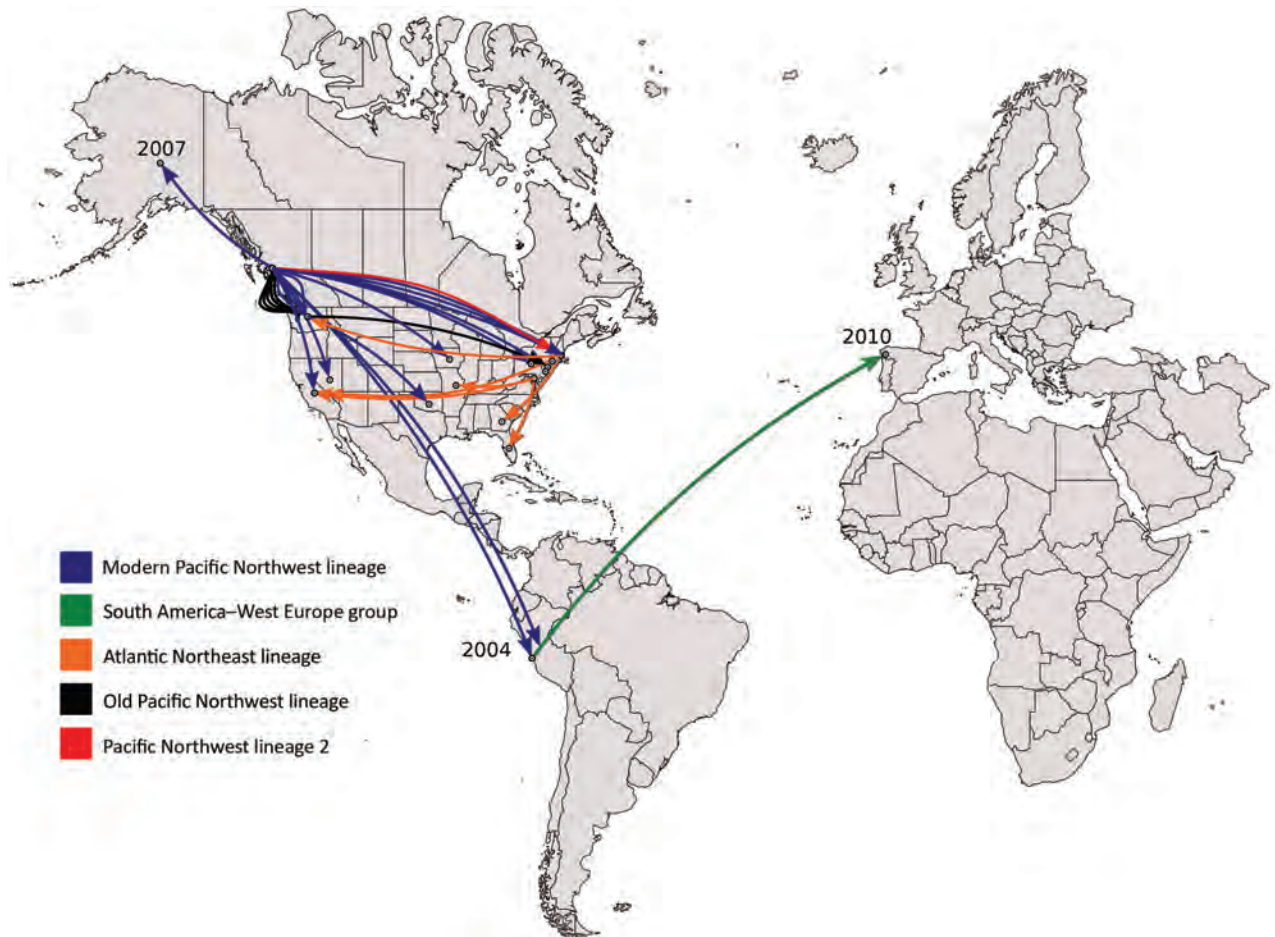


Figure 2. Transcontinental spread of *Vibrio parahaemolyticus* sequence type 36, North America, Peru, and Spain, 1985–2016. Timeline was estimated by using BEAST (Bayesian evolutionary analysis by sampling trees). Years on map indicate the inferred dates of arrival of *V. parahaemolyticus* sequence type 36 to that country. Old Pacific Northwest is the ancestral population (last strain identified in 2002) of the Pacific Northwest lineage complex, which also includes the modern (i.e., currently circulating) Pacific Northwest lineage, Pacific Northwest lineage 2, Atlantic Northeast lineage, and the South America–West Europe group.

(14,15). The arrival of extraordinary weather conditions brought on by El Niño (i.e., a combination of heavy rains and heat waves) provides the ideal conditions for the proliferation of *Vibrio* spp. in the environment. These circumstances, along with disruption of sanitary infrastructure caused by floods and landslides, can help generate the perfect conditions for the explosive emergence of *Vibrio* diseases.

Despite the evidence connecting the epidemiology of *Vibrio* in Peru to El Niño, little is known about the mechanisms of global dispersal and introduction of foreign epidemic clones into the region. Ballast water from cargo ships and marine heat waves have been associated with some instances of disease emergence elsewhere (12). Another mechanism that might be involved in the dispersal of *V. parahaemolyticus* populations is the international trade of shellfish, which was suggested to facilitate the introduction of ST36 into the United States and Spain (12).

Conclusions

We report the transcontinental expansion of ST36 *V. parahaemolyticus* into South America. The presence of ST36 in clinical and environmental settings in Peru emphasizes the exceptional epidemic potential of the Pacific Northwest complex and *V. parahaemolyticus* as a human pathogen. The long-term persistence and presence of environmental isolates suggest the successful establishment of ST36 in environmental reservoirs. ST36's ability for intercontinental dispersal, along with its highly pathogenic nature (1), make this *Vibrio* population a major public health concern. Furthermore, Peru has shown that implementation of systematic surveillance for *Vibrio* species can facilitate the detection of emerging transnational epidemic strains. This strategy will play a crucial role under exceptional climatic conditions, such as those generated by El Niño, where enhanced risk for outbreaks is likely.

This work was funded through the Natural Environment Research Council project NE/P004121/1.

About the Author

Dr. Abanto is a scientist at the Scientific and Technological Bioresource Nucleus, Universidad de la Frontera, Temuco, Chile. His research interests include emerging microbes, genomic epidemiology, and the use of integrative and efficient computational methods applied to the study of the epidemiology and ecology of microorganisms.

References

- Martinez-Urtaza J, Bowers JC, Trinanés J, DePaola A. Climate anomalies and the increasing risk of *Vibrio parahaemolyticus* and *Vibrio vulnificus* illnesses. *Food Res Int*. 2010;43:1780–90. <https://doi.org/10.1016/j.foodres.2010.04.001>

- Marder EP, Griffin PM, Cieslak PR, Dunn J, Hurd S, Jervis R, et al. Preliminary incidence and trends of infections with pathogens transmitted commonly through food – Foodborne Diseases Active Surveillance Network, 10 U.S. sites, 2006–2017. *MMWR Morb Mortal Wkly Rep*. 2018;67:324–8. <https://doi.org/10.15585/mmwr.mm6711a3>
- Newton AE, Garrett N, Stroika SG, Halpin JL, Turnsek M, Mody RK; Centers for Disease Control and Prevention. Increase in *Vibrio parahaemolyticus* infections associated with consumption of Atlantic Coast shellfish – 2013. *MMWR Morb Mortal Wkly Rep*. 2014;63:335–6.
- Scallan E, Hoekstra RM, Angulo FJ, Tauxe RV, Widdowson MA, Roy SL, et al. Foodborne illness acquired in the United States – major pathogens. *Emerg Infect Dis*. 2011;17:7–15. <https://doi.org/10.3201/eid1701.P11101>
- Li Y, Xie X, Shi X, Lin Y, Qiu Y, Mou J, et al. *Vibrio parahaemolyticus*, southern coastal region of China, 2007–2012. *Emerg Infect Dis*. 2014;20:685–8. <https://doi.org/10.3201/eid2004.130744>
- González-Escalona N, Cachicas V, Acevedo C, Rioseco ML, Vergara JA, Cabello F, et al. *Vibrio parahaemolyticus* diarrhea, Chile, 1998 and 2004. *Emerg Infect Dis*. 2005;11:129–31. <https://doi.org/10.3201/eid1101.040762>
- Baker-Austin C, Trinanés JA, Salmenlinna S, Löfdahl M, Siitonen A, Taylor NG, et al. Heat wave-associated vibriosis, Sweden and Finland, 2014. *Emerg Infect Dis*. 2016;22:1216–20. <https://doi.org/10.3201/eid2207.151996>
- Baker-Austin C, Oliver JD, Alam M, Ali A, Waldor MK, Qadri F, et al. *Vibrio* spp. infections. *Nat Rev Dis Primers*. 2018;4:8. <https://doi.org/10.1038/s41572-018-0005-8>
- Nair GB, Ramamurthy T, Bhattacharya SK, Dutta B, Takeda Y, Sack DA. Global dissemination of *Vibrio parahaemolyticus* serotype O3:K6 and its serovariants. *Clin Microbiol Rev*. 2007;20:39–48. <https://doi.org/10.1128/CMR.00025-06>
- Martinez-Urtaza J, Baker-Austin C, Jones JL, Newton AE, Gonzalez-Aviles GD, DePaola A. Spread of Pacific Northwest *Vibrio parahaemolyticus* strain. *N Engl J Med*. 2013;369:1573–4. <https://doi.org/10.1056/NEJMc1305535>
- Martinez-Urtaza J, Powell A, Jansa J, Rey JL, Montero OP, Campello MG, et al. Epidemiological investigation of a foodborne outbreak in Spain associated with U.S. West Coast genotypes of *Vibrio parahaemolyticus*. *Springerplus*. 2016;5:87. <https://doi.org/10.1186/s40064-016-1728-1>
- Martinez-Urtaza J, van Aerle R, Abanto M, Haendiges J, Myers RA, Trinanés J, et al. Genomic variation and evolution of *Vibrio parahaemolyticus* ST36 over the course of a transcontinental epidemic expansion. *MBio*. 2017;8:e01425–17. <https://doi.org/10.1128/mBio.01425-17>
- Martinez-Urtaza J, Trinanés J, Gonzalez-Escalona N, Baker-Austin C. Is El Niño a long-distance corridor for waterborne disease? *Nat Microbiol*. 2016;1:16018. <https://doi.org/10.1038/nmicrobiol.2016.18>
- Speelmon EC, Checkley W, Gilman RH, Patz J, Calderon M, Manga S. Cholera incidence and El Niño-related higher ambient temperature. *JAMA*. 2000;283:3072–4. <https://doi.org/10.1001/jama.283.23.3068i>
- Martinez-Urtaza J, Huapaya B, Gavilan RG, Blanco-Abad V, Ansedé-Bermejo J, Cadarso-Suarez C, et al. Emergence of Asiatic vibrio diseases in South America in phase with El Niño. *Epidemiology*. 2008;19:829–37. <https://doi.org/10.1097/EDE.0b013e3181883d43>

Address for correspondence: Jaime Martinez-Urtaza, The Centre for Environment, Fisheries and Aquaculture Science, The Nothe, Barrack Road, Weymouth, Dorset DT4 8UB, UK; email: jaime.martinez-urtaza@cefas.co.uk

Surge in Anaplasmosis Cases in Maine, USA, 2013–2017

Susan P. Elias, Jessica Bonthius, Sara Robinson, Rebecca M. Robich, Charles B. Lubelczyk, Robert P. Smith, Jr.

Incidence of human granulocytic anaplasmosis is rising in Maine, USA. This increase may be explained in part by adoption of tick panels as a frequent diagnostic test in persons with febrile illness and in part by range expansion of *Ixodes scapularis* ticks and zoonotic amplification of *Anaplasma phagocytophilum*.

Lyme disease is the most common vectorborne disease in Maine. *Borrelia burgdorferi*, the agent of Lyme disease, is transmitted through the bite of infected blacklegged ticks (*Ixodes scapularis*). Lyme disease cases in Maine increased from a single case in 1986 to 1,844 in 2017, reflecting the northward range expansion of *I. scapularis* ticks (1). *Anaplasma phagocytophilum*, the cause of human granulocytic anaplasmosis (HGA), is also transmitted by *I. scapularis* ticks and is the second most common tickborne illness in Maine. Only 45 HGA cases were reported during 2000–2008 (2), but case reports rose dramatically during 2013–2017, generating media attention (3,4). The Maine Center for Disease Control and Prevention (MECDC) reported 663 cases of anaplasmosis in 2017, a 605% increase from 94 cases in 2013, in contrast with Lyme disease cases, which increased by only 33% (1,384 in 2013 to 1,844 in 2017) (5).

We sought to determine whether the increase in anaplasmosis cases reflected broader geographic transmission of *A. phagocytophilum* from ticks to humans through range expansion of *I. scapularis* ticks, increased testing effort through increased use of tick panels that detect multiple pathogens by PCR, or both. Evidence for increased transmission would include geographic range expansion of

HGA incidence and hospitalizations. Evidence of increased testing effort would be increased use of tick panels, which could lead to discovery of mild *A. phagocytophilum* infections, especially pediatric cases, because HGA in children is generally a mild illness (6).

The Study

MECDC provided the number of confirmed and probable cases for Maine residents during 2008–2017, available by county of residence and age of onset. For 2013–2017, we obtained the annual number of hospitalizations for Lyme disease and HGA for Maine residents, with age and county of residence at admission, from the Maine Health Data Organization.

We obtained the annual number of multipathogen (including HGA) PCR tick panel orders during 2013–2017 from NorDx and Mayo Medical Laboratories (MML). NorDx (Scarborough, ME, USA) started using its panel for the agents of HGA and babesiosis in 2015 (H. Webber, NorDx, pers. comm., 2018 Sep 12). All orders were for Maine patients (travel history not specified). MML provided data from 2 branch laboratories, Mayo Clinic Rochester (MCR; Rochester, MN, USA) and Mayo Medical Laboratories, New England (MMLNE; Andover, MA, USA). MML has offered the panel for ≈10 years; the panel contains a PCR test for the agents of human monocytic ehrlichiosis, HGA, babesiosis, and *Borrelia miyamotoi* infections (B. Pritt, MML, pers. comm., 2018 Aug 3). MML data comprised specimens sent to MML from Maine clients, without patient residence or travel history (B. Pritt, A. Boerger, MML, pers. comm., 2018 Oct 8). We were unable to obtain data from other laboratories; however, MML and NorDx combined accounted for 72% of HGA test reports sent to MECDC during 2013–2017. The MML panel had sensitivity and specificity of 1 for detection of *A. phagocytophilum* compared with standard PCR (7). The NorDx panel had sensitivity and specificity of 1 compared

Author affiliations: Maine Medical Center Research Institute, Scarborough, Maine, USA (S.P. Elias, R.M. Robich, C.B. Lubelczyk, R.P. Smith, Jr.); University of Southern Maine, Portland, Maine, USA (J. Bonthius); Maine Center for Disease Control and Prevention, Augusta, Maine, USA (S. Robinson)

DOI: <https://doi.org/10.3201/eid2602.190529>

Table 1. Number of HGA and Lyme disease cases and incidence, Maine, USA, 2008–2017*

Year	HGA								Lyme	
	Cases				Incidence				Cases	Incidence†
	All ages	0–17 y	18–64 y	≥65 y	All ages	0–17 y	18–64 y	≥65 y		
2008	17	0	11	6	1.3	0	1.3	3.0	909	68.3
2009	15	0	9	6	1.1	0	1.1	2.9	976	73.4
2010	17	1	10	6	1.3	0.4	1.2	2.8	752	56.6
2011	26	0	12	14	2.0	0	1.4	6.5	1013	76.3
2012	52	0	37	15	3.9	0	4.4	6.6	1113	83.7
2013	94	0	56	38	7.1	0	6.7	16.2	1384	104.2
2014	191	10	102	79	14.4	3.9	12.3	32.5	1411	106.1
2015	185	9	92	84	13.9	3.5	11.2	33.6	1215	91.4
2016	372	9	206	157	27.9	3.5	25.2	60.8	1497	112.4
2017	663	13	304	346	49.7	5.1	37.3	129.6	1844	138.5
Change 2013–2017‡	605%		443%	811%	602%		454%	701%	33%	33%

*Case data provided by the Maine Center for Disease Control and Prevention. HGA, human granulocytic anaplasmosis.

†Cases/100,000 population.

‡Percentage increase 2013–2017 was calculated when there were nonzero data for 2013.

with panels of MML and other laboratories (H. Webber, pers. comm., 2019 Aug 29).

The HGA incidence rate, hospitalization rate, complications, and death rate increase with age (8), whereas Lyme incidence has a bimodal distribution, with peaks in young children and older adults (9). We tabulated HGA cases and incidence for 2008–2017 overall and by age class and tabulated HGA hospitalizations 2013–2017 overall and by age class and annual laboratory testing effort. For comparison, we included annual overall Lyme incidence and hospitalizations. We compared percentage changes from 2013 to 2017 in disease incidence and hospitalizations. To visualize geographic expansion of HGA, we plotted side-by-side maps of county-level incidence and population-adjusted hospitalization rates for 2013 versus 2017.

During 2013–2017, a total of 1,505 anaplasmosis cases were reported (10). Of these, 85.6% (1,289) were confirmed (1,286 by PCR and 3 by 4-fold antibody titer increase) and 14.4% (216) probable (203 with a single titer result, 8 with <4-fold titer increase, 5 with morulae visualization). Statewide, anaplasmosis incidence rose from 7 cases/100,000 persons in 2013 to 50 cases/100,000 persons in 2017, a 602% increase, compared with a 33% increase for Lyme disease

incidence (Table 1). Hospitalizations for HGA rose from 36 in 2013 to 119 in 2017, a 231% increase, compared with a 27% decline in hospitalizations for Lyme disease (Table 2). Combined tick panel use by MML and NorDx rose from 773 in 2013 to 9,157 in 2017, a 1,085% increase (Table 2).

Among 39 pediatric HGA cases, 1 occurred in 2010 and the remaining 38 during 2014–2017, representing 1.7%–5.2% of total cases per year during 2014–2017 (Table 1). Even though hospitalizations increased for persons 18–64 and ≥65, there were no hospitalizations for children.

Anaplasmosis incidence and hospitalizations underwent geographic range expansion during 2013–2017 (Figures 1, 2). Anaplasmosis incidence was highest in Lincoln and Knox Counties, in Maine's midcoast region, where incidence ranged from 29 cases/100,000 persons in 2013 to 278 cases/100,000 persons in 2017 (Figure 1, panels A, B).

Conclusions

We conclude that the surge in anaplasmosis incidence in Maine, an increase of 602% from 2013 to 2017, was a combination of increased transmission and testing effort, although we cannot partition the relative

Table 2. Number of hospitalizations for HGA and Lyme disease and number of PCR-based tickborne disease panels, Maine, USA, 2013–2017*

Year	Hospitalizations					Tick panels†				
	HGA				Lyme, all ages	MML-R	MML-NE	Total MML	NorDx	All
	All ages	0–17 y	18–64 y	≥65 y						
2013	36	0	9	27	66	0	773	773	0	773
2014	75	0	25	50	55	0	1,479	1,479	0	1,479
2015	68	0	19	49	45	0	1,066	1,066	875	1,941
2016	123	0	42	81	47	596	122	718	5,259	5,977
2017	119	0	24	95	48	973	0	973	8,184	9,157
Change 2013–2017	+231%		+167%	+252%	–27%					+1,085%

*Hospitalizations are Maine hospital inpatient encounters, provided through the Maine Health Data Organization. HGA, human granulocytic anaplasmosis; MML, Mayo Medical Laboratories.

†Tick panels performed at Mayo Clinic Rochester, Rochester, MN, USA (MML-R); MML, New England, Andover, MA, USA (MML-NE, closed in 2016); and NorDx, Scarborough, ME, USA.

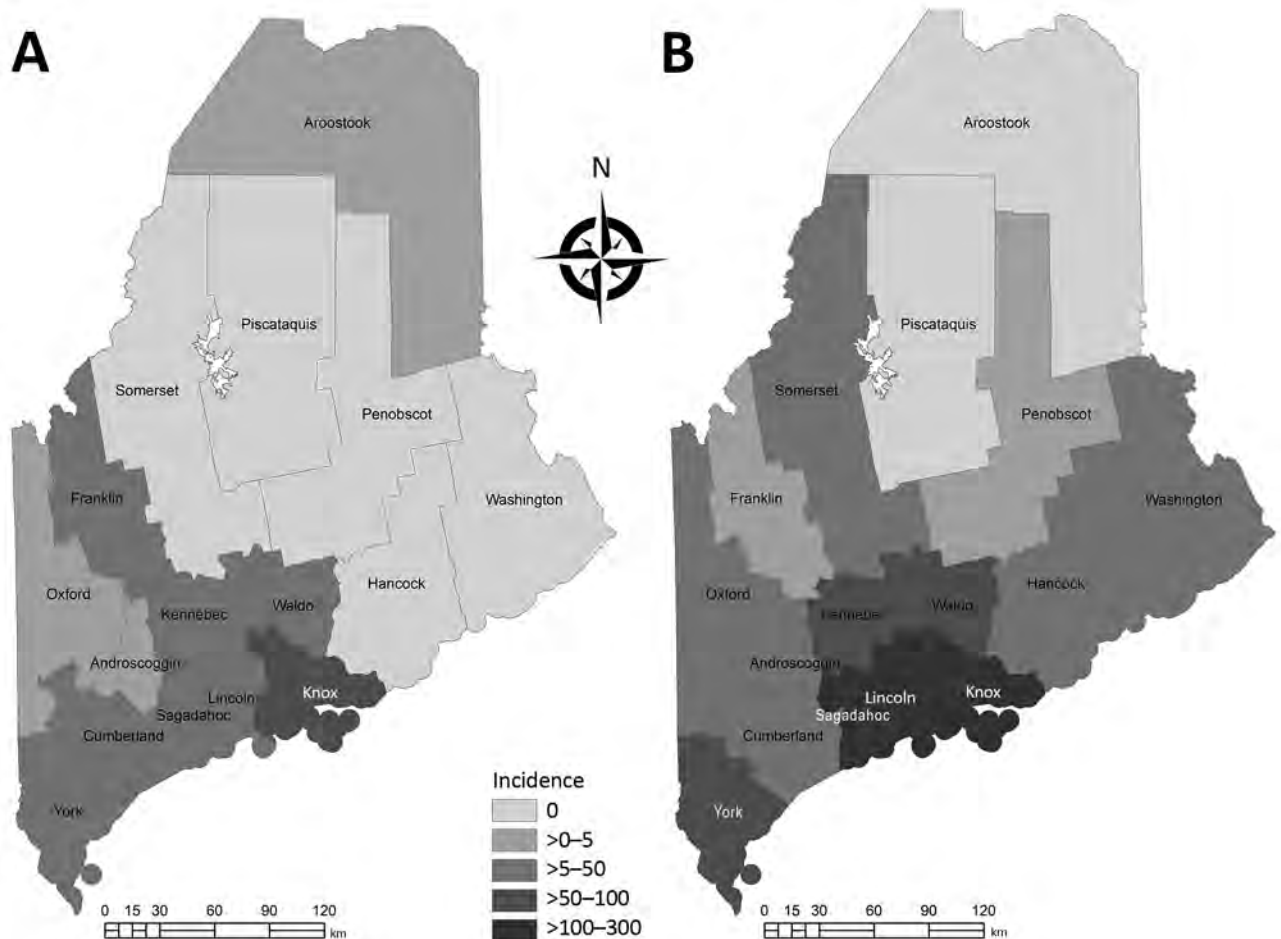


Figure 1. Human granulocytic anaplasmosis incidence (cases/100,000 persons), Maine, USA, 2013 (A) and 2017 (B). Statewide incidence increased 602% during 2013–2017.

contribution of each. The 231% rise in hospitalized patients with HGA and the geographic expansion of HGA incidence and hospitalization indicate increased transmission. Range expansion of *I. scapularis* ticks in Maine likely has contributed to the rise in HGA cases in areas where this tick species is emergent (i.e., a recent colonizer). In addition, zoonotic amplification of *A. phagocytophilum* is likely occurring where *I. scapularis* ticks are established. Because of less efficient enzootic transmission, human infection with *Babesia microti*, the agent of babesiosis, lags behind *B. burgdorferi* transmission over time and space (11). Less efficient enzootic transmission of *A. phagocytophilum* also may be the case, but we know of no confirmatory studies.

Concurrent to increased transmission was the 1,085% increase in tickborne disease panel testing performed by the 2 major providers of testing results to Maine during 2013–2017. Increased testing effort may reflect increased clinician and patient awareness and ready availability of tickborne disease panels that

detect multiple pathogens. These panels may lead to detection of mild *A. phagocytophilum* infections or co-infections in persons with nonspecific febrile illness, as suggested by increased detection of less severely ill persons, such as children. Thirty-eight of 39 pediatric HGA cases were reported after 2013, but there were no pediatric hospitalizations. Before the use of panels, pediatric HGA cases may have been ascribed to another illness with similar symptoms.

Studies relying on diagnostic tests are subject to test sensitivity and specificity. PCR is the most effective diagnostic test during early-stage *A. phagocytophilum* infection with high sensitivity and specificity (12,13). In this study, false positive PCR results were unlikely, based on test specificities reported by Mayo and NorDx.

Collaboration among all state health departments and testing laboratories across New England could help extend our findings. Vermont cases increased 1,078%, from 37 in 2013 to 399 in 2017 (14), and New

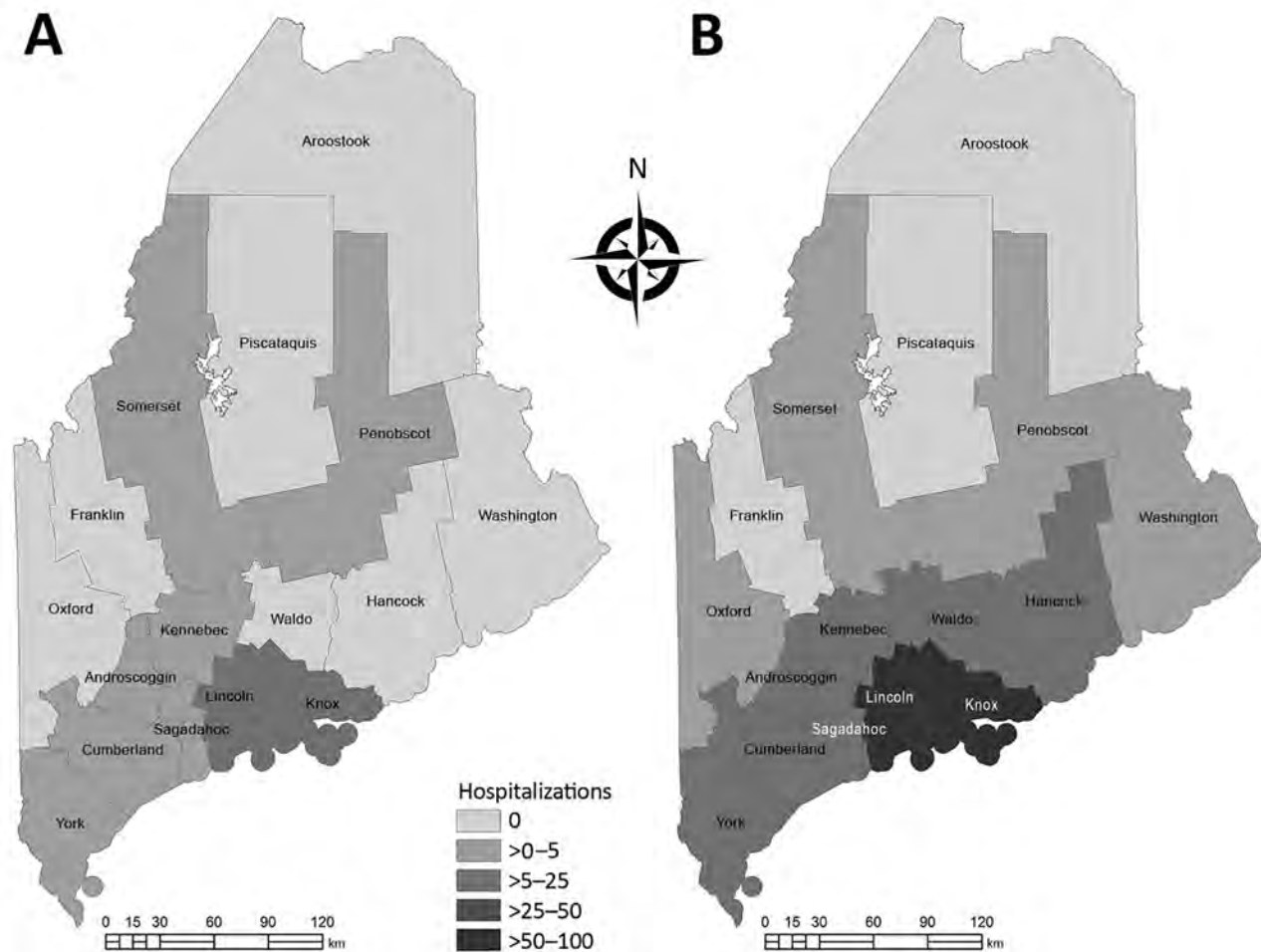


Figure 2. Hospitalizations (per 100,000 persons) for human granulocytic anaplasmosis, Maine, USA, 2013 (A) and 2017 (B). Statewide hospitalizations increased 231% during 2013–2017.

Hampshire cases increased 260%, from 88 in 2013 to 317 in 2017 (15). Correlation between incidence and testing effort at the county level would corroborate a relationship between rising tickborne diseases and testing effort, if panel data included patient county of residence and travel history. Corroborating datasets on density of *A. phagocytophilum*-infected *I. scapularis* ticks would also help clarify the risks posed to human health.

Acknowledgments

For NorDx data, we thank Monica Ianos-Irimie, Haley Webber, and Lisa Webster. For Mayo Medical Laboratories data, we thank Bobbi Pritt and Aimee Boerger. For hospitalization data, we thank the Maine Health Data Organization, as well as Hilary Perrey and Lori Travis.

Partial salary support for co-authors J.B. and S.R. came from the Centers for Disease Control and Prevention grants Building Resilience Against Climate Effects (BRACE) and Epidemiology and Laboratory Capacity (ELC).

About the Author

Dr. Elias is a staff scientist at the Maine Medical Center Research Institute, Lyme and Vector-borne Disease Laboratory, Scarborough, Maine, USA. Her primary research interests include epidemiology and ecology of emergent vectorborne diseases.

References

1. Rand PW, Lacombe EH, Dearborn R, Cahill B, Elias S, Lubelczyk CB, et al. Passive surveillance in Maine, an area emergent for tick-borne diseases. *J Med Entomol*. 2007;44:1118–29. <https://doi.org/10.1093/jmedent/44.6.1118>
2. Cahill B, Lubelczyk C, Smith R, Gensheimer K, Robbins A, Robinson S, et al.; Centers for Disease Control and Prevention (CDC). Anaplasmosis and ehrlichiosis—Maine, 2008. *MMWR Morb Mortal Wkly Rep*. 2009;58:1033–6.
3. Wight P. Tick-borne anaplasmosis on the rise in Maine. 2017 [cited 2019 May 9]. <https://bangordailynews.com/2017/11/13/health/tick-borne-anaplasmosis-on-the-rise-in-maine>

4. Lawlor J. Tick-borne anaplasmosis surging in Maine—and it's worse than Lyme. 2017 [cited 2019 May 9]. <https://www.pressherald.com/2017/11/13/anaplasmosis-cases-surg-ing-in-maine>
5. Maine Center for Disease Control. Reportable infectious diseases in Maine—2017 summary. 2018 [cited 2018 Sep 20]. <https://www.maine.gov/dhhs/mecdc/infectious-disease/epi/publications/#annualreports>
6. Sigurjonsdottir VK, Feder HM Jr, Wormser GP. Anaplasmosis in pediatric patients: case report and review. *Diagn Microbiol Infect Dis*. 2017;89:230–4. <https://doi.org/10.1016/j.diagmicrobio.2017.08.003>
7. Mayo Clinic Laboratories. Test ID: EHRL. Ehrlichia/ anaplasma, molecular detection, PCR, blood [cited 2019 Sep 29]. <https://www.mayocliniclabs.com/test-catalog/Clinical+and+Interpretive/84319>
8. Dahlgren FS, Heitman KN, Drexler NA, Massung RF, Behravesh CB. Human granulocytic anaplasmosis in the United States from 2008 to 2012: a summary of national surveillance data. *Am J Trop Med Hyg*. 2015;93:66–72. <https://doi.org/10.4269/ajtmh.15-0122>
9. Schwartz AM, Hinckley AF, Mead PS, Hook SA, Kugeler KJ. Surveillance for Lyme disease— United States, 2008–2015. *MMWR Surveill Summ*. 2017;66(No. SS-22):1–12. <https://doi.org/10.15585/mmwr.ss6622a1>
10. U.S. Centers for Disease Control and Prevention. Ehrlichiosis and anaplasmosis 2008 case definition [cited 2019 Aug 29]. <https://wwwn.cdc.gov/nndss/conditions/anaplasma-phagocytophilum-infection/case-definition/2008/>
11. Diuk-Wasser MA, Vannier E, Krause PJ. Coinfection by *Ixodes* tick-borne pathogens: ecological, epidemiological, and clinical consequences. *Trends Parasitol*. 2016;32:30–42. <https://doi.org/10.1016/j.pt.2015.09.008>
12. Hansmann Y, Jaulhac B, Kieffer P, Martinot M, Wurtz E, Dukic R, et al. Value of PCR, serology, and blood smears for human granulocytic anaplasmosis diagnosis, France. *Emerg Infect Dis*. 2019;25:996–8. <https://doi.org/10.3201/eid2505.171751>
13. Schotthoefer AM, Meece JK, Ivacic LC, Bertz PD, Zhang K, Weiler T, et al. Comparison of a real-time PCR method with serology and blood smear analysis for diagnosis of human anaplasmosis: importance of infection time course for optimal test utilization. *J Clin Microbiol*. 2013;51:2147–53. <https://doi.org/10.1128/JCM.00347-13>
14. Vermont Department of Health. Anaplasmosis [cited 2018 Sep 25]. <https://www.healthvermont.gov/disease-control/tickborne-diseases/anaplasmosis>
15. New Hampshire Department of Health and Human Services. Tickborne diseases in New Hampshire [cited 2018 Sep 25]. https://www.hanovernh.org/sites/hanovernh/files/uploads/20180518_tickborne_disease_han_with_attachments.pdf

Address for correspondence: Susan P. Elias, Maine Medical Center Research Institute, Lyme and Vector-borne Disease Laboratory, 81 Research Dr, Scarborough, ME 04074, USA; email: susan.elias@maine.edu



EMERGING INFECTIOUS DISEASES®

September 2018

Vectorborne Infections

- Ethics of Infection Control Measures for Carriers of Antimicrobial Drug-Resistant Organisms
- National Surveillance for *Clostridioides difficile* Infection, Sweden, 2009–2016
- Travel-Associated Zika Cases and Threat of Local Transmission during Global Outbreak, California, USA
- Distinguishing Japanese Spotted Fever and Scrub Typhus, Central Japan, 2004–2015
- Event-Based Surveillance at Community and Healthcare Facilities, Vietnam, 2016–2017
- Case Report and Genetic Sequence Analysis of *Candidatus* *Borrelia kalaharica*, Southern Africa
- Novel Orthopoxvirus and Lethal Disease in Cat, Italy
- Emergence of Carbapenemase-Producing *Enterobacteriaceae*, South-Central Ontario, Canada
- From Culturomics to Clinical Microbiology and Forward
- Association of Batai Virus Infection and Encephalitis in Harbor Seals, Germany, 2016
- Use of Favipiravir to Treat Lassa Virus Infection in Macaques
- Aortic Endograft Infection with *Mycobacterium chimaera* and *Granulicatella adiacens*, Switzerland, 2014
- Estimating Frequency of Probable Autochthonous Cases of Dengue, Japan
- Correlation of Severity of Human Tick-borne Encephalitis Virus Disease and Pathogenicity in Mice
- Increasing Prevalence of *Borrelia burgdorferi* sensu stricto-Infected Blacklegged Ticks in Tennessee Valley, Tennessee, USA
- Susceptibility of White-Tailed Deer to Rift Valley Fever Virus
- Outbreak of Pneumococcal Meningitis, Paoua Subprefecture, Central African Republic, 2016–2017

To revisit the September 2018 issue, go to:

<https://wwwnc.cdc.gov/eid/articles/issue/24/9/table-of-contents>

Mycoplasma genitalium Antimicrobial Resistance in Community and Sexual Health Clinic Patients, Auckland, New Zealand

Anna Vesty, Gary McAuliffe, Sally Roberts, Gillian Henderson, Indira Basu

Our retrospective study compared genotypic antimicrobial resistance in *Mycoplasma genitalium*-positive specimens collected from 48 community and 33 sexual health clinic (SHC) patients. Macrolide resistance was similar in community (75%) and SHC (76%) patients. We observed no significant difference in fluoroquinolone resistance between community (19%) and SHC (27%) patients ($p = 0.66$).

Management of *Mycoplasma genitalium* infections is challenging because the limited treatment options have been affected by rapidly evolving resistance to antimicrobial drugs. Molecular approaches are the preferred method of *M. genitalium* detection, and resistance is determined genotypically. 23S rRNA mutations are associated with macrolide resistance and azithromycin treatment failures (1–3), whereas fluoroquinolone resistance is associated with mutations in the quinolone resistance-determining region, specifically in the *gyrA* and *parC* genes (4).

Azithromycin is the first-line treatment for *M. genitalium* infections in New Zealand; second-line treatment relies on moxifloxacin, a fluoroquinolone. A high proportion (72%) of macrolide resistance has been reported in sexual health clinic (SHC) patients in our region (5), and elsewhere in New Zealand fluoroquinolone resistance is reported in 23.3% of *M. genitalium*-positive specimens from SHC attendees (3), consistent with the high prevalence of macrolide and fluoroquinolone resistance in the Asia-Pacific region (1,3,6).

The Study

We performed a retrospective study of all specimens referred to the Microbiology Department at Auckland City Hospital (Auckland, New Zealand) for *M. genitalium* testing in 2017. Referral sites were predominantly general practices in Auckland and SHCs in the Auckland, Northland, and Waikato regions. Ethics approval was granted by the Health and Disability Ethics Committee (approval no. 16/CEN/188).

DNA had been extracted from specimens following a diagnostic workflow and stored at -80°C . We retrieved DNA samples that tested positive for *M. genitalium* using real-time PCR (5,7) for this study. We detected 23S rRNA mutations at nucleotide positions 2058 and 2059 (*Escherichia coli* numbering) by using the commercially available PlexPCR kit Resistance Plus MG (SpeedX, <https://plexpcr.com>) (5) and *gyrA* and *parC* mutations by using PCR amplification of *M. genitalium* nucleotides 172–402 of *gyrA* and 164–483 of *parC* (8), followed by sequencing on the Applied Biosystems 3130xl sequencer (Life Technologies, <https://www.thermofisher.com>). Sequences were aligned against *M. genitalium* reference genes (GenBank accession nos. CP003773 for *gyrA* and *parC* for U25549) by using SeqMan II (DNASTAR, <https://www.dnastar.com>) and the mutations reported by using *M. genitalium* numbering. We compared prevalence of resistance-associated mutations in community and SHC cohorts by using a χ^2 test ($\alpha = 5\%$).

We tested 302 clinical specimens from 247 patients; 33% (101/302) of samples from 34% (84/247) of patients were *M. genitalium* DNA-positive. Four samples from 3 patients were excluded from subsequent analyses because insufficient PCR products were obtained for sequencing. We used the remaining 97

Author affiliations: Auckland City Hospital, Auckland, New Zealand (A. Vesty, G. McAuliffe, S. Roberts, G. Henderson, I. Basu); Labtests, Auckland (G. McAuliffe)

DOI: <https://doi.org/10.3201/eid2602.190533>

Table 1. Prevalence of antimicrobial resistance in *Mycoplasma genitalium* strains from community and SHC patients, Auckland, New Zealand, 2017*

Genotypic-resistance profile	Mutation			Frequency, %		
	23S rRNA	<i>parC</i>	<i>gyrA</i>	Community patients	SHC patients	All patients
Wild type	–	–	–	20.8	24.2	22.2
Macrolide	+	–	–	60.4	48.5	55.6
Macrolide + fluoroquinolone	+	+	–	12.5	12.1	12.3
Macrolide + fluoroquinolone	+	+	+	2.1	15.1	7.4
Fluoroquinolone	–	+	–	4.2	0	2.5

*SHC, sexual health clinic; +, positive; –, negative.

M. genitalium DNA–positive samples obtained from 81 patients to determine macrolide and fluoroquinolone resistance. Specimens were urine samples (92%) or urogenital swabs. The mean (\pm SD) age of patients was 29 (\pm 7.5) years, and 80% (65/81) of patients were men; 59% (48/81) were community patients, and 41% (33/81) were SHC patients.

We detected macrolide mutations in 75% (61/81) of patients (Table 1). We observed no significant difference in the prevalence of macrolide resistance between community (75% [36/48]) and SHC (76% [25/33]) patients ($p = 1.00$). Fluoroquinolone-resistant strains of *M. genitalium* were identified in 22% (18/81) of patients on the basis of the presence of mutations previously associated with phenotypic antimicrobial resistance or treatment failure (Table 2). We observed no significant difference in proportions of fluoroquinolone resistance between community (19% [9/48]) and SHC (27% [9/33]) patients ($p = 0.66$).

Missense mutations in *parC* at amino acid positions 81, 83, or 87 conferred fluoroquinolone resistance (Table 2). Mutations in codon 83 of *parC* are associated with resistance; therefore, the mutation at T249A was presumed to confer fluoroquinolone resistance. The importance of polymorphisms in *parC* at C184T and C356T is uncertain. Mutations in *gyrA* at codon 95 were detected in 6 patients, 5 of whom were

SHC attendees. All 6 patients harbored concomitant *parC* mutations that are associated with fluoroquinolone resistance, meaning that mutations in *gyrA* were not detected in the absence of *parC* mutations. The 5 patients with mutations in *gyrA* at G285A harbored a concurrent *parC* mutation at G248T, suggesting the strains were similar.

We detected dual macrolide and fluoroquinolone resistance in 20% (16/81) of patients (Table 1). Fluoroquinolone-resistant strains were likely to show concurrent macrolide resistance (89%), with the exception of strains from 2 community patients, which harbored only a fluoroquinolone resistance-associated mutation at codon 83 in *parC*.

Repeat specimens from 2 community patients were suggestive of macrolide resistance developing during the sampling period. For 1 patient, 2 of 3 urine samples received at 2-month intervals were negative for 23S rRNA mutations, with a mutation only detected in the most recent of the 3 samples. Another community patient was infected with a strain that harbored a *parC* mutation in codon 83 only; however, a 23S rRNA mutation was later detected in 2 subsequent urine samples collected at 1-month intervals, and the *parC* mutation persisted. A SHC attendee harbored both 23S rRNA and *parC* resistance-associated mutations initially, and a subsequent sample collected 5

Table 2. Position and number of patients with mutations detected in the quinolone resistance–determining regions of the *gyrA* and *parC* genes in *Mycoplasma genitalium* strains from community and SHC patients, Auckland, New Zealand, 2017*

Gene and mutation†	Amino acid change	No. patients with mutation			References
		Community patients	SHC patients	All patients	
<i>gyrA</i>					
G285A	Met → Ile (95)	1	4	5	(1,9)
G285T	Met → Ile (95)	0	1	1	(11)
<i>parC</i>					
C184T‡	Pro → Ser (61)	3	2	5	(1,9,11)
G241T	Gly → Cys (81)	1	0	1	(1,12)
A247C	Ser → Arg (83)	1	0	1	(1,3,9,12)
G248T	Ser → Ile (83)	2	6	8	(1–3,9)
T249A	Ser → Arg (83)	1	0	1	
G259A	Asp → Asn (87)	2	0	2	(1–3,8,9,11)
G259T	Asp → Tyr (87)	2	3	5	(1,2,8,10)
C356T‡	Ala → Val (119)	1	0	1	(11)

*Nucleotide position and amino acid changes shown are based on *M. genitalium* numbering. SHC, sexual health clinic.

†Silent mutations not reported.

‡Fluoroquinolone resistance not determined.

months later harbored a mutation in *gyrA* at G285T in addition to the 23S rRNA and *parC* mutations.

Conclusions

Our findings imply that resistance is common in circulating *M. genitalium* strains in the general population and highlight the limited and declining antimicrobial options for treatment. Few studies have delineated antimicrobial resistance by referrer type, and our results imply that macrolide- and fluoroquinolone-resistant strains are endemic in sexual networks in the general population, rather than confined to, or disproportionately affecting, persons attending SHCs. This information might be useful at local and national levels for informing sexual health treatment guidelines, but a need exists for supranational monitoring and reporting of resistance, given that it varies between countries (13).

Infections caused by strains resistant to both macrolides and fluoroquinolones occurred in 20% of patients, who would require alternative treatment options to obtain clinical and microbiological cure. Although pristinamycin has been successfully used to treat patients with multidrug-resistant infections (14), this treatment is not publicly funded in New Zealand and is only available as an imported medicine by special approval, underscoring the importance of exploring new treatment strategies to manage patients with resistant strains.

The presence of fluoroquinolone resistance in macrolide-sensitive strains in the community is concerning and might signify emergence of circulating fluoroquinolone-monoresistant strains in the region, with consequent implications for future treatment strategies. Although our data do not distinguish between descendants of clonal mutant lineages and de novo variants, we speculate that the introduction of a resistant clone from overseas is likely and that the use of fluoroquinolones in the community contributes to selective pressure for resistant strains.

A limitation of this study was that we did not have patient information regarding treatment of infection or clinical outcomes. This information might help establish whether resistance developed during treatment or occurred through reinfection with a more resistant strain. Another limitation was the inability to establish chain of transmission between patients, which was particularly relevant to the 4 SHC attendees and 1 community patient who harbored similar strains with identical mutations in both the *gyrA* and *parC* genes.

Mutations in the *gyrB* and *parE* genes act synergistically to increase fluoroquinolone resistance when

detected with mutations in *gyrA*, *parC*, or both and might also warrant consideration when screening strains for markers of resistance (15). We found that in genotypically fluoroquinolone-resistant strains, single-nucleotide polymorphisms in *gyrA* were only detected with concomitant *parC* mutations. This finding might support diagnostic laboratories in efforts to target only the 23S rRNA and *parC* genes during their genotypic-resistance testing.

Funding was provided by an Auckland District Health Board Charitable Trust grant (research project no. A+7436).

About the Author

Ms. Vesty is a scientific officer at Auckland City Hospital and a PhD candidate at the University of Auckland, New Zealand. Her research interests include medical microbiology and the human microbiome.

References

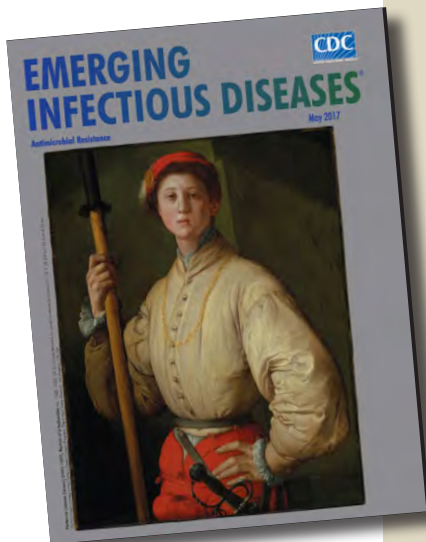
1. Tagg KA, Jeffreys NJ, Couldwell DL, Donald JA, Gilbert GL. Fluoroquinolone and macrolide resistance-associated mutations in *Mycoplasma genitalium*. *J Clin Microbiol*. 2013;51:2245–9. PubMed <https://doi.org/10.1128/JCM.00495-13>
2. Couldwell DL, Tagg KA, Jeffreys NJ, Gilbert GL. Failure of moxifloxacin treatment in *Mycoplasma genitalium* infections due to macrolide and fluoroquinolone resistance. *Int J STD AIDS*. 2013;24:822–8. <https://doi.org/10.1177/0956462413502008>
3. Anderson T, Coughlan E, Werno A. *Mycoplasma genitalium* macrolide and fluoroquinolone resistance detection and clinical implications in a selected cohort in New Zealand. *J Clin Microbiol*. 2017;55:3242–8. <https://doi.org/10.1128/JCM.01087-17>
4. Yamaguchi Y, Takei M, Kishii R, Yasuda M, Deguchi T. Contribution of topoisomerase IV mutation to quinolone resistance in *Mycoplasma genitalium*. *Antimicrob Agents Chemother*. 2013;57:1772–6. <https://doi.org/10.1128/AAC.01956-12>
5. Basu I, Roberts SA, Bower JE, Henderson G, Reid M. High macrolide resistance in *Mycoplasma genitalium* strains causing infection in Auckland, New Zealand. *J Clin Microbiol*. 2017;55:2280–2. <https://doi.org/10.1128/JCM.00370-17>
6. Kikuchi M, Ito S, Yasuda M, Tsuchiya T, Hatazaki K, Takanashi M, et al. Remarkable increase in fluoroquinolone-resistant *Mycoplasma genitalium* in Japan. *J Antimicrob Chemother*. 2014;69:2376–82. <https://doi.org/10.1093/jac/dku164>
7. Jensen JS, Björnelius E, Dohn B, Lidbrink P. Use of TaqMan 5' nuclease real-time PCR for quantitative detection of *Mycoplasma genitalium* DNA in males with and without urethritis who were attendees at a sexually transmitted disease clinic. *J Clin Microbiol*. 2004;42:683–92. <https://doi.org/10.1128/JCM.42.2.683-692.2004>
8. Deguchi T, Maeda S, Tamaki M, Yoshida T, Ishiko H, Ito M, et al. Analysis of the *gyrA* and *parC* genes of *Mycoplasma genitalium* detected in first-pass urine of men with

- non-gonococcal urethritis before and after fluoroquinolone treatment. *J Antimicrob Chemother.* 2001;48:742–4. <https://doi.org/10.1093/jac/48.5.742>
9. Murray GL, Bradshaw CS, Bissessor M, Danielewski J, Garland SM, Jensen JS, et al. Increasing macrolide and fluoroquinolone resistance in *Mycoplasma genitalium*. *Emerg Infect Dis.* 2017;23:809–12. <https://doi.org/10.3201/eid2305.161745>
 10. Shimada Y, Deguchi T, Nakane K, Masue T, Yasuda M, Yokoi S, et al. Emergence of clinical strains of *Mycoplasma genitalium* harbouring alterations in *parC* associated with fluoroquinolone resistance. *Int J Antimicrob Agents.* 2010; 36:255–8. <https://doi.org/10.1016/j.ijantimicag.2010.05.011>
 11. Hamasuna R, Le PT, Kutsuna S, Furubayashi K, Matsumoto M, Ohmagari N, et al. Mutations in *parC* and *gyrA* of moxifloxacin-resistant and susceptible *Mycoplasma genitalium* strains. *PLoS One.* 2018;13:e0198355. <https://doi.org/10.1371/journal.pone.0198355>
 12. Dumke R, Thürmer A, Jacobs E. Emergence of *Mycoplasma genitalium* strains showing mutations associated with macrolide and fluoroquinolone resistance in the region Dresden, Germany. *Diagn Microbiol Infect Dis.* 2016;86:221–3. <https://doi.org/10.1016/j.diagmicrobio.2016.07.005>
 13. Golden MR, Workowski KA, Bolan G. Developing a Public Health Response to *Mycoplasma genitalium*. *J Infect Dis.* 2017;216(suppl_2):S420–6. <https://doi.org/10.1093/infdis/jix200>
 14. Read TRH, Jensen JS, Fairley CK, Grant M, Danielewski JA, Su J, et al. Use of pristinamycin for macrolide-resistant *Mycoplasma genitalium* infection. *Emerg Infect Dis.* 2018;24:328–35. <https://doi.org/10.3201/eid2402.170902>
 15. Bébéar CM, Grau O, Charron A, Renaudin H, Gruson D, Bébéar C. Cloning and nucleotide sequence of the DNA gyrase (*gyrA*) gene from *Mycoplasma hominis* and characterization of quinolone-resistant mutants selected in vitro with trovafloxacin. *Antimicrob Agents Chemother.* 2000;44:2719–27. <https://doi.org/10.1128/AAC.44.10.2719-2727.2000>

Address for correspondence: Indira Basu, Auckland District Health Board, Private Bag 110031, Auckland Hospital, Auckland 1148, New Zealand; email IndiraB@adhb.govt.nz

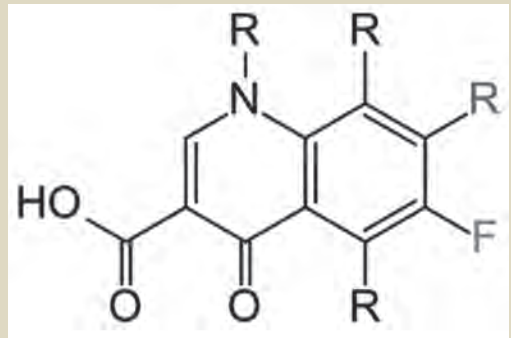
etymologia revisited

Fluoroquinolone [floor"o-kwin'o-lōn]



**Originally published
in May 2017**

The first quinolone (*quinol*[ine] + *-one* [compound related to ketone]), nalidixic acid, was isolated as a by-product of chloroquine (see “quinine,” https://wwwnc.cdc.gov/EID/article/21/7/ET-2107_article) synthesis and was introduced in 1962 to treat urinary tract infections. In 1980, researchers at the Kyorin Pharmaceutical Company showed that the addition of a fluorine atom to the quinolone ring resulted in an antibiotic with broader antimicrobial activity, which was named norfloxacin, the first fluoroquinolone. In 1983, Bayer published data that showed adding a single carbon atom to norfloxacin – what would become ciprofloxacin – further increased activity. Fluoroquinolones are today among the most frequently used antimicrobial drugs to treat infections in humans and animals.



By Reubot, Public domain, Wikimedia Commons, <https://commons.wikimedia.org/w/index.php?curid=14746558>

Sources: See link.

https://wwwnc.cdc.gov/eid/article/23/5/et-2305_article

Early Detection of Public Health Emergencies of International Concern through Undiagnosed Disease Reports in ProMED-Mail

Camille Rolland, Clément Lazarus, Coralie Giese, Bastien Monate, Anne-Sophie Travert, Jérôme Salomon

We conducted a retrospective analysis of all reports in ProMED-mail that were initially classified as undiagnosed diseases during 2007–2018. We identified 371 cases reported in ProMED-mail; 34% were later diagnosed. ProMED-mail could be used to supplement other undiagnosed disease surveillance systems worldwide.

To preserve human health security, a global surveillance system able to rapidly detect, verify, and assess burgeoning outbreaks is key. The World Health Organization (WHO) International Health Regulations (2005) (1) provides an international and legally binding framework for the early detection of, reporting of, and response to any public health threat (e.g., infectious disease outbreaks) that might be of international concern using an all-hazards approach (2).

Event-based surveillance through informal sources now represents a critical source for epidemic intelligence (3). Almost all major outbreaks during 1994–2017 investigated by the WHO were early reported and identified through informal sources (4–7). One of the most valued, internationally acknowledged sources for epidemic intelligence activities that is also available as an open source is ProMED-mail (4,8). By relying on local media, professional networks, and on-the-ground experts, ProMED-mail staff produce reports on occurrences of emerging infectious diseases and outbreaks in near real-time. Specialist moderators curate these reports and provide subject matter expert commentaries.

ProMED-mail captures many reports of undiagnosed diseases (i.e., reports of public health

events for which the diagnosis has not yet been found or reported by field professionals and cannot be classified). Events in these reports take place all around the world, and reports are provided without enough information to formulate a comprehensive risk assessment.

Even though an undiagnosed disease report in ProMED-mail might be an early signal of a major future event (e.g., outbreak), such reports have not been described in the literature. In this study, we aimed to provide a descriptive analysis of reports of undiagnosed disease events related to human health published on ProMED-mail since 2007 to determine whether these reports should be considered in further risk assessments.

The Study

We conducted a retrospective analysis of all reports of undiagnosed diseases in the ProMED-mail registry that were published during January 1, 2007–June 14, 2018 (Figure 1). ProMED-mail staff provided all the archives for undiagnosed diseases and unknown diseases relative to humans, animals, and plants. We also collected data directly from Disease Outbreak News on the WHO website (<https://www.who.int/csr/don/archive/country>) for the period of the study; these data are also open access and disseminated as specified by Article 11 of the International Health Regulations (2005). From ProMED-mail reports, we collected data on case location (WHO zone), source of information, date of publication, number of cases, geographic distribution (i.e., regional, national, or international) of cases, affected population, and final diagnosis. We searched the WHO website for the existence of a related Disease Outbreak News report. We sought information on the confirmation (i.e., biologic confirmation) of the final diagnosis both in subsequent ProMED-mail reports and in Disease Outbreak

Author affiliations: Public Health Emergency Operations Center of the French Ministry of Health, Paris, France (C. Rolland, C. Lazarus, B. Monate, A.-S. Travert); Ministry of Health, Paris (C. Giese, J. Salomon)

DOI: <https://doi.org/10.3201/eid2602.191043>

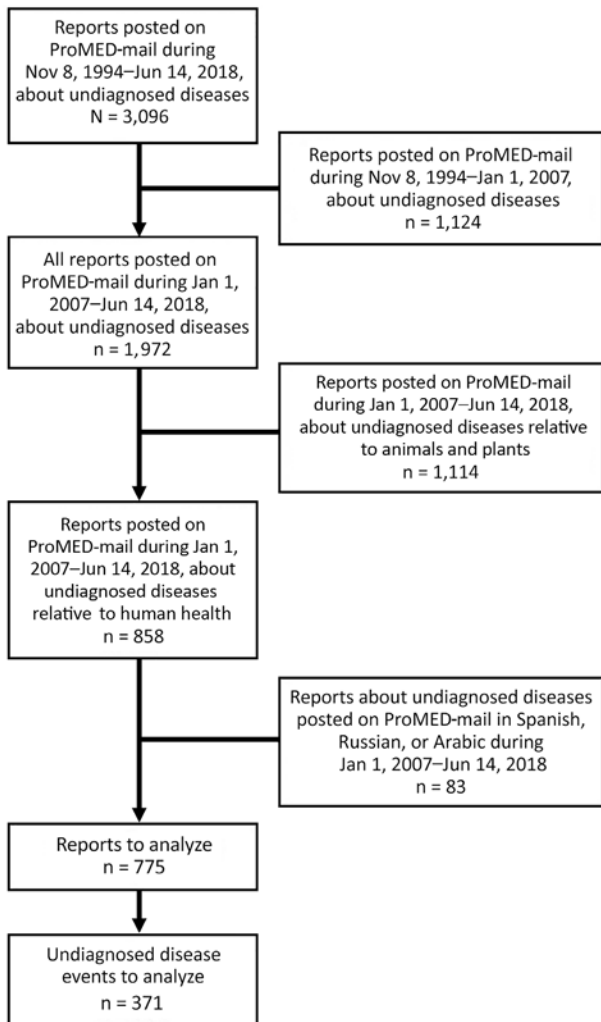


Figure 1. Selection of ProMED-mail reports to analyze for undiagnosed disease events related to human health, January 1, 2007–December 30, 2017.

News reports. When several notifications were linked to 1 undiagnosed disease event, we made the link between notifications using the date of occurrence and location data. We described quantitative variables using median and range and qualitative variables using percentages.

During January 1, 2007–June 14, 2018, a total of 775 ProMED-mail reports accounted for 371 individual undiagnosed disease events in humans (Figure 1). The median number of undiagnosed disease events per year was 34 (range 15–45) (Figure 2). The sources of these reports were mainly the national press (67%, 250/371); 25% (93/371) were from international media, and 8% (28/371) were from experts.

The countries most affected by undiagnosed diseases were India (68/371), Sudan (20/371), Bangladesh (16/371), Nepal (15/371), China (14/371), the Democratic Republic of the Congo (13/371), Uganda (13/371), the United States (13/371), Vietnam (11/371), and Nigeria (9/371) (Appendix Figure, <https://wwwnc.cdc.gov/EID/article/26/2/19-1043-App1.pdf>). Overall, 44% of undiagnosed disease events were in rural areas and 56% were in urban areas; 8% (31/371) took place within a capital city. For 54% (200/371) of undiagnosed disease events, no specific population (e.g., children <18 years of age, persons >65 years of age, health professionals) was identified. For 2.4% (9/371) of undiagnosed disease events, healthcare professionals were affected.

We found a Disease Outbreak News report for 6.5% (24/371) of the undiagnosed disease events described in ProMED-mail. The median delay between the first ProMED-mail notification and the Disease Outbreak News publication was 18.5 (range –1 to 254) days (Table).

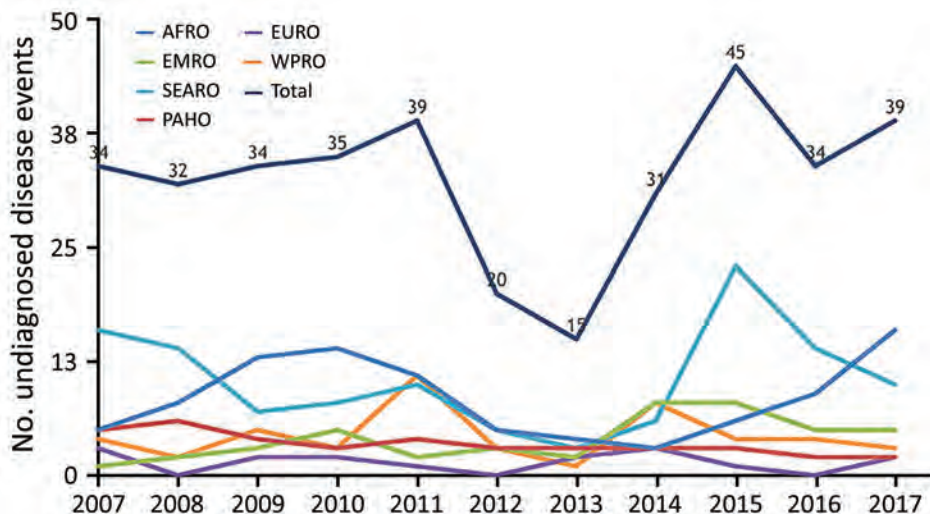


Figure 2. Undiagnosed disease events in humans posted on ProMED-mail, by location (World Health Organization zone), January 1, 2007–December 30, 2017. AFRO, African Regional Office; EMRO, Eastern Mediterranean Regional Office; EURO, Europe Regional Office; PAHO, Pan American Health Organization; SEARO, South-East Asia Regional Office; WPRO, Western Pacific Regional Office.

Table. Characteristics of the 24 undiagnosed disease events posted on ProMED-mail that were also published in Disease Outbreak News, 2007–2018*

ProMED-mail diagnosis date	Country	WHO zone	Diagnosis	Publication date	Period, dt
2007 Sep 1	DRC	AFRO	Ebola	2007 Aug 31	-1
2007 Nov 9	Angola	AFRO	Bromide poisoning	2007 Nov 16	7
2008 Mar 8	Senegal	AFRO	Lead poisoning	2008 Jun 28	112
2008 Jun 23	Senegal	AFRO	Lead poisoning	2008 Jun 28	5
2008 Aug 21	China	WPRO	Powder milk intoxication	2008 Sep 18	28
2008 Oct 5	South Africa	AFRO	Lassa fever	2008 Oct 10	5
2008 Oct 9	DRC	AFRO	Ebola	2008 Dec 26	78
2008 Dec 22	DRC	AFRO	Ebola	2008 Dec 26	4
2010 Sep 27	Pakistan	EMRO	Crimean-Congo hemorrhagic fever	2010 Oct 25	28
2011 Aug 16	Angola	AFRO	Undiagnosed disease	2011 Aug 15	-1
2012 Jul 4	Cambodia	WPRO	Hand, foot and mouth disease	2012 Jul 4	0
2012 Jul 25	Uganda	AFRO	Ebola	2012 Jul 27	2
2012 Aug 2	Uganda	AFRO	Ebola	2012 Aug 3	1
2012 Dec 23	Sudan	EMRO	Yellow fever	2012 Nov 13	-41
2014 Feb 24	USA	PAHO	Human enterovirus infection	2014 Sep 17	205
2015 Feb 9	Brazil	PAHO	Zika virus infection	2015 Oct 21	254
2015 Jul 20	Egypt	EMRO	Dengue fever	2015 Nov 12	115
2015 Aug 15	Egypt	EMRO	Dengue fever	2015 Nov 12	90
2015 Sep 5	Senegal	AFRO	Chikungunya	2015 Sep 14	9
2016 Jun 25	South Sudan	EMRO	Undiagnosed disease	2016 May 19	-38
2016 Jan 22	Angola	AFRO	Yellow fever	2016 Feb 12	21
2017 Mar 8	Nigeria	AFRO	Meningitis	2017 Mar 24	16
2017 Apr 26	Liberia	AFRO	Meningitis	2017 May 5	9
2018 Jan 7	Kenya	AFRO	Chikungunya	2018 Feb 27	51

*AFRO, African Regional Office; DRC, Democratic Republic of the Congo; EMRO, Eastern Mediterranean Regional Office; PAHO, Pan American Health Organization; WHO, World Health Organization; WPRO, Western Pacific Regional Office.

†Time between notification on ProMED-mail and official publication in Disease Outbreak News (<https://www.who.int/csr/don/archive/country>). Negative numbers indicate publication in Disease Outbreak News first.

A final diagnosis was found for 34% (127/371) of undiagnosed disease events (Appendix Table). Among the 127 events for which a final diagnosis could be determined, the most frequent diseases were chikungunya (6/127), leptospirosis (6/127), Nipah virus infection (6/127), Ebola (5/127), meningitis (5/127), yellow fever (5/127), anthrax (4/127), Crimean-Congo hemorrhagic fever (4/127), and nodding disease (4/127).

Undiagnosed diseases might be reported in various medical situations. They often occur in cases of delayed diagnosis of common diseases when access to appropriate medical care or services (e.g., epidemiologic investigations, laboratory testing) is limited. As such, most undiagnosed disease events occurred within low-resource countries. Undiagnosed disease reports less frequently account for unusual or unexpected diseases, such as imported or emerging diseases.

Reporting of undiagnosed diseases through ProMED-mail can be limited by climatic or geopolitical events in the region, which was probably reflected by the yearly and geographic variation in the reporting of undiagnosed disease events we observed. Although informal sources of public health information are valuable, the editorial content of the news sources the reports are based on can strongly limit their usefulness. Hence, our data analysis was limited by missing data.

Conclusions

The impact of ProMED-mail on the public health emergency preparedness response is reflected by the percentage of undiagnosed disease events published through this informal reporting system (6.5%) that were also shared internationally through WHO's Disease Outbreak News website. Regions and countries could benefit from complementing their undiagnosed disease surveillance systems with ProMED-mail (9). Using this approach would help further establish undiagnosed disease event-based monitoring as an invaluable public health tool. ProMED-mail provides critical content and an alternative to standard indicator-based outbreak reporting for undiagnosed diseases (4).

Acknowledgments

We thank the ProMED-mail staff, who made this research possible, and Elsa Dorne for her assistance in reviewing the language of the manuscript.

About the Author

Dr. Rolland is a public health resident who works in the Public Health Emergency Operations Center of the French Ministry of Health in Paris, France. She participates in the operational management of public health alerts in France as well as internationally. Her research interests are infectious diseases (including sexually transmitted infections), emerging diseases, and international health surveillance.

References

1. World Health Organization. International Health Regulations (2005) third edition. 2016 [cited 2019 Jul 22]. <https://apps.who.int/iris/bitstream/handle/10665/246107/9789241580496-eng.pdf>
2. Hartley D, Nelson N, Walters R, Arthur R, Yangarber R, Madoff L, et al. Landscape of international event-based biosurveillance. *Emerg Health Threats J.* 2010;3:7096. <https://doi.org/10.3402/ehth.v3i0.7096>
3. World Health Organization Western Pacific Region. A guide to establishing event-based surveillance. 2008 [cited 2019 Jul 22]. http://www.wpro.who.int/emerging_diseases/documents/docs/eventbasedsurv.pdf
4. Keller M, Blench M, Tolentino H, Freifeld CC, Mandl KD, Mawudeku A, et al. Use of unstructured event-based reports for global infectious disease surveillance. *Emerg Infect Dis.* 2009;15:689–95. <http://dx.doi.org/10.3201/eid1505.081114>
5. Grein TW, Kamara KB, Rodier G, Plant AJ, Bovier P, Ryan MJ, et al. Rumors of disease in the global village: outbreak verification. *Emerg Infect Dis.* 2000;6:97–102. <https://doi.org/10.3201/eid0602.000201>
6. Heymann DL, Rodier GR; World Health Organization Operational Support Team to the Global Outbreak Alert and Response Network. Hot spots in a wired world: WHO surveillance of emerging and re-emerging infectious diseases. *Lancet Infect Dis.* 2001;1:345–53. [https://doi.org/10.1016/S1473-3099\(01\)00148-7](https://doi.org/10.1016/S1473-3099(01)00148-7)
7. Carrion M, Madoff LC. ProMED-mail: 22 years of digital surveillance of emerging infectious diseases. *Int Health.* 2017;9:177–83. <https://doi.org/10.1093/inthealth/ihx014>
8. Krishnan S. Undiagnosed deaths – India (Uttar Pradesh) (02). ProMed. 2006 Aug 14 [cited 2019 Jul 22]. <http://www.promedmail.org>, archive no. 20060814.2279.
9. Woodall JP. Global surveillance of emerging diseases: the ProMED-mail perspective. *Cad Saude Publica.* 2001; 17(Suppl):147–54. <https://doi.org/10.1590/S0102-311X2001000700024>

Address for correspondence: Clément Lazarus, Public Health Emergency Operations Center, 14 Avenue Duquesne, Paris 75007, France; email: clement.lazarus@sante.gouv.fr



EMERGING INFECTIOUS DISEASES™

January 2018

High-Consequence Pathogens

- Zika Virus Testing and Outcomes during Pregnancy, Florida, USA, 2016
- Sensitivity and Specificity of Suspected Case Definition Used during West Africa Ebola Epidemic
- Nipah Virus Contamination of Hospital Surfaces during Outbreaks, Bangladesh, 2013–2014
- Detection and Circulation of a Novel Rabbit Hemorrhagic Disease Virus, Australia
- Drug-Resistant Polymorphisms and Copy Numbers in *Plasmodium falciparum*, Mozambique, 2015
- Increased Severity and Spread of *Mycobacterium ulcerans*, Southeastern Australia
- Emergence of Vaccine-Derived Polioviruses during Ebola Virus Disease Outbreak, Guinea, 2014–2015
- Characterization of a Feline Influenza A(H7N2) Virus
- Japanese Encephalitis Virus Transmitted Via Blood Transfusion, Hong Kong, China
- Changing Geographic Patterns and Risk Factors for Avian Influenza A(H7N9) Infections in Humans, China
- Pneumonic Plague in Johannesburg, South Africa, 1904
- Dangers of Noncritical Use of Historical Plague Databases
- Recognition of Azole-Resistant Aspergillosis by Physicians Specializing in Infectious Diseases, United States
- Melioidosis, Singapore, 2003–2014
- Serologic Evidence of Fruit Bat Exposure to Filoviruses, Singapore, 2011–2016
- Expected Duration of Adverse Pregnancy Outcomes after Zika Epidemic
- Seroprevalence of Jamestown Canyon Virus among Deer and Humans, Nova Scotia, Canada
- Postmortem Findings for a Patient with Guillain-Barré Syndrome and Zika Virus Infection
- Rodent Abundance and Hantavirus Infection in Protected Area, East-Central Argentina
- Two-Center Evaluation of Disinfectant Efficacy against Ebola Virus in Clinical and Laboratory Matrices
- Phylogeny and Immunoreactivity of Human Norovirus GII.P16-GII.2, Japan, Winter 2016–17
- Mammalian Pathogenesis and Transmission of Avian Influenza A(H7N9) Viruses, Tennessee, USA, 2017
- Whole Genome Analysis of Recurrent *Staphylococcus aureus* t571/ST398 Infection in Farmer, Iowa, USA

To revisit the January 2018 issue, go to:

<https://wwwnc.cdc.gov/eid/articles/issue/24/1/table-of-contents>

Ocular *Spiroplasma ixodetis* in Newborns, France

Alexandre Matet, Anne Le Flèche-Matéos, François Doz, Pascal Dureau, Nathalie Cassoux

Cataract and uveitis are rare in newborns but potentially blinding. Three newborns with cataract and severe anterior uveitis underwent cataract surgery. *Spiroplasma ixodetis* was detected in lens aspirates using bacterial 16S-rRNA PCR and transmission electron microscopy. These findings, which suggest maternal–fetal infection, are consistent with previous experimental *Spiroplasma*-induced cataract and uveitis.

Spiroplasma is a genus of Mollicutes, a class of bacteria without cell wall. *Spiroplasma* are intracellular organisms with helical morphology and a small genome (0.78–2.2 Mb) comprising 38 species isolated from insects, crustaceans, and plants (1,2). Ticks, from which *Spiroplasma ixodetis* has been isolated, are abundant sources of *Spiroplasma* (3).

Spiroplasma develop a commensal, pathogenic, or mutualist pathogen–host relationship. The first isolated species (*S. citri*) was described in 1973 (4,5). Two *Spiroplasma* infections have been reported in humans: an intraocular infection in a newborn with Group VI *Spiroplasma*, now known as *S. ixodetis* (6), and a systemic infection in an immunocompromised adult with *S. turonicum* (7). These reports suggest that tetracyclines and macrolides are effective against *Spiroplasma* (6,7). We describe 3 newborns in France who had cataract and intraocular inflammation and in whom *S. ixodetis* was detected in ocular samples (Table).

The Case-Patients

In January 2014, case-patient 1, a 26-day-old girl with unremarkable medical history, was referred for bilateral leukocoria observed by her parents at 20 days of age, suggestive of retinoblastoma. She was born after normal full-term pregnancy without delivery complications (birthweight 2,820 g; Apgar score 10). She had

bilateral anterior uveitis, large keratic precipitates, iris nodules, posterior synechiae, cyclitic membrane, and cataract (Figure 1, panels A, B). Fundus visualization and ocular ultrasonography ruled out retinoblastoma. Physical examination results were unremarkable. Blood cell count showed elevated monocytes ($1.5 \times 10^9/L$ [reference range $0.2\text{--}1.0 \times 10^9/L$]); serologic results for *Toxoplasma gondii*, rubella virus, cytomegalovirus, herpes simplex viruses 1 and 2, HIV-1 and -2, and *Mycoplasma* were negative. Aqueous humor cytologic examination did not reveal malignant cells but identified macrophages, suggesting intraocular infection, as observed in *Tropheryma whipplei*-related uveitis (8). Treatment with topical dexamethasone (8 drops/d with progressive tapering), topical atropine (0.3%, 2 drops/d), and oral josamycin (125 mg 2×/d) was initiated. Anterior chamber inflammation decreased dramatically, and cataract surgery with intraocular lens implantation was performed sequentially in both eyes 4 weeks later. We conducted microbiological investigations of lens and anterior vitreous aspirates from the right eye, including bacteriologic and mycologic cultures, and 16S-rRNA-based PCR for bacterial identification (Appendix, <https://wwwnc.cdc.gov/EID/article/26/2/19-1097-App1.pdf>). Cultures remained negative, but bacterial PCR identified a complete sequence of the *rrs* gene, showing 98.7% similarity to the type strains of *S. ixodetis* (Figure 2). Uveitis did not recur over the next 4 years.

In January 2018, bilateral leukocoria caused by bilateral congenital cataract was detected in an otherwise healthy boy, case-patient 2, on day 3 after full-term birth (birthweight 2,900 g; Apgar score 10). Pregnancy was unremarkable, without maternal seroconversion for toxoplasmosis, rubella, herpes simplex viruses 1 and 2, or cytomegalovirus. Six weeks after birth, ophthalmologic examination under anesthesia revealed a total cataract in each eye with large keratic precipitates, posterior synechiae, and immature dilated iris vessels (Figure 1, panels C, D). Fundus was inaccessible in both eyes. The right eye was slightly microphthalmic. Because of the rarity of uveitis with

Author affiliations: Institut Curie and Université Paris Descartes, Paris, France (A. Matet, F. Doz, N. Cassoux); Institut Pasteur, Paris (A. Le Flèche-Matéos); Fondation Ophthalmologique Adolphe de Rothschild, Paris (P. Dureau)

DOI: <https://doi.org/10.3201/eid2602.191097>

Table. Characteristics of 3 newborns with cataract and anterior uveitis* and 5 controls with congenital cataracts without signs of intraocular infection, France†

ID no.	Sex	Date of diagnosis	Age at diagnosis/lens extraction, mo	Affected eye	Clinical ocular findings	Region of residence (environment)	Travel during pregnancy	Crystalline lens sample volume, μ L	Bacterial 16S-rRNA PCR, % homology to <i>S. ixodeti</i>
Case-patients									
1	F	2014 Jan	1/2	Both	Cataract + anterior uveitis	Hauts-de-France, France (rural area, adjacent to Saint-Gobain Forest)	No	200	98.7
2	M	2018 Jan	0/3	Both	Cataract + anterior uveitis	Centre-Val de Loire, France (rural area, adjacent to Loire-Anjou-Touraine Regional Forest)	No	150	98.6
3	M	2019 Jan	1/2	Left	Cataract + anterior uveitis	Ile-de-France, France (Paris suburban area)	No	100	98.7
Controls									
1	F	2018 Feb	4/5	Right	Cataract	NA	NA	50	Negative
2	M	2018 Apr	4/5	Right	Cataract + nystagmus	NA	NA	10	Negative
3	M	2018 Apr	4/5	Left	Cataract + nystagmus	NA	NA	200	Negative
4	F	2018 Feb	1/2	Left	Cataract	NA	NA	100	Negative
5	F	2018 Mar	0/3	Left	Cataract	NA	NA	50	Negative

*Positive for *Spiroplasma ixodeti* in crystalline lens material by bacterial 16S-rRNA PCR.

†For all case-patients and controls, pregnancy was normal and delivery was uneventful. NA, not applicable.

keratic precipitates and cataract in newborns and the similarity to case-patient 1, the child underwent bilateral cataract extraction without lens implantation, and lens material was sent for bacteriologic investigations.

The 16S-rRNA-based PCR of the *rrs* gene identified in both eyes was 98.6% similar to *S. ixodeti*. Mild, self-resolving bilateral intravitreal hemorrhage developed after cataract surgery. Anterior segment

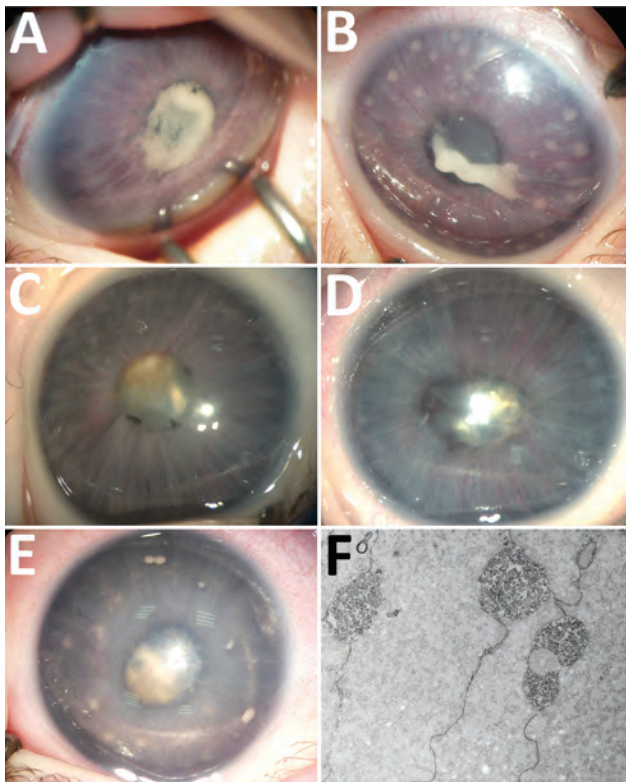


Figure 1. Ocular anterior segment in 3 newborn infants with bilateral total cataract and anterior uveitis related to endogenous *Spiroplasma ixodeti* infection. A, B) Case-patient 1. Right (A) and left (B) eyes of a 4-week-old girl showing total cataract, posterior synechiae due to a cyclitic fibrin membrane, and large keratic precipitates more visible in the left eye. The immature iris vasculature is dilated in the context of anterior segment inflammation. C, D) Case-patient 2. Right (C) and left (D) eyes of a 6-week-old boy showing total cataract, posterior synechiae, dilated immature iris vessels, and few keratic precipitates more visible in the left eye. E) Case-patient 3. Left eye of a 1-month-old boy with multiple retrocorneal white deposits, total cataract, posterior synechiae, and immature dilated iris vessels. F) Case-patient 3. Electron transmission microscopy of crystalline lens material from a 2-month-old boy with total cataract and anterior uveitis, revealing the presence of microorganisms with spiral-like projections highly suggestive of bacteria from the *Spiroplasma* genus.

inflammation resolved under topical dexamethasone (4 drops/d with progressive tapering over 3 months) and atropine (0.3%, 1 drop/d for 1 month) and did not recur over the next 18 months.

In January 2019, case-patient 3, a 1-month-old boy, was referred for left eye leukocoria, first observed 1 week after birth. Pregnancy was uneventful, and delivery was normal at 36 weeks' gestation

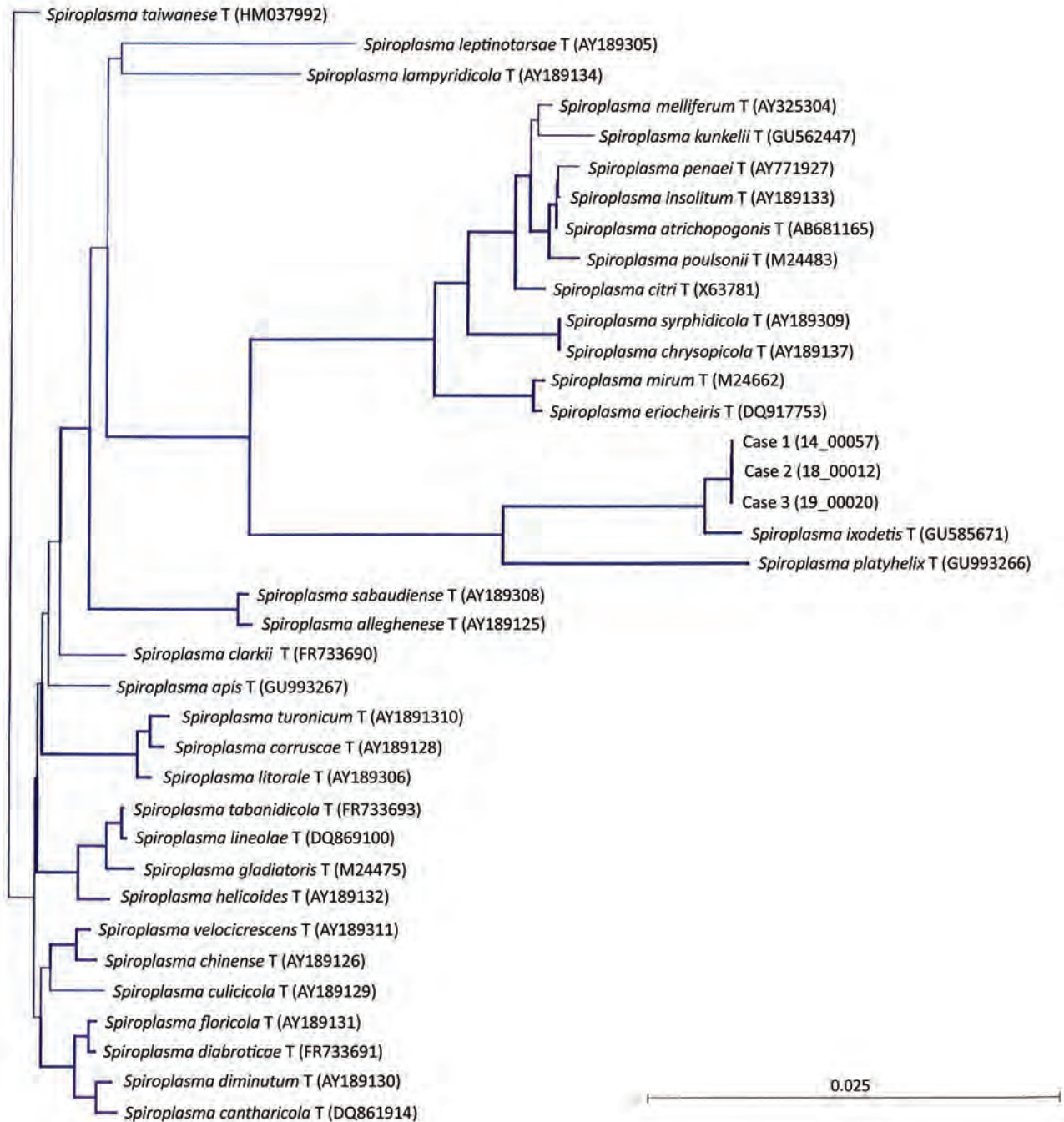


Figure 2. Neighbor-joining unrooted tree based on bacterial *rrs* gene sequences from the crystalline lens samples from 3 newborns with cataract and uveitis (case-patient 1, sample 14_00057; case-patient 2, sample 18_00012; case-patient 3, sample 19_00020). The 14_00057 (case-patient 1) and 19_00020 (case-patient 3) sequences differed by 1 nt along the 1,284-bp bacterial *rrs* gene, and the 18_00012 sequence (case-patient 2) harbored 2 additional nucleotides and differed from 14_00057 by 3 nt and from 19_00020 by 2 nt. At the variation site, the corresponding sequences were __ G (14_00057, case-patient 1), T G A (18_00012, case-patient 2), and __ A (19_00020, case-patient 3). Thick lines indicate bootstrap values >75% (based on 1,000 replicates). Scale bar indicates the proportion of substitutions per nucleotide position.

(birthweight 2,800 g; Apgar score 10). Left eye examination revealed multiple large keratic white deposits, total cataract, posterior synechiae, and immature dilated iris vessels (Figure 1, panel E). Results of a right eye examination were unremarkable. He underwent cataract extraction with synechialysis, without intraocular lens implantation. 16S rRNA-based PCR of the bacterial *rrs* gene performed on crystalline lens aspirates identified *S. ixodetis* with 98.7% similarity. Fresh crystalline lens samples analyzed by electron transmission microscopy revealed microorganisms with spiral-like projections matching the morphology of bacteria from the *Spiroplasma* genus (Figure 1, panel F). Postoperative mild intravitreal hemorrhage developed but self-resolved over 4 weeks. He was treated postoperatively with oral josamycin (125 mg 2×/d for 10 days), topical atropine (0.3% 2×/d for 1 month), and topical drops combining neomycin, polymixin B, and dexamethasone (4×/d with progressive tapering over 1 month). Intraocular inflammation did not recur over the next 6 months.

We conducted all PCRs in *Spiroplasma* DNA-free facilities. Internal negative controls were introduced during DNA manipulation/amplification (Appendix). No control was positive after 16S rRNA PCR amplification, confirming that the detection of *Spiroplasma* sequences did not result from contamination.

To confirm that *S. ixodetis* is absent in intraocular media of newborns with noninflammatory cataracts, we collected crystalline lens samples from 5 newborns with congenital cataracts who underwent surgery before 6 months of age (Table). 16S rRNA-based PCR did not identify any bacterial signature in these samples. The Internal Review Board of the French Society of Ophthalmology approved this study.

Conclusions

Until recently, *Spiroplasma* spp. were considered non-pathogenic in humans. Our observations confirm the reports by Lorenz et al. of an intraocular *Spiroplasma* spp. infection (6), and by Aquilino et al. of a systemic infection (7). Moreover, the congenital presentation of case-patients 1–3 suggests maternal–fetal transmission during pregnancy or delivery, despite the absence of maternal symptoms. Our findings are consistent with those of Lorenz et al., who described a premature baby born at 27 weeks' gestation who, at 4 months of age, had unilateral uveitis with corneal precipitates, posterior synechiae, and cataract. After cataract surgery, bacterial 16S-rRNA PCR of vitreous and lens aspirates identified *Spiroplasma* spp. Group VI (6), now referred to as *S. ixodetis* (9). Electron

microscopy visualized filamentous and helical microorganisms compatible with *Spiroplasma*.

Another clade of *Spiroplasma*, *S. mirum*, phylogenetically close to *S. ixodetis* (Figure 2), initially named suckling mouse cataract agent (9,10), induces rapid cataract formation after intracerebral injection in newborn mice (11), rats (12), and rabbits (13), with variable intraocular inflammation. In these models, adult animals do not develop ocular pathology, suggesting a vulnerability of the immature eye to *Spiroplasma* infection. Moreover, a high rate of microphthalmia developed in these animals, as in case-patient 2, suggesting that *Spiroplasma* infection might interfere with ocular development.

Our observations suggest that intrauterine or early postnatal contamination with *Spiroplasma* spp. might lead to unilateral or bilateral cataract and anterior uveitis in newborns. A similar causative *S. ixodetis* subtype was identified in all 3 infants, without technical contamination. Two of 3 case-patients lived in a rural area adjacent to a forest.

The frequency of this intraocular infection in newborns may be underestimated. *Spiroplasma* are fastidious organisms detectable using PCR techniques not routinely performed on intraocular samples. Because affected infants are at high risk for visual impairment or blindness, pediatricians, ophthalmologists, and microbiologists should be aware of possible *S. ixodetis* ocular infections and collect clinical, bacteriologic, and epidemiologic data on this emerging pathogen. The mechanisms and timing of probable maternal–fetal transmission require further investigations. On the basis of these observations, we recommend systematic bacterial 16S-rRNA PCR analysis on intraocular fluids and lens material from neonates with cataract and uveitis.

About the Author

Dr. Matet is an ophthalmologist and ocular oncology specialist at Institut Curie and Paris Descartes University. His primary research interests include pediatric and adult ocular tumors, radiation therapy, ocular inflammation and infection, and retinal imaging.

References

1. Gasparich GE. Spiroplasmas: evolution, adaptation and diversity. *Front Biosci.* 2002;7:d619–40.
2. Regassa LB, Gasparich GE. Spiroplasmas: evolutionary relationships and biodiversity. *Front Biosci.* 2006;11:2983–3002. <https://dx.doi.org/10.2741/2027>
3. Cisak E, Wójcik-Fatla A, Zajac V, Sawczyn A, Sroka J, Dutkiewicz J. *Spiroplasma* – an emerging arthropod-borne pathogen? *Ann Agric Environ Med.* 2015;22:589–93. <https://dx.doi.org/10.5604/12321966.1185758>
4. Tully JG, Whitcomb RF, Bove JM, Saglio P. Plant mycoplasmas: serological relation between agents associated

- with citrus stubborn and corn stunt diseases. *Science*. 1973;182:827-9. <https://dx.doi.org/10.1126/science.182.4114.827>
5. Whitcomb RF, Tully JG, Bové JM, Saglio P. Spiroplasmas and achleoplasmas: multiplication in insects. *Science*. 1973;182:1251-3. <https://dx.doi.org/10.1126/science.182.4118.1251>
 6. Lorenz B, Schroeder J, Reischl U. First evidence of an endogenous *Spiroplasma* sp. infection in humans manifesting as unilateral cataract associated with anterior uveitis in a premature baby. *Graefes Arch Clin Exp Ophthalmol*. 2002;240:348-53. <https://dx.doi.org/10.1007/s00417-002-0453-3>
 7. Aquilino A, Masiá M, López P, Galiana AJ, Tovar J, Andrés M, et al. First human systemic infection caused by *Spiroplasma*. *J Clin Microbiol*. 2015;53:719-21. <https://dx.doi.org/10.1128/JCM.02841-14>
 8. Touitou V, Fenollar F, Cassoux N, Merle-Beral H, LeHoang P, Amoura Z, et al. Ocular Whipple's disease: therapeutic strategy and long-term follow-up. *Ophthalmology*. 2012;119:1465-9. <https://dx.doi.org/10.1016/j.ophtha.2012.01.024>
 9. Gasparich GE, Whitcomb RF, Dodge D, French FE, Glass J, Williamson DL. The genus *Spiroplasma* and its non-helical descendants: phylogenetic classification, correlation with phenotype and roots of the *Mycoplasma mycoides* clade. *Int J Syst Evol Microbiol*. 2004;54:893-918. <https://dx.doi.org/10.1099/ijs.0.02688-0>
 10. Tully JG, Whitcomb RF, Williamson DL, Clark HF. Suckling mouse cataract agent is a helical wall-free prokaryote (*Spiroplasma*) pathogenic for vertebrates. *Nature*. 1976;259:117-20. <https://dx.doi.org/10.1038/259117a0>
 11. Olmsted E, Prasad S, Sheffer J, Clark HF, Karzon DT. Ocular lesions induced in C57 mice by the suckling mouse cataract agent (SMCA). *Invest Ophthalmol*. 1966;5:413-20.
 12. Friedlaender RP, Barile MF, Kuwabara T, Clark HF. Ocular pathology induced by the suckling mouse cataract agent. *Invest Ophthalmol*. 1976;15:640-7.
 13. Kirchhoff H, Heitmann J, Trautwein G. Pathogenicity of *Spiroplasma* sp. strain SMCA in rabbits: clinical, microbiological, and histological aspects. *Infect Immun*. 1981;33:292-6.

Address for correspondence: Alexandre Matet, Institut Curie, Service d'Ophthalmologie, 26 Rue d'Ulm, F-75248 Paris CEDEX 5, France; email: alexandre.matet@curie.fr

The Public Health Image Library (PHIL)



The Public Health Image Library (PHIL), Centers for Disease Control and Prevention, contains thousands of public health-related images, including high-resolution (print quality) photographs, illustrations, and videos.

PHIL collections illustrate current events and articles, supply visual content for health promotion brochures, document the effects of disease, and enhance instructional media.

PHIL images, accessible to PC and Macintosh users, are in the public domain and available without charge.

Visit PHIL at:
<https://phil.cdc.gov/phil>

Use of Surveillance Outbreak Response Management and Analysis System for Human Monkeypox Outbreak, Nigeria, 2017–2019

Bernard C. Silenou, Daniel Tom-Aba, Olawunmi Adeoye, Chinedu C. Arinze, Ferdinand Oyiri, Anthony K. Suleman, Adesola Yinka-Ogunleye, Juliane Dörrbecker, Chikwe Ihekweazu, Gérard Krause

In November 2017, the mobile digital Surveillance Outbreak Response Management and Analysis System was deployed in 30 districts in Nigeria in response to an outbreak of monkeypox. Adaptation and activation of the system took 14 days, and its use improved timeliness, completeness, and overall capacity of the response.

Human monkeypox is a severe and rare smallpox-like illness that occurs sporadically in remote villages in the tropical rain forest of West and Central Africa (1,2). The causative agent, monkeypox virus, is transmitted by animal-to-human and human-to-human contact (3,4). In September 2017, an outbreak of monkeypox occurred in Nigeria after 40 years of no reported cases in the country. As of October 2017, local health departments in Nigeria had reported 89 cases and 294 contact persons (5,6).

Early in the outbreak, the Nigeria Centre for Disease Control (NCDC) used a conventional surveillance system for the outbreak investigation. That system consisted of paper-based forms transferred manually to databases within the framework of the Integrated Disease Surveillance and Response System (7). As the outbreak expanded, NCDC faced challenges because of information delay and difficulties with updating and verifying case data, integrating laboratory tests, and managing contact tracing in the

conventional system. In October 2017, NCDC decided to implement the Surveillance, Outbreak Response Management and Analysis System (SORMAS) on an ad hoc basis; an earlier prototype of this system had been successfully piloted in Nigeria in 2015 (8). SORMAS is an open-source mHealth (mobile health) system that organizes and facilitates infectious disease control and outbreak management procedures in addition to disease surveillance and epidemiologic analysis for all administrative levels of a public health system (9–11). SORMAS includes specific interfaces for 12 users (e.g., laboratorian, contact tracing officer, epidemiologist), disease-specific process modules for 12 epidemic-prone diseases, and a customizable process module for unforeseen emerging diseases; it adheres to the Integrated Disease Surveillance and Response System. Most users operate SORMAS on mobile digital devices (e.g., smartphone, tablet), bidirectionally synchronized with a central server via mobile telecommunication networks.

We compared SORMAS performance with that of the conventional surveillance system. Here we describe how we adapted and deployed SORMAS, discuss challenges encountered during implementation, and provide recommendations for deployment of similar mHealth tools.

The Study

In the second week of October 2017, we held a 2-day design thinking workshop with clinicians, epidemiologists, and virologists, in which all specific procedures for surveillance and response were defined in accordance with guidelines from the World Health Organization (12). Within 10 days, we translated the findings of the workshop into process models and programmed them into the existing SORMAS. A 2-day field test guided final programming revisions,

Author affiliations: Helmholtz Centre for Infection Research, Braunschweig, Germany (B.C. Silenou, D. Tom-Aba, J. Dörrbecker, G. Krause); PhD Programme “Epidemiology,” Braunschweig-Hannover, Germany (B.C. Silenou, D. Tom-Aba); Nigeria Center for Disease Control, Abuja, Nigeria (O. Adeoye, C.C. Arinze, F. Oyiri, A.K. Suleman, A. Yinka-Ogunleye, C. Ihekweazu); German Center for Infection Research, Braunschweig (G. Krause)

DOI: <https://doi.org/10.3201/eid2602.191139>

Table 1. Qualitative comparison of attributes of SORMAS and the conventional surveillance system in response to monkeypox outbreak in Nigeria, November 2017–July 2019*

Attribute	SORMAS	CS	Comments
Average time for data to arrive at NCDC from LGAs	2 min	2 d	For the CS, the DSNOs sent the paper case forms by post to NCDC, thus requiring longer time for case forms to arrive at NCDC.
Average time to update data (sample results from the laboratory, case classification, outcome, contacts) per case	5 min	20 min	Update in SORMAS requires searching for a case in the case directory and directly updating the fields. For the CS, the database was Excel (https://www.microsoft.com), and each type of case data was stored on a different Excel sheet, thus increasing the time and complexity of updating case data.
Workload to transfer cases from paper forms to database at NCDC	Less	More	With the CS, all case forms were entered in an Excel database at NCDC; with SORMAS, 90 (38%) of the 240 cases were entered directly from the field by DSNOs.
Availability of dashboard and statistics module to generate epidemiologic indicators for disease surveillance (e.g., case classification status, epidemic curve, laboratory test results, fatalities, and map of spatial distribution of cases and contact persons)	Yes	No	SORMAS had a dashboard that displayed the needed surveillance indicators; the CS did not.

*CS, conventional system; DSNOs, district surveillance notification officers; NCDC, Nigeria Centre for Disease Control; LGAs, local government areas; SORMAS, Surveillance Outbreak Response Management and Analysis System.

which took another 2 days before the new module was released. In total, it took 14 days from initial decision to adapt and use SORMAS until its deployment.

In November 2017, we trained the laboratory officers and district surveillance notification officers (DSNOs) in 30 of the most affected local government areas of 8 federal states (Appendix, <https://wwwnc.cdc.gov/EID/article/26/2/19-1139-App1.pdf>); each training session lasted 2 days. DSNOs used the mobile SORMAS version on mobile tablets to notify cases and conduct contact tracing; laboratories used either laptops or tablets to notify test results in SORMAS. We trained staff at the incident command center of the NCDC how to process and analyze data within SORMAS. The incident command center also transferred data into SORMAS received through the conventional system from local government areas not yet using SORMAS. The conventional system frequently involved recontacting DSNOs by phone to correct or update case reports. The dashboard and statistics module in SORMAS generated the epidemiologic indicators needed for weekly situation reports. We used the network package in R software for visualization

and follow-up on chains of transmission (13). We conducted qualitative interviews with the NCDC incident managers of the monkeypox outbreak with regard to timeliness, usefulness, and workload of the conventional system compared with SORMAS. For quantitative evaluation, we used a set of core variables to compare the percentage of completeness in SORMAS versus that of the conventional system.

Yinka-Ogunleye et al. describe the epidemiologic characteristics of the outbreak in detail (14). From September 2017 through July 2019, including the period when SORMAS was not yet available, DSNOs reported 240 cases, either directly digitally in the field via SORMAS ($n = 90$) or via the conventional system ($n = 150$). Comparison of system attributes between SORMAS and the conventional system indicated equal or better performance of SORMAS for all attributes (Tables 1, 2). SORMAS continuously displayed the updated status of cases by case classification, epidemic curve, map of spatial distribution, contact persons, fatalities, and laboratory results, and it reported events in its dashboard within the incident command center (Figure 1). The dashboard also

Table 2. Quantitative comparison of attributes of SORMAS and the conventional surveillance system in response to monkeypox outbreak in Nigeria, November 2017–July 2019*

Data availability for selected variables	SORMAS, %† $n = 90$	CS, %‡ $n = 150$	95% CI for difference
Sex	91	92	(−0.09 to 0.07)
Occupation	84	57	(0.15 to 0.39)
Date of birth	69	55	(0.00 to 0.27)
Onset date of symptoms	89	85	(−0.06 to 0.13)
Body temperature	53	3	(0.39 to 0.62)

*95% CI indicates difference in percentage of completeness determined by using 2-sample χ^2 test. CS, conventional system; SORMAS, Surveillance Outbreak Response Management and Analysis System.

†Percentage of completeness for monkeypox cases notified directly in SORMAS by district surveillance officers in the field.

‡Percentage of completeness for monkeypox cases that arrived at the Nigeria Centre for Disease Control through the conventional system and were retrospectively registered in SORMAS.

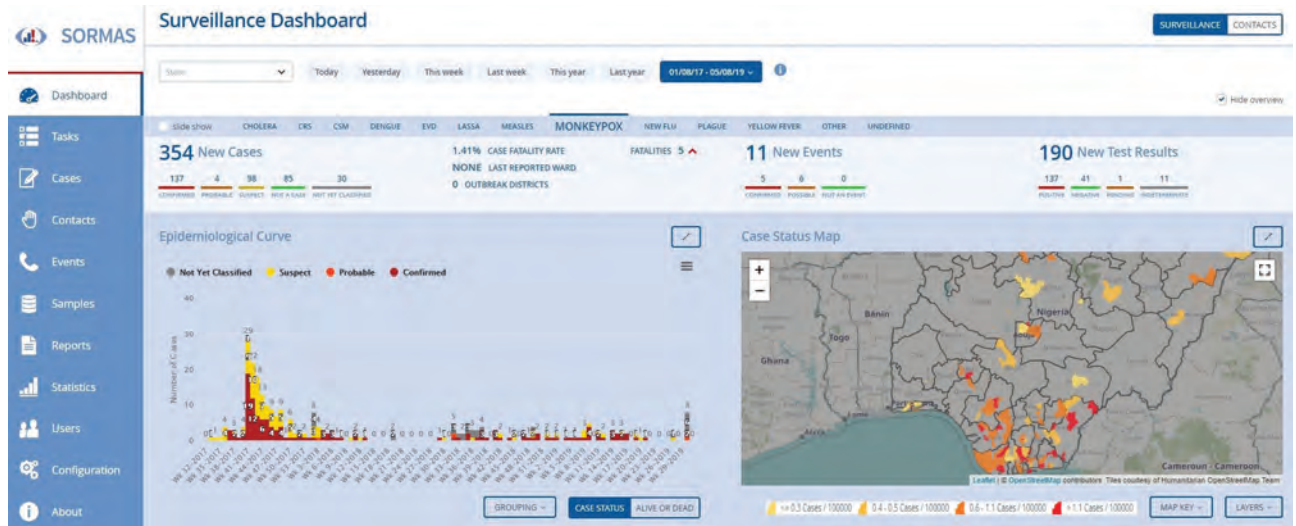


Figure 1. SORMAS dashboard showing monkeypox cases notified September 2017–July 2019 in Nigeria. The map shows the spatial spread of cases with local government area color by incidence proportion/100,000 population. The incidence proportion ranges from 0.1 (quartiles 0.3–0.7) to 8.1. During 2017, the number of cases by epidemic week increases gradually from week 32 to week 39, sharply increases in week 40, and gradually declines until week 53. Exportation of graphs, tables, and other epidemic indicators was generated in the statistic module of SORMAS. SORMAS, Surveillance Outbreak Response Management and Analysis System.

included performance indicators on contact tracing and case follow-up. The network diagrams linking case-patients to contact persons demonstrate that, of 167 contact persons, 12 (7%) converted to case-patients, of which 8 (66%) emerged from 1 chain of transmission (Figure 2).

Conclusions

In this comparison, SORMAS clearly outperformed the conventional surveillance system. SORMAS accelerated visualization and analysis of case reports; expedited data updates and production of daily situation reports; and improved data completeness, timeliness, and several aspects of usefulness. The automated generation of chains of transmission enabled NCDC to assess overall transmissibility and effectiveness of contact tracing and helped with allocation of field staff during the outbreak.

The comparison of data completeness between SORMAS and the conventional system was limited by availability of data from the conventional system only after the incident command center had already executed data revisions and completions. Without this resource-intensive measure, the difference between SORMAS and the conventional system would have been more pronounced.

We also encountered challenges during the deployment phase. The ad hoc deployment of this new digital system in the midst of the outbreak allowed only 2 days of training for DSNOs to become acquainted with the tool. It also resulted in running 2

systems in parallel. Because the SORMAS concept integrates continuous surveillance and response management but has not yet been used routinely, its full potential could not come into play as the outbreak unrolled in this particular situation. Other challenges included the complaint of DSNOs not receiving compensation for transportation to execute follow-up visits for contact tracing, which could result in incomplete information about chains of transmission. This challenge, however, is not inherent to the conventional system or SORMAS, and SORMAS may have mitigated this challenge, given that it did produce chains of transmission that were not available by the conventional system.

Our evaluation was limited to selected attributes and based partly on quantitative analyses. Possibly the most convincing evidence for the added benefit of SORMAS was the ability of NCDC, while still responding to the monkeypox outbreak, to deploy SORMAS in 120 more local government areas of 6 federal states within 2 months. On the basis of the added value experienced through this measure, NCDC has set a goal to fully roll out SORMAS in all 774 local government areas of all 36 federal states plus the Federal Capital Territory in Nigeria by the end of 2021.

Overall, SORMAS has proven to be rapidly deployable and useful in response to multiple outbreaks, including an outbreak of an emerging disease such as monkeypox. For tools that integrate outbreak detection and response process management (such as SORMAS), we recommend their deployment

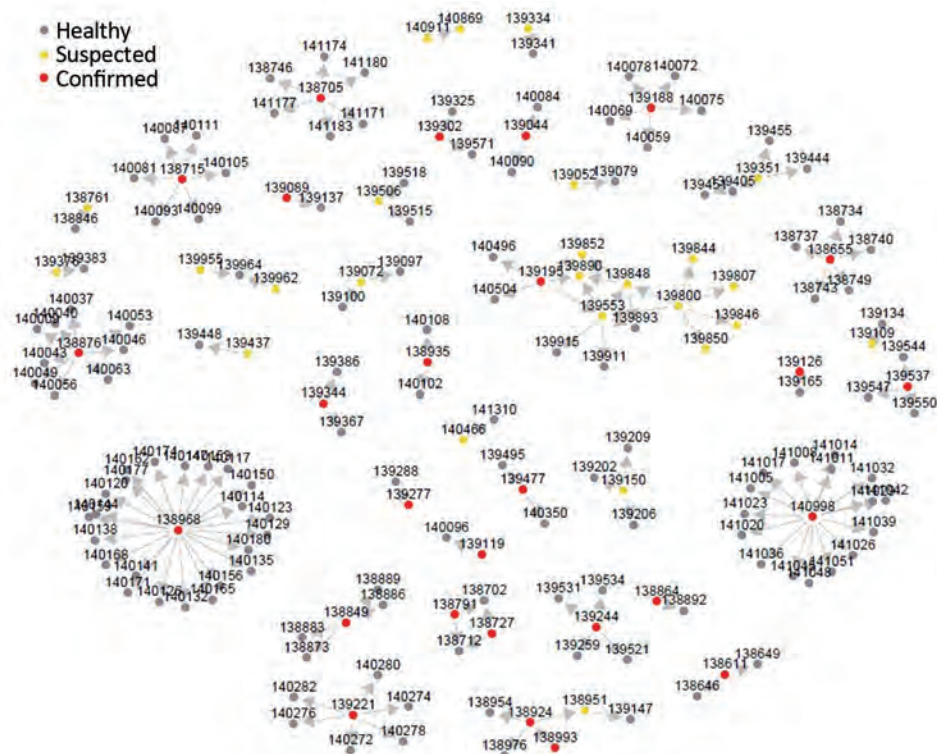


Figure 2. Network diagram for monkeypox cases and contact persons in Nigeria notified November 2017–July 2019. The nodes are labeled with unique identifiers for each person and colored by their classification status. Among case-patients, ≥ 1 contact person was reported for 57 (24%). The average number of contact persons/case-patient was 3 (quartiles 1–4, range 1–23). Arrows show the possible direction of infection transmission.

independently from any response to an acute public health emergency to optimize efficiency of resources for software adaptation, hardware infrastructure, and training. Such a proactive approach will improve not only outbreak response but also early detection of outbreaks, thus further enhancing sustainability.

Acknowledgments

We thank the field investigators and facilitators of the local and state health departments, NCDC, the African Field Epidemiology Network, and Symeda GmbH for contributing to the deployment of SORMAS in this outbreak and for providing valuable feedback for its improvement.

The mobilization of resources needed for the monkeypox-specific SORMAS deployment was made possible through financial support of the German Federal Ministry for Research and Education, the Gesellschaft für Internationale Zusammenarbeit, and the German Center for Infection Research.

About the Author

Mr. Silenou is working toward a PhD degree at the Helmholtz Centre for Infection Research and the Hannover Medical School in Germany. His primary research interests are investigation of the climatic factors that drive infectious disease outbreaks in Africa and research and development of digital surveillance systems.

References

1. Arita I, Jezek Z, Khodakevich L, Ruti K. Human monkeypox: a newly emerged orthopoxvirus zoonosis in the tropical rain forests of Africa. *Am J Trop Med Hyg.* 1985;34:781–9. <https://doi.org/10.4269/ajtmh.1985.34.781>
2. Breman JG, Kalisa-Ruti MV, Steniowski MV, Zanotto E, Gromyko AI, Arita I. Human monkeypox, 1970–79. *Bull World Health Organ.* 1980;58:165–82.
3. Ježek Z, Fenner F. Chapter VI. Epidemiology of human monkeypox. In: Ježek Z, Fenner F, editors. *Human Monkeypox*. Basel (Switzerland): Karger; 1988. p. 81–110.
4. Khodakevich L, Szczeniowski M, Manbu-ma-Disu, Ježek Z, Marennikova S, Nakano J, et al. The role of squirrels in sustaining monkeypox virus transmission. *Trop Geogr Med.* 1987;39:115–22.
5. Nigeria Centre for Disease Control. An update of monkeypox outbreak in Nigeria [cited 2019 May 6]. <https://ncdc.gov.ng/diseases/sitreps/?cat=8&name=An%20Update%20of%20Monkeypox%20Outbreak%20in%20Nigeria>
6. Yinka-Ogunleye A, Aruna O, Ogoina D, Aworabhi N, Eteng W, Badaru S, et al. Reemergence of human monkeypox in Nigeria, 2017. *Emerg Infect Dis.* 2018;24:1149–51. <https://doi.org/10.3201/eid2406.180017>
7. Centers for Disease Control and Prevention. Technical guidelines for integrated disease surveillance and response in the African region [cited 2019 May 6]. <https://stacks.cdc.gov/view/cdc/12082>
8. Adeoye O, Tom-Aba D, Ameh C, Ojo O, Ilori E, Gerado S, et al. Implementing Surveillance and Outbreak Response Management and Analysis System (SORMAS) for public health in West Africa—lessons learnt and future direction. *Int J Trop Dis Health.* 2017;22:1–17. <https://doi.org/10.9734/IJTDH/2017/31584>

9. Fährnich C, Denecke K, Adeoye OO, Benzler J, Claus H, Kirchner G, et al. Surveillance and Outbreak Response Management System (SORMAS) to support the control of the Ebola virus disease outbreak in West Africa. *Euro Surveill.* 2015;20:21071. <https://doi.org/10.2807/1560-7917.ES2015.20.12.21071>

10. Tom-Aba D, Toikkanen SE, Glöckner S, Adeoye O, Mall S, Fährnich C, et al. User evaluation indicates high quality of the Surveillance Outbreak Response Management and Analysis System (SORMAS) after field deployment in Nigeria in 2015 and 2018. *Stud Health Technol Inform.* 2018;253:233–7.

11. Tom-Aba D, Nguku PM, Arinze CC, Krause G. Assessing the concepts and designs of 58 mobile apps for the management of the 2014–2015 West Africa Ebola outbreak: systematic review. *JMIR Public Health Surveill.* 2018;4:e68. <https://doi.org/10.2196/publichealth.9015>

12. World Health Organization. Technical Advisory Group on Human Monkeypox: report of a WHO meeting. Geneva, Switzerland; 1999 Jan 11–12 [cited 2019 May 4]. <https://apps.who.int/iris/handle/10665/65998>

13. Butts CT. network: a package for managing relational data in R. *J Stat Softw.* 2008;24:1–36. <https://doi.org/10.18637/jss.v024.i02>

14. Yinka-Ogunleye A, Aruna O, Dalhat M, Ogoina D, McCollum A, Disu Y, et al.; CDC Monkeypox Outbreak Team. Outbreak of human monkeypox in Nigeria in 2017–18: a clinical and epidemiological report. *Lancet Infect Dis.* 2019;19:872–9. [https://doi.org/10.1016/S1473-3099\(19\)30294-4](https://doi.org/10.1016/S1473-3099(19)30294-4)

Address for correspondence: Gérard Krause, Epidemiology Department, Helmholtz Centre for Infection Research, Inhoffenstraße 7, 38124 Braunschweig, Germany; email: gerard.krause@helmholtz-hzi.de

Featured monthly in **EMERGING INFECTIOUS DISEASES**[®]

<https://wwwnc.cdc.gov/eid/articles/etymologia>

Human Norovirus Infection in Dogs, Thailand

Kamonpan Charoenkul, Chanakarn Nasamran, Taveesak Janetanakit, Ratanaporn Tangwangvivat, Napawan Bunpapong, Supanat Boonyapisitsopa, Kamol Suwannakarn, Apiradee Theamboonler, Watchaporn Chuchaona, Yong Poovorawan, Alongkorn Amonsin

In July 2018, recombinant norovirus GII.Pe-GII.4 Sydney was detected in dogs who had diarrhea in a kennel and in children living on the same premises in Thailand. Whole-genome sequencing and phylogenetic analysis of 4 noroviruses from Thailand showed that the canine norovirus was closely related to human norovirus GII.Pe-GII.4 Sydney, suggesting human-to-canine transmission.

Norovirus infection is a major cause of endemic and epidemic acute gastroenteritis. These viruses have been classified into 7 genogroups on the basis of the major capsid protein, VP1. Noroviruses GI, GII, and GIV can infect humans, GII pigs, GIII and GV ruminants and mice, and GVI and GVII dogs (1). The evolutionary mechanism and typing of noroviruses can be analyzed on the basis of recombination between the genes for RNA-dependent RNA polymerase and VP1 (2). Newly emerged norovirus strains might lead to increasing incidence of infection worldwide (3). The predominant genotype of noroviruses in humans is GII.4. Genetic diversity of noroviruses has been reported in a wide range of animals (e.g., pigs, cattle, and dogs).

In 2007, canine noroviruses in Italy were reported to have the GIV.2 genotype (4). Subsequently, these viruses have been reported to cause diseases in dogs in Asia and Europe (5–8). The seroprevalence of human noroviruses in dogs in the United Kingdom was reported to be 13% (6). The GII.4 genotype (variants GII.4-2006b and GII.4-2008) was reported in dogs in Finland, indicating that human noroviruses could be transmitted to and cause diarrhea in dogs (9). In humans, antibodies against canine norovirus were also reported in veterinarians, who experienced high risk

of exposure (10). However, only a few reports describe human norovirus infections in dogs, and limited numbers of complete genomes of canine noroviruses are available in GenBank. We report evidence of human norovirus infection in dogs from a kennel and children on the same premises in Thailand.

The Study

On July 27, 2018, we investigated acute gastroenteritis in dogs in a dog kennel. An outbreak occurred in a small-scale dog kennel that contained 18 adult dogs in Suphanburi, central Thailand. Clinical signs in bitches and puppies were fever, acute watery diarrhea, and mild dehydration (Appendix Figure 1, <https://wwwnc.cdc.gov/EID/article/26/2/19-1151-App1.pdf>). Information for the outbreak investigation indicated that 2 weeks earlier (July 18), 2 children (8 months and 2 years of age) who lived on the kennel premises were hospitalized because of vomiting and watery diarrhea. These children recovered within 1 week. During hospitalization, human cases were diagnosed and confirmed as norovirus infection by using a rapid test kit (RIDA QUICK Norovirus, <https://clinical.r-biopharm.com>). Five adults, 2 children, and 18 adult dogs were living on the premises. All dogs were housed in the kennel; only 2 apparently pregnant dogs (CU21939 and CU21952) were moved into the house of the owner. The 2 apparently pregnant dogs were kept in close contact with children.

On August 2, 2018, a pregnant dog gave birth to 6 puppies, and the other bitch was found to have a false pregnancy. During the 6 weeks (July 27–September 5) of the norovirus outbreak, 2 (11.11%) of 18 dogs (the 2 apparently pregnant dogs kept in the house of the owner) and 5 (83.33%) of 6 puppies showed clinical signs of infection (Appendix Table 1). After treatment and hygiene management, including separation of dogs, frequent cleaning, and disinfection, all dogs recovered, and no deaths occurred.

Animal samples were collected and examined at the Center of Excellence for Emerging and

Author affiliations: Chulalongkorn University, Bangkok, Thailand (K. Charoenkul, C. Nasamran, T. Janetanakit, R. Tangwangvivat, N. Bunpapong, S. Boonyapisitsopa, A. Theamboonler, W. Chuchaona, Y. Poovorawan, A. Amonsin); Mahidol University, Bangkok (K. Suwannakarn)

DOI: <https://doi.org/10.3201/eid2602.191151>

Table. Characteristics of noroviruses from humans and dogs, Thailand, July 2018*

Virus	Host	Sample	Age	GenBank accession no.
GII/Hu/THA/2018/GII.Pe-GII.4/CU21953	Human	Feces	2 y	MK928496
GII/Hu/THA/2018/GII.Pe-GII.4/CU21954	Human	Feces	8 mo	MK928497
GII/Ca/THA/2018/GII.Pe-GII.4/CU21939	Dog	Rectal swab	2 y	MK928498
GII/Ca/THA/2018/GII.Pe-GII.4/CU21952	Dog	Rectal swab	3 y	MK928499

*Whole-genome sequences were tested for all isolates.

Re-emerging Infectious Diseases in Animals, Chulalongkorn University (Bangkok, Thailand). Studies were approved by the Institutional Animal Care and Use Committee (approval no. 1731074). Human samples were collected and submitted to the Center of Excellence for Clinical Virology under the institutional review board of Chulalongkorn University (Institutional Review Board no. 634/59).

During the 4 visits in the study, we examined 75 samples (4 stool samples from 2 children, 71 rectal swab specimens from 18 adult dogs and 6 puppies). We detected norovirus by using a reverse transcription PCR specific for the RNA-dependent RNA polymerase gene as described (11,12) (Appendix). We detected norovirus in samples from children (4/4), adult dogs (2/53), and puppies (10/18) (Appendix Table 1). All human samples were positive for norovirus at the first (July 27) and third (August 25) visits. The 2 bitches with clinical signs were positive for norovirus at the first visit (July 27). Their puppies (5/6) were positive at the second (August 18) and third (August 25) visits. Our findings are consistent with a previous

report that animals can shed noroviruses for a long period (4). All samples were also tested for canine parvovirus type 2, rotavirus A, canine coronavirus, and canine distemper virus to rule out other canine enteric diseases; all showed negative results (Appendix Table 1).

We selected 4 of the noroviruses, 2 from humans (CU21953 and CU21954) and 2 from dogs (CU21939 and CU21952), for whole-genome sequencing by using oligonucleotide primer sets (Appendix). We then submitted nucleotide sequences for these viruses (GenBank accession nos. MK928496–9) (Table). Phylogenetic analysis showed that the noroviruses in this investigation clustered in genotype GII.4. In general, canine noroviruses are commonly grouped into genogroups GIV, GVI, and GVII. In contrast, noroviruses from these dogs were closely related to human noroviruses and viruses in genogroup GII (Figure 1).

Phylogenetic analysis of partial open reading frame 1 (ORF1) and ORF2 showed that all noroviruses from this investigation clustered with norovirus GII.Pe-GII.4 Sydney 2012, which were reported to be

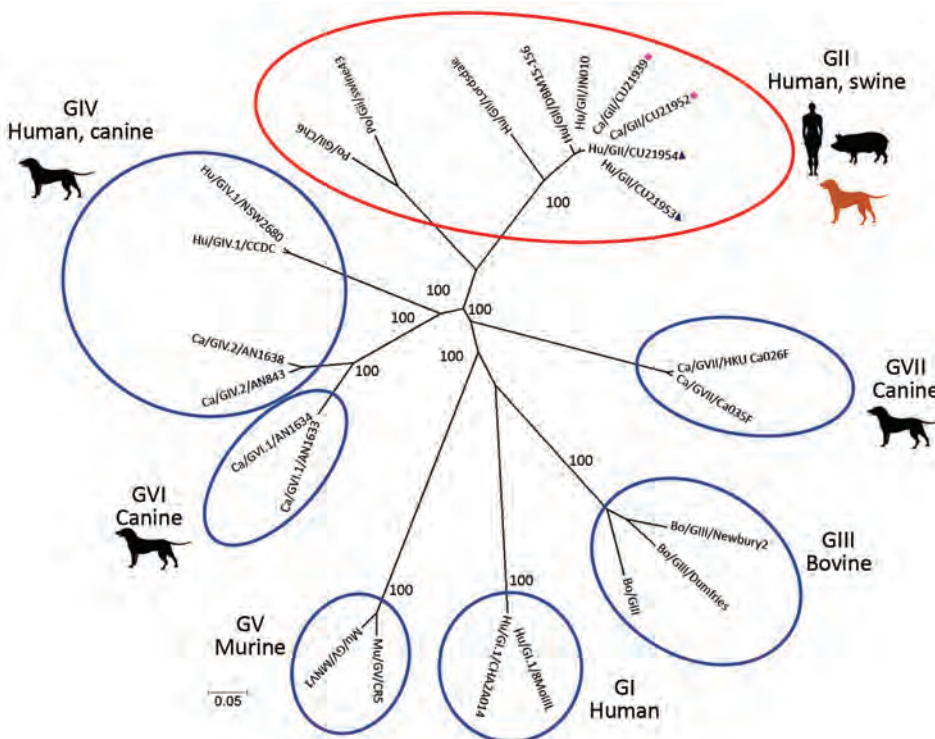


Figure 1. Phylogenetic tree of whole-genome sequences of canine noroviruses (red dots) and human noroviruses (blue triangles) from Thailand and reference sequences. Genogroups GI–GVII are indicated by red oval and blue ovals. The tree was constructed by using MEGA version 7.026 (<https://www.megasoftware.net>) with the neighbor-joining algorithm and bootstrap analysis with 1,000 replications. Numbers along branches are bootstrap values. Scale bar indicates nucleotide substitutions per site.

circulating worldwide (Figure 2; Appendix Figure 2) (3). Noroviruses from dogs in this study (GII.4 Sydney) were in different clusters from canine noroviruses 3-09 (GII.4 Den Haag) and 261-10 and 1C-09 (GII.4 unclassified) reported in Finland (9).

We compared nucleotide and deduced amino acids of the noroviruses from this investigation with reference canine and human noroviruses. On the basis of antigenic epitopes (A–E) of major capsid protein that correlate with blockade of neutralization antibodies,

the noroviruses from Thailand had specific amino acids in specific positions consistent with those for human norovirus *GII.Pe*-*GII.4* Sydney, which were not observed in human norovirus genogroups *GI* and *GIV* and canine norovirus genogroups *GIV* and *GVII* (Appendix Table 2).

Pairwise comparisons of whole-genome sequences showed that the viruses had 99.90% nt identities (only 3 nt differences in ORF2; T1176C [silent mutation 392G], C1354T [silent mutation 452L] and

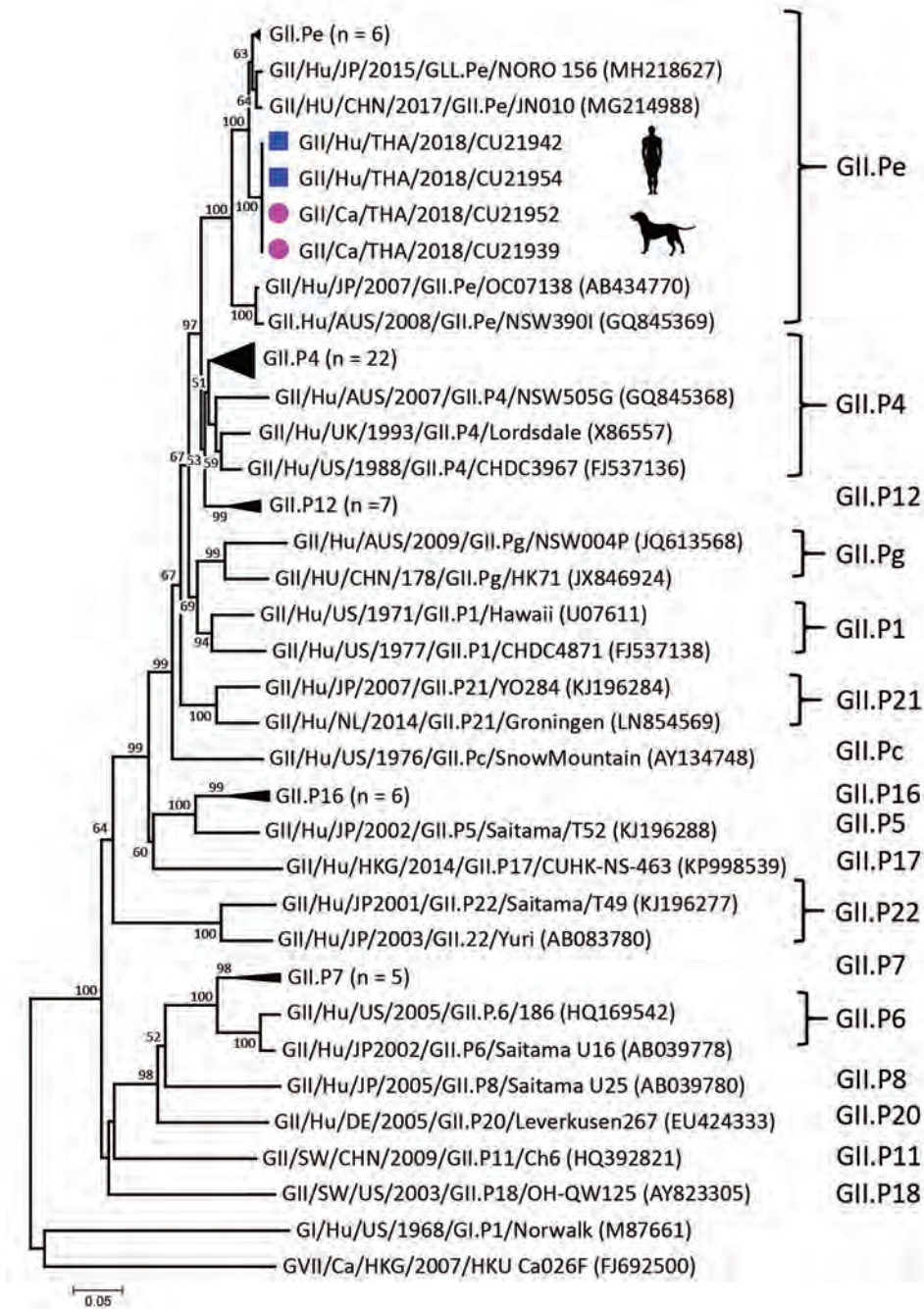


Figure 2. Phylogenetic tree of open reading frame 1 of canine noroviruses (purple dots) and human noroviruses (blue squares) from Thailand and reference sequences. Tree was constructed by using MEGA version 7.026 (<https://www.megasoftware.net>) with the neighbor-joining algorithm and bootstrap analysis with 1,000 replications. Numbers along branches are bootstrap values, and numbers on the right indicate genogroups. Scale bar indicates nucleotide substitutions per site.

in ORF3; T803A [V268E] to each other and highest nucleotide identities to human norovirus from China [99.00%; JN010] and the human norovirus reference Sydney strain [97.6%; NSW0514]). On the basis of partial ORF2 sequences, we showed that the canine noroviruses from this investigation were different from canine noroviruses GII.4 (3-09, 1C-09, and 261-10; 91.6% nt identities) and GIV, GVI, and GVII (52.90%–55.50% nt identities) (Appendix Table 3).

Conclusions

We report infection of dogs with human norovirus GII.4 Sydney. Human noroviruses have been reported in dogs in Finland (GII.4 Den Haag and GII.4 unclassified) (9). Dogs showed mild clinical signs of acute watery diarrhea, similar to that for human norovirus infection, and low levels of illness and death. Similar observations have also been reported in other studies (8,13). In this study, children had been hospitalized 2 weeks before the investigation. Disease developed in dogs and puppies after they shared the same premises and possible direct contact with the children. This observation suggests potential human-to-dog transmission of human noroviruses. Genetic and phylogenetic analyses confirmed that whole genomes of canine and human noroviruses were closely related to human norovirus GII.Pe-GII.4 Sydney, suggesting that a common strain is circulating in Thailand and worldwide (14,15). However, in our study, it is not clear how and when the viruses were introduced to children and dogs.

In summary, we demonstrated evidence of norovirus GII.Pe-GII.4 infection in humans and dogs in Thailand. Dog owners and veterinarians should pay more attention to norovirus infection as a potential zoonotic and reverse zoonotic disease in households, animal hospitals, and shelters. Expanded surveillance for norovirus is needed to determine its status and distribution in human and dog populations.

K.C. received a scholarship from the Royal Golden Jubilee (RGJ) PhD program (RGJ-PHD/0056/2557). Chulalongkorn University provided financial support to the Center of Excellence for Emerging and Re-emerging Infectious Diseases in Animals. A.A. was supported by the Thailand Research Fund (TRF) as a TRF Senior Scholar (RTA6080012).

About the Author

Dr. Charoenkul is a doctoral candidate in the Department of Veterinary Public Health, Faculty of Veterinary Science, Chulalongkorn University, Bangkok, Thailand. Her research interests include emerging and reemerging infectious diseases in animals.

References

1. Chhabra P, de Graaf M, Parra GI, Chan MC, Green K, Martella V, et al. Updated classification of norovirus genogroups and genotypes. *J Gen Virol*. 2019;100:1393–406. <https://doi.org/10.1099/jgv.0.001318>
2. Zheng DP, Ando T, Fankhauser RL, Beard RS, Glass RI, Monroe SS. Norovirus classification and proposed strain nomenclature. *Virology*. 2006;346:312–23. <https://doi.org/10.1016/j.virol.2005.11.015>
3. Cannon JL, Barclay L, Collins NR, Wikswo ME, Castro CJ, Magaña LC, et al. Genetic and epidemiologic trends of norovirus outbreaks in the United States from 2013 to 2016 demonstrated emergence of novel GII.4 recombinant viruses. *J Clin Microbiol*. 2017;55:2208–21. <https://doi.org/10.1128/JCM.00455-17>
4. Martella V, Lorusso E, Decaro N, Elia G, Radogna A, D'Abramo M, et al. Detection and molecular characterization of a canine norovirus. *Emerg Infect Dis*. 2008;14:1306–8. <https://doi.org/10.3201/eid1408.080062>
5. Mesquita JR, Nascimento MS. Molecular epidemiology of canine norovirus in dogs from Portugal, 2007–2011. *BMC Vet Res*. 2012;8:107. <https://doi.org/10.1186/1746-6148-8-107>
6. Caddy S, Emmott E, El-Attar L, Mitchell J, de Rougemont A, Brownlie J, et al. Serological evidence for multiple strains of canine norovirus in the UK dog population. *PLoS One*. 2013;8:e81596. <https://doi.org/10.1371/journal.pone.0081596>
7. Ntakis V, Xylouri E, Radogna A, Buonavoglia C, Martella V. Outbreak of canine norovirus infection in young dogs. *J Clin Microbiol*. 2010;48:2605–8. <https://doi.org/10.1128/JCM.02528-09>
8. Mesquita JR, Barclay L, Nascimento MS, Vinjé J. Novel norovirus in dogs with diarrhea. *Emerg Infect Dis*. 2010;16:980–2. <https://doi.org/10.3201/eid1606.091861>
9. Summa M, von Bonsdorff CH, Maunula L. Pet dogs: a transmission route for human noroviruses? *J Clin Virol*. 2012;53:244–7. <https://doi.org/10.1016/j.jcv.2011.12.014>
10. Mesquita JR, Costantini VP, Cannon JL, Lin SC, Nascimento MS, Vinjé J. Presence of antibodies against genogroup VI norovirus in humans. *Viral J*. 2013;10:176. <https://doi.org/10.1186/1743-422X-10-176>
11. Phumtholsup T, Chieochansin T, Vongpunsawad S, Vuthitanachot V, Payungporn S, Poovorawan Y. Human norovirus genogroup II recombinants in Thailand, 2009–2014. *Arch Virol*. 2015;160:2603–9. <https://doi.org/10.1007/s00705-015-2545-5>
12. Kojima S, Kageyama T, Fukushi S, Hoshino FB, Shinohara M, Uchida K, et al. Genogroup-specific PCR primers for detection of Norwalk-like viruses. *J Virol Methods*. 2002; 100:107–14. [https://doi.org/10.1016/S0166-0934\(01\)00404-9](https://doi.org/10.1016/S0166-0934(01)00404-9)
13. Robilotti E, Deresinski S, Pinsky BA. Norovirus. *Clin Microbiol Rev*. 2015;28:134–64. <https://doi.org/10.1128/CMR.00075-14>
14. Kumthip K, Khamrin P, Maneekarn N. Molecular epidemiology and genotype distributions of noroviruses and sapoviruses in Thailand 2000–2016: a review. *J Med Virol*. 2018;90:617–24. <https://doi.org/10.1002/jmv.25019>
15. Chuchaona W, Chansaenroj J, Wanlapakorn N, Vongpunsawad S, Poovorawan Y. Recombinant GII.Pe-GII.4 norovirus, Thailand, 2017–2018. *Emerg Infect Dis*. 2019;25:1612–4. <https://doi.org/10.3201/eid2508.190365>

Address for correspondence: Alongkorn Amonsin, Center of Excellence for Emerging and Re-emerging Infectious Diseases in Animals, Faculty of Veterinary Science, Chulalongkorn University, Bangkok 10330, Thailand; email: alongkornamonsin1@gmail.com

Hepatitis E Virus in Pigs from Slaughterhouses, United States, 2017–2019

Harini Sooryanarain,¹ Connie L. Heffron,¹ Dolores E. Hill, Jorrell Fredericks, Benjamin M. Rosenthal, Stephen R. Werre, Tanja Opriessnig, Xiang-Jin Meng

Hepatitis E virus (HEV) RNA was detected in 6.3% and HEV IgG in 40% of 5,033 serum samples from market-weight pigs at 25 slaughterhouses in 10 US states. The prevalent HEV genotype was zoonotic genotype 3, group 2. Blood of HEV-viremic pigs from slaughterhouses may contaminate pork supply chains.

Hepatitis E virus (HEV; family *Hepeviridae*, genus *Orthohepevirus A*) comprises at least 8 distinct genotypes (1). In industrialized countries, swine HEV of the zoonotic genotypes 3 and 4 (HEV-3 and HEV-4) is an emerging foodborne pathogen, transmitted by consumption of raw or undercooked pork (2). Recently, HEV-3 has been detected in human blood donors in the United States (3,4). We previously showed that HEV-3 is present in US swine herds (5) and that a small proportion of commercial pork products, such as liver and chitterlings, from US grocery stores contain infectious HEV (6). However, the current HEV infection status of US market-weight pigs at the time of slaughter, the entry point to the food supply chain, remains unknown. We therefore investigated the presence of HEV RNA and HEV IgG prevalence in 5,033 serum samples from market-weight pigs at 25 slaughterhouses in 10 US states.

The Study

During 2017–2019, a comprehensive set of archived serum samples from 22,940 market-weight pigs from 25 slaughterhouses in 10 US states was collected for an unrelated prevalence study of *Toxoplasma*

and *Trichinella*. The samples were collected from slaughterhouses processing adult market-weight pigs ≥ 6 months of age: ≈ 250 -pound market-weight hogs 6 months of age and female pigs >1 year of age. The blood samples were collected on the kill floor at the slaughterhouses, and serum was separated and stored frozen (-20°C) at the US Department of Agriculture–Agricultural Research Service, Beltsville Agricultural Research Center (Beltsville, MD, USA).

For our study, an aliquot of frozen serum samples was sent to Virginia Polytechnic Institute and State University (Blacksburg, VA, USA). From a total of 22,940 samples available, we performed a stratified random selection of 5,033 samples for this study, using the SURVEYSELECT procedure in SAS version 9.4 (<https://www.sas.com>); a combination of state and ZIP code of origin constituted the strata. To detect HEV RNA, we used an established quantitative reverse-transcription PCR (qRT-PCR) (7) and a nested RT-PCR (5). To detect HEV IgG, we used a commercial PrioCHECK Porcine HEV Ab ELISA kit (<https://www.thermofisher.com>), according to the manufacturer's protocol.

Results of qRT-PCR indicated that $\approx 6.3\%$ (318/5,033; 95% CI 5.6%–7.0%) of the market-weight pigs from US slaughterhouses were viremic for HEV RNA at the time of slaughter (Table). Viral loads ranged from <100 to 10^6 copies/mL (mean 8,285 copies/mL; 95% CI 6,210.7–25,397.2 copies/mL). The percentage of HEV-viremic pigs varied among slaughterhouses (range 0%–17.4%) and among states (Table). Higher serum HEV RNA positivity was found in pigs from 3 slaughterhouses in Iowa (17.4%, 9.5%, and 8.3%), 2 in Illinois (8.5% and 7.5%), 1 in North Carolina (7.9%), and 1 in Pennsylvania (7.5%).

To determine HEV genotype in US slaughterhouse pigs, we further tested the 318 serum samples

Author affiliations: Virginia Polytechnic Institute and State University, Blacksburg, Virginia, USA (H. Sooryanarain, C.L. Heffron, S.R. Werre, X.-J. Meng); US Department of Agriculture, Beltsville, Maryland, USA (D.E. Hill, J. Fredericks, B.M. Rosenthal); University of Edinburgh, Midlothian, Scotland, UK (T. Opriessnig)

DOI: <https://doi.org/10.3201/eid2602.191348>

¹These first authors contributed equally to this article.

Table. Detection of HEV IgG and RNA in serum of market-weight pigs from 25 slaughterhouses in 10 US states, 2017–2019*

State, slaughterhouse no.	No. samples tested	Positive for HEV IgG by ELISA, no. (%)	Positive for HEV RNA by qRT-PCR, no. (%)	HEV RNA, copies/mL, range
Oklahoma	455	269 (59.1)	24 (5.3)	<100–1 × 10 ⁴
Tennessee	56	32 (57.1)	1 (1.8)	<100
Virginia	213	89 (41.8)	6 (2.8)	<100–4 × 10 ⁵
Illinois				
1	40	18 (45)	3 (7.5)	102–3,083
2	55	22 (40)	3 (5.5)	<100
3	40	16 (40)	0	0
4	445	118 (26.5)	38 (8.5)	<100–3 × 10 ⁵
5	259	60 (23.3)	2 (0.8)	100
Wisconsin	20	9 (45)	0	0
Iowa				
1	379	135 (35.6)	36 (9.5)	<100–1 × 10 ⁴
2	455	304 (66.8)	23 (5.1)	<100–3 × 10 ⁴
3	70	21 (30)	1 (1.4)	10 ³
4	105	39 (37.1)	1 (1)	<100
5	180	67 (37.2)	15 (8.3)	<100–1 × 10 ⁵
6	37	17 (46.0)	0	0
7	453	153 (33.8)	79 (17.4)	<100–2 × 10 ⁵
8	22	5 (22.7)	0	0
Minnesota	233	76 (32.6)	10 (4.3)	<100–1 × 10 ⁴
North Carolina				
1	245	61 (24.9)	7 (2.9)	<100–3 × 10 ⁴
2	482	266 (55.2)	38 (7.9)	<100–1 × 10 ⁵
Nebraska				
1	223	62 (27.8)	2 (0.9)	100 – 300
2	241	66 (27.49)	9 (3.8)	<100–1 × 10 ⁵
Pennsylvania				
1	50	0	1 (2)	200
2	35	8 (22.9)	1 (2.9)	<100
3	240	94 (39.2)	18 (7.5)	<100–1 × 10 ⁶
Total	5,033	2,007 (39.9)	318 (6.3)	<100–1 × 10 ⁶

*HEV, hepatitis E virus; qRT-PCR, quantitative reverse-transcription PCR.

positive by qRT-PCR by using an established nested RT-PCR (5). We successfully amplified the HEV capsid gene region (348 bp) from 182 samples. Subsequent sequencing and phylogenetic analyses revealed that all 182 HEV sequences belonged to the zoonotic HEV-3 genotype and clustered within group 2 (HEV-3abchij) (Figure). The HEV sequences from slaughterhouse pigs shared ≈90%–94% nt sequence identity with the previously reported US HEV-3 isolates (GenBank accession nos. JN837481 and KF719308). We did not detect any HEV-3-efg subgenotype or HEV-4.

We found that the national average of HEV seropositivity among market-weight pigs in US slaughterhouses is ≈40% (95% CI 38.5%–41.2%). Seroprevalence varied from slaughterhouse to slaughterhouse and from state to state (range 0%–66.8%) (Table). At 1 slaughterhouse in Pennsylvania, all 50 pigs tested were seronegative. Higher HEV seropositivity was found at slaughterhouses in Iowa (68.8%), Oklahoma (59.1%), Tennessee (57.1%), and North Carolina (55.2%) (Table).

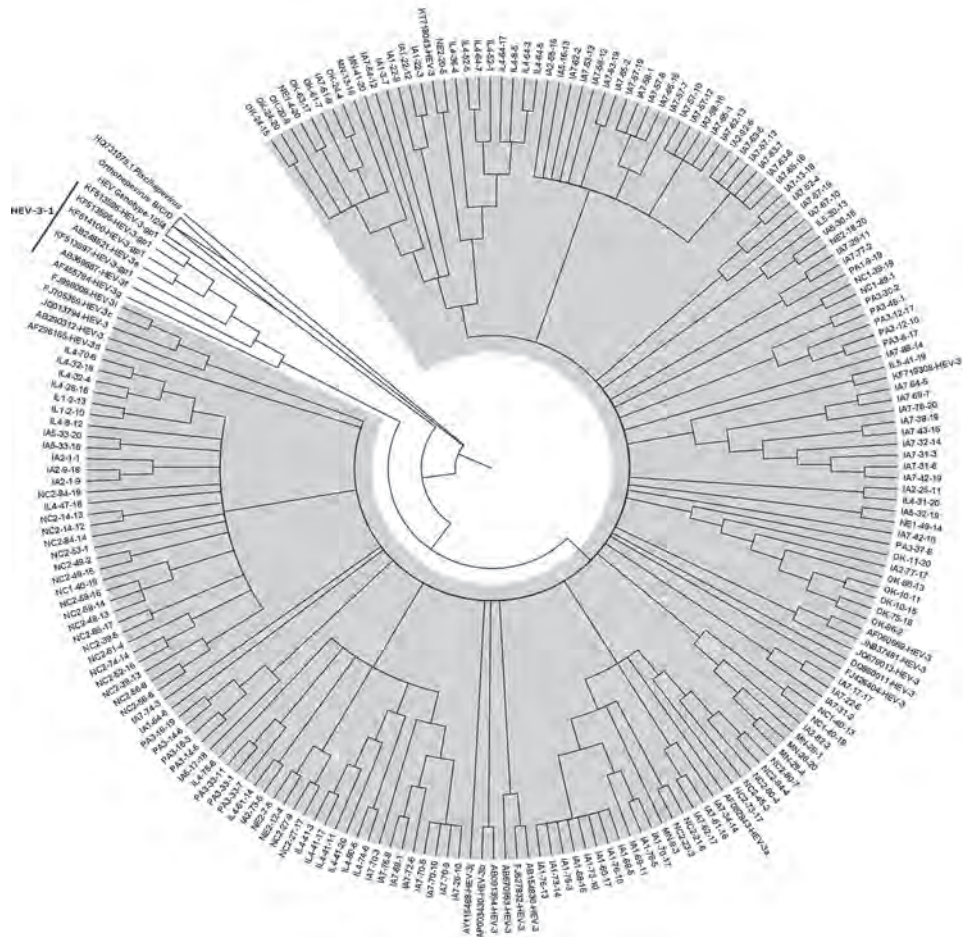
HEV RNA positivity (17.4%) and seropositivity (68.8%) were highest at 1 slaughterhouse in Iowa. Of note, HEV seropositivity was higher in serum

samples from Tennessee, but only 1.8% of these samples were positive for HEV RNA (Table). We performed the Spearman correlation by using SAS version 9.4 and found no apparent correlation between HEV antibody seropositivity and serum HEV RNA positivity in this study (Spearman correlation $R^2 = 0.07$); among 2,007 HEV IgG-positive samples, only 145 were also positive for HEV RNA (7.2%, 95% CI 6.1%–8.3%).

Conclusions

HEV-3 and HEV-4 are zoonotic viruses that infect pigs and humans. In this study, we found that ≈40% of US slaughterhouse pigs were seropositive for HEV, indicating prior HEV infection of the pigs on the farms, which was consistent with prior estimates for farmed US pigs (8,9). Despite the relatively high seropositivity, however, only a small proportion (6%) of the pigs had detectable HEV viremia, probably because HEV viremia is transient and thus the window for detecting HEV RNA in serum is narrow. In addition, active HEV infection occurs naturally in most farm pigs around 2 months of age (5,9). Therefore, most market-weight pigs >6 months of age at the time of slaughter

Figure. Phylogenetic tree of the capsid gene region of reference HEV-1, HEV-2, HEV-3, and HEV-4 strains within species *Orthohepevirus A*, representative HEV strains from species *Orthohepeviruses B, C, and D*, as well as the cutthroat trout virus in the genus *Piscihepevirus*. The phylogenetic analysis was performed by using MEGA6 software (<http://www.megasoftware.net>) and the maximum-likelihood bootstrap method based on the Tamura-Nei model (1). The figure represents a cladogram. The HEV-3abc hij sequences belonging to HEV-3 group 2 (HEV-3-2) are highlighted in gray (n = 182 sequences from slaughterhouse pigs in this study; n = 19 reference sequences from the GenBank database). The HEV-3efg sequences belonging to HEV-3 group 1 (HEV-3-1) are shown on a white background (n = 7 reference sequences from the GenBank database). Reference HEV sequences from genotypes 1/2/4 clade of *Orthohepevirus A*, and *Orthohepevirus B/C/D* clade are also shown as collapsed branches, and the cutthroat trout virus within the genus *Piscihepevirus* is shown as a separate clade. The HEV-3 reference sequences used in the phylogenetic analysis include HEV-3a AF082843, HEV-3b AP003430, HEV-3c FJ705359, HEV-3d AF296165-7, HEV-3e AB248521, HEV-3f AB369687, HEV-3g AF455784, HEV-3h JQ013794, HEV-3i FJ998008, HEV-3j AY115488, HEV-3 AB290312. We also included the following other HEV-3 sequences in the phylogenetic analysis, which were some of the top candidates from our initial BLAST (<https://blast.ncbi.nlm.nih.gov/Blast.cgi>) analysis: AB091394-HEV-3, AB154830-HEV-3, AB670953-HEV-3, DQ860011-HEV-3, FJ426404-HEV-3, FJ527832-HEV-3, JN837481-HEV-3, KF719308-HEV-3, KT718043-HEV-3. HEV, hepatitis E virus.



are no longer actively infected by HEV. Nevertheless, studies have shown that 5.7% of UK (10), and 44.4% of Scotland (11) slaughterhouse market-weight pigs were viremic. A growing number of reported cases of autochthonous HEV-3 and HEV-4 human infection have been attributed to consumption of raw or undercooked pork (12,13), including 1 case acquired from imported HEV-4 in the United States (14).

The HEV sequences we detected all belonged to the zoonotic HEV-3 group 2 (HEV-3abc hij). This finding is consistent with previous reports of detection of HEV-3 in US farm pigs and commercial pork products (5,6). Pigs in Europe are reportedly infected with HEV-3c, 3e, 3f, 3h, and 3i. Because our phylogenetic analysis was based on partial sequences, our results identified the prevalent HEV genotype at the

group level, but more detailed study based on full-length sequence is warranted to definitively identify viral heterogeneity as well as the molecular clock of HEV evolution across the United States. Cases of autochthonous human infection with HEV-3abc hij have been reported in the United Kingdom (13), and low levels of HEV-3abc hij RNA were detected in human blood donor plasma samples in the United States (4). That $\approx 6\%$ of slaughterhouse pigs are still viremic for HEV-3abc hij raises a potential concern about pork safety because blood containing infectious HEV during slaughter may contaminate raw pork products. Therefore, to prevent foodborne HEV infection, pork should be properly cooked before consumption; an internal temperature of 71°C inactivates infectious HEV (15).

Acknowledgments

We thank Nisha Duggal at Virginia Polytechnic Institute and State University for her expert input into the phylogenetic analyses.

This study was supported by a Pork Checkoff grant from the National Pork Board, Des Moines, IA, USA. Sample collection was undertaken by staff from the US Department of Agriculture Animal Parasitic Diseases Laboratory. The laboratory testing, data collection, analysis, and interpretation of the information presented here were undertaken by staff from Virginia Polytechnic Institute and State University.

About the Author

Dr. Sooryanarain is a research scientist in the Department of Biomedical Sciences and Pathobiology at Virginia Polytechnic Institute and State University, Blacksburg, VA. Her research interest focuses on the mechanism of HEV pathogenesis and epidemiology.

References

- Smith DB, Simmonds P, Izopet J, Oliveira-Filho EF, Ulrich RG, Johne R, et al. Proposed reference sequences for hepatitis E virus subtypes. *J Gen Virol*. 2016;97:537–42. <https://doi.org/10.1099/jgv.0.000393>
- Salines M, Andraud M, Rose N. From the epidemiology of hepatitis E virus (HEV) within the swine reservoir to public health risk mitigation strategies: a comprehensive review. *Vet Res (Faisalabad)*. 2017;48:31. <https://doi.org/10.1186/s13567-017-0436-3>
- Ticehurst JR, Pisanic N, Forman MS, Ordak C, Heaney CD, Ong E, et al. Probable transmission of hepatitis E virus (HEV) via transfusion in the United States. *Transfusion*. 2019;59:1024–34. <https://doi.org/10.1111/trf.15140>
- Roth NJ, Schäfer W, Alexander R, Elliott K, Elliott-Browne W, Knowles J, et al. Low hepatitis E virus RNA prevalence in a large-scale survey of United States source plasma donors. *Transfusion*. 2017;57:2958–64. <https://doi.org/10.1111/trf.14285>
- Huang FF, Haqshenas G, Guenette DK, Halbur PG, Schommer SK, Pierson FW, et al. Detection by reverse transcription-PCR and genetic characterization of field isolates of swine hepatitis E virus from pigs in different geographic regions of the United States. *J Clin Microbiol*. 2002;40:1326–32. <https://doi.org/10.1128/JCM.40.4.1326-1332.2002>
- Feagins AR, Opriessnig T, Guenette DK, Halbur PG, Meng XJ. Detection and characterization of infectious hepatitis E virus from commercial pig livers sold in local grocery stores in the USA. *J Gen Virol*. 2007;88:912–7. <https://doi.org/10.1099/vir.0.82613-0>
- Jothikumar N, Cromeans TL, Robertson BH, Meng XJ, Hill VR. A broadly reactive one-step real-time RT-PCR assay for rapid and sensitive detection of hepatitis E virus. *J Virol Methods*. 2006;131:65–71. <https://doi.org/10.1016/j.jviromet.2005.07.004>
- Dong C, Meng J, Dai X, Liang JH, Feagins AR, Meng XJ, et al. Restricted enzooticity of hepatitis E virus genotypes 1 to 4 in the United States. *J Clin Microbiol*. 2011;49:4164–72. <https://doi.org/10.1128/JCM.05481-11>
- Meng XJ, Purcell RH, Halbur PG, Lehman JR, Webb DM, Tsareva TS, et al. A novel virus in swine is closely related to the human hepatitis E virus. *Proc Natl Acad Sci U S A*. 1997;94:9860–5. <https://doi.org/10.1073/pnas.94.18.9860>
- Grierson S, Heaney J, Cheney T, Morgan D, Wyllie S, Powell L, et al. Prevalence of hepatitis E virus infection in pigs at the time of slaughter, United Kingdom, 2013. *Emerg Infect Dis*. 2015;21:1396–401. <https://doi.org/10.3201/eid2108.141995>
- Crossan C, Grierson S, Thomson J, Ward A, Nunez-Garcia J, Banks M, et al. Prevalence of hepatitis E virus in slaughter-age pigs in Scotland. *Epidemiol Infect*. 2015;143:2237–40. <https://doi.org/10.1017/S0950268814003100>
- Tesse S, Lioure B, Fornecker L, Wendling MJ, Stoll-Keller F, Bigaillon C, et al. Circulation of genotype 4 hepatitis E virus in Europe: first autochthonous hepatitis E infection in France. *J Clin Virol*. 2012;54:197–200.
- Said B, Usdin M, Warburton F, Ijaz S, Tedder RS, Morgan D. Pork products associated with human infection caused by an emerging phylotype of hepatitis E virus in England and Wales. *Epidemiol Infect*. 2017;145:2417–23. <https://doi.org/10.1017/S0950268817001388>
- Perumpail RB, Ahmed A, Higgins JP, So SK, Cochran JL, Drobeniuc J, et al. Fatal accelerated cirrhosis after imported HEV genotype 4 infection. *Emerg Infect Dis*. 2015;21:1679–81. <https://doi.org/10.3201/eid2109.150300>
- Feagins AR, Opriessnig T, Guenette DK, Halbur PG, Meng XJ. Inactivation of infectious hepatitis E virus present in commercial pig livers sold in local grocery stores in the United States. *Int J Food Microbiol*. 2008;123:32–7. <https://doi.org/10.1016/j.ijfoodmicro.2007.11.068>

Address for correspondence: Xiang-Jin Meng, Department of Biomedical Sciences and Pathobiology, Virginia Polytechnic Institute and State University, 1981 Kraft Dr, Blacksburg, VA 24061-0913, USA; email: xjmeng@vt.edu

Rapid Nanopore Whole-Genome Sequencing for Anthrax Emergency Preparedness

Heather P. McLaughlin, Julia V. Bugrysheva, Andrew B. Conley, Christopher A. Gulvik, Blake Cherney, Cari B. Kolton, Chung K. Marston, Elke Saile, Erin Swaney, David Lonsway, Amy S. Gargis, Thiphason Kongphet-Tran, Christine Lascols, Pierre Michel, Julie Villanueva, Alex R. Hoffmaster, Jay E. Gee, David Sue

Human anthrax cases necessitate rapid response. We completed *Bacillus anthracis* nanopore whole-genome sequencing in our high-containment laboratory from a human anthrax isolate hours after receipt. The de novo assembled genome showed no evidence of known antimicrobial resistance genes or introduced plasmid(s). Same-day genomic characterization enhances public health emergency response.

Bacillus anthracis causes anthrax, a deadly infectious disease, and is found worldwide, including areas of the United States. Naturally occurring anthrax outbreaks are reported annually in wild and domestic grazing animals, but human transmission is rare (1). Deliberate misuse of *B. anthracis* as a bioweapon could pose an immediate risk to human populations. In such instances, a timely response is critical to reduce morbidity and mortality rates.

After the anthrax incidents during 2001, the Centers for Disease Control and Prevention (CDC) published medical countermeasure recommendations for human anthrax treatment and postexposure prophylaxis using antimicrobial drugs, including amoxicillin, ciprofloxacin, doxycycline, levofloxacin, and penicillin (2). Most *B. anthracis* strains are susceptible to antimicrobial drugs; however, naturally occurring and engineered antimicrobial-resistant strains have been reported (3–5). Laboratory antimicrobial susceptibility testing (AST) by broth microdilution (BMD)

remains the standard method to determine MIC values but requires ≥ 16 hours before results are available. During an anthrax emergency, rapid genomic characterization of the implicated *B. anthracis* strain(s) could identify sequences associated with drug resistance.

Single-nucleotide mutations in chromosomal *B. anthracis* quinolone resistance-determining regions of *gyrA*, *gyrB*, *parC*, and *parE* genes can lead to ciprofloxacin resistance, and gene acquisition can lead to tetracycline and doxycycline resistance (3,4,6). Penicillin resistance can result from a chromosomal mutation in the antisigma factor gene, *rsiP* (5). Most *B. anthracis* strains carrying this signature *rsiP* mutation are resistant to penicillin and amoxicillin (5,7,8). Detection of known antimicrobial resistance (AMR) mutations or other novel gene insertions and deletions (indels) in the clonal *B. anthracis* genome signals genetic anomalies and could influence treatment and postexposure prophylaxis strategies.

Whole-genome sequencing (WGS) can identify gene indels, mutations, or previously undescribed genetic elements, including extrachromosomal plasmid DNA. However, common short-read sequencing (SRS) technologies have difficulty resolving bacterial genome structure because de novo assemblies yield multiple contigs. Long-read nanopore sequencing with the MinION device (Oxford Nanopore Technologies, <https://nanoporetech.com>) can resolve repetitive sequences and structural genomic rearrangements and enables complete bacterial genome finishing (9). Although MinION data are error-prone, especially in homopolymeric regions (10), compared with Illumina (<https://www.illumina.com>)-based SRS, it is available immediately during the sequencing run, enabling rapid assembly and analysis. The technology enables real-time sequencing, including direct pathogen identification from patient specimens, and holds the promise for future point-of-care applications that speed laboratory results reporting (11,12). Portable WGS instruments are

Author affiliations: Centers for Disease Control and Prevention, Atlanta, Georgia, USA (H.P. McLaughlin, J.V. Bugrysheva, C.A. Gulvik, B. Cherney, C.B. Kolton, C.K. Marston, E. Saile, D. Lonsway, A.S. Gargis, T. Kongphet-Tran, C. Lascols, P. Michel, J. Villanueva, A.R. Hoffmaster, J.E. Gee, D. Sue); IHRC–Georgia Tech Applied Bioinformatics Laboratory, Atlanta (A.B. Conley); Texas Department of State Health Services Laboratory, Austin, Texas, USA (E. Swaney)

DOI: <https://doi.org/10.3201/eid2502.191351>

advantageous for laboratories with limited space and remove the need to transfer DNA out of high-containment laboratories for sequencing, mitigating exposure risks to personnel (13).

CDC described a rapid nanopore sequencing approach and custom bioinformatics pipeline for *B. anthracis* that yielded complete chromosome and plasmid assemblies, and detected known AMR genes and mutations in avirulent laboratory strains (13). On the morning of August 2, 2019, our laboratory received a *B. anthracis* culture isolate (Ba0914) from a naturally occurring human anthrax case in Texas. Same-day laboratory WGS and bioinformatics analysis were performed. This study describes the laboratory work and demonstrates the usefulness of rapid WGS to inform time-sensitive public health responses.

The Study

All laboratory work with the *B. anthracis* isolate and nanopore sequencing was performed inside a class II type A2 biological safety cabinet located in a US Federal Select Agent Program registered Biosafety Level 3 laboratory. We performed rapid nanopore sequencing as described by Gargis et al. (13), including silica membrane-based genomic DNA (gDNA) extraction, except

that a bead-beating step was added to speed cell lysis. We extracted Ba0914 gDNA from colonies of an overnight agar culture in 75 min. Within the next hour, fluorometer and microvolume spectrophotometer measurements confirmed that the gDNA extraction was suitable for nanopore sequencing. We prepared a nanopore DNA sequencing library (Rapid Barcoding Sequencing Kit SQK-RBK004; Oxford Nanopore Technologies) and sequencing began <45 min later (MinKNOW, version 18.12.6; Oxford Nanopore Technologies).

Within ≈10 min of sequencing, nanopore data were ready for blastn analysis (<https://blast.ncbi.nlm.nih.gov>), which identified a 13.5-kb read with >91.5% sequence homology with *B. anthracis*. Approximately 120,000 live basecalled reads (average length 4,089 nt, average quality score/read 14.8) were generated in <5 hours of nanopore sequencing. We performed de novo genome assembly (Flye version 2.5; <https://github.com>) by using the first 120,000 nanopore reads and error-corrected with Medaka version 0.6.1 (<https://pypi.org>).

The Ba0914 genome assembly contained single contigs for the chromosome and each plasmid, pXO1 and pXO2 (Figures 1, 2) with ≥54X average depth of coverage and shared >99.75% identity to the Ames Ancestor strain (GenBank accession no. AE017334)

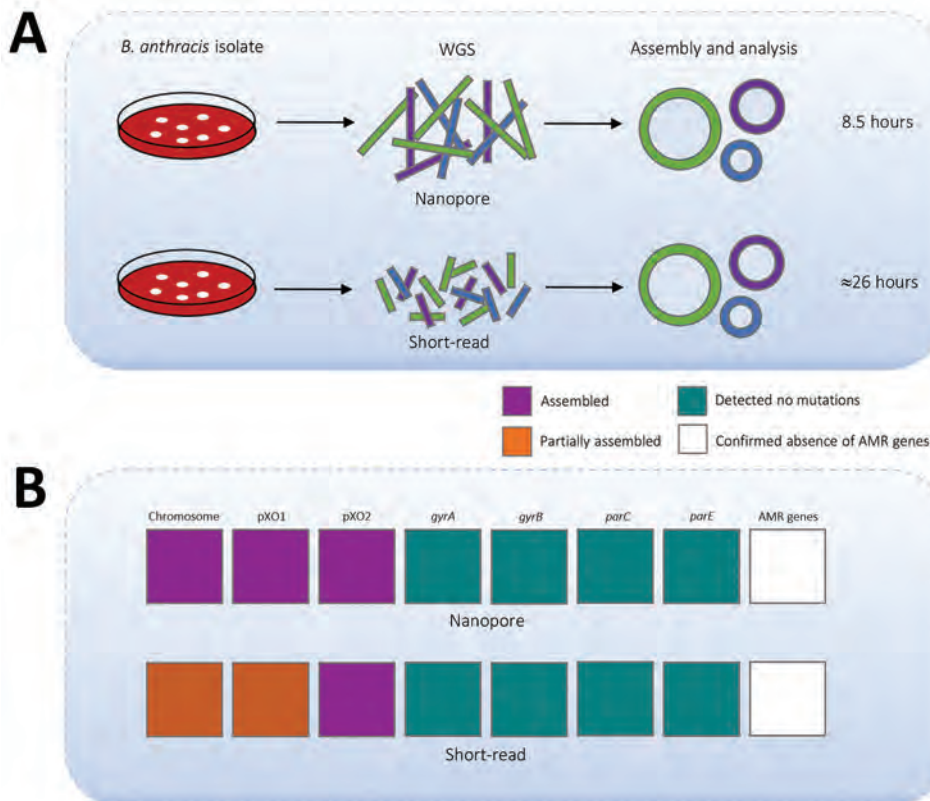


Figure 1. Time required to detect antimicrobial resistance markers in *Bacillus anthracis* strain Ba0914 by using WGS and summary of assembly results. A) Comparison of time to complete rapid nanopore (MinION) and short-read (iSeq) sequencing laboratory workflows. Workflows include DNA extraction, library preparation, WGS, and bioinformatics analysis. B) Comparison of nanopore-based and short-read sequencing-based data used to assemble the *B. anthracis* chromosome and plasmid sequences and to detect known AMR mutations and genes. Mutations associated with fluoroquinolone resistance in *B. anthracis* are located within the quinolone resistance-determining regions of *gyrA*, *gyrB*, *parC*, and *parE* genes. AMR genes contained in the Resfinder database (<https://cge.cbs.dtu.dk>) were queried against the assemblies. The *rsiP* mutation associated with penicillin resistance was not included. The nanopore assembly was generated by using the first 120,000 basecalled reads. AMR, antimicrobial resistance; WGS, whole-genome sequencing.

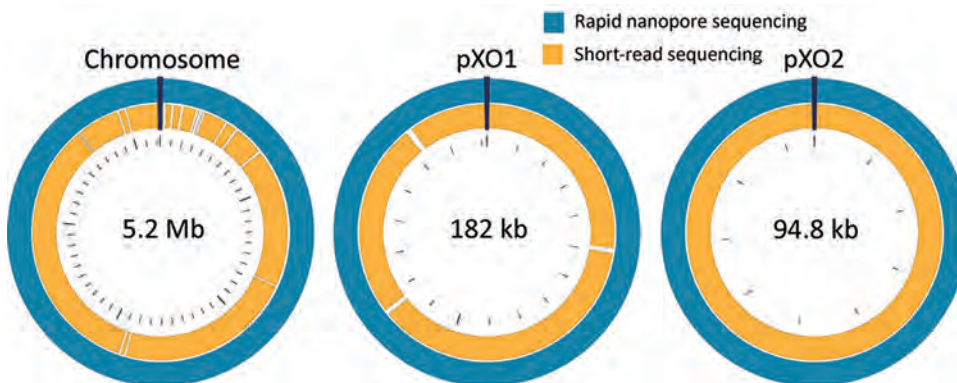


Figure 2. Circular maps of the whole-genome-sequenced *Bacillus anthracis* Ba0914 chromosome and 2 plasmids, pXO1 and pXO2, assembled by using rapid nanopore sequencing and short-read sequencing. (Maps are not to scale.)

(Table). Thousands of indels and nearly 700 mismatches were detected (Table). Conventional BMD testing also began on August 2, 2019, according to guidelines of the Clinical and Laboratory Standards Institute (14), and susceptibility results were ready the following day.

We also performed Illumina-based SRS. We extracted DNA as described by Gargis et al. (7) and prepared the sequencing library (Nextera DNA Flex Library Kit; Illumina) for paired-end 2×150 -bp sequencing by using the iSeq 100 (Illumina). We performed read filtering and assembly as described (15). The SRS-based assembly contained 32 more contigs than nanopore but with higher depths of coverage for the chromosome and plasmids (Table). Alignment to the Ames Ancestor reference strain yielded >99.9% genome identity, with fewer indels and mismatches. SRS-based approaches result in lower error rates and can more reliably detect single-nucleotide polymorphisms in *B. anthracis*, especially in homopolymeric regions, but a same-day laboratory workflow is currently not feasible (Figure 1, panel A). An alignment plot showed gaps in coverage of the chromosome (0.1%) and pXO1 (1.4%) caused by incomplete SRS-based assemblies (Figure 2). Alignment of the nanopore-based assembly to the SRS-based assembly resulted in >99.8% identity but with thousands of indels (Table). All sequencing data were submitted to GenBank under accession no. SAMN12588378.

Only 45 min of bioinformatics analysis (Pima version 01, <https://github.com>) using 120,000 basecalled

nanopore reads was sufficient to assemble and confirm the absence of known AMR genes/markers associated with resistance to quinolones and tetracyclines (Figure 1, panel B) (13). We detected no mutations in *gyrA*, *gyrB*, *parC*, or *parE* genes, identified no AMR genes contained in the Resfinder database (<https://cge.cbs.dtu.dk>), and found no unexpected plasmids. SRS and bioinformatics analysis yielded analogous details about the AMR markers in Ba0914 (Figure 1, panel B). Only the SRS-based assembly, and not the nanopore assembly, was reliable for sequencing *rsiP*. Strain Ba0914 lacked mutations in the homopolymeric *rsiP* region that can confer penicillin resistance. Sequencing of regions containing repetitive nucleotide bases is a known limitation of nanopore technology and, consequently, detection of the *rsiP* mutation was excluded from AMR bioinformatics analysis.

Although genetic analysis is useful for detection of known AMR genes/markers in the *B. anthracis* genome, phenotypic susceptibility testing by BMD remains essential to detect functional resistance (7,13). By using the conventional BMD method, we found that strain Ba0914 was susceptible to ciprofloxacin, levofloxacin, tetracycline, doxycycline, penicillin, and amoxicillin.

Conclusions

Real-time sequencing of the biothreat pathogen *B. anthracis* in a high-containment laboratory demonstrated the speed and usefulness of a rapid, portable

Table. De novo whole-genome assembly metrics for sequencing of *Bacillus anthracis* strain Ba0914*

Aligned to	Mismatches	Indels	Contigs	Nucleotide identity, %; average fold coverage		
				Chromosome	pXO1	pXO2
Ames reference strain						
Nanopore	677	6,411	3	99.83; 54	99.78; 192	99.80; 91
SRS	526	180	35	99.96; 115	99.94; 467	99.94; 220
SRS assembly						
Nanopore	166	6,305	NA	99.86	99.88	99.85

*Mismatches, indels, nucleotide identity, and average fold coverage for chromosomal and plasmid sequences of *B. anthracis* strain Ba0914 were determined on the basis of alignment with the Ames Ancestor reference strain assembly (top) or to the SRS-based Ba0914 strain assembly (bottom). The nanopore assembly was generated by using the first 120,000 live basecalled reads. Contigs, contiguous overlapping DNA segments; Indels, insertions and deletions; NA, not applicable; SRS, short-read sequencing.

nanopore sequencer during an emergency. Long-read sequencing could detect *B. anthracis*-specific DNA sequence from the culture isolate after only 3.5 hours. Although the nanopore-based assembly was error-prone when compared with the SRS-based assembly, as few as 8.5 hours would be required to find evidence of known AMR genes/markers or engineering, including gene insertions and extra-chromosomal plasmids from *B. anthracis*. Although conventional AST remains essential for characterizing functional antimicrobial resistance in *B. anthracis*, nanopore sequencing provided same-day, on-site genomic characterization useful for an anthrax emergency response.

Acknowledgments

We thank scientists in the Zoonoses and Select Agent Laboratory, Division of High-Consequence Pathogens and Pathology, National Center for Emerging and Zoonotic Infectious Diseases (NCEZID), CDC, for performing short-read sequencing; scientists in the Antimicrobial Resistance and Characterization Laboratory, Division of Healthcare Quality Promotion, NCEZID, CDC, for performing conventional BMD AST; and scientists in the Biodefense Research and Development Laboratory, Division of Preparedness and Emerging Infections, NCEZID, CDC, for performing nanopore sequencing.

This study was supported by the CDC Center for Preparedness and Response.

About the Author

Dr. McLaughlin is a scientist at the Biodefense Research and Development Laboratory, Division of Preparedness and Emerging Infections, National Center for Emerging and Zoonotic Infectious Diseases, Centers for Disease Control and Prevention, Atlanta, GA. Her primary research interests are development and evaluation of phenotypic and whole-genome sequencing-based assays to characterize biological threat agents, with an emphasis on rapid detection of antimicrobial resistance in bacteria.

References

- Carlson CJ, Kracalik IT, Ross N, Alexander KA, Hugh-Jones ME, Fegan M, et al. The global distribution of *Bacillus anthracis* and associated anthrax risk to humans, livestock and wildlife. *Nat Microbiol*. 2019;4:1337–43. <https://doi.org/10.1038/s41564-019-0435-4>
- Hendricks KA, Wright ME, Shadomy SV, Bradley JS, Morrow MG, Pavia AT, et al. Workgroup on Anthrax Clinical Guidelines. Centers for disease control and prevention expert panel meetings on prevention and treatment of anthrax in adults. *Emerg Infect Dis*. 2014; 20:e130687. <https://doi.org/10.3201/eid2002.130687>
- Price LB, Vogler A, Pearson T, Busch JD, Schupp JM, Keim P. *In vitro* selection and characterization of *Bacillus anthracis* mutants with high-level resistance to ciprofloxacin. *Antimicrob Agents Chemother*. 2003;47:2362–5. <https://doi.org/10.1128/AAC.47.7.2362-2365.2003>
- Pomerantsev AP, Shishkova NA, Marinin LI. Comparison of therapeutic effects of antibiotics of the tetracycline group in the treatment of anthrax caused by a strain inheriting *tet*-gene of plasmid pBC16 [in Russian]. *Antibiot Khimioter*. 1992;37:31–4.
- Ross CL, Thomason KS, Koehler TM. An extracytoplasmic function sigma factor controls beta-lactamase gene expression in *Bacillus anthracis* and other *Bacillus cereus* group species. *J Bacteriol*. 2009;191:6683–93. <https://doi.org/10.1128/JB.00691-09>
- Weigel LM, Sue D, Michel PA, Kitchel B, Pillai SP. A rapid antimicrobial susceptibility test for *Bacillus anthracis*. *Antimicrob Agents Chemother*. 2010;54:2793–800. <https://doi.org/10.1128/AAC.00247-10>
- Gargis AS, McLaughlin HP, Conley AB, Lascols C, Michel PA, Gee JE, et al. Analysis of whole-genome sequences for the prediction of penicillin resistance and β -lactamase activity in *Bacillus anthracis*. *mSystems*. 2018;3:e00154-18. <https://doi.org/10.1128/mSystems.00154-18>
- Ågren J, Finn M, Bengtsson B, Segerman B. Microevolution during an anthrax outbreak leading to clonal heterogeneity and penicillin resistance. *PLoS One*. 2014;9:e89112. <https://doi.org/10.1371/journal.pone.0089112>
- Wick RR, Judd LM, Gorrie CL, Holt KE. Completing bacterial genome assemblies with multiplex MinION sequencing. *Microb Genom*. 2017;3:e000132. <https://doi.org/10.1099/mgen.0.000132>
- Goodwin S, McPherson JD, McCombie WR. Coming of age: ten years of next-generation sequencing technologies. *Nat Rev Genet*. 2016;17:333–51. <https://doi.org/10.1038/nrg.2016.49>
- Quick J, Loman NJ, Duraffour S, Simpson JT, Severi E, Cowley L, et al. Real-time, portable genome sequencing for Ebola surveillance. *Nature*. 2016;530:228–32. <https://doi.org/10.1038/nature16996>
- Greninger AL, Naccache SN, Federman S, Yu G, Mbala P, Bres V, et al. Rapid metagenomic identification of viral pathogens in clinical samples by real-time nanopore sequencing analysis. *Genome Med*. 2015;7:99. <https://doi.org/10.1186/s13073-015-0220-9>
- Gargis AS, Cherney B, Conley AB, McLaughlin HP, Sue D. Rapid detection of genetic engineering, structural variation, and antimicrobial resistance markers in bacterial bioterror pathogens by nanopore sequencing. *Sci Rep*. 2019;9:13501. <https://doi.org/10.1038/s41598-019-49700-1>
- Clinical and Laboratory Standards Institute. Methods for antimicrobial dilution and disc susceptibility testing of infrequently isolated or fastidious bacteria, 3rd ed. M45. Wayne (PA): The Institute; 2016.
- Nouioui I, Klenk H-P, Igual JM, Gulvik CA, Lasker BA, McQuiston JR. *Streptacidiphilus bronchialis* sp. nov., a ciprofloxacin-resistant bacterium from a human clinical specimen; reclassification of *Streptomyces griseoplanus* as *Streptacidiphilus griseoplanus* comb. nov. and emended description of the genus *Streptacidiphilus*. *Int J Syst Evol Microbiol*. 2019;69:1047–56. <https://doi.org/10.1099/ijsem.0.003267>

Address for correspondence: Heather P. McLaughlin, Centers for Disease Control and Prevention, 1600 Clifton Rd NE, Mailstop H17-5, Atlanta, GA 30329-4027, USA; email: yfq4@cdc.gov

Rickettsia mongolitimonae Encephalitis, Southern France, 2018

María Dolores Corbacho Loarte, Cléa Melenotte,
Nadim Cassir, Serge Cammilleri, Philippe
Dory-Lautrec, Didier Raoult, Philippe Parola

Author affiliations: Hospital Universitario Severo Ochoa, Madrid, Spain (M.D. Corbacho Loarte); Institut Hospitalo-Universitaire–Méditerranée Infection, Marseille, France (M.D. Corbacho Loarte, C. Melenotte, N. Cassir, D. Raoult, P. Parola); Aix-Marseille University, Marseille (M.D. Corbacho Loarte, C. Melenotte, N. Cassir, D. Raoult, P. Parola); Assistance Publique des Hôpitaux de Marseille, Marseille (C. Melenotte, N. Cassir, S. Cammilleri, P. Dory-Lautrec, D. Raoult, P. Parola)

DOI: <https://doi.org/10.3201/eid2602.181667>

We report a case of *Rickettsia sibirica mongolitimonae* infection, an emerging tickborne rickettsiosis, with associated encephalitis in a 66-year-old man. Diagnosis was rapidly confirmed by quantitative PCR obtained from an eschar swab sample. The patient was successfully treated with oral doxycycline.

In July 2018, a 66-year-old man was admitted to the emergency department in Marseille, France, because of fever (40°C) and confusion. His medical history included arterial hypertension controlled with amlodipine and dyslipidemia and coronary artery disease treated with pravastatin and aspirin. He lived in a rural area near Marseille and owned dogs, pigs, pheasants, pigeons, and chickens. In the hospital emergency department, he received acyclovir (1 g every 8 h), amoxicillin (4 g every 6 h), and ceftriaxone (3 g every 12 h) for suspected meningoencephalitis.

At admission to the infectious diseases department, he had a general maculopapular rash over his trunk, palms of his hands, and soles of his feet of 3 days' duration (Figure, panel A). Blood pressure was 130/80 mm Hg. A 15-mm black eschar was noted on his right ankle, associated with rope-like lymphangitis (Figure, panel B). He had a 4/5 right corporal hemiparesis with hemisensory loss and right Babinski sign. Lumbar puncture results were unremarkable, and C-reactive protein was 65.4 mg/L (referent <3 mg/L). Oral doxycycline (300 mg 1×/d) was added to his drug regimen 3 days after symptom onset. Results of brain computed tomography scan were unremarkable. Magnetic resonance imaging showed multiple bilateral brain lesions compatible with acute encephalitis related to vasculitis (Figure, panel C). Positron emission tomographic

scan showed cerebral cortical diffuse hypometabolism (Appendix Figure, <https://wwwnc.cdc.gov/EID/article/26/2/18-1667-App1.pdf>). Results of microbiological tests performed on cerebrospinal fluid and indirect immunofluorescence assay for spotted fever group (SFG) rickettsiae were negative. DNA obtained from eschar swab samples was positive by quantitative PCR for all SFG *Rickettsia* species (*gltA* and *ompA* genes) (1). Positive samples tested with species-specific *R. massiliae*, *R. conorii*, and *R. sibirica mongolitimonae* primers were positive for *R. sibirica mongolitimonae* (35 cycles quantification) (1).

Oral doxycycline was continued for 10 days; other drugs were discontinued. The cutaneous lesions regressed at day 3, and neurologic symptoms progressively improved after administration of doxycycline. A low seroconversion for the SFG rickettsiae was observed (IgM 1:16; IgG 1:16) 3 weeks after symptom onset; at 7 weeks postinfection, serology became negative.

One month after symptom onset, the patient had 4/5 muscular strength in his right leg. Magnetic resonance imaging performed at 7 weeks and 1 year after symptom onset showed cerebral sequelae lesions (Figure, panel C). At 1 year, the Babinski sign in the right foot persisted, but muscular testing was 5/5 with the exception of lifting the right foot, which was 4/5.

R. sibirica mongolitimonae infection is an emerging rickettsiosis; <40 human cases have been described. It is seasonal in France (spring and summer). It has been referred to as lymphangitis-associated rickettsiosis because of the typical rope-like lymphangitis sign (2). Other clinical signs include the classic triad of fever, rash, and eschar. SENLAT (scalp eschar and neck lymphadenopathy after tick bite) also has been reported (3).

Most *R. sibirica mongolitimonae* infections have been reported in the Mediterranean area (France, Spain, Portugal, Greece, and Turkey), Africa (Algeria, Egypt, Cameroon, South Africa), and China (4,5). In Europe, vectors include the tick species *Hyalomma excavatum*, *H. marginatum*, *H. turanicum*, *Rhipicephalus pusillus*, *R. bursa*, and *Haemaphysalis parva* (1,2,4). *R. sibirica mongolitimonae* infection usually causes mild disease, but severe manifestations have been described, including retinal vasculitis, lethargy with hyponatremia, septic shock, myopericarditis, and acute renal failure (2,6).

Only *R. conorii conorii*, *R. rickettsii*, *R. japonica*, and *R. slovaca* have been associated with encephalitis in the literature (Appendix Table); no patients who had received doxycycline were reported to have died. Doxycycline has proven to be superior

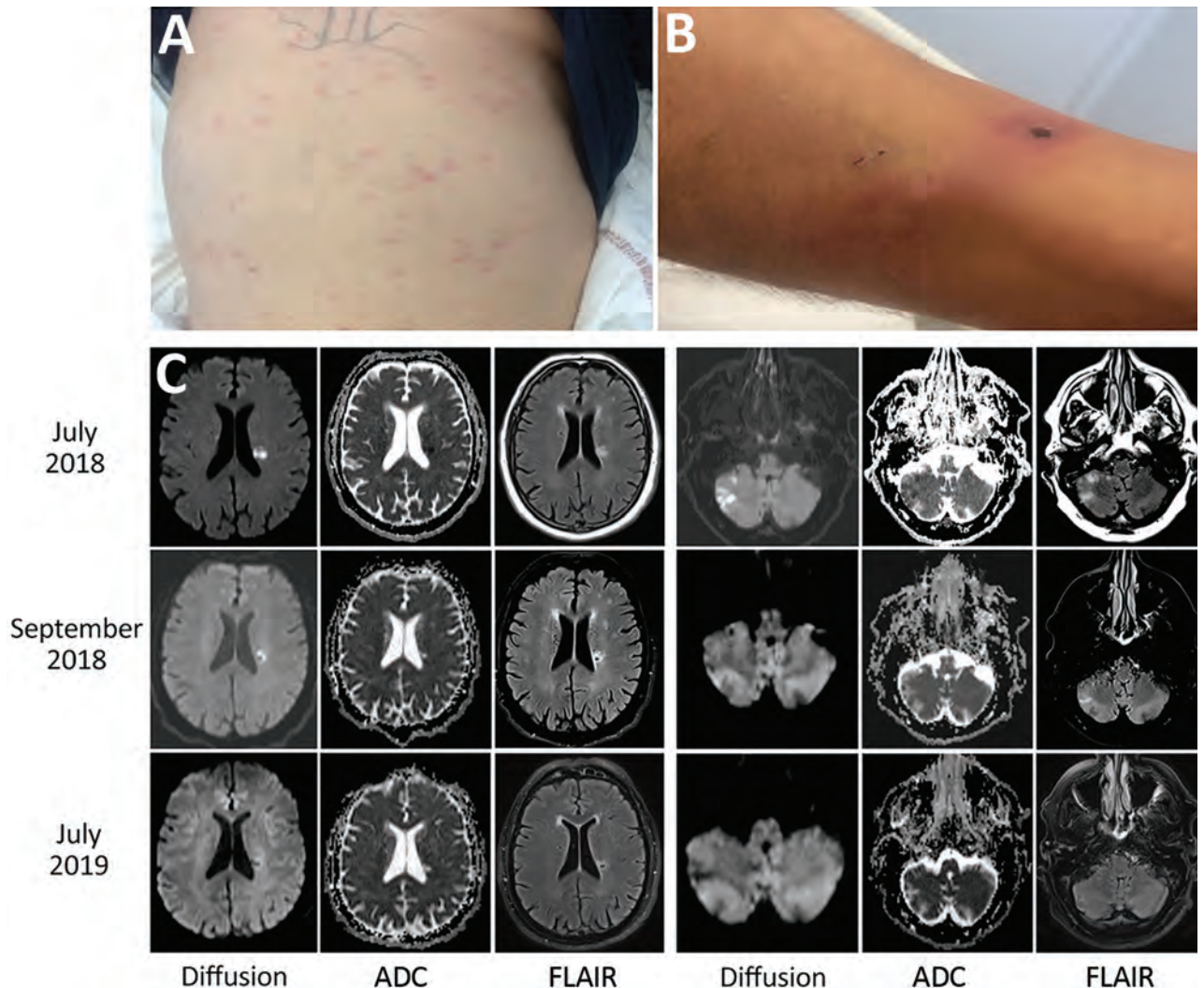


Figure. Clinical manifestations and cerebral magnetic resonance imaging of a 66-year-old man with *Rickettsia sibirica mongolitimonae*-associated encephalitis, southern France, 2018. A) Maculopapular rash. B) Black eschar and rope-like lymphangitis on the right leg. C) Magnetic resonance imaging with diffusion (B1000), ADC, and FLAIR. In July 2018, cytotoxic lesions were observed intra-axially and in the white matter of right cerebellar hemispheres with FLAIR hypersignal and with low ADC signal. In September 2018, these cytotoxic lesions regressed in diffusion with the appearance of a necrotic cavity facing the roof of the left lateral ventricle. In July 2019, disappearance of diffusion anomalies. Small necrotic cavity with after-effects on FLAIR and ADC signals. ADC, apparent diffusion coefficient; FLAIR, fluid-attenuated inversion recovery.

to chloramphenicol and ciprofloxacin in rickettsial infection and should be the treatment of choice for rickettsial-associated encephalitis (1,7).

SFG rickettsiosis can be diagnosed by serology, culture, or molecular assay on blood, skin biopsy, or eschar swab sample. Seroconversion generally appears in the second and third weeks of illness; culture is fastidious and performed only in expert laboratories. Molecular tools using eschar cutaneous swab samples appeared as the best method for detecting and identifying *Rickettsia* spp. (1). The sensitivity of this technique is comparable with that of rickettsial detection on skin biopsy samples using molecular

tools. It is a noninvasive and nonpainful diagnostic method that can be performed easily where molecular facilities are available (3,8).

The discrepancy observed in this case between PCR and serology has been reported in cases of *R. africae* infection, in which seroconversion is delayed (28 days for IgG and 25 days for IgM) and doxycycline treatment within 7 days after symptom onset prevents development of antibodies (9,10). In this patient, we observed very low serologic response 3 weeks after symptom onset, which might have been affected by the early administration of doxycycline. Moreover, the lack of serologic response observed

here may be precisely related to the severity of the disease. The case we described illustrates the rapid efficacy of doxycycline to treat the severe neurologic consequences of rickettsial diseases, as well as the effectiveness and rapidity of the swab sample diagnostic test.

M.D.C.L. received a scholarship from SEIMC (Sociedad Española de Infecciosas y Microbiología Clínica) for a visiting fellowship at the Institut Hospitalo-Universitaire-Méditerranée Infection.

About the Author

Dr. Corbacho Loarte is an internal medicine resident in Madrid and a visiting fellow at the Institut Hospitalo-Universitaire-Méditerranée Infection in Marseille. Her primary research interests are infectious disease, especially zoonoses, neglected tropical diseases, and migrant health.

References

1. Rajoelison P, Mediannikov O, Javelle E, Raoult D, Parola P, Aoun O. *Rickettsia sibirica mongolitimonae* human infection: A diagnostic challenge. *Travel Med Infect Dis*. 2018;26:72–3. <http://dx.doi.org/10.1016/j.tmaid.2018.07.002>
2. Parola P, Paddock CD, Socolovschi C, Labruna MB, Mediannikov O, Kernif T, et al. Update on tick-borne rickettsioses around the world: a geographic approach. *Clin Microbiol Rev*. 2013;26:657–702. <http://dx.doi.org/10.1128/CMR.00032-13>
3. Solary J, Socolovschi C, Aubry C, Brouqui P, Raoult D, Parola P. Detection of *Rickettsia sibirica mongolitimonae* by using cutaneous swab samples and quantitative PCR. *Emerg Infect Dis*. 2014;20:716–8. <http://dx.doi.org/10.3201/eid2004.130575>
4. Kuscü F, Orkun O, Ulu A, Kurtaran B, Komur S, Inal AS, et al. *Rickettsia sibirica mongolitimonae* infection, Turkey, 2016. *Emerg Infect Dis*. 2017;23:1214–6. <http://dx.doi.org/10.3201/eid2307.170188>
5. Nouchi A, Monsel G, Jaspard M, Jannic A, Angelakis E, Caumes E. *Rickettsia sibirica mongolitimonae* infection in a woman travelling from Cameroon: a case report and review of the literature. *J Travel Med*. 2018;25:25. <http://dx.doi.org/10.1093/jtm/tax074>
6. Revilla-Martí P, Cecilio-Irazola Á, Gayán-Ordás J, Sanjoaquin-Conde I, Linares-Vicente JA, Oteo JA. Acute myopericarditis associated with tickborne *Rickettsia sibirica mongolitimonae*. *Emerg Infect Dis*. 2017;23:2091–3. <http://dx.doi.org/10.3201/eid2312.170293>
7. Gikas A, Doukakis S, Pediaditis J, Kastanakis S, Manios A, Tselentis Y. Comparison of the effectiveness of five different antibiotic regimens on infection with *Rickettsia typhi*: therapeutic data from 87 cases. *Am J Trop Med Hyg*. 2004;70:576–9. <http://dx.doi.org/10.4269/ajtmh.2004.70.576>
8. Morand A, Angelakis E, Ben Chaabane M, Parola P, Raoult D, Gautret P. Seek and Find! PCR analyses of skin infections in West-European travelers returning from abroad with an eschar. *Travel Med Infect Dis*. 2018;26:32–6. <http://dx.doi.org/10.1016/j.tmaid.2018.02.009>
9. Fournier P-E, Jensenius M, Laferl H, Vene S, Raoult D. Kinetics of antibody responses in *Rickettsia africae* and *Rickettsia conorii* infections. *Clin Diagn Lab Immunol*. 2002;9:324–8.
10. Jensenius M, Fournier P-E, Kelly P, Myrvang B, Raoult D. African tick bite fever. *Lancet Infect Dis*. 2003;3:557–64. [http://dx.doi.org/10.1016/S1473-3099\(03\)00739-4](http://dx.doi.org/10.1016/S1473-3099(03)00739-4)

Address for correspondence: Maria D. Corbacho Loarte, Aix Marseille University, IHU Méditerranée Infection, Faculté de Médecine Bd Jean Moulin, Marseille 13005, France; email: mdcorbacho@hotmail.com

Human Alveolar Echinococcosis, Croatia

Davorka Dušek, Adriana Vince, Ivan Kurelac, Neven Papić, Klaudija Višković, Peter Deplazes, Relja Beck

Author affiliations: University Hospital for Infectious Diseases, Zagreb, Croatia (D. Dušek, A. Vince, I. Kurelac, N. Papić, K. Višković); University of Zagreb School of Medicine, Zagreb (D. Dušek, A. Vince, N. Papić); University of Zurich, Zurich, Switzerland (P. Deplazes); Croatian Veterinary Institute, Zagreb (R. Beck)

DOI: <https://doi.org/10.3201/eid2602.181826>

Alveolar echinococcosis is a parasitic disease caused by the tapeworm larval stage of *Echinococcus multilocularis*. This zoonotic disease has not been known to occur in Croatia. We report a confirmed case of human alveolar echinococcosis in a patient in Croatia who had never visited a known *E. multilocularis*-endemic area.

A 63-year-old male patient was sent to the University Hospital for Infectious Diseases in Zagreb, Croatia, in September 2017 for treatment of cystic liver lesions and pleural effusion. The patient had grown up and still lived in a rural area in Vukovar (45°21'N, 18°59'E/45.35°N, 18.99°E), where he worked for a waste management company. He spent free time in the woods picking mushrooms.

Before his referral, in November 2014, the patient underwent kidney ultrasonography, which also detected cystic formations in his liver. A subsequent multislice computed tomography (MSCT) scan in

a regional hospital revealed an oval heterogeneous zone in the liver measuring 11 × 8 cm with irregular postcontrast enhancement and an enlarged right suprarenal gland that could not be distinguished from the outer wall of the inferior vena cava. His laboratory results, including tumor markers, were within reference ranges, except for a slightly elevated alkaline phosphatase level.

In March 2015, histopathology of liver tissue excluded malignant disease. The patient tested positive for *Echinococcus* sp. by enzyme immunoassay and Western blotting, but cystic echinococcosis was excluded on the basis of radiologic findings. In June 2015, a second liver biopsy revealed necrotic cells. In November 2015, another MSCT revealed multiple new nodular lesions in the right and left lungs. Thorax and lung biopsies revealed necrotic material.

In 2016, the patient had a bronchoscopy, which showed no malignancy. He had a third diagnostic liver biopsy in October 2016, which revealed acellular, eosinophilic, periodic acid-Schiff–positive histopathology, and morphology that suggested echinococcosis. However, the patient was not seen by an infectious disease physician, nor did he receive treatment for parasites.

An examination in August 2017 showed that his lung nodules had progressed, and a right-sided pleural effusion had enlarged. One month later, the patient's condition worsened. He had a fever (39°C), dyspnea, cough, and sharp pain in the right hemithorax. He was referred to the hospital, where we conducted a cystic lesion biopsy, which indicated suppurative inflammation, but a culture was negative for bacteria. The patient's pleural effusion had eosinophilic exudate, which was negative for bacteria and fungi. The patient had eosinophilia with an average eosinophil count of $2,600 \times 10^9$ cells/L. We analyzed his prior MSCT and magnetic resonance scan results and noted the patient had experienced slow progression of alveolar echinococcosis. The liver lesion had grown from 11 × 8 cm to 13 × 12 × 12 cm during the previous 2.5 years, and the parasite had infiltrated his lungs and right adrenal gland (Figure).

We extracted DNA from pleural exudate and formalin-fixed, paraffin-embedded liver biopsy tissue by using the QIAamp DNA Mini QIAcube system (QIAGEN, <https://www.qiagen.com>). We subjected duplicate samples to PCR and sequenced a 200-bp region in the mitochondrial gene *nad1* (1) and a 395-bp region of the 12S rRNA gene (2). All sequences were identical to isolates of *E. multilocularis* tapeworms from Europe found in GenBank (accession nos. MG755265, MG755266).

Serologic tests using various antigens (3) performed at the University of Zurich (Zurich,

Switzerland) further supported the diagnosis of alveolar echinococcosis. We obtained strongly positive results with genus-specific ELISAs conducted with somatic protoscoleces or cyst fluid from *E. granulosus* sensu stricto and with ELISAs highly specific for *E. multilocularis* tapeworm based on the recombinant Em18 antigen or affinity-purified native EmG11 antigen. Serum analysis conducted by using the Anti-Echinococcus EUROLINE-IgG Western Blot system (EUROIMMUN, <https://www.euroimmun.com>) showed positive results for p7, p28, and Em18.

The patient refused surgery and was treated with oral albendazole (400 mg 2×/d) and intravenous piperacillin/tazobactam (4.5 g 4×/d) for 6 weeks. At discharge, we recommended continued albendazole until clinical and radiologic follow-up 6 months later.

No previous human cases of alveolar echinococcosis have been reported in Croatia, but the *E. multilocularis* tapeworm is endemic in central and eastern Europe and in the Baltic states (4). This patient's infection is surprising because he lived >60 years in eastern Croatia with no international travel. The



Figure. Computed tomography scan of a patient diagnosed with alveolar echinococcosis, Croatia. Arrows indicate right pleural effusion, lung lesions, an enlarged right adrenal gland, and a 13 × 12 × 12 cm lesion in the liver caused by *Echinococcus multilocaris*.

closest reported autochthonous human cases were in southwestern Hungary (5).

E. multilocularis tapeworms have been reported in foxes in western and central Croatia (6) and likely is in eastern areas, such as Vukovar, because it was found in 17.9% of foxes and 14.3% of golden jackals in the region of Serbia directly across the Danube River from Vukovar (7). Since 2013, rabies vaccination has increased in Croatia, which might give the fox population an opportunity to expand and increase transmission of *E. multilocularis* tapeworms to humans, as noted in Switzerland (8).

Correct diagnosis for this patient took 2.5 years because radiologic findings were inconsistent with cystic echinococcosis and clinicians assumed that was the only type of human echinococcosis in Croatia (9). This case highlights the need for clinicians to include alveolar echinococcosis in differential diagnosis of liver lesions. Imaging provides the first-line approach to such a diagnosis and serology provides strong complementary support. Our case also highlights the usefulness of considering pleural effusion and analyzing archival biopsies to retrospectively diagnose alveolar echinococcosis.

About the Author

Dr. Dušek is an attending physician in the University Hospital for Infectious Diseases in Zagreb, Croatia. Her research interests include viral hepatitis and infectious diseases in immunocompromised patients, especially patients with solid organ or stem cell transplants.

References

1. Trachsel D, Deplazes P, Mathis A. Identification of taeniid eggs in the faeces from carnivores based on multiplex PCR using targets in mitochondrial DNA. *Parasitology*. 2007;134:911–20. <https://doi.org/10.1017/S0031182007002235>
2. Stieger C, Hegglin D, Schwarzenbach G, Mathis A, Deplazes P. Spatial and temporal aspects of urban transmission of *Echinococcus multilocularis*. *Parasitology*. 2002;124:631–40. <https://doi.org/10.1017/S0031182002001749>
3. Schweiger A, Grimm F, Tanner I, Müllhaupt B, Bertogg K, Müller N, et al. Serological diagnosis of echinococcosis: the diagnostic potential of native antigens. *Infection*. 2012;40:139–52. <https://doi.org/10.1007/s15010-011-0205-6>
4. Deplazes P, Rinaldi L, Alvarez Rojas CA, Torgerson PR, Harandi MF, Romig T, et al. Global distribution of alveolar and cystic echinococcosis. *Adv Parasitol*. 2017;95:315–493. <https://doi.org/10.1016/bs.apar.2016.11.001>
5. Dezsényi B, Strausz T, Makrai Z, Csomor J, Danka J, Kern P, et al. Autochthonous human alveolar echinococcosis in a Hungarian patient. *Infection*. 2017;45:107–10. <https://doi.org/10.1007/s15010-016-0918-7>
6. Lalošević D, Lalošević V, Simin V, Miljević M, Čabrilo B, Čabrilo OB. Spreading of multilocular echinococcosis in southern Europe: the first record in foxes and jackals in Serbia, Vojvodina Province. *Eur J Wildl Res*. 2016;62:793–6. <https://doi.org/10.1007/s10344-016-1050-9>
7. Morović M. Human hydatidosis in Dalmatia, Croatia. *Epidemiol Infect*. 1997;119:271–6. <https://doi.org/10.1017/S0950268897007760>
8. Schweiger A, Ammann RW, Candinas D, Clavien PA, Eckert J, Gottstein B, et al. Human alveolar echinococcosis after fox population increase, Switzerland. *Emerg Infect Dis*. 2007;13:878–82. <https://doi.org/10.3201/eid1306.061074>
9. Beck R, Mihaljević Ž, Brezak R, Bosnić S, Janković IL, Deplazes P. First detection of *Echinococcus multilocularis* in Croatia. *Parasitol Res*. 2018;117:617–21. <https://doi.org/10.1007/s00436-017-5732-3>

Address for correspondence: Relja Beck, Croatian Veterinary Institute, Department for Bacteriology and Parasitology, Zagreb, Savskacesta 143, 10000 Zagreb, Croatia; email: relja.beck@gmail.com

Two Cases of Newly Characterized *Neisseria* Species, Brazil

Mustapha M. Mustapha, Ana Paula S. Lemos, Marissa P. Griffith, Daniel R. Evans, Ramon Marx, Elizabeth S.F. Coltro, Christian A. Siebra, Loeci Timm, Hamilton Ribeiro, Alessandro Monteiro, A. William Pasculle, Jane W. Marsh, Daria Van Tyne, Lee H. Harrison, Claudio T. Sacchi

Author affiliations: University of Pittsburgh, Pittsburgh, Pennsylvania, USA (M.M. Mustapha, M.P. Griffith, D.R. Evans, A.W. Pasculle, J.W. Marsh, D. Van Tyne, L.H. Harrison); Instituto Adolfo Lutz, São Paulo, Brazil (A.P.S. Lemos, C.T. Sacchi); Hospital Nossa Senhora da Conceição, Porto Alegre, Brazil (R. Marx, A. Monteiro); Hospital do Trabalhador/SESA, Curitiba, Brazil (E.S.F. Coltro); Laboratório Central de Saúde Pública, Curitiba (C.A. Siebra); Laboratório Central de Saúde Pública, Porto Alegre (L. Timm); Paraná Department of Health, Piraquara, Brazil (H. Ribeiro)

DOI: <https://doi.org/10.3201/eid2602.190191>

We describe 2 human cases of infection with a new *Neisseria* species (putatively *N. brasiliensis*), 1 of which involved bacteremia. Genomic analyses found that both isolates were distinct strains of the same species, were closely related to *N. iguanae*, and contained a capsule synthesis operon similar to *N. meningitidis*.

Neisseria is a genus containing diverse organisms; most are rarely pathogenic. *N. meningitidis* and *N. gonorrhoeae* are the most clinically relevant species. The polysaccharide capsule is the most critical meningococcal virulence factor, a vaccine target, and the basis for classifying meningococci into serogroups (1). During routine laboratory-based public health surveillance in Brazil, we identified 2 cases of infection caused by a previously uncharacterized species of the *Neisseria* genus.

Clinicians reported 2 cases to the National Reference Laboratory, Adolfo Lutz Institute (IAL), São Paulo, Brazil. Case-patient 1 was a 64-year-old man from Rio Grande do Sul state, Brazil, who, in June 2016, had congestive heart failure with bilateral pulmonary infiltrates and pleural effusion on chest radiograph. Case-patient 2 was a 74-year-old woman with leprosy from Paraná state, Brazil, who, in February 2016, developed a polymicrobially infected ulcer of the left lower extremity. The 2 cases were separated in time and by >400 km and had no known epidemiologic link.

Overnight cultures of blood from case-patient 1 and ulcer exudate from case-patient 2 on brain-heart infusion agar containing 10% chocolate and horse blood at 37°C in the presence of 5% CO₂ both revealed brownish colonies uncharacteristic of *N. meningitidis*. We identified both isolates (N.95-16, from case-patient 1, and N.177-16, from case-patient 2) as gram-negative glucose-fermenting diplococci with positive catalase and oxidase tests. The isolates fermented maltose, lactose, sucrose, and fructose but not mannose; they reduced nitrate and produced a starch-like polysaccharide detected with Gram's iodine but did not produce DNase. Assessment by matrix-assisted laser desorption/ionization time-of-flight mass spectroscopy found no species match; the closest matches belonged to the *Neisseria* genus for both isolates.

We performed serogrouping by slide agglutination (2) with polyclonal goat or horse antisera prepared at IAL against the *N. meningitidis* capsule groups (ABCEWXYZ), as described previously (3), and confirmed with real-time PCR (4). Isolate N.95-16 had strong agglutination against serogroup X and nonspecific agglutination against serogroups A, B, C, W, Y, E, and Z antisera; isolate N.177-16 had nonspecific agglutination against A, B, C, W, X, Y, E, and Z antisera. Meningococcal serogroup-specific real-time PCR identified isolate 1 as *N. meningitidis* capsular group X and isolate 2 as capsular group B.

We extracted genomic DNA from overnight cultures and performed library preparation and whole-genome sequencing using a combination of Illumina MiSeq (<https://www.illumina.com>) and Oxford

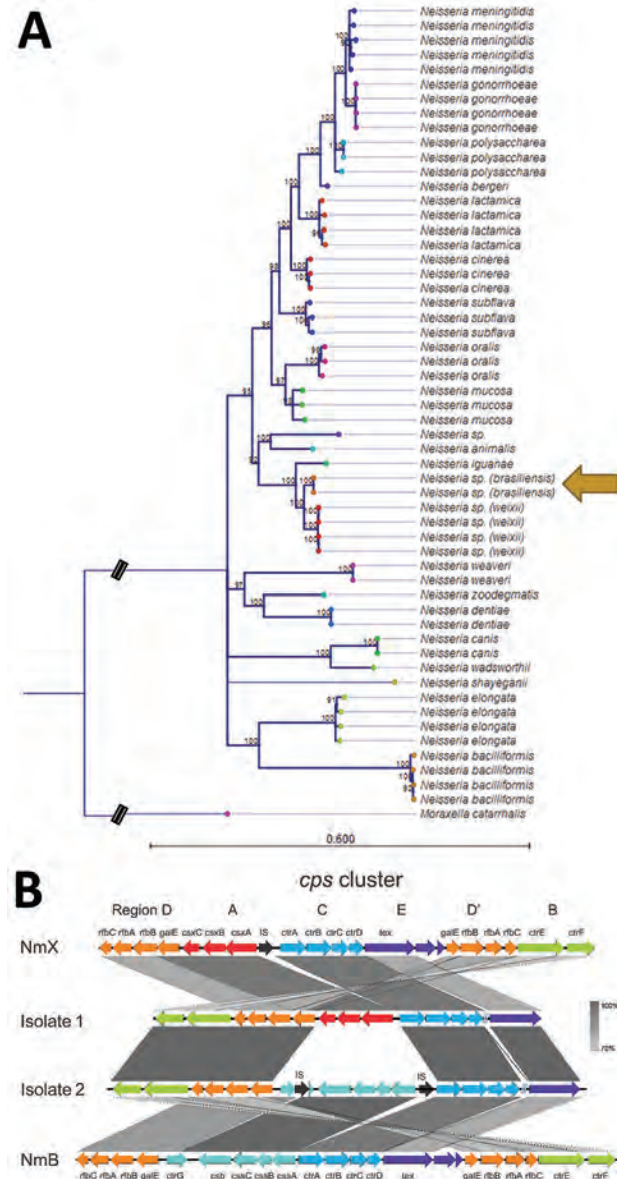
Nanopore MinION (<https://nanoporetech.com>) technologies. Sequencing reads underwent hybrid assembly using Unicycler (5), which generated a high-quality draft assembly for isolate N.95-16 and a complete genome sequence for isolate N.177-16 (GenBank accession nos. WJXO00000000 and CP046027; PubMLST [<https://pubmlst.org>] identification 94178–94179). We performed species investigation by querying sequencing reads and assemblies against the GenBank and PubMLST reference databases (6). We aligned gene sequences corresponding to 53 conserved ribosomal MLST (rMLST) loci (7) across the *Neisseria* genus and constructed a maximum likelihood phylogenetic tree using RAxML with 1,000 bootstrap replicates (Figure, panel A). We calculated average nucleotide identity (ANI) using OrthoANI (8).

Both isolate genomes were 2.5 Mb and had 49.2% guanine-cytosine (GC) content. ANI was 99.3% between the 2 genomes and <86% relative to all other *Neisseria* species. The closest genome matches were *N. iguanae* and the proposed *N. weixii*, isolated from the intestinal contents of a Tibetan Plateau pika (Figure, panel A) (PubMLST identification 56407–56409; GenBank accession no. CP023429). Both genomes shared identical rMLST profiles (rST 61343); the 4 proposed *N. weixii* genomes shared only 1–2 alleles of 53 rMLST loci with these isolate genomes, and *N. iguanae* shared no rMLST alleles. Both genomes contained an intact capsule gene cluster (*cps*) that was similar in gene organization and sequence identity to *N. meningitidis* (Figure, panel B). The *ctrA-cssA/csxA* promoter region was conserved in both isolates. However, both genomes contained only 1 copy of *galE-rfbCAB* (Region D), compared with 2 copies found in meningococcal reference genomes; the *tex* gene was located >10 kb outside *cps*, upstream from *ctrD* (Figure, panel B). The 2 isolates differed in their sequence of sialic acid biosynthesis genes within region A; isolate N.95-16 contained *csxABC* genes that shared 98% amino acid identity with the meningococcal serogroup X reference strain α388 (1), and isolate N.177-16 contained *cssABC-csb* genes that shared 99% amino acid identity with serogroup B reference strain H44/76 (Figure, panel B). The *cps* differences observed between the isolates were similar to the mosaic recombination pattern associated with meningococcal capsular switching (9). Taken together, the presence of *cps* genes sharing substantial similarity to meningococcal homologs suggests that both isolates have the potential to synthesize meningococcal-like capsules.

In summary, we describe 2 sporadic cases of a new *Neisseria* species (which we propose to name

Neisseria brasiliensis), 1 of which also involved bacteremia. Both genomes contain an intact repertoire of genes for capsule synthesis, a key meningococcal virulence factor. The significance of capsule genes

and potential capsule synthesis in nonmeningococcal *Neisseria* is unknown (10). Continued surveillance is required to establish the pathogenic potential and host range for this apparent new species.



Acknowledgments

We thank Maria Vaneide PB. dos Santos, Gladys Maria Zubaran, and Maria Cristina P. Cecconi for assistance in microbiological tests, and Fatima Ali for microbiological and clinical data.

About the Author

Dr. Mustapha is a research assistant professor in the department of medicine and a member of the Microbial Genomic Epidemiology Laboratory at the University of Pittsburgh School of Medicine, Pittsburgh, PA, USA. His research focuses on the genomic epidemiology of bacterial diseases.

References

- Harrison OB, Claus H, Jiang Y, Bennett JS, Bratcher HB, Jolley KA, et al. Description and nomenclature of *Neisseria meningitidis* capsule locus. *Emerg Infect Dis.* 2013;19:566–73. <https://doi.org/10.3201/eid1904.111799>
- Castillo D, Harcourt B, Hatcher C, Jackson M, Katz L, Mair R, et al. Laboratory methods for the diagnosis of meningitis caused by *Neisseria meningitidis*, *Streptococcus pneumoniae*, and *Haemophilus influenzae*, second edition [cited 2019 Dec10]. <https://www.cdc.gov/meningitis/lab-manual/index.html#eref>
- Alkmin MG, Shimizu SH, Landgraf IM, Gaspari EN, Melles CE. Production and immunochemical characterization of *Neisseria meningitidis* group B antiserum for the diagnosis of purulent meningitis. *Braz J Med Biol Res.* 1994;27:1627–34.
- Mothershed EA, Sacchi CT, Whitney AM, Barnett GA, Ajello GW, Schmink S, et al. Use of real-time PCR to resolve slide agglutination discrepancies in serogroup identification of *Neisseria meningitidis*. *J Clin Microbiol.* 2004;42:320–8. <https://doi.org/10.1128/JCM.42.1.320-328.2004>
- Wick RR, Judd LM, Gorrie CL, Holt KE. Unicycler: resolving bacterial genome assemblies from short and long sequencing reads. *PLOS Comput Biol.* 2017;13:e1005595. <https://doi.org/10.1371/journal.pcbi.1005595>
- Bennett JS, Jolley KA, Earle SG, Corton C, Bentley SD, Parkhill J, et al. A genomic approach to bacterial taxonomy: an examination and proposed reclassification of species within the genus *Neisseria*. *Microbiology.* 2012;158:1570–80. <https://doi.org/10.1099/mic.0.056077-0>
- Jolley KA, Bliss CM, Bennett JS, Bratcher HB, Brehony C, Colles FM, et al. Ribosomal multilocus sequence typing: universal characterization of bacteria from domain to strain. *Microbiology.* 2012;158:1005–15. <https://doi.org/10.1099/mic.0.055459-0>
- Lee I, Ouk Kim Y, Park SC, Chun J. OrthoANI: An improved algorithm and software for calculating average nucleotide identity. *Int J Syst Evol Microbiol.* 2016;66:1100–3. <https://doi.org/10.1099/ijsem.0.000760>
- Mustapha MM, Marsh JW, Krauland MG, Fernandez JO, de Lemos APS, Dunning Hotopp JC, et al. Genomic

investigation reveals highly conserved, mosaic, recombination events associated with capsular switching among invasive *Neisseria meningitidis* serogroup W sequence type (ST)-11 strains. *Genome Biol Evol.* 2016;8:2065–75. <https://doi.org/10.1093/gbe/evw122>

10. Clemence MEA, Maiden MCJ, Harrison OB. Characterization of capsule genes in non-pathogenic *Neisseria* species. *Microb Genom.* 2018;4. <https://doi.org/10.1099/mgen.0.000208>

Address for correspondence: Mustapha M. Mustapha, University of Pittsburgh School of Medicine, Division of Infectious Diseases, 3500 Terrace St, S861, Pittsburgh, PA 15261, USA; email: mmm147@pitt.edu

Hepatitis A Virus Genotype IB Outbreak among Internally Displaced Persons, Syria

Malak Kaddoura, Rasmieh Allaham, Abdinasir Abubakar, Amani Ezzeddine, Amal Barakat, Peter Mala, Hassan Zaraket

Author affiliations: American University of Beirut, Beirut, Lebanon (M. Kaddoura, A. Ezzeddine, H. Zaraket); World Health Organization Country Office, Damascus, Syria (R. Allaham); World Health Organization Regional Office for the Eastern Mediterranean, Cairo, Egypt (A. Abubakar, A. Barakat, P. Mala)

DOI: <https://doi.org/10.3201/eid2602.190652>

In 2018, a hepatitis A virus outbreak was identified among internally displaced persons in Syria. Sequence analysis based on the viral protein 1/2A junction revealed that the causative virus belonged to genotype IB. A high displacement rate, deteriorated sanitary and health conditions, and poor water quality likely contributed to this outbreak.

Hepatitis A virus (HAV) is the leading cause of acute hepatitis infections worldwide, infecting ≈1.5 million persons annually (1). Symptoms, which are usually mild, include nausea, vomiting, abdominal pain, restlessness, body weakness, myalgia, loss of appetite, and fever. However, HAV may progress into fulminant liver failure, necessitating liver transplant. Generally, HAV is self-limiting (2). HAV (genus *Hepatovirus*, family *Picornaviridae*) is a nonenveloped virus with a single-stranded, positive-sense

RNA linear genome (7.5 kb). The viral protein (VP) 1/2A junction (168 nt) is used to classify HAV into 6 genotypes: I–III (subgenotypes A and B) of human origin and IV–VI of simian origin (3). Genotype IA is the most commonly reported worldwide, whereas genotype IB is predominant in the Middle East (4–6).

On September 9, 2018, the governorate of Aleppo, Syria, informed the World Health Organization office in Syria that internally displaced persons (IDPs; displaced since early 2018) and local host community members in Tal Refaat, Fafin, and surrounding areas in the northwestern and western parts of Aleppo were experiencing a suspected hepatitis outbreak. The affected area included 17 locations in Azaz and Jabal Sem'an districts in western Aleppo (Appendix, <https://wwwnc.cdc.gov/EID/article/26/2/19-0652-App1.pdf>). Outbreak field investigation found sporadic cases of the disease among IDPs starting July 21, 2018; as of November 8, a total of 638 cases of suspected acute hepatitis infection had been reported. Most patients (98.59%) were <15 years of age and the rest 16–54 years of age. A total of 105 patients (16.5%) were admitted into the Fafin hospital; no fatalities were reported. No field investigations were performed in the first half of 2018 because of the crisis that led to weakness in the routine surveillance system.

A total of 48 unidentified serum and plasma samples were collected from 24 IDP children with suspected hepatitis and sent to the laboratory on October 29. The specimens originated from 3 locations in Syria: 13 from Fafin camp in Aleppo, 6 from eastern rural Daraa, and 5 samples from rural Quneitra. Even though the main outbreak was in the Aleppo governorate, Daraa and Quneitra were also experiencing a notable upsurge in reported cases of suspected acute hepatitis infection. For this reason, additional samples were collected from these governorates.

We analyzed the serum specimens by serology (total HAV antibodies and HAV IgM) using the enzyme-linked fluorescent assay VIDAS (bioMérieux Diagnostics, <https://www.biomerieux-diagnostics.com>) and the plasma specimens by real-time reverse transcription PCR (RT-PCR) for the detection of HAV (using the HAVNET protocol) and hepatitis E virus (HEV) (7). Seven samples had insufficient volume to perform both total HAV antibody and HAV IgM tests; thus, only the IgM test was performed. Overall, 19 plasma specimens were positive for HAV and none for HEV by PCR (Table). Eighteen serum specimens had detectable HAV IgM. All the specimens with sufficient volume (n = 17) were positive for total HAV antibodies. Of these, 5 were from past infections, as indicated by the negative HAV PCR and HAV IgM

Table. Serologic and PCR analysis of serum and plasma specimens from the suspected hepatitis outbreak*

Lab ID	District	Serology		Molecular analysis		Genotype
		HAV IgM	HAV total	HAV vRNA	HEV vRNA	
1	Fafin	+	+	+	–	ND
2	Fafin	+	+	+	–	IB
3	Fafin	+	+	+	–	IB
4	Fafin	+	+	+	–	ND
5	Fafin	+	+	+	–	ND
6	Fafin	+	+	+	–	IB
7	Fafin	+	+	+	–	IB
8	Fafin	+	+	+	–	ND
9	Fafin	–	+	–	–	–
10	Fafin	+	+	+	–	ND
11	Fafin	+	NS	+	–	ND
12	Fafin	–	+	–	–	–
13	Fafin	–	+	–	–	–
14	Quneitra	+	+	+	–	ND
15	Quneitra	–	+	+	–	ND
16	Quneitra	–	+	–	–	–
17	Quneitra	+	+	+	–	ND
18	Quneitra	+	+	+	–	IB
19	Daraa	+	NS	+	–	ND
20	Daraa	+	NS	+	–	ND
21	Daraa	+	NS	+	–	IB
22	Daraa	+	NS	+	–	ND
23	Daraa	+	NS	+	–	ND
24	Daraa	–	NS	–	–	–

*HAV, hepatitis A virus; HEV, hepatitis E virus; ND, not determined; NS, no sufficient volume; +, positive; –, negative.

results. One patient had detectable HAV vRNA but negative HAV IgM, which indicates the early start of acute infection (8). This patient's serum was positive for total HAV antibodies, indicating a previous exposure with a current breakthrough infection.

We successfully sequenced the VP1/2A region for 6 specimens (Table) and used ClustalW in BioEdit 7.0 to align the sequences (9). Sequence-based genotypes were inferred by comparing the obtained sequences with genotype reference and contemporary strains obtained from GenBank. The phylogenetic analysis indicated that all Syria specimens belonged to genotype IB.

The Office for the Coordination of Humanitarian Affairs reported that, as of September 3, 2018, a total of 23,279 families (107,083 persons) were displaced from Afrin to Tel Refaat, Fafin, and surrounding villages. These IDPs were in addition to 4,766 families (38,843 persons) in the host community. Tents, destroyed or empty dwellings, schools, mosques, and warehouses were used as collective shelters but are relatively distant from active frontlines. IDPs had restricted freedom of movement and no access to proper sanitation facilities as a result of infrastructure damage; 70% of the population rely on water trucking services, and 30% live on less than 20 L of water per day. Moreover, 88% of the respondents reported accumulation of solid waste in their areas (World Health Association, unpub. data). A health assessment in the Afrin district found that 153 of 180 (85%) assessed communities have no access to health services. Vaccination

campaigns have been largely suspended since November 2016. These poor living and health conditions render the IDPs highly prone to vaccine-preventable diseases, including hepatitis A, measles, polio, and cholera (10). Although water testing for HAV was not possible in the affected areas, deterioration in water quality was reported down the supply chain and may have contributed to this outbreak (World Health Association, unpub. data).

In summary, we report a large outbreak of hepatitis among IDPs in Syria. Laboratory testing confirmed current HAV IB infection among most screened patients. The high displacement rate, deteriorated sanitary and health conditions, and poor water quality may have all contributed to the increased HAV reports among this population.

Acknowledgments

We thank George Araj and the Clinical Microbiology Laboratory at the American University Medical Center for their help with serologic analysis.

About the Author

Ms. Kaddoura is a research assistant in the virology laboratory at the Department of Experimental Pathology, Immunology, and Microbiology at the American University of Beirut. Her research focuses on molecular epidemiology and evolution of viral infections and antiviral drug discovery.

References

1. Franco E, Meleleo C, Serino L, Sorbara D, Zaratti L. Hepatitis A: epidemiology and prevention in developing countries. *World J Hepatol.* 2012;4:68–73. <https://doi.org/10.4254/wjh.v4.i3.68>
2. Jeong S-H, Lee H-S. Hepatitis A: clinical manifestations and management. *Intervirology.* 2010;53:15–9. <https://doi.org/10.1159/000252779>
3. Lemon SM, Ott JJ, Van Damme P, Shouval D. Type A viral hepatitis: a summary and update on the molecular virology, epidemiology, pathogenesis and prevention. *J Hepatol.* 2017;68:167–84. <https://doi.org/10.1016/j.jhep.2017.08.034>
4. Vaughan G, Goncalves Rossi LM, Forbi JC, de Paula VS, Purdy MA, Xia G, et al. Hepatitis A virus: host interactions, molecular epidemiology and evolution. *Infect Genet Evol.* 2014;21:227–43. <https://doi.org/10.1016/j.meegid.2013.10.023>
5. Hamza H, Abd-Elshafy DN, Fayed SA, Bahgat MM, El-Esnawy NA, Abdel-Mobdy E. Detection and characterization of hepatitis A virus circulating in Egypt. *Arch Virol.* 2017;162:1921–31. <https://doi.org/10.1007/s00705-017-3294-4>
6. Yilmaz H, Karakullukcu A, Turan N, Cizmecigil UY, Yilmaz A, Ozkul AA, et al. Genotypes of hepatitis a virus in Turkey: first report and clinical profile of children infected with sub-genotypes IA and IIIA. *BMC Infect Dis.* 2017; 17:561. <https://doi.org/10.1186/s12879-017-2667-3>
7. Jothikumar N, Cromeans TL, Robertson BH, Meng XJ, Hill VR. A broadly reactive one-step real-time RT-PCR assay for rapid and sensitive detection of hepatitis E virus. *J Virol Methods.* 2006;131:65–71. <https://doi.org/10.1016/j.jviromet.2005.07.004>
8. Bower WA, Nainan OV, Han X, Margolis HS. Duration of viremia in hepatitis A virus infection. *J Infect Dis.* 2000;182:12–7. <https://doi.org/10.1086/315701>
9. Hall TA. BioEdit: a user-friendly biological sequence alignment editor and analysis program for Windows 95/98/NT. 1999 [cited 2019 Apr 17]. <http://brownlab.mbio.ncsu.edu/JWB/papers/1999Hall1.pdf>
10. Connolly MA, Gayer M, Ryan MJ, Salama P, Spiegel P, Heymann DL. Communicable diseases in complex emergencies: impact and challenges. *Lancet.* 2004;364:1974–83. [https://doi.org/10.1016/S0140-6736\(04\)17481-3](https://doi.org/10.1016/S0140-6736(04)17481-3)

Address for correspondence: Hassan Zaraket, American University of Beirut, PO Box 11-0236, Riad El-Solh, Beirut, Lebanon; email: hz34@aub.edu.lb

Rickettsia parkeri and *Candidatus Rickettsia andeanae* in *Amblyomma maculatum* Group Ticks

Bruce H. Noden, Megan A. Roselli, Scott R. Loss

Author affiliation: Oklahoma State University, Stillwater, Oklahoma, USA

DOI: <https://doi.org/10.3201/eid2602.190664>

We determined prevalence of *Rickettsia* spp. in 172 ticks of the *Amblyomma maculatum* group collected from 16 urban sites in Oklahoma City, Oklahoma, USA, during 2017 and 2018. Most ticks (59.3%) were collected from 1 site; 4 (2.3%) were infected with *Rickettsia parkeri* and 118 (68.6%) with *Candidatus Rickettsia andeanae*.

Rickettsia parkeri, part of the spotted fever group *Rickettsia* (SFGR), affects humans throughout much of the southern United States (1). Although *R. parkeri* in an engorged nymph was reported once in Oklahoma, *R. parkeri* has not been reported in adult *A. maculatum* ticks in Oklahoma or Kansas. To date, all test-positive adult ticks in Kansas and Oklahoma have been infected with *Candidatus Rickettsia andeanae* (2). The absence of *R. parkeri* in Oklahoma is surprising because it was detected in *A. maculatum* group ticks recovered from dogs in Arkansas counties bordering eastern Oklahoma (3) and in adult *A. maculatum* ticks in Texas (4), and *A. maculatum* ticks have been present in Oklahoma since the 1940s (4). We collected *A. maculatum* ticks in the Oklahoma City metropolitan area during May–August 2017 and 2018 and tested them for *Rickettsia* spp.

We selected 16 sites as part of a larger study of tickborne disease epidemiology (Figure). We performed collections during May–August by flagging vegetation or using CO₂ traps (5). We completed identification by using established keys (6).

We tested field-collected ticks for rickettsial DNA by using established PCR protocols (7,8). To limit DNA contamination, we conducted DNA extractions by using site-specific reagents in a separate laboratory. After soaking adult ticks in deionized water for 30 minutes and surface-sterilizing with 70% ethanol, we longitudinally bisected ticks; we used one half for DNA extraction and stored the other half at –80°C. DNA extraction followed established protocols (5). In 2017, we screened all ticks by using assays targeting the *gltA* and *ompA* (8) genes and retested positive samples by using an assay targeting the *ompB* gene (primer pair 120–2788/120–3599) (7). In 2018, we

initially screened ticks by using the *gltA* assay and confirmed the results with an *ompB* assay.

We sequenced positive *ompB* amplicons bidirectionally by using an Applied Biosystems 3730 DNA Analyzer (<https://www.thermofisher.com>) at the Oklahoma State University Core Facility to identify bacterial species. We verified each resulting sequence by using BioEdit 7.2 (<https://bioedit.software.informer.com>) and aligned bidirectional sequences to create consensus sequences by using Clustal Omega (<https://www.ebi.ac.uk/Tools/msa/clustalo>). We compared resulting consensus sequences with GenBank submissions by using default conditions on

BLAST (<http://blast.ncbi.nlm.nih.gov/Blast.cgi>), using the highest percentage sequence identity to determine species similarity.

We collected 172 adult ticks in the *A. maculatum* group (112 in 2017, 60 in 2018; 81 male [50 in 2017, 31 in 2018] and 91 female [62 in 2017, 29 in 2018]) from 15/16 sites across Oklahoma City (Figure). Most (59.3%) *A. maculatum* ticks were collected at 1 site in the southwestern metropolitan area consisting of grassland and deciduous shrubland and woodland surrounded by rapidly growing suburban developments (Figure). Most *A. maculatum* tick collections occurred in areas dominated by grassland with few woody plants and trees.

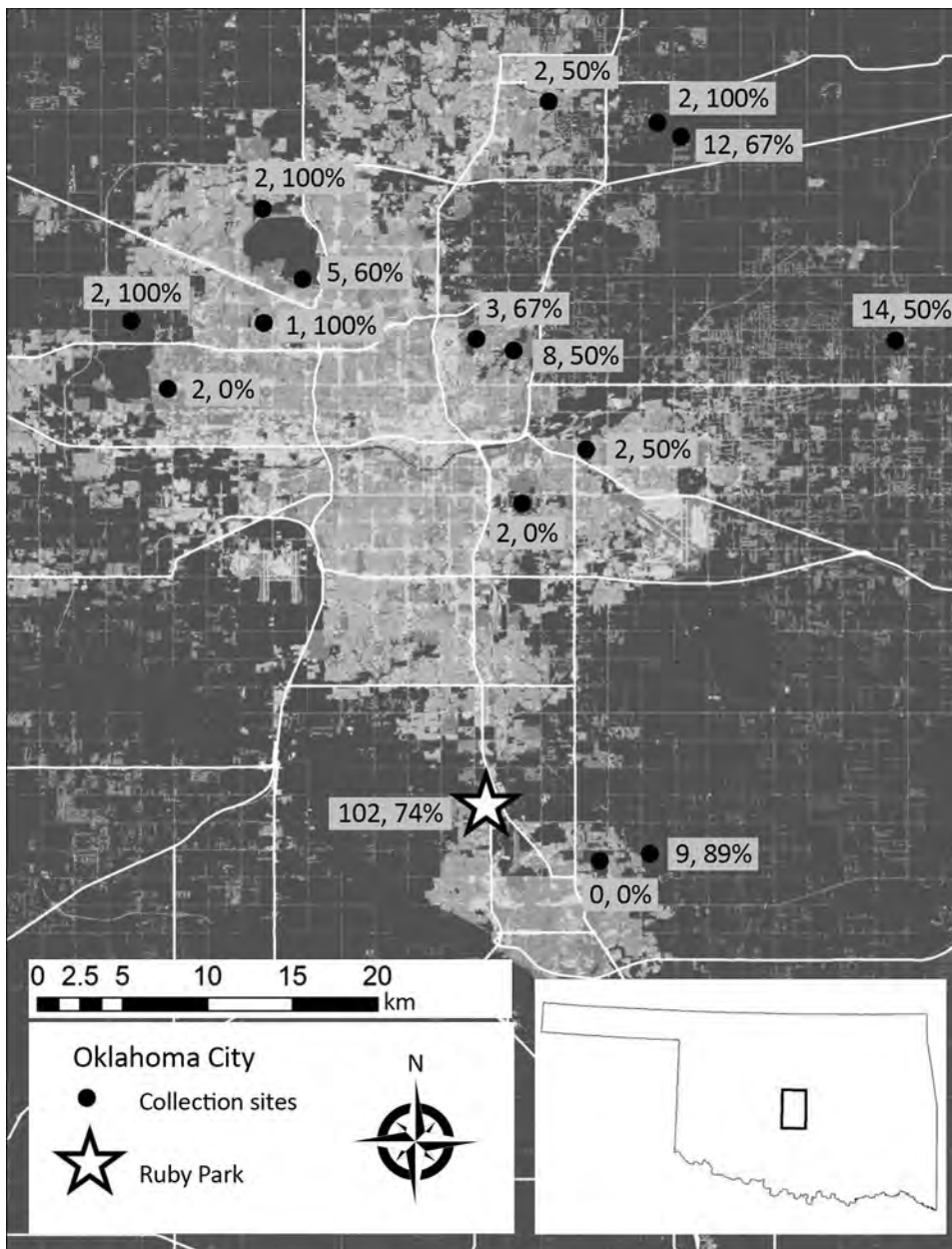


Figure. Locations where ticks of the *Amblyomma maculatum* group were collected (dots) in Oklahoma City, Oklahoma, USA. Numbers of *A. maculatum* ticks collected and percentage infected with *Candidatus R. andeanae* are indicated. Star indicates location where *Rickettsia parkeri*-infected ticks were collected. Figure constructed with ArcMap from highway data from the Environmental Systems Research Institute (Redlands, CA) and the US Geological Survey National Land Cover Database.

Initial screening of the 172 ticks detected 122 positive results, indicating a *Rickettsia* spp. prevalence of 70.9% (76.8% in 2017, 60.0% in 2018). Consensus sequences demonstrating 100% identity with the 850-bp portion of the *ompB* gene of *R. parkeri* Portsmouth (GenBank accession no. CP003341.1) and the 590-bp portion of the *ompA* gene of *R. parkeri* La Paloma (GenBank accession no. MG574938.1) were amplified from 4 (3.3%) positive *A. maculatum* ticks (3 males in 2017, 1 female in 2018). All 4 *R. parkeri*-infected ticks were from 1 site (Figure). The remaining 118 (96.7%) sequences from 122 amplicon-positive *A. maculatum* ticks demonstrated complete identity to homologous 850 bp portions of the *ompB* gene of *Candidatus R. andeanae* (GenBank accession no. GU395297.1). The overall *Candidatus R. andeanae* prevalence by sex was 72.8% for males (74% in 2017, 71% in 2018) and 64.8% for females (74.2% in 2017, 44.8% in 2018). Most *Candidatus R. andeanae*-infected ticks (74/118) were from the park with *R. parkeri*-positive ticks; however, *Candidatus R. andeanae*-positive ticks also were collected in 12 other sites (Figure). No dually infected ticks were identified.

We identified *A. maculatum* group ticks infected with *R. parkeri* and *Candidatus R. andeanae* in the Oklahoma City metropolitan area. Oklahoma lies at the western edge of 1 of the highest-incidence areas of SFGR in the United States (1). To date, no human rickettsiosis cases caused by *R. parkeri* have been reported in Oklahoma, possibly because of treatment based on nonspecific symptoms and the lifting of mandatory reporting to the Centers for Disease Control and Prevention (9). The low prevalence of *R. parkeri* in Oklahoma ticks differs from other areas of the United States, such as Virginia, where prevalence of *R. parkeri* is higher in *A. maculatum* ticks (10). *Candidatus R. andeanae* prevalence in *A. maculatum* ticks varies inversely with *R. parkeri* prevalence in some regions (4). Although *Candidatus R. andeanae* is not known to cause human illness (4), the high prevalence of *Candidatus R. andeanae* in Oklahoma ticks might interfere with *R. parkeri* development, limiting its distribution (2). The potential presence of this human pathogen in the largest metropolitan area in the state, and 1 of the largest in the central United States, necessitates thorough case evaluation of future SFGR cases in this region.

Acknowledgments

We would like to thank Dawn Brown, Caitlin Laughlin, Caleb McKinney, and Liam Whiteman for invaluable help with tick collections. We also thank William Nicholson for providing the positive control *R. rickettsii* DNA.

This work was supported through the Oklahoma Center for the Advancement of Science and Technology (grant no. HR16-038) and US Department of Agriculture National Institute of Food and Agriculture Hatch funds through the Oklahoma Agricultural Experiment Station (grant nos. OKL-03085 and OKL-02915).

About the Author

Dr. Noden is an associate professor of medical and veterinary entomology in the Department of Entomology and Plant Pathology at Oklahoma State University. His research interests include vectorborne diseases involving ticks, mosquitoes, and fleas.

References

- Drexler NA, Dahlgren FS, Heitman KN, Massung RF, Paddock CD, Behravesh CB. National surveillance of spotted fever group rickettsioses in the United States, 2008–2012. *Am J Trop Med Hyg*. 2016;94:26–34. <https://doi.org/10.4269/ajtmh.15-0472>
- Paddock CD, Denison AM, Dryden MW, Noden BH, Lash RR, Abdelghani SS, et al. High prevalence of “*Candidatus Rickettsia andeanae*” and apparent exclusion of *Rickettsia parkeri* in adult *Amblyomma maculatum* (Acari: Ixodidae) from Kansas and Oklahoma. *Ticks Tick Borne Dis*. 2015;6:297–302. <https://doi.org/10.1016/j.ttbdis.2015.02.001>
- Trout R, Steelman CD, Szalanski AL, Williamson PC. Rickettsiae in Gulf Coast ticks, Arkansas, USA. *Emerg Infect Dis*. 2010;16:830–2. <https://doi.org/10.3201/eid1605.091314>
- Paddock CD, Goddard J. The evolving medical and veterinary importance of the Gulf Coast tick (Acari: Ixodidae). *J Med Entomol*. 2015;52:230–52. <https://doi.org/10.1093/jme/tju022>
- Noden BH, Loss SR, Maichak C, Williams F. Risk of encountering ticks and tick-borne pathogens in a rapidly growing metropolitan area in the U.S. Great Plains. *Ticks Tick Borne Dis*. 2017;8:119–24. <https://doi.org/10.1016/j.ttbdis.2016.10.007>
- Keirans JE, Litwak TR. Pictorial key to the adults of hard ticks, family Ixodidae (Ixodida: Ixodoidea), east of the Mississippi River. *J Med Entomol*. 1989;26:435–48. <https://doi.org/10.1093/jmedent/26.5.435>
- Roux V, Raoult D. Phylogenetic analysis of members of the genus *Rickettsia* using the gene encoding the outer-membrane protein rOmpB (*ompB*). *Int J Syst Evol Microbiol*. 2000;50:1449–55. <https://doi.org/10.1099/00207713-50-4-1449>
- Labruna MB, McBride JW, Bouyer DH, Camargo LMA, Camargo EP, Walker DH. Molecular evidence for a spotted fever group *Rickettsia* species in the tick *Amblyomma longirostre* in Brazil. *J Med Entomol*. 2004;41:533–7. <https://doi.org/10.1603/0022-2585-41.3.533>
- Biggs HM, Behravesh CB, Bradley KK, Dahlgren FS, Drexler NA, Dumler JS, et al. Diagnosis and management of tickborne rickettsial diseases: Rocky Mountain Spotted Fever and other spotted fever group rickettsioses, ehrlichioses, and anaplasmosis—United States. *MMWR Recomm Rep*. 2016;65:1–44. <https://doi.org/10.15585/mmwr.rr6502a1>
- Nadolny RM, Wright CL, Sonenshine DE, Hynes WL, Gaff HD. Ticks and spotted fever group rickettsiae of southeastern Virginia. *Ticks Tick Borne Dis*. 2014;5:53–7. <https://doi.org/10.1016/j.ttbdis.2013.09.001>

Address for correspondence: Bruce H. Noden, Oklahoma State University, Entomology and Plant Pathology, 127 Noble Research Center, Stillwater, OK 74078-1010, USA; email: bruce.noden@okstate.edu

Astrovirus in White-Tailed Deer, United States, 2018

Leyi Wang, Huigang Shen, Ying Zheng, Loni Schumacher, Ganwu Li

Author affiliations: University of Illinois, Urbana, Illinois, USA (L. Wang); Iowa State University, Ames, Iowa, USA (H. Shen, Y. Zheng, L. Schumacher, G. Li); Chinese Academy of Agricultural Sciences, Harbin, China (G. Li)

DOI: <https://doi.org/10.3201/eid2602.190878>

We report the identification of astrovirus WI65268 in a white-tailed deer with respiratory disease in the United States in 2018. This virus is a recombinant of Kagoshima1-7 and Kagoshima2-3-2 (both bovine astroviruses from Japan) and was characterized as a potential new genotype. Further surveillance of deer might help identify related isolates.

Astrovirus is a positive-sense, single-stranded RNA virus first identified in feces of children with gastroenteritis in 1975. Since then, astrovirus has been found in a wide variety of mammals and birds (1). The family *Astroviridae* comprises 2 genera, *Mamastrovirus* and *Avastrovirus*, and classification is based on host origin. Astroviruses cause diarrhea and neurologic diseases in mammals and a spectrum of diseases, including diarrhea, hepatitis, and nephritis, in birds (2). Astrovirus is associated with respiratory disease in humans, cattle, and pigs (3–5) and has also been found in fecal samples from roe deer with gastrointestinal illness in Denmark (6). Whether astrovirus circulates in other species of deer remains unclear.

In September 2018, the Veterinary Diagnostic Laboratory at Iowa State University (Ames, Iowa, USA) received 5 sets of tissue samples collected from deer of the same farm for identification of the infectious cause of death of 5 male white-tailed deer 8–14

weeks of age. The pen-raised deer experienced pneumonia and sudden death. Postmortem examinations showed pleural fluid in the lungs, pneumonia, and purple-mottled lungs. Histopathologic observations revealed that 3 deer had necrotizing bronchopneumonia, and 2 had interstitial pneumonia.

Although different combinations of the bacterial pathogens *Bibersteinia trehalosi*, *Tureperella pyogenes*, *Fusobacterium necrophorum*, and *Pasteurella multocida* were found in all cases, an underlying viral cause could not be excluded. Therefore, we used next-generation sequencing, first with pooled lung samples and then with individual lung samples, using Nextera XT DNA Library Preparation Kit with the MiSeq platform and MiSeq Reagent Kit v2 (Illumina, <https://www.illumina.com>). A bioinformatic analysis indicated the presence of an astrovirus along with the bacteria. The complete genome sequence (6,246 nt) of this astrovirus (WI65268; GenBank accession no. MN087316) was found in the pooled lung tissue sample and 1 lung tissue sample, and partial genomes were found in the other 4 lung samples. A complete-genome comparison revealed that BoAstV/JPN/Ishikawa24-6/2013 (bovine isolate from Japan) had the highest identity (60.9%) to WI65268. Further nucleotide sequence analysis revealed that WI65268 had a similar genome organization as other astroviruses (Appendix Figure 1, <https://wwwnc.cdc.gov/EID/article/26/2/19-0878-App1.pdf>).

Sequence comparisons of the amino acid sequences of the 3 open reading frames (ORFs) showed that WI65268 was closely related to 4 bovine astroviruses from Asia: B18 (ORF1a 71.9% sequence identity), Kagoshima1-7 and B76-2 (ORF1b 87.8% sequence identity), and Hokkaido11-55 (ORF2 46.8% sequence identity, distance value 0.479) (Appendix Table). In contrast, WI65268 showed low amino acid sequence identities to US bovine strain BSRI-1 for all 3 ORFs (ORF1a 37.0%, ORF1b 68.3%, ORF2 38.8%) (Appendix Table). The 2 available astrovirus sequences from roe deer (GenBank accession nos. HM447045 and HM447046) from Europe comprised only partial genomic sequences. WI65268 had low identities (34.0% HM447045 and 34.4% HM447046) and pairwise distances (0.787 HM447045 and 0.813 HM447046) to these isolates. On the basis of the International Committee on Taxonomy of Viruses p-distance criteria (new genotypes are assigned at a value of ≥ 0.378) (7), WI65268 represents a novel astrovirus genotype.

Phylogenetic analysis of the complete genome showed that WI65268 is distantly related to other bovine, dromedary, takin, and yak strains (Appendix Figure 2). In phylogenetic analyses of ORF1a and ORF1b protein sequences, WI65268 clustered with

bovine, yak, and takin astrovirus isolates from Asia (Appendix Figure 3). However, in an analysis of ORF2 (capsid) protein, WI65268 clustered with 2 bovine isolates from Japan and was distantly related to the cluster formed by the bovine, yak, and takin isolates from Asia (Figure), strongly indicating that WI65268

is a recombinant. We used Recombination Detection Program 5 (<http://web.cbio.uct.ac.za/~darren/rdp.html>) to confirm that WI65268 was a recombinant and characterize the recombination event (Kagoshima1-7 at 1-5,031 and 5,651-7,967 and Kagoshima2-3-2 at 5,032-5,650; Appendix Figure 4). Reverse transcription

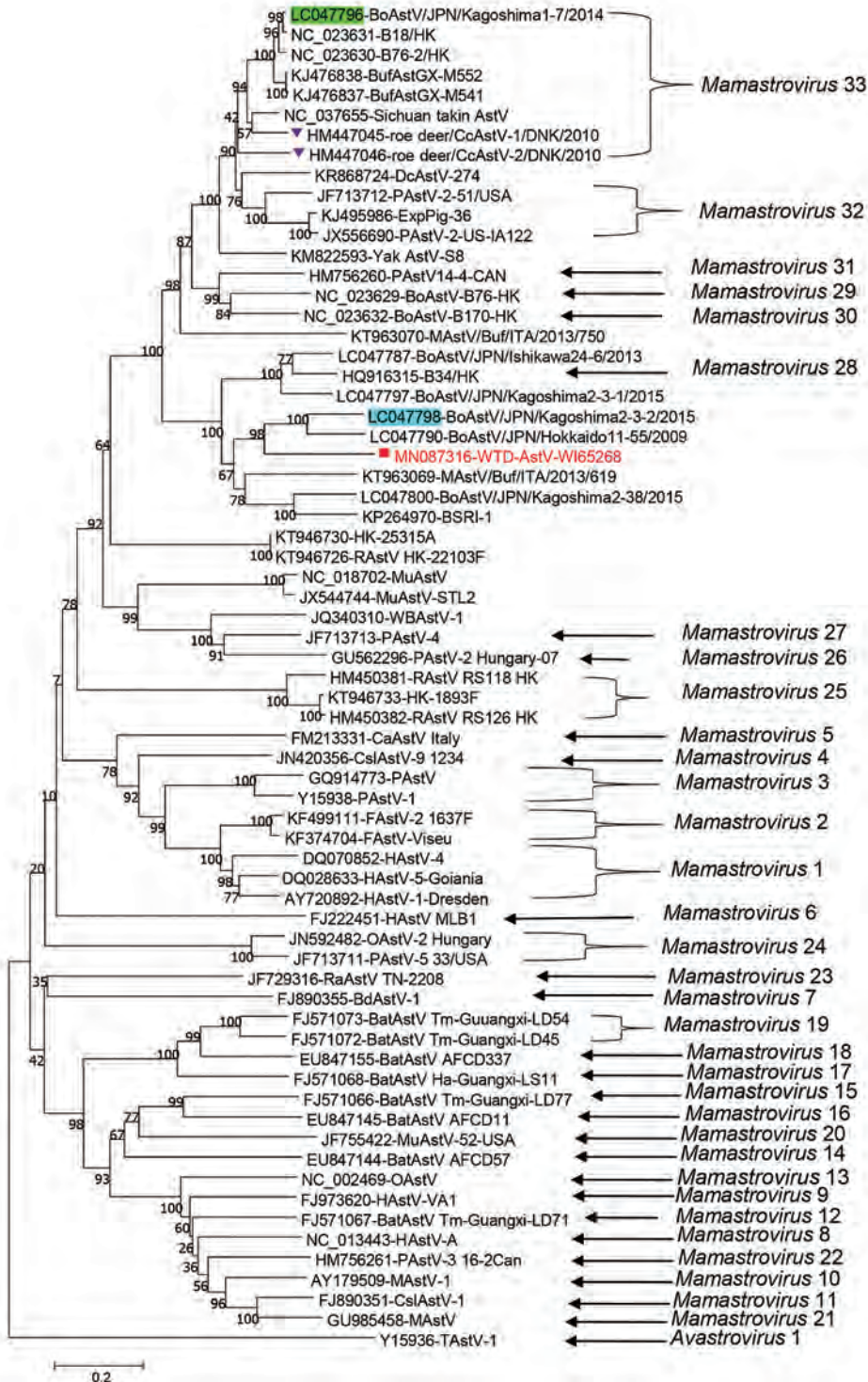


Figure. Phylogenetic analysis of amino acid sequence of open reading frame 2 of WTD-AstV WI65268 from deer in the United States, 2018 (red square), and potential parent viruses, including Kagoshima1-7 (green highlight), Kagoshima2-3-2 (blue highlight), and CcAstVs (purple triangles). Genus type is provided for viruses where that information was known. GenBank accession numbers are indicated, and bootstrap values are provided at nodes. Scale bar indicates amino acid changes per site. AstV, astrovirus; BdAstV, bottlenose dolphin astrovirus; BoAstV, bovine astrovirus; BufAst, water buffalo astrovirus; CaAstV, canine astrovirus; CcAstV, *Capreolus capreolus* astrovirus; CslAstV, California sea lion astrovirus; DcAstV, dromedary camel astrovirus; FAstV, feline astrovirus; HAstV, human astrovirus; MAstV, mink astrovirus; MuAstV, murine astrovirus; OAstV, ovine astrovirus; PAstV, porcine astrovirus; RAstV, rat astrovirus; RaAstV, rabbit astrovirus; TAstV, turkey astrovirus; WBAstV, wild boar astrovirus; WTD, white-tailed deer.

PCR and sequencing results confirmed that sequences at the 2 junctional sites were the same as those found by next-generation sequencing.

Pathogens causing respiratory disease in domesticated animals, such as cattle and pigs, are relatively well studied. However, pathogens causing these diseases in wildlife animals, such as deer, are not well characterized. In this study, the new astrovirus we found or the bacterial pathogens could have contributed to the respiratory disease observed. Whether astrovirus plays a major or just synergistic role in respiratory disease in deer should be explored further.

Astrovirus was previously identified in roe deer with gastrointestinal illness in Europe and found to be closely related to bovine astrovirus isolates from Hong Kong, China, of the same genus (*Mamastrovirus* 33) (7,8). WI65268 was also closely related to bovine isolates from Japan but distantly related to roe deer and Hong Kong bovine astrovirus isolates. An additional analysis of genetic distances of related isolates on the basis of ORF2 tentatively classified WI65268 as a novel species (Appendix Table).

Determining the evolution of WI65268 any further is difficult without further epidemiologic data. Bovine or bovid astroviruses might be able to cross species barriers and replicate in deer, as suggested in a previous study (9), in which a bovine astrovirus isolate clustered with a porcine astrovirus type 5 instead of other bovine astroviruses. Further surveillance of white-tailed deer for astrovirus is needed for field monitoring.

About the Author

Dr. Wang is a clinical assistant professor in the College of Veterinary Medicine at the University of Illinois, Urbana, Illinois, USA. His research interests focus on diagnosis of viral infectious diseases and novel pathogen discovery.

References

1. Bosch A, Pintó RM, Guix S. Human astroviruses. *Clin Microbiol Rev.* 2014;27:1048-74. <https://doi.org/10.1128/CMR.00013-14>
2. Donato C, Vijaykrishna D. The broad host range and genetic diversity of mammalian and avian astroviruses. *Viruses.* 2017;9:102. <https://doi.org/10.3390/v9050102>
3. Ng TF, Kondov NO, Deng X, Van Eenennaam A, Neiberghs HL, Delwart E. A metagenomics and case-control study to identify viruses associated with bovine respiratory disease. *J Virol.* 2015;89:5340-9. <https://doi.org/10.1128/JVI.00064-15>
4. Padmanabhan A, Hause BM. Detection and characterization of a novel genotype of porcine astrovirus 4 from nasal swabs from pigs with acute respiratory disease. *Arch Virol.* 2016;161:2575-9. <https://doi.org/10.1007/s00705-016-2937-1>
5. Cordey S, Brito F, Vu DL, Turin L, Kilowoko M, Kyungu E, et al. Astrovirus VA1 identified by next-generation sequencing in a nasopharyngeal specimen of a febrile Tanzanian child with acute respiratory disease of unknown etiology. *Emerg Microbes Infect.* 2016;5:e99. <https://doi.org/10.1038/emi.2016.98>
6. Smits SL, van Leeuwen M, Kuiken T, Hammer AS, Simon JH, Osterhaus AD. Identification and characterization of deer astroviruses. *J Gen Virol.* 2010;91:2719-22. <https://doi.org/10.1099/vir.0.024067-0>
7. To KKW, Chan WM, Li KSM, Lam CSF, Chen Z, Tse H, et al. High prevalence of four novel astrovirus genotype species identified from rodents in China. *J Gen Virol.* 2017;98:1004-15. <https://doi.org/10.1099/jgv.0.000766>
8. Tse H, Chan WM, Tsoi HW, Fan RY, Lau CC, Lau SK, et al. Rediscovery and genomic characterization of bovine astroviruses. *J Gen Virol.* 2011;92:1888-98. <https://doi.org/10.1099/vir.0.030817-0>
9. Nagai M, Omatsu T, Aoki H, Otomaru K, Uto T, Koizumi M, et al. Full genome analysis of bovine astrovirus from fecal samples of cattle in Japan: identification of possible interspecies transmission of bovine astrovirus. *Arch Virol.* 2015;160:2491-501. <https://doi.org/10.1007/s00705-015-2543-7>

Address for correspondence: Ganwu Li, Department of Veterinary Diagnostic and Production Animal Medicine, College of Veterinary Medicine, Iowa State University, Ames, IA 50011, USA; email: liganwu@iastate.edu

Actinomycetoma Caused by *Actinomadura mexicana*, a Neglected Entity in the Caribbean

Simon Bessis, Latifa Noussair, Veronica Rodriguez-Nava, Camille Jousset, Clara Duran, Alina Beresteanu, Morgan Matt, Benjamin Davido, Robert Carlier, Emmanuelle Bergeron, Pierre-Edouard Fournier, Jean Louis Herrmann, Aurélien Dinh

Author affiliations: Hôpital Universitaire Raymond-Poincaré, Assistance Publique-Hôpitaux de Paris, Garches, France (S. Bessis, L. Noussair, C. Jousset, C. Duran, A. Beresteanu, M. Matt, B. Davido, R. Carlier, J.L. Herrmann, A. Dinh); Claude Bernard University-Lyon I, Lyon, France (V. Rodriguez-Nava, E. Bergeron); Aix-Marseille University, Marseille, France (P.-E. Fournier); Institut Hospitalo-Universitaire Méditerranée Infection, Marseille (P.-E. Fournier); Paris-Saclay University, Versailles, France (J.L. Herrmann)

DOI: <https://doi.org/10.3201/eid2602.191005>

Mycetoma is a chronic infection that is slow to develop and heal. It can be caused by fungi (eumycetoma) or bacteria (actinomycetoma). We describe a case of actinomycetoma caused by *Actinomadura mexicana* in the Caribbean region.

Mycetoma is a neglected tropical disease that poses a major public health problem (1). It is endemic in arid or semiarid regions, such as part of the Indian subcontinent, East and West Africa, and Central and South America (2). Mycetoma when caused by bacteria is called actinomycetoma; when caused by fungi, eumycetoma. The pathogens are found in the environment, often in soil, and usually infect people through minor or undetected trauma, thorn pricks being the most common (3). Bacteria of the *Actinomadura* genus can cause actinomycetoma; the most frequently clinically isolated species are *A. madurae* and *A. pelletieri* (1). We report infection with *A. mexicana* that was acquired in the Caribbean.

A 38-year-old woman from Haiti who had arrived in France with no apparent medical problems was hospitalized a month after her arrival for treatment of multinodular lesions of the left foot and the distal part of the left leg (Figure 1, panel A). She was afebrile but had multiple bulbous nodules of the foot associated with a nodular lesion. The nodules had central pinpoint ulcerations with granular discharge. The woman was experiencing pain and a complete loss of function of her left foot, symptoms that had been evolving for ≈6 months.

Standard radiographs, a computed tomography scan, and magnetic resonance imaging of the affected foot showed symmetrical para-articular marginal erosion in the third and fourth metatarsophalangeal joints, with local inflammation and multiple subcutaneous nodular lesions containing small low-signal foci. A negative result from an HIV serology test and the absence of lymphopenia (2.19 g/L) and

hypogammaglobulinemia indicated that there was no immunosuppression. An inflammatory syndrome, with a C-reactive protein level of 53.93 mg/L and a total leukocyte count of 4.5 g/L (neutrophils 1.7 g/L), was identified.

A sample of the nodules, taken from a punch biopsy, revealed a liquid serum containing white-yellow grains (Figure 1, panel B). Direct examination showed numerous branching gram-positive bacilli, characteristic of actinomycetal bacteria (Figure 1, panel C). Histologic analysis revealed abundant filamentous structures consistent with aerobic actinomycetes. Results from Grocott's methenamine silver staining and Zhiel-Neelssen staining tests were negative at direct examination for mycobacteria and fungus.

We cultured biopsy specimens on Columbia blood agar in an aerobic atmosphere using chocolate Polyvitex agar under 5% CO₂ and Sabouraud and Lowenstein media. After an 8-day incubation, the cultures yielded positive results for bacterial colonies, which were pink to red in color and convex with a wrinkled morphology in shape (Figure 1, panel D). Aerobic and anaerobic blood vials remained negative. A surgical bone biopsy was also performed, and direct examination showed gram-positive branching filaments. Final identification was confirmed by 16S rRNA gene sequencing, as described by Rodriguez-Nava et al. (4), using BLAST (<https://blast.ncbi.nlm.nih.gov/Blast.cgi>) to compare the identified sequence with existing sequences in the GenBank database. The sequence matched ≥95% with *A. mexicana* (GenBank accession no. MN684846).

Antimicrobial susceptibility testing, performed using the agar disk diffusion method (Bio-Rad, <https://www.bio-rad.com>) according to French Microbiology Society guidelines (5), showed susceptibility to amoxicillin, amoxicillin/clavulanate, carbapenems, third-generation cephalosporins, aminosides,

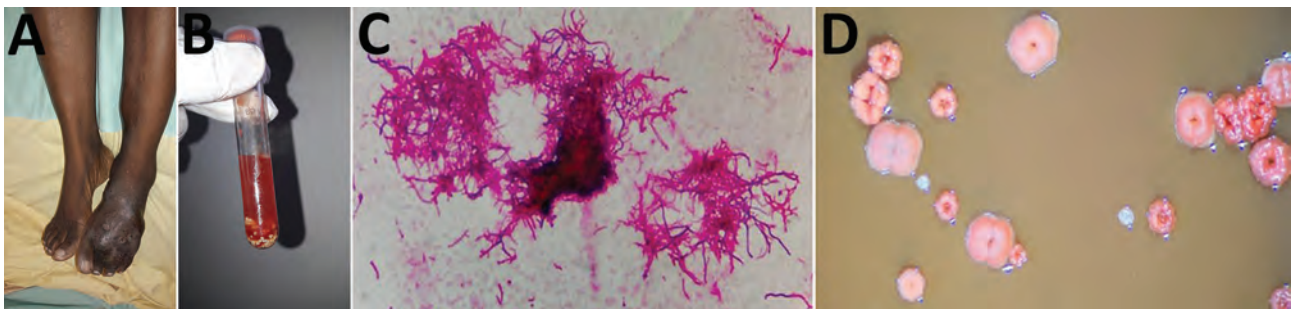


Figure. Actinomycetoma caused by *Actinomadura mexicana* infection in a 38-year-old woman from Haiti, France. A) Multinodular lesions on the dorsal surface of the left foot. B) Liquid from puncture of the nodules, showing white-yellow grains. C) Gram-positive bacilli branching out, characteristic of actinomycetal bacteria (original magnification ×1,000). D) Colonies after an 8-day incubation, showing warty ornamentation, pink to pallid red, convex, with a wrinkled morphology (observed through binocular magnifying glass).

cyclines, erythromycin, linezolid, vancomycin, sulfamethoxazole/trimethoprim, fluoroquinolones, and rifampin. The patient was given amoxicillin/clavulanate (2 g 3×/d) and sulfamethoxazole/trimethoprim (1,600 mg/280 mg 3×/d) for a minimum of 6 months. At her 3-month follow-up, the woman reported reduced pain and doctors found a decrease in the size of the subcutaneous nodules; magnetic resonance imaging confirmed decreased nodule size and indicated no extension of bone damage. No debridement surgery was performed.

The patient used to live in a rural village near the town of Gonaïves in the Artibonite district of Haiti, a semiarid and hot region compatible with actinomycetoma (6), and she mainly walked barefoot or with open shoes, which may explain her exposure to the bacteria. However, no previous case of actinomycetoma caused by *A. mexicana* had been reported in that area. *A. mexicana* was described by Quintana et al. (7) and was isolated with *A. meyerii* from garden soil samples in Mexico in 2003, but a study by Bonifaz et al. published in 2014 found that this species was not identified as a cause of any of the 482 cases of mycetoma recorded in the country during 1980–2013 (8). *A. mexicana* was also not identified as the cause of any mycetoma cases reported during 1991–2014 in Brazil (9). We could find no accounts in the literature of actinomycetoma in the Caribbean region. The only clinical case of mycetoma found, described by Gugnani and Denning in 2016 (10), involved eumycetoma, with etiologic agents such as chromoblastomycoses and *Microsporium canis*. In that article, 2 infections were identified as mycetomas based on case reports in which no laboratory-confirmed microbiological identifications were reported. However, the absence of previous identification might be explained, in part, by lack of access to current molecular biology resources (e.g., matrix-assisted laser desorption/ionization time-of-flight mass spectrometry or PCR).

This case highlights that actinomycetoma may be present but underrecognized in the Caribbean. Because of the severity of mycetoma and the potential for major socioeconomic effects, healthcare providers in this region should remain informed about the potential risk for these infections.

Acknowledgments

We thank the team of the CNR des actinomycétales de Lyon for their help in identifying the strain.

The patient has given free and informed consent for the publication of her data.

About the Author

Dr. Bessis is an assistant clinical fellow, a specialist in infectious and tropical diseases, working in the Infectious Diseases Department of Raymond-Poincaré Hospital, APHP, in Paris.

References

- Zijlstra EE, van de Sande WWJ, Welsh O, Mahgoub ES, Goodfellow M, Fahal AH. Mycetoma: a unique neglected tropical disease. *Lancet Infect Dis*. 2016;16:100–12. [https://doi.org/10.1016/S1473-3099\(15\)00359-X](https://doi.org/10.1016/S1473-3099(15)00359-X)
- van de Sande WWJ. Global burden of human mycetoma: a systematic review and meta-analysis. *PLoS Negl Trop Dis*. 2013;7:e2550. <https://doi.org/10.1371/journal.pntd.0002550>
- Fahal AH, Suliman SH, Hay R. Mycetoma: the spectrum of clinical presentation. *Trop Med Infect Dis*. 2018;3:97–107. <https://doi.org/10.3390/tropicalmed3030097>
- Rodríguez-Nava V, Couble A, Devulder G, Flandrois J-P, Boiron P, Laurent F. Use of PCR-restriction enzyme pattern analysis and sequencing database for hsp65 gene-based identification of *Nocardia* species. *J Clin Microbiol*. 2006;44:536–46. <https://doi.org/10.1128/JCM.44.2.536-546.2006>
- Société Française de Microbiologie (SFM), The European Committee on Antimicrobial Susceptibility Testing (EUCAST). Comité de l'antibiogramme de la Société Française de Microbiologie. Recommendations 2019 v2.0 Mai [in French]. 2019 [cited 2019 May 9]. https://www.sfm-microbiologie.org/wp-content/uploads/2019/05/CASFM2019_V2.0_MAI.pdf
- Mohammadipanah F, Wink J. Actinobacteria from arid and desert habitats: diversity and biological activity. *Front Microbiol*. 2016;6:1541. <https://doi.org/10.3389/fmicb.2015.01541>
- Quintana ET, Trujillo ME, Goodfellow M. *Actinomadura mexicana* sp. nov. and *Actinomadura meyerii* sp. nov., two novel soil sporoactinomycetes. *Syst Appl Microbiol*. 2003;26:511–7. <https://doi.org/10.1078/072320203770865800>
- Bonifaz A, Tirado-Sánchez A, Calderón L, Saúl A, Araiza J, Hernández M, et al. Mycetoma: experience of 482 cases in a single center in Mexico. Reynolds T, editor. *PLoS Negl Trop Dis*. 2014;8:e3102.
- Sampaio FMS, Wanke B, Freitas DFS, Coelho JMCO, Galhardo MCG, Lyra MR, et al. Review of 21 cases of mycetoma from 1991 to 2014 in Rio de Janeiro, Brazil. Vinetz JM, editor. *PLoS Negl Trop Dis*. 2017;11:e0005301.
- Gugnani HC, Denning DW. Burden of serious fungal infections in the Dominican Republic. *J Infect Public Health*. 2016;9:7–12. <https://doi.org/10.1016/j.jiph.2015.04.026>

Address for correspondence: Simon Bessis or Aurélien Dinh, Hôpital Raymond-Poincaré, Service de maladies infectieuses et tropicales, Assistance Publique-Hôpitaux de Paris (AP-HP), 104 Boulevard Raymond Poincaré, Garches 92380, France; email: simon.bessis@aphp.fr or aurelien.dinh@aphp.fr

Antigenic Variant of Highly Pathogenic Avian Influenza A(H7N9) Virus, China, 2019

Wenming Jiang, Guangyu Hou, Jinping Li, Cheng Peng, Suchun Wang, Shuo Liu, Qingye Zhuang, Liping Yuan, Xiaohui Yu, Yang Li, Jingjing Wang, Hualei Liu

Author affiliation: China Animal Health and Epidemiology Center, Qingdao, China

DOI: <https://doi.org/10.3201/eid2602.191105>

In China, influenza A(H7N9) virus appeared in 2013, then mutated into a highly pathogenic virus, causing outbreaks among poultry and cases in humans. Since September 2017, extensive use of the corresponding vaccine, H7-Re1, successfully reduced virus prevalence. However, in 2019, a novel antigenic variant emerged, posing considerable economic and public health threats.

Since mid-2016, influenza A(H7N9), a highly pathogenic avian influenza (HPAI) virus, has led to ≈ 17 outbreaks in poultry in China (1–3). Extensive use of the corresponding vaccine, H7-Re1, substantially reduced the prevalence of H7N9 viruses (4,5). However, in early 2019, active surveillance detected the unprecedented and rapid emergence of a novel HPAI H7N9 virus antigenic variant in several regions of China.

Since 2013, a total of 1,567 cases of human infection with novel H7N9 viruses, associated with a high mortality rate, have been reported in China (6). Studies on circulating H7N9 viruses have suggested that they originated from poultry (7). However, strains isolated from birds at live bird markets displayed low pathogenicity in poultry (8). In early 2017, several outbreaks caused by HPAI H7N9 viruses in poultry were reported. To control infection of poultry and reduce the risk for human exposure to H7N9 virus, development and national use of an inactivated vaccine, H7-Re1, with hemagglutinin (HA) and neuraminidase

(NA) genes derived from A/pigeon/Shanghai/S1069/2013 (H7N9), has since September 2017 substantially decreased prevalence of H7N9 viruses among poultry and humans (5). In December 2018, on the basis of surveillance findings, the original vaccine was replaced with the H7-Re2 vaccine, with HA and NA genes derived from A/chicken/Guangdong/SD098/2017(H7N9).

In 2019, during active surveillance for avian influenza infection in China, we identified 7 strains of H7N9 viruses from 4,226 chicken swab samples. We isolated the strains by inoculating them into 10-day-old specific-pathogen-free chicken embryos and confirmed their identification via reverse-transcription PCR and sequencing. Viruses were from Hebei and Liaoning Provinces and designated A/chicken/China/FQ2/2019(H7N9) (FQ2), A/chicken/China/QHD1/2019(H7N9) (QHD1), A/chicken/China/DL614/2019(H7N9) (DL614), A/chicken/China/AS1/2019(H7N9) (AS1), A/chicken/China/WYG1/2019(H7N9) (WYG1), A/chicken/China/HD1/2019(H7N9) (HD1), and A/chicken/China/DL1/2019(H7N9) (DL1). After determining the HA and NA sequences of the viruses, we deposited the data in GenBank (accession nos. MN700030–43).

According to the deduced amino acid sequence of HA, all strains contained multiple basic amino acids (PKRKRTAR/GLF) at the cleavage site, suggestive of high pathogenicity. This theory was further confirmed by analysis of the intravenous pathogenicity index. In chickens, pathogenicity of the strains was high (index values 2.18, 2.32, 2.28, 2.18, 2.26, 2.30, and 2.36), but in ducks, pathogenicity was low. Although the viruses had replicated in the internal organs (brain, lungs, spleen, liver, intestine, and kidneys) of inoculated ducks on postinoculation days 3 and 5, no deaths or signs of infection were observed within 14 days after inoculation (Appendix Table, <https://wwwnc.cdc.gov/EID/article/26/2/19-1105-App1.pdf>).

We determined that the amino acid residues at the receptor-binding site of HA proteins are A138, V186, P221, and Q226 (H3 numbering), which suggests that these viruses could bind receptors in birds

Table. Efficacy of H7-Re2 vaccine against highly pathogenic avian influenza A(H7N9) viruses in chickens, China, 2019*

Vaccine	Challenge virus	Mean HI titer 21 d after vaccination (\log_2)		Virus shedding				Survival rate
		Challenge virus	H7-Re2	Postchallenge day 3		Postchallenge day 5		
				Trachea	Cloaca	Trachea	Cloaca	
H7-Re2	FQ2	3.2 \pm 0.6	7.7 \pm 0.5	8/8 (2.6 \pm 0.4)	8/8 (2.4 \pm 0.3)	4/4 (2.3 \pm 0.3)	4/4 (2.5 \pm 0.4)	4/10
	DL1	3.3 \pm 0.5	7.9 \pm 0.4	8/8 (2.8 \pm 0.3)	8/8 (2.5 \pm 0.3)	4/4 (2.2 \pm 0.4)	4/4 (2.3 \pm 0.3)	4/10
rFQ2	FQ2	7.6 \pm 0.6	7.0 \pm 0.5	0/10	0/10	0/10	0/10	10/10
	DL1	7.3 \pm 0.5	6.8 \pm 0.4	0/10	0/10	0/10	0/10	10/10
Control	FQ2	<1	<1	4/4 (4.8 \pm 0.5)	4/4 (4.5 \pm 0.4)	NA	NA	0/10
	DL1	<1	<1	4/4 (4.7 \pm 0.4)	4/4 (4.9 \pm 0.5)	NA	NA	0/10

*HI, hemagglutination inhibition; NA, not applicable because of death of chickens.

and humans (9). The phylogenetic tree based on the HA gene showed that all strains belong to the highly pathogenic H7N9 clade but are clearly distinguishable from HPAI H7N9 viruses isolated in 2017 and 2018 (Appendix Figure).

Amino acid identities of the HA gene segments of these strains were 95.8%–96.5% identical to those of H7-Re1 (92.7%–93.7% for HA1) and 97.4%–98.0% identical to those of H7-Re2 (96.2%–97.2% for HA1). To evaluate the antigenicity and protective efficacy of the H7-Re2 vaccine, we vaccinated specific-pathogen-free chickens with H7-Re2 and rFQ2 (a reverse genetic recombinant carrying HA and NA of FQ2 with internal gene segments of PR8). FQ2 and DL1 viruses were selected for subsequent experiments. Cross-reactive hemagglutination inhibition titers of H7-Re2 antiserum against FQ2 and DL1 viruses were 4.5–4.6 log₂ lower than those against the homologous H7-Re2 antigen. In contrast, cross-reactive HI titers of antiserum against H7-Re2 antigens from rFQ2 virus did not differ markedly from those against the 2 homologous H7N9 viruses. These results indicate that the FQ2 and DL1 viruses exhibited rapid antigenic drift and distinct antigenicity relative to the H7-Re2 vaccine strain.

During the 10-day observation period after challenge, H7-Re2-vaccinated birds displayed clinical signs of infection, such as depression, huddling, and decreased consumption of feed and water. Moreover, shed virus was detected in tracheal and cloacal swab samples from all experimentally inoculated chickens on postchallenge days 3 and 5. Only 40.0% of the challenged chickens survived, indicating that the H7-Re2 vaccine had a poor protective effect against FQ2 and DL1.

All rFQ2-vaccinated birds survived with no clinical signs of infection. In addition, no virus shedding was detected in tracheal or cloacal swab samples from any rFQ2-vaccinated chickens on postchallenge days 3 and 5 (Table). Of note, antiserum against the rFQ2 virus showed a broader spectrum of reactivity to other viruses, including H7-Re2, indicating that recombinant rFQ2 offers a better alternative for vaccine development.

In China, vaccination plays a decisive role in the prevention and control of H7N9 virus-mediated infection. Earlier mass vaccination of poultry with H7-Re1 successfully induced a sharp decline in H7N9 infection prevalence among poultry and humans.

However, as of 2019, H7N9 variants have surfaced, posing a considerable economic and public health threat and highlighting the urgent need for new antigen-matched vaccines and more productive measures to eliminate highly pathogenic H7N9 viruses.

About the Author

Dr. Jiang is a veterinary researcher at the China Animal Health and Epidemiology Center. His research interests are epidemiology and control of infectious diseases in animals.

References

1. Wang N, Sun M, Wang W, Ouyang G, Chen Z, Zhang Y, et al. Avian influenza (H7N9) viruses co-circulating among chickens, southern China. *Emerg Infect Dis*. 2017;23:2100–2. <https://doi.org/10.3201/eid2312.170782>
2. Yang L, Zhu W, Li X, Chen M, Wu J, Yu P, et al. Genesis and spread of newly emerged highly pathogenic H7N9 avian viruses in mainland China. *J Virol*. 2017;91:e01277–17. <https://doi.org/10.1128/JVI.01277-17>
3. Shi J, Deng G, Kong H, Gu C, Ma S, Yin X, et al. H7N9 virulent mutants detected in chickens in China pose an increased threat to humans. *Cell Res*. 2017;27:1409–21. <https://doi.org/10.1038/cr.2017.129>
4. Jiang W, Hou G, Li J, Peng C, Wang S, Liu S, et al. Prevalence of H7N9 subtype avian influenza viruses in poultry in China, 2013–2018. *Transbound Emerg Dis*. 2019;66:1758–61. <https://doi.org/10.1111/tbed.13183>
5. Shi J, Deng G, Ma S, Zeng X, Yin X, Li M, et al. Rapid evolution of H7N9 highly pathogenic viruses that emerged in China in 2017. *Cell Host Microbe*. 2018; 24:558–68.
6. Yu D, Xiang G, Zhu W, Lei X, Li B, Meng Y, et al. The re-emergence of highly pathogenic avian influenza H7N9 viruses in humans in mainland China, 2019. *Euro Surveill*. 2019;24.
7. Gao R, Cao B, Hu Y, Feng Z, Wang D, Hu W, et al. Human infection with a novel avian-origin influenza A (H7N9) virus. *N Engl J Med*. 2013;368:1888–97. <https://doi.org/10.1056/NEJMoa1304459>
8. Chen Y, Liang W, Yang S, Wu N, Gao H, Sheng J, et al. Human infections with the emerging avian influenza A H7N9 virus from wet market poultry: clinical analysis and characterisation of viral genome. *Lancet*. 2013;381:1916–25. [https://doi.org/10.1016/S0140-6736\(13\)60903-4](https://doi.org/10.1016/S0140-6736(13)60903-4)
9. Shi Y, Zhang W, Wang F, Qi J, Wu Y, Song H, et al. Structures and receptor binding of hemagglutinins from human-infecting H7N9 influenza viruses. *Science*. 2013;342:243–7. <https://doi.org/10.1126/science.1242917>

Address for correspondence: Hualei Liu, China Animal Health and Epidemiology Center, Laboratory of Surveillance for Avian Diseases, No. 369 Nanjing Rd, Qingdao 266032, China, email: liuhualei@cahec.cn

New Delhi Metallo- β -Lactamase-5–Producing *Escherichia coli* in Companion Animals, United States

Stephen D. Cole, Laura Peak, Gregory H. Tyson, Renate Reimschuessel, Olgica Ceric, Shelley C. Rankin

Author affiliations: University of Pennsylvania School of Veterinary Medicine, Philadelphia, Pennsylvania, USA (S.D. Cole, S.C. Rankin); Louisiana State University, Baton Rouge, Louisiana, USA (L. Peak); US Food and Drug Administration, Silver Spring, Maryland, USA (G.H. Tyson, R. Reimschuessel, O. Ceric)

DOI: <https://doi.org/10.3201/eid2602.191221>

We report isolation of a New Delhi metallo- β -lactamase-5–producing carbapenem-resistant *Escherichia coli* sequence type 167 from companion animals in the United States. Reports of carbapenem-resistant *Enterobacteriaceae* in companion animals are rare. We describe a unique cluster of *bla*_{NDM-5}–producing *E. coli* in a veterinary hospital.

Carbapenems are critically useful antimicrobial drugs that are reserved for treatment of infections caused by multidrug-resistant, gram-negative bacteria (1). Carbapenem-resistant *Enterobacteriaceae* (CRE) have emerged as a major cause of human healthcare-associated infections and are a major clinical and public health problem (1). The most common mechanism of resistance is production of carbapenemases, which hydrolyze carbapenems and many other β -lactams. The genes that encode carbapenemases are found on conjugative plasmids and commonly fall in the following classes: KPC (*Klebsiella pneumoniae* carbapenemase), NDM (New Delhi metallo- β -lactamase), IMP (imipenemase), and VIM (Verona integron-encoded metallo- β -lactamase) (1). Control of these infections in human healthcare settings is a challenge because the organisms colonize the gastrointestinal tract and can go undetected (1). Reports of CRE in animals and animal settings are rare but have been documented in livestock, wildlife, and companion animals (2).

In April 2019, passive surveillance by the Veterinary Laboratory Information and Response Network of the US Food and Drug Administration identified the *bla*_{NDM-5} gene in a carbapenem-resistant *Escherichia coli* isolated from a dog in July 2018. This isolate belonged to sequence type 167 (ST167).

A retrospective review of hospital records showed that, during July 11–August 3, 2018, seven carbapenem-resistant *E. coli* isolates were isolated from 6 animals (Table). Isolates were obtained from 5 dogs and 1 cat; all were from respiratory tract specimens, except for 2 isolates from the urine of 1 dog. All animals were housed in the intensive care unit for ≥ 24 hours (Appendix Figure, <https://wwwnc.cdc.gov/EID/article/26/2/19-1221-App1.pdf>). All animals overlapped with ≥ 1 other affected animal.

We evaluated antimicrobial use; 5/6 animals received ≥ 4 antimicrobial drugs before specimen submission. No animals received a carbapenem drug in the 30-day period before sample submission. A β -lactam was given to 5/6 animals, azithromycin to 5/6 animals, metronidazole to 4/6 animals, and enrofloxacin to 4/6 animals (Table).

The first isolate, *E. coli* 24213-18, was sequenced by using a Pacific Biosciences Sequel Sequencer (<https://www.pacb.com>) and uploaded to GenBank (BioSample SAMN11230749). This testing confirmed *E. coli* ST167 and identified a circular IncFII plasmid of 139,547 bp, which contained the *bla*_{NDM-5} gene and additional resistance genes: *tet(A)*, *aac(6')-Ib-cr*, *aadA5*, *aadA2*, *bla*_{OXA-1'}, *bla*_{CTX-M-15'}, *catB3*, *dfrA17*, *dfrA12*, *sul1* (2 copies), and *mph(A)* (3).

Whole-genome sequencing was performed on all 7 isolates (24213-18, 24920-18, 27025-1-18, 27025-2-18, 27241-18, 27609-18, and 27614-18) by using the Illumina MiSeq platform (<https://www.illumina.com>). We identified antimicrobial resistance genes by using the National Center for Biotechnology Information Pathogen Detection Isolates Browser, which uses AMRFinder (<https://www.ncbi.nlm.nih.gov/pathogens/antimicrobial-resistance/AMRFinder>). The following genes were found in all 7 isolates: *aac 3-IId*, *aac(6')-Ib-cr5*, *aadA2*, *aadA22*, *aadA5*, *bla*_{CTX-M-15'}, *bla*_{NDM-5'}, *bla*_{OXA-1'}, *bla*_{TEM-1}, *ble*, *catB3*, *dfrA12*, *dfrA17*, *mph(A)*, *qacEdelta1*, *sul1*, and *tet(A)*. The *floR* gene was detected in all isolates except 27025-1-18. PlasmidFinder (<https://cge.cbs.dtu.dk/services/PlasmidFinder>) analysis confirmed the presence of an IncFII plasmid in all isolates.

NDM-5–producing *E. coli* have been reported in dogs from Finland, South Korea, and Algeria (3–5). The isolates from Finland were also ST167; the isolates from South Korea and Algeria were obtained from canine feces and identified as ST410 and ST1284. ST1284 is a double-locus variant of ST167, which suggests possible distant relatedness of these isolates; ST410 does not share any multilocus sequence type alleles with ST167 (5). In 2011, the NDM-5 carbapenemase was

Table. Clinical characteristics of New Delhi metallo- β -lactamase-5–producing *Escherichia coli* isolates from 6 companion animals, United States, 2018*

Isolate ID	BioSample accession no.	Source	Species	Breed	Age, y/sex	Concurrent diagnosis	Antimicrobial drugs in the past 30 days	Outcome
24213-18	SAMN11230749	Endotracheal wash	Canine	Great Dane	11/F	Megaesophagus; aspiration pneumonia	AMP, CLI, CAZ, ENR, MTZ	Discharged
24920-18	SAMN12190106	Lung tissue	Canine	Rottweiler	8/M	Pheochromocytoma; aspiration pneumonia	AMP, AZM, ENR, MTZ	Discharged
27025-18-1, 27025-18-2	SAMN12189820, SAMN12190134	Urine (cystocentesis)	Canine	Mixed breed	13/F	Atrioventricular block; acute kidney injury	AMP, AZM, CFZ, ENR, MTZ	Discharged
27241-18	SAMN12190501	Endotracheal wash	Canine	Beagle	5/M	Septic peritonitis after foreign body removal; protein-losing nephropathy; suspected pulmonary thromboembolism	AMP, AZM, FOX, PTZ, MTZ	Euthanized
27609-18	SAMN12190410	Endotracheal wash	Feline	Domestic shorthair	8/F	Asthma	AZM	Discharged
27614-18	SAMN12190436	Endotracheal wash	Canine	Standard poodle	8/F	Laryngeal paralysis; pneumonia	AZM, AMC, ENR	Discharged

*All animals had been spayed or castrated. AMC, amoxicillin/clavulanate; AMP, ampicillin; AZM, azithromycin; CAZ, ceftazidime; CLI, clindamycin; CFZ, cefazolin; ENR, enrofloxacin; FOX, ceftiofur; ID, identification; MTZ, metronidazole; NCBI, National Center for Biotechnology Information; PTZ, piperacillin/tazobactam.

described in an isolate of *E. coli* (ST648) from a human in the United Kingdom who was previously hospitalized in Goa, India (6). In February 2018, three isolates of NDM-5–positive *E. coli* (ST43) were isolated from 2 patients in a skilled nursing facility in New York, New York (7). Spread of NDM-5–positive *E. coli* has occurred globally and included reports of ST167 in persons in Europe and Asia (8,9).

Healthcare-associated spread of this *E. coli* strain in the veterinary intensive care unit emphasizes the need to rapidly identify and characterize carbapenem-resistant isolates from animals. Methods to control the spread of CRE in veterinary medical settings have not yet been studied; these studies are needed to limit the spread of these pathogens in animal populations. Control measures in human healthcare settings include strict hand hygiene, use of personal protective equipment, and environmental decontamination (10). The risk for transmission of CRE from animals to persons is currently poorly understood.

It has been documented that *bla*_{NDM-5} ST167, and carbapenem-resistant *E. coli* strains can infect humans and animals (4). Additional investigations are needed in the context of transmission between humans and animals. Characterization of CRE isolates from animals is needed to build a knowledge base and provide guidance for future studies because CRE will continue to emerge in veterinary medical settings. CRE will be a major challenge across all health fields as these organisms become more prevalent in the community. A One Health approach to antimicrobial resistance surveillance, infection prevention, and

antimicrobial stewardship could limit the spread and potential global dominance of CRE.

This study was supported in part by grant FOA PAR-17-141 and performed in collaboration with the US Food and Drug Administration Veterinary Laboratory Investigation and Response Network (FDA Vet-LIRN) under grant 1 U18 FD006669-01. PacBio sequencing of isolate 24213-18 was supported by the US Food and Drug Administration as part of routine work.

About the Author

Dr. Cole is a veterinary microbiologist and a lecturer at the University of Pennsylvania School of Veterinary Medicine, Philadelphia, PA. His research interests include infectious diseases of dogs and cats and antimicrobial stewardship educational strategies in veterinary medicine.

References

- Gupta N, Limbago BM, Patel JB, Kallen AJ. Carbapenem-resistant *Enterobacteriaceae*: epidemiology and prevention. *Clin Infect Dis*. 2011;53:60–7. <https://doi.org/10.1093/cid/cir202>
- Köck R, Daniels-Haardt I, Becker K, Mellmann A, Friedrich AW, Mevius D, et al. Carbapenem-resistant *Enterobacteriaceae* in wildlife, food-producing, and companion animals: a systematic review. *Clin Microbiol Infect*. 2018;24:1241–50. <https://doi.org/10.1016/j.cmi.2018.04.004>
- Tyson GH, Li C, Ceric O, Reimschuessel R, Cole S, Peak L, et al. Complete genome sequence of a carbapenem-resistant canine *Escherichia coli* isolate with *bla*_{NDM-5} from a dog in the United States. *Microbiol Resour Annot*. 2019;8:e00872–19. <https://doi.org/10.1128/MRA.00872-19>
- Grönthal T, Österblad M, Eklund M, Jalava J, Nykäsenoja S, Pekkanen K, et al. Sharing more than friendship: transmission of NDM-5 ST167 and CTX-M-9 ST69 *Escherichia coli* between dogs and humans in a family, Finland, 2015.

- Euro Surveill. 2018;23. <https://doi.org/10.2807/1560-7917.ES.2018.23.27.1700497>
5. Hong JS, Song W, Park HM, Oh JY, Chae JC, Han JI, et al. First detection of New Delhi metallo- β -lactamase-5-producing *Escherichia coli* from companion animals in Korea. *Microb Drug Resist*. 2019;25:344–9. <https://doi.org/10.1089/mdr.2018.0237>
 6. Yousfi M, Mairi A, Bakour S, Touati A, Hassissen L, Hadjadj L, et al. First report of NDM-5-producing *Escherichia coli* ST1284 isolated from dog in Bejaia, Algeria. *New Microbes New Infect*. 2015;8:17–8. <https://doi.org/10.1016/j.nmni.2015.09.002>
 7. Hornsey M, Phee L, Wareham DW. A novel variant, NDM-5, of the New Delhi metallo- β -lactamase in a multidrug-resistant *Escherichia coli* ST648 isolate recovered from a patient in the United Kingdom. *Antimicrob Agents Chemother*. 2011;55:5952–4. <https://doi.org/10.1128/AAC.05108-11>
 8. Iregui A, Ha K, Meleny K, Landman D, Quale J. Carbapenemases in New York City: the continued decline of KPC, but new emerging threats. *J Antimicrob Chemother*. 2018;73:2997–3000. <https://doi.org/10.1093/jac/dky322>
 9. Giufrè M, Errico G, Accogli M, Monaco M, Villa L, Distasi MA, et al. Emergence of NDM-5-producing *Escherichia coli* sequence type 167 clone in Italy. *Int J Antimicrob Agents*. 2018;52:76–81. <https://doi.org/10.1016/j.ijantimicag.2018.02.020>
 10. Zong Z, Fenn S, Connor C, Feng Y, McNally A. Complete genomic characterization of two *Escherichia coli* lineages responsible for a cluster of carbapenem-resistant infections in a Chinese hospital. *J Antimicrob Chemother*. 2018;73:2340–6. <https://doi.org/10.1093/jac/dky210>

Address for correspondence: Shelley C. Rankin, University of Pennsylvania School of Veterinary Medicine, 3900 Delancey St, Philadelphia, PA 19104, USA; email: srankin@vet.upenn.edu

Hantavirus Infection with Renal Failure and Proteinuria, Colorado, USA, 2019

Swati Chand,¹ Sangharsha Thapa,¹ Shelley Kon, Steven C. Johnson, Eric M. Poeschla, Carlos Franco-Paredes, Alfonso J. Rodríguez-Morales, Salim Mattar, Andrés F. Henao-Martínez

Author affiliations: Kathmandu University School of Medical Sciences, Kathmandu, Nepal (S. Chand, S. Thapa); University of Colorado School of Medicine, Aurora, Colorado, USA (S. Kon, S.C. Johnson, E.M. Poeschla, C. Franco-Paredes,

A.F. Henao-Martínez); Hospital Infantil de México Federico Gómez, Mexico City, Mexico (C. Franco-Paredes); Universidad Tecnológica de Pereira, Pereira, Colombia (A.J. Rodríguez-Morales); Universidad de Córdoba, Montería, Colombia (S. Mattar)

DOI: <https://doi.org/10.3201/eid2602.191349>

In North America, hantaviruses commonly cause hantavirus pulmonary syndrome (HPS). Clinical descriptions of hantavirus-associated renal disease in the Americas are scarce. Herein, we discuss the case of a 61-year-old man whose predominant manifestations were acute kidney injury and proteinuria. Clinical recognition of renal signs in hantavirus infections can reduce risk for death.

In the United States, 20–40 hantavirus cases are reported annually. Human infections result from inhalation of aerosolized secretions of infected rodents. Hantavirus pulmonary syndrome (HPS) is associated with pneumonitis and has a broad clinical spectrum that ranges from mild or no symptoms to fulminant respiratory failure. Hemorrhagic fever with renal syndrome (HFRS) is a characteristic clinical entity that manifests with fever, hypotension, and renal failure (1) and can also manifest as a mild glomerulonephritis and renal insufficiency (2). Eurasian hantaviruses (Hantaan virus, Puumala virus, and Seoul virus [SEOV]) cause HFRS; SEOV has a worldwide distribution (1). However, HPS is the clinical manifestation of most domestically acquired hantavirus infections in the United States.

HFRS in the United States was first reported in 2008 in a 22-year-old man with SEOV infection (2). Investigating a SEOV outbreak in 2017, the Centers for Disease Control and Prevention described 17 human cases in 11 states, including Colorado (3). Of these 17 patients, 9 were asymptomatic, 8 became ill, and 3 were hospitalized and recovered. The index case-patient was an 18-year-old woman with hematuria and mildly elevated creatinine who owned a pet rat (4). Published descriptions of hantavirus infection with renal manifestations in the United States are few, and the clinical characteristics of the renal injury are not often described.

We report a 61-year-old man with predominant renal manifestations of hantavirus who acquired the virus in Colorado, USA, apparently after exposure to aerosolized rodent droppings. He lived on a farm in northeastern Colorado and had cleaned his garage of extensive mouse and rat droppings 2 weeks earlier. He did not wear a mask to clean and did not own pet rats or snakes. He sought care in April 2019 for a 4-day history of fever up to 38.3°C, headache, fatigue, and myalgia. He also reported abdominal pain, anorexia, neck stiffness, and photophobia.

¹These authors contributed equally to this article.

When he arrived he was alert; heart rate was 87 bpm, blood pressure 118/73 mm Hg, respiratory rate 26/min, temperature 37.0°C, and SpO₂ 94%. Physical examination revealed mild abdominal tenderness. Laboratory findings included mild thrombocytopenia ($140 \times 10^9/L$; reference $150\text{--}100 \times 10^9/L$); elevated creatinine (2mg/dL; reference 0.7–1.3 mg/dL); a glomerular filtration rate of 35 mL/min (reference 90–120 mL/min); and increased lactate dehydrogenase (306 units/L, reference 124–271 U/L), fractional excretion of sodium (FeNa) (0.5%), spot albumin-to-creatinine ratio (1,576 mg/G, reference <30 mg/G), and urine protein (100 mg/dL, reference 0–20 mg/dL). A 24-hour total protein excretion was 861 mg/D (reference 0–101 mg/D). Cerebrospinal fluid parameters were within reference values. Chest radiograph showed interstitial prominences and bibasilar patchy opacities (Figure). Renal ultrasound results were normal. Results were negative for blood and cerebrospinal fluid cultures and tests for HIV, hepatitis A/B/C, and lymphocytic choriomeningitis virus. He was admitted for overnight observation; intensive care was not required. Renal function was stable after 24 hours, and he was discharged home without renal replacement or other supportive therapy.

Using a qualitative assay (Quest Diagnostics Infectious Diseases, <http://www.questdiagnostics.com>), we detected IgM and IgG against recombinant hantavirus antigens derived from both Old and New World hantaviruses in patient samples. Testing at the Colorado Public Health Laboratory confirmed Sin Nombre virus (SNV)-specific IgM of 1:6,400 (expected result <1:100). The patient recovered by day 6, with no residual symptoms. Three weeks later, his creatinine was within reference levels (1.07 mg/dL).

This patient's primary manifestations of hantavirus infection were reversible acute kidney injury and proteinuria. Respiratory symptoms were mild; his respiratory rate was slightly elevated, and chest radiograph disclosed interstitial infiltrates suggestive of mild HPS. Clinical HFRS manifestation can range from asymptomatic infection to acute renal failure with proteinuria, hematuria, and oliguria. Severity has been correlated with a specific hantavirus strain (5). Proteinuria is due to hantavirus nephritis, which is transient and usually resolves in 2 weeks (6). When acute interstitial nephritis occurs, it may manifest as acute tubular necrosis with histologic evidence of glomerular and endothelial damage (7).

HFRS caused by Puumala virus (nephropathia epidemica) or SEOV is generally mild and associated with a benign long-term prognosis. Diagnosis is facilitated by a high index of suspicion, a complete history including occupational and travel history, recognition of characteristic clinical symptoms, serologic or PCR testing, and exclusion of other infections. HFRS should be suspected in patients with acute renal failure, fever, hemorrhage, headache, and abdominal, back, or orbital pain; who live in rural areas; or who have possible rodent exposure within the previous 7 weeks. Because hantavirus infection rarely manifests as kidney disease in the United States, clinicians might be less aware of HFRS. At least 1 other SNV case has been reported with renal involvement requiring transient hemodialysis (8). General management is supportive, and most patients recover fully; few develop chronic renal sequelae (9).

Because of serologic cross-reactivity between SNV and SEOV, we lack a final etiology in this case. Our findings are also limited by the absence of viral sequencing and nephritis pathology analysis

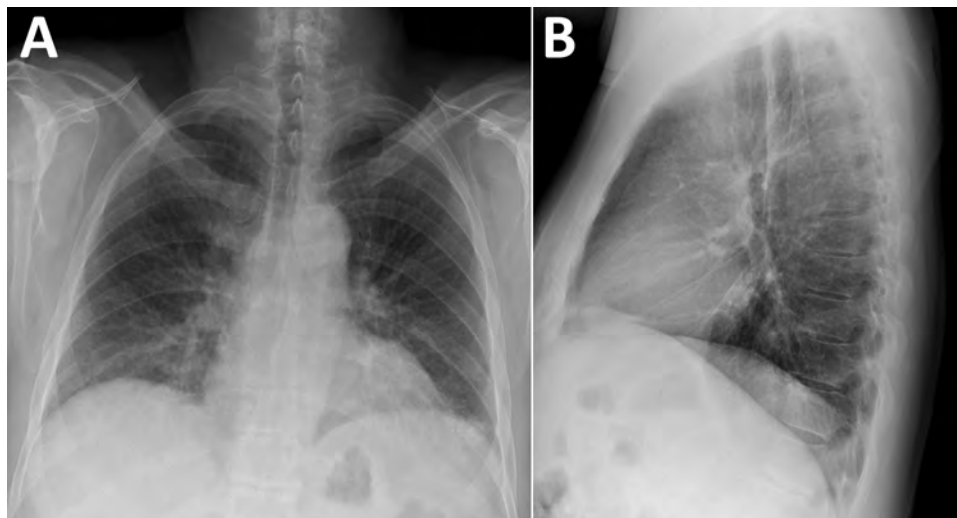


Figure. Chest radiographs displaying bibasilar patchy interstitial opacities in patient with hantavirus pulmonary syndrome, Colorado, USA. A) Posteroanterior view. B) Lateral view.

confirmation. However, our findings indicate that clinical recognition of renal signs and rapid detection of hantavirus infections can reduce risk for serious outcomes.

About the Author

Dr. Chand and Dr. Thapa graduated from Kathmandu University School of Medical Sciences, Kathmandu, Nepal. While completing this work, they are applying to internal medicine residency programs in the United States. Their primary research interests are emerging infectious diseases.

References

1. Avšič-Županc T, Saksida A, Korva M. Hantavirus infections. *Clin Microbiol Infect*. 2019;21S:e6–16. <https://doi.org/10.1111/1469-0691.12291>
2. Woods C, Palekar R, Kim P, Blythe D, de Senarclens O, Feldman K, et al. Domestically acquired Seoul virus causing hemorrhagic fever with renal syndrome—Maryland, 2008. *Clin Infect Dis*. 2009;49:e109–12. <https://doi.org/10.1086/644742>
3. Kerins JL, Koske SE, Kazmierczak J, Austin C, Gowdy K, Dibernardo A, et al.; Seoul Virus Working Group; Canadian Seoul Virus Investigation Group (Federal); Canadian Seoul Virus Investigation Group (Provincial); Contributors. Outbreak of Seoul virus among rats and rat owners—United States and Canada, 2017. *MMWR Morb Mortal Wkly Rep*. 2018;67:131–4. <https://doi.org/10.15585/mmwr.mm6704a5>
4. Fill M-MA, Mullins H, May AS, Henderson H, Brown SM, Chiang C-F, et al. Notes from the field: multiple cases of Seoul virus infection in a household with infected pet rats—Tennessee, December 2016–April 2017. *MMWR Morb Mortal Wkly Rep*. 2017;66:1081–2. <https://doi.org/10.15585/mmwr.mm6640a4>
5. Manigold T, Vial P. Human hantavirus infections: epidemiology, clinical features, pathogenesis and immunology. *Swiss Med Wkly*. 2014;144:w13937. <https://doi.org/10.4414/sm.w.2014.13937>
6. Ferluga D, Vizjak A. Hantavirus nephropathy. *J Am Soc Nephrol*. 2008;19:1653–8. PubMed <https://doi.org/10.1681/ASN.2007091022>
7. Jiang H, Du H, Wang LM, Wang PZ, Bai XF. Hemorrhagic fever with renal syndrome: pathogenesis and clinical picture. *Front Cell Infect Microbiol*. 2016;6:1. <https://doi.org/10.3389/fcimb.2016.00001>
8. Dara SI, Albright RC, Peters SG. Acute Sin Nombre hantavirus infection complicated by renal failure requiring hemodialysis. *Mayo Clin Proc*. 2005;80:703–4. <https://doi.org/10.4065/80.5.703>
9. Krautkrämer E, Zeier M, Plyusnin A. Hantavirus infection: an emerging infectious disease causing acute renal failure. *Kidney Int*. 2013;83:23–7. <https://doi.org/10.1038/ki.2012.360>

Address for correspondence: Andrés F. Henao-Martínez, University of Colorado Denver—Medicine, 12700 E 19th Ave, Mailstop B168, Aurora, CO 80045, USA; email: andres.henaomartinez@cuanschutz.edu

Persistence of Crimean-Congo Hemorrhagic Fever Virus RNA

Leholonolo Mathengtheng,^{1,2} Dominique Goedhals,² Phillip A. Bester, Jacqueline Goedhals, Felicity J. Burt

Author affiliations: National Health Laboratory Service, Bloemfontein, South Africa; University of the Free State, Bloemfontein

DOI: <https://doi.org/10.3201/eid2602.191460>

Crimean-Congo hemorrhagic fever virus (CCHFV) causes severe disease with fatalities. Awareness of potential sources of infection is important to reduce risk to healthcare workers and contacts. We detected CCHFV RNA in formalin-fixed, paraffin-embedded tissues from a spontaneous abortion that were submitted for histology 9 weeks after a suspected CCHFV infection in the mother.

Crimean-Congo hemorrhagic fever virus (CCHFV) has the potential to emerge in areas where competent vectors are present and become a major risk to public health. Because of an absence of registered vaccines or specific antiviral treatment, CCHFV is included as one of the diseases prioritized by the World Health Organization for research and development in public health emergency contexts. Nosocomial infections are one of its transmission routes; thus, awareness of possible sources of infection is important for reducing risk to healthcare workers and other contacts of infected persons.

We detected a case of CCHFV infection in South Africa during a retrospective study, conducted in 2014, of serum samples from patients with suspected tickbite fever and no diagnosis. We retrospectively screened 196 serum samples that were collected during 2008–2011 from acutely ill patients in Free State Province and submitted to the routine serology laboratory of the Department of Medical Microbiology, National Health Laboratory Service (Bloemfontein, South Africa) with suspected rickettsial infection. The University of the Free State Health Science Ethics Committee provided ethics approval to screen residual diagnostic samples (ethics approval no. ETOVS 118/06).

For this screening, RNA was extracted from human serum samples using the QIAamp Viral RNA Mini Kit (QIAGEN, <https://www.qiagen.com>), according to the manufacturer's instructions. We used RNA as template in a nested reverse transcription PCR (RT-PCR) with CCHFV primers designated F2,

¹Deceased.

²These authors contributed equally to this article.

R3 and F3, R2 (1,2). The primers target a 536-bp region (F2, R3) and a 260-bp region (F3, R2) of the small segment using a nested format.

CCHFV RNA was amplified from 1 of the 196 samples. Determination of partial nucleotide sequence of the 260-bp amplicon confirmed that CCHFV RNA

was amplified with 100% nt homology to previously identified South Africa strains (Figure). Because the screening was performed retrospectively on residual samples, no clinical details were available; however, a heat-inactivated aliquot of the serum had a CCHFV IgM titer of 1:40 and IgG titer of 1:10 by immunofluo-

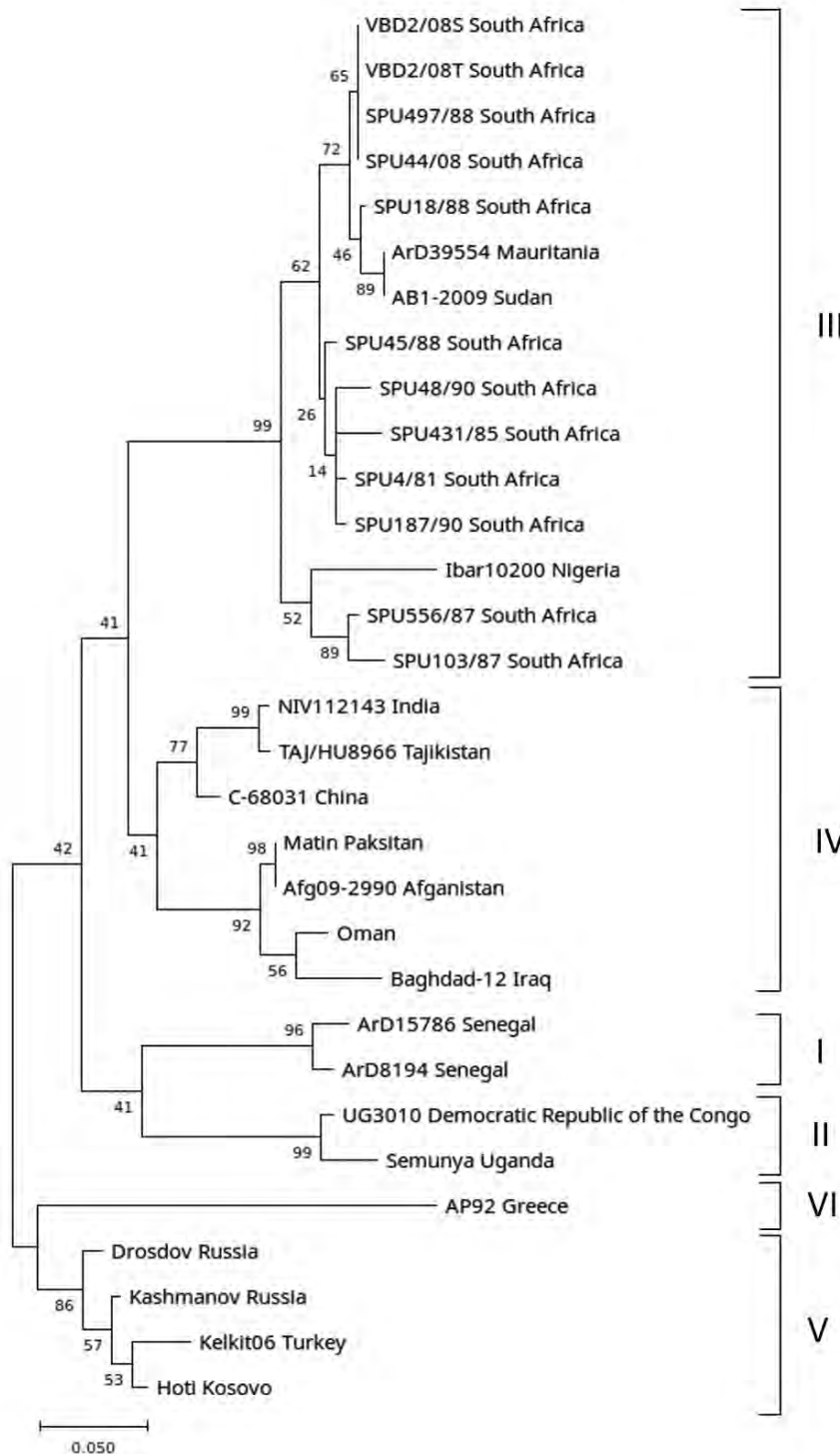


Figure. Detection of Crimean-Congo hemorrhagic fever virus (CCHFV) from a retrospectively tested human serum sample that was among those collected during 2008–2011 from acutely ill patients with suspected rickettsial infection, South Africa. Phylogenetic tree was constructed using a 186-bp region of the CCHFV small gene encoding the nucleoprotein sequence. Nucleotide data were obtained in the study for samples designated VBD2/08S (serum-derived), VBD 2/08T (tissue-derived), and retrieved from GenBank for 29 CCHFV isolates from similar, or geographically distinct, regions (GenBank accession number available on request). The tree was constructed using MEGA X (<https://www.megasoftware.net>) and 1,000 bootstraps. Nodes with values <50 were omitted from the figure. Branch labels are name of isolate and country of origin. Genotypes are indicated at right. Scale bar indicates nucleotide substitutions per site.

rescent antibody assays (EUROIMMUN, <https://www.euroimmun.com>), suggesting an acute infection. Laboratory records indicated that, 9 weeks after the blood sample was collected and submitted, an endometrial curettage sample taken after a spontaneous abortion was sent for histologic examination. Therefore, we retrieved a formalin-fixed paraffin-embedded tissue section of this sample from the archives and tested it retrospectively for evidence of CCHFV RNA using nested RT-PCR. We amplified a short fragment of the gene encoding the CCHFV nucleoprotein and confirmed its identity using nucleotide sequencing (Figure).

Because the biopsy sample contained both endometrial and placental tissue, the sample did not enable cellular localization of viral RNA or antigen and thus did not provide evidence directly linking the viral RNA to fetal demise. Similarly, the absence of retrospective maternal serum samples collected at the time of the spontaneous abortion, or fresh biopsy material, did not enable investigation for viremia. However, detection of viral RNA in tissue biopsy collected 9 weeks after detection of viral RNA in a serum sample suggests persistence of CCHFV RNA.

Persistent viral infection in selected sites has been demonstrated for other RNA viruses. Zika virus RNA is normally detectable in serum samples 3–10 days after symptom onset. Investigations on persistence of Zika virus RNA in formalin-fixed, paraffin-embedded fetal tissue from pregnant mothers with confirmed infection identified a time frame of 119–238 (mean 163) days from maternal symptom onset to detection of RNA by RT-PCR in brains and 15–210 (mean 81) days in placentas (3). The detection of viral RNA in a curettage specimen does not enable distinction between maternal and fetal infection but nevertheless extends the period during which viral RNA is detectable.

Little is known about the clinical course of CCHFV infections in pregnant women. Spontaneous abortions were reported in 24 (58.5%) of 41 mothers with CCHFV infection (4). Similarly, viral hemorrhagic fevers, such as from Ebola and Lassa viruses, during pregnancy have been associated with spontaneous abortion (5,6). Antigenemia has been detected 2–11 days after illness onset, viral RNA has been detected 1–18 days after initial symptoms, and infectious virus has been isolated from samples collected 1–12 days after onset (7). Whether pregnancy influences the duration of viremia is not known.

Although our findings are subject to some limitations and it is not possible to make any assumptions with regard to association between virus infection

and fetal demise or distinguish between maternal and fetal infection, our findings extend the period for detecting CCHFV RNA after infection and raises the potential for nosocomial infections. In addition, because the serum sample we tested was initially submitted for suspected tickbite fever, healthcare workers should consider CCHFV as part of the differential diagnosis for tickbite fever (rickettsial infections) in local patients and travelers returning from CCHFV-endemic regions.

Funding was obtained from the South African Research Chairs Initiative (Vector Borne and Zoonotic Pathogens Research, grant 98346) of the Department of Science and Technology and National Research Foundation.

About the Author

Dr. Mathengtheng was a medical scientist at the National Health Laboratory Service and University of the Free State in Bloemfontein, South Africa, at the time of his death in 2014. His primary research interest was the investigation of mosquito-borne and tick-borne viruses in southern Africa.

References

- Rodriguez LL, Maupin GO, Ksiazek TG, Rollin PE, Khan AS, Schwarz TF, et al. Molecular investigation of a multisource outbreak of Crimean-Congo hemorrhagic fever in the United Arab Emirates. *Am J Trop Med Hyg.* 1997;57:512–8. <https://doi.org/10.4269/ajtmh.1997.57.512>
- Burt FJ. Laboratory diagnosis of Crimean-Congo hemorrhagic fever virus infections. *Future Virol.* 2011;6:831–41. <https://doi.org/10.2217/fvl.11.47>
- Bhatnagar J, Rabeneck DB, Martines RB, Reagan-Steiner S, Ermias Y, Estetter LB, et al. Zika virus RNA replication and persistence in brain and placental tissue. *Emerg Infect Dis.* 2017;23:405–14. <https://doi.org/10.3201/eid2303.161499>
- Pshenichnaya NY, Leblebicioglu H, Bozkurt I, Sannikova IV, Abuova GN, Zhuravlev AS, et al. Crimean-Congo hemorrhagic fever in pregnancy: a systematic review and case series from Russia, Kazakhstan and Turkey. *Int J Infect Dis.* 2017;58:58–64. <https://doi.org/10.1016/j.ijid.2017.02.019>
- Price ME, Fisher-Hoch SP, Craven RB, McCormick JB. A prospective study of maternal and fetal outcome in acute Lassa fever infection during pregnancy. *BMJ.* 1988;297:584–7. <https://doi.org/10.1136/bmj.297.6648.584>
- Black BO, Caluwaerts S, Achar J. Ebola viral disease and pregnancy. *Obstet Med.* 2015;8:108–13. <https://doi.org/10.1177/1753495X15597354>
- Burt FJ, Leman PA, Smith JF, Swanepoel R. The use of a reverse transcription-polymerase chain reaction for the detection of viral nucleic acid in the diagnosis of Crimean-Congo haemorrhagic fever. *J Virol Methods.* 1998;70:129–37. [https://doi.org/10.1016/S0166-0934\(97\)00182-1](https://doi.org/10.1016/S0166-0934(97)00182-1)

Address for correspondence: Felicity J. Burt, National Health Laboratory Service, Division of Virology, PO Box 339 (G23) Bloemfontein 9300, South Africa; email: burtfj@ufs.ac.za

Non-*Leishmania* Parasite in Fatal Visceral Leishmaniasis–like Disease, Brazil

Malgorzata Anna Domagalska, Jean-Claude Dujardin

Author affiliation: Institute of Tropical Medicine, Antwerp, Belgium

DOI: <https://doi.org/10.3201/eid2602.191428>

To the Editor: We read with interest the recent article describing involvement of *Crithidia*-related parasites in visceral leishmaniasis (VL) in Brazil (1). In 2010, we published a similar study about the identification of *Leptomonas* sp., another monoxenous trypanosomatid, among clinical isolates from VL patients in India: of 120 cultured isolates, 111 were typed as *L. donovani* and 9 as *Leptomonas* sp. (2). As in the Brazil study, we infected BALB/c mice with 1 *Leptomonas* isolate; at 45 days postinfection, we found *Leptomonas* and *Leishmania* DNA by PCR in the animals' spleens. Assuming that sterility was preserved during the experiment, we interpreted that original infection in patients resulted from a mixture of the 2 species, *Leptomonas* overgrew *L. donovani* in culture because of substantial growth advantage of the former, and a few remaining *L. donovani* cells in the culture spread in the animals after inoculation because of their higher in vivo fitness.

We suspect a similar phenomenon could have occurred in Brazil, and additional analyses are required to support the authors' conclusions. Given that mice were inoculated with clinical isolates, postanimal typing should have been done. Furthermore, linking genotyping information of cultivated (cloned) strains with a patient phenotype is risky

because of the selection biases of in vitro isolation and maintenance. Using a recently developed method for direct sequencing of *L. donovani* complex parasites in host tissues, we demonstrated that genotypes of parasites in bone marrow samples differed from derived and cultivated isolates. This result most likely was due to polyclonal *L. donovani* infections and differences in fitness of different genotypes in vitro and in vivo. On the basis of this evidence, we recommend direct parasite sequencing in clinical samples in future work. If impossible, results based on cultured isolates should be interpreted with caution. We recommend a follow-up study to verify the possibility of *Crithidia/Leishmania* co-infection and the capacity of *Crithidia* to cause leishmaniasis-like disease as a single infection.

References

1. Maruyama SR, de Santana AKM, Takamiya NT, Takahashi TY, Rogerio LA, Oliveira CAB, et al. Non-*Leishmania* parasite in fatal visceral leishmaniasis-like disease, Brazil. *Emerg Infect Dis*. 2019;25:2088–92. <https://dx.doi.org/10.3201/eid2511.181548>
2. Srivastava P, Prajapati VK, Vanaerschot M, Van der Auwera G, Dujardin JC, Sundar S. Detection of *Leptomonas* sp. parasites in clinical isolates of kala-azar patients from India. *Infect Genet Evol*. 2010;10:1145–50. <https://doi.org/10.1016/j.meegid.2010.07.009>
3. Domagalska MA, Imamura H, Sanders M, Van den Broeck F, Bhattarai NR, Vanaerschot M, et al. Genomes of *Leishmania* parasites directly sequenced from patients with visceral leishmaniasis in the Indian subcontinent. *PLoS Negl Trop Dis*. 2019;13:e0007900. <https://doi.org/10.1371/journal.pntd.0007900>

Addresses for correspondence: Malgorzata Anna Domagalska or Jean-Claude Dujardin, Institute of Tropical Medicine, Molecular Parasitology Unit, Nationalestraat 155, B-2000 Antwerpen, Belgium; email: mdomagalska@itg.be or jcdujardin@itg.be

Social Responses to Epidemics Depicted by Cinema

Qijun Han, Daniel R. Curtis

Films illustrate 2 ways that epidemics can affect societies: fear leading to a breakdown in sociability and fear stimulating preservation of tightly held social norms. The first response is often informed by concern over perceived moral failings within society, the second response by the application of arbitrary or excessive controls from outside the community.

Films related to themes of disease, infection, and contagion often fall into 1 of 3 broad categories connected to fantasy, science fiction, or horror: apocalyptic destruction or near destruction of the whole of humanity, rising concerns over bioterrorism, and the rise of an undead or form of zombie existence (1). Although films traditionally deal sensitively or realistically with the topic of HIV/AIDS (e.g., *Dallas Buyers Club*, *Philadelphia*, *And the Band Played On*, *Kids*), often through melodrama, fewer films have dealt with other epidemic diseases, as either direct subject material or background context. Of these more realistic or semirealistic films about epidemics, scholarly literature has focused on the inadequacy of capturing the correct science behind disease transmission, spread, and illness (2–4) or anachronistic characters in films concerning historical epidemics (5). Notwithstanding broader discussions of society–disease interaction in the media (6), the social responses to various diseases portrayed in films have been discussed less frequently.

In this article, we bring together a sample of films that we manually selected from a consolidated database of epidemic-related films built from assorted scholarly literature and catalogs (2,4,5,7–9). This database was supplemented by accessing “Films about

viral outbreaks” on Wikipedia (https://en.wikipedia.org/wiki/Category:Films_about_viral_outbreaks) and a list of “Apocalyptic, epidemic, pandemic and disaster movies” on the Internet Movie Database (<https://www.imdb.com/list/ls058975821>). We manually selected the films and eliminated those that corresponded to the 3 broad categories mentioned above (i.e., those that are overly fantastical, not based or loosely based on an actual epidemic disease) and focused on films that pay explicit attention to social responses to disease (rather than being a peripheral backdrop to an unrelated story). Furthermore, the absence of comprehensive indexing of films containing narratives around epidemics makes construction of a systematic sample impractical (4).

Scholarly literature that focuses on contemporary disease psychology holds central a connection between fear, panic, and epidemics (10), often focusing on the unique characteristics of infectious diseases themselves (11). Indeed, in an article about the psychosocial effects of diseases, the disproportionate degree of fear was described as connected to the fact that “it is transmitted rapidly and invisibly; historically, it has accounted for major morbidity and mortality; old forms re-emerge and new forms emerge; and both the media and society are often in awe” (12). However, after analyzing this selection of epidemics-related films, we suggest that although social reactions such as panic (an emotive response caused by fear) are typically found in films concerning epidemics, films also remind us that the fear seen during epidemics is often little associated with the disease itself. In fact, films show that epidemics can push societies in 2 directions: fear leading to a breakdown in sociability, but also fear stimulating the preservation of tightly held social norms. The first social response to epidemics is often informed by concern over broader moral failings within society at large, leading, for example, to violence or scapegoating. In accordance with the “outbreak

Author affiliations: Nanjing University of Science and Technology, Nanjing, China (Q. Han); Erasmus University Rotterdam, Rotterdam, the Netherlands (D.R. Curtis)

DOI: <https://doi.org/10.3201/eid2602.181022>

narrative,” a concept developed by Priscilla Wald, a fear of the spread of disease is developed in only 1 direction, from marginalized, deviant, or underdeveloped groups to native, mainstream, or developed society (6). In recent films, this kind of orientalization (perpetuating stereotypes about Middle Eastern, Asian, and North African societies) and othering (viewing or treating others as intrinsically different from and alien to oneself) has been taken a step further as traditional or underdeveloped societies are heroically saved by outsiders. The second social response to epidemics is often informed by the perceived application of arbitrary or excessive controls from above or outside the community in question. Films have shown that epidemics produce active responses such as resistance or unrest—sometimes violent—to paradoxically retain aspects of normal life under threat (often from elites and authorities), such as perceived freedoms and liberties and customary traditions and practices.

Social Morality during Epidemics in Cinema

Many films dealing with epidemics have tended to see panic as an inevitable social response; their main focus has been the process of authorities withholding information to guard against chaos or the circulation of misinformation by the media. For example, in *Panic on the Streets* (1950, directed by Elia Kazan), to avoid mass panic across the city of New Orleans, the US Public Health Service and the police agree to not notify the press of a death resulting from pneumonic plague. Appearing in the same year, *The Killer That Stalked New York* (1950, Earl McEvoy) was based on an actual threat of smallpox that occurred in New York in 1947. In the film, public health officials develop a widespread vaccination program, but after the necessary serum runs out, the city descends into mass panic—after the authorities tried to cover up this information. In the UK film *80,000 Suspects* (1963, Val Guest), the doctor tackling an outbreak of smallpox uses a quarantining process with the explicitly mentioned goal of reducing the chances of public panic. In *Morte a Venezia* (1971, Luchino Visconti), a film based on the 1912 novel by German author Thomas Mann, *Der Tod in Venedig* [*Death in Venice*], the city authorities do not inform those on vacation of cholera problems within the city for fear they will frantically leave—an approach also taken by town officials in John Ford’s depiction of a community during a typhoid epidemic, *Dr. Bull* (1933). Another common feature is defiance of the film’s protagonists against a perceived lack of official information. For example, in *Quiet Killer* (1992, Sheldon Larry), when the

doctor realizes that her patient has succumbed to plague, she tries to push authorities to warn the citizens of New York, against considerable reluctance from the mayor, who envisages widespread panic.

Other films, however, have gone further and tried to examine some of the causes of this fear and panic; in many films, the roots lie in society’s response to perceived declines in social morality. One of the earliest examples is *Die Pest in Florenz* [*The Plague of Florence*] (1918, Fritz Lang), which focused on the real outbreak of the Black Death in Florence in the mid-14th century and portrayed death from plague as a response to immoral behavior and sexual debauchery. The connection between disease and deteriorating social morality came from actual observations of contemporaries at the time, for example, the views of Giovanni Villani (*Nuova Cronica*) and Giovanni Boccaccio (*Decameron*). In several films, the plague became used as an explicit punishment for immorality and wrongdoing: *The Pied Piper* (1972, Jacques Demy), *The Hour of the Pig* (1993, Leslie Megahey), and especially *Anazapta* (2002, Alberto Sciamma), in which plague was a supposed consequence of the brutal rape of a lord’s wife by the village.

Similar kinds of existentialist angst and pessimism over social values in connection with the Black Death were later famously exploited by Ingmar Bergman in *The Seventh Seal* (1957), Lars von Trier in *Epidemic* (1987), Luis Puenzo in *The Plague* (1992), and Christopher Smith in *The Black Death* (2010). Those 4 films focus especially on intolerance in the form of scapegoating and persecution of women as witches, but visualization of dread had already appeared earlier in lesser known films, such as *Singoalla* (1949, Christian-Jaque), *Häxan* (1922, Benjamin Christensen), and *Skeleton on Horseback* (1937, Hugo Haas). In the film *Trollsyn* (1994, Ola Solum), set in Norway, the initial stage of the Black Death outbreak is presented as mass hysteria among the villagers: crying and shouting, desperate prayers, suicides, and frantic searching for buboes and panicked movements. Also, in reference to social decline, one scene shows simultaneously the aggressive inquisition of a female scapegoat while amid the chaos a couple are having sex and others have taken off their clothes and are rolling down a grassy hill.

Many films focusing on outbreaks of epidemic disease focus on outbreaks of senseless violence indicative of a society completely out of control. In *The Horseman on the Roof* (1995, Jean-Paul Rappeneau), set during a cholera epidemic in 19th-century Manosque, southern France, the film’s protagonist, Angelo, is captured by a paranoid mob who accuse him of

poisoning the town fountain and take him to the authorities. Elsewhere, in the *Masque of the Red Death* (1964, Roger Corman [adapted in 1989 by Larry Brand/Jeffrey Delman]), which focuses on a fictional disease with loose parallels to plague, rural villagers become increasingly desperate and seek to escape the devastating death, only to have soldiers shoot them down by crossbow. In *Jezebel* (1939, William Wyler), chaotic and violent scenes of 19th-century New Orleans are overlaid with a dramatic, flashing, capitalized “YELLOW FEVER” text across the screen, as if to heighten the emphasis on uncontrolled panic.

Another aspect of declining social morality is linked to scapegoating; stigmatization and blame have long been connected with epidemics. It is well known that the Black Death brought mass persecution of Jews in various parts of Europe (13), and families were gathered up and burned alive. More recently, Muslims were blamed for poisoning water systems during the 1994 plague outbreak in Surat, India (14), and the HIV/AIDS pandemic from the 1980s led to extreme prejudice against homosexuals and intravenous drug users (15). Globalization and the fear that exotic diseases can be transported into modern urban environments (16), together with increased access to air travel (17), has to some extent heightened these kinds of concerns about scapegoating. Viruses know no borders and thus become easily entangled with contemporary anxieties over migration and refugees (18). Asian populations in Chinatowns of various Western cities were victimized in the wake of severe acute respiratory syndrome (SARS) (19), and studies performed in Hong Kong revealed that the public actually anticipated this kind of outcome (20).

Not surprisingly, then, popular culture has often tended to present epidemics as a foreign invasion (2,21), especially given the moral associations often drawn between disease and social and cultural phenomena through metaphors such as corruption, decay, and pollution (11). For example, in the Sherlock Holmes story *The Giant Rat of Sumatra* (not penned by Conan Doyle), Professor Moriarty prepares to import plague to Britain by acquiring infected rats from Southeast Asia (5). Accordingly, in some recent Hollywood films, the direction of disease movement is typically east to west, or at least from developing to developed countries, and plays on common stereotypes, including concepts of orientalization and othering (4,22). The film *Contagion* (2011, Steven Soderbergh), although widely lauded for its accurate depiction of the mechanisms of disease transmission and epidemiology, can be seen to neatly fit within Wald’s outbreak narrative framework, in which a

pathogen is brought into the developed world after contact with migrants and visitors from lesser developed areas (4,6). Evie Kendal noted that the virus that hit the United States in *Outbreak* (1995, Wolfgang Petersen) was thought to have originated in Africa, whereas in *Contagion* and *The Crazies* (1973, George Romero), the disease originates in Asia (4).

In more recent years, however, the othering narrative has also taken new forms, in which an undeveloped or traditional society under threat of an epidemic is heroically saved by outside forces. This narrative can be seen in the popular film set in China, *Wolf Warrior II* [Zhan lang II] (2017, Jing Wu), which tries to favorably present Chinese attempts to control a fictional disease (lamanla) based on Ebola in Africa. In *The Painted Veil* (2006, John Curran), a 1920s rural village in China is unable to deal with a cholera outbreak until a British bacteriologist comes along to investigate and in the end selflessly gives his own life.

Resistance and Normalcy during Epidemics Depicted in Cinema

Although epidemics can produce panicked responses that lead to the unraveling of the social fabric, this response is not the only outcome, as the literature (both historical and contemporary sociological) has argued (13,23). In a related way, some films have also shown that extreme reactions during epidemics often have a specific purpose, and, paradoxically, elements of unrest (e.g., resistance to authorities and violence) can be society’s way of attempting to return to a state of normalcy and cohesiveness. Indeed, although according to Michel Foucault, sickness and disease became an arena through which authorities and elites tried to exert social controls (24), epidemics can also become a context in which those lower down the social hierarchy vent frustrations, leading to conflict, often as a way of protecting freedoms or traditions and customary practices. Good early cinematic examples of lower class involvement include *The Citadel* (1937, King Vidor), with its scenes of working class miners resisting medical authority during a tuberculosis outbreak, and *1918* (1985, Ken Harrison), in which residents of a small Texas community resolutely try to continue their normal lives, functions, and networks despite the scale of deaths from influenza.

In recent times, more nuanced views about how societies respond to epidemics can be found in films, especially showing how extreme reactions tend to not be intrinsically associated with the disease itself but rather to be a way of dealing with top-down repression impinging on freedoms and liberties. Although perpetuating some elements of othering (6),

the US-based film *Contagion* is a good example of a film that deals with social movements from below, in the process criticizing contemporary trends toward avarice and self-interest, which are further exposed during the epidemic. Throughout the movie, Soderbergh presents collective patterns of behavior during the epidemic, which lead to social discord. However, much of this unrest is connected to unsatisfactory responses to the disease by authorities. Most fears stem from an absence of information from reputable sources, leaving a vacuum for dubious intelligence to emerge on alternative platforms, where intrigue and speculation become almost comparable types of contagion. Overall, a tension emerges between the medical authorities' advised procedure of forcible isolation and quarantine, which conflicts with very contemporary demands for maintenance of ordinary patterns of social networking and communication. This response has strong parallels in history, where communities have been shown to cling strongly to their sociability. Religious rituals such as the Janāza blessing continued unabated in the Middle East during Second Pandemic plagues (25), and the influenza pandemic of 1918–1920 has been cited as the foremost example in modern history of continued social bonds in times of excessive deaths (26).

Another film demonstrating similar issues is *Blindness* (2008, Fernando Meirelles), which deals with a fictional disease that causes epidemic blindness, leading to collective hysteria. Overall, the film considers the human capacity for prejudice, indifference, selfishness, and an easy resort to aggression and violence. As more citizens contract the disease, the normal functioning of society is upturned: strict government quarantines of the infected are imposed by use of physical force. Just as with *Contagion*, however, this action provokes unrest not connected to the disease but to perceived arbitrary and ruthless actions of elites and authorities. We see scenes in which resources such as food begin to be distributed inequitably, and people begin to exploit their positions by withholding food in exchange for other resources, including coerced sex. Most of the violent confrontation stems from hostilities between those subject to quarantines and those managing the confined environments.

These aspects of extreme disdain for the withholding of perceived societal freedoms are not found solely in Western films but in films from Asia too, such as the recent popular movie *Flu* (2013, Kim Sung-su), set in South Korea, which plays on recent experiences with SARS and influenza by focusing on responses to an outbreak of a fictional disease with parallels to the strain of avian influenza A(H5N1)

virus. On the one hand, many scenes capture the frenzied breakdown of social norms. As first details of the disease emerge, the film's protagonist, Ji-goo, is seen in a mall among people frantically making phone calls and rushing to leave the city. After the news is made public on national television, raising the category of the crisis to critical, citizens begin fighting for resources and even exploiting the chaos to loot a supermarket. On the other hand, however, we also see much more focused forms of unrest directed at certain social groups, especially in the process of implementing quarantines. Of note, when infected citizens are forcibly moved to camps, elements of compassion and cohesion develop among camp residents; the most violent reactions come from and are directed toward authorities managing the site. The film also reflects on distrust of elites and authorities with medical knowledge and power; rumors are spread that the infected are killed rather than treated. This same distrust is a theme seen in other films from China, such as *Shen yi bian que* (1985, Yin Cui) and *Fall of Ming* [Da Ming jie] (2013, Jing Wang), about real-life physicians Bian Que and Wu Youke, respectively. This theme again has broad parallels to history and the riots that occurred during 19th- and 20th-century cholera outbreaks, opposing medical staff and governments (27). Note that several films set in China and Hong Kong produced in the immediate aftermath of the 2003 SARS outbreak aimed to present an optimal governmental response: *Profoundly Affecting* [Jingxing dingpo] (2003, Jia Wang/Dong Shen), *Feidian rensheng* (2003, Wai-Man Cheng), and *Golden Chicken 2* [Gam gai 2] (2003, Leung Chun Chiu).

Aside from freedoms and liberties, other films have highlighted how societies sometimes move toward unrest—through either resistance to authorities or physical violence—as a response to perceived infringements on customary and traditional practices that have occurred during an epidemic outbreak. One of the clearest demonstrations of this response appears in the 2006 readaptation of *The Painted Veil*, which follows a British bacteriologist working to prevent the spread of cholera in a small village in rural China in the 1920s, set within a broader context of distrust through heightened nationalist tensions. In this film we see no signs of fear or panic from the local population, despite many deaths within the community; the inhabitants are more concerned about maintaining ordinary patterns of living and sociability. The villagers become incensed for the first time when the foreign doctor tries to move bodies from the cemetery to avoid infecting the water; the villagers believe that the deceased must be nearer to the river to

move swiftly to the afterlife. The decision to remove all corpses and bury them immediately raises further fury because the villagers expect a certain period to elapse while the bodies are laid out in their homes before burial. Although we must be aware of the potential effects of the orientalist imagination when considering a film such as *The Painted Veil*, medical history points to its accuracy. In rural China during the 1920s and 1930s, elite medical reformers' disregard for village internal politics and power dynamics limited the effectiveness of their public health prevention policies, as locals continued the same routines (28). The same issues also appear in older productions set in China; in *Horse Thief* [*Dao ma zei*] (1986, Tian Zhuang-zhuang), set during a disease outbreak in Tibet in the 1920s, people living out in the steppe or grasslands continue their very same daily functions, stopping only to pray for the disease to cease.

Conclusions

Cinema is not reality, and elements of fear leading to panic and chaos are likely to persist in dramatic representations of disease, purely for entertainment value. These representations may be problematic in 2 interrelated ways. First, "the image of a panicked mob makes exciting footage in disaster movies, but it obscures a broad range of possible public reactions" (29). Second, the public perception of how epidemic diseases behave is substantially influenced by the media and popular culture (2,4,6,30); parts of this perception are sometimes adopted as scientific facts (31,32). Similar issues have recently been brought to our attention regarding the widespread and incorrect diagnostic use of images of persons with a disease that is wrongly assumed to be plague (33,34) and media perpetuation of several recent misguided anxieties over how the Ebola virus is spread (35,36).

In this article, however, we have shown that many films focusing on social responses to epidemic disease outbreaks also shine a light on another side of how people react. Although on the one hand, fear and panic can be connected to a perceived breakdown in social morality, on the other hand, disruptive reactions can also work toward societal cohesion to protect freedoms, privileges, and customs under threat. By shifting between the macro scale of humanity or society to the micro scale of individual protagonists and relatable characters—including different social and demographic groups—films can, at times, do an excellent job of showing how disease responses are also shaped by hierarchical relationships (not just the demonstration of power from above but also the

reception of this power from below). In the films mentioned in this article, a recurring lesson is the failure of imposed mass isolation techniques, largely resulting from weak compliance (4). These films also show situations similar to ongoing problems with Ebola in Africa today, where communal suspicions and distrust of the decisions of outside authorities are rife (37–39), violent resistance and outcry occur within communities (40), and localized attempts continue to maintain customary practices in terms of the treatment of the dead (41).

This work was supported by the Netherlands Organisation for Scientific Research grant nos. 275-53-014 and 016.Vidi.185.046; the Chinese National Ministry of Education, Humanities and Social Science grant no. 16YJC760013; the Fundamental Research Funds for the Central Universities grant no. 30919013302; and the Jiangsu Overseas Visiting Scholar Program for University Prominent Young and Middle-aged Teachers and Presidents, China.

About the Authors

Dr. Han is an associate professor at Nanjing University of Science and Technology, Nanjing, China, specializing in film–society interactions. Dr. Curtis is an associate professor at Erasmus University Rotterdam, Rotterdam, the Netherlands, specializing in social responses to historical diseases.

References

- Nasiruddin M, Halabi M, Dao A, Chen K, Brown B. Zombies—a pop culture resource for public health awareness. *Emerg Infect Dis*. 2013;19:809–13. <https://doi.org/10.3201/eid1905.AD1905>
- Pappas G, Seitaridis S, Akritidis N, Tsianos E. Infectious diseases in cinema: virus hunters and killer microbes. *Clin Infect Dis*. 2003;37:939–42. <https://doi.org/10.1086/377740>
- Foreman CH Jr. Editorial commentary: witchcraft science in the cinema of epidemics. *Sci Commun*. 1995;17:3–8. <https://doi.org/10.1177/1075547095017001001>
- Kendal E. Public health crises in popular media: how viral outbreak films affect the public's health literacy. *Med Humanit*. 2019;0:1–9. <https://doi.org/10.1136/medhum-2018-011446>
- Aberth J. Welcome to the apocalypse: Black Death films. In: Aberth J, editor. *A knight at the movies: medieval history on film*. New York: Routledge; 2003. p. 197–254.
- Wald P. *Contagious: cultures, carriers, and the outbreak narrative*. Durham (NC): Duke University Press; 2008.
- Vidal P, Tibayrenc M, Gonzalez J-P. Infectious diseases and arts. In: Tibayrenc M, editor. *Encyclopedia of infectious diseases: modern methodologies*. Hoboken (NJ): Wiley; 2007.
- García Sánchez JE, García Sánchez E, Merino Marcos ML. Antibacterial agents in the cinema. *Rev Esp Quimioter*. 2006;19:397–402.
- Vercruyse T. *The Dark Ages imaginary in European films [dissertation]*. Leuven (Belgium): Katholieke Universiteit Leuven; 2014.

10. Strong P. Epidemic psychology: a model. *Sociol Health Illn.* 1990;12:249–59. <https://doi.org/10.1111/1467-9566.ep11347150>
11. Sontag S. *Illness as metaphor*. New York: Doubleday, 1978.
12. Pappas G, Kiriaze IJ, Giannakis P, Falagas ME. Psychosocial consequences of infectious diseases. *Clin Microbiol Infect.* 2009;15:743–7. <https://doi.org/10.1111/j.1469-0691.2009.02947.x>
13. Cohn SK. *Epidemics: hate and compassion from the plague of Athens to AIDS*. Oxford (UK): Oxford University Press; 2018.
14. Barrett R. The 1994 plague in Western India: human ecology and the risks of misattribution. In: Clunan AL, Lavon PR, Martin SB, editors. *Terrorism, war or disease? Unraveling the use of biological weapons*. Stanford (CA): Stanford University Press; 2008. p 49–71.
15. Kazanjian P. The AIDS pandemic in historic perspective. *J Hist Med Allied Sci.* 2014;69:351–82. <https://doi.org/10.1093/jhmas/jrs061>
16. Covello VT, Peters RG, Wojtecki JG, Hyde RC. Risk communication, the West Nile virus epidemic, and bioterrorism: responding to the communication challenges posed by the intentional or unintentional release of a pathogen in an urban setting. *J Urban Health.* 2001;78:382–91. <https://doi.org/10.1093/jurban/78.2.382>
17. Mangili A, Gendreau MA. Transmission of infectious diseases during commercial air travel. *Lancet.* 2005;365:989–96. [https://doi.org/10.1016/S0140-6736\(05\)71089-8](https://doi.org/10.1016/S0140-6736(05)71089-8)
18. Caduff C. On the verge of death: visions of biological vulnerability. *Annu Rev Anthropol.* 2014;43:105–21. <https://doi.org/10.1146/annurev-anthro-102313-030341>
19. Eichelberger L. SARS and New York's Chinatown: the politics of risk and blame during an epidemic of fear. *Soc Sci Med.* 2007;65:1284–95. <https://doi.org/10.1016/j.socscimed.2007.04.022>
20. Lau JT, Kim JH, Tsui H, Griffiths S. Perceptions related to human avian influenza and their associations with anticipated psychological and behavioral responses at the onset of outbreak in the Hong Kong Chinese general population. *Am J Infect Control.* 2007;35:38–49. <https://doi.org/10.1016/j.ajic.2006.07.010>
21. OToole T. Smallpox: An attack scenario. *Emerg Infect Dis.* 1999;5:540–6. <https://doi.org/10.3201/eid0504.990416>
22. Ostherr K. Contagion and the boundaries of the visible: the cinema of world health. *Camera Obscura.* 2002;17:1–40. https://doi.org/10.1215/02705346-17-2_50-1
23. Quarantelli EL, Smelser N, Baltes PB. The sociology of panic. In: Smelser NJ, Baltes PB, editors. *International encyclopedia of the social & behavioral sciences*. New York: Pergamon; 2001. p. 11010–3.
24. Foucault M. *Discipline and punish: the birth of the prison*. New York: Vintage Books; 1995.
25. Borsch S, Sabraa T. Refugees of the Black Death: quantifying rural migration for plague and other environmental disasters. *Ann Demogr Hist (Paris).* 2017;134:63–93. <https://doi.org/10.3917/adh.134.0063>
26. Crosby A. *Americas forgotten pandemic: the influenza of 1918*. Cambridge (UK): Cambridge University Press; 1989.
27. Cohn SK. Fear and the corpse: cholera and plague riots compared. In: Lyteris C, Evans NHA, editors. *Histories of post-mortem contagion. Medicine and biomedical sciences in modern history*. Cham (Switzerland): Palgrave-Macmillan; 2018. p. 55–82.
28. Merkel-Hess K. The public health of village private life: reform and resistance in early twentieth century rural China. *J Soc Hist.* 2016;49:881–903. <https://doi.org/10.1093/jsh/shv082>
29. Glass TA, Schoch-Spana M. Bioterrorism and the people: how to vaccinate a city against panic. *Clin Infect Dis.* 2002;34:217–23. <https://doi.org/10.1086/338711>
30. Brown B, Nasiruddin M, Dao A, Halabi M. Responsible use of pop culture and communication in the face of Ebola virus. *PLoS Negl Trop Dis.* 2015;9:e0003890. <https://doi.org/10.1371/journal.pntd.0003890>
31. Millard WB. Ebola preparedness: on avoiding making a scary virus scarier. *Ann Emerg Med.* 2015;65:15A–20A. <https://doi.org/10.1016/j.annemergmed.2014.12.024>
32. Freimuth V, Linnan HW, Potter P. Communicating the threat of emerging infections to the public. *Emerg Infect Dis.* 2000;6:337–47. <https://doi.org/10.3201/eid0604.000403>
33. King H, Green MH. On the misuses of medical history. *Lancet.* 2018;391:1354–5. [https://doi.org/10.1016/S0140-6736\(18\)30490-2](https://doi.org/10.1016/S0140-6736(18)30490-2)
34. Jones L, Nevell R. Plagued by doubt and viral misinformation: the need for evidence-based use of historical disease images. *Lancet Infect Dis.* 2016;16:e235–40. [https://doi.org/10.1016/S1473-3099\(16\)30119-0](https://doi.org/10.1016/S1473-3099(16)30119-0)
35. Sinha MS, Parmet WE. The perils of panic: Ebola, HIV, and the intersection of global health and law. *Am J Law Med.* 2016;42:223–55. <https://doi.org/10.1177/0098858816658269>
36. Blakey SM, Reuman L, Jacoby RJ, Abramowitz JS. Tracing fearbola: examining the psychological predictors of anxious responding to the Ebola virus. *Cognit Ther Res.* 2015;39:816–25. <https://doi.org/10.1007/s10608-015-9701-9>
37. Calain P, Poncin M. Reaching out to Ebola victims: coercion, persuasion or an appeal for self-sacrifice? *Soc Sci Med.* 2015; 147:126–33. <https://doi.org/10.1016/j.socscimed.2015.10.063>
38. Kutalek R, Wang S, Fallah M, Wesseh CS, Gilbert J. Ebola interventions: listen to communities. *Lancet Glob Health.* 2015;3:e131. [https://doi.org/10.1016/S2214-109X\(15\)70010-0](https://doi.org/10.1016/S2214-109X(15)70010-0)
39. Pellecchia U, Crestani R, Decroo T, Van den Bergh R, Al-Kourdi Y. Social consequences of Ebola containment measures in Liberia. *PLoS One.* 2015;10:e0143036. <https://doi.org/10.1371/journal.pone.0143036>
40. Cohn S, Kutalek R. Historical parallels, Ebola virus disease and cholera: understanding community distrust and social violence with epidemics. *PLoS Curr.* 2016;8:8. <https://doi.org/10.1371/currents.outbreaks.aaf12b60e8d-43939b43fbd93e1a63a94>
41. Moran M. Missing bodies and secret funerals: the production of safe and dignified burials in the Liberian Ebola crisis. *Anthropol Q.* 2017;90:399–421. <https://doi.org/10.1353/anq.2017.0024>

Address for correspondence: Daniel R. Curtis, Erasmus University Rotterdam, Erasmus School for History, Culture and Communication, Rm M6-31, Burg Oudlaan 50, Rotterdam, 3062PA, the Netherlands; email: curtis@eshcc.eur.nl



Artist Unknown. *A Rajput Warrior with Camel, Possibly Maru Ragini from a Ragamala, 1650–80* (detail). Opaque watercolor, ink, and gold on paper. Ten 1/4 in x 6 15/16 in/26 cm x 17.6 cm. Purchase and partial gift from the Catherine and Ralph Benkaim Collection; Severance and Greta Millikin Purchase Fund. Public domain digital image courtesy of The Cleveland Museum of Modern Art, Cleveland, Ohio.

Veiled Dangers in an Idyllic Setting

Byron Breedlove

The modern word camel is derived from the Latin word *camelus*, the Greek word *kamēlos*, and the Hebrew word *gāmāl*, which means “going without,” in reference to the camel’s ability to survive and function without food or water for days. Camels can “go without” thanks in large measure to their humps, which contain up to 80 pounds of fat that can be broken down into water and energy. This onboard reservoir enables them to travel up to 100 miles through the desert without water. Several other adaptations help camels thrive in dry, desert environments, where temperatures can soar to more than 100°F in summer and plummet to –20°F or colder in winter.

For thousands of years, the people of North Africa and Asia have used the one-humped Arabian camels of the species *Camelus dromedarius* (commonly called dromedaries) for transporting people and conveying goods essential for trade and sustenance. Dromedaries, one of the largest species of domesticated livestock, may reach a shoulder height of 7 feet, and the males typically weigh between 900 and 1,300 pounds. More than serving as beasts of burden, they have also sustained human societies living in inhospitable environments as a source of meat, milk, and leather.

Author affiliation: Centers for Disease Control and Prevention, Atlanta, Georgia, USA

DOI: <https://doi.org/10.3201/eid2602.AC2602>

This month’s cover art, *A Rajput Warrior with Camel, Possibly Maru Ragini from a Ragamala*, celebrates the longstanding relationship between humans and camels. The painting comes from India, the country at the eastern end of the range for this type of camel. Within India, these camels are concentrated in the northwestern state of Rajasthan, and smaller populations are found in the neighboring states of Gujarat and Haryana.

A Rajput Warrior with Camel is an example of ragamala painting, a genre that emerged in medieval India. According to the Metropolitan Museum of Modern Art, “A ragamala, translated from Sanskrit as ‘garland of ragas,’ is a series of paintings depicting a range of musical melodies known as ragas. Its root word, raga, means color, mood, and delight, and the depiction of these moods was a favored subject in later Indian court paintings.” In many cases the mood, or raga, is written as poetry on the margins of the painting, and such works “express the intersections of painting, poetry, and music in Indian court art.” A ragamala typically included 36 or 42 loose-leaf paintings collected in a portfolio by members of various court circles who commissioned the work.

The young warrior portrayed on the painting balances on a fallen tree trunk; his domesticated dromedary compliantly kneels before him. He holds a thin

spear in his right hand and grasps a halter in his left. In addition to his spear, he has a dagger inserted into the sash around his waist and a gold-handled scimitar in a gold-tipped scabbard. Despite this trio of weapons, or perhaps because of them, the young man appears confident and relaxed. He is resplendently garbed in finery from head to toe. The accoutrements and attention to details also accorded to his camel—a decorative bridle, ornate fabric covering its hump, a plumed headdress, and brocade cords—signal privilege and refinement.

The prevailing mood of this scene is benevolence and peace between human and animal. The lush setting adds to the sense of calmness. Pairs of whorled evergreens and broad-leafed tropical trees fill the upper half of the image. Billowing clouds hover over the gentle slope of a hill, and several flowering plants appear throughout. Adding to the restive atmosphere is the bright orange border festooned with an ornate flower motif. If any danger is present, certainly it is far away and not of immediate concern to the warrior or camel.

Perhaps only an epidemiologist or virologist might spot veiled dangers in such an idyllic setting—such as the zoonotic diseases brucellosis and Rift Valley fever—that dromedaries may spread to humans. Some might think of other novel camel-borne diseases, including a prion disease recently found in camels at a slaughterhouse in Algeria.

But the camel-borne zoonotic disease of most concern is a disease that emerged only in the past decade, Middle East respiratory syndrome (MERS). This viral respiratory illness is caused by Middle East respiratory syndrome coronavirus, or MERS-CoV, initially identified in Saudi Arabia in 2012. Dromedary camels are a reservoir host for this zoonotic virus, and researchers believe that the original reservoir hosts may have been bats because similar coronaviruses have been found in bats. More than a third of reported cases have resulted in death. Coronaviruses are a large family of viruses, many of which can cause diseases in humans, ranging from the common cold to severe acute respiratory syndrome (SARS). According to an article published in 2018, researchers also identified dromedary viruses related to human coronavirus (HCoV) 229E, a primarily nonlethal coronavirus that causes some upper and lower respiratory tract infections in humans. These dromedary viruses could replicate in human cells, thus suggesting that HCoV-229E may have descended from camelid-associated viruses.

Almost all modern camels are domesticated, and their population is growing at a faster rate than that

of other domestic livestock such as cattle, horses, sheep, and llamas (though at a lower rate than that for goats). Zoonotic infections such as MERS remind us that for all the shared benefits of long-term human and animal relationships, these close interactions between animals of different species can also yield unwanted consequences and require new protocols and approaches to mitigate disease transmission.

Bibliography

1. Almathen F, Charruau P, Mohandesan E, Mwacharo JM, Orozco-terWengel P, Pitt D, et al. Ancient and modern DNA reveal dynamics of domestication and cross-continental dispersal of the dromedary. *Proc Natl Acad Sci U S A*. 2016;113:6707–12. <https://doi.org/10.1073/pnas.1519508113>
2. Babelhadj B, Di Bari MA, Pirisinu L, Chiappini B, Gaouar SB, Riccardi G, et al. Prion disease in dromedary camels, Algeria. *Emerg Infect Dis*. 2018;24:1029–36. <https://doi.org/10.3201/eid2406.172007>
3. Cleveland Museum of Modern Art. A Rajput warrior with camel, possibly Maru Ragini from a Ragamala, 1650–80 [cited 2019 Dec 16]. <https://www.clevelandart.org/art/2018.168>
4. Corman VM, Muth D, Niemeier D, Drosten C. Hosts and sources of endemic human coronaviruses. *Adv Virus Res*. 2018;100:163–88. <https://doi.org/10.1016/bs.aivir.2018.01.001>
5. Faye B, Bonnet P. Camel sciences and economy in the world: current situation and perspectives. In: *Proceedings of the 3rd Conference of the International Society of Camelid Research and Development*, Muscat, Oman; January 29–February 1, 2012.
6. Killerby ME, Biggs HM, Midgley CM, Gerber SI, Watson JT. Middle East respiratory syndrome coronavirus transmission. *Emerg Infect Dis*. 2020;26:191–8. <https://doi.org/10.3201/eid2602.190697>
7. Köhler-Rollefson I. Camel cultures of India [cited 2019 Dec 29]. <https://www.sahapedia.org/camel-cultures-of-india>
8. Metropolitan Museum of Art. Exhibition overview [cited 2019 Dec 29]. <https://www.metmuseum.org/exhibitions/listings/2014/ragamala>
9. Meyer B, Müller MA, Corman VM, Reusken CB, Ritz D, Godeke GJ, et al. Antibodies against MERS coronavirus in dromedary camels, United Arab Emirates, 2003 and 2013. *Emerg Infect Dis*. 2014;20:552–9. <https://doi.org/10.3201/eid2004.131746>
10. Rooney J. Ragas and *ragamalas*: performance and painting [cited 2019 Dec 29]. <https://www.metmuseum.org/blogs/ruminations/2015/ragas-and-ragamalas>
11. World Health Organization. Frequently asked questions on Middle East respiratory syndrome coronavirus (MERS-CoV) [cited 2020 Jan 3]. https://www.who.int/csr/disease/coronavirus_infections/faq/en
12. World Health Organization. Regional Office for the Eastern Mediterranean. MERS situation update; October 2018 [cited 2020 Jan 3]. <http://www.emro.who.int/pandemic-epidemic-diseases/mers-cov/mers-situation-update-october-2018.html>
13. Zhu S, Zimmerman D, Deem SL. A review of zoonotic pathogens of dromedary camels. *EcoHealth*. 2019;16:356–77. <https://doi.org/10.1007/s10393-019-01413-7>

Address for correspondence: Byron Breedlove, EID Journal, Centers for Disease Control and Prevention, 1600 Clifton Rd NE, Mailstop H16-2, Atlanta, GA 30329-4027, USA; email: wbb1@cdc.gov

EMERGING INFECTIOUS DISEASES®

Upcoming Issue

- Epidemiology of Cryptosporidiosis in New York City, New York, USA, 1995–2018
- *Mycobacterium tuberculosis* Complex Lineage 3 as Causative Agent of Pulmonary Tuberculosis, Eastern Sudan
- Public Health Response to Tuberculosis Outbreak among Persons Experiencing Homelessness, Minneapolis, Minnesota, USA, 2017
- Long-Term Rodent Surveillance after Outbreak of Hantavirus Infection in Yosemite National Park, California, United States, 2012
- Risk Factors for Complicated Lymphadenitis Caused by Nontuberculous Mycobacteria in Children
- Genomic and Phenotypic Variability of Antimicrobial-Susceptible *Neisseria gonorrhoeae*, England
- Hypervirulent Carbapenem-Resistant *Klebsiella pneumoniae* with *blaKPC-2* Gene, Singapore, 2010–2015
- Methicillin-Resistant *Staphylococcus aureus* Bloodstream Infections and Injection Drug Use, Tennessee, USA, 2015–2017
- High Prevalence of and Risk Factors for Latent Tuberculosis among Prisoners, Tianjin, China
- Randomized Trial of 2 Meningococcal B Vaccine Schedules in Adolescents and Young Adults, Canada
- Pregnancy Outcomes among Women Vaccinated with rVSVΔ-ZEBOV-GP Ebola Vaccine during the Sierra Leone Trial to Introduce a Vaccine against Ebola (STRIVE)
- Suspected Locally Acquired Coccidioidomycosis in Resident, Spokane, Washington, USA
- Avian Influenza Virus Detection Rates in Poultry and Environment at Live Poultry Markets, Guangdong, China
- Diphtheria Outbreaks in Schools in Highland Districts of Central Vietnam, 2015–2018
- Novel Techniques for Detection of *Mycobacterium bovis* Infection in a Cheetah
- Geographic Expansion of Sporotrichosis, Brazil
- Three New Cases of Melioidosis, Guadeloupe, French West Indies
- *Chlamydia abortus* in a Pregnant Woman with Acute Respiratory Distress Syndrome

Complete list of articles in the March issue at
<http://www.cdc.gov/eid/upcoming.htm>

Upcoming Infectious Disease Activities

March 8–11, 2020

CROI

Conference on Retroviruses and
Opportunistic Infections
Boston, MA, USA

<https://www.croiconference.org/>

March 9–13, 2020

ASLM

African Society for Laboratory Medicine
7th African Network for Influenza
Surveillance Epidemiology

Livingstone, Zambia

<https://www.anise2020.org>

March 18–20, 2020

International Conference on Reemerging
Infectious Diseases

Addis Ababa, Ethiopia

<http://www.icreid.com>

March 26–30, 2020

Society for Healthcare
Epidemiology of America
Decennial 2020

6th International Conference on
Healthcare Associated Infections
Atlanta, GA, USA

<https://decennial2020.org>

April 18–21, 2020

ECCMID

The European Congress of Clinical
Microbiology and Infectious Diseases
Paris, France

https://www.eccmid.org/eccmid_2020

May 3–6, 2020

ASM Clinical Virology Symposium
West Palm Beach, FL, USA

<https://asm.org/Events/2019-Clinical-Virology-Symposium/Home>

June 18–22, 2020

American Society for Microbiology
ASM Microbe 2020

Chicago, IL, USA

<https://asm.org/Events/ASM-Microbe/Home>

Announcements

Email announcements to EIDEditor
(eideditor@cdc.gov). Include the event's
date, location, sponsoring organization,
and a website.

Earning CME Credit

To obtain credit, you should first read the journal article. After reading the article, you should be able to answer the following, related, multiple-choice questions. To complete the questions (with a minimum 75% passing score) and earn continuing medical education (CME) credit, please go to <http://www.medscape.org/journal/eid>. Credit cannot be obtained for tests completed on paper, although you may use the worksheet below to keep a record of your answers.

You must be a registered user on <http://www.medscape.org>. If you are not registered on <http://www.medscape.org>, please click on the "Register" link on the right hand side of the website.

Only one answer is correct for each question. Once you successfully answer all post-test questions, you will be able to view and/or print your certificate. For questions regarding this activity, contact the accredited provider, CME@medscape.net. For technical assistance, contact CME@medscape.net. American Medical Association's Physician's Recognition Award (AMA PRA) credits are accepted in the US as evidence of participation in CME activities. For further information on this award, please go to <https://www.ama-assn.org>. The AMA has determined that physicians not licensed in the US who participate in this CME activity are eligible for AMA PRA Category 1 Credits™. Through agreements that the AMA has made with agencies in some countries, AMA PRA credit may be acceptable as evidence of participation in CME activities. If you are not licensed in the US, please complete the questions online, print the AMA PRA CME credit certificate, and present it to your national medical association for review.

Article Title

Acute Toxoplasmosis among Canadian Deer Hunters Associated with Consumption of Undercooked Deer Meat Hunted in the United States

CME Questions

1. Which of the following statements regarding the epidemiology of infection with *Toxoplasma gondii* is most accurate?

- A. Its reservoir is limited to mammals
- B. Contact with cat feces is the most common cause of infection among adults
- C. Felines are the only definitive hosts for toxoplasma
- D. Consumption of infected soil does not promote illness among adults

2. Which of the following statements regarding infection with toxoplasma is most accurate?

- A. Infection after birth can be asymptomatic
- B. Toxoplasma is often recognized after development of a characteristic rash
- C. The most common sign is painful and swollen joints
- D. Infection usually resolves within 18 months

3. Which of the following statements regarding the men infected with toxoplasma in the current study is most accurate?

- A. Only men with preexisting conditions developed symptoms
- B. Symptoms began 2 to 3 weeks after returning home from the hunting trip
- C. None of the symptomatic patients were hospitalized
- D. Symptoms included headache, fever, myalgia, and joint pain

4. Which of the following statements about the laboratory assessment of the current cohort of men is most accurate?

- A. All men with symptoms were positive for toxoplasma-immunoglobulin (Ig)M antibodies
- B. Most men with symptoms were positive for toxoplasma-IgG antibodies
- C. Toxoplasma-IgG antibodies were not found among asymptomatic men
- D. Serological assays for brucellosis were positive in half of the cohort

Earning CME Credit

To obtain credit, you should first read the journal article. After reading the article, you should be able to answer the following, related, multiple-choice questions. To complete the questions (with a minimum 75% passing score) and earn continuing medical education (CME) credit, please go to <http://www.medscape.org/journal/eid>. Credit cannot be obtained for tests completed on paper, although you may use the worksheet below to keep a record of your answers.

You must be a registered user on <http://www.medscape.org>. If you are not registered on <http://www.medscape.org>, please click on the “Register” link on the right hand side of the website.

Only one answer is correct for each question. Once you successfully answer all post-test questions, you will be able to view and/or print your certificate. For questions regarding this activity, contact the accredited provider, CME@medscape.net. For technical assistance, contact CME@medscape.net. American Medical Association’s Physician’s Recognition Award (AMA PRA) credits are accepted in the US as evidence of participation in CME activities. For further information on this award, please go to <https://www.ama-assn.org>. The AMA has determined that physicians not licensed in the US who participate in this CME activity are eligible for AMA PRA Category 1 Credits™. Through agreements that the AMA has made with agencies in some countries, AMA PRA credit may be acceptable as evidence of participation in CME activities. If you are not licensed in the US, please complete the questions online, print the AMA PRA CME credit certificate, and present it to your national medical association for review.

Article Title

Characteristics of Patients with Acute Flaccid Myelitis, United States, 2015–2018

CME Questions

1. You are advising a public health department in the United States regarding prevention and management of acute flaccid myelitis (AFM). According to the study by McLaren and colleagues, which of the following statements about the clinical and laboratory characteristics of AFM cases reported in the United States during peak vs. nonpeak years from 2015 through 2018 is correct?

- A. Peak years were 2015 and 2016, followed by nonpeak years in 2017 and 2018
- B. Cases in peak years were older than in nonpeak years (8.3 years vs 5.2 years; $p = 0.02$)
- C. Cases in peak vs. nonpeak years had more cerebrospinal fluid pleocytosis (85% vs. 63%; $p < 0.001$)
- D. Cases in nonpeak vs. peak years had a greater proportion of enterovirus (EV)/rhinovirus (RV)-positive specimens (38% vs. 16%; $p = 0.02$)

2. According to the study by McLaren and colleagues, which of the following statements about clinical and laboratory characteristics of AFM cases reported in the United States during peak years 2016 and 2018 is correct?

- A. Compared with cases with onset in 2018, those in 2016 were more severe and less likely to have cranial nerve lesions
- B. In 2016, more cases had an illness in the 4 weeks preceding limb weakness onset than in 2018

- C. The proportion of confirmed AFM cases that were positive for EV/RV was significantly higher in 2018 than in 2016
- D. Among cases positive for EV/RV, those in 2018 vs 2016 were less likely to be positive for EV-D68 (46% vs. 70%; $p = 0.03$) but more likely to be positive for EV-A71 (18% vs. 6%; $p = 0.13$)

3. According to the study by McLaren and colleagues, which of the following statements about clinical and public health significance of differences in the clinical and laboratory characteristics of AFM cases reported in the United States during peak vs. nonpeak years from 2015 through 2018 is correct?

- A. Differences in clinical and laboratory characteristics of AFM in peak vs. nonpeak years suggest differences in viral etiologies, informing treatment and prevention strategies
- B. Most evidence supports EV-A71 as the most likely pathogen responsible for the new epidemiology of peak years alternating with nonpeak years
- C. AFM surveillance should be restricted to detecting the specific pathogen most likely to be implicated in peak activity
- D. Healthcare providers should report only AFM cases positive for EV-D68 to public health authorities

Earning CME Credit

To obtain credit, you should first read the journal article. After reading the article, you should be able to answer the following, related, multiple-choice questions. To complete the questions (with a minimum 75% passing score) and earn continuing medical education (CME) credit, please go to <http://www.medscape.org/journal/eid>. Credit cannot be obtained for tests completed on paper, although you may use the worksheet below to keep a record of your answers.

You must be a registered user on <http://www.medscape.org>. If you are not registered on <http://www.medscape.org>, please click on the “Register” link on the right hand side of the website.

Only one answer is correct for each question. Once you successfully answer all post-test questions, you will be able to view and/or print your certificate. For questions regarding this activity, contact the accredited provider, CME@medscape.net. For technical assistance, contact CME@medscape.net. American Medical Association’s Physician’s Recognition Award (AMA PRA) credits are accepted in the US as evidence of participation in CME activities. For further information on this award, please go to <https://www.ama-assn.org>. The AMA has determined that physicians not licensed in the US who participate in this CME activity are eligible for AMA PRA Category 1 Credits™. Through agreements that the AMA has made with agencies in some countries, AMA PRA credit may be acceptable as evidence of participation in CME activities. If you are not licensed in the US, please complete the questions online, print the AMA PRA CME credit certificate, and present it to your national medical association for review.

Article Title

Illness Severity in Hospitalized Influenza Patients by Virus Type and Subtype, Spain, 2010–2017

CME Questions

1. You are advising a large hospital in Spain regarding anticipated needs for influenza care and management. According to the retrospective cohort study by Delgado-Sanz and colleagues, which of the following statements about clinical characteristics among severe, hospitalized, confirmed influenza cases (SHCIC) caused by different virus types and subtypes in Spain from 2010 to 2017 is correct?

- A. Approximately one-third of cases were influenza B
- B. Median age was 53 (interquartile, range [IQR] 37–66) years for A(H1N1)pdm09 cases; 73 (IQR 56–83) years for A(H3N2), and 60 (IQR 22–74) years for B cases ($p < 0.001$)
- C. Comorbid medical conditions were most frequent in A(H1N1)pdm09 cases
- D. Median duration from onset of symptoms to hospitalization was longest in A(H3N2) cases

2. According to the retrospective cohort study by Delgado-Sanz and colleagues, which of the following statements about outcomes among SHCIC caused by different virus types and subtypes in Spain from 2010 to 2017 is correct?

- A. Risk for pneumonia did not differ among the subgroups
- B. Risk for intensive care unit (ICU) admission was highest among A(H3N2) cases
- C. Case fatality rate was significantly higher for A(H3N2) than for A(H1N1)pdm09
- D. The associations of ICU admission and death with influenza type and subtype were not independent of other factors

3. According to the retrospective cohort study by Delgado-Sanz and colleagues, which of the following statements about clinical implications of findings regarding SHCIC caused by different virus types and subtypes in Spain from 2010 to 2017 is correct?

- A. Influenza seasons with predominant A(H1N1)pdm09 circulation will result in greater demand for hospital ICUs, especially among hospitalized young adults
- B. Antiviral treatment should be reserved only for confirmed cases with clinical deterioration after 48 hours of supportive care
- C. Data regarding circulating influenza types and subtypes are unlikely to affect healthcare resource allocation
- D. Findings of this study regarding age distribution differ substantially from those of previous reports